ECOPHYSIOLOGY AND BIOGEOCHEMISTRY OF MARINE PLANTS IN THE ANTHROPOCENE

EDITED BY: Kasper Elgetti Brodersen, Stacey Marie Trevathan-Tackett, Fanny Noisette, Mats Björk, Anthony William Larkum, Marianne Holmer and Michael Kühl

PUBLISHED IN: Frontiers in Marine Science and Frontiers in Plant Science

frontiers Research Topics

ISSN 1664-8714
ISBN 978-2-83250-111-5
DOI 10.3389/978-2-83250-111-5

About Frontiers

Frontiers is more than just an open-access publisher of scholarly articles: it is a pioneering approach to the world of academia, radically improving the way scholarly research is managed. The grand vision of Frontiers is a world where all people have an equal opportunity to seek, share and generate knowledge. Frontiers provides immediate and permanent online open access to all its publications, but this alone is not enough to realize our grand goals.

Frontiers Journal Series

The Frontiers Journal Series is a multi-tier and interdisciplinary set of open-access, online journals, promising a paradigm shift from the current review, selection and dissemination processes in academic publishing. All Frontiers journals are driven by researchers for researchers; therefore, they constitute a service to the scholarly community. At the same time, the Frontiers Journal Series operates on a revolutionary invention, the tiered publishing system, initially addressing specific communities of scholars, and gradually climbing up to broader public understanding, thus serving the interests of the lay society, too.

Dedication to Quality

Each Frontiers article is a landmark of the highest quality, thanks to genuinely collaborative interactions between authors and review editors, who include some of the world's best academicians. Research must be certified by peers before entering a stream of knowledge that may eventually reach the public - and shape society; therefore, Frontiers only applies the most rigorous and unbiased reviews.
Frontiers revolutionizes research publishing by freely delivering the most outstanding research, evaluated with no bias from both the academic and social point of view. By applying the most advanced information technologies, Frontiers is catapulting scholarly publishing into a new generation.

What are Frontiers Research Topics?

Frontiers Research Topics are very popular trademarks of the Frontiers Journals Series: they are collections of at least ten articles, all centered on a particular subject. With their unique mix of varied contributions from Original Research to Review Articles, Frontiers Research Topics unify the most influential researchers, the latest key findings and historical advances in a hot research area! Find out more on how to host your own Frontiers Research Topic or contribute to one as an author by contacting the Frontiers Editorial Office: frontiersin.org/about/contact

ECOPHYSIOLOGY AND BIOGEOCHEMISTRY OF MARINE PLANTS IN THE ANTHROPOCENE

Topic Editors:
Kasper Elgetti Brodersen, University of Copenhagen, Denmark
Stacey Marie Trevathan-Tackett, Deakin University, Australia
Fanny Noisette, Université du Québec à Rimouski, Canada
Mats Björk, Stockholm University, Sweden
Anthony William Larkum, University of Technology Sydney, Australia
Marianne Holmer, University of Southern Denmark, Denmark
Michael Kühl, University of Copenhagen, Denmark

Citation: Brodersen, K. E., Trevathan-Tackett, S. M., Noisette, F., Björk, M., Larkum, A. W., Holmer, M., Kühl, M., eds. (2022). Ecophysiology and Biogeochemistry of Marine Plants in the Anthropocene. Lausanne: Frontiers Media SA. doi: 10.3389/978-2-83250-111-5

Table of Contents

frontiers | Frontiers in Marine Science

TYPE Editorial
PUBLISHED 18 August 2022
DOI 10.3389/fmars.2022.1010651

OPEN ACCESS

EDITED AND REVIEWED BY
Angel Borja, Technological Center Expert in Marine and Food Innovation (AZTI), Spain

*CORRESPONDENCE
Kasper Elgetti Brodersen
kasper.elgetti.brodersen@bio.ku.dk

SPECIALTY SECTION
This article was submitted to Marine Ecosystem Ecology, a section of the journal Frontiers in Marine Science

RECEIVED 03 August 2022
ACCEPTED 05 August 2022
PUBLISHED 18 August 2022

CITATION
Brodersen KE, Trevathan-Tackett SM, Noisette F, Björk M, Larkum AWD, Holmer M and Kühl M (2022) Editorial: Ecophysiology and biogeochemistry of marine plants in the anthropocene. *Front. Mar. Sci.* 9:1010651. doi: 10.3389/fmars.2022.1010651

Editorial: Ecophysiology and biogeochemistry of marine plants in the anthropocene

Kasper Elgetti Brodersen[1*], Stacey M. Trevathan-Tackett[2], Fanny Noisette[3], Mats Björk[4], Anthony W. D. Larkum[5], Marianne Holmer[6] and Michael Kühl[1]

[1]Marine Biological Section, Department of Biology, University of Copenhagen, Copenhagen, Denmark, [2]Centre for Integrative Ecology, Deakin University, Geelong, VIC, Australia, [3]nstitut des Sciences de la mer, Université du Québec à Rimouski, Rimouski, QC, Canada, [4]Department of Ecology, Environment and Plant Sciences, Stockholm University, Stockholm, Sweden, [5]Climate Change Cluster (C3), University of Technology Sydney, Sydney, NSW, Australia, [6]Department of Biology, University of Southern Denmark, Odense, Denmark

KEYWORDS

seagrass, macroalgae, ecology, photosynthesis, climate change

Editorial on the Research Topic
Ecophysiology and biogeochemistry of marine plants in the anthropocene

Climate change in the Anthropocene detrimentally effects the livelihood of marine plants and their coastal habitats (Halpern et al., 2008; Waycott et al., 2009; Larkum et al., 2018a; Larkum et al., 2018b), due to increased frequency and severity of extreme environmental events such as: ocean deoxygenation, heatwaves, heavy rain and storm events (Easterling et al., 2000). Hypoxic conditions in the water column, e.g., induced by eutrophication or the shoaling of deoxygenated water (Diaz and Rosenberg, 2008), markedly affect the oxygen availability and internal aeration of marine plants (Colmer, 2003; Greve et al., 2003; Brodersen et al., 2017a), which increases their susceptibility to intrusion of reduced toxic compounds (e.g., hydrogen sulphide) from the sediment (Pedersen et al., 2004; Borum et al., 2005; Holmer and Hasler-Sheetal, 2014; Brodersen et al., 2015a). Coastal eutrophication-driven blooms of epiphytes on seagrass and other marine plant leaves (Borum, 1985) can shade the leaves for light and limit essential gas and nutrient exchange with the water column (Brodersen et al., 2015b; Brodersen et al., 2020; Noisette et al., 2020). Elevated temperature can weaken the blue carbon sink capacity of vegetated coastal ecosystems (Trevathan-Tackett et al., 2020) and can lead to oxygen deficiency in plants living close to their thermal stress threshold (Raun & Borum, 2013; Pedersen et al., 2016). Increased temperature can also lead to decreased seagrass productivity and biomass (George et al., 2018) and elevated microbial activity in the sediment increasing the sulphide pressure on the plants (Blaabjerg et al., 1998; Lamers et al., 2013) and elevated emissions of methane from seagrass sediments (George et al., 2020), further weakening their climate mitigation capacities. Finally, drops in salinity and high ammonium availability can interact synergistically in a negative impact on marine plant fitness (Villazán et al., 2015; Sola et al., 2020).

In light of the above-mentioned threats, future climate conditions will arguably have major impacts on the function and fitness of vegetated coastal ecosystems worldwide and thus on their ecological roles. Gaining a better understanding of the environmental regulation of marine plants and their ecophysiology is thus important for the planning of climate adaptation strategies and development of innovative and sustainable protection strategies for marine plants to better protect and secure vital ecosystem services and functions of vegetated coastal ecosystems in the Anthropocene. The present Research Topic is a compilation of 14 articles that aim to advance our understanding of how changing environmental conditions in the Anthropocene affects the ecophysiology and biogeochemistry of marine plants. The Research Topic is divided into 3 subtopics: (*i*) articles that discuss effects on the phyllosphere and rhizosphere conditions, (*ii*) articles that focus on impacts of ocean warming on marine plants and ecosystems, and (*iii*) articles that studied effects on seagrass metabolism and biogeochemical cycling.

Anthropogenic and climate change-related effects on seagrass phyllosphere and rhizosphere dynamics are discussed in the articles by Brodersen and Kühl, Koop-Jakobsen et al., Martin et al., Scholz et al., and Zhang et al. (*subtopic 1*). Brodersen and Kühl review how epiphytes affect the seagrass phyllosphere. They describe how the phyllosphere micro-habitat is affected by eutrophication-induced epiphytic biofilm communities and changing environmental conditions. Epiphytes impede leaf photosynthesis in light, owing to shading and a combination of induced hyperoxia and reduced CO_2 availability due to phyllosphere basification and epiphytic carbon fixation. Also, absorbed light energy in the epiphyte cover can lead to leaf surface warming, potentially aggravating negative effects of climate change. In darkness, anoxia within the epiphytic biofilm can result in toxic nitric oxide production *via* denitrification. Such phyllosphere stress conditions at night-time may be exacerbated by global warming. Koop-Jakobsen et al. employed planar O_2 optodes to describe rhizosphere oxygenation of high- and low-marsh ecotypes of *Elymus athericus*, a fast-spreading marsh plant. Results revealed oxygen release along the roots and oxic root zones in both marsh ecotypes in light and dark conditions. However, no differences were found in the belowground tissue oxygenation capacity between ecotypes, making *E. athericus* a highly competitive marsh plant in areas affected by fast sea-level rise. Martin et al. used 16S rRNA gene sequencing combined with analysis of seagrass nutrient (e.g., isotopic signatures of C and N) and heavy metal concentrations in tissue to investigate potential links between environmental metal and nutrient pollution to the microbial community associated with seagrass (*Halophila ovalis*) roots collected in an anthropogenically influenced estuary. Results indicate that changes in the composition of the seagrass root microbial community can potentially be used as a bioindicator for environmental conditions, such as pollution and contamination. Scholz et al. review experimental approaches to investigate the seagrass rhizosphere. They describe and discuss microenvironmental analysis techniques such as microsensors, optical sensors (e.g., planar optodes and sensor nanoparticles), and gel sampling methods (e.g., DETs and DGTs). Furthermore, they identify knowledge gaps and potential methodological advances in seagrass research. Studies of geochemical gradients in the seagrass rhizosphere are important as the plant-driven chemical gradients, protect the plants against reduced, anoxic sediment conditions (Brodersen et al., 2018) and can enable nutrient uptake (Brodersen et al., 2017b)while changes in the natural chemical gradients can cause plant stress and die-off (Borum et al., 2005; Brodersen et al., 2015a). Zhang et al. investigated the impact of epiphytic biofilms on the chemical microenvironment of the seagrass (*Z. marina* L.) leaf surface, as measured with microsensors. They demonstrated that the phyllosphere chemistry was mainly affected in the light by the metabolic activity of epiphytes leading to high O_2 concentrations and pH in the seagrass leaf microenvironment, which reduced the CO_2 availability for the seagrass leaf. The study thus advances our understanding of the effects of eutrophication-induced epiphytes on seagrass performance and the leaf surface microenvironment.

Impacts of increasing temperature on seagrass performance, health and abundance are described in articles by Graham et al., Hansen et al., Jueterbock et al., Plaisted et al., and Yucharoen et al. (*subtopic 2*). Graham et al. addressed the effects of seagrass wasting disease infection on eelgrass (*Z. marina* L.) growth and sugar production in a natural meadow in relation to ocean warming under climate change. Seagrass wasting disease impaired eelgrass growth and accumulation of belowground rhizome sugar, suggesting a disease-induced reduction of below-ground carbon accumulation. This study highlights the need to consider pathogen infection effects co-occurring with warmer conditions. Hansen et al. used gas exchange measurements to determine effects of global warming on the photosynthesis, respiration and diel O_2 budget of eelgrass (*Z. marina* L.) leaves with and without epiphytes. Leaves with epiphytes were more affected by elevated seawater temperatures than bare seagrass leaves, as indicated by a lower light use efficiency, higher light requirements and a more negative diel O_2 balance at high seawater temperatures. Epiphytic growth on seagrass leaves can thus aggravate other detrimental effects of climate change on seagrass performance.

Jueterbock et al. utilised a combination of Pulse Amplitude Modulated (PAM) fluorometry and RNA-sequencing to describe the photosynthetic characteristics of eelgrass (*Z. marina* L.) under strong annual fluctuations in day length to investigate adaptations to polar light conditions and the possibility of poleward range expansion into the Arctic region in response to global warming. Results suggested that Norwegian eelgrass populations are able to repress respiration and up-regulate genes related to carbon fixation and chlorophyll synthesis, to tolerate winter dim light conditions *via* metabolic dormancy. Plaisted et al. utilised long-term monitoring data to investigate regional changes in the presence and abundance of eelgrass (*Z. marina* L.) in relation to local sea surface temperatures. They demonstrated that the summer water temperature of the previous year is an important predictor of

eelgrass presence in the region (Northeastern USA), where above average summer temperatures are associated with an increased probability of eelgrass absence, and below average summer temperatures are linked with the highest probability of eelgrass presence in the following year. The study thus delivers new insights on climate change related impacts on seagrass abundance. Yucharoen et al. utilised PAM fluorometry to assess the thermotolerance of tropical shallow-water corals, seagrasses and macroalgae. The study compared the physiological responses to elevated temperature and interspecific sensitivity of species from the different organism groups and furthermore examined the utility of an integrated biomarker response (IBR) approach to evaluate and integrate the candidate responses. Results showed that the IBR index provides a useful tool for assessing the vulnerability of marine organisms to ocean warming and demonstrated that species and organism groups differ in their sensitivity to elevated temperatures. This study underscore that extreme heating events and global warming can have consequences for ecosystem structure and functions in future oceans.

The metabolism of seagrass and their contribution to biogeochemical processes and element cycling in the Anthropocene is described in articles by Apostolaki et al., Asplund et al., Léger-Daigle et al., and Olive et al. (*subtopic 3*). Apostolaki et al. investigated the potential of dead seagrass *Posidonia oceanica* mattes to act as biogeochemical sinks and archives in coastal areas of the Mediterranean. Results indicate that dead *P. oceanica* mattes are sinks for carbon and contaminants and thus contain signals of past environmental change and contamination. The study thus adds important new knowledge of paleoecology to blue carbon research of seagrass sediments. Asplund et al. utilized benthic chambers to determine methane (CH_4) emissions from Nordic seagrasses (*Z. marina* L.) during summer. The authors provide new fundamental insights on the effects of temperature, salinity and soil carbon on net methane emissions from seagrass sediments. Results showed relatively weak methane emissions from Nordic *Z. marina* meadows, where the net methane release was positively affected by the sedimentary carbon content. Thus, the emission of methane from seagrass meadows might increase with elevated temperatures and eutrophication driven increases in sedimentation. Léger-Daigle et al. used PAM fluorometry, pigment content and metabolic measurements to assess photoacclimation and light thresholds of cold temperate seagrasses (*Z. marina* L.). The study provides novel insights into the photoacclimation response of eelgrass to a wide range of light conditions *via* photosynthetic and physiological changes. The authors show that eelgrass is capable of photosynthetic adjustments at irradiances below the threshold between limiting and saturating irradiances, as well as, sustained maximal photosynthesis rates from saturating light down to a photon irradiance of 74 μmol photons m^{-2} s^{-1}. These results highlight the capacity of eelgrass to acclimate to decreasing light conditions in coastal environments, often considered one of the main limiting factors for eelgrass growth and persistence. Finally, Olive et al. assessed the metabolism and nutrient cycling contribution of tropical seagrass (*Syringodium isoetifolium*) in the sediment and benthic community of a tropical reef lagoon. They show that the *S. isoetifolium* meadow was net autotrophic across the lagoon and reduced the heterotrophy of the whole benthic community. However, there was a large variability in the metabolic balance of the benthic components among sites, mainly related to the environmental variability found in the lagoon. This study highlights the need to investigate how community functioning can vary according to environmental variability driven by human activities in changing oceans.

In summary, the articles in this Research Topic elucidate the diverse range of potential negative effects of human activity and climate change related impacts on marine plants in the Anthropocene. Such effects include epiphyte-induced extremes in the seagrass leaf surface microenvironment, as well as ocean warming-induced reduction in seagrass abundance and potential positive correlation with increased seagrass wasting disease, which may reduce belowground carbon accumulation in infected meadows. However, the contributions to this research topic also provide insights into other important aspects such as seagrass paleoecology, factors affecting the microbial community of the rhizosphere, methane emissions, and photoacclimatory responses.

Author contributions

The editorial was written by KEB with contributions from all remaining co-authors.

Funding

KB was supported by a grant from the Villum Foundation (00028156). ST was supported by the Australian Research Council's DECRA Fellowship (DE210101029). MK was supported by grants from the Independent Research Fund Denmark (DFF-8021-00308B) and the Gordon and Betty Moore Foundation through grant no. GBMF9206 to MK (https://doi.org/10.37807/GBMF9206).

Acknowledgments

We thank the Editorial staff of the Frontiers in Marine Science and Frontiers in Plant Science for their invitation and support in producing this Research Topic.

Conflict of interest

The authors declare that the research was conducted in the absence of any commercial or financial relationships that could be construed as a potential conflict of interest.

Publisher's note

References

Blaabjerg, V., Mouritsen, K. N., and Finster, K. (1998). Diel cycles of sulphate reduction rates in sediments of a *Zostera marina* bed (Denmark). *Aquat. Microbial. Ecol.* 15 (1), 97–102. doi: 10.3354/ame015097

Borum, J. (1985). Development of epiphytic communities on eelgrass (*Zostera marina*) along a nutrient gradient in a Danish estuary. *Mar. Biol.* 87 (2), 211–218. doi: 10.1007/BF00539431

Borum, J., Pedersen, O., Greve, T. M., Frankovich, T. A., Zieman, J. C., Fourqurean, J. W., et al. (2005). The potential role of plant oxygen and sulphide dynamics in die-off events of the tropical seagrass, *Thalassia testudinum*. *J. Ecol.* 93, 148–158. doi: 10.1111/j.1365-2745.2004.00943.x

Brodersen, K. E., Hammer, K. J., Schrameyer, V., Floytrup, A., Rasheed, M. A., Ralph, P. J., et al. (2017a). Sediment resuspension and deposition on seagrass leaves impedes internal plant aeration and promotes phytotoxic H_2S intrusion. *Front. Plant Sci.* 8, 657. doi: 10.3389/fpls.2017.00657

Brodersen, K. E., Koren, K., Moßhammer, M., Ralph, P. J., Kühl, M., and Santner, J. (2017b). Seagrass-mediated phosphorus and iron solubilization in tropical sediments. *Environ. Sci. Technol.* 51 (24), 14155–14163. doi: 10.1021/acs.est.7b03878

Brodersen, K. E., Koren, K., Revsbech, N. P., and Kühl, M. (2020). Strong leaf surface basification and CO_2 limitation of seagrass induced by epiphytic biofilm microenvironments. *Plant Cell Environ.* 43 (1), 174–187. doi: 10.1111/pce.13645

Brodersen, K. E., Lichtenberg, M., Paz, L.-C., and Kühl, M. (2015b). Epiphyte-cover on seagrass (*Zostera marina* l.) leaves impedes plant performance and radial O_2 loss from the below-ground tissue. *Front. Mar. Sci.* 2, 58. doi: 10.3389/fmars.2015.00058

Brodersen, K. E., Nielsen, D. A., Ralph, P. J., and Kühl, M. (2015a). Oxic microshield and local pH enhancement protects *Zostera muelleri* from sediment derived hydrogen sulphide. *New Phytol.* 205, 1264–1276. doi: 10.1111/nph.13124

Brodersen, K. E., Siboni, N., Nielsen, D. A., Pernice, M., Ralph, P. J., Seymour, J., et al. (2018). Seagrass rhizosphere microenvironment alters plant-associated microbial community composition. *Environ. Microbiol.* 20 (8), 2854–2864. doi: 10.1111/1462-2920.14245

Colmer, T. D. (2003). Long-distance transport of gases in plants: a perspective on internal aeration and radial oxygen loss from roots. *Plant Cell Environ.* 26, 17–36. doi: 10.1046/j.1365-3040.2003.00846.x

Diaz, R. J., and Rosenberg, R. (2008). Spreading dead zones and consequences for marine ecosystems. *Science* 321 (5891), 926–929. doi: 10.1126/science.1156401

Easterling, D. R., Meehl, G. A., Parmesan, C., Changnon, S. A., Karl, T. R., and Mearns, L. O. (2000). Climate extremes: observations, modeling, and impacts. *Science* 289 (5487), 2068–2074. doi: 10.1126/science.289.5487.2068

George, R., Gullström, M., Mangora, M. M., Mtolera, M. S. P., and Björk, M. (2018). High midday temperature stress has stronger effects on biomass than on photosynthesis: A mesocosm experiment on four tropical seagrass species. *Ecol. Evol.* 8, 4508–4517. doi: 10.1002/ece3.3952

George, R., Gullström, M., Mtolera, M. S., Lyimo, T. J., and Björk, M. (2020). Methane emission and sulfide levels increase in tropical seagrass sediments during temperature stress: A mesocosm experiment. *Ecol. Evol.* 10 (4), 1917–1928. doi: 10.1002/ece3.6009

Greve, T. M., Borum, J., and Pedersen, O. (2003). Meristematic oxygen variability in eelgrass (*Zostera marina*). *Limnol. Oceanogr.* 48 (1), 210–216. doi: 10.4319/lo.2003.48.1.0210

Halpern, B. S., Walbridge, S., Selkoe, K. A., Kappel, CV, Micheli, F, d'Agrosa, C, et al. (2008). A global map of human impact on marine ecosystems. *Science* 319 (5865), 948–952. doi: 10.1126/science.1149345

Holmer, M., and Hasler-Sheetal, H. (2014). Sulfide intrusion in seagrasses assessed by stable sulfur isotopes–a synthesis of current results. *Front. Mar. Sci.* 1, 64. doi: 10.3389/fmars.2014.00064

Lamers, L. P., Govers, L. L., Janssen, I. C., Geurts, J. J., van der Welle, M. E., Van Katwijk, M. M., et al. (2013). Sulfide as a soil phytotoxin–a review. *Front. Plant Sci.* 4. doi: 10.3389/fpls.2013.00268

Larkum, A. W., Kendrick, G. A., and Ralph, P. J. (2018a). *Seagrasses of Australia: Structure, ecology and conservation* (Cham, Switzerland: Springer). (Book).

Larkum, A. W., Pernice, M., Schliep, M., Davey, P., Szabo, M., Raven, J. A., et al. (2018b). Photosynthesis and metabolism of seagrasses. *In: Seagrasses Australia Springer (Book)* pp, 315–342. doi: 10.1007/978-3-319-71354-0_11

Noisette, F., Depetris, A., Kühl, M., and Brodersen, K. E. (2020). Flow and epiphyte growth effects on the thermal, optical and chemical microenvironment in the leaf phyllosphere of seagrass (*Zostera marina*). *J. R. Soc. Interface* 17 (171), 20200485. doi: 10.1098/rsif.2020.0485

Pedersen, O., Binzer, T., and Borum, J. (2004). Sulphide intrusion in eelgrass (*Zostera marina* l.). *Plant Cell Environ.* 27, 595–602. doi: 10.1111/j.1365-3040.2004.01173.x

Pedersen, O., Colmer, T. D., Borum, J., Zavala-Perez, A., and Kendrick, G. A. (2016). Heat stress of two tropical seagrass species during low tides–impact on underwater net photosynthesis, dark respiration and diel *in situ* internal aeration. *New Phytol.* 210 (4), 1207–1218. doi: 10.1111/nph.13900

Raun, A. L., and Borum, J. (2013). Combined impact of water column oxygen and temperature on internal oxygen status and growth of *Zostera marina* seedlings and adult shoots. *J. Exp. Mar. Biol. Ecol.* 441, 16–22. doi: 10.1016/j.jembe.2013.01.014

Sola, J., Sorrell, B. K., Olesen, B., Søndergaard Jørgensen, M., and Lund-Hansen, L. C. (2020). Acute and prolonged effects of variable salinity on growth, gas exchange and photobiology of eelgrass (*Zostera marina* l.). *Aquat. Bot.* 165, 103236. doi: 10.1016/j.aquabot.2020.103236

Trevathan-Tackett, S. M., Brodersen, K. E., and Macreadie, P. I. (2020). Effects of elevated temperature on microbial breakdown of seagrass leaf and tea litter biomass. *Biogeochemistry* 151 (2), 171–185. doi: 10.1007/s10533-020-00715-1

Villazán, B., Salo, T., Brun, F. G., Vergara, J. J., and Pedersen, M. F. (2015). High ammonium availability amplifies the adverse effect of low salinity on eelgrass *Zostera marina*. *Mar. Ecol. Prog. Ser.* 536, 149–162. doi: 10.3354/meps11435

Waycott, M., Duarte, C. M., Carruthers, T. J. B., Orth, RJ, Dennison, WC, Olyarnik, S, et al. (2009). Accelerating loss of seagrasses across the globe threatens coastal ecosystems. *Proc. Natl. Acad. Sci.* 106, 12377–12381. doi: 10.1073/pnas.0905620106

frontiers in Plant Science

ORIGINAL RESEARCH
published: 10 June 2021
doi: 10.3389/fpls.2021.669751

Plant-Mediated Rhizosphere Oxygenation in the Native Invasive Salt Marsh Grass *Elymus athericus*

***Ketil Koop-Jakobsen*[1]*, *Robert J. Meier*[2] *and *Peter Mueller*[3]**

[1]*Wadden Sea Station, Alfred Wegener Institute, Helmholtz Centre for Polar and Marine Research (AWI), List/Sylt, Germany,* [2]*PreSens Precision Sensing GmbH, Regensburg, Germany,* [3]*Institute of Soil Science, Center for Earth System Research and Sustainability, Universität Hamburg, Hamburg, Germany*

In the last decades, the spread of *Elymus athericus* has caused significant changes to the plant community composition and ecosystem services of European marshes. The distribution of *E. athericus* was typically limited by soil conditions characteristic for high marshes, such as low flooding frequency and high soil aeration. However, recently the spread of *E. athericus* has begun to also include low-marsh environments. A high-marsh ecotype and a low-marsh ecotype of *E. athericus* have been described, where the latter possess habitat-specific phenotypic traits facilitating a better adaption for inhabiting low-marsh areas. In this study, planar optodes were applied to investigate plant-mediated sediment oxygenation in *E. athericus*, which is a characteristic trait for marsh plants inhabiting frequently flooded environments. Under waterlogged conditions, oxygen (O_2) was translocated from aboveground sources to the roots, where it leaked out into the surrounding sediment generating oxic root zones below the sediment surface. Oxic root zones were clearly visible in the optode images, and no differences were found in the O_2-leaking capacity between ecotypes. Concentration profiles measured perpendicular to the roots revealed that the radius of the oxic root zones ranged from 0.5 to 2.6 mm measured from the root surface to the bulk anoxic sediment. The variation of oxic root zones was monitored over three consecutive light–dark cycles (12 h/12 h). The O_2 concentration of the oxic root zones was markedly reduced in darkness, yet the sediment still remained oxic in the immediate vicinity of the roots. Increased stomatal conductance improving the access to atmospheric O_2 as well as photosynthetic O_2 production are likely factors facilitating the improved rhizosphere oxygenation during light exposure of the aboveground biomass. *E. athericus'* capacity to oxygenate its rhizosphere is an inheritable trait that may facilitate its spread into low-marsh areas. Furthermore, this trait makes *E. athericus* a highly competitive species in marshes facing the effects of accelerated sea-level rise, where waterlogged sediment conditions could become increasingly pronounced.

Keywords: tidal wetland, plant-soil interaction, sediment oxygenation, ROL, wetland plants, aerenchyma, planar optode, imaging

OPEN ACCESS

Edited by:
Michael Kühl,
University of Copenhagen, Denmark

Reviewed by:
Vincent Scholz,
Aarhus University, Denmark
Brian K. Sorrell,
Aarhus University, Denmark

***Correspondence:**
Ketil Koop-Jakobsen
ketil.koop-jakobsen@awi.de

Specialty section:
This article was submitted to Marine and Freshwater Plants, a section of the Frontiers in Plant Science

Received: *19 February 2021*
Accepted: *03 May 2021*
Published: *10 June 2021*

Citation:
Koop-Jakobsen K, Meier RJ and Mueller P (2021) Plant-Mediated Rhizosphere Oxygenation in the Native Invasive Salt Marsh Grass Elymus athericus. Front. Plant Sci. 12:669751. doi: 10.3389/fpls.2021.669751

INTRODUCTION

Elymus athericus (Link) Kerguélen (henceforth referred to as *Elymus*) is markedly increasing its areal coverage in NW European salt marshes, altering the characteristic plant community composition and becoming a dominant plant species (Leendertse et al., 1997; van Wijnen et al., 1997; Valéry et al., 2017; Hartmann and Stock, 2019). This spread has been described as one of the most significant changes of the NW European salt-marsh landscape in the last decades (Valéry et al., 2004). The spread of *Elymus* may significantly impact the ecosystem services that the salt marshes provide altering the sedimentation and carbon storage capacity (Valéry et al., 2004; Hartmann and Stock, 2019; Nolte et al., 2019) and changing the marshes' role as a nursery for the coastal fish populations (Laffaille et al., 2005).

Elymus is primarily confined to the high marsh, characterized by lower inundation frequency (Bockelmann et al., 2002) and higher soil aeration (Armstrong et al., 1985). The spread of *Elymus* in the high marsh has, in part, occurred in response to the abandonment of grazing practices and increased man-made drainage activities (Rupprecht et al., 2015; Hartmann and Stock, 2019), as well as increased sedimentation enhancing the surface elevation (Nolte et al., 2019). Increased nitrogen loading may also be a driver for the spread of *Elymus* in European marshes (Olff et al., 1997; Van Wijnen and Bakker, 1999; Rozema et al., 2000; Valéry et al., 2017). This is, however, not always the case (Bockelmann and Neuhaus, 1999; Veeneklaas et al., 2013; Nolte et al., 2019).

Strikingly, the spread of *Elymus* is not restricted to the high marsh, and progressive invasion into the low-marsh environments has recently been observed in various studies (Olff et al., 1997; Veeneklaas et al., 2013; Valéry et al., 2017; Nolte et al., 2019; Mueller et al., 2021; Reents et al., 2021). An important factor likely contributing to *Elymus*' competitiveness across a large range of flooding frequencies is the presence of discrete *Elymus* genotypes from high-marsh and low-marsh environments, respectively. These genotypes are reflected in phenotypic characteristics (Bockelmann et al., 2002, 2003). The low-marsh ecotype is characterized by having habitat-specific phenotypic traits, such as higher aboveground biomass production, longer rhizomes, shoots, and leaves, which facilitates a better adaption for inhabiting areas with higher flooding frequencies (Chen, 2020; Reents et al., 2021). Overall, however, the morphological and physiological mechanisms behind *Elymus*' high competitiveness in these frequently flooded environments are poorly understood (Mueller et al., 2021).

The low marsh is frequently flooded by seawater at high tide, and the sediment is primarily waterlogged resulting in anoxic conditions and sulfide accumulation. The marsh plants that inhabit the low marsh have adaptive traits, which enable them to cope with these harsh living conditions (Parent et al., 2008; Pan et al., 2020). Well-developed aerenchyma is a key trait facilitating a rapid supply of oxygen (O_2) from aboveground sources to the belowground roots and rhizomes, where it may leak out and oxygenate the surrounding sediment, generating oxic root zones below the sediment surface (Colmer, 2003; Sorrell and Brix, 2013). Plant-mediated sediment oxygenation is a trait that reduces the phytotoxic impact of sulfide accumulation (Lee et al., 1999; Pezeshki, 2001) and improves nutrient uptake (Bradley and Morris, 1990; Lai et al., 2012). We hypothesize that the *Elymus* low-marsh ecotype, in order to thrive and be competitive in the low marsh, possesses the ability to transport O_2 from aboveground sources to its roots and further into the sediment. In the high marsh, belowground transport of O_2 is not a necessity, as the soils are typically well-drained and aerated (Mueller et al., 2020). In many wetland plants, the porosity of the roots is often lower in plants grown under drained/aerated conditions than plants grown under waterlogged and O_2-deficient conditions (Colmer, 2003). Hence, we hypothesize that the capability of transporting O_2 during events of flooding is limited in the *Elymus* high-marsh ecotype.

In this study, we investigated the formation of oxic root zones during sediment waterlogging in the low-marsh and high-marsh ecotype of *E. athericus*. Planar optodes were applied to image the O_2 haloes evolving around individual roots in the rhizosphere. The effect of light availability of the aboveground biomass on belowground sediment oxygenation was investigated, monitoring oxic root-zone formations during consecutive light–dark cycles.

MATERIALS AND METHODS

Experimental Design

Plant-mediated sediment oxygenation was investigated by imaging oxic roots zones in four replicate plant samples of the low-marsh and high-marsh ecotype, respectively. The impact of light on belowground O_2 dynamics was investigated, monitoring the oxic roots zones during three consecutive light/dark cycles (12 h/12 h). The spatial extension of oxic root zones was measured as O_2 profiles across selected oxic root zones. Both *Elymus* ecotypes were investigated under waterlogged conditions in order to distinguish roots leaking O_2 into the anoxic sediment.

Plant Samples and Cultures

Plants were collected, the Netherlands in April 2015 on the Wadden Sea island of Schiermonnikoog. The sampling was conducted in stands that previously were demonstrated as being genetically distinct populations of *Elymus*, i.e., high-marsh and low-marsh ecotypes (Bockelmann et al., 2003). The two ecotypes were grown under identical conditions in a common-garden setting exposed to natural changes in precipitation and sunlight at the University of Hamburg for 5 years before investigations commenced. Low-marsh and high-marsh ecotypes were still phenotypically distinct after 5 years (Mueller et al., 2021; Reents et al., 2021), which confirms that the morphological differences between the low-marsh and high-marsh ecotypes are indeed caused by genetic differences (Mueller et al., 2021; Reents et al., 2021), as described by Bockelmann et al. (2003).

Planar Optode Imaging

The formation of oxic root zones in the rhizosphere of *Elymus* was investigated using the planar optode system, VisiSens TD

from PreSens – Precision Sensing GmbH, which is a ratiometric optode imaging system allowing for 2D imaging of O_2 (pH and CO_2) distributions. The O_2 optode imaging is based on the dynamic quenching of a luminophore in the presence of O_2. For 2D imaging of plant-mediated sediment oxygenation of the rhizosphere, the plant sample for investigation is placed in a rhizobox with roots facing the transparent front plate of the box. An optode foil, coated with a luminescent O_2-sensitive dye, is placed on the inside of the rhizobox in direct contact with the roots and sediment. The foil is excited by a LED light source, and the luminescent response is recorded with a camera. Through calibration, each pixel in the image is assigned an O_2 value, generating a quantitative 2D image of the O_2 distribution (**Figure 1**). The limit of detection for the VisiSens TD system with SF-RPFu4 O_2 sensing foils is 0.03%.

For a detailed description of the theoretical background behind the ratiometric optode imaging principles used in the VisiSens optode system, we refer to Wang et al. (2010), Tschiersch et al. (2011), and Tschiersch et al. (2012).

Preparation of Plant Samples for Planar Optode Investigations

In preparation for planar optode investigations, single shoots were separated 3 months prior to the optode measurements and cultured in a substrate consisting of 70% sand and 30% potting soil. Salinity was reduced to zero to ensure recovery of shoots after separation. The low-marsh ecotype was kept under permanently waterlogged conditions, and the high-marsh ecotype was kept under moist sediment conditions with regular watering.

For the preparation of a rhizobox with *Elymus* roots placed up against the transparent front plate, the coarse organic matter was washed out of the substrate, and the remaining sandy sediment was slurred and filled in a rhizobox (10 cm × 10 cm × 10 cm) with a detachable front plate. The sediment was allowed to settle for a minimum of 1 day. These procedures were installed to get a uniform sediment with high stability, which allowed for the rhizobox to be turned to a 45° angle and the front plate to be removed, without the sediment collapsing, exposing a well-defined vertical sediment surface. In this way, the roots and rhizomes of the plant sample could manually be distributed over the vertical sediment surface, facing the front plate, allowing for direct contact with the optode foil.

Subsequently, an O_2-sensitive optode foil (SF-RPSu4; 10 cm × 15 cm; range, 0–100% O_2 atm. sat., PreSens GmbH) was attached to the inside of the detached front plate of the rhizobox. Both the front plate and optode foil were placed in a container with water. Under water, the optode foil was pressed up against the front plate, and both items were lifted out of the water together. In this way, a uniform and air-bubble-free water film was generated between the foil and the front plate, holding the foil in place.

The front plate with foil was attached back on the rhizobox, and the rhizobox was then slowly moved back to an upright position, while water was simultaneously added along with the back plate. In this way, the sediment along the front plate was slowly saturated with water from the bottom up, minimizing

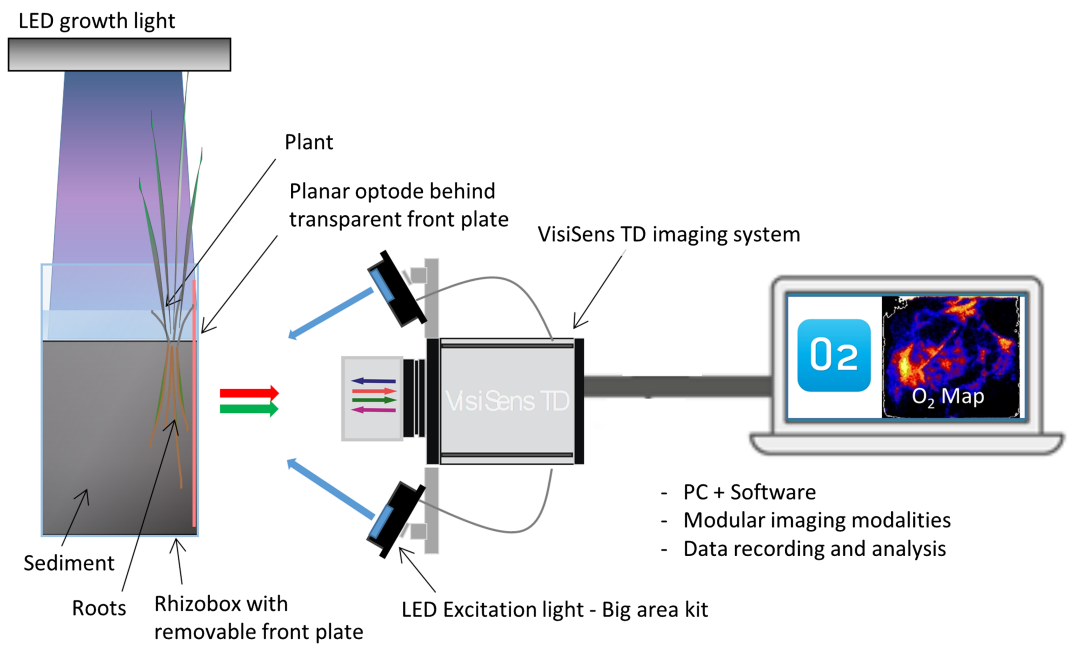

FIGURE 1 | Experimental setup for planar optode investigations of rhizosphere processes with the planar optode system VisiSens TD. A rhizobox with sediment and the sample plant is equipped with a planar luminescent O_2 sensor foil. The aboveground biomass of the plant is illuminated in a day–night cycle with a LED growth light. The O_2 dependent signals of the sensor foil are read out with the VisiSens camera detector under excitation with specific blue excitation light. The recorded signals are transformed into 2D O_2 maps *via* the camera software.

the entrapment of air bubbles along with the optode foil. The water-filled rhizobox had a 3–5 cm water column on top of the sediment with the adult *Elymus* plants being emergent through the water column.

Experimental Setup

Optode imaging of the rhizosphere O_2 distribution was conducted simultaneously on two rhizoboxes, using external LED excitation lights (Big Area Imaging kit, PreSens GmbH). During light periods, the aboveground biomass was illuminated with a LED growth light (Roleadro 270 W LED) placed 40 cm above the plants. Prior to the optode measurements, the sample-prepared rhizobox was run through a minimum of two light–dark cycles, reestablishing normal sediment conditions after the sample preparation. The light conditions under the growth light were too bright for optode imaging, which requires conditions without ambient light. In order to enable optode recordings during the light period, the illumination of the aboveground biomass was turned off for a 3-min period every 30 min, while each optode image was acquired. The optode investigations were conducted in freshwater within a temperature range from 18 to 20°C. At the end of each optode experiment, the front plate with optode foil was detached, and the vertical sediment surface was photographed showing the relative position of the roots. In cases where many roots were partially hidden behind the sediment, the sediment surface was gently rinsed with droplets of water from a Pasteur pipette in order to expose the roots and make them visible in the image.

Image Analysis

The planar optode images were analyzed using the VisiSens ScientifiCal software, which is an integrated part of the optode imaging system. The acquired optode images had a resolution of ~5 pixels per millimeter at the chosen field of view. The internal noise filter was applied to smoothen the optode images with kernel size 2. A two-point calibration was applied, using air-bubbled water for 100% atmospheric equilibrium O_2 (100% atm. sat.) and anoxic sediment for 0% atm. sat. The calibration converted the sensor readout into quantitative 2D images of the O_2 distribution. O_2 concentrations were expressed as the percentage of O_2 saturation at atmospheric equilibrium (% atm. sat.).

For investigation of the impact of light availability on the temporal distribution of oxic root zones, the average O_2 concentration was measured continuously in specific areas of each sample, representing an oxic root zone and the bulk anoxic sediment, respectively. The oxic root zone area was manually selected as a root zone with oxygenation below the sediment surface clearly distinguishable from the bulk anoxic sediment, and likewise, the anoxic bulk sediment area was selected as an anoxic zone without roots below the sediment surface clearly distinguishable from the oxic root zones. This way of measuring temporal variation was conducted using the ScientifiCal software, which allows for the average concentration to be followed over time within a manually selected area of the optode foil.

For investigation of the impact of light availability on the spatial distribution of oxic root zones, cross-sectional concentration profiles were measured perpendicular to selected O_2 leaking roots under light and dark conditions. One profile was measured per sample. Profiles were selected from areas where O_2 leaking from single roots was clearly distinguishable from the background O_2 concentration. In cases with more selectable roots, the root with the highest O_2 concentration was chosen. Larger oxic root zones most often had multiple roots contributing to O_2 leakage; these areas were avoided. This spatial profiling was conducted using the ScientifiCal software (Live Profile plugin). The width of the roots was measured directly from images of the rhizobox using the open-source software ImageJ Fiji (1.53c).

RESULTS

Oxic Root Zones in Low- and High-Marsh Ecotypes

Oxic root zones facilitated by plant-mediated O_2 transport were found in both the low-marsh and the high-marsh ecotype of *Elymus* (**Figures 2, 3**). Although many roots were placed alongside of the rhizobox, only some of these roots were leaking O_2 to the sediment. The size of the oxic root zones ranged from less than a millimeter on either side of a root to larger, centimeter-scale oxic roots zones, where multiple roots contributed to the oxygenation of the sediment.

O_2 leakage was most pronounced in the low-marsh ecotype, where oxic root zones were generated around multiple roots in all four replicates (**Figure 2**). High variation was shown among samples; sediment oxygenation was particularly pronounced in LM1 and LM2, whereas in LM3 and LM4, plant-mediated sediment oxygenation was primarily found near the sediment surface with a few O_2 leaking roots stretching into the sediment. Also, in the high-marsh ecotype (**Figure 3**), oxic root zones were found in all four replicates. Here, plant-mediated sediment oxygenation was primarily associated with roots near the sediment surface. In replicate HM1, HM2, and HM4, oxic root zones were found stretching from the sediment surface into the sediment, whereas HM3 showed very limited sediment oxygenation. Despite the reduction in the size and O_2 concentration during dark periods, the oxic root zones remained visibly distinguishable from the bulk anoxic sediment in the optode images, although they were relatively faint due to low O_2 concentrations (**Figure 2** – dark and **Figure 3** – dark). This demonstrated that *Elymus* is able to maintain oxic conditions around its roots, even without photosynthetic O_2 production.

Impact of Light Availability on the Temporal Variation of Oxic Root Zones

The light conditions of the aboveground biomass markedly affected the belowground oxygenation of the rhizosphere. This was observed in the low-marsh and high-marsh ecotype (**Figure 4**). The average O_2 concentration of the oxic root

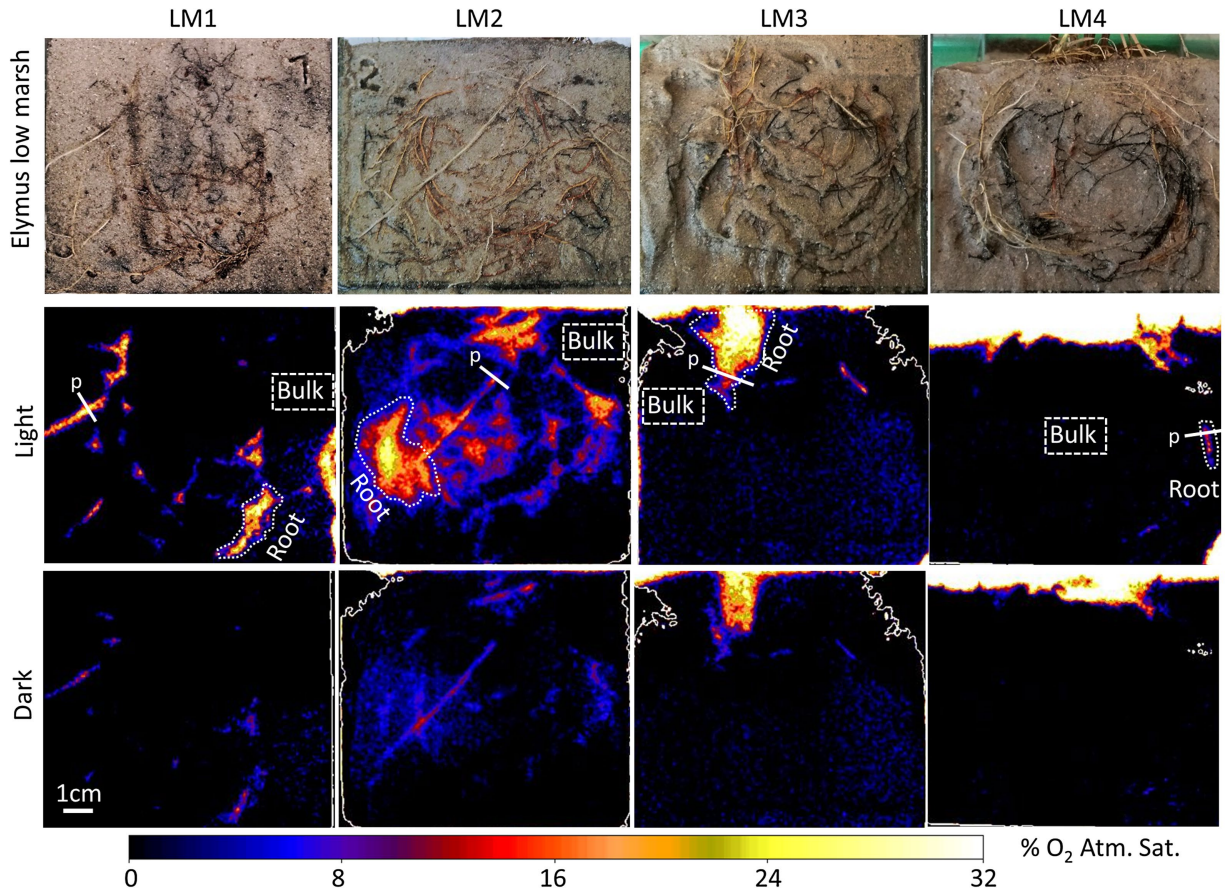

FIGURE 2 | Planar optode images of the O_2 distribution around selected roots of *Elymus athericus* – low-marsh ecotype from four independent samples (LM1–LM4), with and without illumination of the aboveground biomass. "Root" indicates specific oxic root zones, and "Bulk" indicates specific areas with bulk anoxic sediment selected for quantitative measurements shown in **Figure 4**. "p" indicates the locations of the concentration profile shown in **Figure 5**.

zones immediately decreased when light exposure of the aboveground biomass was turned off and immediately increased again when light exposure was turned back on. The reduction in the average O_2 concentration during darkness was highly variable, ranging from 40 to 82% reduction in the low-marsh ecotype and 48–89% in the high-marsh ecotype. Despite the reduction in O_2 concentration during dark periods, the oxic concentrations remained higher in the oxic root zone than in the bulk anoxic sediment (**Figure 4**). There was no statistical difference (*t*-test) between the low-marsh and the high-marsh ecotype in regard to O_2 concentration during the light (t = 1.26, p = 0.26) and the dark period (t = 0.93, p = 0.39) or the reduction in O_2 between light and dark periods (t = 0.33, p = 0.75) (*t*-tests based on data in **Figure 4C**).

Impact of Light Availability on the Spatial Variation of Oxic Root Zones

The spatial distribution of the oxic root zones in the low-marsh ecotype and high-marsh ecotype was affected by changing light conditions, diminishing when the light exposure of the aboveground biomass was turned off (**Figure 5**). The radius of the oxic root zones measured from the O_2 profiles was markedly reduced by 23–57% in the low-marsh ecotype and 35–62% in the high-marsh ecotype. Despite the reduction in the width of the oxic root zones, the sediment remained oxic in the immediate vicinity of the roots during dark periods, and the sediment at the root surface never became fully anoxic (**Figure 5**). There was no statistical difference (*t*-test) between the low-marsh and the high-marsh ecotype in regard to the radius of the oxic root zone during light (t = 1.76, p = 0.13) and dark (t = 1.75, p = 0.13) periods or in the maximum O_2 concentration at the root surface (t = 0.48, p = 0.65) (*t*-tests based on data in **Figure 5C**).

DISCUSSION

Oxic root zones were found in the low-marsh and high-marsh ecotype of *Elymus*. This clearly demonstrated that both ecotypes are genetically disposed to develop roots with the capacity to transport O_2 belowground and oxygenate the sediment. In the optode images, the low-marsh ecotype displayed more and larger oxic root zones and with higher O_2 concentrations below the sediment surface (**Figures 2, 3**). However, the radius of

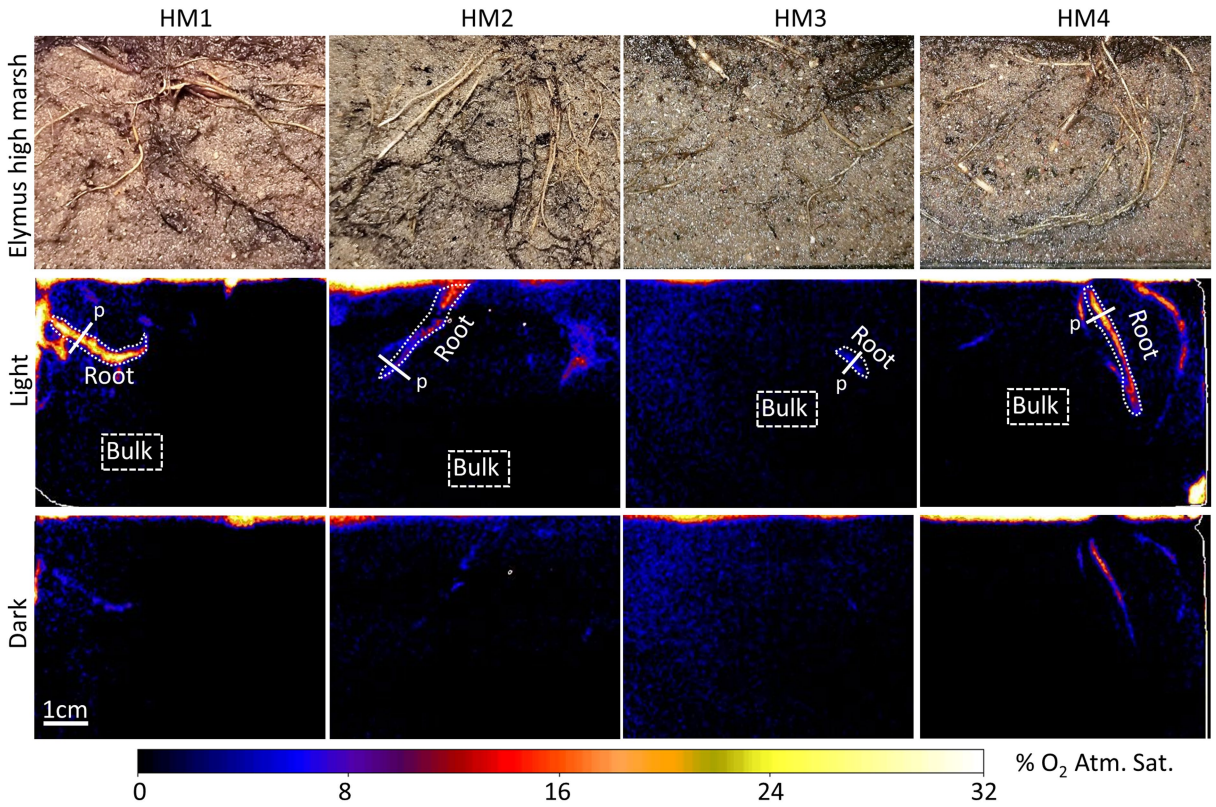

FIGURE 3 | Planar optode images of the O_2 distribution around selected roots of *E. athericus* – high-marsh ecotype from four independent samples (HM1–HM4), with and without illumination of the aboveground biomass. "Root" indicates specific oxic root zones, and "Bulk" indicates specific areas with bulk anoxic sediment selected for quantitative O_2 measurements shown in **Figure 4**. "p" indicates the locations of the concentration profile shown in **Figure 5**.

individual oxic root zones, measured around single roots, showed no difference between ecotypes and ranged from 0.9 to 2.6 mm under illuminated conditions. Hence, our study could not determine any clear distinction in the sediment oxygenation capacity between the two ecotypes. The here observed size range is similar to oxic root zones found in other wetland plants, such as *Spartina anglica* (Koop-Jakobsen et al., 2017) and rice (*Oryza sativa*; Larsen et al., 2015), and in aquatic macrophytes, such as *Ruppia maritima* (Jovanovic et al., 2015) and *Vallisneria spiralis* (Han et al., 2016). In cases where O_2 leaking roots were overlapping (**Figure 2**; LM2 and LM3), larger oxic roots zones developed due to the cumulative contribution, causing O_2 to build up in the sediment. This is often shown in aquatic plants where O_2 leakage occurs from larger parts of the roots, such as the freshwater isoetid *Lobelia dortmanna* (Lenzewski et al., 2018) and rice plants (*O. sativa*; Larsen et al., 2015).

Spatial Variation in Oxygen Leakage from *Elymus* Roots

In many wetland plants, suberin and lignin deposits in the hypodermis/exodermis prevent O_2 leakage from the root into the sediment (Ejiri and Shiono, 2019) as well as intrusion of reduced phytotoxins from the sediment. Plants that develop this O_2-loss barrier are often capable of long-distance O_2 transportation to root tissues deep below the sediment surface, and due to the barrier formation, sediment oxygenation is usually restricted to small areas near the root tips (Colmer, 2003). In the O_2-leaking roots observed in *Elymus*, there was no clear spatial restriction of O_2 loss across the rhizodermis, and O_2 leakage occurred over larger parts of the roots. Therefore, *Elymus* O_2 transport and sediment oxygenation are likely to be limited to the topsoil. Mozdzer et al. (2016) argue that the capacity to develop a deep-reaching root system represents a key trait in many invasive wetland plants that enables them to utilize nutrients below the rooting zone of native plants. However, our results suggest that this invasion strategy may not play a critical role in the spread of *Elymus*.

Sediment phytotoxins, such as low molecular weight carboxylic acids, sulfides, or reduced iron, are known to trigger the formation of a barrier against O_2 loss (Pedersen et al., 2021). As *in situ* phytotoxin concentrations may be higher than those generated in the soils used in our experimental setup, additional research on barrier formation is needed to confirm this notion under field conditions in the waterlogged low marsh.

It is noteworthy that a majority of the roots visible in the rhizobox images (**Figures 2, 3**), which were monitored with the planar optode system, did not leak O_2 at all. Roots without O_2 leakage were present both in the low-marsh and

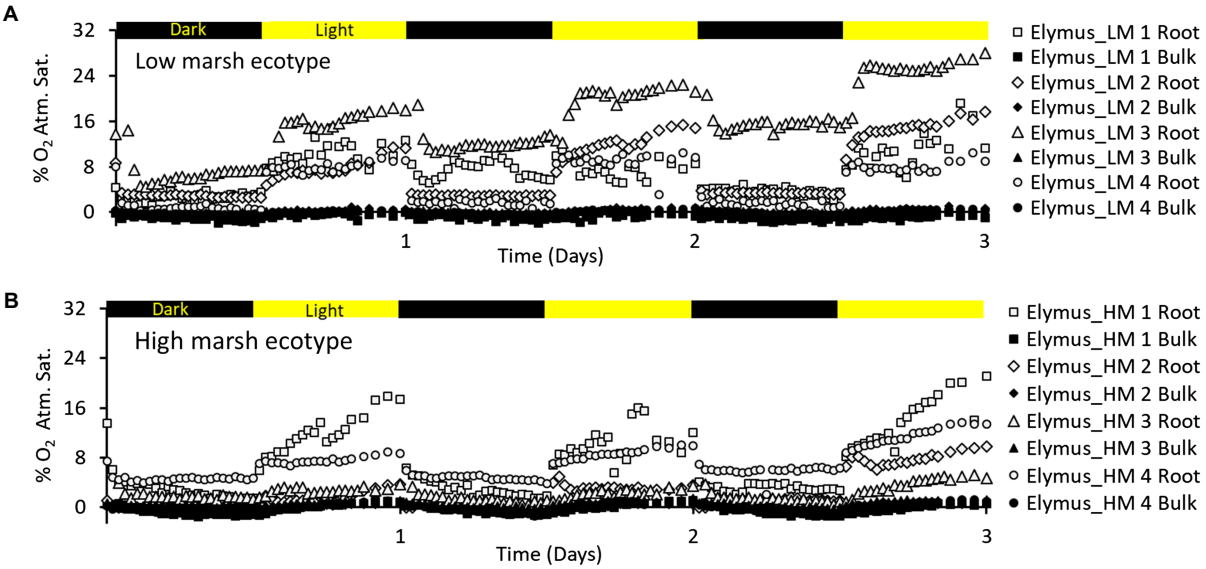

C

	Light period (% O_2 as.±sd)	Dark period (% O_2 as. ±sd)	Reduction
Elymus LM 1	10.9±3.2	3.7±0.6	-66%
Elymus LM 2	14.6±1.9	3.3±0.2	-77%
Elymus LM 3	25.6±1.2	15.4±0.7	-40%
Elymus LM 4	8.0±0.9	1.4±0.7	-82%
Low Marsh			

	Light period (% O_2 as. ±sd)	Dark period (% O_2 as. ±sd)	Reduction
Elymus HM 1	13.9±4.0	3.2±0.5	-77%
Elymus HM 2	7.8±1.0	0.8±0.5	-89%
Elymus HM 3	3.8±0.9	1.2±0.4	-68%
Elymus HM 4	11.3±1.5	5.9±0.9	-48%
High Marsh			

FIGURE 4 | Oxygen dynamics in selected oxic root zones of the *E. athericus* – low-marsh ecotype **(A)** and high-marsh ecotype **(B)** during three light–dark periods (12 h/12 h). The location of the oxic root zones is depicted in the optode images of **Figures 2, 3**. **(C)** Table showing O_2 concentrations [% O_2 atm. sat.(as.)] in selected root zones of the low- and high-marsh ecotype, calculated as an average of the light period (2.5–3 d) and the preceding dark period (2–2.5 d), respectively; ±sd refers to the standard deviation (n = 24). "Reduction" shows the percentage reduction in the average concentration of O_2 between light and dark periods.

high-marsh ecotype. This demonstrates that the sediment-oxygenation capability varied among roots, which can be caused either by insufficient connectivity between the individual roots and the aboveground O_2 resources or by reduction of the permeability of roots, for example, due to the formation of an O_2-loss barrier in the hypodermis/exodermis or the accumulation of metal plaques on the root surface (Povidisa et al., 2009). The latter is particularly shown in older roots. In this study, roots at various life stages were present in the optode images. O_2 leakage was most often associated with newer roots with a clear white root surface and roots with a light brown surface, possibly due to initial precipitation of metal oxides. Older roots colored dark-brown or black showed no or limited O_2 leakage, possibly due to substantial metal-plaque formation given the observed color changes.

Effect of Light on the Development of Oxic Root Zones

The oxic roots zones were highly affected by changing light conditions, resulting in a rapid decrease in the O_2 level (**Figure 4**) and size (**Figure 5**), which occurred immediately (i.e., within 30 min) after the illumination of the aboveground biomass was turned off. However, despite a marked reduction of the oxic root zones, they remained distinguishable in the optode images obtained during dark periods (**Figures 2, 3**). The presence of oxic root zones during dark periods was also confirmed by the quantitative measures, where the O_2 concentration in oxic root zones during dark periods was higher than the anoxic bulk sediment (**Figure 4**). Furthermore, the O_2 profiles also showed the presence of O_2 in darkness (**Figure 5**). This suggests that processes in the aboveground biomass triggered by light availability control belowground rhizosphere oxygenation. In light, stomata will open and provide full access to atmospheric O_2, which will increase the flow of O_2 to roots and rhizomes. In the nighttime, stomata are likely only to be partially opened and restrict access to atmospheric O_2, which can account for the observed decrease in the O_2 level of the oxic root zones during dark periods. However, the stomatal conductance was still sufficient to maintain the oxic root zones and prevent complete anoxia during darkness. Furthermore, photosynthetic O_2 production of the aboveground biomass may increase the internal O_2 concentration and contribute to the belowground O_2 transport during the day. The light-inflicted fluctuations in the O_2 concentration of the oxic root zones varied markedly among the individual roots, ranging from a 40 to 89% reduction

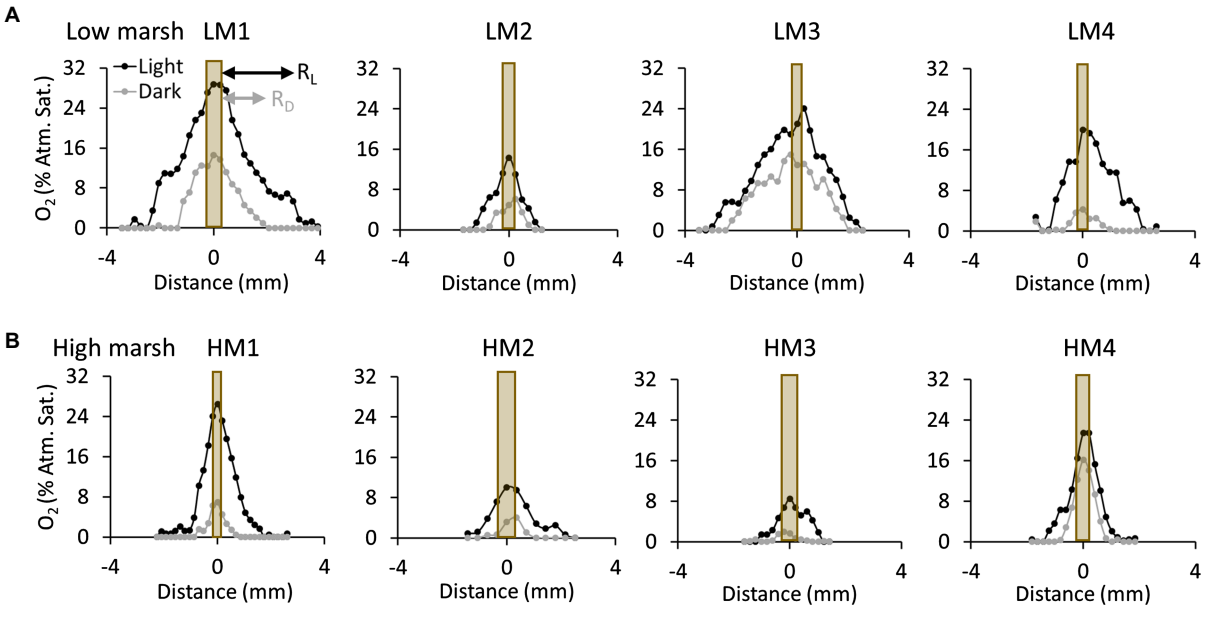

C

	Radius Light R_L (mm)	Radius Dark R_D (mm)	Radius reduction
Elymus LM 1	2.62	1.36	-48%
Elymus LM 2	1.04	0.69	-33%
Elymus LM 3	2.59	2.01	-23%
Elymus LM 4	1.68	0.72	-57%
Low Marsh			

	Radius Light R_L (mm)	Radius Dark R_D (mm)	Radius reduction
Elymus HM 1	1.82	0.69	-62%
Elymus HM 2	1.04	0.68	-35%
Elymus HM 3	0.87	0.46	-47%
Elymus HM 4	1.13	0.72	-36%
High Marsh			

FIGURE 5 | Oxygen concentration profiles measured perpendicular to selected roots of the *E. athericus* low-marsh ecotype **(A)** and high-marsh ecotype **(B)**. The locations of the profiles are depicted in **Figures 2, 3**. The orange bar shows the position of the root relative to the O_2 profile, and the width of the bar represents the relative width of the root investigated. The profiles were measured during the last light cycle (2.5–3 d) and dark cycle (2–2.5 d), respectively, at the time point, when the oxygen concentration at the root surface was highest. **(C)** Table showing the radius of oxic root zones measured from the root surface to the bulk anoxic sediment in the low- and high-marsh ecotype during light and dark periods, respectively.

between light and darkness. This demonstrates a high variability in the O_2 leaking capacity among individual roots. In this study, where the sediment was homogenized removing any variation in the sediment O_2 demand prior to the optode measurements, the variation observed in oxic root zones reflects variation in root properties rather than sediment properties. A variation in root properties can originate from (1) variation in the O_2 transport capability from the atmosphere to roots, (2) continuous root growth which can alter the O_2-leaking capacity during the experiment, and (3) from investigating roots at different levels of maturity expressing differences in barrier formation. Variation in oxic root zones and their development over time has previously been observed in similar optode studies with other aquatic plants (Koop-Jakobsen and Wenzhöfer, 2015; Koop-Jakobsen et al., 2018; Lenzewski et al., 2018).

Methodology

The 2D image series provides detailed information on the spatial and temporal variation in the O_2 content around individual roots over time, which was clearly demonstrated in this study (**Figures 2, 3**). In this way, the planar optode technology is an excellent tool for getting insight into root functions and root-soil interactions, while the roots are still embedded in the soil. However, it should be considered that planar optodes are an experimental tool. In this study, a sandy sediment was deliberately chosen, so the roots could easily be placed in direct contact with the optode foil. Freshwater, rather than saltwater, was used in this study to secure the growth of the individual plants under waterlogged conditions prior to the optode measurement. Growing in the high marsh, *Elymus* is adapted to low-range salinities (<10 ppt) but able to withstand both high salinities during floods and low salinity during rainfalls (Mueller et al., 2021). In our study, *Elymus* thrived in freshwater, and there was no evidence of hyposaline stress from using a low-salt environment.

Furthermore, the O_2 leaking from roots is measured against an optode foil, which acts as a barrier, causing the halo of O_2 around the roots to be slightly skewed compared to normal sediment conditions. Hence, the experimental conditions in

this study differ from the natural sediment conditions in the field. Nevertheless, our optode experiments clearly demonstrate that both the low-marsh and the high-marsh ecotype of *E. athericus* possess the specific trait that enables it to transport O_2 from aboveground sources to its roots and oxygenate the rhizosphere during short-term waterlogging. However, elucidating the impact on the rhizosphere under natural conditions will require further studies *in situ*.

Conclusion and Perspective

Oxic root zones were found in all investigated plants of the low-marsh ecotype. Consequently, we accept our first hypothesis that the low-marsh ecotype possesses the ability to transport O_2 from aboveground sources to its roots and further into the sediment. Oxic root zones were also clearly detectable in all of the investigated plants of the high-marsh ecotype. Hence, we reject our second hypothesis stating that the capability of transporting O_2 is limited in the high-marsh ecotype. Plant-mediated sediment oxygenation is a key trait for aquatic plants facing waterlogged sediment conditions, and this trait is a prerequisite for *Elymus* to spread into the low marsh, potentially making it competitive with other species well adapted for living in waterlogged sediments, such as *Spartina*.

In a world with accelerating sea-level rise, salt marshes will experience more frequent flooding and longer times with waterlogged sediment conditions. As shown in this study, *Elymus* has the ability to improve the chemical environment of its rhizosphere through plant-mediated sediment oxygenation, and thereby, it can be a highly competitive species in a future, wetter salt-marsh environment. This can significantly impact the ecosystem services that the salt marshes provide in terms of coastal protection, carbon storage, and nutrient retention, and further studies are needed on the impact of alterations of the plant community composition caused by external factors, such as climate change.

DATA AVAILABILITY STATEMENT

The raw data supporting the conclusions of this article will be made available by the authors, without undue reservation.

AUTHOR CONTRIBUTIONS

KK-J and PM conceived the research idea. KK-J designed and performed the experiment, analyzed the data, and wrote the manuscript. RM provided the equipment and developed new software applications for image analysis. RM and PM edited the manuscript. All authors contributed to the article and approved the submitted version.

FUNDING

For KK-J, the research was funded in part by The Helmholtz Climate Initiative (HI-CAM). HI-CAM is funded by the Helmholtz Association's Initiative and Networking Funds (10.13039/501100009318). PM was supported by the DAAD (German Academic Exchange Service) PRIME fellowship program funded through the German Federal Ministry of Education and Research (BMBF; 10.13039/501100002347). The authors are responsible for the content of this publication.

ACKNOWLEDGMENTS

We would like to thank Chris Smit and his colleagues from Groningen University for the provision of the plants. Marion Klötzl, Maren Winnacker, and Hao Tang are thanked for culturing plants at Universität Hamburg. KK-J acknowledges the support of the Open Access Publication Funds of Alfred-Wegener-Institut Helmholtz-Zentrum für Polar- und Meeresforschung.

REFERENCES

Armstrong, W., Wright, E. J., Lythe, S., and Gaynard, T. J. (1985). Plant zonation and the effects of the spring-neap tidal cycle on soil aeration in a humber salt marsh. *J. Ecol.* 73, 323–339. doi: 10.2307/2259786

Bockelmann, A.-C., Bakker, J. P., Neuhaus, R., and Lage, J. (2002). The relation between vegetation zonation, elevation and inundation frequency in a Wadden Sea salt marsh. *Aquat. Bot.* 73, 211–221. doi: 10.1016/S0304-3770(02)00022-0

Bockelmann, A.-C., and Neuhaus, R. (1999). Competitive exclusion of *Elymus athericus* from a high-stress habitat in a European salt marsh. *J. Ecol.* 87, 503–513. doi: 10.1046/j.1365-2745.1999.00368.x

Bockelmann, A.-C., Reusch, T. B. H., Bijlsma, R., and Bakker, J. P. (2003). Habitat differentiation vs. isolation-by-distance: the genetic population structure of *Elymus athericus* in European salt marshes. *Mol. Ecol.* 12, 505–515. doi: 10.1046/j.1365-294X.2003.01706.x

Bradley, P. M., and Morris, J. T. (1990). Influence of oxygen and sulfide concentration on nitrogen uptake kinetics in *Spartina alterniflora*. *Ecology* 71, 282–287. doi: 10.2307/1940267

Chen, Q. (2020). Low-marsh ecotypes of a dominant plant may not be better adapted to increased sea level. *Flora* 273, 151722. doi: 10.1016/j.flora.2020.151722

Colmer, T. D. (2003). Long-distance transport of gases in plants: a perspective on internal aeration and radial oxygen loss from roots. *Plant Cell Environ.* 26, 17–36. doi: 10.1046/j.1365-3040.2003.00846.x

Ejiri, M., and Shiono, K. (2019). Prevention of radial oxygen loss is associated with exodermal suberin along adventitious roots of annual wild species of *Echinochloa*. *Front. Plant Sci.* 10:254. doi: 10.3389/fpls.2019.00254

Han, C., Ren, J., Tang, H., Xu, D., and Xie, X. (2016). Quantitative imaging of radial oxygen loss from *Valisneria spiralis* roots with a fluorescent planar optode. *Sci. Total Environ.* 569–570, 1232–1240. doi: 10.1016/j.scitotenv.2016.06.198

Hartmann, K., and Stock, M. (2019). Long-term change in habitat and vegetation in an ungrazed, estuarine salt marsh: man-made foreland compared to young marsh development. *Estuar. Coast. Shelf Sci.* 227:106348. doi: 10.1016/j.ecss.2019.106348

Jovanovic, Z., Pedersen, M., Larsen, M., Kristensen, E., and Glud, R. N. (2015). Rhizosphere O_2 dynamics in young *Zostera marina* and *Ruppia maritima*. *Mar. Ecol. Prog. Ser.* 518, 95–105. doi: 10.3354/meps11041

Koop-Jakobsen, K., Fischer, J., and Wenzhöfer, F. (2017). Survey of sediment oxygenation in rhizospheres of the saltmarsh grass - *Spartina anglica*. *Sci. Total Environ.* 589, 191–199. doi: 10.1016/j.scitotenv.2017.02.147

Koop-Jakobsen, K., Mueller, P., Meier, R. J., Liebsch, G., and Jensen, K. (2018). Plant-sediment interactions in salt marshes–an optode imaging study of O_2, pH, and CO_2 gradients in the rhizosphere. *Front. Plant Sci.* 9:541. doi: 10.3389/fpls.2018.00541

Koop-Jakobsen, K., and Wenzhöfer, F. (2015). The dynamics of plant-mediated sediment oxygenation in *Spartina anglica* rhizospheres - a planar optode study. *Estuar. Coasts* 38, 951–963. doi: 10.1007/s12237-014-9861-y

Laffaille, P., Pétillon, J., Parlier, E., Valéry, L., Ysnel, F., Radureau, A., et al. (2005). Does the invasive plant *Elymus athericus* modify fish diet in tidal salt marshes? *Estuarine Coastal Shelf Sci.* 65, 739–746. doi: 10.1016/j.ecss.2005.07.023

Lai, W.-L., Zhang, Y., and Chen, Z.-H. (2012). Radial oxygen loss, photosynthesis, and nutrient removal of 35 wetland plants. *Ecol. Eng.* 39, 24–30. doi: 10.1016/j.ecoleng.2011.11.010

Larsen, M., Santner, J., Oburger, E., Wenzel, W. W., and Glud, R. N. (2015). O_2 dynamics in the rhizosphere of young rice plants (*Oryza sativa* L.) as studied by planar optodes. *Plant Soil* 390, 279–292. doi: 10.1007/s11104-015-2382-z

Lee, R. W., Kraus, D. W., and Doeller, J. E. (1999). Oxidation of sulfide by *Spartina alterniflora* roots. *Limnol. Oceanogr.* 44, 1155–1159. doi: 10.4319/lo.1999.44.4.1155

Leendertse, P. C., Roozen, A. J. M., and Rozema, J. (1997). Long-term changes (1953–1990) in the salt marsh vegetation at the Boschplaat on Terschelling in relation to sedimentation and flooding. *Plant Ecol.* 132, 49–58. doi: 10.1023/A:1009795002076

Lenzewski, N., Mueller, P., Meier, R. J., Liebsch, G., Jensen, K., and Koop-Jakobsen, K. (2018). Dynamics of oxygen and carbon dioxide in rhizospheres of *Lobelia dortmanna* – a planar optode study of belowground gas exchange between plants and sediment. *New Phytol.* 218, 131–141. doi: 10.1111/nph.14973

Mozdzer, T. J., Langley, J. A., Mueller, P., and Megonigal, J. P. (2016). Deep rooting and global change facilitate spread of invasive grass. *Biol. Invasions* 18, 2619–2631. doi: 10.1007/s10530-016-1156-8

Mueller, P., Do, H. T., Smit, C., Reisdorff, C., Jensen, K., and Nolte, S. (2021). With a little help from my friends: physiological integration facilitates invasion of wetland grass *Elymus athericus* into flooded soils. *Oikos* 130, 431–439. doi: 10.1111/oik.07863

Mueller, P., Granse, D., Nolte, S., Weingartner, M., Hoth, S., and Jensen, K. (2020). Unrecognized controls on microbial functioning in blue carbon ecosystems: the role of mineral enzyme stabilization and allochthonous substrate supply. *Ecol. Evol.* 10, 998–1011. doi: 10.1002/ece3.5962

Nolte, S., Wanner, A., Stock, M., and Jensen, K. (2019). *Elymus athericus* encroachment in Wadden Sea salt marshes is driven by surface elevation change. *Appl. Veg. Sci.* 22, 454–464. doi: 10.1111/avsc.12443

Olff, H., De Leeuw, J., Bakker, J., Platerink, R., and Van Wijnen, H. (1997). Vegetation succession and herbivory in a salt marsh: changes induced by sea level rise and silt deposition along an elevational gradient. *J. Ecol.* 85, 799–814. doi: 10.2307/2960603

Pan, Y., Cieraad, E., Clarkson, B. R., Colmer, T. D., Pedersen, O., Visser, E. J. W., et al. (2020). Drivers of plant traits that allow survival in wetlands. *Funct. Ecol.* 34, 956–967. doi: 10.1111/1365-2435.13541

Parent, C., Nicolas, C., Audrey, B., Crevècoeur, M., and Dat, J. (2008). An overview of plant responses to soil waterlogging. *Plant Stress* 2, 20–27.

Pedersen, O., Sauter, M., Colmer, T. D., and Nakazono, M. (2021). Regulation of root adaptive anatomical and morphological traits during low soil oxygen. *New Phytol.* 229, 42–49. doi: 10.1111/nph.16375

Pezeshki, S. R. (2001). Wetland plant responses to soil flooding. *Environ. Exp. Bot.* 46, 299–312. doi: 10.1016/S0098-8472(01)00107-1

Povidisa, K., Delefosse, M., and Holmer, M. (2009). The formation of iron plaques on roots and rhizomes of the seagrass *Cymodocea serrulata* (R. Brown) Ascherson with implications for sulphide intrusion. *Aquat. Bot.* 90, 303–308. doi: 10.1016/j.aquabot.2008.11.008

Reents, S., Mueller, P., Tang, H., Jensen, K., and Nolte, S. (2021). Plant genotype determines biomass response to flooding frequency in tidal wetlands. *Biogeosciences* 18, 403–411. doi: 10.5194/bg-18-403-2021

Rozema, J., Leendertse, P. C., Bakker, J., and van Wijnen, H. J. (2000). "Nitrogen and vegetation dynamics in European salt marshes" in *Concepts and Controversies in Tidal Marsh Ecology*. ed. M. P. Weinstein (Dortrecht, The Netherlands: Kluwer Academic Publishers), 469–491.

Rupprecht, F., Wanner, A., Stock, M., and Jensen, K. (2015). Succession in salt marshes – large-scale and long-term patterns after abandonment of grazing and drainage. *Appl. Veg. Sci.* 18, 86–98. doi: 10.1111/avsc.12126

Sorrell, B., and Brix, H. (2013). "Gas transport and exchange through wetland plant Aerenchyma" in *Methods in Biogeochemistry of Wetlands*. eds. R. D. DeLaune, K. R. Reddy, C. J. Richardson and J. P. Megonigal (Madison, WI: Soil Science Society of America), 177–196.

Tschiersch, H., Liebsch, G., Borisjuk, L., Stangelmayer, A., and Rolletschek, H. (2012). An imaging method for oxygen distribution, respiration and photosynthesis at a microscopic level of resolution. *New Phytol.* 196, 926–936. doi: 10.1111/j.1469-8137.2012.04295.x

Tschiersch, H., Liebsch, G., Stangelmayer, A., Borisjuk, L., and Rolletschek, H. (2011). "Planar oxygen sensors for non invasive imaging in experimental biology" in *Microsensors*. ed. I. Minin (Rijeka: InTech).

Valéry, L., Bouchard, V., and Lefeuvre, J.-C. (2004). Impact of the invasive native species *Elymus athericus* on carbon pools in a salt marsh. *Wetlands* 24, 268–276. doi: 10.1672/0277-5212(2004)024[0268:IOTINS]2.0.CO;2

Valéry, L., Radureau, A., and Lefeuvre, J.-C. (2017). Spread of the native grass *Elymus athericus* in salt marshes of Mont-Saint-Michel bay as an unusual case of coastal eutrophication. *J. Coast. Conserv.* 21, 421–433. doi: 10.1007/s11852-016-0450-z

Van Wijnen, H. J., and Bakker, J. P. (1999). Nitrogen and phosphorus limitation in a coastal barrier salt marsh: the implications for vegetation succession. *J. Ecol.* 87, 265–272. doi: 10.1046/j.1365-2745.1999.00349.x

van Wijnen, H. J., Bakker, J. P., and de Vries, Y. (1997). Twenty years of salt marsh succession on a Dutch coastal barrier island. *J. Coast. Conserv.* 3, 9–18. doi: 10.1007/BF02908174

Veeneklaas, R. M., Dijkema, K. S., Hecker, N., and Bakker, J. P. (2013). Spatio-temporal dynamics of the invasive plant species *Elytrigia atherica* on natural salt marshes. *Appl. Veg. Sci.* 16, 205–216. doi: 10.1111/j.1654-109X.2012.01228.x

Wang, X. D., Meier, R. J., Link, M., and Wolfbeis, O. S. (2010). Photographing oxygen distribution. *Angew. Chem. Int. Ed.* 49, 4907–4909. doi: 10.1002/anie.201001305

Conflict of Interest: The sensor company, PreSens Precision Sensing GmbH, Regensburg, Germany, provided the planar optode equipment for this study. PreSens GmbH had no restrictive rights in regard to this publication beyond those entitled by their co-authorship. RJM was employed by company PreSens Precision Sensing GmbH.

The remaining authors declare that the research was conducted in the absence of any commercial or financial relationships that could be construed as a potential conflict of interest.

frontiers in Marine Science

ORIGINAL RESEARCH
published: 26 October 2021
doi: 10.3389/fmars.2021.767628

Experimental Assessment of Vulnerability to Warming in Tropical Shallow-Water Marine Organisms

*Mathinee Yucharoen[1,2,3], Sutinee Sinutok[1,2], Ponlachart Chotikarn[1,2,3] and Pimchanok Buapet[2,4]**

[1] Faculty of Environmental Management, Prince of Songkla University, Hat Yai, Thailand, [2] Coastal Oceanography and Climate Change Research Center, Prince of Songkla University, Hat Yai, Thailand, [3] Marine and Coastal Resources Institute, Faculty of Environmental Management, Prince of Songkla University, Hat Yai, Thailand, [4] Division of Biological Science, Faculty of Science, Prince of Songkla University, Hat Yai, Thailand

Tropical shallow-water habitats represent the marine environments with the greatest biodiversity; however, these habitats are the most vulnerable to climate warming. Corals, seagrasses, and macroalgae play a crucial role in the structure, functions, and processes of the coastal ecosystems. Understanding their growth and physiological responses to elevated temperature and interspecific sensitivity is a necessary step to predict the fate of future coastal community. Six species representatives, including *Pocillopora acuta*, *Porites lutea*, *Halophila ovalis*, *Thalassia hemprichii*, *Padina boryana*, and *Ulva intestinalis*, collected from Phuket, Thailand, were subjected to stress manipulation for 5 days. Corals were tested at 27, 29.5, 32, and 34.5°C, while seagrasses and macroalgae were tested at 27, 32, 37, and 42°C. After the stress period, the species were allowed to recover for 5 days at 27°C for corals and 32°C for seagrasses and macroalgae. Non-destructive evaluation of photosynthetic parameters (F_v/F_m, F_v/F_0, ϕPSII and rapid light curves) was carried out on days 0, 3, 5, 6, 8, and 10. Chlorophyll contents and growth rates were quantified at the end of stress, and recovery periods. An integrated biomarker response (IBR) approach was adopted to integrate the candidate responses (F_v/F_m, chlorophyll content, and growth rate) and quantify the overall temperature effects. Elevated temperatures were found to affect photosynthesis, chlorophyll content, and growth rates of all species. Lethal effects were detected at 34.5°C in corals, whereas adverse but recoverable effects were detected at 32°C. Seagrasses and macroalgae displayed a rapid decline in photosynthesis and lethal effects at 42°C. In some species, sublethal stress manifested as slower growth and lower chlorophyll content at 37°C, while photosynthesis remained unaffected. Among all, *T. hemprichii* displayed the highest thermotolerance. IBR provided evidence that elevated temperature affected the overall performance of all tested species, depending on temperature level. Our findings show a sensitivity that differs among important groups of tropical marine organisms inhabiting the same shallow-water environments and highlights the importance of integrating biomarkers across biological levels to assess their vulnerability to climate warming.

Keywords: climate change, temperature sensitivity, coral, seagrass, macroalgae, coastal habitats, tropical, Thailand

OPEN ACCESS

Edited by:
Kasper Elgetti Brodersen, University of Copenhagen, Denmark

Reviewed by:
Mikael Kim, University of Technology Sydney, Australia
Nadine Schubert, University of Algarve, Portugal

***Correspondence:**
Pimchanok Buapet
pimchanok.b@psu.ac.th

Specialty section:
This article was submitted to Marine Ecosystem Ecology, a section of the journal Frontiers in Marine Science

Received: *31 August 2021*
Accepted: *06 October 2021*
Published: *26 October 2021*

Citation:
Yucharoen M, Sinutok S, Chotikarn P and Buapet P (2021) Experimental Assessment of Vulnerability to Warming in Tropical Shallow-Water Marine Organisms. Front. Mar. Sci. 8:767628. doi: 10.3389/fmars.2021.767628

INTRODUCTION

Temperature is one of the key factors that control cellular metabolisms and physiological performance of most marine organisms and consequently affect their growth and survival (Madeira et al., 2018; Savva et al., 2018; Dias et al., 2020). Climate warming and extreme climate events (ECEs) have been identified as among the key drivers of the structural and functional shift of the coastal ecosystems across different bioregions (Smale et al., 2019; Strydom et al., 2020). An increase of more than 1°C in sea surface temperature over the past century has been recorded in the tropical latitudes and even a more rapid increase has been predicted for the next century (Hoegh-Guldberg et al., 2018). Tropical shallow-water marine organisms experience great temporal variability in temperature that is largely influenced by solar radiation and tidal cycles in their natural habitats; temperatures above 40°C have been recorded during spring tides in seagrass meadows (Collier and Waycott, 2014; George et al., 2018), whereas shallow-water coral reefs may experience a temperature up to 34°C (Palumbi et al., 2014). As their surrounding temperature is already reaching their upper thermal threshold, these organisms are particularly susceptible to heat stress due to climate warming and ECEs (Stuart-Smith et al., 2017; Vinagre et al., 2019; Rasmusson et al., 2021). Although acclimation is possible, it may not be fast enough to keep up with the accelerating pace of climate change for most organisms (Collier et al., 2017; Hoegh-Guldberg et al., 2018).

Corals, seagrasses, and macroalgae play critical roles in the structure, functions, and processes of marine ecosystems in shallow areas. They serve as primary producers and habitat builders while providing invaluable ecosystem services, such as provisioning and climate change mitigation (Henderson et al., 2019; Good and Bahr, 2021). Since the 1980s, an alarming decline of these ecosystems has been recorded to be 27% of coral reefs (Cesar et al., 2003) and 35% of the seagrass beds (Waycott et al., 2009), including vast macroalgal coverage areas (Wernberg et al., 2019) that have been lost globally. Heat stress has been found to exacerbate the degradation of marine ecosystems as evidenced by widespread coral bleaching and mortality (Eakin et al., 2019) and the extensive seagrass die-offs during 2014–2017 global heatwaves (Strydom et al., 2020). Responses to thermal stress in these groups of marine species depend on the duration, degree of warming, frequency of the warming event, interspecific variations, and interactions with other environmental factors. Further, these responses are manifested at different biological organization levels (Freeman et al., 2013; Collier and Waycott, 2014; George et al., 2018). Slower growth, changes in phenology, and lower reproductive output have been reported in corals, seagrasses, and macroalgae (Cantin and Lough, 2014; Hughes et al., 2019; Marín-Guirao et al., 2019; Román et al., 2020), whereas the effects on coral and its symbiotic relationship were often revealed as bleaching phenomenon (Robison and Warner, 2006; Hill et al., 2011). It is assumed that physiological acclimation may, to some extent, constitute the ability of thermotolerance and that physiological responses may precede the effects on growth and reproduction (Duarte et al., 2018; Gibbin et al., 2018; Jurriaans and Hoogenboom, 2020). Photosynthesis, a fundamental energy process, is highly sensitive to temperature. Therefore, photosynthetic parameters have been widely used to detect thermal stress (Robison and Warner, 2006; Sinutok et al., 2012; Collier and Waycott, 2014; Rasmusson et al., 2020, 2021; Danaraj et al., 2021). Accumulating evidence has revealed that heat stress lowers the overall photosynthetic efficiency of marine photosynthetic organisms by inhibiting the photosystems, electron transport chain, and carbon fixation (Robison and Warner, 2006; Sinutok et al., 2012; Collier and Waycott, 2014; Rasmusson et al., 2020; Danaraj et al., 2021). Impaired photosynthesis can potentially affect their carbon balance and resource allocation, which, in turn, affects their growth and survival (Tremblay et al., 2016; Collier et al., 2017).

Under the ocean warming scenarios, the vulnerability of marine species, particularly the key habitat builders, to elevated temperature should be closely monitored and managed (Guan et al., 2020; Nguyen et al., 2021). Although comparative studies are scarce, the sensitivity of tropical shallow-water marine organisms to heat is expected to vary among species, life-traits (pioneer vs. climax species), life-forms (calcified vs. non-calcified species), and functional groups (Kilminster et al., 2015; Kram et al., 2016; Anton et al., 2020; Dove et al., 2020). Differences in sensitivity among corals, seagrasses, and macroalgae may be attributed to different ecological and physiological strategies as well as local adaptation (Kilminster et al., 2015; Kram et al., 2016; Savva et al., 2018; Anton et al., 2020; Dove et al., 2020). In this regard, comparative studies on the response of different species with different life-traits or life-forms from different functional groups are needed for the identification of the sensitive species and the prediction of ecosystem structural and functional shift facing climate warming.

This study aimed to establish a comprehensive understanding of the vulnerability of shallow-water marine organisms to warming in a tropical region. We evaluated the effects of increasing temperatures in species representatives of corals (*Pocillopora acuta* and *Porites lutea*), seagrasses (*Halophila ovalis* and *Thalassia hemprichii*), and macroalgae (*Padina boryana* and *Ulva intestinalis*), which are commonly found in shallow habitats in Phuket Province, Thailand. The changes in physiological performances and growth of these marine organisms were examined across the thermal range recorded in their habitats at present and in future scenarios. We further applied the integrated biomarker response index (IBR) approach to elucidate the overall impacts of warming on all the tested species. The results obtained in this study can provide insights on how to prioritize management efforts in mitigating the effects of warming in tropical shallow-water marine ecosystems. This study also provides a valuable tool to support ecological risk assessment in the context of global climate change.

MATERIALS AND METHODS

Sampling and Acclimation of Biological Materials

All biological materials were collected from Phuket, Thailand from May to June 2019. The location map of the sampling sites

is indicated in **Figure 1A**. Marine species belonging to three groups of photosynthetic organisms, including corals, seagrasses, and macroalgae, were selected based on their dominance in the shallow areas of the sampling sites, which makes them more susceptible to warming and consequently relevant candidates for this study. The recorded annual sea surface temperature (SST) of Phuket, Thailand from 2017 to 2020 ranges from 27.45°C ± 0.02°C to 32.00°C ± 0.02°C (**Figure 1B**).

The corals *P. acuta* and *P. lutea* and the lightly-calcified macroalga *P. boryana* were collected from Panwa, Phuket (7°48′6.26″N 98°24′23.75″E). Healthy colonies of *P. acuta* and *P. lutea* were collected from 3 to 5 m depth using a stainless bone cutter, chisel, and hammer. Thalli of *P. boryana* with holdfast intact were hand-picked haphazardly at the sandflat areas at low tide and placed in plastic bags containing the seawater collected on site. The seagrasses *H. ovalis* and *T. hemprichii* and the macroalga *U. intestinalis* were collected from Pakhlok subdistrict, Phuket (8°01′18.3″N 98°24′47.2″E). Monospecific patches of seagrass located at least 5 m apart with similar density were chosen. Intact plants (leaves and root/rhizome complex) with their sediment were collected using a hand shovel, placed in plastic boxes, and covered with wet paper towels. Thalli of *U. intestinalis*, free-floating green tides-forming macroalgae, that are found in the seagrass meadow were hand-picked at low tide and kept in plastic bags containing the seawater collected on the site. All biological materials were transferred with natural seawater to the aquarium facility of the Coastal Oceanography and Climate Change Research Center (COCC), Prince of Songkla University within 12 h of collection. Epiphytes were washed off the collected samples with sterile seawater (salinity of 32 PSU), followed by acclimation, as described below.

All coral colonies were initially acclimated in 600 L holding tank for a week in flowing seawater pumped directly from the seawater stock, prepared from natural seawater filtered with Nomex Filter Bag, and treated with 50 ppm chlorine (50 mg chlorine L^{-1}). Water flow within the tank was generated with recirculating pumps (WP-300M, SOBO, China and AT-107, atman, China). Temperature, salinity, and pH were controlled at levels recorded at the sampling site (29°C, 32 PSU, and pH 8.2). Temperature was regulated using a Heater chiller (CS-160CIRV1, atman, China). Irradiance of 150 μmol photons m^{-2} s^{-1} (measured with Light Sensor Logger, LI-1500, LI-COR, United States) was provided by COB light (TS-A600, Aquarium lamp, China), with 12/12 of light/dark cycle. This irradiance level was non-photoinhibitory (pre-determined in the pilot study) and corresponds to average daily irradiance at the respective sampling periods (155.83 ± 8.81 μmol photons m^{-2} s^{-1} in May and 156.20 ± 7.31 μmol photons m^{-2} s^{-1} in June, **Supplementary Table 1**). After 1 week, coral colonies were cut into nubbins of 3–5 cm and distributed into experimental tanks (36 pieces/species/tank, 60 L/tank). The setting of the experiment tank condition was similar to the holding tank, except for the models of temperature chillers (JMC-02, JBA, China) and water pumps (AP-1200, SONIC, China). The coral nubbins were allowed to acclimate for an additional week. One-fourth of the seawater volume was renewed at the end of the week and all physical and chemical parameters were monitored every 2–3 days throughout the acclimation period.

Three plastic boxes containing sods of each seagrass species (six shoots of *T. hemprichii* or approximately 30 leaf pairs of *H. ovalis* in each box) and sediment were combined into an aquarium (40 L, six boxes in total in each aquarium). All aquaria were filled with sterile seawater (salinity of 32 PSU, pH 8.2). Seawater in the aquaria was regularly mixed and filtered using a submersible pump coupled with a microfiber filter (Atman HF-0600, China). Non-photoinhibitory irradiance (pre-determined in the pilot study) was provided by aquarium LEDs (A601, Chihiros, China) set at approximately 200 μmol photons m^{-2} s^{-1} and 12/12 light/dark cycle. This level corresponds to average daily irradiance at the respective sampling period (199.80 ± 43.59 μmol photons m^{-2} s^{-1}, **Supplementary Table 1**) and is comparable to minimal saturating irradiances [E_k], pre-determined *in situ* from the RLCs (218.39 ± 19.72 μmol photons m^{-2} s^{-1} in *T. hemprichii* and 225.09 ± 19.79 μmol photons m^{-2} s^{-1} in *H. ovalis*, Diving-PAM, Walz, Effeltrich, Germany). A constant temperature at 30°C throughout the acclimation period of the aquaria was maintained using submersible heating rods (EHEIM 3617, EHEIM, Germany). The acclimation period lasted 5 days.

Approximately 20 g of each macroalgal species were placed in each glass container and anchored to the bottom of the containers with plastic mesh. Other settings followed the seagrass setups.

Experimental Design

As this study aims to evaluate vulnerability to warming in shallow-water marine organisms, we focused on their stress responses to an increase in temperature within a range recorded in their natural settings encompassing the future warming scenarios. The testing temperatures were chosen based on past SST (27.45 ± 0.02°C to 32.00 ± 0.02°C, **Figure 1B**), records of temperature profiles of the sampling sites (28.84–30.25°C in shallow water coral reefs and 26.96–36.70°C in tidal flat areas at the respective sampling periods, **Supplementary Table 1**), our previous investigations (Rasmusson et al., 2020, 2021; unpublished data) and other studies from the tropical shallow waters (Sutthacheep et al., 2013a; Collier and Waycott, 2014; Pedersen et al., 2016; George et al., 2018; Kong et al., 2019). Extreme temperatures, exceeding 40°C, have been reported in tropical seagrass meadows (Collier and Waycott, 2014; Pedersen et al., 2016; George et al., 2018) whereas the highest temperature reported in shallow water coral reefs in Thailand was 32.7°C (Sutthacheep et al., 2013a). As corals are exposed to smaller thermal variations *in situ* compared to seagrasses and macroalgae (**Supplementary Table 1**), narrower range of temperature with smaller increment was thus adopted for coral experimental design.

The experiment was continued in the same setups for acclimatization and divided into two phases: 5 days of stress and 5 days of recovery. The stress period consisted of four treatments (1) 27°C (2) 29.5°C (2) 32°C, and (4) 34.5°C for corals and (1) 27°C (2) 32°C (2) 37°C, and (4) 42°C for seagrasses and macroalgae. During the stress period, the maximum quantum yield of photosystem II (F_v/F_m) and photosystem II potential

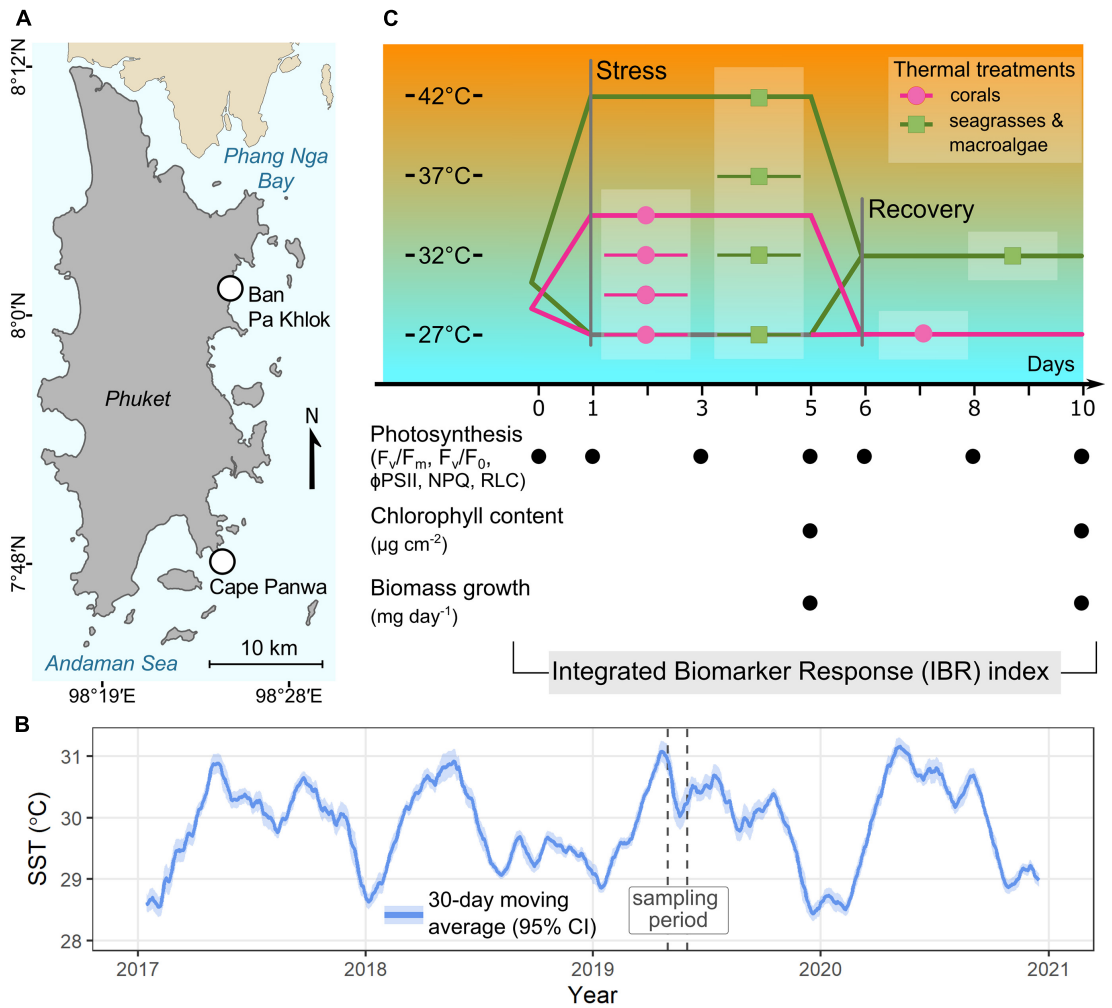

FIGURE 1 | (A) Locations of the sampling sites, **(B)** average sea surface temperature (SST) in coastal water of Phuket recorded from 2017 to 2020 and **(C)** experimental design, timeline and investigated parameters. Sea surface temperatures were retrieved from GHRSST Level 4 MUR Global Foundation Sea Surface Temperature Analysis (v4.1) (https://podaac.jpl.nasa.gov/dataset/MUR-JPL-L4-149GLOB-v4.1 accessed on July 01, 2021).

activity (F_v/F_0) were assessed on days 0, 3, and 5 before the light was turned on, whereas the effective quantum yield (ϕPSII) and RLCs were assessed in the middle of the photoperiod on the same day. At the end of the stress period, the biological materials were randomly collected from all treatments for further analysis of photosynthetic pigments, while zooxanthellae density was assessed in the coral samples. Growth rates and biomass loss rates (when applicable) were determined at the end of the stress period (as detailed below). A recovery period was initiated by adjusting the temperature of all aquaria to 27°C for corals and 32°C for seagrasses and macroalgae (pre-determined in the preliminary study as the optimal temperature). All species were subjected to the new temperature regime for an additional 5 days and the same measurements were done as described for the stress period. The seawater was renewed before starting the stress period and before starting the recovery period. Salinity was measured every day using a refractometer and, when necessary, adjusted to 32 PSU by adding distilled water. The experimental design and timeline for the measurements are summarized in **Figure 1C**.

Measurement Protocols

Chlorophyll Fluorescence

The parameters associated with the integrity of photosystem II; F_v/F_m, and F_v/F_0 were assessed before the light was turned on using a Pulse Amplitude Modulated Fluorometer (Diving-PAM, Walz, Effeltrich, Germany). The two parameters F_v/F_m and F_v/F_0 were calculated from $(F_m - F_0)/F_m$ and $(F_m - F_0)/F_0$, respectively; where F_0 represents minimum fluorescence of dark-adapted biological materials and F_m represents maximum fluorescence after saturating pulse is applied.

The ϕPSII and RLC were constructed in the middle of the photoperiod (Diving-PAM, Walz, Effeltrich, Germany). Measurements in the light were assisted by distant leaf clip (Distance Clip 60° 2010-A, Walz, Effeltrich, Germany), which

kept the angle and distance between the Diving-PAM optical fiber and coral surface and the algal thalli and plant leaves fixed. The ϕPSII was calculated from $(F'_m - F)/F'_m$; where F represents minimum fluorescence of light-adapted biological materials and F'_m represents maximum fluorescence after saturating pulse is applied.

For RLCs, a series of photosynthetic active radiation (PAR) was provided by the optical fiber ranging from 45 to 617 μmol photons m^{-2} s^{-1} and with 20 s increment step. The ϕPSII was determined after each PAR step. The electron transport rates (ETR) were subsequently calculated by multiplying ϕPSII by PAR and 0.5 (based on the assumption that absorbed photons are equally divided between photosystems I and photosystem II) and by the preset absorption factor (AF = 0.84). The ETRs, as the functions of PAR, were plotted and fitted using the equation of Platt et al. (1980) from which the photosynthetic parameters, including asymptotic maximum levels of ETR (ETR_{max}), the initial slope of the light response curve (α), and minimum saturating irradiance (E_k), were estimated.

Diving-PAM settings for measurements taken in corals were as follows: intensity of measuring light 2 (MEAS-INT), electronic signal gain 3 (GAIN), saturation pulse intensity 8 (SAT-INT), width of saturating light pulse 0.6 s (SATWIDTH). Measurements done in seagrasses and macroalgae followed the settings used in corals except for GAIN which was lowered to 2. The photosynthetic parameters were measured in three replicate tanks with three sub-replicates. As it has been shown that photosynthetic characteristics vary significantly depending on age and position of the photosynthetic tissues (e.g., along the thallus or leaf blade) (Colombo-Pallota et al., 2006; Schubert et al., 2015), the same areas of the same individuals were used for the determination of chlorophyll fluorescence parameters throughout the experiment. The coral surface areas were randomly selected. The photosynthetic parameters of *H. ovalis* were measured in the middle area of the leaf, whereas those of *T. hemprichii* were measured at the middle section of the second youngest leaf. The photosynthetic parameters of macroalgae were measured at the middle section of the algal thallus.

Determination of Zooxanthellae Density

Coral tissue was removed from the skeleton using an airbrush and the slurry was centrifuged for 10 min at 1,500 rpm and 4°C to obtain a well-mixed sample. A hemocytometer was used to count the zooxanthellae cells within a 1 ml aliquot under a light microscope (40×). All coral skeletons were completely bleached in 10% Sodium Hypochlorite and washed several times. The surface area was determined using the paraffin wax technique on bleached skeleton and quantified using a standard curve (Hill and Ralph, 2007; Veal et al., 2010). The zooxanthellae density was calculated as the total number of cells per unit coral surface area.

Determination of Photosynthetic Pigments

Total chlorophylls of corals were determined in the remaining solution after the cell number was determined, as described above. The slurry was centrifuged for 5 min at 5,000 rpm and 4°C and the supernatant was discarded. The algal pellets were re-suspended in 90% acetone and stored in darkness for 24 h at 4°C. The centrifugation was subsequently repeated, and the obtained supernatant was collected. Total chlorophylls (chlorophyll $a + c_2$) were determined using the standard spectrophotometric method of Ritchie (2006), with absorbance measured at 630, 664, and 750 nm. Total chlorophylls were normalized against coral surface area pre-determined using the paraffin wax technique, as mentioned above.

Seagrass and macroalgal tissues were ground using a mortar and pestle in 80% acetone. The homogenate was kept in darkness for 72 h and then centrifuged at 1,000 × g for 10 min before the absorbance was measured at 664, 647, and 470 nm (Metertech SP-8001 UV/Visible Spectrophotometer, Taiwan). Before the extraction, photographs of all the samples were promptly taken and the wet weight was recorded. The surface areas of the algal thallus and seagrass leafs were estimated using the ImageJ program[1]. Total chlorophylls (chlorophyll $a + b$) were calculated according to the method described by Porra (2002) and normalized against the surface area.

Determination of Growth-Related Attributes

As the three groups of organisms used for this study exhibit varying growth forms, different approaches were adopted to measure their growth-related attributes. All measurements were done in a non-destructive manner, such that the same individuals were used for growth assessment at the end of the stress period as well as at the end of the recovery period. Growth rates of corals and macroalgae were expressed as a net increase in biomass (mg) per day, whereas growth-related attributes of seagrasses were expressed as an increase in biomass per day and senescent biomass per day.

The buoyant weight technique was used to measure the coral skeleton growth rate (Jokiel and Guinther, 1978). The same coral nubbin was weighted at the start, end of stress period, and at end of the recovery period using a 4-digit precision balance (Ohaus, United States). In each measurement, the seawater temperature and salinity were recorded for the calculation of seawater density, and glass reference was weighed in both sea water and air (Davies, 1989). The skeleton bulk densities of *P. lutea* and *P. acuta* were calculated according to the methods described by Ng et al. (2019), respectively. Coral growth rates were expressed as net increases in biomass (mg) per day. Negative values were shown when there was a net loss in the biomass weight.

At the beginning of the experiment, at the end of the stress period, and at the end of the recovery period, photographs of *H. ovalis* in each box were taken and the number of living and dead leaves were later counted. Both growth rates and senescence rates were recorded as an increase in the number of viable leaves and an increase in the number of dead leaves, respectively. At the end of the experiment, leaf fresh weight was measured to give an estimate of the weight per leaf (n = 50). This value was used to convert the growth rates and senescence rates into an increase in biomass (mg) and senescent biomass (mg) per day, respectively. For *T. hemprichii*, leaf area gained was assessed using the leaf marking method (Short and Duarte, 2001). In brief, all of the leaves in each shoot were punched

[1]http://rsb.info.nih.gov/ij/

using hypodermic needles at the meristematic tissue at the base of the shoot. The first mark provided an initial reference level and new growth increments were measured at the end of the stress period. The same steps were applied for the recovery period. The leaf growth rate expressed as $mm^2\ day^{-1}$ was subsequently obtained. Similarly, weight per area of the green leaves of *T. hemprichii* was determined ($n = 50$) and this constant was used to estimate an increase in biomass (mg) per day. The biomass loss of *T. hemprichii* was determined from both the dead areas of undetached leaves and the weight of shed leaves during the stress and recovery period. The dead areas of undetached leaves were converted to biomass using the same constant for the viable leaf. Senescence rates were expressed as biomass (mg) loss per day.

At the beginning of the experiment, at the end of the stress period, and at the end of the recovery period, the wet weight of *P. boryana* and *U. intestinalis* was recorded. The algal thalli were carefully dried using paper towels before weighing with a 4-digit precision balance (Ohaus, United States). Their growth rates were expressed as net increase in biomass (mg) per day. Negative values were shown when there was a net loss in the algal biomass.

Integrated Biomarker Response

Integrated Biomarker Response (IBR) approach was used to quantify the overall effects of temperature on each species through an integrated response of F_v/F_m, chlorophyll content, and growth rate. The biomarkers used in this analysis were chosen as the representatives for the responses at physiological, biochemical, and whole-organism levels. The IBR indices were analyzed according to the method of Beliaeff and Burgeot (2002) as described by Madeira et al. (2018). For each biomarker, the general mean (m) and standard deviation (s) of all treatments combined were calculated and standardized (Y) as $Y = (X - m)/s$; where X is the mean value for the biomarker at a given treatment. Z was then calculated as $Z = -Y$ or $Z = Y$ in the case of biological effects corresponding to inhibition or activation, respectively. The score (S) was computed as $S = Z + |\mathrm{Min}|$; where $S \geq 0$ and $|\mathrm{Min}|$ is the absolute value for the minimum of all Y calculated in a given biomarker. The score results (S) were presented as star plots and used to calculate the IBR as:

$$\mathrm{IBR} = \sum_{i=1}^{n} A_i \quad (1)$$

$$A_i = \frac{S_i}{2}\sin\beta(S_i\cos\beta + S_{i+1}\sin\beta) \quad (2)$$

Where

$$\beta = \tan^{-1}\left(\frac{S_{i+1}\sin\alpha}{S_i - S_{i+1}\cos\alpha}\right) \quad (3)$$

Where Si and S_{i+1} are two consecutive clockwise scores (radius coordinates) of a given star plot; A_i corresponds to the area connecting two scores; n is the number of biomarkers used for the calculations; and $\alpha = 2\pi/n$ (Beliaeff and Burgeot, 2002; Madeira et al., 2018).

Statistical Analysis

All statistical analyses were performed separately for each group of organisms (corals, macroalgae, or seagrasses). The photosynthetic parameters derived by PAM measurements (F_v/F_m, F_v/F_0, ϕPSII, ETR_{max}, E_k, and α) and growth rates were analyzed by repeated-measures analysis of variance (ANOVA) using time of measurements as the within-group factor and thermal treatments and species as the categorical factors. The statistical significance of differences in total chlorophyll content and coral zooxanthellae density was determined by factorial ANOVA using temperatures, species, and treatment period (stress and recovery) as categorical factors. Fisher's least significant difference (LSD) test was used for *post hoc* comparisons. Cochran's test was used to test the assumption of homogeneity of variances before performing the ANOVAs. All analyses were performed with Statistica Academic Version 13.0.

RESULTS

Both temperature and time of exposure were found to affect the overall performance of all species, which manifested as a reduction in photosynthesis, pigment content, and growth rates (for complete ANOVA statistical results, see **Supplementary Table 2**). However, the sensitivity differed among species. The highest temperature applied in the present study (34.5°C for corals and 42°C for seagrasses and macroalgae) had lethal effects on all the tested species.

Photosynthetic Responses

Maximum Quantum Yield of PSII (F_v/F_m), PSII Potential Activity (F_v/F_0) and Effective Quantum Yield (Psi PSII)

Repeated-measures ANOVA (repeated ANOVA) showed significant effects of temperature ($p < 0.001$), time of measurement ($p < 0.001$), and interaction of these factors ($p < 0.001$) on the maximum quantum yield of PSII (F_v/F_m) of corals. At 27°C and 29.5°C, F_v/F_m showed slight variations among days, but these variations were not statistically significant. In contrast, exposure to 32 and 34.5°C resulted in a significant decrease in F_v/F_m (**Figure 2A**), with a more rapid decline and lethal effect at 34.5°C (Fisher's LSD test). Both *P. acuta* and *P. lutea* pre-exposed to 32°C fully recovered on day 3 of the recovery period. There were significant effects of temperature (repeated ANOVA, $p < 0.001$), species (repeated ANOVA, $p < 0.001$), time of measurement (repeated ANOVA, $p < 0.001$), and interaction of these factors (repeated ANOVA, $p < 0.001$) on PSII potential activity (F_v/F_0) of corals. Although F_v/F_0 followed a similar trend as observed in F_v/F_m, it exhibited higher variability and higher sensitivity (**Figure 2B**). In other words, a significant decrease in F_v/F_0 than F_v/F_m was detected earlier and at a lower temperature. Full recovery was observed in the samples pre-exposed to 29.5°C, whereas partial recovery was observed in the samples exposed to 32°C.

Repeated ANOVA revealed significant effects of temperature ($p < 0.001$), species ($p < 0.001$), time of measurement ($p < 0.001$), and interaction of these factors ($p < 0.05$) on the

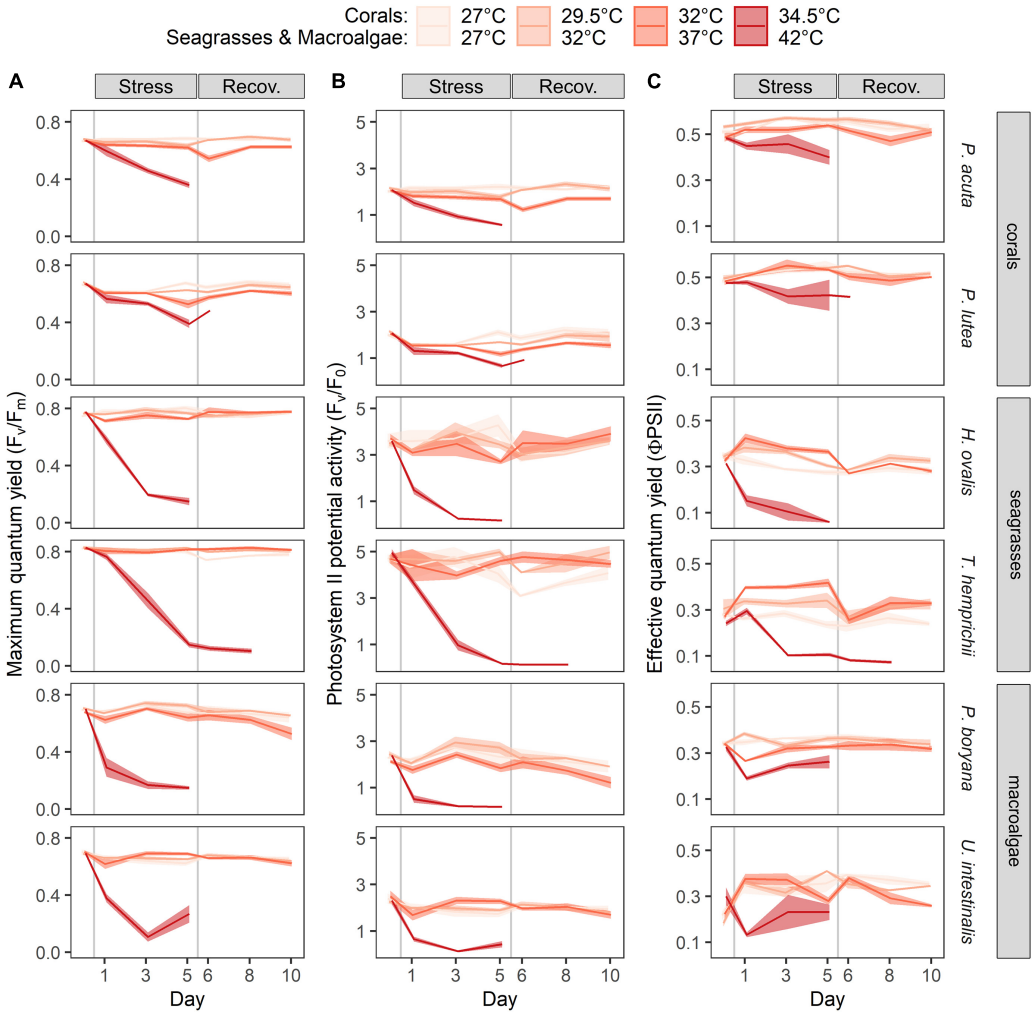

FIGURE 2 | Time course of the warming effects on the photosynthetic parameters of corals, seagrasses and macroalgae. **(A)** Maximum quantum yield (F_v/F_m), **(B)** PSII potential activity (F_v/F_0) and **(C)** effective quantum yield (ϕPSII). Values are shown as mean ± SE (n = 3). For each replicate, 3 individuals were assessed. Corals were subjected to 27–34.5°C in stress period and 27°C in recovery period. Seagrasses and macroalgae were subjected to 27–42°C in stress period and 32°C in recovery period.

F_v/F_m and F_v/F_0 of seagrasses (**Figures 2A,B**). At 27, 32, and 37°C, F_v/F_m showed slight variations among the days; however, these variations were not statistically significant. In contrast, exposure to 42°C resulted in a significant decrease in F_v/F_m (**Figure 2A**). *H. ovalis* exposed to 42°C showed a decrease in F_v/F_m compared to the initial values on day 1 after treatment (Fisher's LSD test), followed by a drastic decline in F_v/F_m until it was not detectable after day 5. *T. hemprichii* appeared to be more resistant to thermal stress (following exposure of the plants to 42°C), showing a decrease in F_v/F_m compared to the initial values on day 3 after treatment (Fisher's LSD test), followed by a drastic decline until it was not detectable after day 3 of the recovery period. The F_v/F_0 in seagrasses also showed a higher sensitivity than F_v/F_m, since a significant decrease was observed at both 37 and 42°C (**Figure 2B**, Fisher's LSD test). While mortality was seen in plants exposed to 42°C, complete recovery was detected in plants pre-exposed to 37°C. In addition, *T. hemprichii* also showed a reduction in F_v/F_0 when exposed to 27°C; however, full recovery was achieved at the end of the recovery period.

There were significant effects of temperature (repeated ANOVA, $p < 0.001$), time of measurement ($p < 0.001$), and interaction of these factors ($p < 0.05$) on the F_v/F_m and F_v/F_0 of macroalgae (**Figure 2A**). At 27, 32, and 37°C, F_v/F_m showed slight variations among the days; however, these variations were not statistically significant, with an exception in *P. boryana* exposed to 37°C, where a marginal difference from the initial value was detected on day 5 of the recovery period. Both macroalgae exposed to 42°C displayed a drastic decline in F_v/F_m compared to the initial values on day 1 after treatment, followed by a steady decline, which became undetectable after day 5. Similar trend was observed in F_v/F_0 (**Figure 2B**).

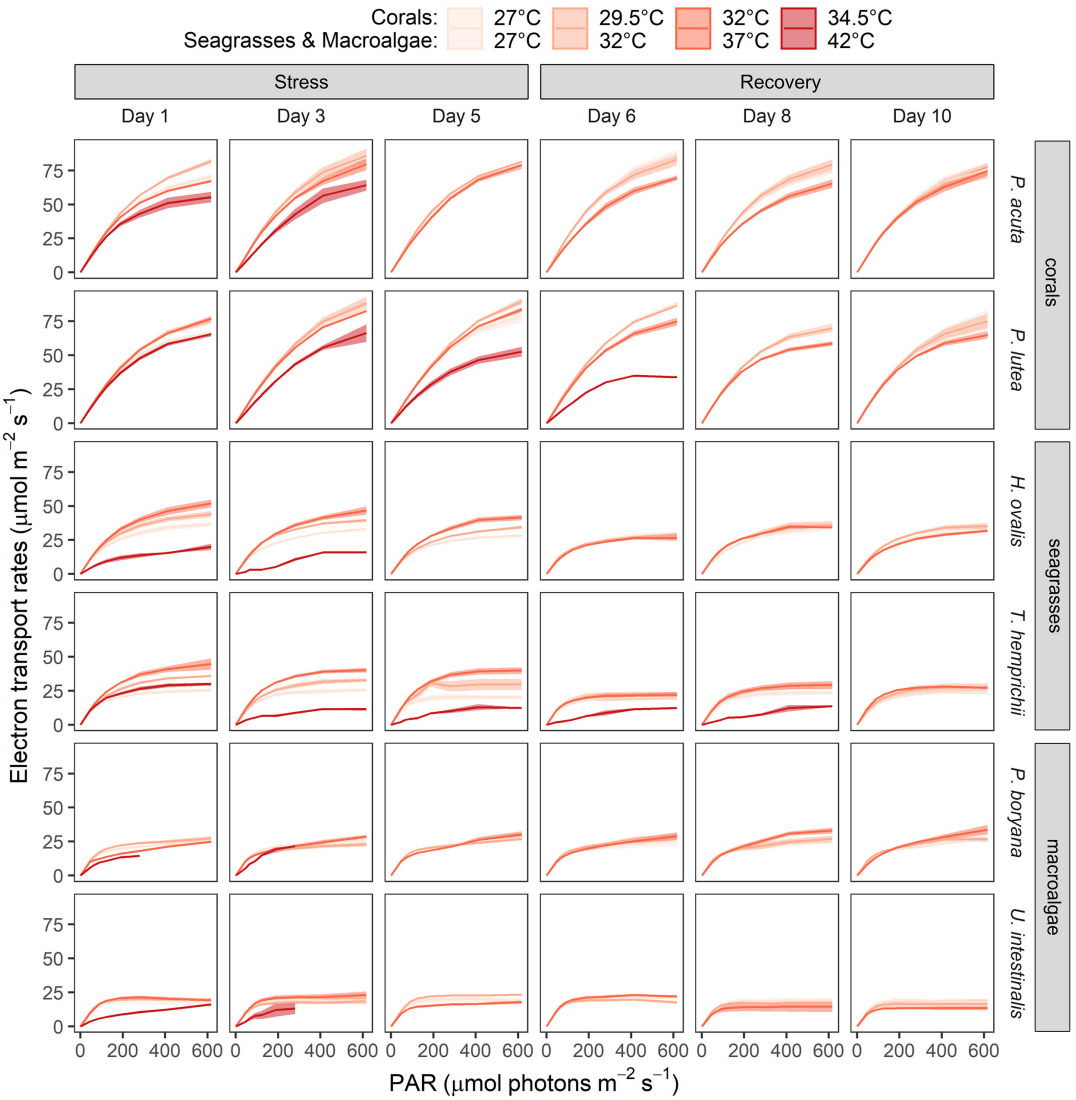

FIGURE 3 | Time course of the warming effects on the rapid light response curves of corals, seagrasses and macroalgae. Values are shown as mean ± SE (n = 3). For each replicate, 3 individuals were assessed. Corals were subjected to 27–34.5°C in stress period and 27°C in recovery period. Seagrasses and macroalgae were subjected to 27–42°C in stress period and 32°C in recovery period.

The response pattern of the effective quantum yield (ϕPSII) in all species followed that of F_v/F_m except for *T. hemprichii* of which an increase in ϕPSII was observed as temperature increased from 27 to 37°C (**Figure 2C**, Fisher's LSD test).

Rapid Light Curves

Increasing temperatures also exerted negative effects on light use efficiency, which was measured as rapid light curve-derived parameters (**Figure 3**, data are shown in **Supplementary Table 3**). The highest temperatures applied in the present study (34.5°C for corals and 42°C for seagrasses and macroalgae) had lethal effects on all the tested species. Toward the end of the stress period of these temperatures, the RLCs of some species did not show any functional response fitted for the equations used and were therefore omitted from the dataset.

All parameters, including the asymptotic maximum levels of ETR (ETR_{max}), initial slope of the light response curve (α), and minimum saturating irradiance (E_k) of all organisms varied according to temperature, time of exposure, and among species (**Supplementary Table 3**). As ETR_{max} exhibited the most obvious temperature-dependent response among the three parameters, it was selected as a proxy to describe the effects of heat stress on the photosynthetic capacity of the marine organisms tested in the present study (**Table 1**).

In corals, ETR_{max} were affected by temperature (repeated ANOVA, $p < 0.001$), duration of exposure ($p < 0.001$), and interactions of these factors ($p < 0.05$). While temporal variations were detected (Fisher's LSD test), the comparison of the values measured on the same day revealed a lower ETR_{max} at 32 and 34.5°C (Fisher's LSD test, **Table 1**). At the

TABLE 1 | The maximum electron transport rates (μmol m^{-2} s^{-1}, ETR_{max}) derived from the rapid light curves (mean ± SE, n = 3).

Species/treatments	Day 0	Stress period			Recovery period		
		Day 1	Day 3	Day 5	Day 6	Day 8	Day 10
Pocillopora acuta							
• 27°C	64.24 ± 3.68	70.38 ± 1.84	84.37 ± 1.51	80.58 ± 1.51	87.05 ± 2.84	74.83 ± 2.39	76.02 ± 4.90
• 29.5°C	63.43 ± 2.677	81.83 ± 1.83	85.68 ± 5.16	81.47 ± 0.85	82.97 ± 4.27	79.45 ± 3.78	74.79 ± 5.60
• 32°C	62.74 ± 3.94	67.25 ± 1.04	79.59 ± 4.35	74.23 ± 0.90	69.51 ± 1.78	65.30 ± 3.24	74.78 ± 3.56
• 34.5°C	76.34 ± 0.50	55.42 ± 3.86	65.53 ± 2.61	–	–	–	–
Porites lutea							
• 27°C	55.32 ± 2.196	66.33 ± 2.04	85.50 ± 3.95	78.81 ± 4.56	88.11 ± 1.40	71.86 ± 2.05	75.64 ± 7.58
• 29.5°C	62.18 ± 2.20	75.49 ± 2.18	88.42 ± 4.63	89.68 ± 2.33	86.76 ± 1.06	70.02 ± 2.89	75.29 ± 5.34
• 32°C	61.26 ± 2.21	76.98 ± 1.81	82.52 ± 0.50	83.66 ± 1.67	74.80 ± 2.91	58.62 ± 1.73	64.95 ± 2.69
• 34.5°C	61.49 ± 0.66	65.54 ± 1.60	70.29 ± 2.93	52.68 ± 3.60	33.91*	–	–
Halophila ovalis							
• 27°C	34.41 ± 0.95	35.01 ± 1.96	31.12 ± 0.79	26.82 ± 1.09	27.95 ± 2.09	33.19 ± 2.38	30.89 ± 2.28
• 32°C	31.10 ± 1.13	42.38 ± 2.14	37.87 ± 1.00	32.72 ± 0.91	2728 ± 0.72	35.15 ± 2.94	34.36 ± 1.94
• 37°C	36.57 ± 1.67	50.39 ± 3.04	45.05 ± 2.72	40.86 ± 2.18	25.91 ± 1.32	33.83 ± 1.11	30.18 ± 0.98
• 42°C	40.21 ± 2.43	19.17 ± 1.62	12.07 ± 4.50	–	–	–	–
Thalassia hemprichii							
• 27°C	23.66 ± 1.21	24.13 ± 1.12	24.87 ± 1.30	20.35 ± 1.81	20.26 ± 1.99	23.33 ± 1.46	23.27 ± 0.53
• 32°C	21.47 ± 1.11	34.66 ± 0.76	31.61 ± 1.68	29.10 ± 4.19	20.82 ± 3.12	27.24 ± 1.46	27.05 ± 2.98
• 37°C	24.46 ± 0.62	43.32 ± 4.03	39.22 ± 1.65	39.48 ± 2.33	21.42 ± 1.81	28.86 ± 2.71	27.50 ± 0.85
• 42°C	26.80 ± 3.64	28.68 ± 1.45	11.60 ± 0.60	13.38 ± 1.01	13.01 ± 3.07	13.01 ± 3.60	–
Padina boryana							
• 27°C	22.74 ± 1.48	25.14 ± 0.36	26.18 ± 0.31	28.03 ± 2.88	25.20 ± 3.08	26.28 ± 2.78	27.03 ± 0.82
• 32°C	23.69 ± 1.24	27.26 ± 1.79	23.02 ± 1.72	27.02 ± 0.57	28.75 ± 1.57	26.94 ± 2.51	27.02 ± 1.38
• 37°C	22.82 ± 0.83	25.23 ± 0.86	28.69 ± 1.24	30.40 ± 2.26	28.97 ± 2.81	33.48 ± 1.92	33.99 ± 3.46
• 42°C	22.71 ± 1.79	24.80 ± 0.29	21.63 ± 1.36	–	–	–	–
Ulva intestinalis							
• 27°C	13.13 ± 1.07	20.22 ± 2.92	20.49 ± 2.51	20.54 ± 2.50	22.83 ± 1.20	20.26 ± 2.29	19.72 ± 1.19
• 32°C	14.56 ± 1.38	20.75 ± 1.10	18.29 ± 1.18	23.15 ± 0.84	20.19 ± 1.24	17.46 ± 0.54	18.61 ± 3.53
• 37°C	13.89 ± 0.50	21.48 ± 1.25	22.18 ± 2.16	18.65 ± 2.02	20.91 ± 3.00	15.33 ± 3.70	13.72 ± 1.03
• 42°C	13.85 ± 2.57	16.24 ± 0.58	13.16 ± 4.05	–	–	–	–

For each replicate, 3 individuals were assessed.
Asterisk (*) indicates the treatment in which there was only one replicate of fitted rapid light curve (n = 1).

end of the recovery period, *P. acuta* pre-exposed to 32°C fully recovered, whereas photoinhibition in *P. lutea* pre-exposed to 32°C was not alleviated (Fisher's LSD test). In seagrasses, ETR_{max} was affected by temperature (repeated ANOVA, $p < 0.001$), duration of exposure ($p < 0.001$), species ($p < 0.001$), and interactions of these factors ($p < 0.05$). From 27 to 37°C, ETR_{max} of *H. ovalis* and *T. hemprichii* showed an increasing trend with increasing temperature when comparing the values measured on the same day, while exposure to 42°C led to a significant decline in ETR_{max} (Fisher's LSD test), which is in line with the response of ϕPSII. Nevertheless, plants pre-exposed to 27–37°C exhibited a comparable ETR_{max} in the recovery period. In macroalgae, the effect of sublethal temperature was less prominent (**Figure 3** and **Table 1**). ETR_{max} was affected by the duration of exposure (repeated ANOVA, $p < 0.001$) and species ($p < 0.001$), but not temperature. Nevertheless, *post hoc* comparisons (Fisher's LSD test) showed that *U. intestinalis,* at 42°C, had the lowest ETR_{max} on days 1 and 3 of the stress period.

Chlorophyll Content

Total chlorophylls in both coral species (**Figure 4**) varied according to temperature (factorial ANOVA, $p < 0.05$), time of sampling ($p < 0.001$), and interactions between the two factors ($p < 0.001$). At the end of the stress period, total chlorophyll of *P. acuta* exposed to 27, 29.5, and 32°C remained similar and was higher than total chlorophyll of individuals exposed to 34.5°C (Fisher's LSD test). A further decline in the total chlorophyll after the recovery period was detected in individuals pre-exposed to 34.5°C (Fisher's LSD test). On the other hand, chlorophyll content of *P. lutea* decreased after exposure to 32 and 34.5°C, showing a significant difference between the two treatments (Fisher's LSD test). Nevertheless, no further change in the total chlorophyll was detected at the end of the recovery period. A reduction in chlorophyll content in coral species was in accordance with a reduction in zooxanthellae density and bleaching (**Supplementary Figure 1**). Total chlorophylls in seagrasses exhibited differences according to temperature (factorial ANOVA, $p < 0.001$) and species ($p < 0.001$). At the end

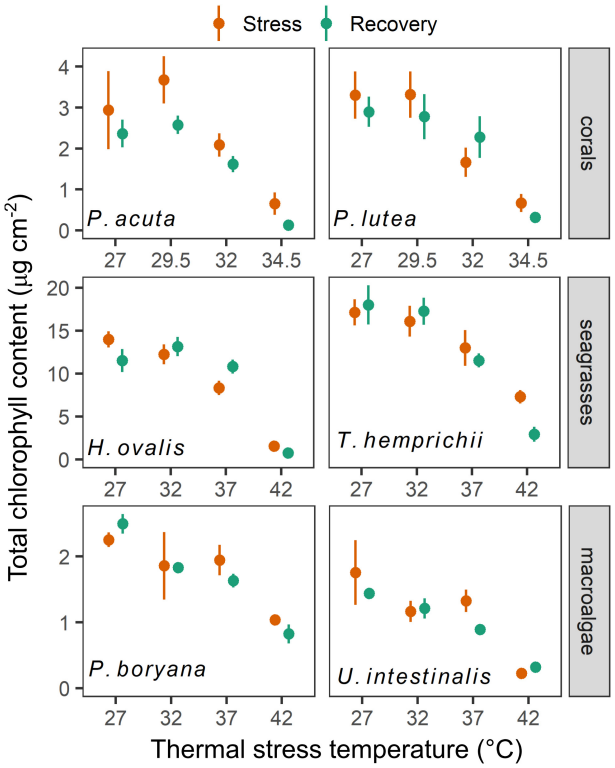

FIGURE 4 | The effects of experimental temperatures on total chlorophyll content of corals, seagrasses and macroalgae at the end of stress and recovery periods. Values are shown as mean ± SE (n = 3). For each replicate, 3 individuals were sampled. Corals were subjected to 27–34.5°C in stress period and 27°C in recovery period. Seagrasses and macroalgae were subjected to 27–42°C in stress period and 32°C in recovery period.

of the stress period, a decrease in total chlorophyll in *H. ovalis* was found at 37 and 42°C (Fisher's LSD test). A recovery was observed in the plants exposed to 37°C. At the end of the stress period, a decrease in total chlorophyll in *T. hemprichii* was found only at 42°C, which showed a further decline at the end of the recovery period (Fisher's LSD test). Total chlorophylls in macroalgae exhibited differences according to temperature (factorial ANOVA, $p < 0.001$) and species ($p < 0.001$). Both macroalgae showed a significant decrease in total chlorophyll only at 42°C treatment (Fisher's LSD test). While *P. boryana* showed no significant change in total chlorophyll at the end of the recovery period, a further decline in the total chlorophyll was detected in *U. intestinalis* pre-exposed to 37°C (Fisher's LSD test).

Growth Rates and Growth-Related Attributes

Growth rates of all species were affected by increasing temperature (**Figure 5**). Growth rates of the corals (**Figure 5A**) were influenced by species (repeated ANOVA, $p < 0.05$), temperature ($p < 0.01$), time of measurement ($p < 0.001$), and interactions between these factors ($p < 0.001$). At the end of the stress period, the net biomass increments of *P. acuta* exposed to 27, 29.5, and 32°C remained similar, whereas a significant decline was observed in individuals exposed to 34.5°C (Fisher's LSD test). At this temperature, *P. acuta* exhibited a net loss in biomass. No significant change was detected after the recovery period. On the other hand, the growth rates of *P. lutea* showed a stepwise decline at 27–34.5°C (Fisher's LSD test), reaching negative values at 34.5°C indicating a net loss in biomass. Complete recovery was seen in individuals pre-exposed to 29.5 and 32°C, whereas growth rates of the individuals pre-exposed to 34.5°C did not improve.

The growth rates in seagrasses (**Figure 5B**) showed differences according to species (repeated ANOVA, $p < 0.01$), temperature ($p < 0.001$), time of measurement ($p < 0.001$), and interactions between these factors ($p < 0.001$). The biomass increments of *H. ovalis* measured at the end of the stress period decreased linearly with increasing temperature from 27 to 42°C (Fisher's LSD test). Further reductions in growth rates were detected in plants pre-exposed to 27°C at the end of the recovery period (Fisher's LSD test). On the contrary, negative effects of temperature on biomass increments of *T. hemprichii* were detected only at 42°C (Fisher's LSD test). Further reductions in biomass increments were detected in individuals pre-exposed to 37 and 42°C at the end of the recovery period (Fisher's LSD test). In addition, a negative effect of moderate warming (37°C) was also seen in senescence rates in *T. hemprichii*, which was alleviated after the recovery period (**Figure 5C**). The highest senescence rates were found in *H. ovalis* at 42°C, which was likely due to mortality.

The growth rates in macroalgae (**Figure 5D**) showed differences according to temperature (repeated ANOVA, $p < 0.001$), species ($p < 0.01$), and interaction of the two factors ($p < 0.001$). At the end of the stress period, the net biomass increments of *P. boryana* exposed to 27 and 32°C were comparable, whereas a net loss in biomass was observed at 37 and 42°C (Fisher's LSD test). No significant change was detected after the recovery period. On the other hand, a negative effect of increasing temperature on growth rates of *U. intestinalis* was detected only at 42°C (Fisher's LSD test), where there was a net loss in biomass (**Figure 5D**). In the recovery period, *U. intestinalis* pre-exposed to 37°C suffered a further decline in growth, resulting in a net loss in biomass (Fisher's LSD test).

Integrated Biomarker Response

For all categories, the most sensitive species to increases in temperature were *P. lutea*, *H. ovalis*, and *P. boryana*, as indicated by higher IBR index at 32 and 34.5°C for coral and at 37 and 42°C for seagrass and macroalga. There was recovery at 37 and 32°C only in *H. ovalis* and *P. lutea*, while all species showed no recovery capacity after exposure to the highest temperatures (**Figure 6A**). The most responsive biomarkers during the stress period were growth in *P. lutea*, *H. ovalis,* and *P. boryana* and chlorophyll content in *P. acuta, T. hemprichii*, and *U. intestinalis*. The most responsive biomarkers during the recovery period were growth in *P. acuta*, *H. ovalis*, and *P. boryana* and chlorophyll content in *P. lutea*, *T. hemprichii*, and *U. intestinalis*. On the other hand, $\underline{F}_v/F_m$ was a less responsive biomarker during the stress and recovery period in all species (**Figure 6B**).

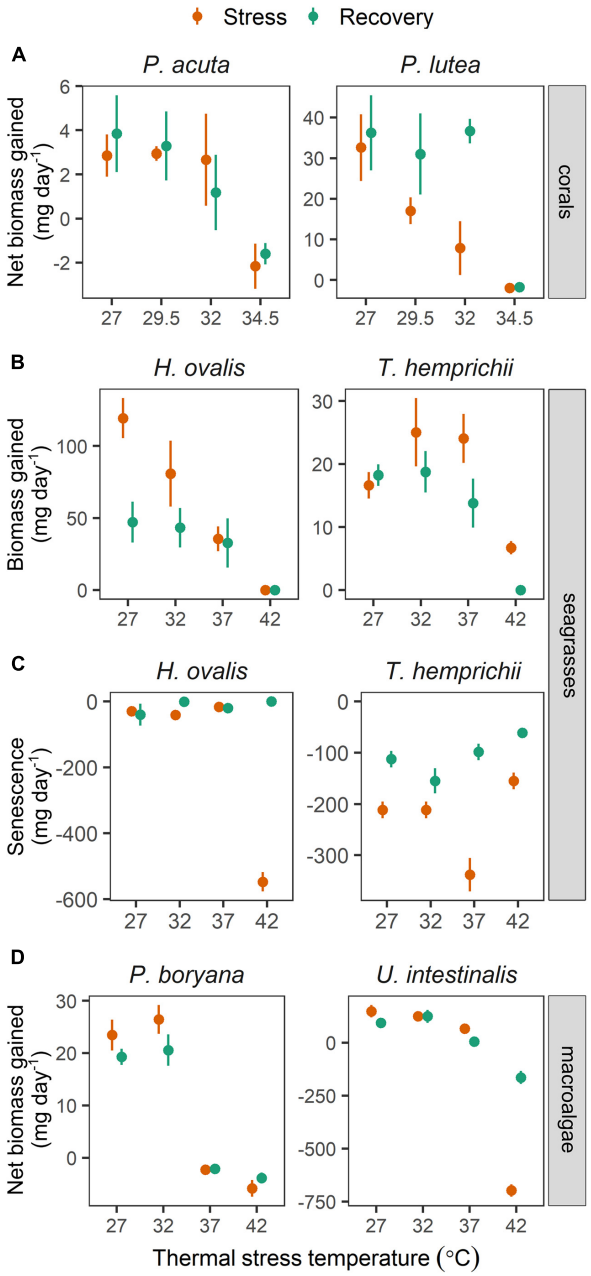

FIGURE 5 | The effects of experimental temperatures on growth rates of corals, seagrasses and macroalgae during stress and recovery periods. **(A)** Net biomass increase in corals, **(B)** biomass increase in seagrasses, **(C)** senescence (biomass loss) in seagrasses and **(D)** net biomass increase in macroalgae. Values are shown as mean ± SE (n = 3). For each replicate, 3 individuals were examined. Corals were subjected to 27–34.5°C in stress period and 27°C in recovery period. Seagrasses and macroalgae were subjected to 27–42°C in stress period and 32°C in recovery period.

DISCUSSION

Under warming scenarios, seagrasses and macroalgae could outcompete shallow-water corals, owing to their greater thermal tolerance (Anton et al., 2020; Roth et al., 2021). While the present study supports this notion, our results also show that temperature extremes could affect the photosynthesis and growth of seagrasses and macroalgae, resulting in irrecoverable damage and mortality. IBR provides further support that warming imposes an impact of manifold magnitude on the overall health of the tested species, depending on the temperature. As vulnerability to warming varies both among groups of organisms and species, ECEs are expected to have consequences on the structure, functions, and processes of coastal ecosystems.

Effects of Warming on Overall Performance of Shallow-Water Marine Organisms

In line with previous studies (Robison and Warner, 2006; Sinutok et al., 2012; Collier and Waycott, 2014; Rasmusson et al., 2020; Danaraj et al., 2021), our results suggest that short duration of elevated temperature poses significant adverse effects on the tropical shallow-water corals, seagrasses, and macroalgae. The heat stress effects, though complex, were manifested as lower efficiency of photosynthesis and photoprotection, chlorophyll degradation, slower growth, and mortality. Our results suggested that heat stress threshold lies between 37 and 42°C in seagrasses and macroalgae and between 32 and 34.5°C in corals, where the photosynthetic performance and growth were significantly affected. Our results are comparable to the thermal optima and threshold in tropical shallow-water organisms reported in previous studies (Mayfield et al., 2013; Collier et al., 2014; Buerger et al., 2015; Kong et al., 2019; George et al., 2020; Rasmusson et al., 2020, 2021; Keng et al., 2021).

It is established that photosynthesis is a major target of heat stress, since its associated components are heat sensitive (Allakhverdiev et al., 2008). Based on F_v/F_m and F_v/F_0, corals showed partial photoinhibition at 32°C, with subsequent recovery and irreversible photodamage at 34.5°C. On the contrary, the effect of increasing temperature on seagrass and macroalgae went from no effect or a slightly positive effect from 27 to 37°C to an acute and lethal effect at 42°C. These were accompanied by a decrease in RLC-derived parameters (ETR_{max}, E_k, and α) and chlorophylls contents, indicating an overall decline in photosynthetic activity. As an increase in temperature from 27 to 42°C can lead to a significant reduction in HCO_3^- in seawater (Pierrot et al., 2006), such HCO_3^- limitation may also contribute to a decrease in photosynthetic activities and growth rates observed in this study, particularly in HCO_3^- users (Beer and Rehnberg, 1997; Sinutok et al., 2011, 2012). The impacts on photosynthetic functions were worsened with the experimental duration, indicating accumulative stress effects. It is worth noting that F_v/F_0, although showed higher variability, provided a more sensitive indication of heat stress, which is in agreement with the recent study by Rasmusson et al. (2020), in which F_v/F_0 instead of F_v/F_m was adopted to trace the effects of warming in temperate and tropical seagrasses. In addition, a decrease in chlorophyll content implies that the ability of the photosynthetic tissue to absorb light also decreased. By using constant absorption factor (AF), the ETR values in RLC fittings were likely to be over-estimated. Direct comparison of ETR_{max} across treatments

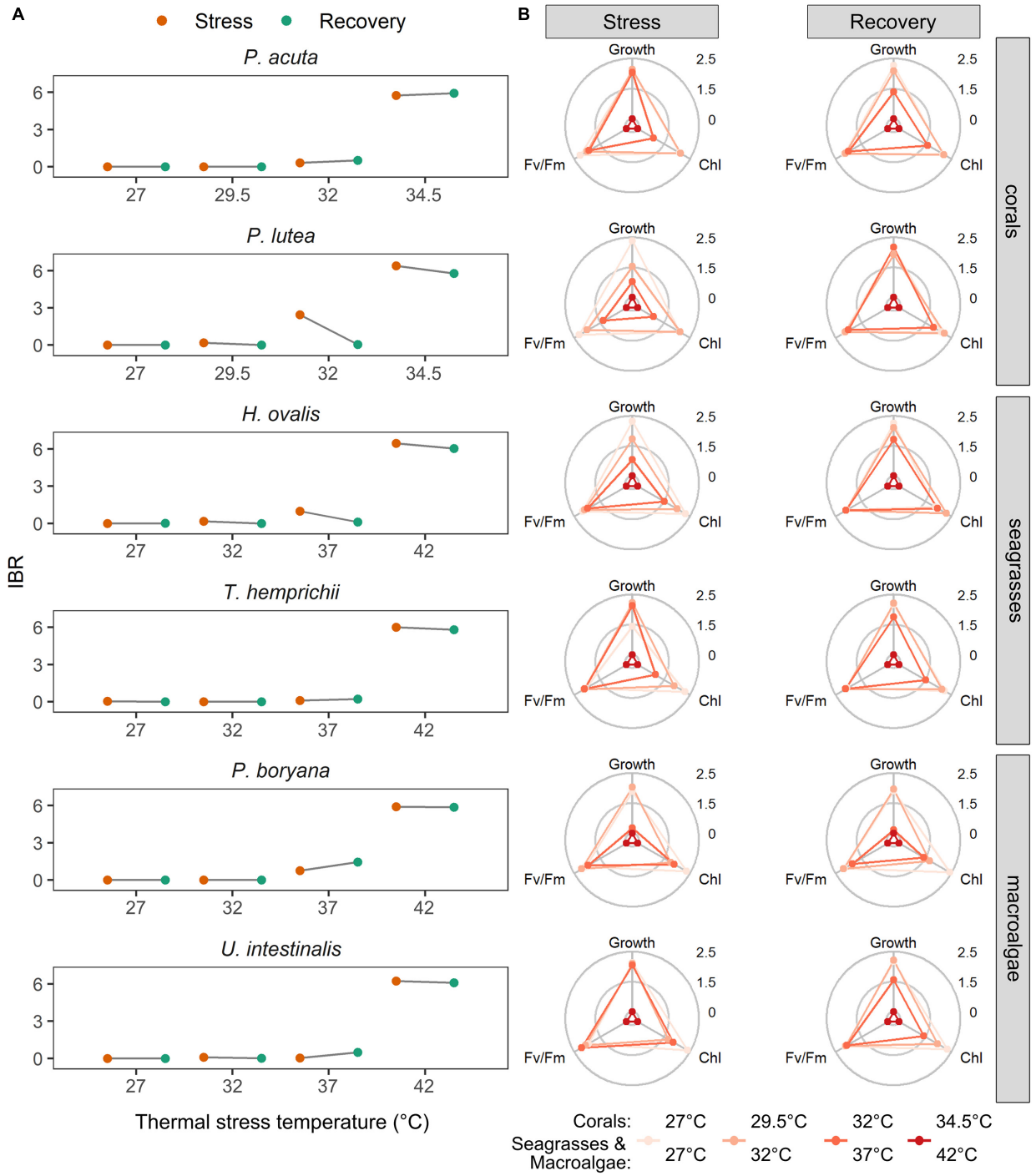

FIGURE 6 | (A) The effects of experimental temperatures on the integrated biomarker response (IBR) indices calculated from F_v/F_m, chlorophyll contents and growth rates of corals, seagrasses and macroalgae. **(B)** Star plots with mean scores for F_v/F_m, chlorophyll contents and growth rates in all tested species. Chl – total chlorophyll content. Growth – growth rates measured as an increase in biomass. Corals were subjected to 27–34.5°C in stress period and 27°C in recovery period. Seagrasses and macroalgae were subjected to 27–42°C in stress period and 32°C in recovery period.

(**Table 1**) should be interpreted with care as heat stress may have more pronounced effects on ETR than reported in our results. This points to limitation of the use of RLCs in repeated measurements in experiment which may induce variation in AF, in line with previous discussions by Enríquez and Borowitzka (2010) and González-Guerrero et al. (2021).

Negative effects were also observed in growth rates of all the tested organisms, which appeared to be more heat

sensitive than photosynthesis. This may be linked to the negative carbon balance caused by higher respiratory carbon consumption relative to photosynthetic carbon assimilation (Scheufen et al., 2017; Hammer et al., 2018; Rasmusson et al., 2020; Costa et al., 2021), while photorespiratory activity, a competing process with carbon fixation, is known to be enhanced by increased temperature (Zhang et al., 2018; Hu et al., 2020). In addition, metabolic depression and energy allocation to certain defensive mechanisms (Bernardet et al., 2019; Marín-Guirao et al., 2019; Innis et al., 2021) may have long-term consequences on energetic balance and growth. Previous studies highlight that maintaining metabolic balance in coral holobionts (host, symbiotic algae, and associated microbes) is crucial under stress conditions (Levas et al., 2013). Undoubtedly, energy deficiency could be exacerbated during bleaching in corals (Innis et al., 2021), which was visible at 34.5°C. As coral calcification is known to be tightly coupled with photosynthetic and carbon translocation rates (Tremblay et al., 2016), a decrease in integrated photosynthetic capacity (photodamage, chlorophyll content, and zooxanthellae density) is likely to be among the key drivers for a decline in growth rates in the two corals at this temperature.

A more prominent heat stress effects on growth rates than on photosynthesis was also reported in other tropical species (Sinutok et al., 2012; Terada et al., 2016), including *P. acuta*, and *T. hemprichii* (George et al., 2018; Poquita-Du et al., 2020; Ho et al., 2021). This implies that the general notion that photosynthesis is one of the most sensitive physiological processes (Bhagooli et al., 2021) and that its response may precede the response at growth level may not entirely hold true for heat stress or could not be supported by the chlorophyll fluorescence parameters measured in the present study. Tropical shallow-water organisms may be able to maintain an intact photosynthetic machinery during warming events, albeit slower biomass production, which may persist in some species after the warming period is over (e.g., *H. ovalis*; *P. boryana,* and *U. intestinalis* at 37°C). In seagrasses, senescence was found to be among the significant effects of warming; not only seen as higher number of dead leaves in the two species, but higher number of shed leaves in *T. hemprichii* at 37°C. Anoxia in intercalary meristematic tissue has been identified as among the mechanisms contributing to detachment of shoots in seagrasses subjected to heat stress (Hammer et al., 2018). From our results, we proposed that whole-organism-related parameters, such as growth rates and senescence, may serve as good measurements for heat stress responses in relatively fast-growing species. These parameters are not only quantifiable but also ecologically relevant since they give an integrated indication of the organism's performance and health status (Madeira et al., 2018; Dias et al., 2020).

Differences in Sensitivity to Warming Among Important Groups of Tropical Marine Organisms and Species and Its Ecological Relevance

Different sensitivities to warming in conjunction with biotic interactions are likely to be the key predictors of climate change impacts on shallow-water marine ecosystems. Among the six species from three different groups of organisms, the seagrass *T. hemprichii* may be the least affected by future warming, whereas the coral *P. lutea* appears to be the most sensitive to increments in temperature.

Coral bleaching and mortality generally occur when the ambient temperature exceeds the thermal thresholds (Skirving et al., 2019). Mass bleaching of shallow-water corals in Thai waters corresponded to the thermal anomalies, with an average SST of 30.1°C in 1991 and 1995, 30.4°C in 1998, and 31.1°C in 2010 and 2016 (Brown et al., 1996; Phongsuwan and Chansang, 2012; Sutthacheep et al., 2013b; Putchim et al., 2017). In addition, a long-term comparative study conducted in Phuket in 1984–1986 and 2003–2005 revealed that a gradual increase in temperature resulted in a significant reduction in skeletal growth of the coral *P. lutea* (Tanzil et al., 2009). The average SSTs showed an increasing trend during the past three decades (Brown et al., 1996; Tanzil et al., 2009; Phongsuwan and Chansang, 2012; Sutthacheep et al., 2013b; Putchim et al., 2017) and is expected to reach 32°C in the near future (Hoegh-Guldberg et al., 2018). Our field records of variability in temperatures in the natural setting indicate that shallow-water corals are already exposed to an occasional rise in ambient temperature to 32°C (Unpublished data by authors). The future scenarios may drive radical change of local reef structure as recorded in the Great Barrier Reef (Hughes et al., 2018). Such higher thermal sensitivity observed in corals compared to seagrasses and macroalgae might be because they often grow in deeper habitats, thus experiencing smaller fluctuations in temperature and are rarely exposed during low tide (Smale et al., 2019; Roth et al., 2021). Although seagrasses and macroalgae can withstand a wide range of increasing temperature, a rapid deleterious effect was observed when the testing temperature reached 42°C, implying that the irregular warming events, in which temperature rises above 40°C, though uncommon and brief, will put immense pressure on intertidal seagrasses and macroalgae, thereby affecting productivity and leading to mortality. Although the seagrass and macroalgal die-off as a result of warming event was never reported in Thailand, it has been recorded in other locations in the tropical bioregions (Carlson et al., 2018; Buckee et al., 2021).

It is therefore expected that, as a result of moderate warming, seagrasses and macroalgae could outcompete shallow-water corals as the temperature increases (Anton et al., 2020; Roth et al., 2021). Although our results suggest that *T. hemprichii* might be the most persistent species in warming scenarios because of their relatively high thermotolerance, successful expansion, and colonization in the subtidal areas requires acclimation to different arrays of environmental factors (Beca-Carretero et al., 2020). One of the key limiting factors is light availability, which has been identified as the fundamental driver for growth and distribution of many marine primary producers (Falkowski and Knoll, 2007). Due to their relatively higher light requirement, slower growth rate, and preference for soft substrates (Collier et al., 2012; Badalamenti et al., 2015), seagrasses are less likely to expand to deeper coral reef areas, implying that direct interaction between corals and seagrasses is improbable. On the contrary, there is growing evidence of enhanced algal occupation of coral reefs following warming events (Hughes et al., 2019;

Anton et al., 2020; Wasim et al., 2021). This interaction with macroalgae has been shown to worsen coral health status and physiological performance and is often associated with coral reef degradation (Fong and Todd, 2021; Roth et al., 2021). Although they appear less tolerant to extreme warming, opportunistic characteristics, such as rapid nutrient uptake, effective carbon utilization, and high reproduction capacity of *Ulva* species and their free-floating trait (Buapet et al., 2008, 2013; Zhang et al., 2019; Kambey et al., 2020), may allow them to proliferate in the coral reef habitat under moderate warming scenarios, particularly where eutrophication is not properly regulated. As previously stated, light is one of the key controlling factors (Falkowski and Knoll, 2007) and studies have shown that interaction with light availability can determine heat stress responses in marine species (Dove et al., 2006; Moreno-Marín et al., 2018; Costa et al., 2021). The extrapolation of our results obtained from controlled experiment using a single non-photoinhibitory level of irradiance to natural conditions, where organisms are exposed to different light environments, must be taken with caution.

When comparing the two species of corals, *P. acuta* maintained their photosynthesis and growth rates relatively well when facing moderate heat stress (29.5–32°C), although more rapid bleaching (**Supplementary Figure 1**) and earlier mortality were observed in 34.5°C compared to *P. lutea*. Other biological attributes, such as photosynthetic efficiency and growth rates, suggested that *P. lutea* was more sensitive to warming, particularly at moderate levels. It has been suggested that *Pocillopora* species are more susceptible to thermal stress than the massive *Porites* species (Hill et al., 2012). This is evident in the mass coral bleaching events from 1998 to 2010 during which severe bleaching and mortality of pocilloporids in Thai waters were recorded (Yeemin et al., 2009; Chavanich et al., 2012; Sutthacheep et al., 2013b). Nevertheless, their susceptibility seems to reduce as they were repeatedly exposed to thermal stress (Pratchett et al., 2013; McClanahan, 2017; Putchim et al., 2017). Association with Clade D types of zooxanthellae, a more heat-resistant clade, which have been increasingly reported in Thai coastal reefs (Chankong et al., 2018, 2020), may contribute to their enhanced thermotolerance (Cunning et al., 2015; Wham et al., 2017). On the contrary, field records showed that *P. lutea* often suffered partial bleaching and mortality (Phongsuwan and Chansang, 2012; Brown et al., 2014) and that this phenomenon has gradually increased during the past decade (Putchim et al., 2017). Significant impacts of warming on *Porites* species were manifested as a decline in calcification measured as linear extension, density, and hiatus (Cantin and Lough, 2014; Xu et al., 2018), which is in line with our results. It is worth noting that growth rates of *P. lutea* pre-exposed to 32°C displayed complete recovery, thus corroborating previous investigations reporting the subsequent recovery of *P. lutea* after thermal stress in their natural settings (Phongsuwan and Chansang, 2012; Brown et al., 2014).

The different life traits of the two seagrasses may contribute to their difference in thermotolerance. *Halophila* are considered the colonizing species, while *Thalassia* are considered the persistent ones (Kilminster et al., 2015; O'Brien et al., 2018). It has been suggested that the former often exhibit lower physiological resistance to environmental disturbances compared to the latter (Kilminster et al., 2015; O'Brien et al., 2018). This notion agrees with the findings in the present study and is in line with our previous investigations in which *H. ovalis* showed lower physiological tolerance to stressors, such as desiccation and high irradiance, than *T. hemprichii* (Wuthirak et al., 2016; Phandee and Buapet, 2018). Nevertheless, colonizing species are expected to recover from stress more rapidly than persistent species, owing to their fast growth rates and usually large seed banks (Kilminster et al., 2015; O'Brien et al., 2018; Ong et al., 2020). Even at a short duration of recovery, physiological improvement was already seen in *H. ovalis* exposed to 37°C. In this study, while growth rates were not yet restored, their photosynthesis and chlorophyll contents showed almost complete recovery after 5 days at optimal temperature.

Padina species are lightly-calcified brown macroalgae (Wichachucherd et al., 2010), whereas *Ulva* species are green macroalgae known for their opportunistic traits and capacity to generate "green tides" (Zhang et al., 2019; Kambey et al., 2020). Higher thermotolerance in *U. intestinalis* compared to *P. boryana* may be a result of their local acclimation. In their respective sampling sites, *U. intestinalis* were mostly found free-floating or attached to seagrass leaf blades or mangrove roots and directly exposed to sunlight and heat at low tide, while *P. boryana* remained attached to the substrate, forming assemblage structure, which may buffer drastic changes in environmental factors influenced by tidal cycle. Underlying mechanisms of heat tolerance in *Ulva* species have been extensively studied and vast arrays of molecular regulations and metabolic adjustment pathways have been identified (Fan et al., 2017; He et al., 2018). Previous studies also provide evidence that calcified macroalgae are more negatively affected by warming than fleshy macroalgae (Kram et al., 2016; Dove et al., 2020), partly due to the sensitivity of the calcification process to heat (Sinutok et al., 2011, 2012). Although *P. boryana* and *U. intestinalis* did not show recovery potential after 5 days at optimal temperature, both species have high reproductive outputs and high recruitment potential (Wichachucherd et al., 2010; Mayakun, 2019), which may support their long-term recolonization once the environmental factors become favorable.

Devastating loss of ecosystem services are expected if the corals, seagrasses, and macroalgae undergo degradation. As *Porites* and *Pocillopora* species serve as dominant reef-building corals in Thai waters (Yeemin et al., 2009; Chavanich et al., 2012; Sutthacheep et al., 2013b; Putchim et al., 2017), negative effects on their productivity and growth may be translated to an overall decrease in the health of coral habitats, thereby affecting a range of services, such as nursery ground (Lin et al., 2021), fisheries (Edgar et al., 2014), and coastal protection (Zhao et al., 2019). In addition to these services, seagrass meadows and some macroalgal habitats contribute as effective sinks for CO_2 (Krause-Jensen and Duarte, 2016), and their decline would eventually reduce the overall capacity for carbon sequestration and promote a release of greenhouse gasses (Arias-Ortiz et al., 2018). Thus, the effects

of warming may not only limit to coastal habitat degradation but may also accelerate the changing climate. While recovery by recolonization is possible, reports suggest that ecosystem services provided by fast-growing pioneer species may differ from those provided by the climax species (Kilminster et al., 2015; O'Brien et al., 2018). Therefore, long-term shifts of structure, functions, and processes of coastal ecosystems may be expected following ECEs.

Integrated Biomarker Response and Application for Monitoring and Management Efforts

The IBR index was adopted to quantify and visualize an overall integrated stress effect of warming on all shallow-water marine organisms. This tool has been successfully applied in assessing the health of corals, reef calcifiers, and marine invertebrates exposed to climate change related stressors, including warming (Madeira et al., 2018; Dias et al., 2020; Marques et al., 2020; Zhang et al., 2021); however, its application in seagrass and macroalgal research is yet to be explored. It is established that various biomarkers at different biological organization levels, ranging from cellular to organismal levels, are affected by increasing temperatures (George et al., 2018; Madeira et al., 2018; Savva et al., 2018; Dias et al., 2020). Early investigations on corals and other marine invertebrates also suggested that biomarkers both associated with cellular mechanisms and whole-organism performance should be combined in IBR indices to better elucidate the effects of heat stress (Madeira et al., 2018; Dias et al., 2020). Therefore, we tested the IBR approach using F_v/F_m, chlorophyll content, and growth rate as biomarkers encompassing physiological, biochemical, and organismal responses, respectively.

In general, the IBR index increased with increasing temperature in all tested organisms (**Figure 6A**). The highest IBR index was found at 34.5°C in corals and at 42°C in seagrasses and macroalgae, which indicates the highest stress level at this temperature. These integrative analyses, which corroborate the previously discussed results, indicate that an increase of 2.5°C from the maximum SST (32°C) will produce lethal effects in corals, while an increase of 10°C from the maximum SST will potentially cause seagrasses and macroalgae to die-off. In addition, a slightly higher IBR value was observed at 32°C in the coral *P. lutea* and at 37°C in the seagrass *H. ovalis* and the macroalga *P. boryana*, thus suggesting a higher sensitivity of these species under moderate heat stress. Therefore, poorer health of these organisms may be already seen within a range of the current maximum SST to an increase in the maximum SST by 5°C. Recovery from five consecutive days of moderate heat stress, however, was observed in *P. lutea* and *H. ovalis*, implying that the overall health status can be restored once the warming period is over. This emphasizes that the ability of the organisms to recover from stress significantly contributes to their resilience to moderate warming (Brown et al., 2014; Xu et al., 2020; Nguyen et al., 2021) and that recovery should be considered when evaluating the potential impacts of ECEs.

The IBR analysis showed an inhibition of photosynthetic activity, degradation of chlorophyll, and slower growth in all the tested species (**Figure 6B**). Deleterious effects at 34.5°C for corals and 42°C for seagrasses and macroalgae were manifested as a marked decline of all three biomarkers, while sublethal effects (32°C in the corals and 37°C in the seagrasses and macroalgae) were largely driven by growth rate and chlorophyll content for most of the tested species. These results, which support the suggestions made by previous studies (Madeira et al., 2018; Dias et al., 2020; Marques et al., 2020; Zhang et al., 2021), highlight the importance of using multiple biomarkers across the biological organizations and inclusion of the biomarkers at the organismic level.

Our results demonstrate that the IBR approach provides quantifiable indices for monitoring the health status of shallow-water marine organisms under warming scenarios and is therefore proven a useful tool for both research and management. Nevertheless, improvement of its efficiency is warranted, and careful consideration is necessary when interpreting the results within complex environments of a natural setting. While the biomarker suite adopted in the present study seems sufficient to elucidate the overall stress effects in the tested species, since it displayed a temperature-dependent response, all biomarkers are not specific to heat stress. Incorporations of biomarkers, such as heat shock proteins, energy metabolisms-related makers, and certain regulatory molecules (van Oppen and Oakeshott, 2020; Danaraj et al., 2021; Innis et al., 2021), particularly those at the molecular level, will enhance the precision and resolution of the IBR index. However, the selection of suitable biomarkers relies on advanced knowledge of the cause-effect relationship between temperature and complex biological responses of given species and populations, which remains inadequate, particularly in the tropical Southeast Asian region (Guan et al., 2020; Nguyen et al., 2021). An in-depth understanding of the underlying physiological mechanisms associated with warming will therefore not only be crucial for predicting how future warming scenarios will affect the coastal ecosystems, but also for developing a more effective tool to assess and mitigate the long-term impact of warming events on shallow-water marine organisms.

DATA AVAILABILITY STATEMENT

The raw data supporting the conclusions of this article will be made available by the authors, without undue reservation.

AUTHOR CONTRIBUTIONS

All authors contributed to the conceptualization of the study. MY, SS, PC, and PB planned and conducted the experiments, analyzed the samples, interpreted the data, performed the statistical analysis, and wrote the manuscript. All authors read and approved the submitted manuscript.

FUNDING

This research was supported by National Science, Research and Innovation Fund (NSRF) and Prince of Songkla University (Grant Number: ENV6405083M).

ACKNOWLEDGMENTS

The authors wish to thank Jenjira Sudprang, Chutima Tongchu, Pimrak Moungkeaw, and Long Ying for their helpful assistance in the laboratory and Michael Jenke for support in data visualization.

SUPPLEMENTARY MATERIAL

The Supplementary Material for this article can be found online at: https://www.frontiersin.org/articles/10.3389/fmars.2021.767628/full#supplementary-material

REFERENCES

Allakhverdiev, S. I., Kreslavski, V. D., Klimov, V. V., Los, D. A., Carpentier, R., and Mohanty, P. (2008). Heat stress: an overview of molecular responses in photosynthesis. *Photosynth. Res.* 98, 541–550. doi: 10.1007/s11120-008-9331-0

Anton, A., Randle, J. L., Garcia, F. C., Rossbach, S., Ellis, J. I., Weinzierl, M., et al. (2020). Differential thermal tolerance between algae and corals may trigger the proliferation of algae in coral reefs. *Glob. Chang. Biol.* 26, 4316–4327. doi: 10.1111/gcb.15141

Arias-Ortiz, A., Serrano, O., Masqué, P., Lavery, P. S., Mueller, U., Kendrick, G. A., et al. (2018). A marine heatwave drives massive losses from the world's largest seagrass carbon stocks. *Nat. Clim. Chang.* 8, 338–344. doi: 10.1038/s41558-018-0096-y

Badalamenti, F., Alagna, A., and Fici, S. (2015). Evidences of adaptive traits to rocky substrates undermine paradigm of habitat preference of the Mediterranean seagrass *Posidonia oceanica*. *Sci. Rep.* 5:8804. doi: 10.1038/srep08804

Beca-Carretero, P., Teichberg, M., Winters, G., Procaccini, G., and Reuter, H. (2020). Projected rapid habitat expansion of tropical seagrass species in the Mediterranean Sea as climate change progresses. *Front. Plant Sci.* 11:555376. doi: 10.3389/fpls.2020.555376

Beer, S., and Rehnberg, J. (1997). The acquisition of inorganic carbon by the seagrass *Zostera marina*. *Aquat. Bot.* 56, 277–283. doi: 10.1016/S0304-3770(96)01109-6

Beliaeff, B., and Burgeot, T. (2002). Integrated biomarker response: a useful tool for ecological risk assessment. *Environ. Toxicol. Chem.* 21, 1316–1322. doi: 10.1002/etc.5620210629

Bernardet, C., Tambutté, E., Techer, N., Tambutté, S., and Venn, A. A. (2019). Ion transporter gene expression is linked to the thermal sensitivity of calcification in the reef coral *Stylophora pistillata*. *Sci. Rep.* 9:18676. doi: 10.1038/s41598-019-54814-7

Bhagooli, R., Mattan-Moorgawa, S., Kaullysing, D., Louis, Y. D., Gopeechund, A., Ramah, S., et al. (2021). Chlorophyll fluorescence–a tool to assess photosynthetic performance and stress photophysiology in symbiotic marine invertebrates and seaplants. *Mar. Pollut. Bull.* 165:112059. doi: 10.1016/j.marpolbul.2021.112059

Brown, B. E., Dunne, R. P., and Chansang, H. (1996). Coral bleaching relative to elevated seawater temperature in the Andaman Sea (Indian Ocean) over the last 50 years. *Coral Reefs* 15, 151–152. doi: 10.1007/BF01145885

Brown, B. E., Dunne, R. P., Phongsuwan, N., Patchim, L., and Hawkridge, J. M. (2014). The reef coral *Goniastrea aspera*: a 'winner' becomes a 'loser' during a severe bleaching event in Thailand. *Coral Reefs* 33, 395–401. doi: 10.1007/s00338-013-1120-3

Buapet, P., Hiranpan, R., Ritchie, R. J., and Prathep, A. (2008). Effect of nutrient inputs on growth, chlorophyll, and tissue nutrient concentration of Ulva reticulata from a tropical habitat. *Sci. Asia* 34:245. doi: 10.2306/scienceasia1513-1874.2008.34.245

Buapet, P., Rasmusson, L. M., Gullström, M., and Björk, M. (2013). Photorespiration and carbon limitation determine productivity in temperate seagrasses. *PLoS One* 8:e83804. doi: 10.1371/journal.pone.0083804

Buckee, J., Hetzel, Y., Nyegaard, M., Evans, S., Whiting, S., Scott, S., et al. (2021). Catastrophic loss of tropical seagrass habitats at the Cocos (Keeling) islands due to multiple stressors. *Mar. Pollut. Bull.* 170:112602. doi: 10.1016/j.marpolbul.2021.112602

Buerger, P., Schmidt, G. M., Wall, M., Held, C., and Richter, C. (2015). Temperature tolerance of the coral *Porites lutea* exposed to simulated large amplitude internal waves (LAIW). *J. Exp. Mar. Biol. Ecol.* 471, 232–239. doi: 10.1016/j.jembe.2015.06.014

Cantin, N. E., and Lough, J. M. (2014). Surviving coral bleaching events: porites growth anomalies on the Great Barrier Reef. *PLoS One* 9:e88720. doi: 10.1371/journal.pone.0088720

Carlson, D. F., Yarbro, L. A., Scolaro, S., Poniatowski, M., McGee-Absten, V., and Carlson, P. R. (2018). Sea surface temperatures and seagrass mortality in Florida Bay: spatial and temporal patterns discerned from MODIS and AVHRR data. *Remote Sens. Environ.* 208, 171–188. doi: 10.1016/j.rse.2018.02.014

Cesar, H. S. J., Burke, L. M., and Pet-Soede, L. (2003). *The Economics of Worldwide Coral Reef Degradation*. Arnhem: Cesar Environmental Economics Consulting (CEEC).

Chankong, A., Kongjandtre, N., Senanan, W., and Manthachitra, V. (2018). Genetic diversity of Symbiodiniaceae associated with *Porites lutea* and *Pocillopora damicornis* in the Gulf of Thailand inferred from nucleotide sequences of internal transcribed spacer-2. *J. Fish. Environ.* 42, 66–79.

Chankong, A., Kongjandtre, N., Senanan, W., and Manthachitra, V. (2020). Community composition of Symbiodiniaceae among four scleractinian corals in the eastern Gulf of Thailand. *Reg. Stud. Mar. Sci.* 33:100918. doi: 10.1016/j.rsma.2019.100918

Chavanich, S., Viyakarn, V., Adams, P., Klammer, J., and Cook, N. (2012). Reef communities after the 2010 mass coral bleaching at Racha Yai Island in the Andaman Sea and Koh Tao in the Gulf of Thailand. *Phuket Mar. Biol. Center Res. Bull.* 71, 103–110.

Collier, C. J., and Waycott, M. (2014). Temperature extremes reduce seagrass growth and induce mortality. *Mar. Pollut. Bull.* 83, 483–490. doi: 10.1016/j.marpolbul.2014.03.050

Collier, C. J., Ow, Y. X., Langlois, L., Uthicke, S., Johansson, C. L., O'Brien, K. R., et al. (2017). Optimum temperatures for net primary productivity of three tropical seagrass species. *Front. Plant Sci.* 8:1446. doi: 10.3389/fpls.2017.01446

Collier, C. J., Villacorta-Rath, C., van Dijk, K., Takahashi, M., and Waycott, M. (2014). Seagrass proliferation precedes mortality during hypo-salinity events: a stress-induced morphometric response. *PLoS One* 9:e94014. doi: 10.1371/journal.pone.0094014

Collier, C. J., Waycott, M., and Ospina, A. G. (2012). Responses of four Indo-West Pacific seagrass species to shading. *Mar. Pollut. Bull.* 65, 342–354. doi: 10.1016/j.marpolbul.2011.06.017

Colombo-Pallota, M. F., García-Mendoza, E., and Ladah, L. B. (2006). Photosynthetic performance, light absorption, and pigment composition of *Macrocystis pyrifera* (Laminariales, Phaephyceae) blades from different depths. *J. Phycol.* 42, 1225–1234. doi: 10.1111/j.1529-8817.2006.00287.x

Costa, M. M., Silva, J., Barrote, I., and Santos, R. (2021). Heatwave effects on the photosynthesis and antioxidant activity of the seagrass *Cymodocea nodosa* under contrasting light regimes. *Oceans* 2, 448–460. doi: 10.3390/oceans2030025

Cunning, R., Silverstein, R. N., and Baker, A. C. (2015). Investigating the causes and consequences of symbiont shuffling in a multi-partner reef coral symbiosis under environmental change. *Proc. R. Soc. B* 282:20141725. doi: 10.1098/rspb.2014.1725

Danaraj, J., Ayyappan, S., Mariasingarayan, Y., Packiyavathy, I. A. S. V., and Dharmadhas, J. S. (2021). Chlorophyll fluorescence, dark respiration and

metabolomic analysis of *Halodule pinifolia* reveal potential heat responsive metabolites and biochemical pathways under ocean warming. *Mar. Environ. Res.* 164:105248. doi: 10.1016/j.marenvres.2020.105248

Davies, P. S. (1989). Short-term growth measurements of corals using an accurate buoyant weighing technique. *Mar. Biol.* 101, 389–395. doi: 10.1007/BF00428135

Dias, M., Madeira, C., Jogee, N., Ferreira, A., Gouveia, R., Cabral, H., et al. (2020). Integrative indices for health assessment in reef corals under thermal stress. *Ecol. Indic.* 113:106230. doi: 10.1016/j.ecolind.2020.106230

Dove, S. G., Brown, K. T., Van Den Heuvel, A., Chai, A., and Hoegh-Guldberg, O. (2020). Ocean warming and acidification uncouple calcification from calcifier biomass which accelerates coral reef decline. *Commun. Earth. Environ.* 1:55. doi: 10.1038/s43247-020-00054-x

Dove, S., Ortiz, J. C., Enríquez, S., Fine, M., Fisher, P., Iglesias-Prieto, R., et al. (2006). Response of holosymbiont pigments from the scleractinian coral *Montipora monasteriata* to short-term heat stress. *Limnol. Oceanogr.* 51, 1149–1158. doi: 10.4319/lo.2006.51.2.1149

Duarte, B., Martins, I., Rosa, R., Matos, A. R., Roleda, M. Y., Reusch, T. B. H., et al. (2018). Climate change impacts on seagrass meadows and macroalgal forests: an integrative perspective on acclimation and adaptation potential. *Front. Mar. Sci.* 5:190. doi: 10.3389/fmars.2018.00190

Eakin, C. M., Sweatman, H. P. A., and Brainard, R. E. (2019). The 2014–2017 global-scale coral bleaching event: insights and impacts. *Coral Reefs* 38, 539–545. doi: 10.1007/s00338-019-01844-2

Edgar, G. J., Stuart-Smith, R. D., Willis, T. J., Kininmonth, S., Baker, S. C., Banks, S., et al. (2014). Global conservation outcomes depend on marine protected areas with five key features. *Nature* 506, 216–220. doi: 10.1038/nature13022

Enríquez, S., and Borowitzka, M. A. (2010). "The use of the fluorescence signal in studies of seagrasses and macroalgae," in *Chlorophyll a Fluorescence in Aquatic Sciences: Methods and Applications*, eds D. J. Suggett, O. Prášil, and M. A. Borowitzka (Dordrecht: Springer), 187–208.

Falkowski, P. G., and Knoll, A. H. (2007). "An introduction to primary producers in the sea: who they are, what they do, and when they evolved," in *Evolution of Primary Producers in the Sea*, eds P. G. Falkowski and A. H. Knoll (Amsterdam: Elsevier), 1–6. doi: 10.1016/B978-012370518-1/50002-3

Fan, M., Sun, X., Xu, N., Liao, Z., Li, Y., Wang, J., et al. (2017). Integration of deep transcriptome and proteome analyses of salicylic acid regulation high temperature stress in Ulva prolifera. *Sci Rep* 7:11052. doi: 10.1038/s41598-017-11449-w

Fong, J., and Todd, P. A. (2021). Spatio-temporal dynamics of coral–macroalgal interactions and their impacts on coral growth on urbanised reefs. *Mar. Pollut. Bull.* 172:112849.

Freeman, L. A., Kleypas, J. A., and Miller, A. J. (2013). Coral reef habitat response to climate change scenarios. *PLoS One* 8:e82404. doi: 10.1371/journal.pone.0082404

George, R., Gullström, M., Mangora, M. M., Mtolera, M. S. P., and Björk, M. (2018). High midday temperature stress has stronger effects on biomass than on photosynthesis: a mesocosm experiment on four tropical seagrass species. *Ecol. Evol.* 8, 4508–4517. doi: 10.1002/ece3.3952

George, R., Gullström, M., Mtolera, M. S. P., Lyimo, T. J., and Björk, M. (2020). Methane emission and sulfide levels increase in tropical seagrass sediments during temperature stress: a mesocosm experiment. *Ecol. Evol.* 10, 1917–1928. doi: 10.1002/ece3.6009

Gibbin, E. M., Krueger, T., Putnam, H. M., Barott, K. L., Bodin, J., Gates, R. D., et al. (2018). Short-term thermal acclimation modifies the metabolic condition of the coral holobiont. *Front. Mar. Sci.* 5:10. doi: 10.3389/fmars.2018.00010

González-Guerrero, L. A., Vásquez-Elizondo, R. M., López-Londoño, T., Hernán, G., Iglesias-Prieto, R., and Enríquez, S. (2021). Validation of parameters and protocols derived from chlorophyll a fluorescence commonly utilised in marine ecophysiological studies. *Funct. Plant. Biol.* doi: 10.1071/FP21101 [Epub ahead of print].

Good, A. M., and Bahr, K. D. (2021). The coral conservation crisis: interacting local and global stressors reduce reef resiliency and create challenges for conservation solutions. *SN Appl. Sci.* 3:312. doi: 10.1007/s42452-021-04319-8

Guan, Y., Hohn, S., Wild, C., and Merico, A. (2020). Vulnerability of global coral reef habitat suitability to ocean warming, acidification and eutrophication. *Glob. Chang. Biol.* 26, 5646–5660. doi: 10.1111/gcb.15293

Hammer, K. J., Borum, J., Hasler-Sheetal, H., Shields, E. C., Sand-Jensen, K., and Moore, K. A. (2018). High temperatures cause reduced growth, plant death and metabolic changes in eelgrass *Zostera marina*. *Mar. Ecol. Prog. Ser.* 604, 121–132. doi: 10.3354/meps12740

He, Y., Hu, C., Wang, Y., Cui, D., Sun, X., Li, Y., et al. (2018). The metabolic survival strategy of marine macroalga Ulva prolifera under temperature stress. *J. Appl. Phycol.* 30, 3611–3621. doi: 10.1007/s10811-018-1493-3

Henderson, C. J., Stevens, T., Lee, S. Y., Gilby, B. L., Schlacher, T. A., Connolly, R. M., et al. (2019). Optimising seagrass conservation for ecological functions. *Ecosystems* 22, 1368–1380. doi: 10.1007/s10021-019-00343-3

Hill, R., and Ralph, P. J. (2007). Post-bleaching viability of expelled zooxanthellae from the scleractinian coral Pocillopora damicornis. *Mar. Ecol. Prog. Ser.* 352, 137–144. doi: 10.3354/meps07159

Hill, R., Brown, C. M., DeZeeuw, K., Campbell, D. A., and Ralph, P. J. (2011). Increased rate of D1 repair in coral symbionts during bleaching is insufficient to counter accelerated photo-inactivation. *Limnol. Oceanogr.* 56, 139–146. doi: 10.4319/lo.2011.56.1.0139

Hill, R., Larkum, A. W. D., Prášil, O., Kramer, D. M., Szabó, M., Kumar, V., et al. (2012). Light-induced dissociation of antenna complexes in the symbionts of scleractinian corals correlates with sensitivity to coral bleaching. *Coral Reefs* 31, 963–975. doi: 10.1007/s00338-012-0914-z

Ho, M., McBroom, J., Bergstrom, E., and Diaz-Pulido, G. (2021). Physiological responses to temperature and ocean acidification in tropical fleshy macroalgae with varying affinities for inorganic carbon. *ICES J. Mar. Sci.* 78, 89–100. doi: 10.1093/icesjms/fsaa195

Hoegh-Guldberg, O., Jacob, D., Taylor, M., Bindi, M., Brown, S., Camilloni, I., et al. (2018). "Impacts of 1.5°C global warming on natural and human systems," in *Global Warming of 1.5°C.* An IPCC Special Report on the impacts of global warming of 1.5°C above pre-industrial levels and related global greenhouse gas emission pathways, in the context of strengthening the global response to the threat of climate change, sustainable development, and efforts to eradicate poverty, eds V. Masson-Delmotte, P. Zhai, H.-O. Pörtner, D. Roberts, J. Skea, P. R. Shukla, et al. (Geneva: World Meteorological Organization Technical Document).

Hu, S., Ding, Y., and Zhu, C. (2020). Sensitivity and responses of chloroplasts to heat stress in plants. *Front. Plant Sci.* 11:375. doi: 10.3389/fpls.2020.00375

Hughes, T. P., Kerry, J. T., Baird, A. H., Connolly, S. R., Chase, T. J., Dietzel, A., et al. (2019). Global warming impairs stock–recruitment dynamics of corals. *Nature* 568, 387–390. doi: 10.1038/s41586-019-1081-y

Hughes, T. P., Kerry, J. T., Baird, A. H., Connolly, S. R., Dietzel, A., Eakin, C. M., et al. (2018). Global warming transforms coral reef assemblages. *Nature* 556, 492–496. doi: 10.1038/s41586-018-0041-2

Innis, T., Allen−Waller, L., Brown, K. T., Sparagon, W., Carlson, C., Kruse, E., et al. (2021). Marine heatwaves depress metabolic activity and impair cellular acid–base homeostasis in reef−building corals regardless of bleaching susceptibility. *Glob. Chang. Biol.* 27, 2728–2743. doi: 10.1111/gcb.15622

Jokiel, P. L., and Guinther, E. B. (1978). Effects of temperature on reproduction in the hermatypic coral *Pocillopora damicornis*. *Bull. Mar. Sci.* 28, 786–789.

Jurriaans, S., and Hoogenboom, M. (2020). Seasonal acclimation of thermal performance in two species of reef-building corals. *Mar. Ecol. Prog. Ser.* 635, 55–70. doi: 10.3354/meps13203

Kambey, C. S. B., Kang, J. W., and Chung, I. K. (2020). Impact of temperature, low pH and NH4+ enrichment on ecophysiological responses of a green tide species Ulva australis Areschoug. *Ocean Sci. J.* 55, 115–127. doi: 10.1007/s12601-020-0005-y

Keng, F. S.-L., Phang, S.-M., Abd Rahman, N., Yeong, H.-Y., Malin, G., Leedham Elvidge, E., et al. (2021). Halocarbon emissions by selected tropical seaweeds exposed to different temperatures. *Phytochemistry* 190:112869. doi: 10.1016/j.phytochem.2021.112869

Kilminster, K., McMahon, K., Waycott, M., Kendrick, G. A., Scanes, P., McKenzie, L., et al. (2015). Unravelling complexity in seagrass systems for management: Australia as a microcosm. *Sci. Total Environ.* 534, 97–109. doi: 10.1016/j.scitotenv.2015.04.061

Kong, E., Ow, Y. X., Lai, S., Yaakub, S. M., and Todd, P. (2019). Effects of shading on seagrass morphology and thermal optimal of productivity. *Mar. Freshw. Res.* 71, 913–921. doi: 10.1071/MF19173

Kram, S. L., Price, N. N., Donham, E. M., Johnson, M. D., Kelly, E. L. A., Hamilton, S. L., et al. (2016). Variable responses of temperate calcified and

fleshy macroalgae to elevated pCO2 and warming. *ICES J. Mar. Sci.* 73, 693–703. doi: 10.1093/icesjms/fsv168

Krause-Jensen, D., and Duarte, C. M. (2016). Substantial role of macroalgae in marine carbon sequestration. *Nat. Geosci.* 9, 737–742. doi: 10.1038/ngeo2790

Levas, S. J., Grottoli, A. G., Hughes, A., Osburn, C. L., and Matsui, Y. (2013). Physiological and biogeochemical traits of bleaching and recovery in the mounding species of coral *Porites lobata*: implications for resilience in mounding corals. *PLoS One* 8:e63267. doi: 10.1371/journal.pone.0063267

Lin, Y.-J., Rabaoui, L., Basali, A. U., Lopez, M., Lindo, R., Krishnakumar, P. K., et al. (2021). Long-term ecological changes in fishes and macro-invertebrates in the world's warmest coral reefs. *Sci. Total Environ.* 750:142254. doi: 10.1016/j.scitotenv.2020.142254

Madeira, C., Mendonça, V., Leal, M. C., Flores, A. A. V., Cabral, H. N., Diniz, M. S., et al. (2018). Environmental health assessment of warming coastal ecosystems in the tropics–application of integrative physiological indices. *Sci. Total Environ.* 643, 28–39. doi: 10.1016/j.scitotenv.2018.06.152

Marín-Guirao, L., Entrambasaguas, L., Ruiz, J. M., and Procaccini, G. (2019). Heat-stress induced flowering can be a potential adaptive response to ocean warming for the iconic seagrass *Posidonia oceanica*. *Mol. Ecol.* 28, 2486–2501. doi: 10.1111/mec.15089

Marques, J. A., Abrantes, D. P., Marangoni, L. F. B., and Bianchini, A. (2020). Ecotoxicological responses of a reef calcifier exposed to copper, acidification and warming: a multiple biomarker approach. *Environ. Pollut.* 257:113572. doi: 10.1016/j.envpol.2019.113572

Mayakun, J. (2019). Spatial variation in early patterns of algal recruitment in a tropical intertidal community. *Songklanakarin J. Sci. Technol.* 41, 254–489. doi: 10.14456/SJST-PSU.2019.60

Mayfield, A. B., Fan, T.-Y., and Chen, C.-S. (2013). Physiological acclimation to elevated temperature in a reef-building coral from an upwelling environment. *Coral Reefs* 32, 909–921. doi: 10.1007/s00338-013-1067-4

McClanahan, T. (2017). Changes in coral sensitivity to thermal anomalies. *Mar. Ecol. Prog. Ser.* 570, 71–85. doi: 10.3354/meps12150

Moreno-Marín, F., Brun, F. G., and Pedersen, M. F. (2018). Additive response to multiple environmental stressors in the seagrass *Zostera marina* L. *Limnol. Oceanogr.* 63, 1528–1544. doi: 10.1002/lno.10789

Ng, C. S. L., Lim, J. X., Sam, S. Q., Kikuzawa, Y. P., Toh, T. C., Wee, T. W., et al. (2019). Variability in skeletal bulk densities of common hard corals in Southeast Asia. *Coral Reefs* 38, 1133–1143. doi: 10.1007/s00338-019-01852-2

Nguyen, H. M., Ralph, P. J., Marín-Guirao, L., Pernice, M., and Procaccini, G. (2021). Seagrasses in an era of ocean warming: a review. *Biol. Rev. Camb. Philos. Soc.* 96, 2009–2030. doi: 10.1111/brv.12736

O'Brien, K. R., Waycott, M., Maxwell, P., Kendrick, G. A., Udy, J. W., Ferguson, A. J. P., et al. (2018). Seagrass ecosystem trajectory depends on the relative timescales of resistance, recovery and disturbance. *Mar. Pollut. Bull.* 134, 166–176. doi: 10.1016/j.marpolbul.2017.09.006

Ong, G. H. M., Lai, S., Yaakub, S. M., and Todd, P. (2020). Depauperate seed banks in urban tropical seagrass meadows. *Mar. Freshw. Res.* 71:935. doi: 10.1071/MF19204

Palumbi, S. R., Barshis, D. J., Traylor-Knowles, N., and Bay, R. A. (2014). Mechanisms of reef coral resistance to future climate change. *Science* 344, 895–898. doi: 10.1126/science.1251336

Pedersen, O., Colmer, T. D., Borum, J., Zavala-Perez, A., and Kendrick, G. A. (2016). Heat stress of two tropical seagrass species during low tides–impact on underwater net photosynthesis, dark respiration and diel in situ internal aeration. *New Phytol.* 210, 1207–1218. doi: 10.1111/nph.13900

Phandee, S., and Buapet, P. (2018). Photosynthetic and antioxidant responses of the tropical intertidal seagrasses *Halophila ovalis* and *Thalassia hemprichii* to moderate and high irradiances. *Bot. Mar.* 61, 247–256. doi: 10.1515/bot-2017-0084

Phongsuwan, N., and Chansang, H. (2012). Repeated coral bleaching in the Andaman Sea, Thailand, during the last two decades. *Phuket Mar. Biol. Center Res. Bull.* 71, 19–41.

Pierrot, D., Lewis, E., and Wallace, D. W. R. (2006). *MS Excel Program Developed for CO2 System Calculations*. Oak Ridge, TN: Dioxide Information Analysis Center, Oak Ridge National Laboratory, U.S. Department of Energy.

Platt, T., Gallegos, C. L., and Harrison, W. G. (1980). Photoinhibition of photosynthesis in natural assemblages of marine phytoplankton. *J. Mar. Res.* 38, 687–701.

Poquita-Du, R. C., Goh, Y. L., Huang, D., Chou, L. M., and Todd, P. A. (2020). Gene expression and photophysiological changes in *Pocillopora acuta* coral holobiont following heat stress and recovery. *Microorganisms* 8:1227. doi: 10.3390/microorganisms8081227

Porra, R. J. (2002). The chequered history of the development and use of simultaneous equations for the accurate determination of chlorophylls a and b. *Photosynth. Res.* 73, 149–156. doi: 10.1023/A:1020470224740

Pratchett, M. S., McCowan, D., Maynard, J. A., and Heron, S. F. (2013). Changes in bleaching susceptibility among corals subject to ocean warming and recurrent bleaching in Moorea, French Polynesia. *PLoS One* 8:e70443. doi: 10.1371/journal.pone.0070443

Putchim, L., Phongsuwan, N., Yaemarunpattana, C., Thongtham, N., and Richter, C. (2017). Long-term changes in the susceptibility of corals to thermal stress around Phuket, Thailand. *PeerJ Preprints* 5:e2979v1. doi: 10.7287/peerj.preprints.2979v1

Rasmusson, L. M., Buapet, P., George, R., Gullström, M., Gunnarsson, P. C. B., and Björk, M. (2020). Effects of temperature and hypoxia on respiration, photorespiration, and photosynthesis of seagrass leaves from contrasting temperature regimes. *ICES J. Mar. Sci.* 77, 2056–2065. doi: 10.1093/icesjms/fsaa093

Rasmusson, L. M., Nualla-ong, A., Wutiruk, T., Björk, M., Gullström, M., and Buapet, P. (2021). Sensitivity of photosynthesis to warming in two similar species of the aquatic angiosperm Ruppia from tropical and temperate habitats. *Sustainability* 13:9433. doi: 10.3390/su13169433

Ritchie, R. J. (2006). Consistent sets of spectrophotometric chlorophyll equations for acetone, methanol and ethanol solvents. *Photosynth. Res.* 89, 27–41. doi: 10.1007/s11120-006-9065-9

Robison, J. D., and Warner, M. E. (2006). Differential impacts of photoacclimation and thermal stress on the photobiology of four different phylotypes of *Symbiodinium* (Pyrrhophyta). *J. Phycol.* 42, 568–579. doi: 10.1111/j.1529-8817.2006.00232.x

Román, M., Román, S., Vázquez, E., Troncoso, J., and Olabarria, C. (2020). Heatwaves during low tide are critical for the physiological performance of intertidal macroalgae under global warming scenarios. *Sci. Rep.* 10:21408. doi: 10.1038/s41598-020-78526-5

Roth, F., Rädecker, N., Carvalho, S., Duarte, C. M., Saderne, V., Anton, A., et al. (2021). High summer temperatures amplify functional differences between coral− and algae−dominated reef communities. *Ecology* 102:e03226. doi: 10.1002/ecy.3226

Savva, I., Bennett, S., Roca, G., Jordà, G., and Marbà, N. (2018). Thermal tolerance of Mediterranean marine macrophytes: vulnerability to global warming. *Ecol. Evol.* 8, 12032–12043. doi: 10.1002/ece3.4663

Scheufen, T., Krämer, W. E., Iglesias-Prieto, R., and Enríquez, S. (2017). Seasonal variation modulates coral sensibility to heat-stress and explains annual changes in coral productivity. *Sci. Rep.* 7:4937. doi: 10.1038/s41598-017-04927-8

Schubert, N., Colombo-Pallota, M. F., and Enríquez, S. (2015). Leaf and canopy scale characterization of the photoprotective response to high-light stress of the seagrass *Thalassia testudinum*. *Limnol. Oceanogr.* 60, 286–302. doi: 10.1002/lno.10024

Short, F. T., and Duarte, C. M. (2001). "Methods for the measurement of seagrass growth and production," in *Global Seagrass Research Methods*, eds F. T. Short and R. G. Coles (Amsterdam: Elsevier), 155–182. doi: 10.1016/B978-044450891-1/50009-8

Sinutok, S., Hill, R., Doblin, M. A., Kühl, M., and Ralph, P. J. (2012). Microenvironmental changes support evidence of photosynthesis and calcification inhibition in Halimeda under ocean acidification and warming. *Coral Reefs* 31, 1201–1213. doi: 10.1007/s00338-012-0952-6

Sinutok, S., Hill, R., Doblin, M. A., Wuhrer, R., and Ralph, P. J. (2011). Warmer more acidic conditions cause decreased productivity and calcification in subtropical coral reef sediment-dwelling calcifiers. *Limnol. Oceanogr.* 56, 1200–1212. doi: 10.4319/lo.2011.56.4.1200

Skirving, W. J., Heron, S. F., Marsh, B. L., Liu, G., De La Cour, J. L., Geiger, E. F., et al. (2019). The relentless march of mass coral bleaching: a global perspective of changing heat stress. *Coral Reefs* 38, 547–557. doi: 10.1007/s00338-019-01799-4

Smale, D. A., Wernberg, T., Oliver, E. C. J., Thomsen, M., Harvey, B. P., Straub, S. C., et al. (2019). Marine heatwaves threaten global biodiversity and the

provision of ecosystem services. *Nat. Clim. Chang.* 9, 306–312. doi: 10.1038/s41558-019-0412-1

Strydom, S., Murray, K., Wilson, S., Huntley, B., Rule, M., Heithaus, M., et al. (2020). Too hot to handle: unprecedented seagrass death driven by marine heatwave in a World Heritage Area. *Glob. Chang. Biol.* 26, 3525–3538. doi: 10.1111/gcb.15065

Stuart-Smith, R. D., Edgar, G. J., and Bates, A. E. (2017). Thermal limits to the geographic distributions of shallow-water marine species. *Nat. Ecol. Evol.* 1, 1846–1852. doi: 10.1038/s41559-017-0353-x

Sutthacheep, M., Saenghaisuk, C., Pengsakun, S., Donsomjit, W., and Yeemin, T. (2013a). Quantitative studies on the 2010 mass coral bleaching event in Thai waters. *Galaxea* 15, 379–390. doi: 10.3755/galaxea.15.379

Sutthacheep, M., Yucharoen, M., Klinthong, W., Pengsakun, S., Sangmanee, K., and Yeemin, T. (2013b). Impacts of the 1998 and 2010 mass coral bleaching events on the Western Gulf of Thailand. *Deep Sea Res. 2 Top. Stud. Oceanogr.* 96, 25–31. doi: 10.1016/j.dsr2.2013.04.018

Tanzil, J. T. I., Brown, B. E., Tudhope, A. W., and Dunne, R. P. (2009). Decline in skeletal growth of the coral *Porites lutea* from the Andaman Sea, South Thailand between 1984 and 2005. *Coral Reefs* 28, 519–528. doi: 10.1007/s00338-008-0457-5

Terada, R., Vo, T. D., Nishihara, G. N., Shioya, K., Shimada, S., and Kawaguchi, S. (2016). The effect of irradiance and temperature on the photosynthesis and growth of a cultivated red alga *Kappaphycus alvarezii* (Solieriaceae) from Vietnam, based on in situ and in vitro measurements. *J. Appl. Phycol.* 28, 457–467. doi: 10.1007/s10811-015-0557-x

Tremblay, P., Gori, A., Maguer, J. F., Hoogenboom, M., and Ferrier-Pagès, C. (2016). Heterotrophy promotes the re-establishment of photosynthate translocation in a symbiotic coral after heat stress. *Sci. Rep.* 6:38112. doi: 10.1038/srep38112

van Oppen, M. J. H., and Oakeshott, J. G. (2020). A breakthrough in understanding the molecular basis of coral heat tolerance. *Proc. Natl. Acad. Sci. U.S.A.* 117, 28546–28548. doi: 10.1073/pnas.2020201117

Veal, C. J., Carmi, M., Fine, M., and Hoegh-Guldberg, O. (2010). Increasing the accuracy of surface area estimation using single wax dipping of coral fragments. *Coral Reefs* 29, 893–897. doi: 10.1007/s00338-010-0647-9

Vinagre, C., Dias, M., Cereja, R., Abreu-Afonso, F., Flores, A. A. V., and Mendonça, V. (2019). Upper thermal limits and warming safety margins of coastal marine species–indicator baseline for future reference. *Ecol. Indic.* 102, 644–649. doi: 10.1016/j.ecolind.2019.03.030

Wasim, M. d., Pandey, A. C., Kumar, A., and Dwivedi, C. S. (2021). Spatio-temporal mapping to investigate coral bleaching in Andaman and Nicobar Islands, India using geoinformatics. *J. Indian Soc. Remote Sens.* 49, 1879–1894. doi: 10.1007/s12524-021-01345-2

Waycott, M., Duarte, C. M., Carruthers, T. J. B., Orth, R. J., Dennison, W. C., Olyarnik, S., et al. (2009). Accelerating loss of seagrasses across the globe threatens coastal ecosystems. *Proc. Natl. Acad. Sci. U.S.A.* 106, 12377–12381. doi: 10.1073/pnas.0905620106

Wernberg, T., Krumhansl, K., Filbee-Dexter, K., and Pedersen, M. F. (2019). "Status and trends for the world's kelp forests," in *World Seas: An Environmental Evaluation*, ed. C. Sheppard (Amsterdam: Elsevier), 57–78. doi: 10.1016/B978-0-12-805052-1.00003-6

Wham, D. C., Ning, G., and LaJeunesse, T. C. (2017). *Symbiodinium glynnii* sp. nov., a species of stress-tolerant symbiotic dinoflagellates from pocilloporid and montiporid corals in the Pacific Ocean. *Phycologia* 56, 396–409. doi: 10.2216/16-86.1

Wichachucherd, B., Liddle, L. B., and Prathep, A. (2010). Population structure, recruitment, and succession of the brown alga, *Padina boryana* Thivy (Dictyotales, Heterokontophyta), at an exposed shore of Sirinart National Park and a sheltered area of Tang Khen Bay, Phuket Province, Thailand. *Aquat. Bot.* 92, 93–98. doi: 10.1016/j.aquabot.2009.10.008

Wuthirak, T., Kongnual, R., and Buapet, P. (2016). Desiccation tolerance and underlying mechanisms for the recovery of the photosynthetic efficiency in the tropical intertidal seagrasses *Halophila ovalis* and *Thalassia hemprichii*. *Bot. Mar.* 59, 387–396. doi: 10.1515/bot-2016-0052

Xu, H., Feng, B., Xie, M., Ren, Y., Xia, J., Zhang, Y., et al. (2020). Physiological characteristics and environment adaptability of reef-building corals at the Wuzhizhou Island of South China Sea. *Front. Physiol.* 11:390. doi: 10.3389/fphys.2020.00390

Xu, S., Yu, K., Tao, S., Wu, C.-C., Wang, Y., Jiang, W., et al. (2018). Evidence for the thermal bleaching of *Porites* corals from m 4.0 ka B.P. in the northern South China Sea. *J. Geophys. Res. Biogeosci.* 123, 79–94. doi: 10.1002/2017JG004091

Yeemin, T., Saenghaisuk, C., Sutthacheep, M., Pengsakun, S., Klinthong, W., and Saengmanee, K. (2009). Conditions of coral communities in the Gulf of Thailand: a decade after the 1998 severe bleaching event. *Galaxea* 11, 207–217. doi: 10.3755/galaxea.11.207

Zhang, T., Qu, Y., Zhang, Q., Tang, J., Cao, R., Dong, Z., et al. (2021). Risks to the stability of coral reefs in the South China Sea: an integrated biomarker approach to assess the physiological responses of *Trochus niloticus* to ocean acidification and warming. *Sci. Total Environ.* 782:146876. doi: 10.1016/j.scitotenv.2021.146876

Zhang, Y., He, P., Li, H., Li, G., Liu, J., Jiao, F., et al. (2019). Ulva prolifera green-tide outbreaks and their environmental impact in the Yellow Sea, China. *Natl. Sci. Rev.* 6, 825–838. doi: 10.1093/nsr/nwz026

Zhang, Y.-P., Shen, C., Li, F., Shen, Y.-C., and Liu, L. (2018). Ultrastructural changes of endosymbiotic Symbiodinium of *Galaxea astreata* under thermal stress and after short time recovery process. *J. Mar. Sci. Res. Dev.* 8:6. doi: 10.4172/2155-9910.1000262

Zhao, M., Zhang, H., Zhong, Y., Jiang, D., Liu, G., Yan, H., et al. (2019). The status of coral reefs and its importance for coastal protection: a case study of northeastern Hainan Island, South China Sea. *Sustainability* 11:4354. doi: 10.3390/su11164354

Conflict of Interest: The authors declare that the research was conducted in the absence of any commercial or financial relationships that could be construed as a potential conflict of interest.

Publisher's Note: All claims expressed in this article are solely those of the authors and do not necessarily represent those of their affiliated organizations, or those of the publisher, the editors and the reviewers. Any product that may be evaluated in this article, or claim that may be made by its manufacturer, is not guaranteed or endorsed by the publisher.

frontiers in Marine Science

MINI REVIEW
published: 29 October 2021
doi: 10.3389/fmars.2021.771382

Resolving Chemical Gradients Around Seagrass Roots—A Review of Available Methods

Vincent V. Scholz[1], Kasper E. Brodersen[2], Michael Kühl[2] and Klaus Koren[3]**

[1] Section for Microbiology, Department of Biology, Center for Electromicrobiology, Aarhus University, Aarhus, Denmark, [2] Marine Biological Section, Department of Biology, University of Copenhagen, Helsingør, Denmark, [3] Section for Microbiology, Department of Biology, Aarhus University Centre for Water Technology (WATEC), Aarhus University, Aarhus, Denmark

Steep geochemical gradients surround roots and rhizomes of seagrass and protect the plants against the harsh conditions in anoxic sediment, while enabling nutrient uptake. Imbalance of these gradients, due to e.g., low plant performance and/or changing sediment biogeochemical conditions, can lead to plant stress and large-scale seagrass meadow die-off. Therefore, measuring and mapping the dynamic gradients around seagrass roots and rhizomes is needed to better understand plant responses to human impact and environmental changes. Historically, electrochemical microsensors enabled the first measurements of important chemical species like O_2, pH or H_2S with high sensitivity and spatial resolution giving important insights to the seagrass rhizosphere microenvironment; however, such measurements only provide information in one dimension at a time. In recent years, the use of reversible optical sensors (in the form of planar optodes or nanoparticles) and accumulative gel sampling methods like Diffusive Gradients in Thin films (DGT) have extended the array of analytes and allowed 2-D mapping of chemical gradients in the seagrass rhizosphere. Here, we review and discuss such microscale methods from a practical angle, discuss their application in seagrass research, and point toward novel experimental approaches to study the (bio)geochemistry around seagrass roots and rhizomes using a combination of available techniques, both in the lab and *in situ*.

Keywords: planar-optode, microsensor, rhizosphere, geochemistry, imaging, multidimensional, DGT, DET

OPEN ACCESS

Edited by:
Lars Wörmer, University of Bremen, Germany

Reviewed by:
Marshall Wayne Bowles, Louisiana Universities Marine Consortium, United States
Ketil Koop-Jakobsen, Alfred Wegener Institute Helmholtz Centre for Polar and Marine Research (AWI), Germany

****Correspondence:***
Vincent V. Scholz
vincent.scholz@bio.au.dk
Klaus Koren
klaus.koren@bio.au.dk

Specialty section:
This article was submitted to Marine Biogeochemistry, a section of the journal Frontiers in Marine Science

Received: *06 September 2021*
Accepted: *08 October 2021*
Published: *29 October 2021*

Citation:
Scholz VV, Brodersen KE, Kühl M and Koren K (2021) Resolving Chemical Gradients Around Seagrass Roots—A Review of Available Methods. Front. Mar. Sci. 8:771382. doi: 10.3389/fmars.2021.771382

INTRODUCTION

Seagrass meadows are important ecosystems that play an important role for marine biodiversity (Bertelli and Unsworth, 2014), coastal protection (Fonseca and Cahalan, 1992) and not the least sediment biogeochemistry and carbon sequestration (Mcleod et al., 2011; Fourqurean et al., 2012). Photo-assimilated carbon moves from the seagrass leaves to the roots, and into the anoxic sediment, where the anoxic conditions prevent rapid microbial mineralization (Duarte et al., 2005). Besides plant debris, organic carbon from plant excretions involving sugars and organic acids can have a major impact on the carbon sequestration capability (Wetzel and Penhale, 1979; Long et al., 2008).

Up to 40% of the dissolved organic carbon under seagrass meadows was recently estimated to be in the form of plant-derived sucrose that accumulates in the seagrass rhizosphere and seems to largely escape from microbial degradation due to the concomitant excretion of phenolic compounds (Sogin et al., 2021). However, the organic carbon can also find its way back to the atmosphere through re-mobilization, e.g., via the continuous emission of the greenhouse gas methane from seagrass meadows (Garcias-Bonet and Duarte, 2017) or via physical disturbance by humans that exposes the reduced sediment to O_2 and thereby stimulates aerobic mineralization processes with faster carbon turnover rates and complete oxidation of organic carbon to CO_2 (Brodersen et al., 2019). Nevertheless, plant-microbe and other microbial interactions in the seagrass rhizosphere are not well understood and it is important to resolve biogeochemical element cycling underneath seagrass meadows and its role for seagrass plant fitness.

Growth of seagrass roots into reduced, anoxic sediment relies strongly on gas-filled plant tissue layers, aerenchyma, which allows O_2 in the seagrass leaves, originating either via photosynthesis or via diffusion from the water column, to reach and ventilate the belowground tissue (Brodersen et al., 2018a). While the mature parts of the seagrass roots develop a gas-impermeable tissue layer—a Casparian band-like structure mainly composed of suberin—that enables efficient internal transport of O_2 and prevents radial O_2 loss (ROL) and influx of phytotoxins such as sulfide (H_2S) into the plant tissue (Barnabas, 1996; Colmer, 2003), O_2 eventually leaks from the growing root tips and the root/shoot junctions and oxidizes the rhizosphere (Jensen et al., 2005; Brodersen et al., 2015b; Koren et al., 2015). For instance, Jensen et al. (2005) reported that O_2 diffused from the roots 2 mm into the sediment. The extent of the radial O_2 loss varies with changing light conditions and root age resulting in hetereogenous and dynamic distributions of oxic zones underneath a seagrass meadow (Frederiksen and Glud, 2006). However, the extent of radial O_2 loss is not only determined by the capacity of the root to leak O_2 but also by the capability of the sediment to consume the released O_2 (i.e., the sediment O_2 demand). For example, if seagrass is transplanted into oligotrophic sediment with less bacterial density, the O_2 released from roots will diffuse further into the sediment before it is consumed by abiotic and biotic oxidation reactions than in highly reduced, sulfidic sediment with a high content of organic material and resulting high bacterial density. Taken together, the presence of organic carbon from plant debris and root exudates together with the spatially restricted oxic zones create hotspots of microbial activity below a seagrass meadow (Blaabjerg et al., 1998; Nielsen et al., 2001; Jensen et al., 2007; Brodersen et al., 2018b), which renders the seagrass rhizosphere into a diurnally changing, mosaic of steep geochemical gradients.

Despite their ability to sustain the harsh geochemical conditions of anoxic sediment, seagrasses are currently challenged by human impact such as coastal development and eutrophication, which lead to increased water turbidity and hypoxia, as well as, increased epiphyte growth on seagrass leaves (Erftemeijer and Robin Lewis, 2006; Orth et al., 2006; Waycott et al., 2009). This results in prolonged, low-light availability for photosynthesis altering the balance of the chemical gradients that form around the roots protecting seagrasses and enabling nutrient uptake (Brodersen et al., 2015a, 2017a). The source of the stress originates from above the meadow through human impact and environmental changes, but the resulting danger often comes from underneath and that is H_2S (Holmer and Bondgaard, 2001). Under healthy conditions, the aeration of the below-ground tissues and oxygenation of the rhizosphere around the root tips, root/shoot junctions and the base of the shoot (i.e., the basal leaf meristem) facilitates the abiotic and microbial oxidation of the toxic H_2S (Brodersen et al., 2018b). However, during periods of low water-column O_2 content, e.g., during nighttime when photosynthesis-driven O_2 production is halted, the supply of O_2 to the below-ground tissues cannot counterbalance the H_2S intrusion. Thus, prolonged O_2 limitations initiate large-scale seagrass meadow die-off (Borum et al., 2005). Therefore, it is important to determine how human impact can change geochemical gradients in the seagrass meadow sediment and rhizosphere.

Vertical concentration gradients in sediments of a broad variety of analytes can be determined by analyzing extracted porewater (e.g., McGlathery et al., 2001). Typically, cylindrical push cores have been used to section the sediment horizons on the cm-scale (Toshihiro et al., 2001; Sogin et al., 2021). However, this technique provides average concentrations from large sample volumes; hence, steep gradients in the mm-range, as well as, small-scale heterogeneities are overlooked (Huang et al., 2019). To fully account for the pronounced structural and chemical heterogeneity of the seagrass rhizosphere it is thus necessary to employ tools for microenvironmental sensing and analysis at high spatio-temporal resolution. In the following, we review experimental tools for exploring the seagrass rhizosphere microenvironment ranging from one-dimensional measurements of chemical concentration gradients with different types of microsensors, to mapping of the two-dimensional distribution of chemical species in the rhizosphere using optode-based chemical imaging and gel-sampling techniques. We exemplify how these techniques have been used to study the seagrass rhizosphere and discuss future needs and possibilities for multidimensional sensing approaches to further resolve how the seagrass rhizosphere microenvironment modulates plant fitness and sediment biogeochemistry.

ONE-DIMENSIONAL PROBING OF THE SEAGRASS RHIZOSPHERE MICROENVIRONMENT

Microsensors

Electrochemical and fiber-optic microsensors enable measurements of concentration profiles in 1-D with high sensitivity and spatial resolution owing to the small tip sizes in the μm-range. The available gas, ion, bio and micro-optode sensors cover a wide range of analytes (Kühl and Revsbech, 2001; Revsbech, 2021), but electrochemical O_2 and H_2S microsensors (Revsbech and Jørgensen, 1986; Revsbech, 1989;

Jeroschewski et al., 1996) are still the most used ones in the context of seagrass ecology (Jensen et al., 2005; Trevathan-Tackett et al., 2017; Schrameyer et al., 2018; Brodersen et al., 2019). Further information on the working principles of microsensors and their application in plant biology can be found in recent reviews by Pedersen et al. (2020) and Revsbech (2021).

Microsensors are usually guided vertically into the sediment using a micromanipulator to measure depth profiles, from which the analyte fluxes between sediment and water and inside the sediment can be calculated or modeled (e.g., Berg et al., 1998). The μm tip diameter and the slender shaft of microsensors enable minimally invasive measurements of the steep chemical gradients in the sediment. For example, Schrameyer et al. (2018) carried out an *in situ* shading experiment and used microsensors to measure H_2S and O_2 in retrieved sediment cores in the laboratory, among others, to calculate the diffusive O_2 uptake. It is more convenient to carry out microsensor probing on retrieved cores in aquaria in the laboratory (see an example setup in **Figure 1A**). For instance, in the laboratory the sensor tip can be positioned on the sediment surface by using a dissecting microscope, which serves as a reference point during profiling. Anyhow, *in situ* microsensor measurements are cumbersome but feasible (e.g., Brodersen et al., 2017a; **Figure 1C**). The analyst should then be experienced enough to handle the sensors and judge the sensor position in the sediment by following the signal response. In this way, microsensor tips can be positioned within the root tissue or in the base of the leaf under field conditions (Borum et al., 2005). The microsensor tips are typically robust enough to penetrate root and rhizome/leaf tissue but break if they hit a solid surface like a bivalve shell or larger, motile infauna. Using microsensors in un-sieved, natural sediment is thus risky, albeit microsensors often break due to incautious handling during (dis)mounting.

One of the main challenges is to relate the position of the sensor tip in the sediment to the below-ground root structures if the roots cannot be visually seen. In order to know the sensor tip proximity to the roots during measurements, Jensen et al. (2005) placed a seagrass root horizontally on the sediment, positioned the microsensor tip at the root surface as reference point, and covered the roots again with sediment. However, this approach is very time-consuming as profiles can only commence when the geochemical gradients have re-established (often after more than 3 h depending on the analyte) and the connection between sensor and root is often lost during the sediment re-covering process. To accommodate this, artificial, transparent sediment can be used, for example, in a split flow chamber which enables approaching the roots with the microsensors from various angles (Brodersen et al., 2014, 2015b; **Figure 1B**). However, the use of non-natural sediment, with e.g., different redox conditions, microbial communities, and O_2 demand, for laboratory incubations should be carefully considered as this can deviate the measured gradients from the ones which would be found in natural sediment. One way to alleviate this experimental limitation is, e.g., to utilize a reducing agent such as H_2S, which can be applied to the artificial sediment to function as an O_2 scavenger (Brodersen et al., 2014). Moreover, it is possible to perform spatial measurements of 2-D transects and 3-D grids of concentration profiles with microsensors using dedicated motorized microprofiling setups (e.g., Lichtenberg et al., 2017; Herschend et al., 2018), but such approach has limited applicability for rhizosphere studies, where the exact position of the plant biomass in the sediment is uncertain. Although this to some extent can be alleviated by employing artificial, transparent sediment it is a very time-consuming process, especially if the whole rhizosphere and/or several analytes are analyzed. Despite the fast response time (time that is needed for a stable read-out) of microsensors, typically in the range of seconds, recording one profile can take more than a few minutes. The time for acquiring one concentration profile will depend on the sensor response time, the amount of datapoints recorded, i.e., the given step size between data points, and the motor velocity used for positioning. The lowest possible step size is roughly the diameter of the sensor tip. During prolonged measuring periods roots can grow into new sediment regions (e.g., root growth of 5 mm day^{-1} for *Z. marina*; cf. Jensen et al., 2005) and thus can lead to difficulties to overlay the results from subsequently recorded profiles. Therefore, it is recommended to aim for chemical hotspots like the root tip region and root/shoot junction when analyzing the seagrass rhizosphere with detailed microsensor measurements.

In summary, microsensors cannot fully resolve the complex spatial heterogeneity of chemical gradients around seagrass roots but allow detailed, local measurements within the plant tissue, as well as local measurements of concentration profiles between the plant and surrounding sediment at very high spatio-temporal resolution. The commercial availability of microsensors for a wide array of analytes are additional benefits. In fact, for several analytes of interest microsensors represent the only option for microscale measurements (e.g., H_2S, N_2O, H_2, CH_4 and most ionic species).

MULTI-DIMENSIONAL MAPPING OF THE SEAGRASS RHIZOSPHERE MICROENVIRONMENT

Optode-Based Techniques for Reversible, Chemical Imaging

In contrast to microsensors, the use of planar optical sensors (planar optodes) in combination with imaging enables the measurement of analytes in 2-D and can therefore visualize dynamic changes in the chemical microenvironment and link them to small-scale heterogeneities around seagrass roots. For seagrass, planar optodes sensitive to O_2 (Jensen et al., 2005; Frederiksen and Glud, 2006; Jovanovic et al., 2015) and pH (Brodersen et al., 2017b) have been used, whereas CO_2-sensitive optodes have only been used for other aquatic and saltmarsh plants (Koop-Jakobsen et al., 2018; Lenzewski et al., 2018). The rectangular planar optode foils need to be brought in close contact with the below-ground plant tissue in the sediment. In order to ensure such close contact, planar optodes can be integrated in custom-made chambers with a flat, transparent wall. For instance, Martin et al. (2018) used narrow (2 cm wide) chambers that were placed in an aquarium and incubated in a tilted position to encourage root growth against the detachable

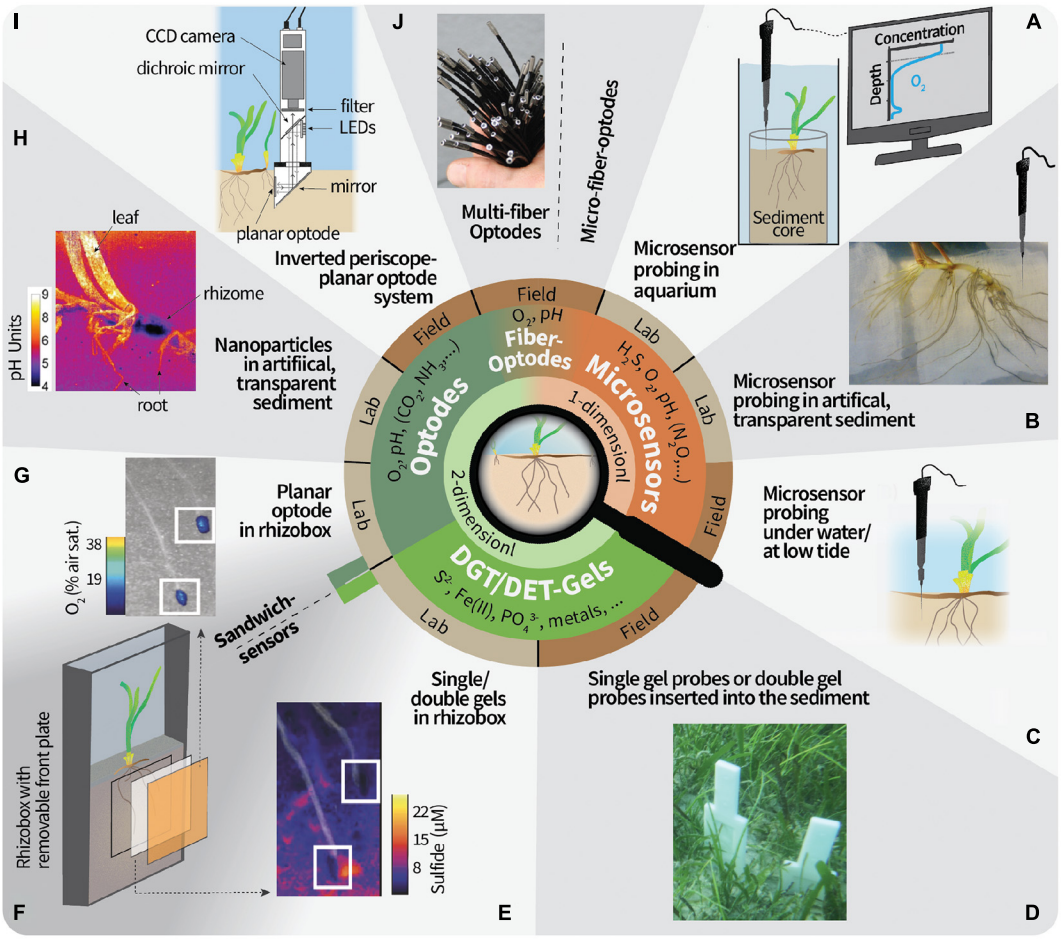

FIGURE 1 | Overview of 1- and 2-D techniques to study the geochemistry in the seagrass rhizosphere microenvironment. **(A)** Microsensor probing on sediment cores retrieved from the field or seagrass transplanted into sediment in the laboratory. The conceptual microsensor profile of O_2 is taken vertically through the upper layers of the sediment core and allows the calculation of, for example, the sediment diffusive O_2 uptake and the O_2 penetration depth. O_2 excursions below the O_2 penetration depth could be from radial O_2 loss from roots/rhizomes or ventilated fauna burrows. **(B)** Artificial, transparent sediment in a custom-made split flow chamber (Brodersen et al., 2015b) allows to approach the roots with microsensors from different directions. **(C)** Microsensor probing under submerged conditions or when the seagrass plants are emerged during low tide have been proven challenging but feasible. **(D)** Gel probes or gel-sandwich (double) probes have been proven to be a robust field technique. **(E)** Example result of a sulfide-sensitive gel from a laboratory deployment. The image is modified from Martin et al. (2018) and white squares mark the root tips. **(F)** Gels can be mounted in between the sediment and planar optodes. **(G)** Example result of an O_2-sensitive planar optode. An imaging system needs to be brought in position for the excitation in the dark and read-out of the planar optode. The image is modified from Martin et al. (2018) and white squares mark the root tips. **(H)** Optode nanoparticles in artificial, transparent sediment overcomes limitations of planar optodes, but cannot be done in natural sediment. Image is taken from Brodersen et al. (2016). **(I)** *In situ* instrument for planar optode measurements. Note that this has not yet been deployed in seagrass meadows. Image was modified from Glud et al. (2001). **(J)** O_2 multi-fiber optode system for the simultaneous recording of 100 datapoints in the field. Note that this has not yet been deployed in seagrass meadows. Image was modified from Fischer and Koop-Jakobsen (2012). Micro-fiber optodes are more robust but with a lower resolution due to the bigger tip size than microsensors made out of glass.

glass wall mounted with a planar optode (**Figure 1F**). A practical video tutorial for the assembly of a similar incubation chamber has been published by Moßhammer et al. (2019b).

Planar optodes consist of an analyte-sensitive indicator dye dispersed in a polymer matrix and coated on solid supports such as plastic foils (Larsen et al., 2011). They are excited externally with a light source, and an image is taken quantifying either the emitted luminescence intensity or the decay time (Schäferling, 2012; Koren and Kühl, 2018), which change as function of the analyte concentration. Data acquisition can rely on simple ratiometric imaging (e.g., Larsen et al., 2011), or more advanced measurements, such as the luminescence decay time (e.g., Koren et al., 2019) and hyperspectral imaging (i.e., the recording of the continuous spectrum of light in each pixel of the image, which allows the simultaneous analysis of emissions from different analyte-sensitive indicators, see Zieger et al., 2021, for more details). The acquired images can be transformed into a calibrated, color-coded image of analyte concentration distributions, which can be aligned with the underlying root/rhizome structure. Hence, hotspots of enhanced biogeochemical reactions can be identified based on where distinct concentration variations are seen (e.g., Jensen et al., 2005;

Frederiksen and Glud, 2006) (example result can be seen in **Figure 1G**). In order to link the measured gradients to the actual below-ground tissue, a photograph should be taken of the sediment cross-section that faced the planar optode after disassembly. If the optode foil is transparent enough, the root structures and positions can also be followed directly during measurement (Frederiksen and Glud, 2006; Martin et al., 2018). Generally, planar optodes have high spatial resolution (μm^2-range), can be made in large sizes (>400 cm^2) to cover the entire area of interest, and have a response time in the range of seconds to a few minutes depending on the type of planar optode and the thickness of the sensor layer and/or the optical isolation layer on top of the sensor layer (Santner et al., 2015). The response time, however, is often not a critical factor in seagrass studies, as the planar optode stays in the same position during the experiment and high measuring frequencies (more than one image per minute) is usually not needed. Besides the preparation of the imaging and incubation setup, calibration is one of the most laborious steps of planar optode measurements and is usually carried out in sediment-free aquaria prior to measurements. The imaging step itself only takes a few seconds. Therefore, once the setup is ready, dynamic changes over day and night cycles can be easily monitored due to the fully reversible response of the planar optodes to e.g., O_2 or pH. For example, Frederiksen and Glud (2006) measured O_2 distributions at regular time intervals around roots of *Zostera marina* over 44 h and showed that O_2 release was reduced by 60% during darkness. We note that the excellent long-term stability of O_2 optodes and their temperature sensitivity, enabling temperature compensated measurements during deployment, allows for measuring over weeks and even months (e.g., Rickelt et al., 2014). Simple, yet powerful planar optode systems can be assembled from commercially available components (e.g., Larsen et al., 2011; Staal et al., 2011) and are also commercially available as complete systems. Instrumentation for underwater *in situ* imaging with planar optodes has also been developed (Glud et al., 2001, 2005; **Figure 1I**), but awaits first applications in seagrass meadows.

When assembling the planar optode-seagrass chambers close contact of the optode with the root biomass is important, because otherwise the true distribution of gradients cannot be resolved. Another challenge during the assembly is to avoid air bubbles trapped on either side of the optode foil. Furthermore, the plant tissue and the microbial community around the roots should be given time to recover after assembly of the incubation chamber. While gradients from purely abiotic sources to sinks establish relatively fast, the biotic components of the rhizosphere can sometimes need several weeks to recover from manipulation/disturbance (Wang et al., 2021). This could e.g., be due to the recovery of root hairs that were broken off during transplantation or the slow re-establishment of a microbial network including filamentous bacteria (Scholz et al., 2021) and fungal associations (Borovec and Vohník, 2018). The plant itself can also experience stress during sampling and separation into single shoots followed by transplantation into the experimental chamber.

One constraint of planar optode-based imaging is that the diffusive fluxes are cut off by the solid support on one side which can distort the true analyte gradients around a 3-D structure positioned against the planar optode (Li et al., 2019). An alternative approach to coating the optode matrix on a solid support is to use optode-nanoparticles (Moßhammer et al., 2019a), e.g., in combination with magnetite to force the optode particles against the seagrass leaves in a magnetic field (Brodersen et al., 2020) or dispersed in a transparent, artificial sediment embedding the below-ground tissues of a seagrass plant (Koren et al., 2015; Brodersen et al., 2016; **Figure 1H**). Such dispersed optical sensor nanoparticle approaches are read out by the same imaging systems as planar optodes, but alleviate the limitations of planar optodes by avoiding the sudden cut off of gradients at the plastic foil on which the optode is coated and the need to ensure close contact between the optode foil and the sample. Sensor nanoparticles have, for example, been used to resolve radial O_2 loss from below-ground seagrass tissues on an entire rhizosphere level and how this is affected by changing light and water-column O_2 conditions (Koren et al., 2015).

In summary, optode-based imaging of the below-ground chemical microenvironment with planar optodes or dispersed sensor nanoparticles is fast and reversible, enabling time-series measurements. The incubation chambers can be custom-made and flexibly adjusted to fit the experimental needs, but challenges are to ensure close contact of root/rhizome tissue with the optode and to avoid air bubbles being trapped behind the foil during assembly. Once the setup is ready, small-scale heterogeneities and spatio-temporal dynamics can be visualized. Optical nanoparticles to study O_2 dynamics around the below-ground structure of seagrass circumvents drawbacks of the planar optode technique, but requires the incubation in artificial, transparent sediment. Currently, such reversible optode-based imaging is limited to a handful of analytes (mainly O_2, pH, CO_2). Novel optodes for important analytes like NH_3 are being developed (Merl and Koren, 2020), but so far have not been used in seagrass research. Also, multi-analyte optodes exist (Moßhammer et al., 2016) and novel imaging approaches are promising to push multi-parameter chemical mapping in the rhizosphere even further (Koren and Zieger, 2021).

Irreversible Chemical Mapping With Gel Probes

Gel-sampling methodologies using either Diffusive Gradients in Thin-films (DGT) or Diffusive Equilibration in Thin-Films (DET) enable irreversible, spatial 2-D mapping of chemical species after sample exposure to the gel for a defined time interval (see Davison et al., 2000; Santner et al., 2015 for a more detailed account of these experimental methods). Both techniques rely on passive diffusion of the sediment solutes from the target area into a gel, where they are either continuously accumulated (DGT) or in equilibrium with the porewater concentrations (DET). Hence, similar experimental incubation chambers as explained for the planar optode systems can be used (**Figure 1F**). But in contrast to the planar optodes, the gels can relatively easily be deployed *in situ* and subsequently analyzed after retrieval (**Figure 1D**). One of the most targeted analytes for single-analyte-binding DGT gel analysis in the seagrass rhizosphere

is H_2S (Brodersen et al., 2017b; Martin et al., 2018; **Figure 1E**), which can e.g., be mapped with a silver iodide gel which continuously binds ΣH_2S (i.e., H_2S, HS^-, and S^{2-}) from the porewater through a precipitation reaction to silver sulfide (Teasdale et al., 1999). The precipitation reaction induces a dark coloration, which can then be analyzed after incubation by computer imaging densitometry (CID), e.g., using a common flatbed scanner. In contrast to DGT gels, the DET gels do not bind the analyte and hence concentrations within the gel represent porewater concentrations at the time of retrieval. One of the most common analytes for DET gels in seagrass beds is Fe(II) (Pagès et al., 2012; Kankanamge et al., 2017, 2020), where the analyte concentrations can be quantified by covering the gel with a ferrozine reagent staining gel after sampling to induce a colorimetric reaction (Jézéquel et al., 2007; Robertson et al., 2008; Bennett et al., 2012). This staining reaction is not necessary if the gels are directly analyzed after drying (in the case for DET gels, the analytes must be immobilized after sampling) using a beam technology such as laser ablation inductively coupled mass spectrometer (LA-ICP-MS), which allows to simultaneously analyze and map the distribution of several ionic species in the seagrass rhizosphere with a spatial resolution of around 100 μm (Brodersen et al., 2017b).

When the DGT and DET gels are deployed in incubation chambers (as described above for planar optodes) the following practical aspects should be considered: (1) close contact of the gel with the root/rhizome tissue, (2) avoiding entrapment of air pockets between gel and sediment, and (3) sufficient pre-incubation for the recovery of plant and microbial community, as well as, chemical gradients after transplanting. A defined onset of gel incubation can be accommodated by placing a retrievable, sterilized plastic foil in between the sample/sediment and the gel (Brodersen et al., 2017b), which can be removed to initiate sample contact to the gel when steady state biogeochemical conditions have been reached. While planar optodes allow continuous and dynamic recording of data over time using the same optode foil, measurements with DGT gels represent accumulated signals during a defined incubation time, i.e., a one-time irreversible readout. Another drawback of DGT gels is the continuous removal of the analyte that can affect processes within the sediment, which is especially critical e.g., at low solute concentrations. Hence, careful planning of the cultivation/measuring period is required. This is not the case for DET gels, because the solutes are not bound and accumulated within gel. But therefore, it is also crucial to process the DET gels immediately after sampling, as otherwise the analyte diffuses within the gel in all directions and blurs the actual gradients and distributions.

These passive gel-sampling techniques can also be used *in situ*, as probes of single gels and even combined DET-DGT and DET-DET gels can be pushed into the seagrass sediment when the meadow is exposed at low-tide (Simpson et al., 2018) or under water (Brodersen et al., 2017b; **Figure 1D**). The combination of multiple gels in one probe with *in situ* deployment enables the simultaneous measurement of multiple analytes over similar temporal and spatial scales, which can visualize the chemical heterogeneity below a seagrass meadow, including the contribution from multiple seagrass shoots and bioturbation. The *in situ* gel deployments and sandwich-gel approaches of combined DGT-DET or DET-DET gels also have several drawbacks, which should be considered when interpreting the imaging results. First, pushing the gel probes into the sediment can drag upper sediment layers deeper down causing artifacts (Santner et al., 2015). Second, no structural photographs can be taken from the measured cross-section of the sediment and hence correlations of solute distributions with below-ground structures such as roots or burrows are speculative. Third, DGT gels provide integrated and averaged concentrations over the entire deployment time, while DET gels represent the porewater concentrations over the last period of the deployment time. Therefore, the combination and deployment of DGT and DET gels at the same time may lead to artifacts depending on the change of gradients during the deployment time (Robertson et al., 2008). An alternative to circumvent this issue for H_2S is a novel DET gel (Kankanamge et al., 2020), which allows to deploy a DET(H_2S)-DET probe rather than a DGT(H_2S)-DET-probe.

One simple but yet elegant approach was reported by Marzocchi et al. (2019), who investigated the PO_4^{3-} and NH_4^+ porewater concentrations around roots of the freshwater plant *Vallisneria spiralis* by assembling a sediment sandwich with 96-well microplates covered with a membrane on each side. The microtiter plates can be considered a variant of DET gels, where each well goes in equilibrium with the porewater concentrations. After deployment, the analyte concentrations were quantified by standard colorimetric reactions. With this approach, the spatial resolution is limited by the diameter of the wells (approximately 7 mm) and the spacing between the wells (approximately 1 mm).

In summary, gels are passive sampling techniques that extend the array of analytes for 2-D mapping. In contrast to reversible optodes, the gel-based approaches allow only the read-out of analyte distributions at a given time period. However, for several key analytes such as sulfide, metals and other ionic species these gel-sampling techniques are presently the only option for 2-D mapping in the seagrass rhizosphere. Advantages of these techniques include the versatility of the gels as they can be deployed in various configurations including as sandwich sensors and for *in situ* measurements.

FUTURE DEVELOPMENTS

A better understanding of the heterogeneous distribution of geochemical hotspots around seagrass roots/rhizome, and their dynamic changes over day/night and seasonal cycles is instrumental for enhancing our knowledge about how the seagrass plant is adapted to life in sediments and how it is affected by environmental stress. As mentioned above, the seagrass rhizosphere is a dynamic chemical environment where several chemical parameters exhibit changes at different time scales and with different interdependences. Hence, the analysis of multiple analytes in the same spatial area and time is needed. This can be achieved through various approaches.

For instance, Brodersen et al. (2017b) used a narrow sandwich chamber (width: 1 cm) design for the deployment of O_2

and/or pH planar optodes on one side of the below-ground tissue structures and single- or multi-binding DGT gels on the other side. With this approach the authors could show that the release of O_2 and organic compounds from the roots and rhizome stimulate nutrient mobilization in the rhizosphere, where (i) protolytic dissolution (protons generated from protective sulfide oxidation stimulated through radial O_2 loss from the roots and rhizome) mobilized phosphate mainly in the light and (ii) reductive dissolution [reduction of insoluble Fe(III)oxyhydroxides to dissolved Fe(II) driven by sulfide generated by sulfate reducing bacteria that are stimulated by organic carbon exudations from the roots] mobilized phosphate and increases Fe(II) availability mainly in the dark. These are important seagrass-driven nutrient mobilization mechanisms that are further supported by the release of organic acids (Long et al., 2008) and microbial Fe(III) reduction linked to organic carbon oxidation. However, optodes can also be directly coated with a sampling gel (**Figure 1F**). By means of such a combined optode-gel-sensor, Martin et al. (2018) monitored the O_2 concentrations and ensured sediments remained anoxic during deployment of the H_2S-sensitive DGT gel. Other sensor combinations are the above-mentioned DGT-DET and DET-DET gel-sandwiches, which can also be applied in the field (Robertson et al., 2008; Pagès et al., 2012). Moreover, dual optode sensors for pH and O_2 measurements (Moßhammer et al., 2016) and the advances in hyperspectral imaging (Zieger et al., 2021) will facilitate further development and applications of multi-analyte optodes in future studies. A comprehensive model example of combining multidimensional techniques has been provided by Williams et al. (2014), who measured the O_2 or pH and metal distributions around rice roots by using combined optode-DGT gel sensors.

Microbial communities drive geochemical changes and conditions in the rhizosphere, but their specific associations with hotspots along the roots/rhizome and in different distances away from seagrass root/rhizome surfaces have only been poorly resolved. One approach for the sampling of microbial communities and correlation with geochemical gradients measured with microsensors has been reported by Brodersen et al. (2018b). The authors made use of artificial, transparent sediment with added porewater microbes in the previously reported, custom made split flow chamber (Brodersen et al., 2014). Moreover, Martin et al. (2018) used O_2-sensitive planar optodes to distinguish microbial communities on O_2-releasing and non-leaking roots with particular focus on cable bacteria, which are filamentous, cm-long bacteria that change their surrounding sediment geochemistry with major impact on the pH and sulfur-cycle (Pfeffer et al., 2012). The colonization pattern of cable bacteria and their geochemical impact in surface sediments and around worm tubes have been visualized using combinations of planar optodes and gels (Aller et al., 2019; Yin et al., 2021a,b). Interestingly, cable bacteria appear to be a common member of the root microbiome of various seagrass species (Scholz et al., 2021) but their potential geochemical impact in the seagrass rhizosphere has not yet been shown. The identification of hotspots by multidimensional imaging could also be used for targeted sampling for metabolomics or chemical analyses.

Last, not least, there is a strong need for better *in situ* mapping of the seagrass rhizosphere microenvironment. Microenvironmental analyses of the seagrass rhizosphere have mostly been done in the laboratory, with the exception of (i) diver-operated *in situ* microsensor measurements, typically positioned in seagrass leaf meristems to follow the O_2 and H_2S status of the plant over diel cycles (e.g., Brodersen et al., 2017a; Olsen et al., 2018), and (ii) the *in situ* deployment of gel samplers (e.g., Pagès et al., 2012; Brodersen et al., 2017b, see **Supplementary Table 1** for an overview of selected key references). However, laboratory measurements cannot fully replicate the dynamic environmental conditions found *in situ* and often involve manipulation of the rhizosphere and surrounding sediment during assembly of the setup and sampling. This can potentially change redox conditions and other aspects of the *in situ* microenvironment including the spatial arrangement of microbes relative to the plant roots. Thus, it should be kept in mind that measurements in laboratory setups with sieved, homogenized sediment and mainly on a single shoot do not represent the natural environment below a seagrass meadow, where bioturbation, multiple shoots, and plant debris cause even more heterogenous distributions of gradients (Edward and Mark, 1998; Simpson et al., 2018). While *in situ* mapping of chemical species over hours/days with planar optodes mounted on dedicated underwater imaging platforms and in mesocosms is well established in soil and sediment biogeochemistry (Glud et al., 2001; Askaer et al., 2010; Santner et al., 2015) such technologies have, surprisingly, not yet been applied in seagrass meadows. For instance, potential issues to be solved are how to avoid scratching and other damage of the planar optode surface when inserting it into the tough matrix of seagrass covered sediments. The insertion would also break the root/rhizome network and disrupt the gradients in a seagrass meadow. But this could be overcome if the instrument would be deployed at the fringe of a seagrass bed or in newly restored seagrass beds where seagrass seedlings were just transplanted. It should be noted that no perfect alignment of roots and rhizome to the measuring devices (planar optodes or gel probes) can be assured under *in situ* conditions, but rather the natural distribution of gradients will be determined. Also more long-term *in situ* measurements, e.g., of seasonal changes in the seagrass rhizosphere or long-term changes due to environmental impacts such as dredging, heat waves or hypoxia events, remain to be realized. A suitable starting point for such measurements could, e.g., be based on systems for distributed sensing with fiber-optic optode arrays (e.g., Fischer and Koop-Jakobsen, 2012; **Figure 1J**) that can be inserted into the sediment at various positions/depths to monitor rhizosphere oxygenation over hours/days (Koop-Jakobsen et al., 2017) or robust spears with defined measuring spots that are able to monitor, e.g., O_2 and temperature profiles in soils and sediment over several months (Rickelt et al., 2014). Adaptation and expansion of such techniques for optode-based, long-term *in situ* measurements of key parameters like O_2, pH and temperature in seagrass rhizospheres is a promising research direction, which

will enhance insight to *in situ* characteristics of the seagrass rhizosphere and could become a valuable tool for environmental monitoring and management (e.g., as an early warning system for environmental stress in seagrass meadows).

AUTHOR CONTRIBUTIONS

VVS, KEB, MK, and KK developed the concept for this review. VVS wrote the manuscript with input from all co-authors. All authors approved the submitted version.

FUNDING

We acknowledge financial support by the Danish National Research Foundation (DNRF136 to VVS), the Grundfos Foundation (KK), the Independent Research Fund Denmark (DFF-8048-00057B to KK), (DFF-8022-00301B and DFF-8021-00308B to MK), and the Villum Foundation (00028156 to KEB).

ACKNOWLEDGMENTS

Lars Peter Nielsen and Nils Risgaard-Petersen are thank for discussions about potential novel directions in seagrass research, as well as Silvia Zieger and Fabian Steininger for discussions about the figure design. We also acknowledge the input from Belinda C. Martin in regard to the potential root hair breakage during seagrass transplantation.

SUPPLEMENTARY MATERIAL

The Supplementary Material for this article can be found online at: https://www.frontiersin.org/articles/10.3389/fmars.2021.771382/full#supplementary-material

REFERENCES

Aller, R. C., Aller, J. Y., Zhu, Q., Heilbrun, C., Klingensmith, I., and Kaushik, A. (2019). Worm tubes as conduits for the electrogenic microbial grid in marine sediments. *Sci. Adv.* 5:eaaw3651. doi: 10.1126/sciadv.aaw3651

Askaer, L., Elberling, B., Glud, R. N., Kühl, M., Lauritsen, F. R., and Joensen, H. P. (2010). Soil heterogeneity effects on O2 distribution and CH4 emissions from wetlands: in situ and mesocosm studies with planar O2 optodes and membrane inlet mass spectrometry. *Soil Biol. Biochem.* 42, 2254–2265. doi: 10.1016/j.soilbio.2010.08.026

Barnabas, A. D. (1996). Casparian band-like structures in the root hypodermis of some aquatic angiosperms. *Aquat. Bot.* 55, 217–225. doi: 10.1016/S0304-3770(96)01072-8

Bennett, W. W., Teasdale, P. R., Welsh, D. T., Panther, J. G., and Jolley, D. F. (2012). Optimization of colorimetric DET technique for the in situ, two-dimensional measurement of iron(II) distributions in sediment porewaters. *Talanta* 88, 490–495. doi: 10.1016/j.talanta.2011.11.020

Berg, P., Risgaard-Petersen, N., and Rysgaard, S. (1998). Interpretation of measured concentration profiles in sediment pore water. *Limnol. Oceanogr.* 43, 1500–1510. doi: 10.4319/lo.1998.43.7.1500

Bertelli, C. M., and Unsworth, R. K. F. (2014). Protecting the hand that feeds us: seagrass (*Zostera marina*) serves as commercial juvenile fish habitat. *Mar. Pollut. Bull.* 83, 425–429. doi: 10.1016/j.marpolbul.2013.08.011

Blaabjerg, V., Mouritsen, K. N., and Finster, K. (1998). Diel cycles of sulphate reduction rates in sediments of a *Zostera marina* bed (Denmark). *Aquat. Microb. Ecol.* 15, 97–102. doi: 10.3354/ame015097

Borovec, O., and Vohník, M. (2018). Ontogenetic transition from specialized root hairs to specific root-fungus symbiosis in the dominant Mediterranean seagrass *Posidonia oceanica*. *Sci. Rep.* 8:10773. doi: 10.1038/s41598-018-28989-4

Borum, J., Pedersen, O., Greve, T., Frankovich, T., Zieman, J., Fourqurean, J. W., et al. (2005). The potential role of plant oxygen and sulphide dynamics in die-off events of the tropical seagrass, *Thalassia testudinum*. *J. Ecol.* 93, 148–158. doi: 10.1111/j.1365-2745.2004.00943.x

Brodersen, K. E., Hammer, K. J., Schrameyer, V., Floytrup, A., Rasheed, M. A., Ralph, P. J., et al. (2017a). Sediment resuspension and deposition on seagrass leaves impedes internal plant aeration and promotes phytotoxic H2S intrusion. *Front. Plant Sci.* 8:657. doi: 10.3389/fpls.2017.00657

Brodersen, K. E., Koren, K., Moßhammer, M., Ralph, P. J., Kühl, M., and Santner, J. (2017b). Seagrass-mediated phosphorus and iron solubilization in tropical sediments. *Environ. Sci. Technol.* 51, 14155–14163. doi: 10.1021/acs.est.7b03878

Brodersen, K. E., Koren, K., Lichtenberg, M., and Kühl, M. (2016). Nanoparticle-based measurements of pH and O2 dynamics in the rhizosphere of *Zostera marina L.*: effects of temperature elevation and light-dark transitions. *Plant Cell Environ.* 39, 1619–1630. doi: 10.1111/pce.12740

Brodersen, K. E., Kühl, M., Nielsen, D. A., Pedersen, O., and Larkum, A. W. D. (2018a). "Rhizome, root/sediment interactions, aerenchyma and internal pressure changes in seagrasses," in *Seagrasses of Australia: Structure, Ecology and Conservation*, eds A. W. D. Larkum, G. A. Kendrick, and P. J. Ralph (Cham: Springer International Publishing), 393–418.

Brodersen, K. E., Siboni, N., Nielsen, D. A., Pernice, M., Ralph, P. J., Seymour, J., et al. (2018b). Seagrass rhizosphere microenvironment alters plant-associated microbial community composition. *Environ. Microbiol.* 20, 2854–2864. doi: 10.1111/1462-2920.14245

Brodersen, K. E., Kühl, M., Trampe, E., and Koren, K. (2020). Imaging O2 dynamics and microenvironments in the seagrass leaf phyllosphere with magnetic optical sensor nanoparticles. *Plant J.* 104, 1504–1519. doi: 10.1111/tpj.15017

Brodersen, K. E., Nielsen, D. A., Ralph, P. J., and Kühl, M. (2014). A split flow chamber with artificial sediment to examine the below-ground microenvironment of aquatic macrophytes. *Mar. Biol.* 161, 2921–2930. doi: 10.1007/s00227-014-2542-3

Brodersen, K., Lichtenberg, M., Paz, L.-C., and Kühl, M. (2015a). Epiphyte-cover on seagrass (*Zostera marina L.*) leaves impedes plant performance and radial O2 loss from the below-ground tissue. *Front. Mar. Sci.* 2:58. doi: 10.3389/fmars.2015.00058

Brodersen, K. E., Nielsen, D. A., Ralph, P. J., and Kühl, M. (2015b). Oxic microshield and local pH enhancement protects *Zostera muelleri* from sediment derived hydrogen sulphide. *New Phytol.* 205, 1264–1276. doi: 10.1111/nph.13124

Brodersen, K. E., Trevathan-Tackett, S. M., Nielsen, D. A., Connolly, R. M., Lovelock, C. E., Atwood, T. B., et al. (2019). Oxygen consumption and sulfate reduction in vegetated coastal habitats: effects of physical disturbance. *Front. Mar. Sci.* 6:14. doi: 10.3389/fmars.2019.00014

Colmer, T. D. (2003). Long-distance transport of gases in plants: a perspective on internal aeration and radial oxygen loss from roots. *Plant Cell Environ.* 26, 17–36. doi: 10.1046/j.1365-3040.2003.00846.x

Davison, W., Fones, G., Harper, M., Teasdale, P., and Zhang, H. (2000). "Dialysis, DET and DGT: in situ diffusional techniques for studying water, sediments and soils," in *In Situ Monitoring of Aquatic Systems: Chemical Analysis and Speciation*, eds J. Buffle and G. Horvai (New York, NY: John Wiley & Sons), 495–569.

Duarte, C. M., Middelburg, J. J., and Caraco, N. (2005). Major role of marine vegetation on the oceanic carbon cycle. *Biogeosciences* 2, 1–8. doi: 10.5194/bg-2-1-2005

Edward, C. T., and Mark, S. F. (1998). Bioturbation as a potential mechanism influencing spatial heterogeneity of North Carolina seagrass beds. *Mar. Ecol. Prog. Ser.* 169, 123–132. doi: 10.3354/meps169123

Erftemeijer, P. L. A., and Robin Lewis, R. R. (2006). Environmental impacts of dredging on seagrasses: a review. *Mar. Pollut. Bull.* 52, 1553–1572. doi: 10.1016/j.marpolbul.2006.09.006

Fischer, J. P., and Koop-Jakobsen, K. (2012). The multi fiber optode (MuFO): a novel system for simultaneous analysis of multiple fiber optic oxygen sensors. *Sens. Actuators B Chem.* 168, 354–359. doi: 10.1016/j.snb.2012.04.034

Fonseca, M. S., and Cahalan, J. A. (1992). A preliminary evaluation of wave attenuation by four species of seagrass. *Estuar. Coast. Shelf Sci.* 35, 565–576. doi: 10.1016/S0272-7714(05)80039-3

Fourqurean, J. W., Duarte, C. M., Kennedy, H., Marbà, N., Holmer, M., Mateo, M. A., et al. (2012). Seagrass ecosystems as a globally significant carbon stock. *Nat. Geosci.* 5, 505–509. doi: 10.1038/ngeo1477

Frederiksen, M. S., and Glud, R. N. (2006). Oxygen dynamics in the rhizosphere of Zostera marina: a two-dimensional planar optode study. *Limnol. Oceanogr.* 51, 1072–1083. doi: 10.4319/lo.2006.51.2.1072

Garcias-Bonet, N., and Duarte, C. M. (2017). Methane production by seagrass ecosystems in the red sea. *Front. Mar. Sci.* 4:340. doi: 10.3389/fmars.2017.00340

Glud, R. N., Tengberg, A., Kühl, M., Hall, P. O. J., and Klimant, I. (2001). An in situ instrument for planar O2 optode measurements at benthic interfaces. *Limnol. Oceanogr.* 46, 2073–2080. doi: 10.4319/lo.2001.46.8.2073

Glud, R. N., Wenzhöfer, F., Tengberg, A., Middelboe, M., Oguri, K., and Kitazato, H. (2005). Distribution of oxygen in surface sediments from central Sagami Bay, Japan: in situ measurements by microelectrodes and planar optodes. *Deep Sea Res. I Oceanogr. Res. Pap.* 52, 1974–1987. doi: 10.1016/j.dsr.2005.05.004

Herschend, J., Koren, K., Røder, H. L., Brejnrod, A., Kühl, M., Burmølle, M., et al. (2018). In vitro community synergy between bacterial soil isolates can be facilitated by pH stabilization of the environment. *Appl. Environ. Microbiol.* 84, e01450–18. doi: 10.1128/AEM.01450-18

Holmer, M., and Bondgaard, E. J. (2001). Photosynthetic and growth response of eelgrass to low oxygen and high sulfide concentrations during hypoxic events. *Aquat. Bot.* 70, 29–38. doi: 10.1016/S0304-3770(00)00142-X

Huang, J., Franklin, H., Teasdale, P. R., Burford, M. A., Kankanamge, N. R., Bennett, W. W., et al. (2019). Comparison of DET, DGT and conventional porewater extractions for determining nutrient profiles and cycling in stream sediments. *Environ. Sci. Process. Impacts* 21, 2128–2140. doi: 10.1039/C9EM00312F

Jensen, S. I., Kühl, M., and Priemé, A. (2007). Different bacterial communities associated with the roots and bulk sediment of the seagrass *Zostera marina*. *FEMS Microbiol. Ecol.* 62, 108–117. doi: 10.1111/j.1574-6941.2007.00373.x

Jensen, S. I., Kühl, M., Glud, R. N., Jørgensen, L. B., and Priemé, A. (2005). Oxic microzones and radial oxygen loss from roots of *Zostera marina*. *Mar. Ecol. Prog. Ser.* 293, 49–58. doi: 10.3354/meps293049

Jeroschewski, P., Steuckart, C., and Kühl, M. (1996). An amperometric microsensor for the determination of H2S in aquatic environments. *Anal. Chem.* 68, 4351–4357. doi: 10.1021/ac960091b

Jézéquel, D., Brayner, R., Metzger, E., Viollier, E., Prévot, F., and Fiévet, F. (2007). Two-dimensional determination of dissolved iron and sulfur species in marine sediment pore-waters by thin-film based imaging. Thau lagoon (France). *Estuar. Coast. Shelf Sci.* 72, 420–431. doi: 10.1016/j.ecss.2006.11.031

Jovanovic, Z., Pedersen, M., Larsen, M., Kristensen, E., and Glud, R. N. (2015). Rhizosphere O2 dynamics in young *Zostera marina* and *Ruppia maritima*. *Mar. Ecol. Prog. Ser.* 518, 95–105. doi: 10.3354/meps11041

Kankanamge, N. R, Bennett, W. W., Teasdale, P. R., Huang, J., and Welsh, D. T. (2017). Comparing in situ colorimetric DET and DGT techniques with ex situ core slicing and centrifugation for measuring ferrous iron and dissolved sulfide in coastal sediment pore waters. *Chemosphere* 188, 119–129. doi: 10.1016/j.chemosphere.2017.08.144

Kankanamge, N. R., Bennett, W. W., Teasdale, P. R., Huang, J., and Welsh, D. T. (2020). A new colorimetric DET technique for determining mm-resolution sulfide porewater distributions and allowing improved interpretation of iron(II) co-distributions. *Chemosphere* 244:125388. doi: 10.1016/j.chemosphere.2019.125388

Koop-Jakobsen, K., Fischer, J., and Wenzhöfer, F. (2017). Survey of sediment oxygenation in rhizospheres of the saltmarsh grass - *Spartina anglica*. *Sci. Total Environ.* 589, 191–199. doi: 10.1016/j.scitotenv.2017.02.147

Koop-Jakobsen, K., Mueller, P., Meier, R. J., Liebsch, G., and Jensen, K. (2018). Plant-sediment interactions in salt marshes–an optode imaging study of O2, pH, and CO2 gradients in the rhizosphere. *Front. Plant Sci.* 9:541. doi: 10.3389/fpls.2018.00541

Koren, K., and Kühl, M. (2018). "Optical O2 sensing in aquatic systems and organisms," in *Quenched-Phosphorescence Detection of Molecular Oxygen: Applications in Life Sciences*, eds D. B. Papkovsky and R. I. Dmitriev (London: The Royal Society of Chemistry), 145–174.

Koren, K., and Zieger, S. E. (2021). Optode based chemical imaging—possibilities, challenges, and new avenues in multidimensional optical sensing. *ACS Sensors* 6, 1671–1680. doi: 10.1021/acssensors.1c00480

Koren, K., Brodersen, K. E., Jakobsen, S. L., and Kühl, M. (2015). Optical sensor nanoparticles in artificial sediments–a new tool to visualize O2 dynamics around the rhizome and roots of seagrasses. *Environ. Sci. Technol.* 49, 2286–2292. doi: 10.1021/es505734b

Koren, K., Moßhammer, M., Scholz, V. V., Borisov, S. M., Holst, G., and Kühl, M. (2019). Luminescence lifetime imaging of chemical sensors—a comparison between time-domain and frequency-domain based camera systems. *Anal. Chem.* 91, 3233–3238. doi: 10.1021/acs.analchem.8b05869

Kühl, M., and Revsbech, N. P. (2001). "Biogeochemical microsensors for boundary layer studies," in *The Benthic Boundary Layer: Transport Processes and Biogeochemistry*, eds B. P. Boudreau and B. B. Jørgensen (Oxford: Oxford University Press), 180–210.

Larsen, M., Borisov, S. M., Grunwald, B., Klimant, I., and Glud, R. N. (2011). A simple and inexpensive high resolution color ratiometric planar optode imaging approach: application to oxygen and pH sensing. *Limnol. Oceanogr.* 9, 348–360. doi: 10.4319/lom.2011.9.348

Lenzewski, N., Mueller, P., Meier, R. J., Liebsch, G., Jensen, K., and Koop-Jakobsen, K. (2018). Dynamics of oxygen and carbon dioxide in rhizospheres of *Lobelia dortmanna* – a planar optode study of belowground gas exchange between plants and sediment. *New Phytol.* 218, 131–141. doi: 10.1111/nph.14973

Li, C., Ding, S., Yang, L., Zhu, Q., Chen, M., Tsang, D. C. W., et al. (2019). Planar optode: a two-dimensional imaging technique for studying spatial-temporal dynamics of solutes in sediment and soil. *Earth Sci. Rev.* 197:102916. doi: 10.1016/j.earscirev.2019.102916

Lichtenberg, M., Nørregaard, R. D., and Kühl, M. (2017). Diffusion or advection? Mass transfer and complex boundary layer landscapes of the brown alga *Fucus vesiculosus*. *J. R Soc. Interface* 14:20161015. doi: 10.1098/rsif.2016.1015

Long, M. H., McGlathery, K. J., Zieman, J. C., and Berg, P. (2008). The role of organic acid exudates in liberating phosphorus from seagrass-vegetated carbonate sediments. *Limnol. Oceanogr.* 53, 2616–2626. doi: 10.4319/lo.2008.53.6.2616

Martin, B. C., Bougoure, J., Ryan, M. H., Bennett, W. W., Colmer, T. D., Joyce, N. K., et al. (2018). Oxygen loss from seagrass roots coincides with colonisation of sulphide-oxidising cable bacteria and reduces sulphide stress. *ISME J.* 13, 707–719. doi: 10.1038/s41396-018-0308-5

Marzocchi, U., Benelli, S., Larsen, M., Bartoli, M., and Glud, R. N. (2019). Spatial heterogeneity and short-term oxygen dynamics in the rhizosphere of *Vallisneria spiralis*: implications for nutrient cycling. *Freshw. Biol.* 64, 532–543. doi: 10.1111/fwb.13240

McGlathery, K. J., Berg, P., and Marino, R. (2001). Using porewater profiles to assess nutrient availability in seagrass-vegetated carbonate sediments. *Biogeochemistry* 56, 239–263. doi: 10.1023/A:1013129811827

Mcleod, E., Chmura, G. L., Bouillon, S., Salm, R., Björk, M., Duarte, C. M., et al. (2011). A blueprint for blue carbon: toward an improved understanding of the role of vegetated coastal habitats in sequestering CO2. *Front. Ecol. Environ.* 9:552–560. doi: 10.1890/110004

Merl, T., and Koren, K. (2020). Visualizing NH3 emission and the local O2 and pH microenvironment of soil upon manure application using optical sensors. *Environ. Int.* 144:106080. doi: 10.1016/j.envint.2020.106080

Moßhammer, M., Scholz, V. V., Holst, G., Kühl, M., and Koren, K. (2019b). Luminescence lifetime imaging of O2 with a frequency-domain-based camera system. *J. Vis. Exp.* 154:e60191. doi: 10.3791/60191

Moßhammer, M., Brodersen, K. E., Kühl, M., and Koren, K. (2019a). Nanoparticle- and microparticle-based luminescence imaging of chemical species and temperature in aquatic systems: a review. *Microchim. Acta* 186:126. doi: 10.1007/s00604-018-3202-y

Moßhammer, M., Strobl, M., Kühl, M., Klimant, I., Borisov, S. M., and Koren, K. (2016). Design and application of an optical sensor for simultaneous imaging of pH and dissolved O2 with low cross-talk. *ACS Sensors* 1, 681–687. doi: 10.1021/acssensors.6b00071

Nielsen, L. B., Finster, K., Welsh, D. T., Donelly, A., Herbert, R. A., De Wit, R., et al. (2001). Sulphate reduction and nitrogen fixation rates associated with roots, rhizomes and sediments from *Zostera noltii* and *Spartina maritima* meadows. *Environ. Microbiol.* 3, 63–71. doi: 10.1046/j.1462-2920.2001.00160.x

Olsen, Y. S., Fraser, M. W., Martin, B. C., Pomeroy, A., Lowe, R., Pedersen, O., et al. (2018). In situ oxygen dynamics in rhizomes of the seagrass *Posidonia sinuosa*: impact of light, water column oxygen, current speed and wave velocity. *Mar. Ecol. Prog. Ser.* 590, 67–77. doi: 10.3354/meps12477

Orth, R. J., Carruthers, T. J. B., Dennison, W. C., Duarte, C. M., Fourqurean, J. W., Heck, K. L., et al. (2006). A global crisis for seagrass ecosystems. *BioScience* 56, 987–996.

Pagès, A., Welsh, D. T., Robertson, D., Panther, J. G., Schäfer, J., Tomlinson, R. B., et al. (2012). Diurnal shifts in co-distributions of sulfide and iron(II) and profiles of phosphate and ammonium in the rhizosphere of *Zostera capricorni*. *Estuar. Coast. Shelf Sci.* 115, 282–290. doi: 10.1016/j.ecss.2012.09.011

Pedersen, O., Revsbech, N. P., and Shabala, S. (2020). Microsensors in plant biology – in vivo visualization of inorganic analytes with high spatial and/or temporal resolution. *J. Exp. Bot.* 71, 3941–3954. doi: 10.1093/jxb/eraa175

Pfeffer, C., Larsen, S., Song, J., Dong, M., Besenbacher, F., Meyer, R. L., et al. (2012). Filamentous bacteria transport electrons over centimetre distances. *Nature* 491:218. doi: 10.1038/nature11586

Revsbech, N. P. (1989). An oxygen microsensor with a guard cathode. *Limnol. Oceanogr.* 34, 474–478. doi: 10.4319/lo.1989.34.2.0474

Revsbech, N. P. (2021). Simple sensors that work in diverse natural environments: the micro-Clark sensor and biosensor family. *Sens. Actuators B Chem.* 329:129168. doi: 10.1016/j.snb.2020.129168

Revsbech, N. P., and Jørgensen, B. B. (1986). "Microelectrodes: their use in microbial ecology," in *Advances in Microbial Ecology*, ed. K. C. Marshall (Boston, MA: Springer), 293–352.

Rickelt, L. F., Askaer, L., Walpersdorf, E., Elberling, B., Glud, R. N., and Kühl, M. (2014). An optode sensor array for long-term in situ oxygen measurements in soil and sediment. *J. Environ. Qual.* 43:1821. doi: 10.2134/jeq2012.0334er

Robertson, D., Teasdale, P. R., and Welsh, D. T. (2008). A novel gel-based technique for the high resolution, two-dimensional determination of iron (II) and sulfide in sediment. *Limnol. Oceanogr. Methods* 6, 502–512. doi: 10.4319/lom.2008.6.502

Santner, J., Larsen, M., Kreuzeder, A., and Glud, R. N. (2015). Two decades of chemical imaging of solutes in sediments and soils – a review. *Anal. Chim. Acta* 878, 9–42. doi: 10.1016/j.aca.2015.02.006

Schäferling, M. (2012). The art of fluorescence imaging with chemical sensors. *Angew. Chem. Int. Edn.* 51, 3532–3554. doi: 10.1002/anie.201105459

Scholz, V. V., Martin, B. C., Meyer, R., Schramm, A., Fraser, M. W., Nielsen, L. P., et al. (2021). Cable bacteria at oxygen-releasing roots of aquatic plants: a widespread and diverse plant–microbe association. *New Phytol.* (in press). doi: 10.1111/nph.17415

Schrameyer, V., York, P. H., Chartrand, K., Ralph, P. J., Kühl, M., Brodersen, K. E., et al. (2018). Contrasting impacts of light reduction on sediment biogeochemistry in deep- and shallow-water tropical seagrass assemblages (Green Island, Great Barrier Reef). *Mar. Environ. Res.* 136, 38–47. doi: 10.1016/j.marenvres.2018.02.008

Simpson, A. G., Tripp, L., Shull, D. H., and Yang, S. (2018). Effects of *Zostera marina* rhizosphere and leaf detritus on the concentration and distribution of pore-water sulfide in marine sediments. *Estuar. Coast. Shelf Sci.* 209, 160–168. doi: 10.1016/j.ecss.2018.05.024

Sogin, E. M., Michellod, D., Gruber-Vodicka, H., Bourceau, P., Geier, B., Meier, D. V., et al. (2021). Sugars dominate the seagrass rhizosphere. *bioRxiv* [Preprint]. doi: 10.1101/797522

Staal, M., Prest, E. I., Vrouwenvelder, J. S., Rickelt, L. F., and Kühl, M. (2011). A simple optode based method for imaging O2 distribution and dynamics in tap water biofilms. *Water Res.* 45, 5027–5037. doi: 10.1016/j.watres.2011.07.007

Teasdale, P. R., Hayward, S., and Davison, W. (1999). In situ, high-resolution measurement of dissolved sulfide using diffusive gradients in thin films with computer-imaging densitometry. *Anal. Chem.* 71, 2186–2191. doi: 10.1021/ac981329u

Toshihiro, M., Masahiro, S., Yu, U., and Isao, K. (2001). Microbiological nitrogen transformation in carbonate sediments of a coral-reef lagoon and associated seagrass beds. *Mar. Ecol. Prog. Ser.* 217, 273–286. doi: 10.3354/meps217273

Trevathan-Tackett, S. M., Seymour, J. R., Nielsen, D. A., Macreadie, P. I., Jeffries, T. C., Sanderman, J., et al. (2017). Sediment anoxia limits microbial-driven seagrass carbon remineralization under warming conditions. *FEMS Microbiol. Ecol.* 93:fix033. doi: 10.1093/femsec/fix033

Wang, L., English, M. K., Tomas, F., Mueller, R. S., and Cann, I. (2021). Recovery and community succession of the *Zostera marina* rhizobiome after transplantation. *Appl. Environ. Microbiol.* 87, e02326–20. doi: 10.1128/AEM.02326-20

Waycott, M., Duarte, C. M., Carruthers, T. J. B., Orth, R. J., Dennison, W. C., Olyarnik, S., et al. (2009). Accelerating loss of seagrasses across the globe threatens coastal ecosystems. *Proc. Natl. Acad. Sci. U.S.A.* 106, 12377–12381. doi: 10.1073/pnas.0905620106

Wetzel, R. G., and Penhale, P. A. (1979). Transport of carbon and excretion of dissolved organic carbon by leaves and roots/rhizomes in seagrasses and their epiphytes. *Aquat. Bot.* 6, 149–158. doi: 10.1016/0304-3770(79)90058-5

Williams, P. N., Santner, J., Larsen, M., Lehto, N. J., Oburger, E., Wenzel, W., et al. (2014). Localized flux maxima of arsenic, lead, and iron around root apices in flooded lowland rice. *Environ. Sci. Technol.* 48, 8498–8506. doi: 10.1021/es501127k

Yin, H., Aller, R. C., Zhu, Q., and Aller, J. Y. (2021b). The dynamics of cable bacteria colonization in surface sediments: a 2D view. *Sci. Rep.* 11:7167. doi: 10.1038/s41598-021-86365-1

Yin, H., Aller, R. C., Zhu, Q., and Aller, J. Y. (2021a). Biogenic structures and cable bacteria interactions: redox domain residence times and the generation of complex pH distributions. *Mar. Ecol. Prog. Ser.* 669, 51–63. doi: 10.3354/meps13722

Zieger, S. E., Mosshammer, M., Kühl, M., and Koren, K. (2021). Hyperspectral luminescence imaging in combination with signal deconvolution enables reliable multi-indicator-based chemical sensing. *ACS Sensors* 6, 183–191. doi: 10.1021/acssensors.0c02084

Conflict of Interest: The authors declare that the research was conducted in the absence of any commercial or financial relationships that could be construed as a potential conflict of interest.

Publisher's Note: All claims expressed in this article are solely those of the authors and do not necessarily represent those of their affiliated organizations, or those of the publisher, the editors and the reviewers. Any product that may be evaluated in this article, or claim that may be made by its manufacturer, is not guaranteed or endorsed by the publisher.

frontiers in Marine Science

BRIEF RESEARCH REPORT
published: 10 November 2021
doi: 10.3389/fmars.2021.768668

Effects of Seagrass Wasting Disease on Eelgrass Growth and Belowground Sugar in Natural Meadows

Olivia J. Graham[1†], Lillian R. Aoki[1†], Tiffany Stephens[2], Joshua Stokes[3], Sukanya Dayal[4], Brendan Rappazzo[5], Carla P. Gomes[5] and C. Drew Harvell[1]*

[1] Department of Ecology and Evolutionary Biology, College of Agriculture and Life Sciences, Cornell University, Ithaca, NY, United States, [2] Seagrove Kelp Co., Ketchikan, AK, United States, [3] Department of Biology, Southeast Missouri State University, Cape Girardeau, MO, United States, [4] Department of Natural Resources, College of Agriculture and Life Sciences, Cornell University, Ithaca, NY, United States, [5] Department of Computer Science, College of Arts and Sciences, Cornell University, Ithaca, NY, United States

OPEN ACCESS

Edited by:
Stacey Marie Trevathan-Tackett, Deakin University, Australia

Reviewed by:
Janina Brakel, Scottish Association for Marine Science, United Kingdom
Luísa Magalhães, University of Aveiro, Portugal
Forest Schenck, Massachusetts Division of Marine Fisheries, United States

****Correspondence:***
Olivia J. Graham
ojg5@cornell.edu

†These authors have contributed equally to this work and share first authorship

Specialty section:
This article was submitted to Marine Ecosystem Ecology, a section of the journal Frontiers in Marine Science

Received: *01 September 2021*
Accepted: *21 October 2021*
Published: *10 November 2021*

Citation:
Graham OJ, Aoki LR, Stephens T, Stokes J, Dayal S, Rappazzo B, Gomes CP and Harvell CD (2021) Effects of Seagrass Wasting Disease on Eelgrass Growth and Belowground Sugar in Natural Meadows. Front. Mar. Sci. 8:768668. doi: 10.3389/fmars.2021.768668

Seagrass meadows provide valuable ecosystem benefits but are at risk from disease. Eelgrass (*Zostera marina*) is a temperate species threatened by seagrass wasting disease (SWD), caused by the protist *Labyrinthula zosterae*. The pathogen is sensitive to warming ocean temperatures, prompting a need for greater understanding of the impacts on host health under climate change. Previous work demonstrates pathogen cultures grow faster under warmer laboratory conditions and documents positive correlations between warmer ocean temperatures and disease levels in nature. However, the consequences of disease outbreaks on eelgrass growth remain poorly understood. Here, we examined the effect of disease on eelgrass productivity in the field. We coupled *in situ* shoot marking with high-resolution imagery of eelgrass blades and used an artificial intelligence application to determine disease prevalence and severity from digital images. Comparisons of eelgrass growth and disease metrics showed that SWD impaired eelgrass growth and accumulation of non-structural carbon in the field. Blades with more severe disease had reduced growth rates, indicating that disease severity can limit plant growth. Disease severity and rhizome sugar content were also inversely related, suggesting that disease reduced belowground carbon accumulation. Finally, repeated measurements of diseased blades indicated that lesions can grow faster than healthy tissue *in situ*. This is the first study to demonstrate the negative impact of wasting disease on eelgrass health in a natural meadow. These results emphasize the importance of considering disease alongside other stressors to better predict the health and functioning of seagrass meadows in the Anthropocene.

Keywords: *Zostera marina*, *Labyrinthula zosterae*, specific productivity, non-structural carbon, climate change

INTRODUCTION

Rapid environmental changes significantly impact and reshape our oceans. Elevated temperatures can alter marine host-pathogen dynamics by increasing host stress and pathogen virulence, expanding pathogen ranges, and altering host ranges, thus triggering increased occurrence and severity of disease outbreaks (Harvell et al., 2002; Burge et al., 2014; Cohen et al., 2018; Burge and Hershberger, 2020). Climate-driven disease outbreaks can be especially devastating

when they target foundation species—like seagrass and corals—that structure nearshore communities and play vital roles in ecosystem function (Harvell and Lamb, 2020). This paper examines the impacts of seagrass wasting disease (SWD) on eelgrass (*Zostera marina*) health and productivity.

Seagrass wasting disease historically shaped eelgrass meadows and continues to persist today. In the 1930s, SWD outbreaks decimated up to 90% of eelgrass meadows throughout the North Atlantic (Renn, 1936; Short et al., 1987; Muehlstein, 1989), reducing waterfowl, shrimp, scallop, and fish populations (Renn, 1936; Stauffer, 1937; Moffitt and Cottam, 1941; Milne and Milne, 1951) and compromising eelgrass ecosystem services (Orth et al., 2006). These and subsequent die-offs were traced to *Labyrinthula zosterae* (Muehlstein et al., 1988), which is now recognized as a virulent pathogen in eelgrass (Groner et al., 2014, 2016; Martin et al., 2016) and other seagrasses worldwide (reviewed in Sullivan et al., 2018). Given that eelgrass creates nursery and feeding grounds (Orth et al., 1984), filters and oxygenates seawater (Costanza et al., 1997; Hasegawa et al., 2008), stabilizes sediments (Fonseca et al., 1983), efficiently stores carbon (Duarte et al., 2005; Röhr et al., 2018), and plays important roles in nutrient cycling in nearshore communities (reviewed in Moore and Short, 2006), SWD can compromise the health of eelgrass individuals, populations, and entire coastal communities.

Understanding the impact of SWD on eelgrass health and productivity under field conditions is particularly pertinent, given the synergistic relationship between warming temperatures *L. zosterae* (Rasmussen, 1977; Muehlstein, 1992; Bull et al., 2012; Bockelmann et al., 2013; Dawkins et al., 2018; Groner et al., in press; Aoki et al., in review). Laboratory studies indicate the pathogen grows faster *in vitro* under elevated temperatures (Dawkins et al., 2018), and warmer temperatures coincided with historic (Rasmussen, 1977) and more recent disease outbreaks (Bull et al., 2012; Bockelmann et al., 2013). More recently, field surveys of natural eelgrass meadows in the San Juan Islands, Washington, United States indicate that elevated levels of SWD and declines in meadow density were significantly correlated with warmer winter (Groner et al., in press) and summer temperatures (Aoki et al., in review).

Despite the growing body of literature on *L. zosterae* biology and ecology and continued monitoring of SWD in natural eelgrass meadows (Bockelmann et al., 2012; Groner et al., 2014, 2016, in press; Jakobsson-Thor et al., 2018; Aoki et al., in review), little is known about the impacts of SWD on eelgrass under natural conditions. Laboratory studies have shown that *L. zosterae* attacks and consumes plant chloroplasts (Muehlstein, 1992), reduces photosynthetic capabilities of tissue (Ralph and Short, 2002), and creates large areas of necrotic tissue (Pokorny, 1967; Short et al., 1986). SWD therefore likely compromise eelgrass growth rates and ability to accumulate non-structural carbon in rhizomes, which contain high concentrations of sugar. Normally, this sugar accumulates during the summer growing season and fuels regrowth in spring (Burke et al., 1996). However, since SWD prevalence peaks during warm summer months (Bockelmann et al., 2013), disease could reduce these valuable sugar reserves and impair eelgrass growth the subsequent year. Here, we coupled ecological surveys and image analysis using artificial intelligence to determine the effect of SWD on eelgrass growth, health, and rhizome sugar in the field.

Eelgrass meadows are considered bioindicators of health within the Salish Sea, an inland sea spanning the United States-Canada border in the northeastern Pacific Ocean (Dennison et al., 1993; McManus et al., 2020), and have experienced high levels of SWD in recent years (Groner et al., 2014, 2016, in press; Aoki et al., in review), making this region an important location for understanding the ecological impacts of SWD. The aim of this study was to examine the effect of SWD on aboveground eelgrass growth and productivity and belowground sugar. We measured blade-level disease status (healthy or diseased), site-level disease prevalence (proportion of shoots with SWD), severity (proportion of tissue damaged by wasting disease lesions), and specific productivity (percentage of new blade area produced per day). Given the significant historical role of *L. zosterae* in the extirpation of many eelgrass meadows globally, we expected SWD to compromise eelgrass growth. Specifically, we expected plants with elevated levels of disease to have reduced blade growth rates and rhizome sugar concentrations compared to eelgrass with lower disease levels.

MATERIALS AND METHODS

Field Study 1: Eelgrass Growth

To determine temporal differences and interactions between eelgrass growth, productivity, and SWD, we conducted field trials in June and July 2019 at Fourth of July Beach, San Juan Island, WA (48°28′01.4″ N, 123°00′00.4″ W). We selected this site because its intertidal eelgrass has had consistently high levels of SWD since monitoring began in 2017 (Aoki et al., in review) and remains exposed for several hours during extreme low tides, providing ample time for fieldwork. Each month, we deployed three, 30-m transects spaced approximately 5 m apart in the shallow, intertidal eelgrass meadow at low tide, using a compass to maintain consistent headings and depth gradients for each. We targeted eelgrass in the interior of the meadow to avoid any potential edge effects, since eelgrass growth can vary with nutrients, hydrodynamics, and sediment dynamics within a meadow (Bell et al., 2007). Using neon flagging tape, we tagged individual eelgrass shoots at 1-m intervals along each transect (n = 90 shoots/month, **Supplementary Figure 1**) to minimize heavily impacting any one area (ex: tagging many shoots in a quadrat), since all shoots were ultimately destructively sampled. We marked each tagged shoot for shoot-specific growth rate measurements using the needle punch method (Short and Duarte, 2001), a standard approach for measuring direct, short-term growth rates in seagrasses. At 5-m intervals along each transect, we recorded eelgrass shoot densities. We also scanned a subset of tagged shoots from each transect for baseline disease measurements (n = 4 in June, n = 25 in July) and to track lesion development following 6 days of growth in the field. To do so, we removed epiphytes from the third-rank blade of the shoot and carefully scanned it at high resolution (600 dpi) using a photocopy scanner (Canon CanoScan LiDE 220) whilst the shoot was still rooted in the sediment. We also deployed

2 HOBO Pendant loggers in the eelgrass meadow to capture *in situ* temperatures.

After 6 days, we collected all tagged shoots ($n = 90$ in each month). In lab, we removed epiphytes from all shoots and separated the blades from each shoot by age; each shoot contained 3–7 blades. The needle-punch method enabled us to easily separate old growth—the blade area above the needle scar—from the new growth—the blade area below the scar (**Supplementary Figure 1**). We scanned all blades ($n = 434$ in June, $n = 398$ in July) to measure disease and blade areas (**Supplementary Figure 1**). We also measured canopy height, number of blades, and sheath length for each shoot. We calculated blade growth rates (specific productivity) as the percentage of daily new blade area (mm^2d^{-1}).

Field Study 2: Non-structural Carbon Analyses

We collected belowground rhizomes to determine the effect of SWD on sugar reserves in July 2019. We targeted three sites in the San Juan Islands—Fourth of July Beach, Indian Cove (48°33′47.6″ N, 122°56′11.2″ W), False Bay (48°28′57.9″ N, 123°04′25.0″ W)—known for having variable levels of SWD (Groner et al., 2016, in press; Aoki et al., in review). At each site, we deployed three, 30-m transects at the same tidal height in the intertidal, where we measured shoot densities and collected five shoots with intact rhizomes at 0, 15, and 30 m ($n = 45$ shoots/site, $n = 135$ total). We targeted rhizomes at least 15 cm long to ensure sufficient sample biomass for subsequent non-structural carbon analyses. We scanned the third-rank (third youngest, Short and Duarte, 2001) blade of each shoot for disease analyses. To analyze belowground sugar content (non-structural carbon), we dried rhizomes at 60°C, homogenized with a mortar and pestle, and extracted sugars using the hot ethanol extraction method with 2% phenol and concentrated sulfuric acid. We determined total sugar concentrations based on the absorbance at 490 nm using a glucose-fructose-galactose standard curve according to published protocols (Chow and Landhausser, 2004).

Disease Analyses

A state-of-the-art computer learning algorithm, the Eelgrass Lesion Image Segmentation Application (EeLISA), identified and measured the total area of wasting disease lesions and the total area of healthy tissue on all scanned eelgrass images. We used these to determine blade-level disease status (healthy or diseased), and to calculate SWD prevalence (proportion of shoots with SWD lesions), and blade- and site-level severity (proportion of blade area covered in SWD lesions). Details on EeLISA development and training are provided elsewhere (Rappazzo et al., 2021; Aoki et al., in review). EeLISA was trained on over 789 expert-labeled scanned eelgrass images that distinguished SWD lesions from other forms of damage (Rappazzo et al., 2021). Other forms of damage, including desiccation stress and herbivore grazing scars, are distinctive and readily distinguished from SWD lesions, which have been well characterized (Short et al., 1986, 1987; Muehlstein et al., 1988; Burdick et al., 1993). Using ImageJ, we measured the areas of new and old growth for each blade by hand (**Supplementary Figure 1**).

We compared lesion growth rates and blade growth rates on individual blades using the 29 blades scanned for disease in the field at the start of the marking period and in the lab at the end of the marking period. Using the output from EeLISA for initial and final lesion area, we determined lesion growth rates (mm^2d^{-1}) and compared them to the blade growth rates (mm^2d^{-1}) calculated from the old and new blade areas at the end of the marking period.

We validated pathogen presence using qPCR to detect *L. zosterae* DNA in samples of diseased eelgrass tissue. In July 2019, we collected lesion tissue samples from the three field sites and processed the samples using established extraction and qPCR methods (Bockelmann et al., 2013; Groner et al., 2018).

Statistical Analyses

We performed all statistical analyses in R (v. 1.4.1106). To compare the growth rates between all blades from the eelgrass growth study, we ran a generalized linear mixed model (GLMM) with a gamma distribution and log link using the "glmmTMB" package (Brooks et al., 2017), with specific productivity as the response variable. We included blades of all ages (youngest to oldest) in this model to capture the variation in growth rates with respect to disease. Since we measured multiple blades from the same individual shoot, we included shoot identifier as a random effect; fixed effects were blade rank (i.e., age), disease status (healthy or diseased), blade area, total blades per shoot, shoot density (measured at the transect level), and month. We also included an interaction between disease status and blade rank; we compared the full model to simpler models (excluding the interaction and individual terms) using AIC and removed model terms based on $\Delta AIC > 2$. The best-performing model by AIC did not include the interaction term but did include all individual fixed effects. We used a gamma distribution, since there was high variation in growth rates and included a dispersion term, as young blades had a greater spread in growth rates. Blades with growth rates of zero were excluded from these analyses, leaving 530 blades in the model.

To determine the impacts of severity on blade growth, we standardized our measurements by targeting the third-rank (third youngest) blades from each shoot ($n = 176$). These blades provided useful disease estimates because third-rank blades contained both healthy and diseased tissue and grew at a measurable rate, in contrast to the oldest blades which were often deteriorating and the youngest blades which rarely had any visually apparent lesions. Third-rank blades are also recognized as the best indicators of recent environmental conditions (Sand-Jensen, 1975), including disease (Aoki et al., in review). We used a quantile regression model using the package "quantreg" (Koenker, 2021) to assess the relationship between third-rank blade growth rate and severity. For the third-rank blades ($n = 29$) for which we had initial and final disease and blade area measurements, we used a paired *t*-test to compare the lesion and blade growth rates.

To assess disease impacts on belowground non-structural carbon, we ran a linear model with rhizome sugar content as the

response variable and disease severity, blade area, shoot density, site, and an interaction between site and severity as fixed effects; site was treated as a fixed effect due to the low number of sites sampled ($n = 3$). Data met assumptions for normality and homoscedasticity.

RESULTS

Site Characteristics

Temperature loggers deployed at Fourth of July Beach in the intertidal meadow documented daily temperature ranges of 11–20°C during the June marking period and 11–23°C during the July marking period. Daily mean (12.5°C) and median (11.8°C) temperatures were similar during the two marking periods. Maximum daily temperatures occurred when the meadow was exposed during midday low tides. Across the three meadows, shoot densities were lowest at Fourth of July Beach (60 ± 28 shoots m^{-2}, mean ± SD) and were similar at False Bay (106 ± 28 shoots m^{-2}) and Indian Cove (103 ± 28 shoots m^{-2}). Molecular analysis confirmed the presence of *L. zosterae* DNA in diseased eelgrass tissue from all three sites, supporting the presence of *L. zosterae* as an infectious pathogen (**Supplementary Table 1**).

Disease Prevalence and Severity

Wasting disease was prevalent at Fourth of July Beach, in both June and July 2019. In both months, disease prevalence (number of infected shoots/total number of shoots) was approximately 95%. Shoot-level severity (total lesion area of all blades on a shoot/total blade area for the shoot) was also similar between the two months, ranging from 0–36% in June and 0–39% in July and averaging 9% in June and 10% in July. Overall, these disease metrics indicated a substantial presence of the pathogen and potential for meadow-wide impacts from disease.

Disease and Blade Growth Rates

Blade-level disease status and blade rank (age), standardized blade area, and the total number of blades per shoot were significant predictors of blade growth rates (**Figure 1** and **Supplementary Table 2**). Diseased and older blades grew significantly slower than healthy and younger blades (glmm, $p < 0.001$). A diseased, first-rank (youngest) blade grew at approximately 82% of the rate of a healthy, first-rank blade (**Supplementary Figure 2**). Blade growth rates steadily decreased in both diseased and healthy blades with increasing blade age; second-rank blades grew at 17% the rate of first-rank blades. Total number of leaves per shoot and blade area were also significant in the best performing model; smaller blades and shoots with more leaves had faster relative growth (**Supplementary Figure 2**). Shoot density and month were not significant predictors of growth rates.

Disease severity ranged from 0–70% for third-rank blades across June and July. Blades with more severe SWD (larger proportion of blade tissue damaged) had reduced growth rates compared to blades with less severe SWD, as predicted. Quantile regression showed that this effect was larger for blades with higher disease levels (**Figure 2**). In higher quantiles with elevated severity, the slopes of the regression lines were steeper than lower quantiles, indicating larger effects. This was also reflected by severity coefficients, which sharply increased in magnitude at higher quantiles (**Supplementary Figure 3**).

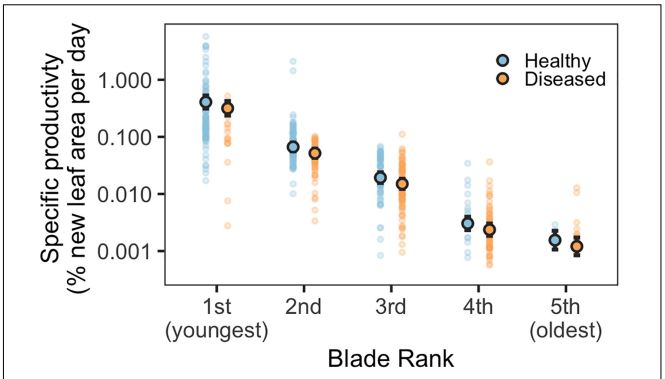

FIGURE 1 | Predicted specific productivity for diseased and healthy eelgrass blades of different ages, modeled as a function of blade rank (age) and disease status (note the log scale). Blade rank refers to blade age and position on each shoot (1st rank = youngest, 5th rank = 5th youngest). Outlined circles indicate mean predicted values, solid circles indicate underlying data. Error bars indicate 95% confidence intervals of the prediction.

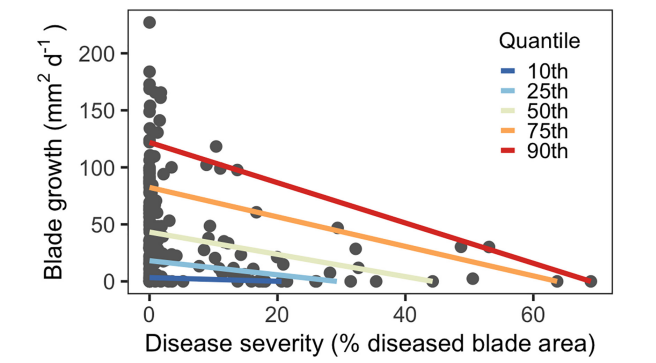

FIGURE 2 | Quantile regression model showing decreasing blade growth in response to disease severity for third-rank blades ($n = 176$).

Lesion Growth Rates

Repeated measurements of diseased blades indicated that lesion growth rates can significantly exceed blade growth rates *in situ* for third-rank (third youngest) blades (**Figure 3**, paired *t*-test, $p < 0.05$). Mean lesion growth rates were 51 mm^2d^{-1}, with a maximum rate of 371 mm^2d^{-1}. In comparison, the mean absolute blade growth rate for this subset of third-rank blades was 16 mm^2d^{-1} and the maximum growth rate was 71 mm^2d^{-1}.

Non-structural Carbon Analyses

Across the three meadows, disease severity and rhizome sugar content (mg per g rhizome dry weight) were inversely related (**Figure 4**). Disease severity ranged from 0–10% at Indian Cove and from 0–20% at Fourth of July Beach and False Bay. Both disease severity and site were significant predictors for rhizome sugar concentrations, together explaining roughly 50% of variation in sugar content (**Supplementary Table 3**). Shoot density was not a significant predictor of belowground sugar

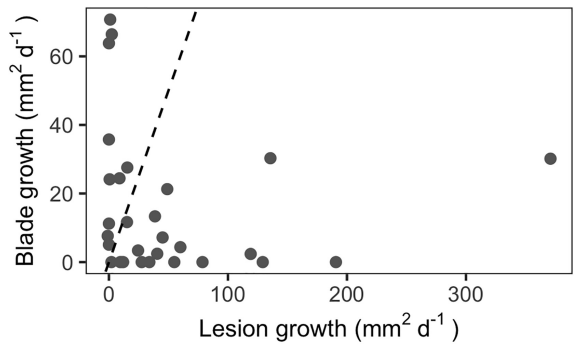

FIGURE 3 | *In situ* lesion growth rates outpaced blade growth rates among third-rank blades (n = 29). Dashed line indicates the 1:1 line.

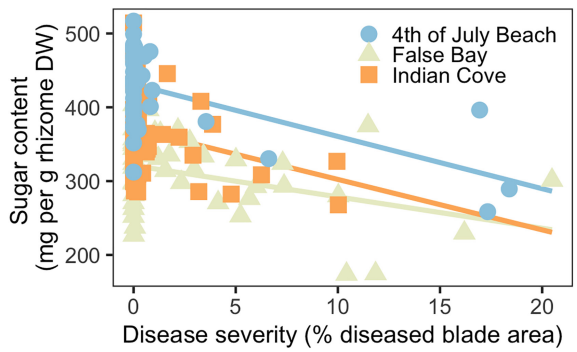

FIGURE 4 | Rhizome sugar content declined as a function of disease severity (n = 135) at three eelgrass meadows.

content. Mean (± SD) sugar content was highest at Fourth of July Beach (419 ± 56 mg per g rhizome dry weight) and similar at Indian Cove (311 ± 53 mg per g) and False Bay (356 ± 54 mg per g). Despite the variation between sites, the overall pattern was consistent: at higher disease severities, rhizome sugar concentrations decreased significantly.

DISCUSSION

Globally, seagrasses are declining under pressure from coastal development, climate change, and disease (Orth et al., 2006; Waycott et al., 2009; Dunic et al., 2021). To sustain and conserve these crucial habitats and their ecosystem services, we must determine the impacts of disease on eelgrass health. Though laboratory studies have identified the impact of SWD on eelgrass photosynthesis (Ralph and Short, 2002) and necrosis (Pokorny, 1967; Short et al., 1986; Muehlstein, 1992) and field surveys continue to highlight outbreak-levels of disease (Groner et al., 2014, 2016, in press; Jakobsson-Thor et al., 2018; Aoki et al., in review), the direct impact of SWD on eelgrass growth and sugar reserves in natural meadows remains unknown. Here we show that SWD predicts reduced blade growth rates and rhizome sugar concentrations in natural meadows. However, given the observational nature of this field study, reverse causality could account for the reduced blade growth among eelgrass with elevated SWD severity. For example, slower growing eelgrass could be more susceptible to SWD compared to faster-growing eelgrass. The observed reduced blade growth rates also could be due to other confounding factors like blade-level differences in epiphyte loads, which have been associated with higher probabilities of eelgrass having SWD (Groner et al., 2016). Shading due to epiphytes could then impact both SWD severity and eelgrass growth.

Our observed SWD prevalence and severity levels were higher than historical measurements from nearby sites. Previously, intertidal field surveys from 2012–2013 found disease prevalence ranged from 6–79% (Groner et al., 2014, 2016) elsewhere in the San Juan Islands, WA. These disparities may in part be due to different methods for calculating prevalence. Groner et al. (2014) measured prevalence—the proportion of diseased blades relative to total number of blades—based on the longest blade on each shoot, while Groner et al. (2016) used the second-oldest intact blade on each shoot. Our results based on the proportion of diseased shoots relative to the total number of shoots indicated elevated SWD levels, like observed prevalence of 95.8–100% in intertidal Swedish eelgrass (Jakobsson-Thor et al., 2018). While some spatiotemporal variation is expected, the near-100% prevalence we observed at Fourth of July Beach could be in part linked to warmer ocean temperatures in 2019 (Aoki et al., in review; Amaya et al., 2020). In comparison to historical sea surface temperature records, summer 2019 temperatures were warmer locally in the San Juan Islands (Aoki et al., in review) and more broadly for the North Pacific (Amaya et al., 2020). This is important for eelgrass growth and health, since warm temperatures are associated with reduced production of phenolic compounds (Vergeer et al., 1995), which are used in microbial defense. Among eelgrass, thermal stress during warmer summer months can also increase respiration compared to photosynthesis, altering photosynthetic and growth rates (Phillips and Menez, 1988; Lee et al., 2007). Taxed by thermal stress and compromised growth, eelgrass could be more susceptible to SWD in certain conditions. Indeed, warming temperatures have recently been suggested to contribute to SWD outbreaks (Groner et al., 2014, in press; Martin et al., 2016; Sullivan et al., 2018; Aoki et al., in review).

While outbreaks of SWD have been implicated in meadow decline and collapse, understanding how disease impacts at individual blade- and shoot-levels scale across eelgrass populations and ecosystems remains unclear. Our results suggest that consequences of disease may have ecosystem-wide effects under natural conditions. Diseased, first-rank blades grew nearly 25% slower than healthy, first-rank blades. Because blade growth is concentrated in the youngest two blades (Sand-Jensen, 1975), our findings suggest SWD in natural meadows may limit shoot size at maturity by compromising the growth of the young, fast-growing blades. Disease on mature blades may also reduce total shoot growth. Although third-rank blades have lower specific productivity rates (blade elongation as a percent of existing blade area per day), absolute blade growth rates could exceed 200 mm^{2}d^{-1} for third-rank blades. These growth rates declined significantly with more severe SWD, suggesting that greater disease severity could limit plant growth. Rapidly spreading SWD may further influence total shoot

physiology by interrupting transport of oxygen, photosynthesis products, and/or nutrients (Ralph and Short, 2002). The reduced rhizome sugar concentrations in severely diseased plants indicate SWD likely affected belowground carbon accumulation. Indeed, reduced non-structural carbon reserves were likely related to the observed, compromised blade growth, as diseased eelgrass has reduced photosynthetic capacity and may dedicate more resources to immune response (Vergeer et al., 1995). Ultimately, the combination of compromised growth and diminished sugar stores may reduce shoot survival, and in meadows such as this study site, where almost every plant had SWD, the impacts could accumulate at the ecosystem scale.

Reduced blade growth and rhizome sugars associated with severe SWD suggest that the disease can limit the persistence of entire eelgrass meadows over time. Some eelgrass meadows experience increased thermal and pathogen stress during warmer summer months (Young, 1943; Bockelmann et al., 2013; Aoki et al., in review). Taken together, this could reduce not only immediate eelgrass growth, which normally peaks in summer (Sand-Jensen, 1975), but also alter seasonal patterns in eelgrass productivity. Heavily diseased eelgrass with compromised growth and rhizome sugars may be vulnerable to environmental stressors over winter or early spring when eelgrass draws upon critical carbohydrate reserves from the previous summer (Burke et al., 1996). Less robust plants may be further vulnerable to SWD the following summer, creating a reinforcing feedback loop that could drive meadow-wide declines. Prior studies have noted that while SWD outbreaks can cause large-scale meadow die-offs, other meadows can support widespread disease without collapsing (Short et al., 1987; Jakobsson-Thor et al., 2018). The results from this study show how SWD may negatively impact the health of a meadow without immediately causing an ecosystem collapse. A precipitating disturbance or change in environmental conditions may then trigger widespread die-offs of vulnerable eelgrass. The global losses of eelgrass in the 1930s likely resulted from some combination of SWD and environmental stressors (Sullivan et al., 2013). However, studies testing the combined effects of SWD and stressors such as light availability, salinity, and temperature tend to occur in short-term laboratory mesocosms experiments (e.g., Brakel et al., 2019; Jakobsson-Thor et al., 2020). While these allow for carefully controlled testing of multiple stressors, they do not fully capture the long-term effects of SWD and environmental conditions in natural meadows. Additional field-based studies are needed to better understand these dynamic interactions over time.

In addition to making meadows more vulnerable to collapse, SWD may also impair meadow recovery following disturbance. At the meadow scale, reduced growth rates and carbohydrate reserves may limit regrowth of diseased shoots compared to healthy shoots. Rapid regrowth following disturbance is key to maintaining seagrass ecosystem services, such as carbon sequestration and biodiversity (Nowicki et al., 2017; Aoki et al., 2021); slower recovery rates may also increase meadow vulnerability to repeated disturbance, such as successive marine heat waves. By both increasing vulnerability and impairing recovery, SWD reduces the ecological resilience of eelgrass meadows and may impede conservation of existing meadows. Given the significant role of eelgrass in structuring coastal ecosystems and driving biogeochemical processes (reviewed in Moore and Short, 2006), reduced meadow resilience will have negative consequences for habitat provisioning, nutrient cycling, and other ecosystem services. Better understanding of the impact of chronic SWD on meadow trajectories through time is needed to optimize seagrass conservation and restoration efforts.

Further work is needed to understand the complex interactions between climate change, SWD, and eelgrass meadow resilience. The effects of environmental stressors on eelgrass, including changes in sea surface temperatures, salinity, ocean acidification, and altered light availability due to sea level rise, are not well understood (Short et al., 2016). Recent field surveys indicate positive associations between temperature and SWD (Groner et al., in press; Aoki et al., in review), while others suggest the relationship may be more bell-shaped, given the optimal thermal ranges for *L. zosterae* (Young, 1943; Olsen et al., 2015). Furthermore, the interactions between SWD and other environmental stressors remains unclear. Some reports indicate future conditions may reduce the effects of disease (Brakel et al., 2019), while others determined SWD is correlated with salinity (Jakobsson-Thor et al., 2018) and may be sensitive to pH (Groner et al., 2018). Certainly, interactions between temperature and other aspects of climate change may influence SWD but necessitate further research to understand these complex relationships and determine drivers of eelgrass resilience.

This study emphasizes the importance of considering disease alongside other climate change stressors to better predict the health and functioning of seagrass meadows in the Anthropocene. To the best of our knowledge, this is the first project to demonstrate that *L. zosterae* can significantly compromise eelgrass growth and belowground, non-structural carbohydrates in natural meadows. This work broadens our understanding of the effects of SWD on eelgrass productivity and is particularly relevant given mounting environmental stressors. Of course, these analyses were limited to eelgrass in one region over one summer growing season. Furthermore, at a site there can be multiple *L. zosterae* strains, which can vary in virulence (Martin et al., 2016) and produce significant differences in disease severity (Dawkins et al., 2018). Other groups of seagrass pathogens, including oomycetes and Phytomyxea (reviewed in Sullivan et al., 2018), should also be considered in the context of eelgrass health and productivity. As such, more studies are needed to examine these plant-pathogen relationships across the range of environmental conditions of existing eelgrass meadows. Eelgrass is a foundation species of critical coastal habitat across the northern hemisphere. Understanding the vulnerability of these meadows to disease is essential to their conservation across the species' range and in a changing climate.

DATA AVAILABILITY STATEMENT

The datasets presented in this study can be found in online repositories. The names of the repository/repositories and accession number(s) can be found below: The datasets analyzed

for this study can be found in the Zenodo repository (https://doi.org/10.5281/zenodo.5339331).

AUTHOR CONTRIBUTIONS

OG, TS, and CH conceived of this study. OG, LA, and SD developed the methods. OG, LA, TS, and JS collected and processed samples in the laboratory. BR and CG developed EeLISA. BR processed images. LA analyzed the data. OG and LA wrote the manuscript. CG and CH provided resources and supervision. CH helped in the field. All authors contributed to editing this manuscript.

FUNDING

SD and JS received support from the National Science Foundation's Research Experience for Undergraduates (NSF-REU) program. The Friday Harbor Labs Research Fellowship Endowment provided support for OG. LA was supported by NSF award OCE-1829921.

ACKNOWLEDGMENTS

We would like to thank Jack Novak for help with collecting and processing samples, and to the University of Washington's Friday Harbor Laboratories community, which supports collaborative research like this! We would also like to thank three reviewers for their thoughtful, constructive feedback.

SUPPLEMENTARY MATERIAL

The Supplementary Material for this article can be found online at: https://www.frontiersin.org/articles/10.3389/fmars.2021.768668/full#supplementary-material

REFERENCES

Amaya, D. J., Miller, A. J., Xie, S.-P., and Kosaka, Y. (2020). Physical drivers of the summer 2019 North Pacific marine heatwave. *Nat. Commun.* 11:1903. doi: 10.1038/s41467-020-15820-w

Aoki, L. R., McGlathery, K. J., Wiberg, P. L., Oreska, M. P. J., Berger, A. C., Berg, P., et al. (2021). Seagrass recovery following marine heat wave influences sediment carbon stocks. *Front. Mar. Sci.* 7:576784. doi: 10.3389/fmars.2020.576784

Aoki, L., Rappazzo, B., Beatty, D., Domke, L., Eckert, G., Eisenlord, M., et al. (in review). *Continental scale disease surveillance by artificial intelligence links seagrass wasting disease to ocean warming. (In review at Limnology and Oceanography)*.

Bell, S., Fonesca, M., and Stafford, N. (2007). "Seagrass Ecology: New Contributions from a Landscape Perspective," in *Seagrasses: Biology, Ecology, and Conservation*, eds A. Larkum, R. Orth, and C. Duarte (Netherland: Springer), 625–645. doi: 10.1007/1-4020-2983-7_26

Bockelmann, A. C., Beining, K., and Reusch, T. (2012). Widespread occurrence of endophytic *Labyrinthula* spp. in northern European eelgrass *Zostera marina* beds. *Mar. Ecol. Prog. Ser.* 445, 109–116. doi: 10.3354/meps09398

Bockelmann, A. C., Tams, V., Ploog, J., Schubert, P. R., and Reusch, T. B. H. (2013). Quantitative PCR reveals strong spatial and temporal variation of the wasting disease pathogen, *Labyrinthula zosterae* in Northern European eelgrass (*Zostera marina*) beds. *PLoS One* 8:e62169. doi: 10.1371/journal.pone.0062169

Brakel, J., Jakobsson-Thor, S., Bockelmann, A. C., and Reusch, T. B. H. (2019). Modulation of the eelgrass – *Labyrinthula zosterae* interaction under predicted ocean warming, salinity change and light limitation. *Front. Mar. Sci.* 6:268. doi: 10.3389/fmars.2019.00268

Brooks, M. E., Kristensen, K., van Benthem, K. J., Magnusson, A., Berg, C. W., Nielsen, A., et al. (2017). glmmTMB balances speed and flexibility among packages for zero-inflated generalized linear mixed modeling. *R. J.* 9, 378–400. doi: 10.32614/rj-2017-066

Bull, J. C., Kenyon, E. J., and Cook, K. J. (2012). Wasting disease regulates long-term population dynamics in a threatened seagrass. *Oecologia* 169, 135–142. doi: 10.1007/s00442-011-2187-6

Burdick, D. M., Short, F. T., and Wolf, J. (1993). An index to assess and monitor the progression of wasting disease in eelgrass Zostera marina. *Mar. Ecol. Prog. Series.* 94, 83–90.

Burge, C. A., Eakin, M. C., Friedman, C. S., Froelich, B., Hershberger, P. K., Hofmann, E. E., et al. (2014). Climate change influences on marine infectious diseases: Implications for management and society. *Ann. Rev. Mar. Sci.* 6, 249–277. doi: 10.1146/annurev-marine-010213-135029

Burge, C. A., and Hershberger, P. K. (2020). "Climate change can drive marine diseases," in *Marine Disease Ecology*, eds D. C. Behringer, B. R. Silliman, and K. D. Lafferty (Oxford: Oxford University Press), 83–94.

Burke, M., Dennison, W., and Moore, K. (1996). Non-structural carbohydrate reserves of eelgrass *Zostera marina*. *Mar. Ecol. Prog. Ser.* 137, 195–201. doi: 10.3354/meps137195

Chow, P. S., and Landhausser, S. M. (2004). A method for routine measurements of total sugar and starch content in woody plant tissues. *Tree Phys.* 24, 1129–1136. doi: 10.1093/treephys/24.10.1129

Cohen, R., James, C., Lee, A., Martinelli, M., Muraoka, W., Ortega, M., et al. (2018). Marine host-pathogen dynamics: Influences of global climate change. *Oceanography* 31:201. doi: 10.5670/oceanog.2018.201

Costanza, R., d'Arge, R., de Groot, R., Farber, S., Grasso, M., Hannon, B., et al. (1997). The value of the world's ecosystem services and natural capital. *Ecol. Eco.* 25, 3–15. doi: 10.1016/S0921-8009(98)00020-2

Dawkins, P., Eisenlord, M., Yoshioka, R., Fiorenza, E., Fruchter, S., Giammona, F., et al. (2018). Environment, dosage, and pathogen isolate moderate virulence in eelgrass wasting disease. *Dis. Aquat. Org.* 130, 51–63. doi: 10.3354/dao03263

Dennison, W. C., Orth, R. J., Moore, K. A., Stevenson, J. C., Carter, V., Kollar, S., et al. (1993). Assessing water quality with submersed aquatic vegetation. *Biosci* 43, 86–94.

Duarte, C. M., Middelburg, J. J., and Caraco, N. (2005). Major role of marine vegetation on the oceanic carbon cycle. *Biogeosciences* 2, 1–8. doi: 10.1371/journal.pone.0052932

Dunic, J. C., Brown, C. J., Connolly, R. M., Turschwell, M. P., and Côté, I. M. (2021). Long−term declines and recovery of meadow area across the world's seagrass bioregions. *Glob. Change Biol.* 27, 4096–4109. doi: 10.1111/gcb.15684

Fonseca, M. S., Zieman, J. C., Thayer, G. W., and Fisher, J. S. (1983). The role of current velocity in structuring eelgrass (*Zostera marina* L.) meadows. *Estuar. Coast. Shelf Sci.* 17, 367–380. doi: 10.1016/0272-7714(83)90123-3

Groner, M., Burge, C. A., Couch, C., Kim, C., Siegmund, G., Singhal, S., et al. (2014). Host demography influences the prevalence and severity of eelgrass wasting disease. *Dis. Aquat. Org.* 108, 165–175. doi: 10.3354/dao02709

Groner, M., Burge, C. A., Kim, C., Rees, E., Van Alstyne, K., Yang, S., et al. (2016). Plant characteristics associated with widespread variation in eelgrass wasting disease. *Dis. Aquat. Org.* 118, 159–168. doi: 10.3354/dao02962

Groner, M., Eisenlord, M., Yoshioka, R., Fiorenza, E., Dawkins, P., Graham, O., et al. (in press). Warming sea surface temperatures fuel summer epidemics of eelgrass wasting disease. *Mar. Ecol. Prog. Ser.* doi: 10.3354/meps13902

Groner, M. L., Burge, C. A., Cox, R., Rivlin, N. D., Turner, M., Van Alstyne, K. L., et al. (2018). Oysters and eelgrass: potential partners in a high pCO_2 ocean. *Ecology* 99, 1802–1814. doi: 10.1002/ecy.2393

Harvell, C. D., and Lamb, J. B. (2020). *"Disease outbreaks can threaten marine biodiversity," in Marine Disease Ecology*. Oxford: Oxford University Press, 141–158.

Harvell, C. D., Mitchell, C., Ward, J., Altizer, S., Dobson, A., Ostfeld, R., et al. (2002). Climate warming and disease risks for terrestrial and marine biota. *Science* 296, 2158–2162. doi: 10.1126/science.1063699

Hasegawa, N., Hori, M., and Mukai, H. (2008). Seasonal changes in eelgrass functions: current velocity reduction, prevention of sediment resuspension, and control of sediment–water column nutrient flux in relation to eelgrass dynamics. *Hydrobiologia* 596, 387–399. doi: 10.1007/s10750-007-9111-4

Jakobsson-Thor, S., Brakel, J., Toth, G. B., and Pavia, H. (2020). Complex interactions of temperature, light and tissue damage on seagrass wasting disease in *Zostera marina*. *Front. Mar. Sci.* 7:575183. doi: 10.3389/fmars.2020.575183

Jakobsson-Thor, S., Toth, G., Brakel, J., Bockelmann, A., and Pavia, H. (2018). Seagrass wasting disease varies with salinity and depth in natural *Zostera marina* populations. *Mar. Ecol. Prog. Ser.* 587, 105–115. doi: 10.3354/meps12406

Koenker, R. (2021). *quantreg: Quantile Regression. R package version 5.85*. https://CRAN.R-project.org/package=quantreg.

Lee, K.-S., Park, S. R., and Kim, Y. K. (2007). Effects of irradiance, temperature, and nutrients on growth dynamics of seagrasses: a review. *J. Exp. Mar. Biol. Ecol.* 350, 144–175. doi: 10.1016/j.jembe.2007.06.016

Martin, D. L., Chiari, Y., Boone, E., Sherman, T. D., Ross, C., Wyllie-Echeverria, S., et al. (2016). Functional, phylogenetic, and host-geographic signatures of *Labyrinthula* spp. provide for putative species delimitation and a global-scale view of seagrass wasting disease. *Estuar. Coast.* 39, 1403–1421. doi: 10.1007/s12237-016-0087-z

McManus, E., Durance, K., and Khan, S. (2020). *Revisions to Puget Sound vital signs and indicators*. Seattle: Ross Strategic.

Milne, L., and Milne, M. (1951). The eelgrass catastrophe. *Sci. Am.* 184, 52–55. doi: 10.1038/scientificamerican0151-52

Moffitt, J., and Cottam, C. (1941). *Eelgrass depletion on the Pacific coast and its effect upon the Black Brant*. Virginia: US Department of Interior Fish and Wildlife Service.

Moore, K. A., and Short, F. T. (2006). "*Zostera*: Biology, ecology, and management," in *Seagrasses: Biology, Ecology, and Conservation*, ed. A. W. D. Larkum (Netherlands: Springer), 361–386. doi: 10.1007/1-4020-2983-7_16

Muehlstein, L. K. (1989). Perspectives on the wasting disease of eelgrass *Zostera marina*. *Dis. Aquat. Org.* 7, 211–221. doi: 10.3354/dao007211

Muehlstein, L. K. (1992). The host – pathogen interaction in the wasting disease of eelgrass. *Zostera marina*. *Can. J. Bot.* 70, 2081–2088. doi: 10.1139/b92-258

Muehlstein, L. K., Porter, D., and Short, F. T. (1988). Labyrinthula sp., a marine slime mold producing the symptoms of wasting disease in eelgrass, *Zostera marina*. *Mar. Biol.* 99, 465–472. doi: 10.1007/bf00392553

Nowicki, R., Thomson, J., Burkholder, D., Fourqurean, J., and Heithaus, M. (2017). Predicting seagrass recovery times and their implications following an extreme climate event. *Mar. Ecol. Prog. Ser.* 567, 79–93. doi: 10.3354/meps12029

Olsen, Y. S., Potouroglou, M., Garcias-Bonet, N., and Duarte, C. M. (2015). Warming reduces pathogen pressure on a climate-vulnerable seagrass species. *Estuar. Coast.* 38, 659–667. doi: 10.1007/s12237-014-9847-9

Orth, R. J., Carruthers, T. J. B., Dennison, W. C., Duarte, C. M., Fourqurean, J. W., Heck, K. L., et al. (2006). A global crisis for seagrass ecosystems. *BioScience* 56:987. doi: 10.1641/0006-3568

Orth, R. J., Heck, K. L., and van Montfrans, J. (1984). Faunal communities in seagrass beds: A review of the influence of plant structure and prey characteristics on predator: prey relationships. *Estuaries* 7:339. doi: 10.2307/1351618

Phillips, R. C., and Menez, E. G. (1988). Seagrasses. *Smithsonian Contr. Mar. Sci.* 34, 1–104.

Pokorny, K. S. (1967). Labyrinthula. *J. Protozool.* 14, 697–708. doi: 10.1111/j.1550-7408.1967.tb02065.x

Ralph, P., and Short, F. (2002). Impact of the wasting disease pathogen, *Labyrinthula zosterae*, on the photobiology of eelgrass *Zostera marina*. *Mar. Ecol. Prog. Ser.* 226, 265–271. doi: 10.3354/meps226265

Rappazzo, B. H., Eisenlord, M. E., Graham, O. J., Aoki, L. R., Dawkins, P. D., Harvell, C. D., et al. (2021). EeLISA: Combating global warming through the rapid analysis of eelgrass wasting disease. *Proc. AAAI Confer. Artif. Intel.* 35, 15156–15165.

Rasmussen, E. (1977). "The wasting disease of eelgrass (*Zostera marina*) and its effects on environmental factors and fauna," in *Seagrass Ecosystems: A Scientific Perspective*, eds C. P. McRoy and C. Helfferich (New York: Marcel Dekker), 1–52.

Renn, C. (1936). The wasting disease of *Zostera marina*: A phytological investigation of the diseased plant. *Biol. Bull.* 70, 148–158. doi: 10.2307/1537320

Röhr, M. E., Holmer, M., Baum, J. K., Björk, M., Boyer, K., Chin, D., et al. (2018). Blue carbon storage capacity of temperate eelgrass (*Zostera marina*) meadows. *Glob. Biogeochem. Cycles* 32, 1457–1475. doi: 10.1029/2018GB005941

Sand-Jensen, K. (1975). Biomass, net production, and growth dynamics in an eelgrass (*Zostera marina* L.) population in Vellerup Vig, Denmark. *Ophelia* 14, 185–201. doi: 10.1080/00785236.1975.10422501

Short, F. T., and Duarte, C. M. (2001). "*Methods for the measurement of seagrass growth and production in Global Seagrass Research Methods*. Amsterdam: Elsevier, 155–182. doi: 10.1016/B978-044450891-1/50009-8

Short, F. T., Kosten, S., Morgan, P. A., Malone, S., and Moore, G. E. (2016). Impacts of climate change on submerged and emergent wetland plants. *Aqua. Bot.* 135, 3–17. doi: 10.1016/j.aquabot.2016.06.006

Short, F. T., Mathieson, A., and Nelson, J. (1986). Recurrence of the eelgrass wasting disease at the border of New Hampshire and Maine. *USA Mar. Ecol. Prog. Ser.* 29, 89–92. doi: 10.3354/meps029089

Short, F. T., Muehlstein, L. K., and Porter, D. (1987). Eelgrass wasting disease: Cause and recurrence of a marine epidemic. *Biol. Bull.* 173, 557–562. doi: 10.2307/1541701

Stauffer, R. C. (1937). Changes in the invertebrate community of a lagoon after disappearance of the eel grass. *Ecology* 18, 427–431. doi: 10.2307/1931212

Sullivan, B. K., Sherman, T. D., Damare, V. S., Lilje, O., and Gleason, F. H. (2013). Potential roles of *Labyrinthula* spp. in global seagrass population declines. *Fung. Ecol.* 6, 328–338. doi: 10.1016/j.funeco.2013.06.004

Sullivan, B. K., Trevathan-Tackett, S. M., Neuhauser, S., and Govers, L. L. (2018). Review: Host-pathogen dynamics of seagrass diseases under future global change. *Mar. Poll. Bull.* 134, 75–88. doi: 10.1016/j.marpolbul.2017.09.030

Vergeer, L. H. T., Aarts, T. L., and de Groot, J. D. (1995). The 'wasting disease' and the effect of abiotic factors (light intensity, temperature, salinity) and infection with *Labyrinthula zosterae* on the phenolic content of *Zostera marina* shoots. *Aquat. Bot.* 52, 35–44. doi: 10.1016/0304-3770(95)00480-N

Waycott, M., Duarte, C. M., Carruthers, T. J. B., Orth, R. J., Dennison, W. C., Olyarnik, S., et al. (2009). Accelerating loss of seagrasses across the globe threatens coastal ecosystems. *Proc. Nat. Acad. Sci.* 106, 12377–12381. doi: 10.1073/pnas.0905620106

Young, E. (1943). Studies on labyrinthula. the etiologic agent of the wasting disease of eel-grass. *Am. J. Bot.* 30, 586–593. doi: 10.2307/2437469

Conflict of Interest: TS is employed by Seagrove Kelp Co.

The remaining authors declare that the research was conducted in the absence of any commercial or financial relationships that could be construed as a potential conflict of interest.

Publisher's Note: All claims expressed in this article are solely those of the authors and do not necessarily represent those of their affiliated organizations, or those of the publisher, the editors and the reviewers. Any product that may be evaluated in this article, or claim that may be made by its manufacturer, is not guaranteed or endorsed by the publisher.

frontiers in Plant Science

ORIGINAL RESEARCH
published: 02 December 2021
doi: 10.3389/fpls.2021.745855

Adaptation of Temperate Seagrass to Arctic Light Relies on Seasonal Acclimatization of Carbon Capture and Metabolism

Alexander Jueterbock[1], Bernardo Duarte[2,3], James Coyer[4], Jeanine L. Olsen[5], Martina Elisabeth Luise Kopp[6], Irina Smolina[6], Sophie Arnaud-Haond[7], Zi-Min Hu[8] and Galice Hoarau[6]*

[1]Algal and Microbial Biotechnology Division, Faculty of Biosciences and Aquaculture, Nord University, Bodø, Norway, [2]Marine and Environmental Sciences Centre, Faculty of Sciences of the University of Lisbon, Lisbon, Portugal, [3]Departamento de Biologia Vegetal da Faculdade de Ciências da Universidade de Lisboa, Lisbon, Portugal, [4]Shoals Marine Laboratory, University of New Hampshire, Durham, NH, United States, [5]Ecological Genetics-Genomics Group, Groningen Institute of Evolutionary Life Sciences, University of Groningen, Groningen, Netherlands, [6]Marine Molecular Ecology Group, Faculty of Biosciences and Aquaculture, Nord University, Bodø, Norway, [7]UMR MARBEC Marine Biodiversity Exploitation and Conservation, Univ Montpellier, CNRS, IFREMER, IRD, Montpellier, France, [8]Ocean School, Yantai University, Yantai, China

OPEN ACCESS

Edited by:
Kasper Elgetti Brodersen, University of Copenhagen, Denmark

Reviewed by:
Manoj Kumar, Indian Institute of Toxicology Research (CSIR), India
Matthew William Fraser, University of Western Australia, Australia

***Correspondence:**
Alexander Jueterbock
Alexander-Jueterbock@web.de

Specialty section:
This article was submitted to Functional Plant Ecology, a section of the journal Frontiers in Plant Science

Received: *22 July 2021*
Accepted: *29 October 2021*
Published: *02 December 2021*

Citation:
Jueterbock A, Duarte B, Coyer J, Olsen JL, Kopp MEL, Smolina I, Arnaud-Haond S, Hu Z-M and Hoarau G (2021) Adaptation of Temperate Seagrass to Arctic Light Relies on Seasonal Acclimatization of Carbon Capture and Metabolism. Front. Plant Sci. 12:745855. doi: 10.3389/fpls.2021.745855

Due to rising global surface temperatures, Arctic habitats are becoming thermally suitable for temperate species. Whether a temperate species can immigrate into an ice-free Arctic depends on its ability to tolerate extreme seasonal fluctuations in daylength. Thus, understanding adaptations to polar light conditions can improve the realism of models predicting poleward range expansions in response to climate change. Plant adaptations to polar light have rarely been studied and remain unknown in seagrasses. If these ecosystem engineers can migrate polewards, seagrasses will enrich biodiversity, and carbon capture potential in shallow coastal regions of the Arctic. Eelgrass (*Zostera marina*) is the most widely distributed seagrass in the northern hemisphere. As the only seagrass species growing as far north as 70°N, it is the most likely candidate to first immigrate into an ice-free Arctic. Here, we describe seasonal (and diurnal) changes in photosynthetic characteristics, and in genome-wide gene expression patterns under strong annual fluctuations of daylength. We compared PAM measurements and RNA-seq data between two populations at the longest and shortest day of the year: (1) a Mediterranean population exposed to moderate annual fluctuations of 10–14 h daylength and (2) an Arctic population exposed to high annual fluctuations of 0–24 h daylength. Most of the gene expression specificities of the Arctic population were found in functions of the organelles (chloroplast and mitochondrion). In winter, Arctic eelgrass conserves energy by repressing respiration and reducing photosynthetic energy fluxes. Although light-reactions, and genes involved in carbon capture and carbon storage were upregulated in summer, enzymes involved in CO_2 fixation and chlorophyll-synthesis were upregulated in winter, suggesting that winter metabolism relies not only on stored energy resources but also on active use of dim light conditions. Eelgrass is unable to use excessive amounts of light during summer and

demonstrates a significant reduction in photosynthetic performance under long daylengths, possibly to prevent photoinhibition constrains. Our study identified key mechanisms that allow eelgrass to survive under Arctic light conditions and paves the way for experimental research to predict whether and up to which latitude eelgrass can potentially migrate polewards in response to climate change.

Keywords: eelgrass (*Zostera marina*), climate change, Arctic light, respiration, photosynthesis, carbon capture, daylength, energy storage

INTRODUCTION

Climate-change induced increases in surface temperatures are causing a worldwide poleward shift of temperature isotherms (McMahon and Hays, 2006) and concomitantly, distribution limits (Wernberg et al., 2013; Melbourne-Thomas et al., 2020), and spring phenology of species (Clausen and Clausen, 2013; Poloczanska et al., 2013). Furthermore, polar regions are warming at a particularly high rate (Høye et al., 2007; Burrows et al., 2011). For example, Arctic sea ice has melted at a rate of 6% per decade since the late 1970 (Cai et al., 2021), opening thermally suitable habitats with unoccupied niches available for colonizing species from the south (Cheung et al., 2009).

Whether a temperate species can immigrate into ice-free Arctic regions depends not only on finding thermally suitable conditions but also on its ability to tolerate extreme Arctic light conditions (Huffeldt, 2020). Constant daylight or darkness can be particularly challenging for sessile autotrophs. To what extent constant summer daylight inhibits cellular respiration (Kok effect; Griffin and Heskel, 2013; Heskel et al., 2013), growth, productivity, and photosynthesis in plants (Kallio and Valanne, 1975) remains controversial and may depend on the species (Sysoeva et al., 2010). A poleward range shift further implies that growth and reproduction are triggered in suboptimal seasons if temperate species follow the same photoperiodic changes as specific life cycle triggers when immigrating into the Arctic (Taulavuori et al., 2010). Yet, research and, thus, knowledge on physiological adjustments of temperate plants to Arctic light conditions is scarce in both terrestrial, and marine systems (Huffeldt, 2020).

Seagrasses comprise a polyphyletic group of marine flowering plants inhabiting shallow subtidal shores from subarctic to tropical regions. Seagrass meadows provide habitat and food that support a diverse food web, as well as important ecosystem services such as nutrient fixation, protection of the shoreline from erosion, nursery grounds for commercially important fishes, and carbon sequestration of ca. 104 Tg C year^{-1} (Duarte and Krause-Jensen, 2017), or 1% of the global annual carbon emissions (ca. 9.8 Gt C year^{-1}; Friedlingstein et al., 2020). Thus, if seagrass can grow under Arctic light conditions, its predicted northward shift (Wilson and Lotze, 2019) will likely enrich biodiversity and introduce drastic functional changes in future Arctic coastal ecosystems, food webs, fish/invertebrate stocks, and biogeochemical cycles (Krause-Jensen and Duarte, 2014).

The eelgrass *Zostera marina* is the most widely distributed seagrass species, occurring in suitable habitats along shores of all five continents in the northern hemisphere (Green and Short, 2004). Eelgrass meadows grow in coastal waters from subtropical regions at latitudes as low as 36°N (e.g., southern Iberia; Green and Short, 2004) to polar regions at latitudes as high as *ca.* 70°N (e.g., Greenland at 64.5° N; Olesen et al., 2015) and northern Norway at 69.8° N (Olsen et al., 2013).

Temperature, optimally from 15–25°C (Boström et al., 2004; Staehr and Borum, 2011; Zhang et al., 2016), is considered as the most important factor controlling phases of eelgrass sexual reproduction (Blok et al., 2018). Photoperiod appears to not control eelgrass reproduction because the eelgrass genome lacks the phytochrome C gene (PHYC; Olsen et al., 2016) that is involved in the photoperiodic control of flowering in most terrestrial plants (Chen et al., 2014; Woods et al., 2014). Accordingly, the species' northern distribution limit probably is limited by cool summer water temperatures <13.5°C that prevent seed maturation (Blok et al., 2018). As its seed germination is not regulated by photoperiodic rhythms (Moore et al., 1993), eelgrass seeds are likely to develop and disperse in a warming Arctic and contribute to a seed-driven northward shift of eelgrass meadows under projected climate change (Clausen et al., 2014; Blok et al., 2018). Temperature also is one of the most important factors for eelgrass growth (Clausen et al., 2014; Zhang et al., 2016). For example, increased investment in below-ground rhizomes contributes to larger annual biomass in populations from high latitudes compared with populations from warmer waters (Clausen et al., 2014).

Below-ground rhizomes provide stored energy to fuel eelgrass metabolism under low-light conditions during Arctic winter (Olesen and Sand-Jensen, 1993; Burke et al., 1996) and the concentration of stored carbohydrates in eelgrass beds increases with latitude (Colarusso, 2007; Novak et al., 2020). However, rising temperatures may lead to a mismatch between peak growth – advancing to winter darkness – and available solar radiation in spring (Clausen et al., 2014). The mismatch, in combination with an increased annual biomass turnover under warmer temperatures (Olesen et al., 2015), requires eelgrass to store sufficient resources to fuel winter metabolism and the higher and earlier production of shoots at the onset of the growing season (Clausen et al., 2014). Thus, poleward migrating eelgrass will have strong implications for the dynamics of below-ground carbon sinks.

The minimum light requirement for long-term survival and growth – meeting respiratory and metabolic energy demands – ranges between 11 and 34% surface irradiance (Ochieng et al., 2010), corresponding to 1.2–12.6 mol photons m^{-2} day^{-1} (Gattuso et al., 2006). Six hours daily of saturating irradiance (Hk) was suggested to be the minimum allowing for eelgrass growth and survival (Dennison and Alberte, 1985). Furthermore, shaded eelgrass showed significantly higher mortality rates under increased temperatures (16% at 20°C vs. 0.57% at 12°C; Eriander, 2017).

Most previous research has focused on the impact of modest light reductions or depth limits of eelgrass (e.g., Ralph et al., 2007), although a period of 30 days at 10% surface irradiance (<3 mol photons m^{-2} d^{-1}) limited the survival of eelgrass transplants in estuarine temperate systems (Moore et al., 1997). The potential for poleward migration into the Arctic remains unknown because eelgrass survival under extreme light periods remains understudied. In order to investigate to what extent extreme Arctic photoperiods may present an energetic constraint to projected northward range shifts of eelgrass, we compared photosynthetic characteristics and gene expression patterns between two populations at the longest and shortest day of the year: (1) a Mediterranean population experiencing moderate annual fluctuations of 10–14 h daylength and 2) an Arctic population experiencing high annual fluctuations of 0–24 h daylength. The specific objectives were to:

1. Characterize energy-saving mechanisms (in photosynthetic and metabolic pathways) that may allow eelgrass to survive during long Arctic winter nights.
2. Determine possible adaptive mechanisms of Arctic eelgrass to compensate for energy loss during winter with increased investment in energy storing mechanisms during summer.

Differences in gene expression between summer and winter or day and night samples from a single population are interpreted as resulting from seasonal or diurnal acclimatization (**Box 1**). Our study cannot identify whether gene-expression or photosynthetic specificities of the Norwegian population (not replicated in the French population) are acclimatizations resulting from phenotypic plasticity or whether they are genetic adaptations (**Box 1**) that evolved under polar light regimes. Thus, in this manuscript, we use the term "adaptation" when referring to either acclimatization or genetic adaptation (**Box 1**).

BOX 1 | Glossary of adaptation-related terms

Acclimatization – Phenotypic change over the life span of an organism induced by epigenetic regulation in response to environmental cues.

Adaptation – All plastic and genetically adaptive changes that reduce the negative effects of unfamiliar and undesirable external environment. This includes both acclimatization and genetic adaptation.

Genetic adaptation – Evolution of genetically determined heritable traits in a population across generations in response to natural selection.

MATERIALS AND METHODS

Site Characteristics

Eelgrass shoots were sampled in Norway (Røvik, 67°16′06.2" N, 15°15′38.4″ E) and France (Sète, Thau Lagoon, 43°25′08.0" N, 3°40′03.9″ E). The youngest two shoots of each of six plants were collected at each site at noon and the following midnight around summer solstice (June 21) and winter solstice (December 21) 2017. Intact shoots were placed in RNAlater (ThermoFisher) and stored after 1–2 days at −20°C.

Defining Zeitgeber Times ZTs (time after an environmental time cue that entrains circadian rhythms, such as sunlight) that correspond between the French and Norwegian samples is complicated by the fact that the two latitudes do not only differ in diurnal light rhythms but also in light quantity and quality (Taulavuori et al., 2010) (i.e., light conditions at dawn at the French site do not correspond to dawn light conditions at the Norwegian site and, thus may mark different ZTs in the circadian cycle). We chose midday and midnight as time points to compare samples from the two locations as these represent times at which the plants from both locations had the potential to receive most/least light of the day in both seasons, and the time that is at equal temporal distance from sunset and sunrise. This implies, however, that differences between the Norwegian and French samples at corresponding time points may be partly explained by them being at different ZTs within their circadian rhythm. However, differences in ZTs are less affecting seasonal differences between the Norwegian and French, because we compared daily averages that involved measurements from both midday and midnight samplings.

Snapshots of temperature (°C) and light (Lux; **Table 1**) were taken at each sampling event in ca. 20 cm water depth with Pendant data loggers (Onset HOBO UA-002). Annual variation of temperature (°C), salinity, and Lux conditions at the Norwegian sampling site were recorded from spring 2016 to spring 2017 with data loggers (HOBO U24-002-C for salinity/temperature with 30 min intervals, and HOBO UA-002 for light/temperature with 10 min intervals) anchored ca. 30 cm above sandy substrate during low tide. At low tide, the light/temperature loggers were falling dry. Temperature (°C) and salinity conditions in the Thau Lagoon (43° 22′ 44.4" N, 3° 34′ 17.4″ E) were downloaded for year 2016 from the marine environmental station database of Thau Lagoon (Messiaen et al., 2018) on July 31, 2020, which were recorded every 30 min with data loggers (WTW) at 1–2 m water depth. Light (PAR µmol m^2 s^{-1}) conditions were recorded with dataloggers (SKUW 215 PAR Sensor, Skye Instruments) every 30 min for December 2015–July 2016 at the Thau Lagoon Observatory (43°24′53" N, 3°41′16″ E; Trombetta et al., 2019) and were downloaded from Sea scientific open data publication (www.seanoe.org, accessed on July 31, 2020). To make the light conditions comparable between the Norwegian and French sampling sites, Lux values were converted to approximate PAR (photosynthetically active radiation) values by applying a multiplication factor of 0.019, an approximation for the spectral power distribution of sunlight (6,000 K; Creswell, 2010).

TABLE 1 | Snapshots of temperature and light conditions measured at the sampling events.

Measurement	Population	June		December	
		Night	Day	Night	Day
Temperature (°C)	Norway (Røvik)	15.1	16.0	−1.9	−1.6
	France (Sète)	22.8	21.7	7.3	8.2
Light (μmol m^{-2} s^{-1})	Norway (Røvik)	6.3	235.6	0.0	0.0
	France (Sète)	0.0	327.2	0.2	535.4

Seasonal variation in light levels was greater in Norway, where PAR levels remained close to zero from mid-November to mid-January, but reached ca. 1,000 μmol m^{-2} s^{-1} in summer, similar to France (**Figures 1C**,**D**,**E**; **Supplementary Table 1**). In summer, light levels showed a diurnal rhythm in both Norway and France, but – as expected – reached slightly higher nocturnal levels in Norway.

Summer temperatures were ca. 10°C higher in France (20–25°C) compared to Norway (10–15°C; **Supplementary Figure 1**; **Supplementary Table 1**). Stronger Norwegian diurnal temperature variations likely reflected the differences between air and water temperatures around spring tides when the dataloggers may have been shortly exposed to air during low-tides but submerged during high-tides. In contrast, the eelgrass meadow in the Thau lagoon was constantly submerged. Accordingly, the data loggers revealed relatively constant salinity throughout the year at ca. 37 PSU (**Supplementary Figure 2**; **Supplementary Table 6**), while the high fluctuation (10–30 PSU) in Norway was due to seasonal rainfall, freshwater runoff, ice formation, and melting.

Photosynthesis

At each sampling event, we assessed leaf photochemistry using a Chlorophyll *a* Pulse Amplitude Modulated (PAM) Fluorometer (FluorPen FP100, Photon Systems Instruments), by measuring the increase in chlorophyll *a* fluorescence upon illumination after a 10-min dark period induced by leaf-clips (OJIP curve; Bussotti et al., 2010; (Duarte et al., 2017). using a saturating pulse at 455 nm from 10 seagrass shoots.

When a dark-adapted leaf is illuminated with a saturating light intensity, it exhibits a so-called OJIP curve from a state where all reaction centers are opened (all quinone acceptors are oxidized and can accept electrons) to a state where all quinone acceptors are reduced and chlorophyll fluorescence reaches its maximum. The rise in fluorescence transient along this polyphasic OJIP curve depicts the rate of reduction kinetics of various components of Photosystem II (PSII). The OJIP curve provides information on the processes involved in photon absorption at the PSII antennae (ABS), transformation into an exciton and its free energy flux (RE), and transduction of its energy in the form of electronic potential vial electron transport (ET) from the donor side of the PSII to the electron acceptor of the PSI. The analysis of this OJIP transient (JIP test) allows to estimate the energy fluxes, involving absorption, entrapment in the PSII, transport to the quinone pool, and dissipation in the form of heat or fluorescence that helps to avoid photoinhibition damages. The formulae and definitions of terms derived from the JIP-test (chlorophyll *a* induction curves, or Kautsky curves measurements; **Supplementary Table 2**) are listed in **Table 2**.

Differences in these photosynthetic characteristics between populations (day/night/season) were tested for significance with Wilcoxon rank sum tests followed by correcting the values of *p* for multiple pairwise comparisons using the Benjamini-Hochberg method with the R package "rstatix" v0.6.0 (Kassambara, 2020). Multivariate differences in photochemistry were estimated from photochemical raw data using a canonical analysis of principal coordinates (CAP) with Euclidean distances with the Primer 6 software (Clarke and Gorley, 2005). This multivariate approach is insensitive to heterogeneous data and frequently used to compare different sample groups (Duarte et al., 2017; Cruz de Carvalho et al., 2020). Differences in the overall photochemical metabolism were estimated from normalized photochemical raw data with a canonical analysis of principal coordinates (Duarte et al., 2017). Multivariate differences were visualized as Euclidean distances along the first two principal coordinates.

RNA Preparation

RNA was extracted from small pieces of stored samples (RNAlater; ThermoFisher) that were homogenized (PowerLyzer 24; Qiagen) and processed according to the standard protocol of the RNeasy PowerPlant Kit (Qiagen). We consistently excised the mid portion of the youngest fully mature leaf in the shoot (usually the second-rank leaf), so that tissue-age dependent within- or among-leaf variations were unlikely to explain differences in gene expression (Ruocco et al., 2019a,b). RNA concentrations were measured with Qubit™ RNA HS Assays (ThermoFisher) using a Qubit 4 fluorometer. RNA integrity was verified on TapeStation 2200 with RNA ScreenTape. RIN values were >3.6.

RNA libraries were prepared from 1 μg of extracted RNA with NEBNext® Ultra™ II Directional RNA Library Prep Kit for Illumina (New England Biolabs) following the polyA mRNA workflow of the kit protocol. Libraries were verified on TapeStation 2200 using High Sensitivity D1000 ScreenTape. Paired-end (2×150 bp) RNA sequencing (RNASeq) data were generated using a NextSeq 500/550 High Output Kit v2 (Illumina) on an Illumina NextSeq 500 platform at Nord University.

Sequence Data Analysis

Raw reads were trimmed for low quality (Phred score Q < 20, 99% base call accuracy), and TruSeq adapter sequences

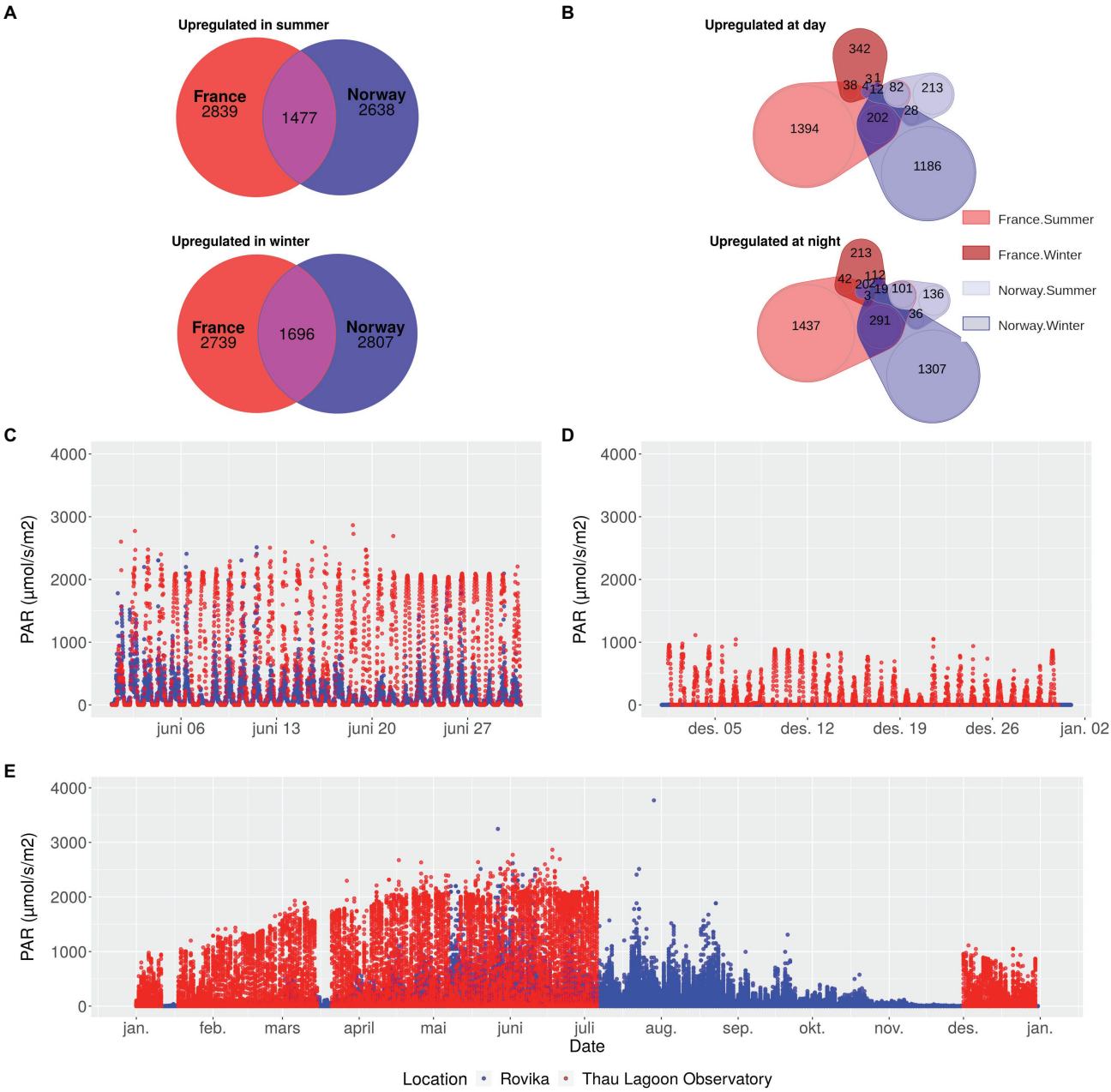

FIGURE 1 | Seasonal and diurnal gene expression changes of the Norwegian and French population of the seagrass *Zostera marina* in relation to differences in annual light conditions at the sampling sites. Number of genes upregulated in summer, and winter **(A)** in France and in Norway, or upregulated during day, and night **(B)**, separately for summer and winter. The subset of genes in A and B are independent from each other but partly overlapping. Light levels in June **(C)**, December **(D)**, and over the entire year **(E)** at the Norwegian sampling site (blue) and at an observatory station in the Thau Lagoon close to the French sampling site (red). In the Thau Lagoon, values are missing from July to December. PAR: Photosynthetically active radiation.

(overlap > 3 bp) before reads <25 bp were removed with TrimGalore! v 0.6.0.[1] Read quality was checked with FastQC v 0.11.8 to control for aberrant read base content, length distribution, duplication and over-representation.[2]

Trimmed reads were mapped to the genome of *Z. marina* (Olsen et al., 2016) v 2.2 from ORCAE (Sterck et al., 2012) and the organellar genomes (chloroplast and mitochondria) of *Z. marina* v2.1 from ORCAE (Sterck et al., 2012) with the splice-aware RNA-seq aligner STAR v 2.7.2a (sjdbOverhang 149; Dobin et al., 2013, 2016), guided by gff3 gene annotations v2.2 from ORCAE (Sterck et al., 2012), converted to gtf with

[1]https://www.bioinformatics.babraham.ac.uk/projects/trim_galore/
[2]http://www.bioinformatics.babraham.ac.uk/projects/fastqc/

TABLE 2 | Formulae and definitions of terms derived from the JIP test.

Term	Formula	Definition
PI_{ABS}	$[\gamma_{RC}{}^{1}(1-\gamma RC)] \times [\varphi_{Po}{}^{2}/(1-\varphi_{Po})] \times [\psi_{o}{}^{3}/(1-\psi_{o})]$	Performance Index reflecting the overall photosynthetic performance by combining three parameters: (1) the density of reaction centers, (2) the electron transport at the onset of illumination, and (3) the maximum energy flux reaching the reaction center in PS II.
ABS/CS	$F_0{}^{4}$	Absorbed energy flux measured as the minimal fluoresence intensity in a dark adapted frond when all reaction centers are opened (all quinone acceptors are oxidized and can accept electrons)
ET/CS	$\varphi_{Po} \times \psi_{o} \times$ (ABS/CS)	Electron transport energy flux
TR_0/CS	$\varphi_{Po} \times$ (ABS/CS)	Trapped energy flux
DI_0/CS	(ABS/CS) – (TR_0/CS)	Dissipated energy flux
Area	Extracted from the recorded OJIP	Size of the oxidized quinone pool; total complementary area between the fluorescence induction curve and $F = F_M$
RC_0/CS	$\varphi_{Po} \times (V_J{}^{5}/M_0{}^{6}) \times$ ABS/CS	Density of photosystem II oxidized reaction centers per excited cross-section
TR_0/DI_0		Contribution of the light reactions for primary photochemistry
$\Psi_0/(1-\Psi_0)$		Contribution of the dark reactions for primary photochemistry

[1] $\gamma_{RC} = Chl_{RC}/Chl_{total} = RC/(ABS+RC)$, *the probability that a PSII Chl molecule functions as reaction center (RC).*

[2] $\varphi_{Po} = TR_0/ABS = [1-(F_0/F_M)]$, *the maximum quantum yield for primary photochemistry, with* F_M *representing the maximum fluorescence intensity when all reaction centers are closed (all quinone acceptors are reduced).*

[3] $\psi_0 = ET_0/TR_0 = (1-V_J)$, *efficiency/probability for electron transport (ET), or the probability that an electron moves further than* Q_A *(the primary quinone acceptor).*

[4] F_0, *minimal fluorescence when all PSII RCs are open.*

[5] V_J $(F_j - F_0)/(F_M - F_0)$, *with* F_j *representing the fluorescence intensity at the J-step (at 2 ms).*

[6] M_0 *Slope of the origin of the fluorescence rise. Maximal rate of accumulation of the fraction of closed reaction centers.*

Based on Zhu et al. (2005) and Duarte et al., (2017).

the program gffread.[3] Alignments that contained noncanonical splice junctions were filtered out. Duplication rates were checked with the R package "dupRadar" v1.14.0 (Sayols et al., 2016).

[3]https://github.com/gpertea/gffread

Read counts for 21,069 genes (**Supplementary Table 3**) were obtained with featureCounts in the R package "Rsubread" v1.34.6 (Liao et al., 2019) with the non-default settings minOverlap = 3, MinMQS = 20, strandSpecific = 2, isPairedEnd = TRUE. Genes of low expression (library average < 5, $n = 7{,}023$) were excluded from subsequent analyses to avoid potential artefacts from sequencing errors.

Gene IDs of the *Z. marina* genome v2.2 (Olsen et al., 2016) were annotated with gene descriptions, Gene Ontology (GO) terms, KEGG Orthology groups (KO), and Enzyme Commission (EC) numbers (based on enzyme nomenclature) from the ORCAE database (Sterck et al., 2012). Gene ontology terms assign genes to one or more categories related to the molecular function, cellular component or biological process of the gene products. KEGG Orthology groups assign gene products to their function in a biological pathway of molecular interactions. The EC number classifies genes numerically based on the chemical reactions they catalyze.

Multivariate Clustering of Gene Expression

To characterize overall transcriptomic differentiation, we clustered the samples hierarchically by the first five principal components of gene coverage (14,046 genes), which together explained 73.4% of the variation, using the R package "FactoMineR" v. 1.42 (Lê et al., 2008). For Principal Component Analysis (PCA), the scale.unit was set to FALSE not to scale the expression values to unit variance. Prior to PCA, we regularized log-transformed gene count values (**Supplementary Table 4**) with DESeq2 v 1.24.0 (Love et al., 2014) in order to assure homoscedasticity and to account for differences in sequencing depth.

Differential Gene Expression

We tested for differential gene expression between summer and winter samples (day and night samples combined) and between day and night samples in France and Norway, respectively, with DESeq2 v1.24.0 (Love et al., 2014). The values of p were adjusted with Independent Hypothesis Filtering based on the R package "IHW" v1.14.0 (Ignatiadis et al., 2016). We plotted overlaps of differentially expressed genes between seasons and locations with the R package "eulerr" v6.1.0 (Larsson, 2019) and "nVennR" v0.2.1 (Pérez-Silva et al., 2018).

For each population, we tested (Fisher's exact test) for enriched gene ontology terms (biological process, cellular component, and molecular function) in genes that were differentially expressed between day and night samples or between summer and winter samples with the R package "topgo" (Alexa and Rahnenführer, 2010). Significance levels were adjusted with the Benjamini and Hochberg correction (Benjamini and Hochberg, 1995), using the p.adjust function in R (R Core Team, 2019), to control for the false discovery rate when conducting multiple comparisons.

The adjusted-log10 of the values of p of significantly enriched GO-terms were visualized for each population in heatmaps using the heatmap.2 function of the R package "gplots" v.3.0.3 (Warnes et al., 2020). GO terms were hierarchically clustered

with the R package "goSTAG" v1.12.0 (Bennett and Bushel, 2017) based on euclidean distances and Ward's minimum variance clustering method with Ward's (Ward, 1963) clustering criterion implemented (ward.D2 option; Murtagh and Legendre, 2014). The sample dendrogram was based on Euclidean distances and a complete linkage clustering method.

Enriched/perturbed KEGG metabolic pathways in the fold-change matrices of differentially expressed genes were identified using the R package "gage" v2.37.0 (Luo et al., 2009). Nuclear genes were mapped to KO (Kegg Orthology)-terms by translating EC numbers from the genome annotation to corresponding KO-terms based on the KEGG API list http://rest.kegg.jp/link/ec/ko. For organellar genes, EC numbers and, thus KO-terms were not annotated. For pathways perturbed ($p < 0.05$) in at least one of the populations and seasons, we plotted the significant fold-changes of molecular functions (KO-terms) for all populations and seasons with the R package "pathview" v3.11 (Luo and Brouwer, 2013). When several genes referred to the same KO-term, we plotted their average fold-change in the respective pathway.

RESULTS

Photosynthesis

Overall photosynthetic performance, represented by the photochemical performance index (PI_{ABS}; **Figure 2A**) showed inverse seasonal shifts in Norway and France. While the French population performed significantly better during summer, the Norwegian population performed significantly better during winter. The reduced summer performance of the Norwegian population was associated with peculiar photosynthetic characteristics. In contrast to the French population and the Norwegian winter samples, light harvesting ability increased in the Norwegian summer samples under non-saturating light levels during night-time, as represented by the increase in absorbed (ABS/CS; **Figure 2C**) and trapped (TR_0/CS; **Figure 2D**) energy flux, and in the number of oxidized reaction centers per leaf cross section (RC_0/CS; **Figure 2G**). The contribution of dark reactions to the overall photochemistry [$\Psi_0/(1\text{-}\Psi_0)$; **Figure 2I**] decreased significantly during summer nights. However, despite readiness of the electron transport chain (ETC) for electron transport, as indicated by the significant increase in the size of the oxidized quinone pool during Norwegian summer nights (Area; **Figure 2B**), the electron transport energy flux (ET_0/CS; **Figure 2E**) did not increase significantly. During winter, despite a significant increase in the contribution of light and dark reactions to the primary photochemistry [TR_0/DI_0, and $\Psi_0/(1-\Psi_0)$; **Figures 2H,I**], the Norwegian population showed a significant reduction in all energy fluxes, particularly during night-time (ABS/CS, TR_0/CS, and ET_0/CS; **Figures 2C–E**), including dissipated energy loss (DI_0/CS; **Figure 2F**).

The samples clustered well by sampling location and daylength (78 of 80 samples correctly identified) along the first two principal components showing that the photochemical traits from the chlorophyll *a* induction curves could well classify the samples (**Figure 3**). The Norwegian summer samples grouped into one cluster, irrespective of whether they were collected at day or night. The Norwegian winter samples collected during nighttime formed another distinct cluster. Winter daytime samples from France and Norway grouped close together, indicating that winter had a prevalent effect over location.

Gene Expression

On average, 76% of 1 million raw reads (average per library) mapped to exons (**Supplementary Table 5**). Based on the expression of 13,932 genes covered >5 times, the samples grouped into four clusters, separated by location (France/Norway) and season (Summer/Winter; **Figure 4**). The most distinct gene expression patterns were recorded in the winter samples from Norway (NW). Gene expression was most similar between winter samples from France (FS) and summer samples from Norway (NS; **Figure 4**). Strictly distinct clusters of gene expression between day and night were only observed in France during summer (FS).

Seasonal differences in gene expression were found in 8652 genes in the French population and in 8569 genes in the Norwegian population (**Supplementary Table 6**). In summer, 4,274 genes were upregulated in France, and 4,084 genes in Norway, of which 1,475 overlapped between the two populations (**Figure 1A**). In winter, 2,691 genes were upregulated in France, and 2,798 genes in Norway, of which 1,687 overlapped between the two populations (**Figure 1A**).

Diurnal differences in expression were strongest (>3,000 genes) in, and most similar (>500 genes shared) between the French summer samples and the Norwegian winter samples (**Figure 1B**). In contrast, the number of genes with diurnal expression differences was an order of magnitude lower (ca. 600 genes) in the French winter samples or the Norwegian summer samples (**Figure 1B**). All genes with diurnal differences in gene expression are characterized in **Supplementary Table 7**.

Functional Changes

Genes involved in photosynthesis, carbon fixation (dark reactions of photosynthesis; **Supplementary Figure 3**), and sugar metabolism (fructose and mannose metabolism: **Supplementary Figure 4** and glycolysis: **Supplementary Figure 5**) showed contrasting seasonal patterns between the Norwegian and French seagrass populations. Those are likely to explain the functional basis of the strong transcriptome similarity between Norwegian winter samples and French summer samples (**Figure 4**). Summer upregulation/winter downregulation of most of the organellar functions, both related to the chloroplast and the mitochondrion, characterizes the functional transcriptome specificities of the Norwegian samples (**Figure 5**). All pathways enriched for seasonal or diurnal differentially expressed genes are listed in **Supplementary Table 8**.

Photosynthesis and Carbon Sequestration

The Norwegian samples upregulated in summer genes related to photosynthesis and ATP metabolism (**Figure 6**;

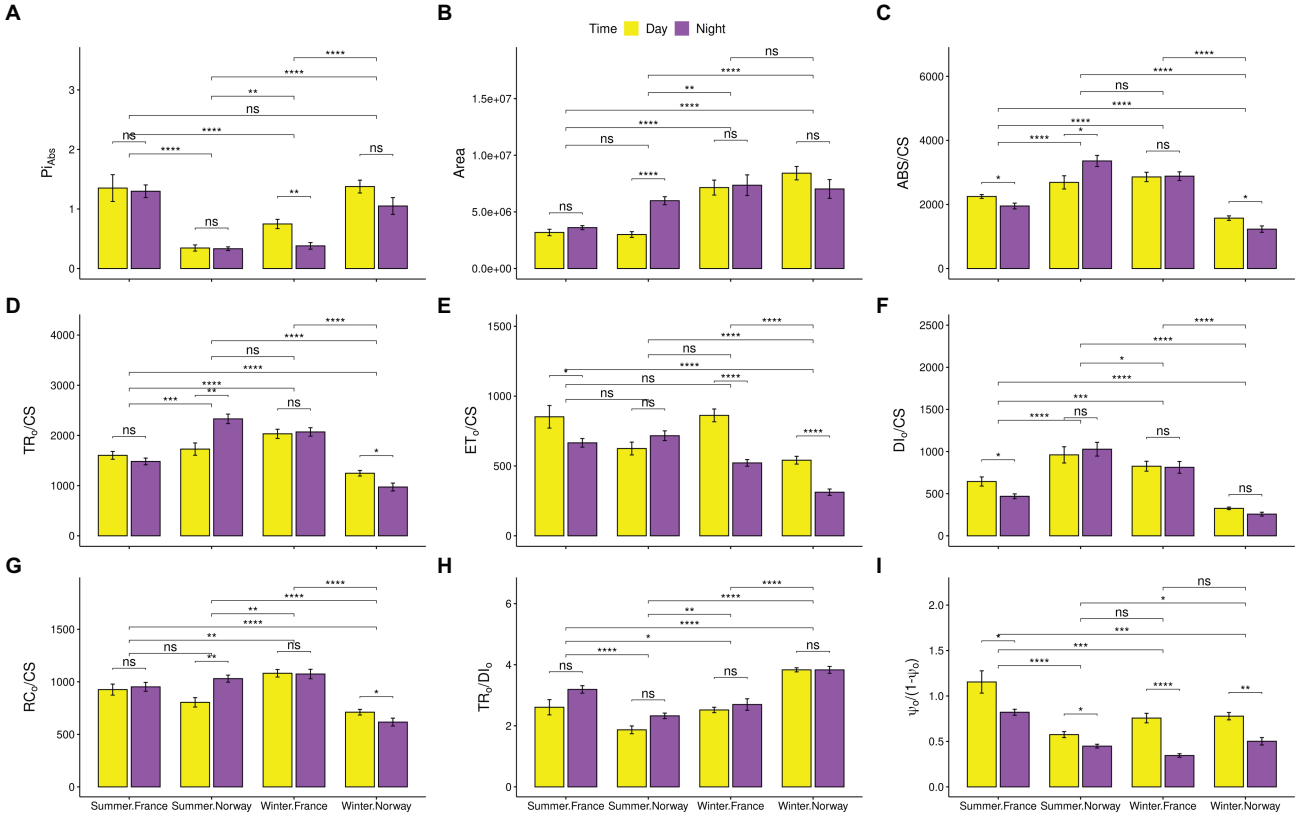

FIGURE 2 | Photosynthetic characteristics. Snapshots of photosynthetic characteristics with standard error bars and indications for significant differences between populations, day and night, or summer and winter. Significance codes after the value of *p* correction (Benjamini-Hochberg) for multiple comparisons: "<0.05": *, "<0.01": **, "<0.001": ***, "<0.0001": ****. **(A)** Index of photosynthetic performance (PI_{ABS}). **(B)** Size of the oxidized quinone pool (Area). **(C)** Absorption per excited cross-section (ABS/CS). **(D)** Trapping per excited cross-section (TR_0/CS). **(E)** Electron transport per excited cross-section (ET_0/CS), **(F)** Dissipated energy flux per excited cross section (DI_0/CS). **(G)** Oxidized reaction centers per excited cross-section (RC_0/CS). **(H)** Contribution of the light reactions to the primary photochemistry (TR_0/DI_0). **(I)** Contribution of the dark reactions to the primary photochemistry [$\Psi_0/(1-\Psi_0)$].

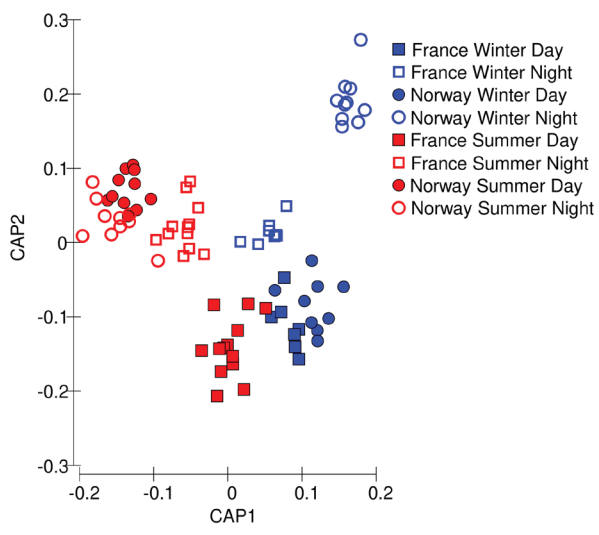

FIGURE 3 | Multivariate differences among samples in photochemical data, visualized as Euclidean distances along the first two principal coordinates.

Supplementary Figure 6), photosystem, and photosynthetic membrane (**Supplementary Figure 6**), especially during the day (**Figure 7**; **Supplementary Figures 7**,**8**). Moreover, the Norwegian summer samples showed enrichment ($p < 0.05$) of genes with significant upregulation in the fructose and mannose metabolism (ko00051; **Supplementary Figure 4**). While significantly lower expressed in winter, genes involved in photosynthesis (**Figure 7**), chlorophyll binding (**Supplementary Figure 7**), chloroplast, photosystem, and photosynthetic membrane (**Supplementary Figure 8**) were significantly upregulated in winter nights as compared with winter days. During summer nights, the Norwegian samples showed the upregulation of trehalose biosynthesis (**Figure 7**).

The carbon fixation pathway in photosynthetic organisms (ko00710; **Supplementary Figure 3**) was enriched ($p < 0.05$) for genes that were upregulated in the Norwegian samples during summer but in the French samples during winter. The French samples upregulated during winter days genes involved in oxidoreduction (**Figure 7**; **Supplementary Figure 7**), as well as chloroplast genes

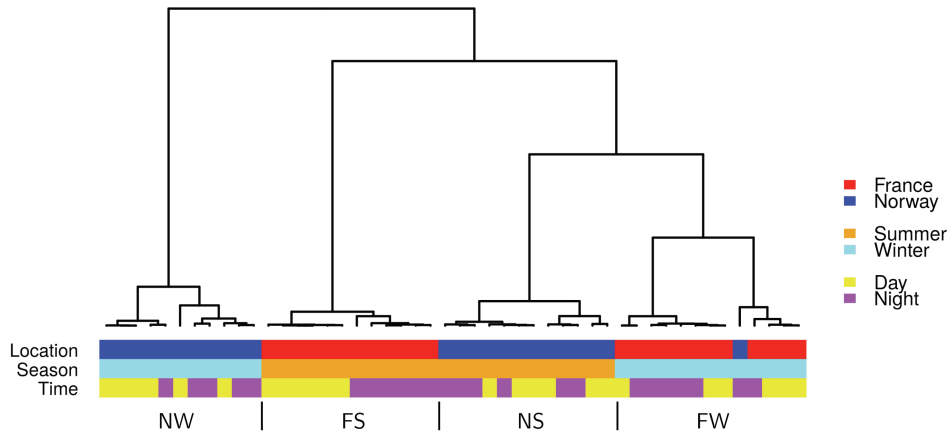

FIGURE 4 | Hierarchical cluster of all 48 samples based on the first five principal components of expression in 13,932 genes. FS: France Summer, FW: France Winter, NS: Norway Summer, NW: Norway Winter.

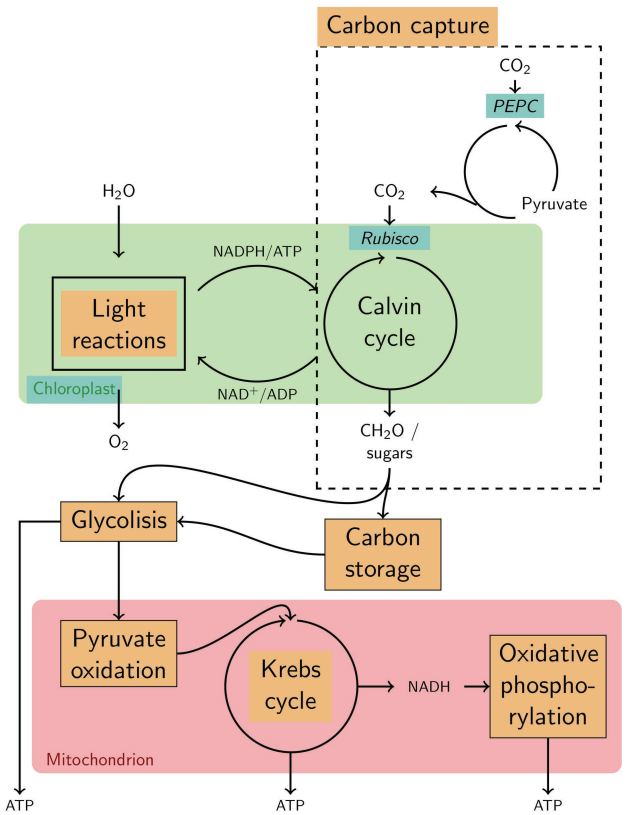

FIGURE 5 | Highly simplified overview of various functions that characterize the specificities in seasonal variation of gene expression in the Norwegian population of *Zostera marina*. Functions, enzymes and components upregulated in winter are highlighted with a blue background; such upregulated in summer are highlighted with an orange background.

(**Supplementary Figure 8**), and were enriched for upregulated genes in the pentose phosphate pathway (ko00030; **Supplementary Figure 9**).

Respiration

The French samples upregulated in winter genes related to respiration, including GO-terms of cellular respiration (**Figure 6**), mitochondria (**Supplementary Figure 6**), and oxidoreductase activity (**Supplementary Figure 10**). Moreover, the French winter samples were enriched for genes involved in glycolysis/gluconeogenesis (ko00010; **Supplementary Figure 5**).

In contrast, the Norwegian upregulated genes related to mitochondria (**Supplementary Figure 6**) and showed enrichment ($p < 0.05$) of genes with significant upregulation in glycolysis/gluconeogenesis (ko00010; **Supplementary Figure 5**) in summer. Only genes involved in the mitochondrial inner membrane were upregulated in the Norwegian samples during winter (**Supplementary Figure 8**).

Peptide Synthesis

In winter, the Norwegian samples upregulated functions and processes involved in gene expression, including peptide synthesis, translation, RNA processing (**Figure 6**), binding of nucleic acids and catalytic activities on RNA and tRNA (**Supplementary Figure 10**), as well as genes involved in intracellular organelles such as the ribosome (**Supplementary Figure 6**). During winter days, the Norwegian samples had upregulated genes involved in protein maturation, peptidyl-lysine modification (**Figure 7**), NAD^+ kinase, and phosphatidyl-inositol phospholipase C activity (**Supplementary Figure 7**).

The French samples showed diurnal changes in the expression of genes related to protein synthesis during summer, when genes involved in translation, amid biosynthesis, (**Figure 7**), as well as the ribosome (**Supplementary Figure 8**) were upregulated during the day.

DISCUSSION

Our results provide the first assessment of seasonal (and diurnal) changes in photosynthetic and genome-wide gene expression

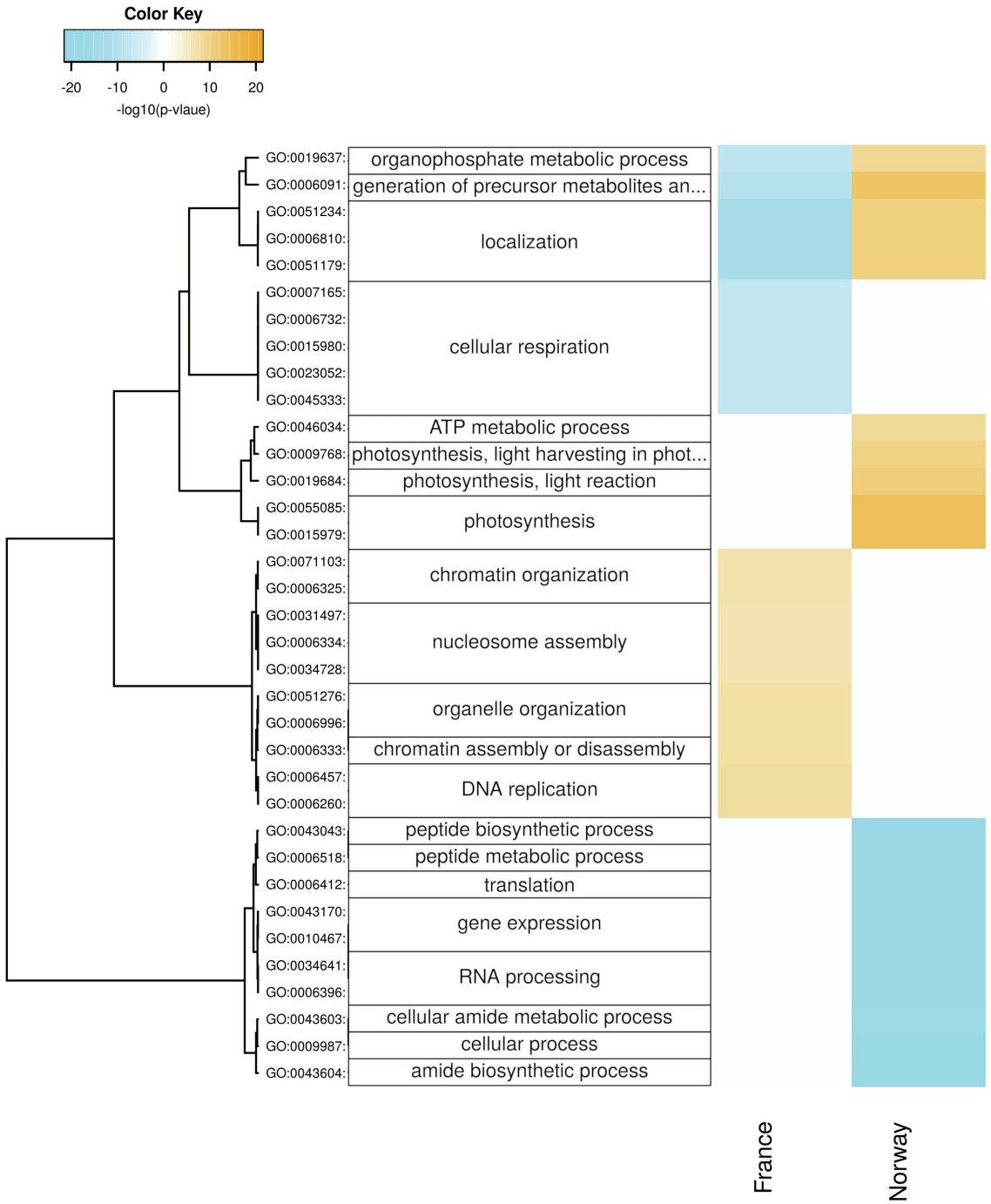

FIGURE 6 | Seasonal changes in biological processes. Enriched processes are shown for each population with positive-log10 (*p*) for genes upregulated in summer (orange) and with negative-log10 (*p*) for genes upregulated in winter (cyan). The hierarchical cluster of GO terms is based on Euclidean distance and a ward.D2 clustering algorithm (Ward's minimum variance method).

patterns specific to a population growing above the Arctic circle that contrast patterns observed in a Mediterranean (control) population. Our results indicate that adaptation to polar light regimes involves continued photosynthesis, carbon fixation and energy conservation during long winter nights, and carbon storage during the polar summer.

Strategies to Survive Long Winter Nights

Photosynthesis and Carbon Fixation in Winter

Despite reduced rhythmicity in daylight levels during the Arctic winter, our Norwegian winter samples appeared to still follow a day-night rhythm in gene expression (**Figure 1B**). Indeed, the Norwegian population showed, in contrast to the French

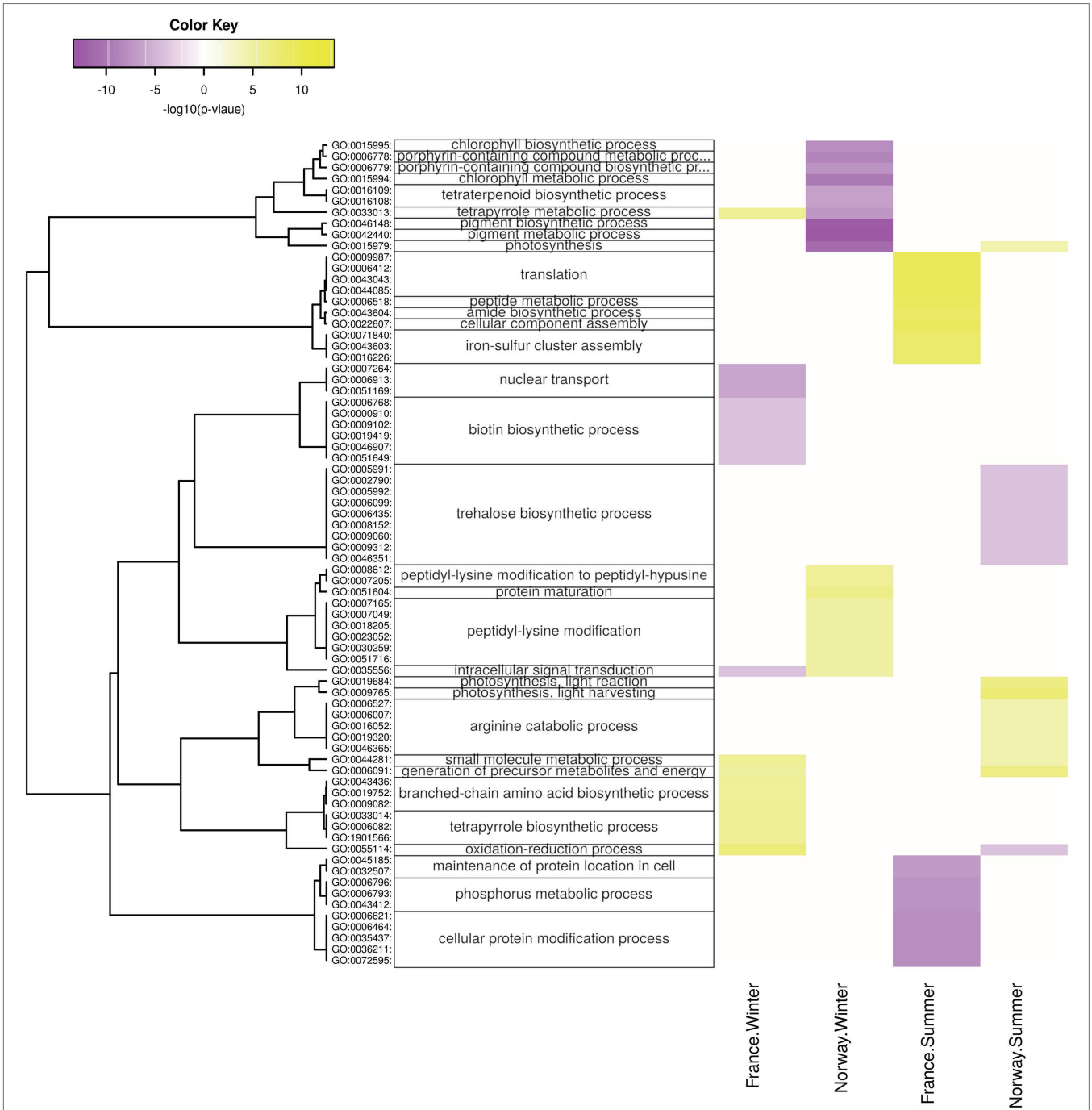

FIGURE 7 | Diurnal changes in biological processes. Enriched processes are shown for each population x season with positive-log10 (*p*) for genes upregulated at day (yellow) and with negative-log10 (*p*) for genes upregulated at night (violet). The hierarchical cluster of GO terms is based on Euclidean distance and a ward.D2 clustering algorithm (Ward's minimum variance method).

population, a far higher number of genes with diurnal expression differences during winter (3,099; **Figure 1B**) than during summer (657; **Figure 1B**). Increased night-time expression of genes related to the synthesis of chloroplasts and chlorophyll (**Figure 7**) is in line with earlier field observations of enhanced chlorophyll in winter acclimatized eelgrass (Thom et al., 2008), and suggests that the Norwegian population actively synthesizes photosynthesis-relevant proteins to capture the smallest amounts of photosynthetically active radiation in winter.

Efficient use of very dim Arctic winter light in the Norwegian samples is suggested by a significant increase in the photochemical performance index (PI_{ABS}; **Figure 2A**), and in the contribution

of both light and dark reactions (**Figures 2H,I**) to the primary photochemistry during winter. Adjustments that may contribute to photosynthesis under low light levels include an increase in chlorophyll *b* levels in comparison to chlorophyll *a*, thus increasing photosystem II antennae size, and maximizing the photon harvesting probability (Ort et al., 2011) with a simultaneous increase (by chlorophyll *b*) in the affinity for harvesting light of long wavelengths that protrudes to greater water depths (Lee et al., 2007; Eriander, 2017). Moreover, under low light levels, eelgrass plants invest more energy into vertical leaf growth, compensating the low light levels with large photosynthetic surfaces and a reduction in canopy depth (Ochieng et al., 2010; Wong et al., 2021). While energy fluxes (ABS/CS and TR_0/CS; **Figures 2C,D**) during the Norwegian winter cannot match fluxes occurring in summer, they are likely to prevent the depletion of assembled carbohydrate storages. Accordingly, winter survival of eelgrass at its lower depth distribution in the Great Bay Estuary (New Hampshire, United States), depended primarily on adaptations that allowed for continued photosynthesis under extreme low light conditions (e.g., increase in leaf size, chlorophyll a, and maximum quantum yield of PSII; Chapter IV in Ochieng, 2008). Thus, adaptation to the Arctic appears to involve seasonal acclimatization that allows to actively use the smallest amounts of winter light *via* photosynthesis.

Accordingly, the Norwegian population appears to present the physiological potential to capture carbon in winter. For example, ribulose-bisphosphate carboxylase (RuBisCO, K01601), the initial carboxylase of the Calvin cycle that fixes atmospheric CO_2, was expressed at higher levels during winter than during summer (**Figure 5**; **Supplementary Figure 3**). This contrasts with 30% under-expression of RuBisCO in *Posidonia oceanica* leaves adapted to low light-levels (Mazzuca et al., 2009) and shows that winter gene expression in an Arctic population is not comparable with gene expression characteristics of seagrass experiencing low light levels in turbid waters year-round. In addition, the enzyme RuBisCO activase, although showing significantly higher expression in the Norwegian population during summer (Zosma13g01130, **Supplementary Table 6**), was still expressed during winter (Zosma294g00110, Zosma13g01130, and Zosma88g00030 in **Supplementary Table 7**). The presence of this activator, which removes the RuBisCO inhibitor CAP (2-carboxylarabinitol-1,5-bisphosphate), suggests that the Norwegian population could indeed maintain carbon fixation during the dark winter period. If increased RuBisCO expression in Norwegian winter samples is related to cold-acclimation, as shown in maize (Salesse-Smith et al., 2020), then warmer winters could hinder carbon assimilation and, thus, survival in the future Arctic.

Furthermore, the Norwegian winter samples had upregulated the enzyme phosphoenolpyruvate carboxylase (PEPC, K01595; **Figure 5**), which can catalyze CO_2 fixation with phosphoenolpyruvate to produce oxaloacetate and inorganic phosphate. This suggests that *Z. marina*, although being characterized as a C3 plant that fixes CO_2 primarily *via* RuBisCo (Koch et al., 2013), can fix some carbon during winter independent from photosynthesis, although at much lower levels than RuBisCo would allow (Raven and Farquhar, 1990). PEPC CO_2 fixation is not uncommon in C3 plants (Chi et al., 2014), given that enzymes involved in the C4 photosynthetic biochemistry have functions in C3 plants other than in C4 photosynthesis, including the supply of carbon skeletons (*via* the intermediates oxaloacetate and malate) to the citric acid cycle (Lepiniec et al., 1994; Aubry et al., 2011; **Figure 5**) for the formation of new tissue. Thus, we suggest that PEP-carboxylase may present a key enzyme that allows for winter growth by decoupling photosynthesis and biomass formation not only in polar algae (Wiencke et al., 2007, 2009) but also in Arctic eelgrass.

Active growth in winter would explain the presence of freshly grown seagrass leaves in the dark season in the Norwegian population (**Supplementary Figure 11**). Eelgrass reaches light saturation between ca. 70 and 900 $\mu mol\, m^{-2}\, s^{-1}$, and compensation above ca. 1–36 $\mu mol\, m{-}^{2}\, s^{-1}$ (Ochieng, 2008). Given that photosynthetically active radiation exceeded 10 $\mu mol\, m^{-2}\, s^{-1}$ in the Norwegian population only for short mid-day periods on two December days in 2016 (**Supplementary Table 1**), photosynthesis-driven carbon dioxide assimilation is expected to be very low in the Norwegian winter.

Winter growth, therefore, is expected as a result of light-independent carbon fixation and the usage of stored carbohydrates mobilized from below-ground tissues (Burke et al., 1996). For example, strong activation of sucrose synthase, of which the products can drive many metabolic pathways, has been shown in sink-tissues of eelgrass under negative carbon balances (Alcoverro et al., 1999). Sustained growth during periods of negative carbon balance (respiratory C loss exceeding photosynthetic C gain) – fueled by mobilized carbohydrate storages – has been shown in both eelgrass (Wium-Andersen and Borum, 1984; Olesen and Sand-Jensen, 1993), and the Mediterranean seagrass *P. oceanica* (Alcoverro et al., 2001). In conclusion, our results suggest that the use of low light levels and light-independent carbon fixation count among the adaptations that allow for eelgrass to grow during winter without fully depleting their stored carbohydrates.

Energy Conservation Strategies in Winter

The Norwegian population appears to conserve energy during winter, as indicated by a significant reduction in all photosynthetic energy fluxes (ABS/CS, TR_0/CS and ET_0/CS; **Figures 2C–E**), resulting in a significantly reduced loss of energy *via* dissipation (DI_0/CS; **Figure 2F**). Such state of metabolic dormancy, limiting the enzymatic reactions of photosynthesis, may be adaptive to the combination of low light availability and low winter temperatures.

Moreover, the respiratory breakdown of carbohydrates must have been reduced in the Norwegian population during winter, given that genes related to glycolysis, ATP metabolism (**Figure 6**; **Supplementary Figure 5**), and the fructose and mannose metabolism (**Supplementary Figure 4**; e.g., fructose-bisphosphate-aldolase K01623; **Figures 6, 7**) were downregulated. Accordingly, while upregulated during winter in the French population (**Figure 6**), genes involved in cellular respiration were significantly downregulated in the Norwegian population during winter (e.g.,

malate dehydrogenase, pyruvate dehydrogenase, and Cytochrome c oxidase subunit 5b; **Supplementary Table 6**; **Figure 6**), suggesting a shutdown of catabolic pathways during the Norwegian winter. Thus, our results provide the first molecular support for winter-acclimatization in eelgrass that explains an increase in photosynthesis-to-respiration ratios, in line with reports of a greater net primary productivity in eelgrass acclimatized to winter than to summer conditions (Thom et al., 2008). Acclimatization of eelgrass to low light conditions, further involves reduced rhizome and root growth, lower production of new shoots through lateral branching, shoot density, biomass, and sheath length (Ochieng et al., 2010; Wong et al., 2021), all of which reduce the respiratory burden. Furthermore, active reduction in respiration rates likely accompanies other factors, such as increased chlorophyll *a* content and lower epiphytic growth, in photo-adaptive processes that are involved in lowering light-saturation and compensation points in winter-acclimatized eelgrass (Ochieng, 2008; Thom et al., 2008). Such seasonal acclimatization may to some degree counteract the respiratory burden of rising temperatures by decreasing respiration rates and critical light requirements (Zimmerman et al., 1989; Staehr and Borum, 2011).

Glycolysis (**Figure 5**; **Supplementary Figure 5**) is a catabolic pathway providing energy in the form of NADH, ATP, and pyruvate, the latter being further catabolized in the citric acid cycle as part of oxidative respiration. Its downregulation during winter in this study contrasts with upregulation of genes involved in carbohydrate catabolism (e.g., 1-fructose-bisphosphate aldolase) in low-light adapted seagrass leaves of the species *P. oceanica* (Mazzuca et al., 2009). Downregulation in our study may be explained by the ability of our low-light (winter) eelgrass to build up carbon storages during summer and, thus, to obtain carbon-storages during winter from storage tissues such as roots and rhizomes, instead of from the above-ground leaf tissue. In other words, while carbon catabolism was low in the seagrass leaves, we cannot know what processes were active in the below-ground organs, in which sucrose and starch can be depleted by 50 and 23%, respectively, after a 3-week shading period (Eriander, 2017).

That carbon storages were built up over summer was suggested by the significantly increased expression of enzymes involved in carbon fixation (**Supplementary Figure 3**) and by significantly increased summer expression of two genes encoding for sucrose-phosphate synthase (Zosma255g00080, Zosma87g00120, **Supplementary Table 6**). This enzyme is involved in the synthesis of sucrose, the dominant storage carbohydrate in seagrasses (Touchette and Burkholder, 2000). Reduced carbohydrate cleavage in the sampled winter leaves is likely to contribute to the ability of the Norwegian population to survive long dark periods as the reduced demand for metabolic energy prevents depletion of carbon storages.

Carbon Storage and Stress Under Polar Summer Light

Upregulation of photosynthesis-related genes in the Norwegian population during summer (**Figure 6**) was also shown in the seagrass *P. oceanica* when exposed to high light levels (Dattolo et al., 2014) and is likely to enable the plants to process the increased amount of captured light energy (Walters, 2005). Upregulation of genes with functions in carbon capture during summer in the Norwegian (but not the French) samples (**Supplementary Figure 3**) is necessary for the rapid build-up of stored carbohydrates during the short summer period, and provides a molecular explanation for increasing autumn starch content with latitude (in *Zostera noltii*; Soissons et al., 2018).

Surprisingly, the light intensity at the Norwegian sampling site showed a clear day-night rhythm during summer. Even though the summer sun does not set below the horizon, shading by mountain ridges and the low sun angle during night-time appears to create a short, but clearly noticeable drop in available photosynthetically active radiation. This diurnal light rhythm was paralleled by diurnal changes in gene expression. For example, the daytime upregulation of arginine catabolism (**Figure 7**) may mobilize nitrogen storages and thus, allow for active growth under nitrogen limitation (Winter et al., 2015). In addition, the nighttime upregulation of trehalose biosynthesis (**Figure 7**), in which the intermediate compound trehalose-6-phosphate acts as a sensor for available sucrose, is likely involved in the regulation of sucrose-levels that have built up over the day (Lunn et al., 2014; Figueroa and Lunn, 2016) and plays a role in plant growth, development, and protection against various environmental stressors (Lunn et al., 2014; Joshi et al., 2020). Thus, the diurnal changes in gene expression during summer are likely related to active growth and processing of assembled sugars. Local geography, e.g., the presence of mountain ridges, may play an important role in allowing eelgrass to process a dark phase in high latitudes.

Despite diurnal fluctuations in daylight levels, the lack of complete darkness during summer significantly lowers the photosynthetic performance (PI_{ABS}) of the Norwegian samples (**Figure 2A**), in contrast to the seasonal change in photosynthetic performance in the French population (with significantly higher values during summer: **Figure 2A**). Particularly during summer nights, the Norwegian population showed a significant increase in absorbed (ABS/CS; **Figure 2C**), trapped (TR_0/CS; **Figure 2D**), and electron transport (ET_0/CS) energy fluxes, as well as the size of the oxidized quinone pool (ABS) and the number of oxidized reaction centers per leaf cross section (RC_0/CS; **Figure 2G**). Although these photosynthetic adjustments increase the light harvesting ability and efficiency to use low-light, the Norwegian samples also showed a significant increase in energy dissipation (DI/CS), suggesting an inability to use excessive amounts of light energy in summer.

Low light intensities during the polar summer nights appear to have allowed the Norwegian plants to process a dark phase to recycle intermediates of the Krebs cycle (such as malic acid) that are consumed during the light phase of photosynthesis. The dark phase is triggered by an inhibitor (2-carboxylarabinitol-1,5-bisphosphate, CAP) that is only produced under low light when the chloroplast pH shifts from acid to basic. It was not found in any of the genes showing diurnal differential expression (**Supplementary Table 7**). A crucial limit to the northward shift of seagrass may be set by the latitude at which the sunlight is too strong to allow the procession of a dark phase. The

existence and identification of this latitude, however, relies on future studies involving transplant experiments to a range of increasing latitudes.

The Metabolic Dilemma of Carbon Storage Tissue

Our findings suggest that eelgrass can store sufficient energy reserves to survive dark periods lasting longer than those at 67°N (our Norwegian sampling site). In fact, if sugar levels were depleted in mid-winter, we would have expected to see an upregulation of genes involved in protein degradation, as autophagic protein degradation has been suggested as an alternative energy source under sugar depletion in eelgrass (Mochida et al., 2019). As the expected upregulation was not observed, a poleward shift of eelgrass should not be hindered by the potential to store sufficient photosynthates. In order to test this hypothesis, future studies must evaluate carbohydrate reserves in autumn, a good indicator of winter survival in the seagrass *Zostera noltii* (Govers et al., 2015), and reserve depletion over long dark periods directly in below-ground rhizomes.

While energy storing rhizomes allow eelgrass to survive dark periods, they also represent respiratory burdens that can increase light requirements, potentially preventing poleward migration (Olesen and Sand-Jensen, 1993; Lee et al., 2007). This is particularly true as respiration increases under rising temperatures (Lee et al., 2007; McMinn and Martin, 2013), faster than photosynthesis (higher Q10; Thom et al., 2008; Staehr and Borum, 2011). The respiratory demands of seagrass roots and rhizomes explain the relatively high amounts of light (10–30% surface irradiance; Ochieng et al., 2010) required for long-term survival, as compared with 1–5% for many species of phytoplankton and algae (Kenworthy and Fonseca, 1996). Below-ground rhizomes in eelgrass consume up to 15% of the carbon fixed, and up to 25% at the deepest range-margin (Kraemer and Alberte, 1993). Moreover, even if carbohydrate concentrations are not depleted, seagrass originating from 36°N cannot survive extreme experimental winter light limitation (2 h irradiance saturated photosynthesis), presumably through the effects of anoxia on increased translocation of energy reserves (Alcoverro et al., 1999). Thus, increasing carbohydrate storage does not guarantee long-term survival in the dark.

The need of eelgrass to elevate carbon storage in warming Arctic oceans may be lowered by thermal acclimatization that increases respiratory energy efficiency, as has been shown in terrestrial Arctic tundra species (Kornfeld et al., 2013), or by increasing CO_2 levels (Zimmerman et al., 1997). Eelgrass is generally carbon limited, because it cannot efficiently use the inorganic carbon from the water column ($HCO3^-$; Lee et al., 2007). Thus, increasing CO_2 levels are expected to increase photosynthetic rates without affecting respiration (Zimmerman et al., 1997). If turbidity does not hinder long-term survival (Moore et al., 1997) in the future Arctic, increasing CO_2 levels will reduce the need for producing high below-ground biomass by shortening the seasonal period during which eelgrass experiences a negative carbon balance.

Conclusion and Perspectives

In this study, we show that distinct seasonal expression patterns of an eelgrass population from the Norwegian subarctic are driven by genes encoding functions of the organelles (chloroplast and mitochondrion). These are likely to provide key physiological adaptations that allow eelgrass to endure the polar dark season, and suggest metabolic strategies to enhance restoration success in turbid waters. The two most prominent features were:

1. Active carbon capture in winter. Winter expression of genes encoding for functions related to carbon capture, including Rubisco and PEP-carboxylase (**Figure 5**), may allow for eelgrass growth and carbon fixation during the polar dark season. This resembles the season-anticipator strategy of polar algae to fix carbon and grow even under the ice during Arctic darkness when nutrient conditions are highest (Berge et al., 2015).
2. Metabolic dormancy in winter. Downregulation of genes related to cellular respiration/carbohydrate cleavage provides the first molecular support for winter-acclimatization in eelgrass that explains an increase in photosynthesis-to-respiration ratios as compared with summer conditions (Thom et al., 2008) and is likely to prevent depletion of carbohydrate storages during the dark period.

This study alone, based on two meadows and an assessment of metabolic and transcriptomic responses, does not allow us to predict whether eelgrass will be able to migrate poleward into a warming, ice-free Arctic. Although this study reveals specificities that are functionally relevant at the species' current northernmost range of distribution, its potential to migrate further poleward depends on the plastic and/or adaptive potential of the identified key functions. While genetic adaptations would rely on standing genetic diversity that allows for evolutionary change over several generations, acclimatization – which can build up within the lifetime of an organism (Kelly et al., 2012; Donelson et al., 2019) – would allow eelgrass to immediately occupy niches that open up in the Arctic. For example, in the seagrass *Thalassia testudinum*, phenotypic variation among subpopulations across an environmental gradient in the Florida Bay were mainly ascribed to phenotypic plasticity because gene flow was high within 50 km distance (Bricker et al., 2011). Further studies are needed to identify to what degree the north–south differences that we identified result from acclimatization or genetic adaptation (**Box 1**):

1. Reciprocal transplantation of individuals between northern to southern latitudes would allow to identify genetic adaptations as features in photosynthesis and gene expression as such remaining distinct in northern/southern populations and adaptive to northern/southern latitudes even one or more generations after the populations had been transplanted (to minimize non-genetic confounding effects; Kawecki and Ebert, 2004; Pazzaglia et al., 2021).
2. Genetic tests for outlier loci will identify genomic regions that have responded to natural selection in polar regions with exceptionally low allelic variation in 2 high-latitude populations and high genetic divergence from 2 low-latitude

populations (Luikart et al., 2003; Narum and Hess, 2011). Functions associated with genes located in these regions are likely to have adapted genetically to polar conditions. For example, outlier tests identified genes related to growth and immunity as putatively adaptive to varying temperature and light conditions along latitudinal and bathymetric gradients in the seagrass *P. oceanica* (Jahnke et al., 2019).

In order to test whether the reaction norm of eelgrass is wide enough to acclimatize to a warming Arctic, we need to expose eelgrass to a simulation of near-future polar conditions. For example, seagrass meadows in Australia (*Halodule pinifolia* and *Halophila ovalis*) were shown to die at >38 days at 0.1 mol photons m^{-2} d^{-1} (0.35% SI; Longstaff and Dennison, 1999). To determine the latitude at which eelgrass would lack sufficient daylight throughout the year, we would need an equivalent study that imitates future temperature and CO_2 levels at different daylight lengths in a common-garden setup and, ideally, includes a variety of genotypes – since these can differ in their dark tolerance (Salo et al., 2015).

DATA AVAILABILITY STATEMENT

The datasets presented in this study can be found in online repositories. The names of the repository/repositories and accession number(s) can be found at:

https://figshare.com/projects/Adaptation_of_temperate_seagrass_to_Arctic_light_relies_on_seasonal_acclimatization_of_carbon_capture_and_metabolism/117825

https://www.ncbi.nlm.nih.gov/, PRJNA745558

https://dataview.ncbi.nlm.nih.gov/object/PRJNA745558?reviewer=d8qlenvsni8uvdohe3mik9n00s.

AUTHOR CONTRIBUTIONS

GH (project leader) and AJ planned the project and designed the sampling design. AJ, GH, and SA-H collected the shoots. AJ and BD analyzed the data and wrote the manuscript. JC performed the RNA extraction. MK and IS performed the library preparation and sequencing. SA-H, JO, and Z-MH were involved in data interpretation. All authors contributed to the article and approved the submitted version.

FUNDING

This work was funded by the Norwegian Research Council (Havkyst project 243916). JC was supported by a visiting researcher grant from the Norwegian Research Council (project 281153). Research in the Marine and Environmental Sciences Centre (MARE) was funded by "Fundação para a Ciência e Tecnologia (FCT)" UIDB/04292/2020 and Mar2020 program (VALPRAD project, MAR-01.04.02-FEAMP-0007). BD was supported by FCT throughout an Investigator Contract (CEECIND/03869/2018).

SUPPLEMENTARY MATERIAL

The Supplementary Material for this article can be found online at https://www.frontiersin.org/articles/10.3389/fpls.2021.745855/full#supplementary-material

REFERENCES

Alcoverro, T., Manzanera, M., and Romero, J. (2001). Annual metabolic carbon balance of the seagrass *Posidonia oceanica*: The importance of carbohydrate reserves. *Mar. Ecol. Prog. Ser.* 211, 105–116. doi: 10.3354/meps211105

Alcoverro, T., Zimmerman, R. C., Kohrs, D. G., and Alberte, R. S. (1999). Resource allocation and sucrose mobilization in light-limited eelgrass *Zostera marina*. *Mar. Ecol. Prog. Ser.* 187, 121–131. doi: 10.3354/meps187121

Alexa, A., and Rahnenführer, J. (2010). Enrichment analysis for Gene Ontology. R Packag. "topGO" v2.16.0. Available at: http://www.bioconductor.org/packages/2.11/bioc/html/topGO.html (Accessed November 02, 2020).

Aubry, S., Brown, N. J., and Hibberd, J. M. (2011). The role of proteins in C 3 plants prior to their recruitment into the C 4 pathway. *J. Exp. Bot.* 62, 3049–3059. doi: 10.1093/jxb/err012

Benjamini, Y., and Hochberg, Y. (1995). Controlling the false discovery rate - a practical and powerful approach to multiple testing. *J. R. Stat. Soc. Ser. B* 57, 289–300. doi: 10.2307/2346101

Bennett, B. D., and Bushel, P. R. (2017). goSTAG: gene ontology subtrees to tag and annotate genes within a set. *Source Code Biol. Med.* 12, 6–13. doi: 10.1186/s13029-017-0066-1

Berge, J., Renaud, P. E., Darnis, G., Cottier, F., Last, K., Gabrielsen, T. M., et al. (2015). In the dark: A review of ecosystem processes during the Arctic polar night. *Prog. Oceanogr.* 139, 258–271. doi: 10.1016/j.pocean.2015.08.005

Blok, S. E., Olesen, B., and Krause-jensen, D. (2018). Life history events of eelgrass *Zostera marina* L. populations across gradients of latitude and temperature. *Mar. Ecol. Prog. Ser.* 590, 79–93. doi: 10.3354/meps12479

Boström, C., Roos, C., and Rönnberg, O. (2004). Shoot morphometry and production dynamics of eelgrass in the northern Baltic Sea. *Aquat. Bot.* 79, 145–161. doi: 10.1016/j.aquabot.2004.02.002

Bricker, E., Waycott, M., Calladine, A., and Zieman, J. C. (2011). High connectivity across environmental gradients and implications for phenotypic plasticity in a marine plant. *Mar. Ecol. Prog. Ser.* 423, 57–67. doi: 10.3354/meps08962

Burke, M. K., Dennison, W. C., and Moore, K. A. (1996). Non-structural carbohydrate reserves of eelgrass *Zostera marina*. *Mar. Ecol. Prog. Ser.* 137, 195–201. doi: 10.3354/meps137195

Burrows, M. T., Schoeman, D. S., Buckley, L. B., Moore, P., Poloczanska, E. S., Brander, K. M., et al. (2011). The pace of shifting climate in marine and terrestrial ecosystems. *Science* 334, 652–655. doi: 10.1126/science.1210288

Bussotti, F., Desotgiu, R., Pollastrini, M., and Cascio, C. (2010). The JIP test: a tool to screen the capacity of plant adaptation to climate change. *Scand. J. For. Res.* 25, 43–50. doi: 10.1080/02827581.2010.485777

Cai, Q., Wang, J., Beletsky, D., Overland, J. E., Ikeda, M., and Wan, L. (2021). Summer Arctic Sea ice decline during 1850-2017 and the amplified Arctic warming during the recent decades. *Environ. Res. Lett.* 16. doi: 10.1088/1748-9326/abdb5f

Chen, A., Li, C., Hu, W., Lau, M. Y., Lin, H., Rockwell, N. C., et al. (2014). PHYTOCHROME C plays a major role in the acceleration of wheat flowering under long-day photoperiod. *Proc. Natl. Acad. Sci. U. S. A.* 111, 10037–10044. doi: 10.1073/pnas.1409795111

Cheung, W. W. L., Lam, V. W. Y., Sarmiento, J. L., Kearney, K., Watson, R., and Pauly, D. (2009). Projecting global marine biodiversity impacts under climate change scenarios. *Fish Fish.* 10, 235–251. doi: 10.1111/j.1467-2979.2008.00315.x

Chi, S., Wu, S., Yu, J., Wang, X., Tang, X., and Liu, T. (2014). Phylogeny of C4-photosynthesis enzymes based on algal transcriptomic and genomic data supports an archaeal/proteobacterial origin and multiple duplication for most C4-related genes. *PLoS One* 9, e110154. doi: 10.1371/journal.pone.0110154

Clarke, K. R., and Gorley, R. N. (2005). PRIMER 6: Getting Started with v6. researchgate.net, 1–12. Available at: https://www.researchgate.net/file.PostFileLoader.html?id=5656d8ce5dbbbdcba28b459f&assetKey=AS:299979836018691@1448532174760 (Accessed April 12, 2021).

Clausen, K. K., and Clausen, P. (2013). Earlier Arctic springs cause phenological mismatch in long-distance migrants. *Oecologia* 173, 1101–1112. doi: 10.1007/s00442-013-2681-0

Clausen, K. K., Krause-Jensen, D., Olesen, B., and Marbà, N. (2014). Seasonality of eelgrass biomass across gradients in temperature and latitude. *Mar. Ecol. Prog. Ser.* 506, 71–85. doi: 10.3354/meps10800

Colarusso, (2007). Natural and stress-induced changes in non-structural carbohydrate concentrations in eelgrass {Zostera marina L.). Ph. D. thesis, Marine Science Center, Northestern University, Nahant Massachusetts, USA, 88.

Creswell, L. (2010). Phytoplankton culture for aquaculture feed. *South. Reg. Aquac. Cent.*, 1–55.

Cruz de Carvalho, R., Feijão, E., Kletschkus, E., Marques, J. C., Reis-Santos, P., Fonseca, V. F., et al. (2020). Halophyte bio-optical phenotyping: A multivariate photochemical pressure index (multi-PPI) to classify salt marsh anthropogenic pressures levels. *Ecol. Indic.* 119, 106816. doi: 10.1016/j.ecolind.2020.106816

Dattolo, E., Ruocco, M., Brunet, C., Lorenti, M., Lauritano, C., D'Esposito, D., et al. (2014). Response of the seagrass *Posidonia oceanica* to different light environments: insights from a combined molecular and photo-physiological study. *Mar. Environ. Res.* 101, 225–236. doi: 10.1016/j.marenvres.2014.07.010

Dennison, W., and Alberte, R. (1985). Role of daily light period in the depth distribution of *Zostera marina* (eelgrass). *Mar. Ecol. Prog. Ser.* 25, 51–61. doi: 10.3354/meps025051

Dobin, A., Davis, C. A., Schlesinger, F., Drenkow, J., Zaleski, C., Jha, S., et al. (2013). STAR: Ultrafast universal RNA-seq aligner. *Bioinformatics* 29, 15–21. doi: 10.1093/bioinformatics/bts635

Dobin, A., Gingeras, T. R., Spring, C., Flores, R., Sampson, J., Knight, R., et al. (2016). Mapping RNA-seq with STAR. *Curr. Protoc. Bioinforma.* 51, 586–597. doi: 10.1002/0471250953.bi1114s51

Donelson, J. M., Sunday, J. M., Figueira, W. F., Gaitán-Espitia, J. D., Hobday, A. J., Johnson, C. R., et al. (2019). Understanding interactions between plasticity, adaptation and range shifts in response to marine environmental change. *Philos. Trans. R. Soc. B Biol. Sci.* 374:20180186. doi: 10.1098/rstb.2018.0186

Duarte, C. M., and Krause-Jensen, D. (2017b). Export from seagrass meadows contributes to marine carbon sequestration. *Front. Mar. Sci.* 4:13. doi: 10.3389/fmars.2017.00013

Duarte, B., Pedro, S., Marques, J. C., Adão, H., and Caçador, I. (2017a). Zostera noltii development probing using chlorophyll a transient analysis (JIP-test) under field conditions: integrating physiological insights into a photochemical stress index. *Ecol. Indic.* 76, 219–229. doi: 10.1016/j.ecolind.2017.01.023

Eriander, L. (2017). Light requirements for successful restoration of eelgrass (*Zostera marina* L.) in a high latitude environment – acclimatization, growth and carbohydrate storage. *J. Exp. Mar. Bio. Ecol.* 496, 37–48. doi: 10.1016/j.jembe.2017.07.010

Figueroa, C. M., and Lunn, J. E. (2016). A tale of two sugars: Trehalose 6-phosphate and sucrose. *Plant Physiol.* 172, 7–27. doi: 10.1104/pp.16.00417

Friedlingstein, P., O'Sullivan, M., Jones, M. W., Andrew, R. M., Hauck, J., Olsen, A., et al. (2020). Global carbon budget 2020. *Earth Syst. Sci. Data* 12, 3269–3340. doi: 10.5194/essd-12-3269-2020

Gattuso, J.-P., Gentili, B., Duarte, C. M., Kleypas, J. A., Middelburg, J. J., and Antoine, D. (2006). Light availability in the coastal ocean: impact on the distribution of benthic photosynthetic organisms and contribution to primary production. *Biogeosci. Discuss.* 3, 895–959. doi: 10.5194/bgd-3-895-2006

Govers, L. L., Suykerbuyk, W., Hoppenreijs, J. H. T., Giesen, K., Bouma, T. J., and Van Katwijk, M. M. (2015). Rhizome starch as indicator for temperate seagrass winter survival. *Ecol. Indic.* 49, 53–60. doi: 10.1016/j.ecolind.2014.10.002

Green, E. P., and Short, F. (2004). World Atlas of Seagrasses. Berkeley, USA: University of California Press.

Griffin, K. L., and Heskel, M. (2013). Breaking the cycle: how light, CO_2 and O_2 affect plant respiration. *Plant Cell Environ.* 36, 498–500. doi: 10.1111/pce.12039

Heskel, M. A., Atkin, O. K., Turnbull, M. H., and Griffin, K. L. (2013). Bringing the Kok effect to light: a review on the integration of daytime respiration and net ecosystem exchange. *Ecosphere* 4, art98–art14. doi: 10.1890/ES13-00120.1

Høye, T. T., Post, E., Meltofte, H., Schmidt, N. M., and Forchhammer, M. C. (2007). Rapid advancement of spring in the high Arctic. *Curr. Biol.* 17, R449–R451. doi: 10.1016/j.cub.2007.04.047

Huffeldt, N. P. (2020). Photic barriers to Poleward range-shifts. *Trends Ecol. Evol.* 35, 652–655. doi: 10.1016/j.tree.2020.04.011

Ignatiadis, N., Klaus, B., Zaugg, J. B., and Huber, W. (2016). Data-driven hypothesis weighting increases detection power in genome-scale multiple testing. *Nat. Methods* 13, 577–580. doi: 10.1038/nmeth.3885

Jahnke, M., D'Esposito, D., Orrù, L., Lamontanara, A., Dattolo, E., Badalamenti, F., et al. (2019). Adaptive responses along a depth and a latitudinal gradient in the endemic seagrass *Posidonia oceanica*. *Heredity* 122, 233–243. doi: 10.1038/s41437-018-0103-0

Joshi, R., Sahoo, K. K., Singh, A. K., Anwar, K., Pundir, P., Gautam, R. K., et al. (2020). Enhancing trehalose biosynthesis improves yield potential in marker-free transgenic rice under drought, saline, and sodic conditions. *J. Exp. Bot.* 71, 653–668. doi: 10.1093/jxb/erz462

Kallio, P., and Valanne, N. (1975). "*On the Effect of Continuous Light on Photosynthesis in Mosses*," in (Springer, Berlin, Heidelberg), 149–162.

Kassambara, A. (2020). rstatix: Pipe-Friendly Framework for Basic Statistical Tests. Available at: https://cran.r-project.org/package=rstatix (Accessed September 18, 2020).

Kawecki, T. J., and Ebert, D. (2004). Conceptual issues in local adaptation. *Ecol. Lett.* 7, 1225–1241. doi: 10.1111/j.1461-0248.2004.00684.x

Kelly, S. A., Panhuis, T. M., and Stoehr, A. M. (2012). Phenotypic plasticity: molecular mechanisms and adaptive significance. *Compr. Physiol.* 2, 1417–1439. doi: 10.1002/cphy.c110008

Kenworthy, W. J., and Fonseca, M. S. (1996). Light requirements of seagrasses Halodule wrightii and Syringodium filiforme derived from the relationship between diffuse light attenuation and maximum depth distribution. *Estuaries* 19, 740–750. doi: 10.2307/1352533

Koch, M., Bowes, G., Ross, C., and Zhang, X. H. (2013). Climate change and ocean acidification effects on seagrasses and marine macroalgae. *Glob. Chang. Biol.* 19, 103–132. doi: 10.1111/j.1365-2486.2012.02791.x

Kornfeld, A., Heskel, M., Atkin, O. K., Gough, L., Griffin, K. L., Horton, T. W., et al. (2013). Respiratory flexibility and efficiency are affected by simulated global change in Arctic plants. *New Phytol.* 197, 1161–1172. doi: 10.1111/nph.12083

Kraemer, G. P., and Alberte, R. S. (1993). Age-related patterns of metabolism and biomass in subterranean tissues of *Zostera marina* (eelgrass). *Mar. Ecol. Prog. Ser.* 95, 193–203. doi: 10.3354/meps095193

Krause-Jensen, D., and Duarte, C. M. (2014). Expansion of vegetated coastal ecosystems in the future Arctic. *Front. Mar. Sci.* 1:77. doi: 10.3389/fmars.2014.00077

Larsson, J. (2019). eulerr: Area-Proportional Euler and Venn Diagrams with Ellipses. R package version 6.0.0. Available at: https://cran.r-project.org/package=eulerr (Accessed November 10, 2020).

Lê, S., Josse, J., and Husson, F. (2008). FactoMineR: an R package for multivariate analysis. *J. Stat. Softw.* 35, 253–258. doi: 10.1016/j.envint.2008.06.007

Lee, K. S., Park, S. R., and Kim, Y. K. (2007). Effects of irradiance, temperature, and nutrients on growth dynamics of seagrasses: a review. *J. Exp. Mar. Bio. Ecol.* 350, 144–175. doi: 10.1016/j.jembe.2007.06.016

Lepiniec, L., Vidal, J., Chollet, R., Gadal, P., and Crétin, C. (1994). Phosphoenolpyruvate carboxylase: structure, regulation and evolution. *Plant Sci.* 99, 111–124. doi: 10.1016/0168-9452(94)90168-6

Liao, Y., Smyth, G. K., and Shi, W. (2019). The R package Rsubread is easier, faster, cheaper and better for alignment and quantification of RNA sequencing reads. *Nucleic Acids Res.* 47:e47. doi: 10.1093/nar/gkz114

Longstaff, B. J., and Dennison, W. C. (1999). Seagrass survival during pulsed turbidity events: The effects of light deprivation on the seagrasses *Halodule pinifolia* and *Halophila ovalis*. *Aquat. Bot.* 65, 105–121. doi: 10.1016/S0304-3770(99)00035-2

Love, M. I., Huber, W., and Anders, S. (2014). Moderated estimation of fold change and dispersion for RNA-seq data with DESeq2. *Genome Biol.* 15, 550. doi: 10.1186/s13059-014-0550-8

Luikart, G., England, P. R., Tallmon, D., Jordan, S., and Taberlet, P. (2003). The power and promise of population genomics: from genotyping to genome typing. *Nat. Rev. Genet.* 4, 981–994. doi: 10.1038/nrg1226

Lunn, J. E., Delorge, I., Figueroa, C. M., Van Dijck, P., and Stitt, M. (2014). Trehalose metabolism in plants. *Plant J.* 79, 544–567. doi: 10.1111/tpj.12509

Luo, W., and Brouwer, C. (2013). Pathview: An R/bioconductor package for pathway-based data integration and visualization. *Bioinformatics* 29, 1830–1831. doi: 10.1093/bioinformatics/btt285

Luo, W., Friedman, M. S., Shedden, K., Hankenson, K. D., and Woolf, P. J. (2009). GAGE: generally applicable gene set enrichment for pathway analysis. *BMC Bioinformatics* 10:161. doi: 10.1186/1471-2105-10-161

Mazzuca, S., Spadafora, A., Filadoro, D., Vannini, C., Marsoni, M., Cozza, R., et al. (2009). Seagrass light acclimation: 2-DE protein analysis in Posidonia leaves grown in chronic low light conditions. *J. Exp. Mar. Bio. Ecol.* 374, 113–122. doi: 10.1016/j.jembe.2009.04.010

McMahon, C. R., and Hays, G. C. (2006). Thermal niche, large-scale movements and implications of climate change for a critically endangered marine vertebrate. *Glob. Chang. Biol.* 12, 1330–1338. doi: 10.1111/j.1365-2486.2006.01174.x

McMinn, A., and Martin, A. (2013). Dark survival in a warming world. *Proc. R. Soc. Biol. Sci.* 280:20122909. doi: 10.1098/rspb.2012.2909

Melbourne-Thomas, J., Audzijonyte, A., Brasier, M. J., Cresswell, K., Fogarty, H. E., Haward, M., et al. (2020). Poleward bound: adapting to climate-driven species redistribution. *Rev. Fish Biol. Fish.* doi: 10.1007/s11160-021-09641-3 [Epub ahead of print]

Messiaen, G., Mortreux, S., Le Gall, P., Crottier, A., and Lagarde, F. (2018). Marine environmental station database of Thau lagoon. *Seanoe*. doi: 10.17882/52404

Mochida, K., Hano, T., Onduka, T., Ito, K., and Yoshida, G. (2019). Physiological responses of eelgrass (*Zostera marina*) to ambient stresses such as herbicide, insufficient light, and high water temperature. *Aquat. Toxicol.* 208, 20–28. doi: 10.1016/j.aquatox.2018.12.018

Moore, K. A., Orth, R. J., and Nowak, J. F. (1993). Environmental regulation of seed germination in *Zostera marina* L. (eelgrass) in Chesapeake Bay: effects of light, oxygen and sediment burial. *Aquat. Bot.* 45, 79–91. doi: 10.1016/0304-3770(93)90054-Z

Moore, K. A., Wetzel, R. L., and Orth, R. J. (1997). Seasonal pulses of turbidity and their relations to eelgrass (*Zostera marina* L.) survival in an estuary. *J. Exp. Mar. Bio. Ecol.* 215, 115–134. doi: 10.1016/S0022-0981(96)02774-8

Murtagh, F., and Legendre, P. (2014). Ward's hierarchical agglomerative clustering method: which algorithms implement Ward's criterion? *J. Classif.* 31, 274–295. doi: 10.1007/s00357-014-9161-z

Narum, S. R., and Hess, J. E. (2011). Comparison of FST outlier tests for SNP loci under selection. *Mol. Ecol. Resour.* 11, 184–194. doi: 10.1111/j.1755-0998.2011.02987.x

Novak, A. B., Pelletier, M. C., Colarusso, P., Simpson, J., Gutierrez, M. N., Arias-Ortiz, A., et al. (2020). Correction to: factors influencing carbon stocks and accumulation rates in eelgrass meadows Across New England, USA. *Estuar. Coasts* 43, 2183–2184. doi: 10.1007/s12237-020-00815-z (Estuaries and Coasts, (2020), 43, 8, (2076–2091), 10.1007/s12237-020-00754-9)

Ochieng, C. A. (2008). Suvival Strategies of Eelgrass in Reduced Light. Vasa. Available at: http://medcontent.metapress.com/index/A65RM03P4874243N.pdf (Accessed March 08, 2021).

Ochieng, C. A., Short, F. T., and Walker, D. I. (2010). Photosynthetic and morphological responses of eelgrass (*Zostera marina* L.) to a gradient of light conditions. *J. Exp. Mar. Bio. Ecol.* 382, 117–124. doi: 10.1016/j.jembe.2009.11.007

Olesen, B., Krause-Jensen, D., Marbà, N., and Christensen, P. B. P. (2015). Eelgrass *Zostera marina* in subarctic Greenland: dense meadows with slow biomass turnover in cold waters. *Mar. Ecol. Prog. Ser.* 518, 107–121. doi: 10.3354/meps11087

Olesen, B., and Sand-Jensen, K. (1993). Seasonal acclimatization of eelgrass *Zostera marina* growth to light. *Mar. Ecol. Prog. Ser.* 94, 91–99. doi: 10.3354/meps094091

Olsen, J. L., Coyer, J. A., Stam, W. T., Moy, F. E., Christie, H., and Jørgensen, N. M. (2013). Eelgrass *Zostera marina* populations in northern Norwegian fjords are genetically isolated and diverse. *Mar. Ecol. Prog. Ser.* 486, 121–132. doi: 10.3354/meps10373

Olsen, J. L., Rouzé, P., Verhelst, B., Lin, Y., Bayer, T., Collen, J., et al. (2016). The genome of the seagrass *Zostera marina* reveals angiosperm adaptation to the sea. *Nature* 530, 331–335. doi: 10.1038/nature16548

Ort, D. R., Zhu, X., and Melis, A. (2011). Optimizing antenna size to maximize photosynthetic efficiency. *Plant Physiol.* 155, 79–85. doi: 10.1104/pp.110.165886

Pazzaglia, J., Reusch, T. B. H., Terlizzi, A., Marín-Guirao, L., and Procaccini, G. (2021). Phenotypic plasticity under rapid global changes: The intrinsic force for future seagrasses survival. *Evol. Appl.* 14, 1181–1201. doi: 10.1111/eva.13212

Pérez-Silva, J. G., Araujo-Voces, M., and Quesada, V. (2018). NVenn: Generalized, quasi-proportional Venn and Euler diagrams. *Bioinformatics* 34, 2322–2324. doi: 10.1093/bioinformatics/bty109

Poloczanska, E. S., Brown, C. J., Sydeman, W. J., Kiessling, W., Schoeman, D. S., Moore, P. J., et al. (2013). Global imprint of climate change on marine life. *Nat. Clim. Chang.* 3, 919–925. doi: 10.1038/nclimate1958

R Core Team (2019). R: A Language and Environment for Statistical Computing. Available at: https://www.r-project.org/ (Accessed Febraury 05, 2021).

Ralph, P. J., Durako, M. J., Enríquez, S., Collier, C. J., and Doblin, M. A. (2007). Impact of light limitation on seagrasses. *J. Exp. Mar. Bio. Ecol.* 350, 176–193. doi: 10.1016/j.jembe.2007.06.017

Raven, J. A., and Farquhar, G. D. (1990). The influence of N metabolism and organic acid synthesis on the natural abundance of isotopes of carbon in plants. *New Phytol.* 116, 505–529. doi: 10.1111/j.1469-8137.1990.tb00536.x

Ruocco, M., De Luca, P., Marín-Guirao, L., and Procaccini, G. (2019a). Differential leaf age-dependent thermal plasticity in the keystone Seagrass *Posidonia oceanica*. *Front. Plant Sci.* 10. doi: 10.3389/fpls.2019.01556

Ruocco, M., Marín-Guirao, L., and Procaccini, G. (2019b). Within- and among-leaf variations in photo-physiological functions, gene expression and DNA methylation patterns in the large-sized seagrass *Posidonia oceanica*. *Mar. Biol.* 166, 1–18. doi: 10.1007/s00227-019-3482-8

Salesse-Smith, C. E., Sharwood, R. E., Busch, F. A., and Stern, D. B. (2020). Increased Rubisco content in maize mitigates chilling stress and speeds recovery. *Plant Biotechnol. J.* 18, 1409–1420. doi: 10.1111/pbi.13306

Salo, T., Reusch, T. B. H., and Boström, C. (2015). Genotype-specific responses to light stress in eelgrass *Zostera marina*, a marine foundation plant. *Mar. Ecol. Prog. Ser.* 519, 129–140. doi: 10.3354/meps11083

Sayols, S., Scherzinger, D., and Klein, H. (2016). dupRadar: A bioconductor package for the assessment of PCR artifacts in RNA-Seq data. *BMC Bioinformatics* 17:428. doi: 10.1186/s12859-016-1276-2

Soissons, L. M., Haanstra, E. P., Van Katwijk, M. M., Asmus, R., Auby, I., Barillé, L., et al. (2018). Latitudinal patterns in european seagrass carbon reserves: influence of seasonal fluctuations versus short-term stress and disturbance events. *Front. Plant Sci.* 9. doi: 10.3389/fpls.2018.00088

Staehr, P. A., and Borum, J. (2011). Seasonal acclimation in metabolism reduces light requirements of eelgrass (*Zostera marina*). *J. Exp. Mar. Bio. Ecol.* 407, 139–146. doi: 10.1016/j.jembe.2011.05.031

Sterck, L., Billiau, K., Abeel, T., Rouzé, P., and Van de Peer, Y. (2012). ORCAE: online resource for community annotation of eukaryotes. *Nat. Methods* 9:1041. doi: 10.1038/nmeth.2242

Sysoeva, M., Markovskaya, E., and Shibaeva, T. (2010). Plants under continuous light: A review. *Plant Stress* 4, 5–17.

Taulavuori, K., Sarala, M., and Taulavuori, E. (2010). "Growth responses of trees to arctic light environment" in *Progress in Botany* . eds. U. Lüttge, W. Beyschlag, B. Büdel and D. Francis (Berlin, Heidelberg: Springer), 157–168.

Thom, R. M., Southard, S. L., Borde, A. B., and Stoltz, P. (2008). Light requirements for growth and survival of eelgrass (*Zostera marina* L.) in Pacific northwest (USA) estuaries. *Estuar. Coasts* 31, 969–980. doi: 10.1007/s12237-008-9082-3

Touchette, B. W., and Burkholder, J. A. M. (2000). Overview of the physiological ecology of carbon metabolism in seagrasses. *J. Exp. Mar. Bio. Ecol.* 250, 169–205. doi: 10.1016/S0022-0981(00)00196-9

Trombetta, T., Vidussi, F., Mas, S., Parin, D., Simier, M., and Mostajir, B. (2019). Water temperature drives phytoplankton blooms in coastal waters. *PLoS One* 14, e0214933. doi: 10.1371/journal.pone.0214933

Walters, R. G. (2005). Towards an understanding of photosynthetic acclimation. *J. Exp. Bot.* 56, 435–447. doi: 10.1093/jxb/eri060

Ward, J. H. (1963). Hierarchical grouping to optimize an objective function. *J. Am. Stat. Assoc.* 58, 236–244. doi: 10.1080/01621459.1963.10500845

Warnes, G. R., Bolker, B., Bonebakker, L., Gentleman, R., Huber, W., Liaw, A., et al. (2020). gplots: Various R Programming Tools for Plotting Data. Available at: https://cran.r-project.org/package=gplots (Accessed June 16, 2021)..

Wernberg, T., Smale, D., and Tuya, F. (2013). An extreme climatic event alters marine ecosystem structure in a global biodiversity hotspot. *Nat. Clim.* 3, 78–82. doi: 10.1038/nclimate1627

Wiencke, C., Clayton, M. N., Gómez, I., Iken, K., Lüder, U. H., Amsler, C. D., et al. (2007). Life strategy, ecophysiology and ecology of seaweeds in polar waters. *Life Extrem. Environ.* 6, 213–244. doi: 10.1007/978-1-4020-6285-8-13

Wiencke, C., Gómez, I., and Dunton, K. (2009). Phenology and seasonal physiological performance of polar seaweeds. *Bot. Mar.* 52, 585–592. doi: 10.1515/BOT.2009.078

Wilson, K. L., and Lotze, H. K. (2019). Climate change projections reveal range shifts of eelgrass *Zostera marina* in the Northwest Atlantic. *Mar. Ecol. Prog. Ser.* 620, 47–62. doi: 10.3354/meps12973

Winter, G., Todd, C. D., Trovato, M., Forlani, G., and Funck, D. (2015). Physiological implications of arginine metabolism in plants. *Front. Plant Sci.* 6:534. doi: 10.3389/fpls.2015.00534

Wium-Andersen, G., and Borum, J. (1984). Biomass variation and autotrophic production of an epiphyte-macrophyte community in a coastal danish area: I. eelgrass (*Zostera marina* L.) biomass and net production. *Ophelia* 23, 33–46. doi: 10.1080/00785236.1984.10426603

Wong, M. C., Vercaemer, B. M., and Griffiths, G. (2021). Response and recovery of eelgrass (*Zostera marina*) to chronic and episodic light disturbance. *Estuar. Coasts* 44, 312–324. doi: 10.1007/s12237-020-00803-3

Woods, D. P., Ream, T. S., Minevich, G., Hobert, O., and Amasino, R. M. (2014). PHYTOCHROME C is an essential light receptor for photoperiodic flowering in the temperate grass, Brachypodium distachyon. *Genetics* 198, 397–408. doi: 10.1534/genetics.114.166785

Zhang, P. D., Liu, Y. S., Guo, D., Li, W. T., and Zhang, Q. (2016). Seasonal variation in growth, morphology, and reproduction of eelgrass *Zostera marina* on the eastern coast of the Shandong peninsula, China. *J. Coast. Res.* 318, 315–322. doi: 10.2112/JCOASTRES-D-14-00117.1

Zhu, X. G., Govindjee, , Baker, N. R., DeSturler, E., Ort, D. R., and Long, S. P. (2005). Chlorophyll a fluorescence induction kinetics in leaves predicted from a model describing each discrete step of excitation energy and electron transfer associated with photosystem II. *Planta* 223, 114–133. doi: 10.1007/s00425-005-0064-4

Zimmerman, R. C., Kohrs, D. G., Steller, D. L., and Alberte, R. S. (1997). Impacts of CO2 enrichment on productivity and light requirements of eelgrass. *Plant Physiol.* 115, 599–607. doi: 10.1104/pp.115.2.599

Zimmerman, R. C., Smith, R. D., and Alberte, R. S. (1989). Thermal acclimation and whole-plant carbon balance in *Zostera marina* L. (eelgrass). *J. Exp. Mar. Bio. Ecol.* 130, 93–109. doi: 10.1016/0022-0981(89)90197-4

Conflict of Interest: The authors declare that the research was conducted in the absence of any commercial or financial relationships that could be construed as a potential conflict of interest.

Publisher's Note: All claims expressed in this article are solely those of the authors and do not necessarily represent those of their affiliated organizations, or those of the publisher, the editors and the reviewers. Any product that may be evaluated in this article, or claim that may be made by its manufacturer, is not guaranteed or endorsed by the publisher.

frontiers in Marine Science

ORIGINAL RESEARCH
published: 18 January 2022
doi: 10.3389/fmars.2021.811533

Methane Emissions From Nordic Seagrass Meadow Sediments

Maria E. Asplund[1], Stefano Bonaglia[2], Christoffer Boström[3], Martin Dahl[4], Diana Deyanova[1], Karine Gagnon[3], Martin Gullström[4], Marianne Holmer[5] and Mats Björk[6]**

[1] Department of Biological and Environmental Sciences, University of Gothenburg, Fiskebäckskil, Sweden, [2] Department of Marine Sciences, University of Gothenburg, Gothenburg, Sweden, [3] Faculty of Science and Engineering, Environmental and Marine Biology, Åbo Akademi University, Åbo, Finland, [4] School of Natural Sciences, Technology and Environmental Studies, Södertörn University, Huddinge, Sweden, [5] Department of Biology, Danish Institute for Advanced Study, University of Southern Denmark, Odense, Denmark, [6] Department of Ecology, Environment and Plant Sciences, Stockholm University, Stockholm, Sweden

OPEN ACCESS

Edited by:
Elva G. Escobar-Briones, National Autonomous University of Mexico, Mexico

Reviewed by:
Fernanda Adame, Australian Rivers Institute, Griffith University, Australia
Ian MacDonald, Florida State University, United States

***Correspondence:**
Maria E. Asplund
maria.asplund@gu.se
Mats Björk
mats.bjork@su.se

Specialty section:
This article was submitted to Marine Ecosystem Ecology, a section of the journal Frontiers in Marine Science

Received: *08 November 2021*
Accepted: *15 December 2021*
Published: *18 January 2022*

Citation:
Asplund ME, Bonaglia S, Boström C, Dahl M, Deyanova D, Gagnon K, Gullström M, Holmer M and Björk M (2022) Methane Emissions From Nordic Seagrass Meadow Sediments. Front. Mar. Sci. 8:811533. doi: 10.3389/fmars.2021.811533

Shallow coastal soft bottoms are important carbon sinks. Submerged vegetation has been shown to sequester carbon, increase sedimentary organic carbon (C_{org}) and thus suppress greenhouse gas (GHG) emissions. The ongoing regression of seagrass cover in many areas of the world can therefore lead to accelerated emission of GHGs. In Nordic waters, seagrass meadows have a high capacity for carbon storage, with some areas being recognized as blue carbon hotspots. To what extent these carbon stocks lead to emission of methane (CH_4) is not yet known. We investigated benthic CH_4 emission (i.e., net release from the sediment) in relation to seagrass (i.e. *Zostera marina*) cover and sedimentary C_{org} content (%) during the warm summer period (when emissions are likely to be highest). Methane exchange was measured *in situ* with benthic chambers at nine sites distributed in three regions along a salinity gradient from ∼6 in the Baltic Sea (Finland) to ∼20 in Kattegat (Denmark) and ∼26 in Skagerrak (Sweden). The net release of CH_4 from seagrass sediments and adjacent unvegetated areas was generally low compared to other coastal habitats in the region (such as mussel banks and wetlands) and to other seagrass areas worldwide. The lowest net release was found in Finland. We found a positive relationship between CH_4 net release and sedimentary C_{org} content in both seagrass meadows and unvegetated areas, whereas no clear relationship between seagrass cover and CH_4 net release was observed. Overall, the data suggest that Nordic *Zostera marina* meadows release average levels of CH_4 ranging from 0.3 to 3.0 μg CH_4 m^{-2} h^{-1}, which is at least 12–78 times lower (CO_2 equivalents) than their carbon accumulation rates previously estimated from seagrass meadows in the region, thereby not hampering their role as carbon sinks. Thus, the relatively weak CH_4 emissions from Nordic *Z. marina* meadows will not outweigh their importance as carbon sinks under present environmental conditions.

Keywords: seagrass, greenhouse gas, blue carbon, nordic, *Zostera marina*

INTRODUCTION

Methane (CH_4) is a very potent greenhouse gas (GHG), with a global warming potential that is estimated to be 28–34 times higher than carbon dioxide (CO_2) per mole of carbon over a 100-year period (Myhre et al., 2013). It has been estimated that about half of the global CH_4 emissions generate from aquatic sources, although there is high variability between regions and ecosystems (Saunois et al., 2020; Rosentreter et al., 2021). Oceanic shelves, although marginal in area compared to deep oceans, contribute to about 75% of the CH_4 emission from oceans worldwide (Bange et al., 1994). Methane in the marine environment is mainly produced in sediments during anaerobic degradation of organic matter by methanogenic archaea (Bakker et al., 2014; Wilson et al., 2020). The produced CH_4 may be oxidized to CO_2 in the sediment or released to the water column in solution by diffusion, via plant–tissue or as gas bubbles (Reeburgh, 2007; Jeffrey et al., 2019). Generally, only a small portion of the produced CH_4 eventually reaches the atmosphere, since most CH_4 is oxidized by microorganisms in the sediment and water column (Reeburgh, 2007). Seeping bubbles released from sediments lose most of their CH_4 content during their passage through the water column and the extent of that loss depends on the bubble size and water depth (Weber et al., 2019). This explains why most marine CH_4 emissions derive from the nearshore coastal environment, where there is less likelihood that the CH_4 is oxidized before reaching the atmosphere (Weber et al., 2019).

Natural wetlands, i.e., vegetated ecosystems where the soil is water-saturated for most part of the year and which store large amount of carbon in their soils, account for 20–30% of the global yearly CH_4 emissions and are thus the single largest non-anthropogenic source of CH_4, adding up to 164 Tg yr^{-1} to the atmosphere (IPCC, 2001; Bridgham et al., 2013; He et al., 2015). In the coastal zone, vegetated habitats (i.e. saltmarshes, mangroves, and seagrass meadows) are estimated to emit around 4 Tg yr^{-1} (Al-Haj and Fulweiler, 2020). This emission level is hence low compared to their terrestrial counterparts, although greater than the release from open oceans, which are estimated to release between 0.4 and 1.8 Tg yr^{-1} (Rhee et al., 2009; Borges et al., 2016). Photosynthetically derived oxygen from submerged plants can potentially be used by methane-oxidizing bacteria (MOBs) in the sediment and water column, converting CH_4 to CO_2, and thereby hinder emission of CH_4 to the atmosphere in these submerged vegetated ecosystems (Laanbroek, 2010). This may contrast with conditions in terrestrial and coastal wetlands where vegetation is emerged, i.e., in direct contact with the atmosphere, and therefore CH_4 will be released without being processed in the water phase by MOBs (Laanbroek, 2010). Up to 90% of the CH_4 produced in sediments with submerged vegetation can be reoxidized in the water column (King et al., 1990), but if the oxygen levels are low, due to for instance stagnant waters and during high consumption rates, the CH_4 may be emitted to the atmosphere.

High organic loading and anoxic sediments provide conditions for long-term storage of refractory carbon. Consequently, coastal vegetated ecosystems such as saltmarshes, mangroves, and seagrass meadows are efficient sinks of atmospheric CO_2 and referred to as blue carbon habitats (e.g., Mcleod et al., 2011; Duarte, 2017; Howard et al., 2017). However, the same conditions that make these habitats ideal for carbon storage also provide the potential for CH_4 production (Al-Haj and Fulweiler, 2020). Conditions that favor methanogenesis could tip these coastal habitats from sinks to sources of CO_2 and CH_4 and thereby accelerate the greenhouse effect. It is therefore of great importance to understand the conditions governing the release of CH_4 and other GHGs from these habitats. Studies from tidal saltmarshes show that CH_4 emission is strongly salinity dependent, with significantly lower emissions at salinities over 18 (Poffenbarger et al., 2011), while in fresh- to brackish water marshes such a salinity-driven threshold has been reported to occur already at salinities above 10 (Wang et al., 2017). In peatlands, sulfate reduction inhibits methanogenesis and the release of CH_4 is low (Dowrick et al., 2006). However, in anoxic marine sediments, sulfate reduction and methanogenesis may co-occur (Oremland and Taylor, 1978; Holmer and Kristensen, 1994; Sela-Adler et al., 2017).

Seagrass meadows have been reported to naturally emit low to moderate levels of CH_4, ranging from 2–5 (Oremland, 1975) to 378 $\mu g\ m^{-2}\ h^{-1}$ (Garcias-Bonet and Duarte, 2017). This is substantially lower than what has been observed in other marine habitats; for example, saltmarshes can emit over 10,000 $\mu g\ m^{-2}\ h^{-1}$ (Whiting and Chanton, 1993). However, stressors (such as light reduction, habitat fragmentation, and warming) can dramatically increase CH_4 emission in seagrass systems (Lyimo et al., 2018; Burkholz et al., 2020; George et al., 2020). Vegetation loss or alteration in macrophyte species composition may also stimulate methanogenesis in the sediment (Sutton-Grier and Megonigal, 2011; Lyimo et al., 2018; Al-Haj and Fulweiler, 2020).

In the Nordic region, seagrass meadows have high capacity for storing large amounts of carbon in the sediment, in particular, some sites along the Swedish Skagerrak coast are suggested to be global hotspots for blue carbon (Dahl et al., 2016; Röhr et al., 2018; Moksnes et al., 2021). It is previously known from the coastal southern Baltic Sea that CH_4 emissions are positively correlated to the organic carbon content in sediments (Heyer and Berger, 2000). Therefore, it is of particular interest to study blue carbon habitats, such as seagrass meadows, that may store large amounts of organic carbon (C_{org}) in their sediments to understand the fate of stored carbon as potential sources for GHG emissions. No previous reports have, however, focused on CH_4 emissions from *Zostera marina* beds in northern European coastal waters. In the current study, we aimed to investigate (i) the extent and variability in CH_4 (g) emission from seagrass (*Z. marina*) dominated coastal soft bottom sediments in three regions along the salinity gradient from the Baltic Sea to the North Sea, (ii) to what degree vegetation cover (in terms of *Z. marina*) modifies CH_4 (g) emission from the substrate, and (iii) whether CH_4 (g) emission is correlated to the sedimentary organic carbon content.

MATERIALS AND METHODS

Study Area

Nordic coastal areas are of particular interest since they stretch from the Baltic Sea, which is a semi-enclosed water body and one of the largest brackish water areas in the world, to the marine environments of Skagerrak and Kattegat through the Danish straits (Storebælt, Lillebælt, and Öresund). The region is therefore characterized by a strong, large-scale salinity gradient from freshwater conditions (0–2) in the Bothnian Bay to marine conditions (∼34) in the North Sea (Helcom 2017-2018)[1]. Coastal shallow habitats in northern areas are deemed by climate scenario models to be exposed to faster warming than the global average, with an expected temperature increase ranging from 2°C in the southern part of the Baltic Sea to 4°C in the northern part by the end of this century (i.e., year 2100, Andersson et al., 2015), which may influence CH_4 emissions from coastal blue carbon habitats in the future. Further, the coastal waters of the Baltic Sea, the Kattegat and Skagerrak are surrounded by nine countries and human activities in the area, adding pressure on the seagrass ecosystems (Boström et al., 2014). For instance, severe seagrass loss of about 60% has been reported on the Swedish west coast between 1980s and 2000s (Baden et al., 2003; Nyqvist et al., 2009). From some of these areas in Sweden where historical losses have occurred, it has been estimated that the resulting loss of carbon from the sediments could be up to 60 Mg C ha^{-1} (Moksnes et al., 2021).

[1]http://stateofthebalticsea.helcom.fi/

The current study was carried out during a warm summer period (with water temperatures ranging from 20 to 23.5°C; see **Supplementary Table 1**) in August 2018 in *Z. marina* meadows and adjacent unvegetated areas within three regions, along the salinity gradient stretching from the Baltic Sea archipelago west of Turku in Finland (three sites) to the fjords east of Fyn Odense in Denmark (two sites) and the Gullmar Fjord on the Swedish Skagerrak coast (four sites) (see **Figure 1** and **Table 1**). At the Finnish study area, *Z. marina* grows at the lower end of its salinity propagation limit (∼6), while the Danish sites have intermediate salinities (∼20) and the Swedish sites have salinities varying between 18 and 30 in the surface waters, with a yearly average of ∼26. Water temperatures were between 20 and 23.5°C in all study areas during the sampling period. In Finland, the sites are moderately exposed, and the sediment consists mainly of fine to coarse sand with low levels of organic content. In Denmark, the Nyborg site is exposed to easterly winds and the sediment is sandy with a low organic content, while the Holckenhavn Fjord is sheltered, and the sediment is siltier with a low organic content. In Sweden, the sites are situated in shallow bays exposed to different levels of hydrodynamic forces and the topmost layers in the sediments are sandy, silty, or muddy.

Incubation Chambers for Sampling CH_4 at Sediment–Water Interface

Incubation chambers, produced by transparent Plexiglas cores (inner diameter: 4.7 cm, height: 45 cm; **Figure 2**) containing an air-filled gas pocket with a gas-tight septum for extraction of

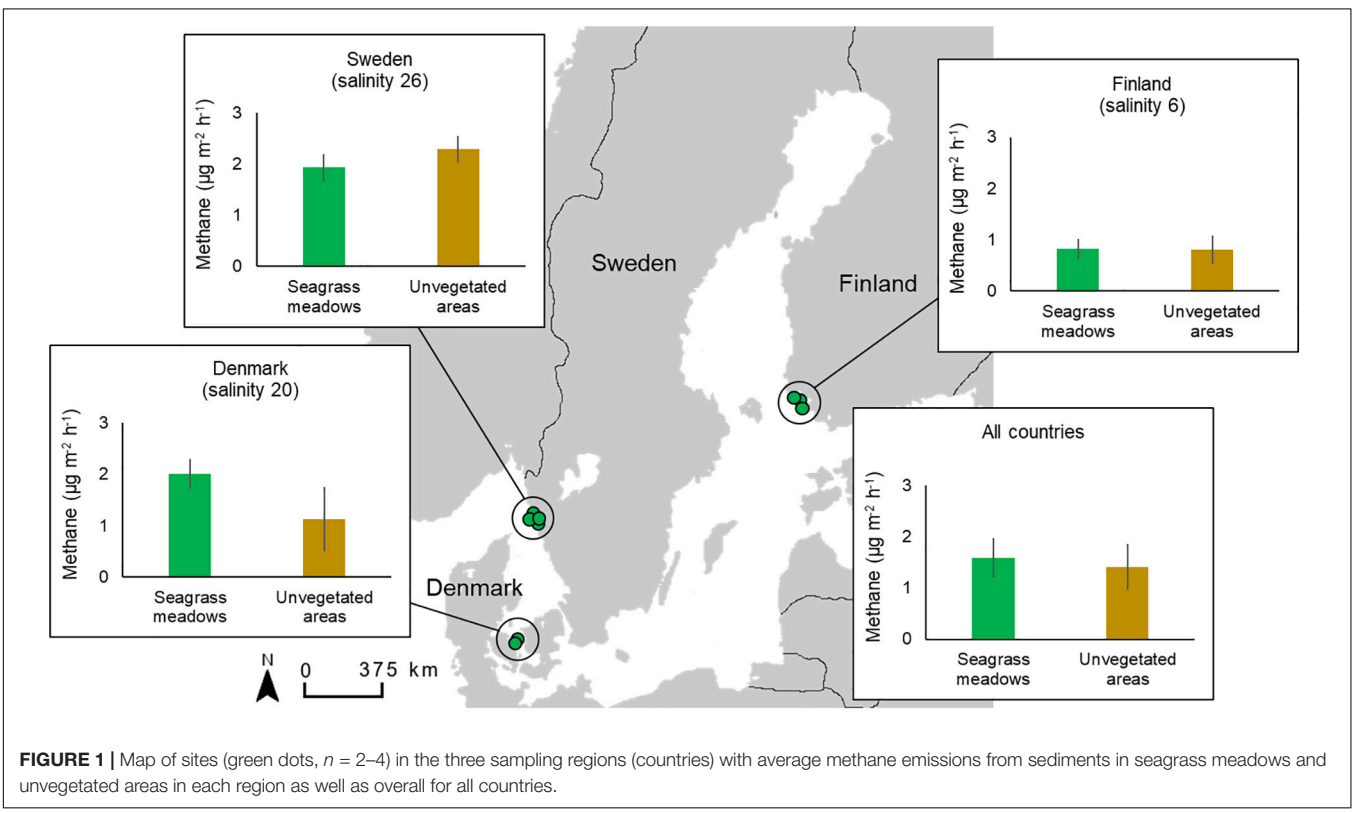

FIGURE 1 | Map of sites (green dots, n = 2–4) in the three sampling regions (countries) with average methane emissions from sediments in seagrass meadows and unvegetated areas in each region as well as overall for all countries.

TABLE 1 | Sampling design showing number of replicates, water depth and water temperature in seagrass meadows and adjacent unvegetated habitats at the different sampling sites, and mean salinity for each of the three sampling regions.

Sampling regions Sites	Seagrass replicates (*n*)	Unveg. replicates (*n*)	Seagrass depth (m)	Unveg. depth (m)	Temp. (°C)	Salinity (mean)
Finland (Fin)						6
Fårö	6	6	2	2	20	
Hummelskär	6	6	2.1–2.2	2.3–2.4	20	
Ängsö	6	6	2–2.3	2–2.1	20	
Denmark (Den)						20
Holckenhavn Fjord	6	6	2	2	21	
Nyborg	5	5	2.5	2.5	23.5	
Sweden (Swe)						26
Getevik	6	6	2.2	2.6	21.5	
Kristineberg	6	4	3.1	3.5	21.6	
Skallhavet	6	6	2.2	2	22.3	
Gåsö	6	6	2.5	2.7	23.5	

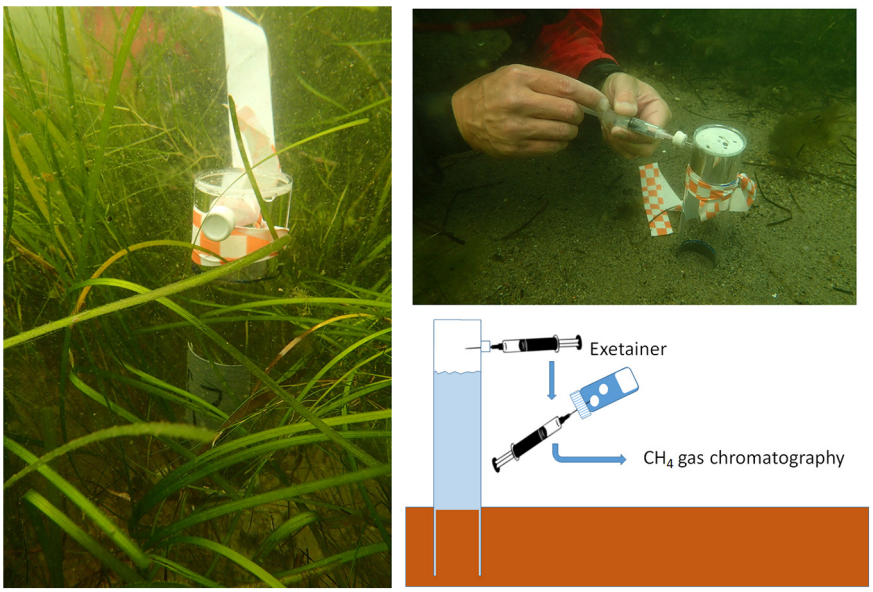

FIGURE 2 | Deployed incubation chamber in a seagrass meadow (left) and collection of a gas sample (top right). Illustration (bottom right) of the sampling methodology using an incubation chamber inserted 15 cm into sediment with a 20 cm water column above the sediment. On the top, a 5 cm air-pocket is connected to a gas-tight septum from where a gas-sample (including methane) released from the sediment could be collected (using a syringe). Gas-samples were extracted periodically after insertion from the chamber and stored in gas-tight exetainers until analyzed with gas-chromatography (GC). Photos: K. Gagnon.

gas samples, were placed in seagrass meadows (n = 6) and in adjacent unvegetated areas (n = 5 or 6) at 2–3 m water depth using scientific (SCUBA) diving. For details of the sampling regions and sites, see **Table 1**. The start time for incubations was set to around 10 am to catch the midday hours when productivity is expected to be highest. The chamber cores were pushed down 15 cm into the sediment, leaving a 20-cm water column and a 5-cm gas pocket (volume: 87 cm^3) above the water in the chamber. A "start" gas sample (5 mL) was withdrawn from the pocket about 10 minutes after placing the chamber into the sediment and the time was noted. The incubations were conducted for about 5–6 h, whereafter an "end" gas sample was extracted from the gas pocket and the ending time was noted. The gas samples were directly transferred into gas-tight exetainers containing 58.3 mM zinc chloride (aq) for storage and to prevent any potential bacterial breakdown of CH_4 until analysis. The exetainers were stored upside-down in the refrigerator (4°C) until analysis. At the Swedish sites, the development of CH_4 release in the chambers was observed at several time points during the incubation period to follow and confirm linearity in the CH_4 release.

Salinities and temperatures were measured at each site prior to incubations. In the seagrass sites, seagrass shoot density (shoots per m^2) were either measured, in field, in quadrats (25 × 25 cm, n = 6) or measurements from previous studies (Gullström et al., 2012; Staveley et al., 2017) (see **Supplementary Table 1**) were used.

Analysis of Methane

The gas in the collected exetainer samples were analyzed by means of headspace analysis and gas chromatography (GC). Briefly, 1 mL headspace was injected into a gas chromatographer (GC 8A, Shimadzu Corporation) equipped with a Porapak N column (80–100 mesh) and a flame ionization detector (FID). The carrier gas for the FID was nitrogen, while the fuel gas was hydrogen and the oxidant air. For calibration, certified standards at atmospheric concentration (1.9 ppm) and with 49.9 ppm CH_4 (AirLiquide Gas AB) were used. Using the Ideal Gas Law (PV = nRT), the ppm concentrations were converted into molar concentrations (μmol CH_4 L^{-1}), which were plotted against incubation time. The CH_4 emissions per surface area of the sediments were calculated as the total amount of CH_4 accumulating over time within the gas-filled pocket of the incubation chamber and reported as μg CH_4 m^{-2} h^{-1}. Since measurements were only conducted during daytime, values were not extrapolated to full diurnal estimates.

Collection of Sediment Cores

After incubation, a sediment core was collected adjacent to each incubation chamber using a push corer (diameter: 4.7 cm, height: 60 cm). The cores were sliced into three different depth sections: 0–1 cm representing the oxidized zone, 1–15 cm representing the rhizosphere and below 15 cm representing the sediment without living seagrass. Sediment compression was accounted for in all cores by measuring the distance from the top of the core to the sediment surface, inside and outside the core after being inserted into the sediment (Glew et al., 2002).

Analysis of Organic Carbon Content in the Sediment

Sediment core slices were weighed wet, homogenized and a subsample of 60 mL from each depth was then dried (60° C, ∼48 h) until constant weight, whereafter the dry bulk density (g DW cm^{-3}) was calculated. The dry sediment samples were grinded to a powder using a Retch 400 mixing mill for subsequent carbon analyses. The total carbon and nitrogen content (% C and % N) in each sediment depth section was analyzed using a carbon–nitrogen elemental analyzer (Flash 2000, Thermo Fisher Scientific). Previous research in the studied regions have documented that the inorganic carbon content generally is low (<5%) and was therefore not accounted for Röhr et al. (2016); Dahl et al. (2020).

Data Analysis

Variations in CH_4 emission rates were compared between the different regions for the two habitat types, i.e., seagrass meadows *vs.* unvegetated areas separately, and then overall between seagrass meadows and unvegetated areas, using non-parametric Kruskal–Wallis tests (since with the $\log_{10}[x + 1]$ transformation, homogeneity of variance was not achieved). A Bonferroni correction of the significance level was applied for multiple testing to limit the probability of Type 1 error (Holm, 1979). Potential relationships between CH_4 emission and environmental variables such as sedimentary C_{org} content and seagrass shoot density, respectively were tested with linear regression analysis. All data analyses were performed in IBM SPSS statistics (version 27).

RESULTS

The CH_4 emissions were generally low but varied substantially both within and between sites, resulting in a net release of CH_4 to the air phase ranging from 0.3 to 1.8 μg CH_4 m^{-2} h^{-1} at the Finnish sites to 2.0–2.5 μg CH_4 m^{-2} h^{-1} at the Danish sites and 0.4–3.0 μg CH_4 m^{-2} h^{-1} at the Swedish sites (**Figures 1**, **3**). Pairwise comparisons showed that the overall CH_4 emissions from seagrass meadows were significantly higher in both the Swedish and Danish sites when compared to the Finnish sites, while there was no significant difference between the Swedish and Danish sites (**Table 2**). For the unvegetated areas, CH_4 emissions were significantly higher in the Swedish sites compared to the Finnish sites (**Table 2**). Overall, there was no difference in emissions between seagrass covered- and unvegetated sediments, even though differences between these habitat types occurred at some sites within each region (**Table 2** and **Figure 3**).

Methane emission increased along the salinity gradient (**Figures 1**, **4**), although this pattern likely also is reflecting the inherent conditions of the three regions. The mean integrated (0-15 cm) organic carbon (C_{org}) content in the sediment varied between 0.1 and 6%, with the largest levels found in the Swedish sites (**Supplementary Tables 1**, **2**). There were linear

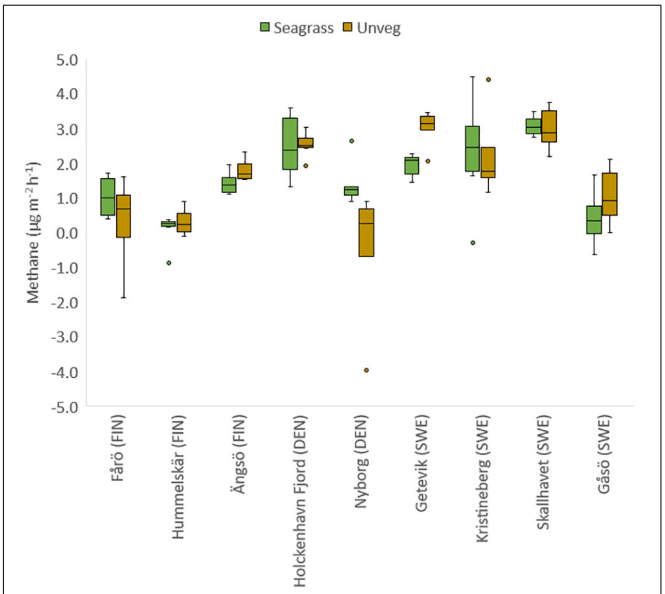

FIGURE 3 | Box-and-whisker-plot showing the variation of methane emission from the sediment to the gas-filled pocket in the incubation chambers of seagrass meadows and adjacent unvegetated areas in Finland (FIN), Denmark (DEN), and Sweden (SWE). The solid lines within the boxes indicate median values, the boxes represent the 25th to the 75th percentiles and the vertical whisker bars show the 5th and 95th percentiles of the data.

TABLE 2 | Summary of non-parametric Kruskal–Wallis tests of methane emissions among regions within (seagrass meadows and unvegetated areas) and between habitats.

Pairwise comparison	Test statistic	Std. error	Std. test statistic	Adj p
Region-seagrass (total N = 51, df = 2, model p = ***0.005****)*				
Fin vs **Den**	14.483	5.823	2.487	**0.039**
Fin vs **Swe**	−14.479	4.798	−3.018	**0.008**
Den vs Swe	0.004	5.413	0.001	1.000
Region-unvegetated (total N = 47, df = 2, model p = ***0.002****)*				
Fin vs Den	7.321	5.443	1.345	1.000
Fin vs **Swe**	−16.010	4.635	−3.454	**0.003**
Den vs Swe	−8.688	5.103	−1.703	0.532
Habitat (total N = 98, df = 1, model p = 0.806)				

Significant values ($p < 0.05$) are shown in bold. Countries with bolded text indicate the higher values in the pairwise comparisons. Std. error, standard error, Adj p, Adjusted p-value.

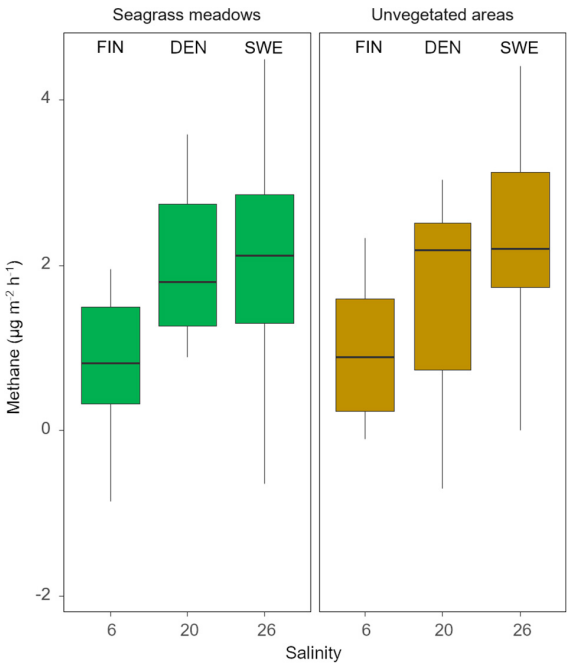

FIGURE 4 | Box-and-whisker plot summarizing methane emissions from the sediment to the gas-filled pocket in the incubation chambers in seagrass meadows and adjacent unvegetated areas in relation to average salinities in the different regions. The solid lines within the boxes indicate median values, the boxes represent the 25th to the 75th percentiles and the vertical whisker bars show the 5th to the 95th percentiles of the data.

relationships between sedimentary C_{org} and CH_4 emissions in seagrass meadows (Adj R^2 = 0.12, p = 0.01, **Supplementary Figure 1A**) and in unvegetated areas (Adj R^2 = 0.21, $p < 0.01$, **Supplementary Figure 1B**), respectively, although the adjusted R^2 value were low indicating that there are other factors influencing the CH_4 mean net release.

Seagrass meadows average shoot densities, as presented in previous works, varied from 101 to 652 shoots m^{-2} (**Supplementary Table 1**). There was no significant relationship between the average seagrass shoot density and CH_4 emission in the current study.

DISCUSSION

This study shows that CH_4 emissions from cold-temperate Nordic seagrass meadows are relatively low, both when compared to seagrass areas worldwide and when compared to other shallow-water habitats in the Nordic region. The amount of C_{org} stored in the sediment appeared to influence the emissions, as there was a positive correlation between CH_4 emission and the sedimentary organic carbon content. The relatively low explanatory value suggests that besides the sedimentary C_{org} content, there must be other factors that are of major importance for methane release from these coastal sediments. Nevertheless, we found no significant influence of vegetation or salinity on CH_4 emissions. The current study was conducted during the warm high-productive season, when also the net release of methane is expected to peak, and represents the first survey of methane emissions from seagrass meadow sediments in Nordic coastal waters.

Methane net release from *Z. marina* meadow sediments varied from 0.3 to 3.0 $\mu g\ m^{-2}\ h^{-1}$. These values are in the lower range of what is reported from seagrass habitats globally, which can reach up to 378 $\mu g\ m^{-2}\ h^{-1}$ (see **Table 3**). It is further drastically lower than reported emissions from other shallow-water habitats in Nordic waters like estuarine wetlands (8,583 $\mu g\ m^{-2}\ h^{-1}$) or brackish-water reed (*Phragmites*) belts (15,200 $\mu g\ m^{-2}\ h^{-1}$), (**Table 3**). The relatively low CH_4 emission levels measured in our study agree well with those reported for coastal bare sediments (1.2–2.3 $\mu g\ CH_4\ m^{-2}\ h^{-1}$) of the Baltic proper (Bonaglia et al., 2017). Those sediments had similar carbon content as on the Swedish west coast (5.5%) and similar salinities as in the Finnish areas (6.8), but were sampled deeper (50 m) and at much lower temperature (8.0°C) compared to our study (range: 20–23.5°C, **Supplementary Table 1**). The good agreement in rates may thus be explained by the fact that most of the CH_4 generated deep inside the sediment is efficiently oxidized by the community of methane-oxidizing archaea and sulfate-reducing bacteria before it can reach the sediment water-interface (Orphan et al., 2001). Up to 90% of the CH_4 produced in marine sediments are consumed already in the sediment phase (Reeburgh et al., 1993).

Most studies where high emissions from seagrass habitats have been reported are from warmer (warm-temperate or tropical) waters (**Table 3**). This could be due to a temperature dependence of CH_4 production as well as differences in organic matter quality and quantity, and in the microbial community composition. Temperature is known to significantly influence CH_4 production both in tropical (Burkholz et al., 2020; George et al., 2020) and cold-temperate waters (Heyer and Berger, 2000). In the present study, water temperatures were similar across regions; nevertheless, differences in water temperature on local spatial (cm to m) and temporal (day to seasonal) scales could still influence the variation in emission rates, but this was not investigated here.

We found no significant influence of vegetation cover on CH_4 emission from the sediments in the seagrass meadows,

TABLE 3 | Sediment methane (CH_4) emission rates from seagrass meadows worldwide and other shallow-water habitats in Nordic waters, using sediment-to-air filled pocket chamber techniques, reported in the literature and in the current study.

Region	Habitat type	Ranges (or average*) of emission rates, ($\mu g\ CH_4\ m^{-2}\ h^{-1}$)	References
Seagrass meadows worldwide			
Global estimation	Seagrass in general	54*	Rosentreter et al., 2021
Portugal, Atlantic coast	*Zostera noltii*	71(at night) –111 (in day)	Bahlmann et al., 2014
Florida bay	*Thalassia testudinum*	14–185	Barber and Carlson, 1993
France, Atlantic coast	*Zostera* spp	66 *	Deborde et al., 2010
Red Sea	*Halophila stipulacea* and *Halodule unervis*	16–74	Garcias-Bonet and Duarte, 2017
	Thalassodendron ciliatum	0.067–4.6	
	Thalassia hemprichii	0.20–11	
	Halophila decipiens	0.47–11	
	Enhalus acoroides	−8.0 to 181	
	Cymodocea serrulata and *Halodule uniervis*	91–378	
	Halodule unervis	17–40	
Western Indian Ocean	*Thalassia hemprichii*	50 * (controls), 224–291 (disturbed)	Lyimo et al., 2018
Florida Keys	*Syringodium* sp.	2–5	Oremland, 1975
	Thalassia testudinum	29–30	
Nordic waters	*Zostera marina*	0.3–3.0	Current study
Other shallow-water habitats in Nordic waters			
North-Eastern Germany	Brackish fen, *Phragmites australis*	538–15,200	Koch et al., 2014
Gulf of Bothnia	Eustarine wetlands	8,583*	Liikanen et al., 2009

and unvegetated sediments had similar emissions as the vegetated areas. There are, however, reports that submerged vegetation, such as seagrasses and other rooted macrophytes, significantly influences the microbial composition and actions in the sediments (Jensen et al., 2007; Santos-Fonseca et al., 2015; Cúcio et al., 2016), with potential effects on the GHG balance. Seagrasses have been reported to reduce CH_4 emissions by their photosynthetic oxygen production (Oremland, 1975; George et al., 2020) and also by symbiotic CH_4 oxidizers associated with the plants.

In some coastal habitats, such as in tidal saltmarshes, CH_4 emission is strongly affected by salinity, with lower emissions at higher salinities (Poffenbarger et al., 2011; Wang et al., 2017). It has been suggested that the higher levels of sulfate found in sediments of higher salinity will increase sulfate reduction, which in turn could inhibit CH_4 production in vegetated habitats (e.g., Koebsch et al., 2018). Methane emissions from marine areas could hence be expected to be low. In contrast, we found the highest emission levels within the region with highest salinities, i.e., at the Swedish sites. When the organic carbon loading is high, it can be that the inhibitory effect of sulfate reduction plays a minor role and sulfate reduction and methanogenesis can co-occur (Holmer and Kristensen, 1994; Santos-Fonseca et al., 2015). Therefore, CH_4 production can occur in marine areas with high organic carbon content, which is also confirmed in the current study.

Even though the emissions we measured from both vegetated and adjacent unvegetated sediments were low, the CH_4 emissions partly counteract the seagrass meadows' capacity to function as carbon sinks. The only published data on carbon accumulation rates for seagrasses in the Nordic area (Röhr et al., 2016) show annual mean values of 0.05 t C ha^{-1} yr^{-1} for Finland, and 0.35 t C ha^{-1} yr^{-1} for Denmark, while no accumulation data for Sweden has been published. Given in the same units and calculated as e-CO_2 at a GWP100 of 34 (Myhre et al., 2013), the CH_4 emissions in this study ranged from 0.0007 to 0.0040 in Finland, from 0.0045 to 0.0056 in Denmark, and from 0.0009 to 0.0067 t eCO_2-C ha^{-1} yr^{-1} in Sweden. Thus, the carbon accumulation rate in Finland was between 12 and 75 times higher, and in Denmark between 63 and 78 times higher, than the estimated C emissions from CH_4. We therefore conclude that the relatively weak emissions of CH_4 from Nordic *Z. marina* meadows will not outweigh their importance as carbon sinks under present environmental conditions.

Climate simulations for the Baltic Sea ecosystems indicate a 2–4°C warming and a significant increase in precipitation by the year 2100 that may increase land runoff of allochthonous organic matter and decrease salinity (Andersson et al., 2015). This might have multifaceted effects on the seagrass systems. While healthy seagrass meadows contribute to mitigate the effects of runoff and capture part of the increased input of nutrients and organic matter, an increased organic content in the sediments might result in increased respiration and lower oxidation state of the sediment. A lower oxidation will in turn favor anaerobic respiration and might thus lead to increased production and emissions of CH_4 and other GHGs. As temperatures are predicted to increase more drastically in the Nordic region than on a global scale (Andersson et al., 2015), this may accelerate CH_4 emissions from blue carbon habitats such as seagrass meadows (Yvon-Durocher et al., 2011). It has previously been shown in tropical seagrass sediments that CH_4 emissions more than doubled during high temperature stress (George et al., 2020). The Nordic seagrass systems, today functioning as effective sinks for atmospheric CO_2, might thus be hampered by climate change effects so that their carbon capture capacity is reduced while their emission of GHGs is increased. This may eventually turn Nordic seagrass meadows from sinks to sources of CO_2.

In conclusion, the relative low net release of methane from Nordic seagrass meadows presented in this study may reinforce

their capacity as natural blue carbon sinks. To fully understand the extent of emissions of methane and other GHGs from Nordic coastal habitats, multiple spatial (from microhabitat to seascape level) and temporal (diurnal and seasonal) aspects should be considered in future studies.

DATA AVAILABILITY STATEMENT

The original contributions presented in the study are included in the article/**Supplementary Material**, further inquiries can be directed to the corresponding author.

AUTHOR CONTRIBUTIONS

MA, MB, SB, MG, CB, and MH conceived and designed the study. MA, MB, DD, MG, CB, and KG carried out the fieldwork. MA, SB, and MD carried out the lab work and analysis. MA and MB wrote the first draft of the manuscript with aid from MD and MG. All authors contributed to the final version of the manuscript.

FUNDING

The research was partly funded by the Bolin Centre for Climate Research. SB was supported by the Swedish Research Council Formas (grant number: 2017-01513). CB was funded by the Åbo Akademi University Foundation SR. KG was funded by the European Union's Horizon 2020 Research and Innovation Programe as part of the project MERCES: Marine Ecosystem Restoration in Changing European Seas (grant number: 689518).

ACKNOWLEDGMENTS

Thanks to Nellie Stjärnkvist for assistance with laboratory analyses and also Lukas Meysick and Luca Rugiu for assistance in the field and with laboratory work.

SUPPLEMENTARY MATERIAL

The Supplementary Material for this article can be found online at: https://www.frontiersin.org/articles/10.3389/fmars.2021.811533/full#supplementary-material

REFERENCES

Al-Haj, A. N., and Fulweiler, R. W. (2020). A synthesis of methane emissions from shallow vegetated coastal ecosystems. *Glob. Change Biol.* 26, 2988–3005. doi: 10.1111/gcb.15046

Andersson, A., Meier, H. E. M., Ripszam, M., Rowe, O., Wikner, J., Haglund, P., et al. (2015). Projected future climate change and Baltic Sea ecosystem management. *Ambio* 44, 345–356. doi: 10.1007/s13280-015-0654-8

Baden, S., Gullström, M., Lundén, B., Pihl, L., and Rosenberg, R. (2003). Vanishing seagrass (*Zostera marina*, L.) in Swedish coastal waters. *Ambio* 32, 374–377. doi: 10.1579/0044-7447-32.5.374

Bahlmann, E., Weinberg, I., Lavrič, J., Eckhard, T., Michaelis, W., Santos, R., et al. (2014). Tidal controls on trace gas dynamics in a seagrass meadow of the Ria Formosa lagoon (southern Portugal). *Biogeosci. Discuss.* 11, 10571–10603. doi: 10.5194/bg-12-1683-2015

Bakker, D. C. E., Bange, H. W., Gruber, N., Johannessen, T., Upstill-Goddard, R. C., Borges, A. V., et al. (2014). "Air-sea interactions of natural long-lived greenhouse gases (CO2, N2O, CH4) in a changing climate," in *Ocean-Atmosphere Interactions of Gases and Particles*, eds P. S. Liss and M. T. Johnson (Berlin: Springer), doi: 10.1007/978-3-642-25643-1_3

Bange, H. W., Bartell, U. H., Rapsomanikis, S., and Andreae, M. O. (1994). Methane in the Baltic and North Seas and a reassessment of the marine emissions of methane. *Glob. Biogeochem. Cycl.* 8, 465–480. doi: 10.1029/94GB02181

Barber, T. R., and Carlson, P. R. Jr. (1993). "Effects of seagrass die-off on benthic fluxes and porewater concentrations of $\sum$ CO2, $\sum$ H2S, and CH4 in Florida Bay sediments," in *Biogeochemistry of Global Change: Radiatively Active Trace Gases*, ed. R. S. Oremland (New York, NY: Chapman and Hall), 530–550. doi: 10.1007/978-1-4615-2812-8_29

Bonaglia, S., Brüchert, V., Callac, N., Vicenzi, A., Fru, E. C., and Nascimento, F. J. A. (2017). Methane fluxes from coastal sediments are enhanced by macrofauna. *Sci. Rep.* 7:13145. doi: 10.1038/s41598-017-13263-w

Borges, A. V., Champenois, W., Gypens, N., Delille, B., and Harlay, J. (2016). Massive marine methane emissions from near-shore shallow coastal areas. *Sci. Rep.* 6:27908. doi: 10.1038/srep27908

Boström, C., Baden, S., Bockelmann, A.-C., Dromph, K., Fredriksen, S., Gustafsson, C., et al. (2014). Distribution, structure and function of Nordic eelgrass (Zostera marina) ecosystems: implications for coastal management and conservation. *Aquatic. Conserv. Mar. Freshw. Ecosyst.* 24, 410–434. doi: 10.1002/aqc.2424

Bridgham, S. D., Cadillo-Quiroz, H., Keller, J. K., and Zhuang, Q. (2013). Methane emissions from wetlands: biogeochemical, microbial, and modeling perspectives from local to global scales. *Glob. Change Biol.* 19, 1325–1346. doi: 10.1111/gcb.12131

Burkholz, C., Garcias-Bonet, N., and Duarte, C. M. (2020). Warming enhances carbon dioxide and methane fluxes from Red Sea seagrass (*Halophila stipulacea*) sediments. *Biogeosci.* 17, 1717–1730. doi: 10.5194/bg-17-1717-2020

Cúcio, C., Engelen, A. H., Costa, R., and Muyzer, G. (2016). Rhizosphere microbiomes of European seagrasses are selected by the plant, but are not species specific. *Front. Microbiol.* 7:440. doi: 10.3389/fmicb.2016.00440

Dahl, M., Asplund, M. E., Deyanova, D., Franco, J. N., Koliji, A., Infantes, E., et al. (2020). High seasonal variability in sediment carbon stocks of cold–temperate seagrass meadows. *J. Geophys. Res. Biogeosci.* 125, 1–13. doi: 10.1029/2019JG005430

Dahl, M., Deyanova, D., Guetschow, S., Asplund, M. E., Lyimo, L. D., Karamfilov, V., et al. (2016). Sediment properties as important predictors of carbon storage in *Zostera marina* meadows: a comparison of four European areas. *PLoS One* 11:e0167493. doi: 10.1371/journal.pone.0167493

Deborde, J., Anschutz, P., Guérin, F., Poirier, D., Marty, D., Boucher, G., et al. (2010). Methane sources, sinks and fluxes in a temperate tidal Lagoon: the Arcachon lagoon (SW France). *Estuar. Coast. Shelf Sci.* 89, 256–266. doi: 10.1016/j.ecss.2010.07.013

Dowrick, D. J., Freeman, C., Lock, M. A., and Reynolds, B. (2006). Sulphate reduction and the suppression of peatland methane emissions following summer drought. *Geoderma* 132, 384–390. doi: 10.1016/j.geoderma.2005.06.003

Duarte, C. M. (2017). Reviews and syntheses: Hidden forests, the role of vegetated coastal habitats in the ocean carbon budget. *Biogeosciences* 14, 301–310. doi: 10.5194/bg-14-301-2017

Garcias-Bonet, N., and Duarte, C. M. (2017). Methane production by seagrass ecosystems in the Red Sea. *Front. Mar. Sci.* 4:340. doi: 10.3389/fmars.2017.00340

George, R., Gullström, M., Mtolera, M. S. P., Lyimo, T. J., and Björk, M. (2020). Methane emission and sulfide levels increase in tropical seagrass sediments during temperature stress: a mesocosm experiment. *Ecol. Evol.* 10, 1917–1928. doi: 10.1002/ece3.6009

Glew, J. R., Smol, J. P., and Last, W. M. (2002). "Sediment core collection and extrusion," in *Tracking Environmental Change Using lake Sediments, Developments in Paleoenvironmental Research*, Vol. 1, eds W. M. Last and J. P. Smol (Dordrecht: Springer), 73–105. doi: 10.3791/54363

Gullström, M., Baden, S., and Lindegarth, M. (2012). Spatial patterns and environmental correlates in epiphytic assemblages of temperate seagrass (*Zostera marina*) meadows. *Mar. Biol.* 159, 413–425. doi: 10.1007/s00227-011-1819-z

He, S., Malfatti, S. A., McFarland, J. W., Anderson, F. E., Pati, A., Huntemann, M., et al. (2015). Patterns in wetland microbial community composition and functional gene repertoire associated with methane emissions. *mBio* 6:e00066-15. doi: 10.1128/mBio.00066-15

Heyer, J., and Berger, U. (2000). Methane emission from the coastal area in the southern Baltic Sea. *Estuar. Coast. Shelf Sci.* 51, 13–30. doi: 10.1006/ecss.2000.0616

Holm, S. (1979). A simple sequentially rejective multiple test procedure. *Scan. J. Stat.* 6, 65–70.

Holmer, M., and Kristensen, E. (1994). Coexistence of sulfate reduction and methane production in an organic-rich sediment. *Mar. Ecol. Prog. Ser.* 107, 177–177. doi: 10.3354/meps107177

Howard, J., Sutton-Grier, A., Herr, D., Kleypas, J., Landis, E., Mcleod, E., et al. (2017). Clarifying the role of coastal and marine systems in climate mitigation. *Front. Ecol. Environ.* 15:42–50. doi: 10.1002/fee.1451

IPCC (2001). "Climate change 2001: the scientific basis," in *Contribution of Working Group I to the Third Assessment Report Of The Intergovernmental Panel on Climate Change*, eds J. T. Houghton, Y. Ding, D. J. Griggs, M. Noguer, P. J. van der Linden, X. Dai, et al. (Cambridge: Cambridge University Press). doi: 10.1111/j.1461-0248.2005.00854.x

Jeffrey, L. C., Maher, D. T., Johnston, S. G., Kelaher, B. P., Steven, A., and Tait, D. R. (2019). Wetland methane emissions dominated by plant-mediated fluxes: contrasting emissions pathways and seasons within a shallow freshwater subtropical wetland. *Limnol. Oceanogr.* 64, 1895–1912. doi: 10.1002/lno.11158

Jensen, S. I., Kühl, M., and Priemé, A. (2007). Different bacterial communities associated with the roots and bulk sediment of the seagrass *Zostera marina*. *FEMS Microbiol. Ecol.* 62, 108–117. doi: 10.1111/j.1574-6941.2007.00373.x

King, G. M., Roslev, P., and Skovgaard, H. (1990). Distribution and rate of methane oxidation in sediments of the Florida Everglades. *Appl. Environ. Microbiol.* 56, 2902–2911. doi: 10.1128/aem.56.9.2902-2911.1990

Koch, S., Jurasinski, G., Koebsch, F., Koch, M., and Glatzel, S. (2014). Spatial variability of annual estimates of methane emissions in a phragmites australis (cav.) trin. ex steud. dominated restored coastal brackish fen. *Wetlands* 34, 593–602. doi: 10.1007/s13157-014-0528-z

Koebsch, F., Winkel, M., Liebner, S., Liu, B., Westphal, J., Schmiedinger, I., et al. (2018). Sulfate deprivation triggers high methane production in a disturbed and rewetted coastal peatland. *Biogeosci. Discuss.* 16, 1938–1953. doi: 10.5194/bg-2018-416

Laanbroek, H. J. (2010). Methane emission from natural wetlands: interplay between emergent macrophytes and soil microbial processes: a mini-review. *Ann. Bot.* 105, 141–153. doi: 10.1093/aob/mcp201

Liikanen, A., Silvennoinen, H., Karvo, A., Rantakokko, P., and Martikainen, P. J. (2009). Methane and nitrous oxide fluxes in two coastal wetlands in the northeastern Gulf of Bothnia. *Baltic Sea. Bor. Environ. Res.* 14, 351–368.

Lyimo, L. D., Gullström, M., Lyimo, T. J., Deyanova, D., Dahl, M., Hamisi, M. I., et al. (2018). Shading and simulated grazing increase the sulphide pool and methane emission in a tropical seagrass meadow. *Mar. Poll. Bull.* 134, 89–93. doi: 10.1016/j.marpolbul.2017.09.005

Mcleod, E., Chmura, G. L., Bouillon, S., Salm, R., Björk, M., Duarte, C. M., et al. (2011). A blueprint for blue carbon: toward an improved understanding of the role of vegetated coastal habitats in sequestering CO2. *Front. Ecol. Environ.* 9:552–560. doi: 10.1890/110004

Moksnes, P.-O., Röhr, M. E., Holmer, M., Eklöf, J. S., Eriander, L., Infantes, E., et al. (2021). Major impacts and societal costs of seagrass loss on sediment carbon and nitrogen stocks. *Ecosphere* 12:e03658. doi: 10.1002/ecs2.3658

Myhre, G., Shindell, D., and Pongratz, J. (2013). ""Anthropogenic and natural radiative forcing," in *Climate change 2013: The Physical Science Basis. Working Group I Contribution to the Fifth Assessment Report of the Intergovernmental Panel on Climate Change*, ed. T. Stocker (Cambridge: Cambridge University Press), 659–740. doi: 10.1017/cbo9781107415324.018

Nyqvist, A., André, C., Gullström, M., Baden, S. P., and Åberg, P. (2009). Dynamics of seagrass meadows on the Swedish Skagerrak coast. *Ambio* 38, 85–88. doi: 10.1579/0044-7447-38.2.85

Oremland, R. S. (1975). Methane production in shallow-water, tropical marine sediments. *Appl. Microbiol.* 30, 602–608. doi: 10.1128/am.30.4.602-608.1975

Oremland, R. S., and Taylor, B. F. (1978). Sulfate reduction and methanogenesis in marine sediments. *Geochim. Cosmochim. Acta.* 42, 209–214. doi: 10.1016/0016-7037(78)90133-3

Orphan, V. J., Hinrichs, K.-U., Ussler Iii, W., Paull, C. K., Taylor, T., Sylva, S. P., et al. (2001). Comparative analysis of methane-oxidizing archaea and sulfate-reducing bacteria in anoxic marine sediments. *Appl. Environ. Microbiol.* 67, 1922–1934. doi: 10.1128/AEM.67.4.1922-1934.2001

Poffenbarger, H., Needelman, B., and Megonigal, P. (2011). Salinity influence on methane emissions from tidal marshes. *Wetlands* 31, 831–842. doi: 10.1007/s13157-011-0197-0

Reeburgh, W. S. (2007). Oceanic methane biogeochemistry. *Chem. Rev.* 107, 486–513. doi: 10.1021/cr050362v

Reeburgh, W. S., Whalen, S. C., and Alperin, M. J. (1993). "The role of methylotrophy in the global methane budget," in *Microbial Growth on C1 Compounds. Proceedings of the 7th International Symposium. American Society for Microbiology*, eds J. C. Murrell and D. P. Kelly (Washington, DC: Intercept Press), 1–14. doi: 10.1038/s41564-019-0534-2

Rhee, T. S., Kettle, A. J., and Andreae, M. O. (2009). Methane and nitrous oxide emissions from the ocean: a reassessment using basin-wide observations in the Atlantic. *J. Geophys. Res.* 114:D12304. doi: 10.1029/2008JD011662

Röhr, M. E., Boström, C., Canal-Vergés, P., and Holmer, M. (2016). Blue carbon stocks in Baltic Sea eelgrass (*Zostera marina*) meadows. *Biogeosciences* 13, 6139–6153. doi: 10.5194/bg-13-6139-2016

Röhr, M. E., Holmer, M., Baum, J. K., Björk, M., Boyer, K., Chin, D., et al. (2018). Blue carbon storage capacity of temperate eelgrass (*Zostera marina*) meadows. *Glob. Biogeochem. Cycl.* 32, 1457–1475. doi: 10.1029/2018GB005941

Rosentreter, J. A., Borges, A. V., Deemer, B. R., Holgerson, M. A., Liu, S., Song, C., et al. (2021). Half of global methane emissions come from highly variable aquatic ecosystem sources. *Nat. Geosci.* 14, 225–230. doi: 10.1038/s41561-021-00715-2

Santos-Fonseca, A., Cardoso Marinho, C., and Assis Esteves, F. (2015). Aquatic macrophytes detritus quality and sulfate availability shape the methane production pattern in a dystrophic coastal lagoon. *Amer. J. Plant Sci.* 6, 1675–1684. doi: 10.4236/ajps.2015.610167

Saunois, M., Stavert, A. R., Poulter, B., Bousquet, P., Canadell, J. G., Jackson, R. B., et al. (2020). The global methane budget 2000–2017. *Earth Syst. Sci. Data* 12, 1561–1623. doi: 10.5194/essd-12-1561-2020

Sela-Adler, M., Ronen, Z., Herut, B., Antler, G., Vigderovich, H., Eckert, W., et al. (2017). Co-existence of methanogenesis and sulfate reduction with common substrates in sulfate-rich estuarine sediments. *Front. Microbiol.* 8:766. doi: 10.3389/fmicb.2017.00766

Staveley, T. A. B., Perry, D., Lindborg, R., and Gullström, M. (2017). Seascape structure and complexity influence temperate seagrass fish assemblage composition. *Ecography* 40, 936–946. doi: 10.1111/ecog.02745

Sutton-Grier, A. E., and Megonigal, J. P. (2011). Plant species traits regulate methane production in freshwater wetland soils. *Soil Biol. Biochem.* 43, 413–420. doi: 10.1016/j.soilbio.2010.11.009

Wang, C., Tong, C., Chambers, L. G., and Liu, X. (2017). Identifying the salinity thresholds that impact greenhouse gas production in subtropical tidal freshwater marsh soils. *Wetlands* 37, 559–571. doi: 10.1007/s13157-017-0890-8

Weber, T., Wiseman, N. A., and Kock, A. (2019). Global ocean methane emissions dominated by shallow coastal waters. *Nat. Comm.* 10:4584. doi: 10.1038/s41467-019-12541-7

Whiting, G., and Chanton, J. (1993). Primary production control of methane emission from wetlands. *Nature* 364, 794–795. doi: 10.1038/364794a0

Wilson, S. T., Al-Haj, A. N., Bourbonnais, A., Frey, C., Fulweiler, R. W., Kessler, J. D., et al. (2020). Ideas and perspectives: a strategic assessment of methane and nitrous oxide measurements in the marine environment. *Biogeosci.* 17, 5809–5828. doi: 10.5194/bg-17-5809-2020

Yvon-Durocher, G., Montoya, J. M., Woodward, G., Jones, J. I., and Trimmer, M. (2011). Warming increases the proportion of primary production emitted as methane from freshwater mesocosms. *Glob. Change Biol.* 17, 1225–1234. doi: 10.1111/j.1365-2486.2010.02289.x

Conflict of Interest: The authors declare that the research was conducted in the absence of any commercial or financial relationships that could be construed as a potential conflict of interest.

Publisher's Note: All claims expressed in this article are solely those of the authors and do not necessarily represent those of their affiliated organizations, or those of the publisher, the editors and the reviewers. Any product that may be evaluated in this article, or claim that may be made by its manufacturer, is not guaranteed or endorsed by the publisher.

frontiers in Marine Science

ORIGINAL RESEARCH
published: 27 January 2022
doi: 10.3389/fmars.2021.768864

Composition of Seagrass Root Associated Bacterial Communities Are Linked to Nutrients and Heavy Metal Concentrations in an Anthropogenically Influenced Estuary

Belinda C. Martin[1,2,3], Jen A. Middleton[1,3], Grzegorz Skrzypek[1], Gary A. Kendrick[1,2], Jeff Cosgrove[4] and Matthew W. Fraser[1,2]*

[1] School of Biological Sciences, The University of Western Australia, Crawley, WA, Australia, [2] UWA Oceans Institute, The University of Western Australia, Crawley, WA, Australia, [3] Ooid Scientific, South Fremantle, WA, Australia, [4] Department of Biodiversity, Conservation and Attractions, WA Government, Kensington, WA, Australia

OPEN ACCESS

Edited by:
Anthony William Larkum, University of Technology Sydney, Australia

Reviewed by:
Shunyan Cheung, Hong Kong University of Science and Technology, Hong Kong SAR, China
Perran Cook, Monash University, Australia

***Correspondence:**
Belinda C. Martin
Belinda.martin@uwa.edu.au

Specialty section:
This article was submitted to Marine Biogeochemistry, a section of the journal Frontiers in Marine Science

Received: *01 September 2021*
Accepted: *31 December 2021*
Published: *27 January 2022*

Citation:
Martin BC, Middleton JA, Skrzypek G, Kendrick GA, Cosgrove J and Fraser MW (2022) Composition of Seagrass Root Associated Bacterial Communities Are Linked to Nutrients and Heavy Metal Concentrations in an Anthropogenically Influenced Estuary. Front. Mar. Sci. 8:768864. doi: 10.3389/fmars.2021.768864

Seagrasses are globally recognized as bioindicators of marine eutrophication and contamination. Seagrasses also harbor a distinct root microbial community that largely reflects the conditions of the surrounding environment as well as the condition of the seagrass. Hence monitoring changes in the root microbial community could act as an additional biological indicator that reflects both the seagrass health condition, as well as potential deterioration in coastal waters. We used 16S rRNA gene sequencing combined with analysis of seagrass nutrients (C, N, $\delta^{15}N$, $\delta^{13}C$) and tissue metal concentrations to investigate potential links between seagrass (*Halophila ovalis*) root bacteria and seagrass nutrient and metal concentrations within an anthropogenically influenced estuary. We found seagrass tissue nitrogen (%) and $\delta^{15}N$ values were 2–5 times higher than global averages for this species. Seagrass root associated bacteria formed distinct communities that clustered by site and were correlated to both seagrass nutrient and metal concentration, with some putative sulfide oxidizing bacteria (*Sulfurimonas* and *Sulfurovum*) correlated with greater nutrient concentrations, and putative iron cycling bacteria (*Lewinella* and *Woeseia*) correlated with greater Fe and As concentrations. Our findings shed further light on the relationship between seagrass and their microbes, as well as provide additional assessment of the use of both seagrass and their microbes as indicators of estuarine and seagrass condition.

Keywords: microbiome, stable isotopes, nitrogen, carbon, 16S rRNA, arsenic, iron

INTRODUCTION

Estuaries, which are transitional zones between the land and the sea, trap sediments and pollutants from rivers and streams and reduce the extent to which these pollutants enter the ocean. However, poor catchment management can lead to increased sediment, nutrient and pollutant loads to estuaries which can cause a decline in the health of the estuary and increase pollution export to the

ocean (Dafforn et al., 2012; Statham, 2012). Excess nutrients and heavy metals are both common and serious pollutants of estuaries (Jiang et al., 2001; Sutherland et al., 2017). Excess nutrients in estuaries can lead to cultural eutrophication and associated deoxygenation events, which is a leading cause of impairment of freshwater and coastal ecosystems globally (Statham, 2012). Heavy metals can accumulate in estuaries naturally through the weathering of rocks and soils and anthropogenically *via* urban and industrial run-off, sewage, and poor agricultural practices (Birch et al., 2018b). Heavy metals can be in dissolved or particulate form and often accrue in sediments (Burton and Johnston, 2010). Under certain physicochemical conditions (e.g., water hypoxia and anoxia), these contaminated sediments can become a source of continued pollution for estuarine ecosystems (Bennett et al., 2012).

Seagrasses are foundation species within many estuaries across the globe, providing habitat, and performing many essential ecological functions (Short et al., 2007; Orth et al., 2017). Seagrasses can uptake nutrients and heavy metals from the sediment *via* their roots or from the water column *via* their shoots. The canopies of seagrass meadows also enhance particle trapping which can further facilitate the accumulation of metals in seagrass sediments (De Boer, 2007). Seagrasses have been used as valuable indicators of estuarine condition and contamination because concentrations of metals and nutrients (and their associated isotope signatures) in seagrass tissue often reflect the concentrations of the surrounding environment (Govers et al., 2014; Kilminster et al., 2014; Bonanno and Orlando-Bonaca, 2017; Orth et al., 2017; Lee et al., 2019). However, whilst seagrasses are considered foundational species of marine ecosystems, microbes are the foundational units of Earth; responsible for balancing and maintaining global biogeochemical cycles. Because of this, microbes (predominantly bacteria) have been used to assess ecological conditions of various natural and man-made systems (Birrer et al., 2019; Filippini et al., 2019) and have recently been used to also assess the health of seagrass (Martin et al., 2020a). As microbes respond rapidly to changes in their environment, developing microbial indicators enhances our capacity to detect potential ecosystem deterioration before lethal impacts have occurred on macroorganisms.

The Swan-Canning estuary flows through Perth the capital city of Western Australia and has seen increased levels of nutrients (above natural levels) due to rapid population growth and intensive agriculture in the surrounding catchment. These excess nutrients have contributed to observed signs of eutrophication (e.g., algal blooms and deoxygenation events) (Robson and Hamilton, 2003). Sediments have also continued to accumulate in the estuary which are enriched in both nutrients and some heavy metals (Gerritse et al., 1998; Rate et al., 2000; Nice, 2009). Historical practice of using riverside wetland areas as rubbish tips, then infilling for parkland or development has also left areas of increased contamination in close proximity to, and leaching into, the estuarine environment (Brearly, 2006). One area of concern is the Alfred Cove Marine Park, which is in close proximity to historic waste disposal sites. Seagrasses in the Alfred Cove Marine Park have previously been found to be in poor condition, to have low C:N ratios as well as elevated $\delta^{15}N$ compared to seagrass in other areas of the Swan-Canning estuary, indicating potentially elevated local inputs of nitrogen to the area (Kilminster and Forbes, 2014). A subsequent groundwater sampling program at Alfred Cove Marine Park confirmed that nitrogen and metal contamination (namely iron, copper, chromium and mercury) exists in this area and that there is potential for this to impact seagrass and the wider estuarine ecology (Vogwill and Oldmeadow, 2018). The aims of this study were to; (i) assess whether concentrations of nutrients (carbon and nitrogen), stable isotopes of carbon and nitrogen, and metals of seagrass tissue correlate with estuary and/or groundwater quality, and (ii) investigate links between seagrass root bacterial communities and seagrass nutrient and seagrass metal concentrations to assess the suitability of bacteria as an additional indicator of seagrass and estuary condition.

MATERIALS AND METHODS

Site Description

The study sites were located within the Swan-Canning estuary which flows through Perth, Western Australia (31.95°S, 115.86°E) and drains a catchment area of approximately 2,090 km^2. The Swan-Canning estuary has a small tidal range and tributaries generally only flow during winter and spring. *Halophila ovalis* is the dominant seagrass growing in the Swan-Canning estuary. The main study area of Alfred Cove Marine Park is one of three marine parks within the Swan-Canning estuary and covers an area ∼ 2 square km (**Figure 1** and **Supplementary Table 1**). The marine park encompasses mudflats, seagrass meadows and intertidal vegetation, which provides habitats for a variety of animals including internationally important migratory wading birds.

The low topography of the area makes it subject to groundwater flow and stormwater runoff and there are several suburban drains which enter the area (**Figure 1**). There are two known historic waste disposal sites in the area (**Figure 1**, marked with red crosses) that were used for domestic and building wastes between 1952 and 1964. During this same decade (1950–1960), the foreshore was cleared of riparian vegetation, the riverbed was dredged with the spoil used to fill in the foreshore.

Sample Collection

A total of 5 seagrass sites, three stormwater drains and two groundwater bores were sampled along the foreshore in January 2019 (Austral summer). All seagrass sites were in water depths between 0.5 and 1.5 m (**Figure 1**). Temperature, salinity, dissolved oxygen and electrical conductivity of each of the sites (except site 4) were recorded *in situ* at the time of collection using a YSI Pro and YSI ProODO. Groundwater was accessed *via* pumping valves on bores that were purged for 5 min before retrieving a water sample. Water samples were also collected from each site and immediately filtered either through a 0.45 μm Polyethersulphone (PES) syringe filter (for $\delta^{15}N$-NO_3 and $\delta^{18}O$-NO_3 analysis) or PES syringe 0.2 μm (for dissolved nutrient analysis). Sampling syringes and containers were rinsed twice with deionized water and with new sample water prior to

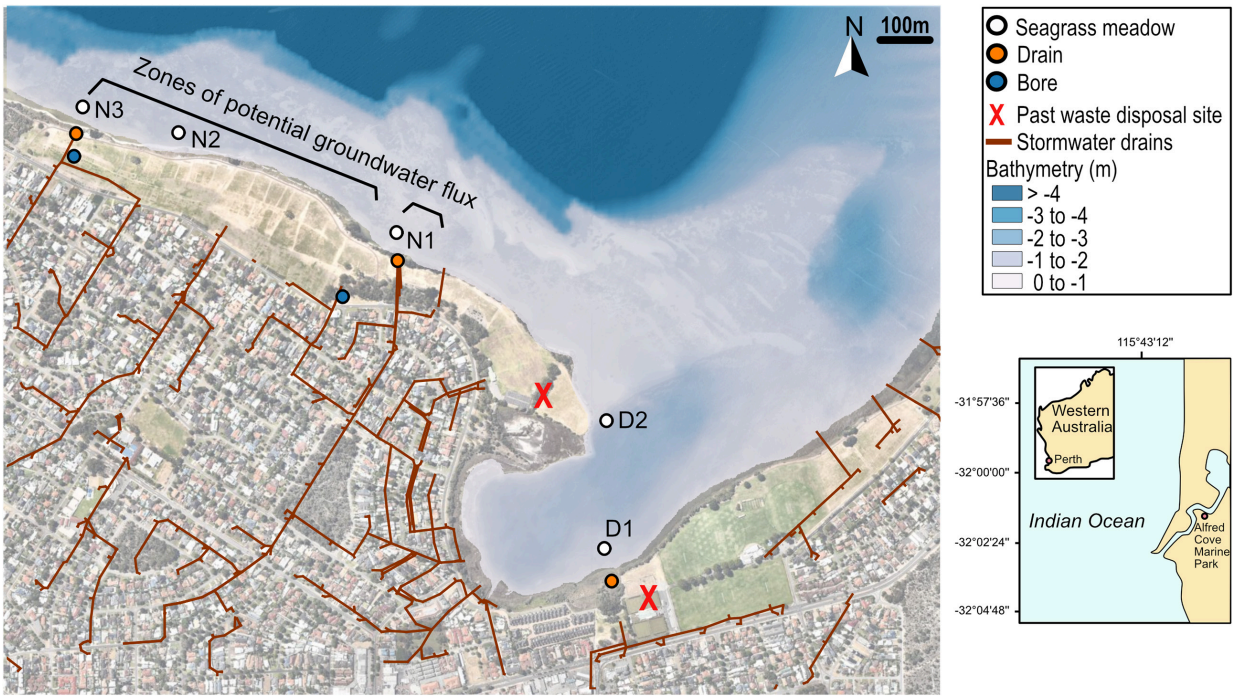

FIGURE 1 | Site names and locations along the Alfred Cove Marine Park with stormwater drainage channels, bathymetry and aerial imagery overlain, where D1 and D2 are closest to old waste disposal sites and N1, N2, and N3 are in the line of the modeled zone of groundwater flux potential. Zones of flux potential of groundwater throughflow have been adapted from Cahill et al. (2017), which were estimated from conductivity-depth profiles. Two historical domestic and building waste disposal sites which were operating in the 1950's are marked with red crosses. Underlying map imagery © 2022 Google, Imagery © 2022 CNES/ Airbus, Maxar Technologies.

sampling. All collected water samples were cooled immediately on ice, stored at 4°C, and were analyzed within 2 weeks of collection (see below).

Four replicate seagrass tissue and sediment samples were collected at each of the seagrass sites using cores (96 mm diameter, 15 cm deep). Sediment was sieved (2 mm) in the field before cooling immediately on ice. Upon returning to the laboratory, the sediment samples were directly frozen, whilst the seagrass tissue was first rinsed in DI water, epiphytes were gently removed and then the tissue frozen. Seagrass biomass (root, rhizome and shoot) was estimated from drying (60°C) and weighing *Halophila ovalis* collected from cores. This dry biomass was also used for $\delta^{15}N$, $\delta^{13}C$, nutrient, and metal analysis (see below).

An additional four replicate apical shoots of *H. ovalis* (with roots attached) were removed from the meadows using the same cores. The two youngest roots (the first and second root) were gently washed from the sediment *in situ* (i.e., some sediment grains were still attached to the root hairs), cut from the rhizome using sterile scissors and gloves, placed into Whirl-paks® (Nasco, Wisconsin) then immediately into liquid nitrogen. Upon returning to the laboratory, these samples were transferred to a −80°C freezer until DNA extraction.

$\delta^{15}N$, $\delta^{13}C$, Nutrient, and Metal Analysis

Dissolved nitrate, ammonium and soluble reactive phosphorus (SRP) were analyzed from filtered (0.2 μm) water samples. Nitrate and ammonium were measured with a colorimetric detection method on a Bran-Luebbe Autoanalyzer 3 (Bran and Luebbe, Norderstedt, Germany) and digital Colorimeter (Technicon, Tarrytown, New York). SRP was determined colorimetrically using the ascorbic acid–molybdate technique (Murphy and Riley, 1962). Dissolved nitrate in water samples was also analyzed for $\delta^{15}N$ (‰, Air) and $\delta^{18}O$ (‰, VSMOW-SLAP) using a modification of the denitrifier method (Sigman et al., 2001; Casciotti et al., 2002) on a continuous flow stable isotope ratio mass spectrometer (Delta V Plus, Thermo-Finnigan, Germany), and the results reported after normalization vs. international standards ($\delta^{15}N$—N2, IAEA-NO-3, USGS32, USGS34, USGS35). The combined uncertainty of analyses (1 std dev) for $\delta^{15}N$ and $\delta^{18}O$ was 0.25‰.

The first and second shoot, rhizome and root from the apex of *H. ovalis* (youngest tissue), as well as sediment were analyzed for $\delta^{15}N$, $\delta^{13}C$,% C, and % N. Frozen seagrass tissue and sediment were dried (60°C) and ground into a fine powder using zirconia balls and a SPEX SamplePrep 2010 Geno/Grinder. Additionally, the sediments were treated with 4% HCl to remove carbonates. Ground samples were then analyzed using a continuous flow system consisting of a Delta V Plus mass spectrometer connected with a Thermo Flush 1112 *via* Conflo IV (Thermo-Finnigan, Germany). All values are given in per mil; $\delta^{13}C$ (‰, VPDB) and $\delta^{15}N$ (‰, Air) according to delta notation (Coplen et al., 2006). Multi-point normalization and international reference materials ($\delta^{13}C$: NBS22, USGS24, NBS19, IAEA600, USGS40;

δ^{15}N—N1, N2, USGS32, IAEA600, USGS40) were used to reduce raw values to the international scales (Skrzypek, 2013). The combined analytical uncertainty (1 std dev) for δ^{13}C was 0.10‰ and for δ^{15}N was 0.10‰.

The first and second shoot, rhizome and root from the apex of *H. ovalis* (youngest tissue) were also analyzed for Al, As, Cd, Cu, Fe, Pb, and Zn. Dried and ground tissue was digested with HNO_3 and $HClO_4$ (0.1 g 10 mL^{-1}) according to Simmons (1975). Analysis of digests was performed using a Perkin Elmer Nexion 1000 (Shelton, Connecticut United States) Inductively Coupled Plasma—Mass Spectrometer. Detection limits (mg kg^{-1}) for metals were as follows; Al (10), As (0.10), Cd (0.02), Cu (1.0), Fe (1.0), Pb (0.1), and Zn (0.5). These metal concentrations were also compared with metal concentrations analyzed from *H. ovalis* tissue and sediments in site N1 in June 2019 (austral winter) using the same method and instrument.

DNA Extraction, Sequencing, and Bioinformatics

DNA was extracted from ∼0.1 g of apical roots using the DNeasy PowerSoil DNA kit (QIAGEN) according to the manufacturer's instructions. A FastPrep-24 bead beater (MP Biomedicals) set at 4.5 ms^{-1} for 60 s was used to lyse microbial cells prior to DNA extraction. Extracted DNA was then eluted in 50 μL nuclease-free water. Microbial communities were profiled using the primers 341F–806R that target the V3-V4 hypervariable region of the 16S rRNA gene. These primers predominantly amplify bacterial taxa but also amplify some members of archaea and have lower off-target amplification of plant chloroplasts (Muyzer et al., 1993; Muhling et al., 2008; Caporaso et al., 2011). Sequencing of pooled amplicons was performed by the Australian Genome Research Facility (AGRF) on the MiSeq platform, using Nextera XT v2 indices and 300 bp paired end sequencing chemistry. Primers were trimmed using cutadapt (version 1.16) (Martin, 2011) and trimmed reads were processed in DADA2 (version 1.9)[1] (Callahan et al., 2016). Taxonomy was assigned following the DADA2 pipeline with the Ribosomal Database Project (RDP) classifier and the SILVA SSU Ref NR 132 database (Quast et al., 2013). Amplicon sequence variants (ASVs) identified in less than 1% of the reads were removed (filter defined by investigating prevalence plots) as well as ASVs identified as chloroplast or mitochondria. Archaea were not filtered out.

PICRUSt2 (Douglas et al., 2020) accompanied by EPA-ng (Barbera et al., 2019), gappa (Czech et al., 2020), castor (Louca and Doebeli, 2018), and MinPath (Ye and Doak, 2009) were used to assign filtered sequencing reads to functional orthologs (KEGG orthologs; KOs) and infer functional pathways. The recommended maximum NSTI cut-off of 2 was implemented in PICRUSt2 to prevent unconsidered interpretation of overly speculative inferences. The NSTI values in our dataset ranged from 0.0001 to 1.3343, indicating a well characterized microbial community in relation to isolate genomes. All pathways were subsequently classified to broader functional categories (i.e., higher pathways) using a custom mapping file created using the MetaCyc database (Caspi et al., 2016). General sequencing statistics can be found in **Supplementary Table 2**. All raw sequences and meta-data have been uploaded to NCBI Sequence Read Archive (SRA) under BioProject ID: PRJNA663104.

[1]https://benjjneb.github.io/dada2/

Data Analysis

Differences in seagrass biomass, seagrass and sediment δ^{15}N, δ^{13}C, C (%), and N (%) among sites were tested with one-way ANOVA's. Normality and homogeneity of variances were checked, and data were log transformed where required. Tukey's HSD was used for multi-comparisons if a significant difference among sites was found. A constrained ordination (Canonical Analysis of Principal Coordinates; CAP) using Bray-Curtis dissimilatory measure on non-rarified ASVs was used to explore the association between root bacterial communities and seagrass root parameters (∼root biomass + root metal concentrations + root nutrients) among sites. A CAP model using Bray-Curtis dissimilatory measures was also built to explore the association between predicted bacterial functions and seagrass root parameters among sites. The significance of the CAP models were assessed using permutation tests with 999 permutations. Correlation analysis between the top 40 most abundant ASVs and predicted functions (agglomerated to Genus and level 2 KEGG functional categories, respectively) and root variables was performed using Pearson's correlation coefficient with *p*-values adjusted for multiple testing (Bonferroni correction).

All statistical analysis was carried out in R (version 4.0.2) (R Development Core Team, 2011) using the Phyloseq (version 1.24.2) (McMurdie and Holmes, 2013), ggplot2 (version 3.3.2) (Wickham, 2009), and vegan packages (version 2.5–6) (Oksanen et al., 2016).

RESULTS

Water Quality

Dissolved oxygen (DO) concentration of seagrass beds ranged from 7.9 mg L^{-1} (99% air saturation) to 15.5 mg L^{-1} (202% air saturation), whilst DO in stormwater drains flowing into seagrass meadows ranged from 0.1 mg L^{-1} (1% air saturation) to 2.8 mg L^{-1} (32% air saturation). The stormwater drains tended to have high concentrations of soluble reactive phosphorus (SRP) and N-NH_4 compared to the seagrass meadows in the estuary, with some of these nutrient values above the Australian and New Zealand guidelines for fresh and marine water quality (ANZECC and ARMCANZ; **Table 1**). The groundwater also had levels of SRP and dissolved inorganic nitrogen that exceeded guidelines (**Table 1**), with the bore sampled closest to site N1 having relatively high levels of N-NH_4 (2.03 mg L^{-1}) and the bore sampled closest to site N3 having high levels of N-NO_3 (0.20 mg L^{-1}). The δ^{15}N-NO_3 values (where N-NO_3 was above the detection limit) ranged from 5.8 to 11.0‰, with the highest value measured in the stormwater drain at S5. The δ^{18}O-NO_3 values ranged from –2.9 to 3.7‰, with the highest value measured in the stormwater drain at S5.

TABLE 1 | Water quality parameters of seagrass meadows, stormwater drains, and groundwater.

Site ID	Location	Temp (°C)	Salinity (ppt)	DO (mg L^{-1})	EC (µS cm^{-1})	Time of day	SRP (mg L^{-1})	N-NO_3 (mg L^{-1})	N-NH_4 (mg L^{-1})	δ^{15}N-NO_3 (‰ AIR)	δ^{18}O-NO_3 (‰ VSMOW)
D1	Seagrass meadow	27.1	34.6	9.6	54,687	1310	**0.019**	BDL	**0.072**	7.2	2.7
D1	Stormwater drain	20.8	0.4	0.3	679	1300	**0.101**	BDL	**0.798**	NA	NA
N1	Seagrass meadow	29.0	33.1	15.5	54,550	1200	**0.006**	BDL	**0.054**	NA	NA
N1	Stormwater drain	22.1	0.7	2.8	1,253	1200	0.005	0.002	0.005	5.8	–2.9
N1	Bore	21.7	0.5	4.4	979	1145	**0.021**	BDL	**2.028**	NA	NA
N3	Seagrass meadow	22.5	32.8	8.9	50,560	1230	**0.014**	BDL	0.034	6.4	2.6
N3	Stormwater drain	22.2	13.7	0.1	21,780	1500	**0.072**	BDL	**0.231**	11.0	3.4
N3	Bore	21.7	0.6	7.5	1,070	1130	**0.018**	**0.202**	**0.069**	6.8	3.7

Values above guidelines for estuaries in south-west Australia (ANZECC and ARMCANZ guidelines, 2000) for SRP (0.005 mg L^{-1}), N-NOx (0.045 mg L^{-1}), and N-NH4 + (0.040 mg L^{-1}) are outlined in bold typeface. DO, dissolved oxygen; SRP, soluble reactive phosphate; BDL, Below detection limit.

Seagrass Biomass and Nutrients

Belowground biomass of *Halophila ovalis* recovered from cores (live roots and rhizomes) was significantly lower at site D1 than sites N2 and N3 (with a general increasing trend from D1 to N3), but aboveground biomass was not significantly different (**Figure 2**).

The sediment at site D2 had significantly higher nitrogen ($\overline{x}$ = 0.1% DW) and carbon content ($\overline{x}$ = 0.9% DW) compared to all other sites (**Figure 3**). Nitrogen% dry weight (DW) was also greatest in seagrass shoots ($\overline{x}$ = 3.0% DW) and roots ($\overline{x}$ = 1.4% DW) growing at site N2 compared to other sites, with exception to shoot nitrogen at N2 which had an average high mean shoot N of 3.2% DW (**Figure 3**). δ^{13}C of seagrass tissue (shoots, rhizomes and roots) was significantly higher at site D2 compared to all other sites, while δ^{15}N was significantly lower (**Figure 3**). The seagrass tissue (shoots, rhizomes and roots) at sites N1 to N3 were all higher in δ^{15}N compared to other sites; with a maximum value across these sites of 8.9‰ measured from shoot tissue at site N3 (**Figure 3**).

Seagrass Heavy Metals

Seagrass tissue metal concentrations differed according to the metal analyzed, the tissue type, and the site (**Figure 4**). With exception of zinc and cadmium, metals were higher in the belowground tissue than aboveground (**Figure 4**). Several metal concentrations in seagrass roots were highly positively correlated, including arsenic and iron ($p < 0.001$, $r = 0.98$) and copper and lead ($p < 0.001$, $r = 0.71$).

Site D1 had some of the highest metal tissue concentrations of all the sites, including for arsenic (As in roots $\overline{x}$ = 20.5 mg kg^{-1}), aluminum (Al in roots $\overline{x}$ = 4,162 mg kg^{-1}), and iron (Fe in roots $\overline{x}$ = 16, 585 mg kg^{-1}). Site N1 had the highest tissue concentrations of copper, cadmium and zinc, though these values were highly variable (**Figure 4**). There are currently no environmental guidelines for heavy metals of aquatic plants in Australia, but some of the heavy metal concentrations measured from *H. ovalis* tissue exceeded the sediment toxicant guidelines in Australia and New Zealand, including arsenic, cadmium and zinc (**Figure 4**). The tissue concentrations of cobolt and zinc when averaged across all sites within the marine park were within the range of those recorded from *H. ovalis* within the highly urbanized Sydney estuary, but were lower for lead, copper and arsenic (**Figure 5**). Regression analysis between root concentrations of heavy metals and sediment heavy metals collected in winter from the current study area showed a significant positive relationship for arsenic [(As) roots = −8.12 + 26.39*(As) Sediment; $p < 0.01$, $R^2 = 0.87$] and a significant negative relationship for lead [(Pb) roots = 20.26 −4.27 *(Pb) Sediment; $p < 0.01$, $R^2 = 0.84$]. Several metal concentrations in seagrass tissues were negatively correlated with total seagrass biomass including arsenic ($p < 0.01$, $r = -0.62$), iron ($p < 0.01$, $r = -0.62$) and aluminum ($p < 0.05$, $r = -0.50$).

Seagrass Root Bacterial Communities

A total of 3128 ASVs were recovered from *H. ovalis* roots. These root bacterial communities were grouped distinctly by site, and this grouping was associated with differences in root nutrients, biomass and metal concentrations (permutation test of constrained analysis $p < 0.001$; **Figure 6A**). Root bacterial communities at Site D2 were associated with higher levels of arsenic and iron, whilst bacterial communities at site N2 and N3 were associated with higher root biomass (**Figure 6A**). Bacterial communities at site N3 were associated with higher δ^{15}N root tissue values, whilst those at site D2 were mostly associated with higher N%, δ^{13}C, and C% (**Figure 6A**).

Agglomerating ASVs to the genus level reduced the number of ASVs to 462. Within this dataset, the top 40 ASVs comprised 71.4% of the community. Of these, the top three ASVs with the highest relative abundance in the *H. ovalis* root microbiome across all sites were related to putative sulfide oxidizing nitrogen fixers [Ca. *Thiodiazotropha* (*Sedimenticolaceae*), Ca. *Electrothrix* (*Desulfobulbaceae*), and *Sulfurimonas* (*Sulfurimonadaceae*); **Figure 6B**]. Of these top genera, *Sulfurimonas* was correlated to seagrass N%, δ^{13}C and lead, and negatively correlated to δ^{15}N (**Figure 6C**). This pattern was also mirrored by related putative sulfide oxidizers of the genus *Sulfurovum* (*Sulfurovaceae*). Several of the top 40 most abundant ASVs were positively correlated with As and Fe concentrations in seagrass roots including, *Lewinella* (*Saprospiraceae*), Marine methylotrophic group 3 (*Methylophagaceae*), *Woeseia* (*Woeseiaceae*), and subgroup 10 of *Thermoanaerobaculaceae*.

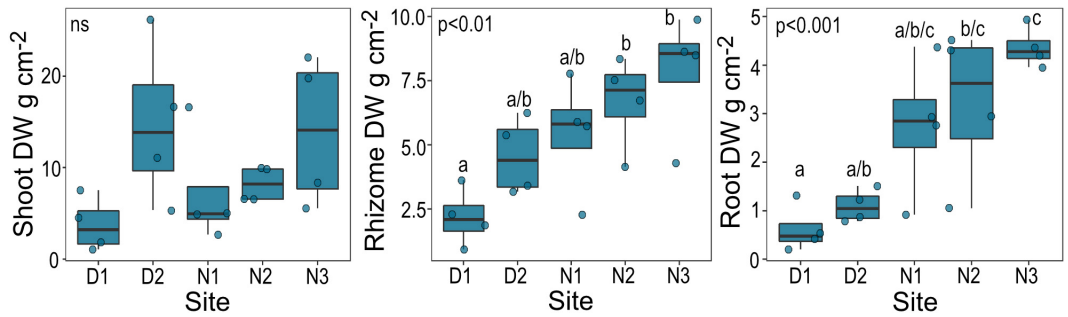

FIGURE 2 | Biomass (DW, dry weight) of *H. ovalis* by site. Data are boxplots with datapoints overlain. Significant *post hoc* comparisons between individual sites are indicated by lowercase letters. Ns, no significant difference among sites.

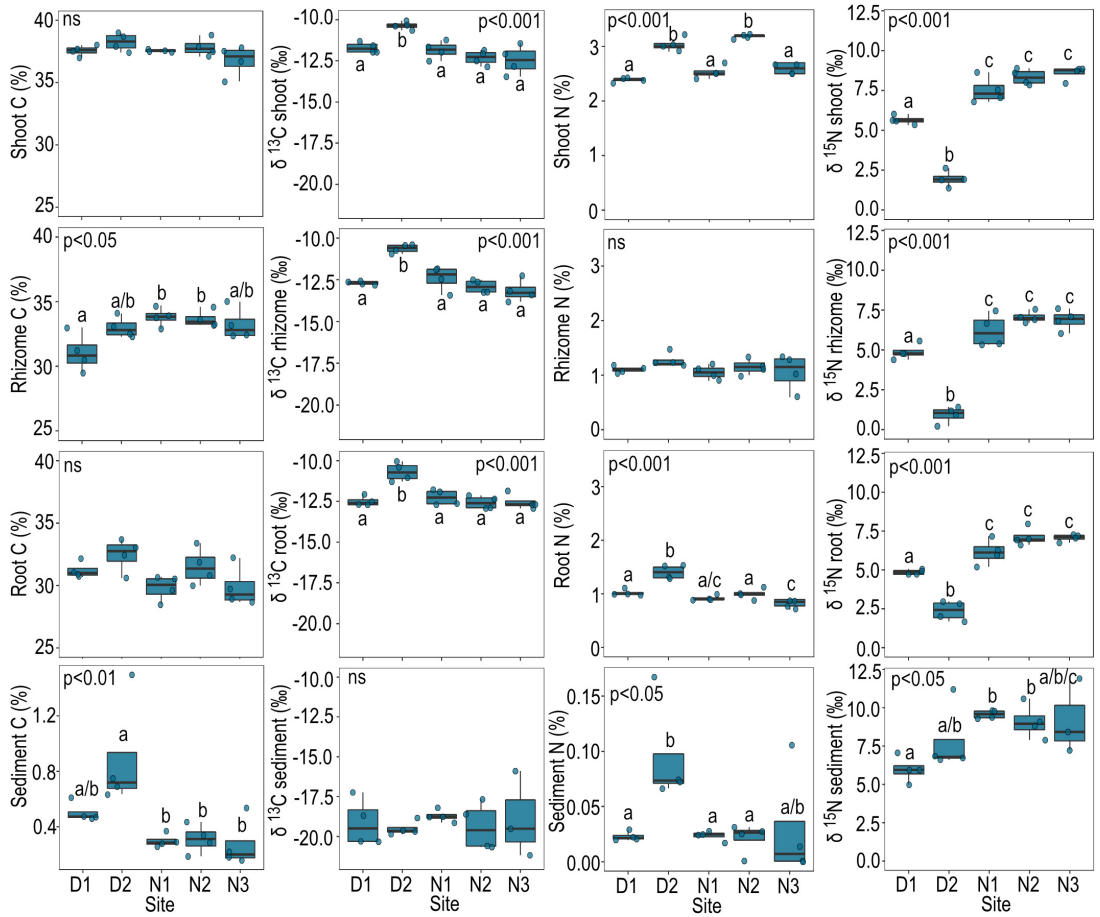

FIGURE 3 | Carbon (%), $\delta^{13}C$, nitrogen (%), and $\delta^{15}N$ of seagrass tissue and sediment by site. Data are boxplots with datapoints overlain. Significant *post hoc* comparisons are indicated by lowercase letters. Ns, no significant difference among sites.

The predicted functions of the root bacterial communities also grouped by site, although less distinctly than the grouping observed for ASVs (permutation test of constrained analysis $p < 0.05$; **Figure 7A**). Predicted bacterial functions from site D2 were particularly variable (**Figure 7A**). The most common predicted bacterial functions of *H. ovalis* root microbiome across sties were related to biosynthesis, including amino acid biosynthesis and fatty acid biosynthesis (**Figure 7B**). Functions related to respiration were also common, as were functions related to the utilization of C1 compounds (**Figure 7B**). Predicted functions relating to bacterial respiration and carbohydrate biosynthesis were positively correlated to root N% and $\delta^{13}C$ (**Figure 7C**). Microbial functions related to fatty acid and lipid biosynthesis were negatively correlated to root biomass, but were

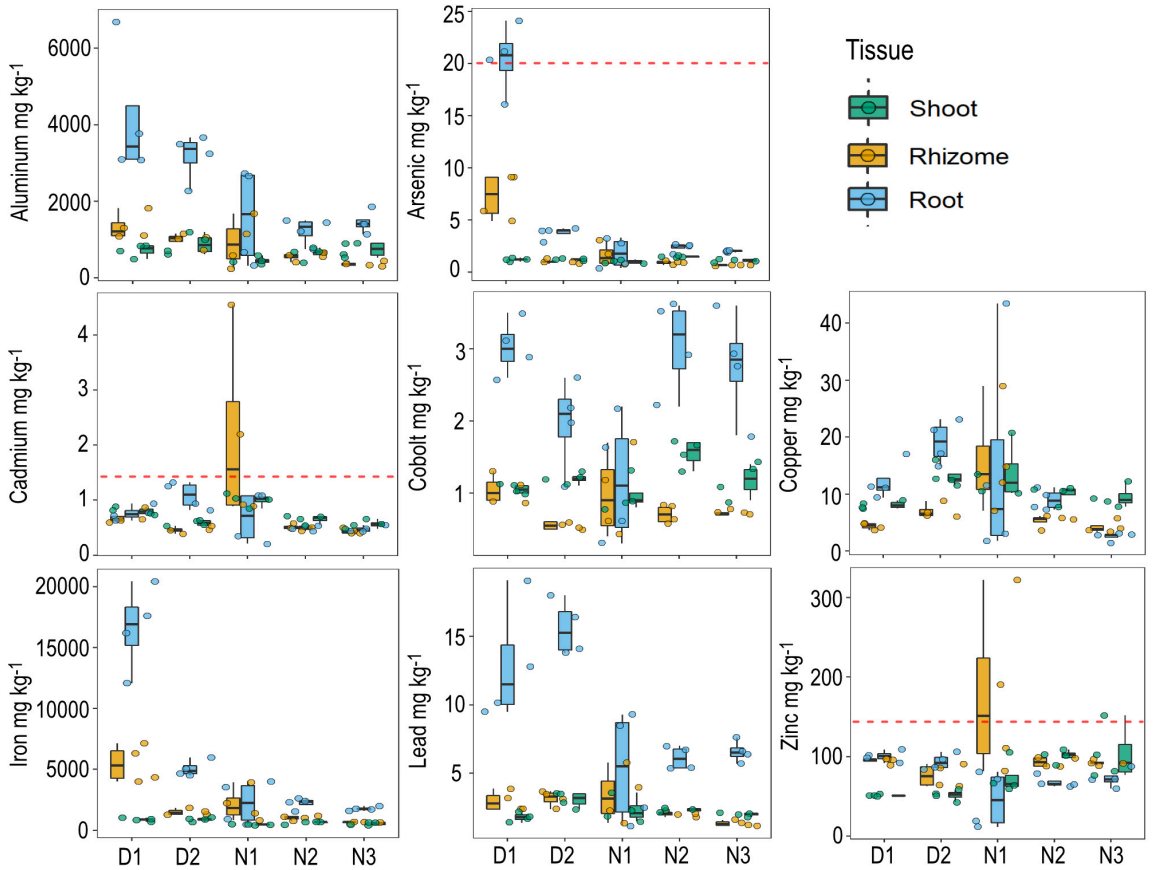

FIGURE 4 | Metal concentrations in seagrass tissue (shoot, rhizome, and roots) by site. Data are boxplots with datapoints overlain. The dashed red line indicates the default value guideline (the concentrations below which there is a low risk of unacceptable effects occurring) for toxicants in sediment according to the Australian and New Zealand Guidelines for Fresh and marine water quality.

positively correlated with root concentrations of Al, As and Fe (**Figure 7C**).

DISCUSSION

Biological monitoring tools (either individual organisms or communities) are increasingly used in integrated assessments of contaminant exposure and for assessing environmental degradation in ecosystems. Here we show that seagrass nutrient and metal status is reflective of an anthropogenically influenced estuary (elevated nutrients and metals). Seagrass root associated bacteria also correlated with the nutrient and metal status of seagrass, thus providing an additional potential monitoring tool for assessing both seagrass and estuarine health.

Seagrass Nutrients as Indicators for Dissolved Inorganic Nitrogen Sources

The δ^{15}N and N% values of *H. ovalis* leaves in this study are among the highest recorded for this species globally, but are in line with previous reports of *H. ovalis* from the Swan-Canning estuary (Hillman et al., 1995). Leaf N% of *H. ovalis* has been previously found to range from 0.75 to 2.68% dry weight (DW) (Birch, 1975; Terrados et al., 1999; Yamamuro et al., 2001, 2003; Mellors et al., 2005), with nutrient limitation estimated to occur with leaf $N < 1.8\%$ DW (Duarte, 1990). All N% leaf values in the current study were $> 2\%$ DW, with some as high as 3.2% DW, which aligns with the nutrient enriched status of the Alfred Cove Marine Park, and more generally of the Swan-Canning estuary (Hillman et al., 1995; Gerritse et al., 1998).

δ^{15}N values of *H. ovalis* leaves have been reported to range from −1.4 to 3.2‰, with a global mean of ∼ 2‰ (Yamamuro et al., 2001, 2003; Christiaen et al., 2014). The average δ^{15}N value of *H. ovalis* leaves in the current study was 6.3‰, with a maximum value of 8.9‰. These δ^{15}N values were also greater than those recorded from the Leschenault estuary (mean = 2.13 ± 0.58‰, $n = 30$, data unpublished), which is an estuary also dominated by *H. ovalis* and located 150 km south of the Swan-Canning estuary. Higher δ^{15}N values in seagrass leaves have been used to indicate anthropogenic nitrogen [dissolved inorganic N; dissolved inorganic nitrogen (DIN)] from sources such as sewage. The δ^{15}N isotope is typically higher in wastewater effluent compared to DIN in natural systems due to enzymatic preference for ^{14}N by bacteria during nitrogen transformations (Lepoint et al., 2004). For example, elevated

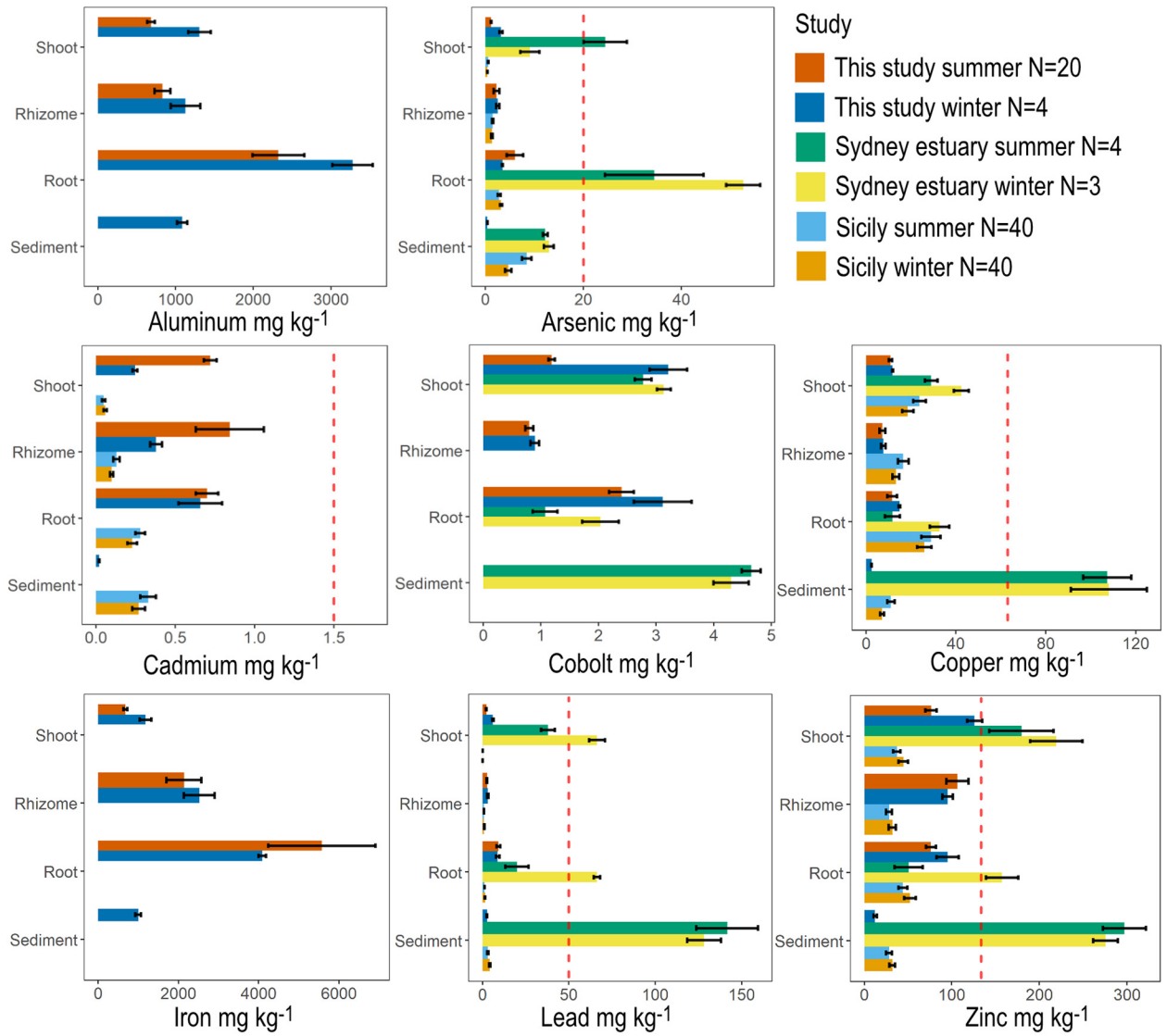

FIGURE 5 | Metal concentrations in seagrass tissue (shoot, rhizome and roots) across all sites compared with mean values recorded from the literature for *Halophila* species. Seagrass tissue at site N1 was also analyzed for metals during June (winter). The dashed red line indicates the default value guideline (the concentrations below which there is a low risk of unacceptable effects occurring) for toxicants in sediment according to the Australian and New Zealand Guidelines for Fresh and marine water. Values for the Sydney estuary were taken from Birch et al. (2018a) and values from Sicily were taken from Bonanno and Raccuia (2018).

$\delta^{15}N$ signatures in stream biota have previously been used to indicate DIN from leaking septic tanks of an urban watershed that was entering *via* groundwater (Steffy and Kilham, 2004). Groundwater modeling of the current study area at Alfred Cove Marine park indicated flux potential of groundwater directly over sites N1 to N3 (**Figure 1**; Cahill et al., 2017). These sites also had the highest $\delta^{15}N$ in seagrass tissues and in the sediment of all the sites which indicates groundwater is a likely source of DIN for these seagrass. The groundwater N-NH_4 concentrations near these same sites were between 30–60 times greater than the N-NH_4 concentrations in surface water at the seagrass meadows (**Table 1**). Ammonium is considered the dominant form of DIN for seagrass uptake, particularly for uptake from the roots (Touchette and Burkholder, 2000). Such relatively high concentrations of N-NH_4 in the groundwater are likely a result of denitrification within the aquifer or during infiltration through unsaturated sediments, which also elevates the δ^{15}N-NO_3 value as NO_3 is consumed (Mariotti et al., 1988). However, the contribution of legacy DIN entering the groundwater from old septic tank systems (which are now largely disused in the region) cannot be ruled out. For this study, the only δ^{15}N-NO_3 value that could be estimated from the groundwater at Alfred Cove Marine Park was 6.8‰, but this was from the section of the aquifer that had lower N-NH_4 concentrations, and so this value is likely to be higher closer to site N3. Additionally, the stormwater drain entering site N3 had a δ^{15}N-NO_3 value of 11‰, which may indicate leaching highly denitrified residual nitrogen that is mobilized from the urban catchment during high rainfall

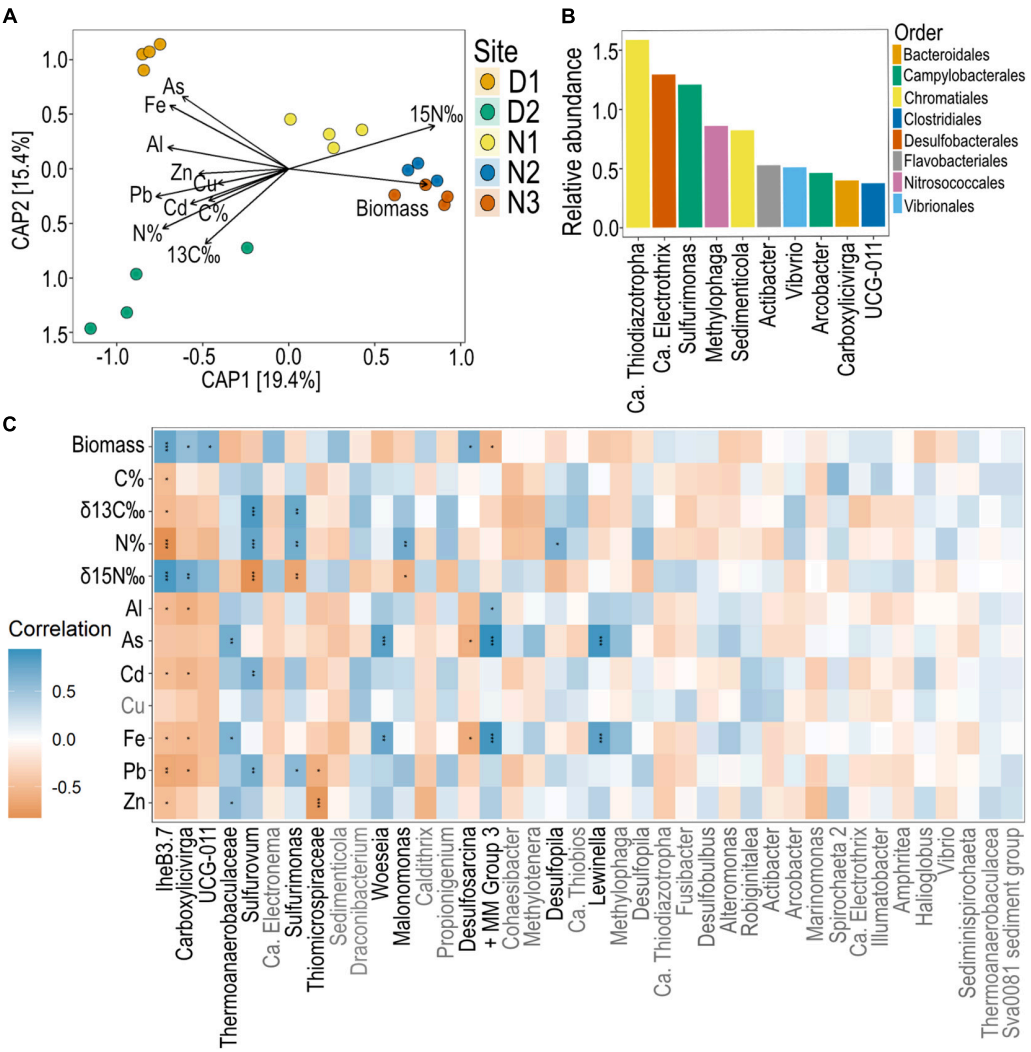

FIGURE 6 | Seagrass root bacteria across sites and their correlation with seagrass nutrient and metal concentrations. **(A)** CAP of Bray-Curtis dissimilatory measures of ASVs constrained by root properties (root biomass, root nutrients and root metal concentrations). **(B)** Top 10 most abundant ASVs across all sites of seagrass roots (agglomerated to genus). **(C)** Pearson's correlation analysis between the top 40 most abundant ASVs (agglomerated to genus) and seagrass root parameters with significant Bonferroni corrected *p*-values indicated with a *, where * = 0.05, ** < 0.01, *** < 0.001. All metal concentrations are mg kg^{-1}. $^{+}$ MM Group 3, Marine methylotrophic group 3.

events. Several factors influence the $\delta^{15}N$ values of seagrasses including temperature, nitrogen availability and the influence of denitrification (higher $\delta^{15}N$) vs. fertilizer run-off (lower $\delta^{15}N$) and nitrogen from biological nitrogen fixation ($\delta^{15}N$ close to 0‰) (Lepoint et al., 2004; Glibert et al., 2019). Further investigation of fractionation effects due to denitrification processes in the aquifer and in the rhizosphere would increase confidence in the interpretation of these results and allow more definitive conclusions as to the elevated $\delta^{15}N$ observed in the current study.

Seagrasses as Indicators for Heavy Metals

Heavy metal concentrations of the Swan-Canning estuary have been previously reported to be highly heterogenous within the estuary, with some sites around the city center contaminated with zinc, lead and copper at levels exceeding Australian and New Zealand sediment quality trigger values (Rate et al., 2000; Nice, 2009). Additionally, groundwater from disused waste disposal sites along the Swan-Canning estuary, including from the site under study, has been found to be contaminated with lead, aluminum, chromium, copper, zinc, arsenic, cadmium, manganese, nickel, and iron (Evans, 2009; Vogwill and Oldmeadow, 2018). Heavy metal analysis of mussels in the Swan-Canning estuary found that zinc was present at the highest concentrations of all metals tested (average across sites = 29.3 mg kg^{-1}), and that these mussels had concentrations of cadmium, copper and zinc that were approximately twice as high as the nearby embayment of Cockburn Sound (Shute, 2007). Some heavy

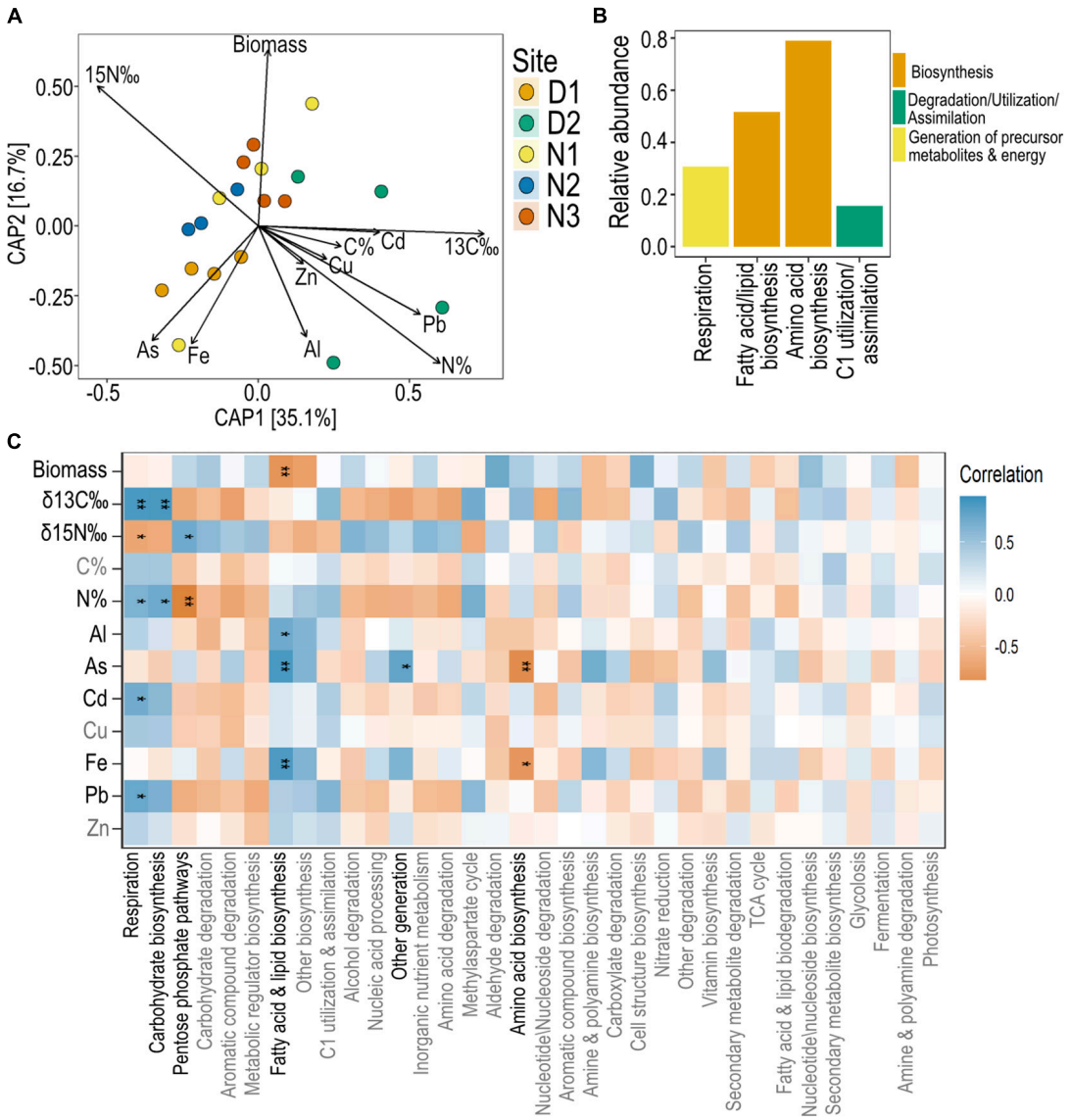

FIGURE 7 | Predicted bacterial functions of seagrass root microbiomes and their correlation with nutrient and metal concentrations. **(A)** Constrained Analysis of Principal Coordinates (CAP) model of PICRUSt2 predicted functions constrained by root properties (root biomass, root nutrients and root metal concentrations). **(B)** Top 10 most abundant predicted functions across all sites of seagrass roots at level 2. **(C)** Pearson's correlation analysis between the top 40 most abundant PICRUSt2 predicted functions (agglomerated to level 2 functions) and seagrass root parameters with significant Bonferroni corrected *p*-values indicated with a *, where * = 0.05, ** < 0.01.

metal concentrations in *H. ovalis* tissue in this study were above sediment guidelines (e.g., arsenic, cadmium and zinc), but were not the highest recorded for this species. The highest literature values of heavy metal concentrations for *H. ovalis* tissue were recorded from Sydney estuary, which is heavily urbanized with an extensive history of industrial use and subsequent contamination events (Birch et al., 2018a). However, few studies exist with reported values of heavy metal concentrations for *Halophila* species (see Nienhuis, 1986; Birch et al., 2018a; Bonanno and Raccuia, 2018), which makes global comparisons limited.

There is little information on how heavy metals impact seagrass physiology and their potential to biomagnify through food chains; especially for *H. ovalis*. Of the few toxicity studies that have been completed, heavy metals have been found to predominantly impact the photosynthetic apparatus of seagrasses (Ralph and Burchett, 1995; Prange and Dennison, 2000). In the current study, aluminum, iron and arsenic were all negatively correlated with seagrass biomass, which could be indicative of photosystem damage. However, this correlation may also be due to other parameters known to impact seagrass biomass (e.g., sulfide and light) that could be co-correlated with metal

concentration. In the case of arsenic, increased uptake of arsenic in macrophytes has been linked with phosphorus deficiency which may impact growth (Chen et al., 2015). This is because plants can uptake arsenic unintentionally *via* phosphate and silicone transporters. A range of freshwater plants including *Vallisneria natans*, which is in the same family as *H. ovalis*, have been shown to hyperaccumulate arsenic (Chen et al., 2015; Wagner et al., 2020), and their potential for use in phytoremediation of wetlands is being explored (Rahman and Hasegawa, 2011). In both the current study and that of Birch et al. (2018a), *H. ovalis* roots contained total arsenic concentrations that were between two and seven times higher than those in the sediments, which may indicate that *H. ovalis* is also able to accumulate arsenic from sediments. Groundwater surrounding the Perth region is thought to be enriched in arsenic due to the exposure of pyritic sediments caused by a combination of dewatering activities, groundwater abstraction, and reduced rainfall; all of which lower the water table (Appleyard et al., 2006). Iron concentration is commonly correlated with arsenic, as was the situation in the current study, as Fe (III) minerals are strong scavengers of arsenic *via* surface sorption and coprecipitation (Johnston et al., 2011). Additionally, the formation of Fe (III) minerals on seagrass roots (so called iron plaques) may be driven by oxygen loss from seagrass roots (Jensen et al., 2005; Brodersen et al., 2014; Martin et al., 2019), as has been shown for rice (Wang et al., 2013; Cheng et al., 2014). Reductive dissolution of Fe (III) minerals can occur in anoxic conditions (e.g., when root oxygen loss ceases at night), which can then release arsenic to the water column (Bennett et al., 2012). Plaque formation and dissolution may also be driven by the activities root associated bacteria *via* elemental cycling (discussed in section below).

It should be stated that the concentrations of metals in seagrass tissues presented here may not necessarily reflect the levels present in the sediment, as whilst seagrass may accumulate some metals, they may also exclude others. Indeed, using the sediment and seagrass metal data collected from the current study site in winter, only concentrations of arsenic and lead were found to be significantly related to the concentrations in the sediment. Additionally, metal bioavailability in sediments is largely controlled by sediment geochemistry. In the current study, the concentrations of cadmium and lead in seagrass roots were significantly correlated to sediment C% (cadmium: $p = 0.03$, $r = 0.48$, lead: $p < 0.01$, $r = 0.64$). However, the interpretation of this is further complicated by the fact that seagrass are also capable of uptake of some metals from the water column through their shoots (Luy et al., 2012; Malea et al., 2018). The advantage of focusing on seagrass tissue rather than sediment or water concentrations is that it provides an integrated measurement of exposure over a period of time rather than just a snapshot which is highly biased by flow, sediment re-suspension/re-working, mixing, tides and other geochemical properties of the sediment. Another benefit of measuring seagrass tissue directly, is that it provides a measure of the total metal concentrations that organisms feeding on seagrass may be exposed to. In fact, the effect of heavy metal contamination in seagrass ecosystems may have a greater impact on the organisms that feed on seagrasses if these metals biomagnify through food webs. Black swans (*Cygnus atratus*) are significant grazers of *H. ovalis* in the Swan-Canning estuary; removing up to 23% of total seagrass production (Eklof et al., 2009). Whilst heavy metal accumulation has been demonstrated for various fauna inhabiting the Swan-Canning estuary such as mussels and bony fish (Shute, 2007; Ranaldi and Gagnon, 2008), heavy metal accumulation in black swans has not been investigated. Recently, scales from wetland snakes collected across wetlands surrounding the Swan-Canning estuary showed contamination of various heavy metals including Mn, As, and Se, which suggests these metals could be accumulating to levels of concern in top predators (Lettoof et al., 2021). Further research on metal biomagnification and biotransference in seagrass ecosystems, as well as understanding the forms that these metals are in (e.g., organic vs. inorganic) is warranted to understand the environmental implications of seagrasses that may accumulate metals of concern.

Linking Seagrass Root Bacteria to Root Tissue Nutrients and Root Tissue Metals

The composition and predicted functions of the root associated bacteria of *H. ovalis* were linked to both seagrass root nutrients (N%, C%, $\delta^{13}C$, $\delta^{15}N$) and seagrass root metal concentrations (particularly As and Fe). For example, some putative sulfide oxidizers including *Sulfurimonas* and *Sulfurovum* were positively correlated to root N% and C%. *Sulfurimonas* related sequences have been recovered previously from seagrass roots, and have been shown to respond to environmental perturbations such as light and oxygen availability (Fahimipour et al., 2017; Martin et al., 2018, 2019). Their relatively high abundance in seagrass roots combined with their apparent response to environmental conditions could make them a good candidate indicator of change across different seagrass species and environments.

Several studies have also shown that metal pollution can impact microbial (bacteria and phytoplankton) communities by decreasing diversity, biomass, and activity (Chodak et al., 2013; Chen et al., 2014; Gołębiewski et al., 2014), which may affect overall nutrient cycling and productivity. Here, both As and Fe were highly correlated to the seagrass root bacterial community structure as well as predicted functions. Of the most abundant bacteria present in the seagrass root microbiome (top 40 ASVs), the genera *Lewinella* and the *Marine methylotrophic group 3* were strongly positively correlated with seagrass root concentrations of As and Fe. Methylotrophic bacteria use reduced one-carbon compounds (such as methane, methanol and other methylated compounds) as the carbon source for their growth and are key players in the global carbon cycle, while *Lewinella* strains are capable of hydrolysis and utilization of complex carbon substrates (McIlroy and Nielsen, 2014). Whilst these genera are significantly correlated with these metals in the current study, this does not imply a cause-effect relationship. However, it does suggest that these bacteria are at least resistant to environments with greater arsenic and iron concentrations which implies they may prove promising candidates for tracking these metals in seagrass and coastal ecosystems.

The speciation and mobility of metals in the environment is also highly influenced by redox activities of microbes. For

example, ferrous iron and arsenite can serve as electron donors for several chemolithotrophic microbes that use oxygen or nitrate as electron acceptors (Hassan et al., 2015). Sulfur-cycling bacteria and methane oxidizers can also impact arsenic and iron mobilization in sediments (Glodowska et al., 2020). As reported previously (Cúcio et al., 2018; Scholz et al., 2019; Tarquinio et al., 2019; Martin et al., 2020a,b), the seagrass root bacterial community was overwhelmingly dominated by putative sulfur cyclers, particularly sulfide oxidizers such as [Ca. *Thiodiazotropha* (*Sedimenticolaceae*), Ca. *Electrothrix* (*Desulfobulbaceae*), and *Sulfurimonas* (*Sulfurimonadaceae*). Sulfide intrusion, and sulfide tissue concentrations of *H. ovalis* and of sediments in the Swan-Canning estuary have previously been found to be greater than sulfide intrusion of *H. ovalis* in another estuary in the southwest of Australia (the Leschenault estuary) (Kilminster et al., 2014; Martin et al., 2020a). This difference is likely due to the higher degree of nutrient and organic matter enrichment in the more urbanized Swan-Canning estuary. These sulfur cycling microbes were associated with sites experiencing higher degree of sediment stress (predominantly measured as greater sulfide intrusion). Sulfide concentrations and sulfide intrusion were not measured in the current study, but would be playing an important role in influencing the composition of the root bacterial communities of *H. ovalis* seen here. The role of sulfur cycling bacteria in influencing seagrass health is an important ongoing research area with implications for improving both environmental monitoring and seagrass restoration (Martin et al., 2020b; Scholz et al., 2021).

Whilst the development of microbial indicators using next-generation sequencing technologies shows great promise for increasing the scope and sensitivity of environmental monitoring, their true success will only be realized when combined with experimental approaches to unravel mechanistic links between microbial taxonomy and function, which have been confirmed from isolated cultures. These mechanistic links are also necessary for predicting microbial responses to pollutants across a range of environments. However, despite the well-known limitations of sequencing technology, the integration of microbial parameters into current monitoring programs is still a worthwhile exercise for hypothesis generation regarding pollution impacts on ecosystems functions. Future advances in sequencing technology will also likely facilitate the uptake of this technology by more diverse end users; either as a result of decreased sequencing costs or increased accuracy of data (e.g., long read sequencing) and improvements in database accuracy. As such, complementary use of biochemical and molecular indicator tools shows great promise as another line of evidence in helping understand ecosystem response to environmental perturbations and ultimately aid in predicting and mitigating impacts of future change.

DATA AVAILABILITY STATEMENT

The datasets presented in this study can be found in online repositories. The names of the repository/repositories and accession number(s) can be found below: https://www.ncbi.nlm.nih.gov/, PRJNA663104.

AUTHOR CONTRIBUTIONS

BM: study design and conception, method development, data collection, data analysis, drafting the manuscript, and approval of final submission. JM: method development, data collection, data analysis, drafting the manuscript, and approval of final submission. MF, GK, and JC: study design and conception, method development, drafting the manuscript, and approval of final submission. GS: study design and conception, data analysis, drafting the manuscript, and approval of final submission. All authors contributed to the article and approved the submitted version.

FUNDING

This research was funded through WA Department of Biodiversity Conservation and Attractions (DBCA). MF was supported by the Robson and Robertson postdoctoral fellowship awarded by the Jock Clough Marine Foundation. This research was partly supported by the Integrated Coastal Analyses and Sensor Technology (ICoAST) project with funding from the Indian Ocean Marine Research Centre, a joint partnership between The University of Western Australia (UWA), the Australian Institute of Marine Science (AIMS), the Commonwealth Scientific and Industrial Research Organisation (CSIRO), and the Department of Primary Industries and Regional Development (DPIRD) WA.

ACKNOWLEDGMENTS

We thank Liam Kelly, Natalie Joyce, and City of Melville for their assistance with fieldwork and collection of data. We also thank the reviewers who have improved this manuscript through review. We also acknowledge the use of WABC and UWA-SAGE, as well as the technical assistance of Douglas Ford, Kate Bowler, and Michael Smirk for stable isotope and metal analysis. We acknowledge the use of the services and facilities of AGRF and PWIS for many fruitful discussions. We acknowledge that this work was completed on Noongar land, and that Noongar people remain the spiritual and cultural custodians of their land, and continue to practice their values, languages, beliefs and knowledge. We pay our respects to the traditional owners of the lands on which we live and work across Western Australia and Australia.

SUPPLEMENTARY MATERIAL

The Supplementary Material for this article can be found online at: https://www.frontiersin.org/articles/10.3389/fmars.2021.768864/full#supplementary-material

REFERENCES

Appleyard, S. J., Angeloni, J., and Watkins, R. (2006). Arsenic-rich groundwater in an urban area experiencing drought and increasing population density, Perth, Australia. *Appl. Geochem.* 21, 83–97. doi: 10.1016/j.apgeochem.2005.09.008

Barbera, P., Kozlov, A. M., Czech, L., Morel, B., Darriba, D., Flouri, T., et al. (2019). EPA-ng: massively parallel evolutionary placement of genetic sequences. *Syst. Biol.* 68, 365–369. doi: 10.1093/sysbio/syy054

Bennett, W. W., Teasdale, P. R., Panther, J. G., Welsh, D. T., Zhao, H., and Jolley, D. F. (2012). Investigating arsenic speciation and mobilization in sediments with DGT and DET: a mesocosm evaluation of oxic-anoxic transitions. *Environ. Sci. Technol.* 46, 3981–3989. doi: 10.1021/es204484k

Birch, G. F., Cox, B. M., and Besley, C. H. (2018a). Metal concentrations in seagrass (*Halophila ovalis*) tissue and ambient sediment in a highly modified estuarine environment (Sydney estuary, Australia). *Mar. Pollut. Bull.* 131, 130–141. doi: 10.1016/j.marpolbul.2018.04.010

Birch, G. F., Cox, B. M., and Besley, C. H. (2018b). The relationship between metal concentrations in seagrass (*Zostera capricorni*) tissue and ambient fine sediment in modified and near-pristine estuaries (Sydney estuaries, Australia). *Mar. Pollut. Bull.* 128, 72–81. doi: 10.1016/j.marpolbul.2018.01.006

Birch, W. R. (1975). Some chemical and calorific properties of tropical marine angiosperms compared with those of other plants. *J. Appl. Ecol.* 12, 201–212.

Birrer, S. C., Dafforn, K. A., Sun, M. Y., Williams, R. B. H., Potts, J., Scanes, P., et al. (2019). Using meta-omics of contaminated sediments to monitor changes in pathways relevant to climate regulation. *Environ. Microbiol.* 21, 389–401. doi: 10.1111/1462-2920.14470

Bonanno, G., and Orlando-Bonaca, M. (2017). Trace elements in Mediterranean seagrasses: accumulation, tolerance and biomonitoring. A review. *Mar. Pollut. Bull.* 125, 8–18. doi: 10.1016/j.marpolbul.2017.10.078

Bonanno, G., and Raccuia, S. A. (2018). Comparative assessment of trace element accumulation and bioindication in seagrasses *Posidonia oceanica*, *Cymodocea nodosa* and *Halophila stipulacea*. *Mar. Pollut. Bull.* 131, 260–266. doi: 10.1016/j.marpolbul.2018.04.039

Brearly, A. (2006). *Ernest Hodgkin's Swanland: Estuaries and Coastal Lagoons of South-Western Australia*. Perth, WA: UWA Publishing.

Brodersen, K. E., Nielsen, D. A., Ralph, P. J., and Michael, K. (2014). Oxic microshield and local pH enhancement protects *Zostera muelleri* from sediment derived hydrogen sulphide. *New Phytol.* 205, 1264–1276. doi: 10.1111/nph.13124

Burton, G. A., and Johnston, E. L. (2010). Assessing contaminated sediments in the context of multiple stressors. *Environ. Toxicol. Chem.* 29, 2625–2643. doi: 10.1002/etc.332

Cahill, K., Rutherford, J., Farmer, D., and Munday, T. (2017). *Ground-Based Geophysics: Results from an Investigation Near Lucky Bay*. Perth, WA: CSIRO.

Callahan, B. J., McMurdie, P. J., Rosen, M., Han, A. W., Johnson, A. J. A., and Holmes, S. (2016). DADA2: high resolution sample inference from Illumina amplicon data. *Nat. Methods* 13, 581–583. doi: 10.1038/nmeth.3869.DADA2

Caporaso, J. G., Lauber, C. L., Walters, W. A., Berg-Lyons, D., Lozupone, C. A., Turnbaugh, P. J., et al. (2011). Global patterns of 16S rRNA diversity at a depth of millions of sequences per sample. *Proc. Natl. Acad. Sci. U.S.A.* 108, 4516–4522. doi: 10.1073/pnas.1000080107

Casciotti, K. L., Sigman, D. M., Hastings, M. G., Böhlke, J. K., and Hilkert, A. (2002). Measurement of the oxygen isotopic composition of nitrate in seawater and freshwater using the denitrifier method. *Anal. Chem.* 74, 4905–4912. doi: 10.1021/ac020113w

Caspi, R., Billington, R., Ferrer, L., Foerster, H., Fulcher, C. A., Keseler, I. M., et al. (2016). The MetaCyc database of metabolic pathways and enzymes and the BioCyc collection of pathway/genome databases. *Nucleic Acids Res.* 44, D471—D480. doi: 10.1093/nar/gkv1164

Chen, G., Liu, X., Brookes, P. C., and Xu, J. (2015). Opportunities for phytoremediation and bioindication of arsenic contaminated water using a submerged aquatic plant: *Vallisneria natans* (lour.) Hara. *Int. J. Phytoremediation* 17, 249–255. doi: 10.1080/15226514.2014.883496

Chen, J., He, F., Zhang, X., Sun, X., Zheng, J., and Zheng, J. (2014). Heavy metal pollution decreases microbial abundance, diversity and activity within particle-size fractions of a paddy soil. *FEMS Microbiol. Ecol.* 87, 164–181. doi: 10.1111/1574-6941.12212

Cheng, H., Wang, M., Wong, M. H., and Ye, Z. (2014). Does radial oxygen loss and iron plaque formation on roots alter Cd and Pb uptake and distribution in rice plant tissues? *Plant Soil* 375, 137–148. doi: 10.1007/s11104-013-1945-0

Chodak, M., Gołębiewski, M., Morawska-Płoskonka, J., Kuduk, K., and Niklińska, M. (2013). Diversity of microorganisms from forest soils differently polluted with heavy metals. *Appl. Soil Ecol.* 64, 7–14. doi: 10.1016/j.apsoil.2012.11.004

Christiaen, B., Bernard, R. J., Mortazavi, B., Cebrian, J., and Ortmann, A. C. (2014). The degree of urbanization across the globe is not reflected in the δ15N of seagrass leaves. *Mar. Pollut. Bull.* 83, 440–445. doi: 10.1016/j.marpolbul.2013.06.024

Coplen, T. B., Brand, W. A., Gehre, M., Gröning, M., Meijer, H. A. J., Toman, B., et al. (2006). New guidelines for δ13C measurements. *Anal. Chem.* 78, 2439–2441. doi: 10.1021/ac052027c

Cúcio, C., Overmars, L., Engelen, A. H., and Muyzer, G. (2018). Metagenomic analysis shows the presence of bacteria related to free-living forms of sulfur-oxidizing chemolithoautotrophic symbionts in the rhizosphere of the seagrass *Zostera marina*. *Front. Mar. Sci.* 5:171. doi: 10.3389/fmars.2018.00171

Czech, L., Barbera, P., and Stamatakis, A. (2020). Genesis and Gappa: processing, analyzing and visualizing phylogenetic (placement) data. *Bioinformatics* 36, 3263–3265. doi: 10.1093/bioinformatics/btaa070

Dafforn, K. A., Simpson, S. L., Kelaher, B. P., Clark, G. F., Komyakova, V., Wong, C. K. C., et al. (2012). The challenge of choosing environmental indicators of anthropogenic impacts in estuaries. *Environ. Pollut.* 163, 207–217. doi: 10.1016/j.envpol.2011.12.029

De Boer, W. F. (2007). Seagrass-sediment interactions, positive feedbacks and critical thresholds for occurrence: a review. *Hydrobiologia* 591, 5–24. doi: 10.1007/s10750-007-0780-9

Douglas, G. M., Maffei, V. J., Zaneveld, J. R., Yurgel, S. N., Brown, J. R., Taylor, C. M., et al. (2020). PICRUSt2 for prediction of metagenome functions. *Nat. Biotechnol.* 38, 685–688. doi: 10.1038/s41587-020-0548-6

Duarte, C. (1990). Seagrass nutrient content. *Mar. Ecol. Prog. Ser.* 67, 201–207. doi: 10.3354/meps067201

Eklof, J. S., McMahon, K., and Lavery, P. S. (2009). Effects of multiple disturbances in seagrass meadows: shading decreases resilience to grazing. *Mar. Freshw. Res.* 60, 1317–1327. doi: 10.1071/MF09008

Evans, S. (2009). *A Baseline Study of Contaminants in Groundwater at Disused Waste Disposal Sites in the Swan Canning Catchment*. Perth, WA: Department of Water and Environmental Regulation.

Fahimipour, A. K., Kardish, M. R., Lang, J. M., Green, J. L., Eisen, J. A., and Stachowicz, J. J. (2017). Global-scale structure of the eelgrass microbiome. *Appl. Environ. Microbiol.* 83:e03391-16. doi: 10.1128/AEM.03391-16

Filippini, G., Bugnot, A. B., Johnston, E. L., Ruszczyk, J., Potts, J., Scanes, P., et al. (2019). Sediment bacterial communities associated with environmental factors in Intermittently Closed and Open Lakes and Lagoons (ICOLLs). *Sci. Total Environ.* 693:133462. doi: 10.1016/j.scitotenv.2019.07.268

Gerritse, R. G., Wallbrink, P. J., and Murray, A. S. (1998). Accumulation of phosphorus and heavy metals in the Peel-Harvey Estuary in Western Australia: results of a preliminary study. *Estuar. Coast. Shelf Sci.* 47, 679–693. doi: 10.1006/ecss.1998.0392

Glibert, P. M., Middelburg, J. J., Mcclelland, J. W., and Vander Zanden, M. J. (2019). Stable isotope tracers: enriching our perspectives and questions on sources, fates, rates, and pathways of major elements in aquatic systems. *Limnol. Oceanogr.* 66, 950–981. doi: 10.1002/lno.11087

Glodowska, M., Stopelli, E., Schneider, M., Rathi, B., Straub, D., Lightfoot, A., et al. (2020). Arsenic mobilization by anaerobic iron-dependent methane oxidation. *Commun. Earth Environ.* 1:42. doi: 10.1038/s43247-020-00037-y

Gołębiewski, M., Deja-Sikora, E., Cichosz, M., Tretyn, A., and Wróbel, B. (2014). 16S rDNA pyrosequencing analysis of bacterial community in heavy metals polluted soils. *Microb. Ecol.* 67, 635–647. doi: 10.1007/s00248-013-0344-7

Govers, L. L., Lamers, L. P. M., Bouma, T. J., Eygensteyn, J., de Brouwer, J. H. F., Hendriks, A. J., et al. (2014). Seagrasses as indicators for coastal trace metal pollution: a global meta-analysis serving as a benchmark, and a Caribbean case study. *Environ. Pollut.* 195, 210–217. doi: 10.1016/j.envpol.2014.08.028

Hassan, Z., Sultana, M., van Breukelen, B. M., Khan, S. I., and Röling, W. F. M. (2015). Diverse arsenic- and iron-cycling microbial communities in arsenic-contaminated aquifers used for drinking water in Bangladesh. *FEMS Microbiol. Ecol.* 91:fiv026. doi: 10.1093/femsec/fiv026

Hillman, K., McComb, A. J., and Walker, D. I. (1995). The distribution, biomass and primary production of the seagrass *Halophila ovalis* in the Swan/Canning Estuary, Western Australia. *Aquat. Bot.* 51, 1–54. doi: 10.1016/0304-3770(95)00466-D

Jensen, S. I., Kühl, M., Glud, R. N., Jørgensen, L. B., and Priemé, A. (2005). Oxic microzones and radial oxygen loss from roots of *Zostera marina*. *Mar. Ecol. Prog. Ser.* 293, 49–58. doi: 10.3354/meps293049

Jiang, Y., Kirkman, H., and Hua, A. (2001). Megacity development: managing impacts on marine environments. *Ocean Coast. Manag.* 44, 293–318. doi: 10.1016/S0964-5691(01)00052-7

Johnston, S. G., Keene, A. F., Burton, E. D., Bush, R. T., and Sullivan, L. A. (2011). Iron and arsenic cycling in intertidal surface sediments during wetland remediation. *Environ. Sci. Technol.* 45, 2179–2185. doi: 10.1021/es103403n

Kilminster, K., and Forbes, V. (2014). *Seagrass as an Indicator of Estuary Condition in the Swan-Canning Estuary, Water Science Technical Series, Report No. 62.* Perth, WA: Department of Water.

Kilminster, K., Forbes, V., and Holmer, M. (2014). Development of a 'sediment-stress' functional-level indicator for the seagrass *Halophila ovalis*. *Ecol. Indic.* 36, 280–289. doi: 10.1016/j.ecolind.2013.07.026

Lee, G., Suonan, Z., Kim, S. H., Hwang, D. W., and Lee, K. S. (2019). Heavy metal accumulation and phytoremediation potential by transplants of the seagrass *Zostera marina* in the polluted bay systems. *Mar. Pollut. Bull.* 149:110509. doi: 10.1016/j.marpolbul.2019.110509

Lepoint, G., Dauby, P., and Gobert, S. (2004). Applications of C and N stable isotopes to ecological and environmental studies in seagrass ecosystems. *Mar. Pollut. Bull.* 49, 887–891. doi: 10.1016/j.marpolbul.2004.07.005

Lettoof, D. C., Rankenburg, K., McDonald, B. J., Evans, N. J., Bateman, P. W., Aubret, F., et al. (2021). Snake scales record environmental metal(loid) contamination. *Environ. Pollut.* 274:116547. doi: 10.1016/j.envpol.2021.116547

Louca, S., and Doebeli, M. (2018). Efficient comparative phylogenetics on large trees. *Bioinformatics* 34, 1053–1055. doi: 10.1093/bioinformatics/btx701

Luy, N., Gobert, S., Sartoretto, S., Biondo, R., Bouquegneau, J. M., and Richir, J. (2012). Chemical contamination along the Mediterranean French coast using *Posidonia oceanica* (L.) Delile above-ground tissues: a multiple trace element study. *Ecol. Indic.* 18, 269–277. doi: 10.1016/j.ecolind.2011.11.005

Malea, P., Kevrekidis, T., Chatzipanagiotou, K. R., and Mogias, A. (2018). Cadmium uptake kinetics in parts of the seagrass *Cymodocea nodosa* at high exposure concentrations. *J. Biol. Res.* 25:5. doi: 10.1186/s40709-018-0076-4

Mariotti, A., Landreau, A., and Simon, B. (1988). 15N isotope biogeochemistry and natural denitrification process in groundwater: application to the chalk aquifer if northern France. *Geochim. Cosmochim. Acta* 52, 1869–1878. doi: 10.1016/0016-7037(88)90010-5

Martin, B. C., Alarcon, M. S., Gleeson, D., Middleton, A., Fraser, M. W., Ryan, M. H., et al. (2020a). Root microbiomes as indicators of seagrass health. *FEMS Microbiol. Ecol.* 96:fiz201. doi: 10.1093/femsec/fiz201

Martin, B. C., Middleton, J. A., Fraser, M. W., Marshall, I. P. G., Scholz, V. V., and Schmidt, H. (2020b). Cutting out the middle clam: lucinid endosymbiotic bacteria are also associated with seagrass roots worldwide. *ISME J.* 14, 2901–2905. doi: 10.1038/s41396-020-00771-3

Martin, B. C., Bougoure, J., Ryan, M. H., Bennett, W. W., Colmer, T. D., Joyce, N. K., et al. (2019). Oxygen loss from seagrass roots coincides with colonisation of sulphide-oxidising cable bacteria and reduces sulphide stress. *ISME J.* 13, 707–719. doi: 10.1038/s41396-018-0308-5

Martin, B. C., Gleeson, D., Statton, J., Siebers, A. R., Grierson, P., Ryan, M. H., et al. (2018). Low light availability alters root exudation and reduces putative beneficial microorganisms in seagrass roots. *Front. Microbiol.* 8:2667. doi: 10.3389/fmicb.2017.02667

Martin, M. (2011). Cutadapt removes adapter sequences from high-throughput sequencing reads. *EMBnet J.* 7, 2803–2809. doi: 10.1089/cmb.2017.0096

McIlroy, S. J., and Nielsen, P. H. (2014). "The family *Saprospiraceae*," in *The Prokaryotes*, eds E. Rosenberg, E. F. DeLong, S. Lory, E. Stackebrandt, and F. Thompson (Berlin: Springer), 863–889. doi: 10.1007/978-3-642-38954-2_138

McMurdie, P. J., and Holmes, S. (2013). phyloseq: an R package for reproducible interactive analysis and graphics of microbiome census data. *PLoS One* 8:e61217. doi: 10.1371/journal.pone.0061217

Mellors, J., Waycott, M., and Marsh, H. (2005). Variation in biogeochemical parameters across intertidal seagrass meadows in the central Great Barrier Reef region. *Mar. Pollut. Bull.* 51, 335–342. doi: 10.1016/j.marpolbul.2004.10.046

Muhling, M., Woolven-Allen, J., Murrell, J. C., and Joint, I. (2008). Improved group-specific PCR primers for denaturing gradient gel electrophoresis analysis of the genetic diversity of complex microbial communities. *ISME J.* 2, 379–392. doi: 10.1038/ismej.2007.97

Murphy, J., and Riley, J. P. (1962). A modified single solution method for the determination of phosphate in natural waters. *Anal. Chim. Acta* 27, 31–36. doi: 10.1016/S0003-2670(00)88444-5

Muyzer, G., De Waal, E. C., and Uitterlinden, A. G. (1993). Profiling of complex microbial populations by denaturing gradient gel electrophoresis analysis of polymerase chain reaction-amplified genes coding for 16S rRNA. *Appl. Environ. Microbiol.* 59, 695–700. doi: 10.1128/aem.59.3.695-700.1993

Nice, H. (2009). *A Baseline Study of Contaminants in the Sediments of the Swan and Canning Estuaries*. Perth, WA: Department of Water and Environmental Regulation.

Nienhuis, P. H. (1986). Background levels of heavy metals in nine tropical seagrass species in Indonesia. *Mar. Pollut. Bull.* 17, 508–511. doi: 10.1016/0025-326X(86)90640-5

Oksanen, J., Blanchet, F., Friendly, M., Kindt, R., Legendre, P., McGlinn, D., et al. (2016). *Vegan: Community Ecology Package. R package Version. 2.0-10.*

Orth, R. J., Dennison, W. C., Lefcheck, J. S., Gurbisz, C., Hannam, M., Keisman, J., et al. (2017). Submersed aquatic vegetation in chesapeake bay: sentinel species in a changing world. *BioScience* 67, 698–712. doi: 10.1093/biosci/bix058

Prange, J. A., and Dennison, W. C. (2000). Physiological responses of five seagrass species to trace metals. *Mar. Pollut. Bull.* 41, 327–336. doi: 10.1016/S0025-326X(00)00126-0

Quast, C., Pruesse, E., Yilmaz, P., Gerken, J., Schweer, T., Yarza, P., et al. (2013). The SILVA ribosomal RNA gene database project: improved data processing and web-based tools. *Nucleic Acids Res.* 41, 590–596. doi: 10.1093/nar/gks1219

R Development Core Team (2011). *R: A Language and Environment for Statistical Computing*. Vienna: R Foundation for Statistical Computing.

Rahman, M. A., and Hasegawa, H. (2011). Aquatic arsenic: phytoremediation using floating macrophytes. *Chemosphere* 83, 633–646. doi: 10.1016/j.chemosphere.2011.02.045

Ralph, P. J., and Burchett, M. D. (1995). Photosynthetic responses of the seagrass *Halophila ovalis* (R. Br.) Hook. f. to high irradiance stress, using chlorophyll a fluorescence. *Aquat. Bot.* 51, 55–66. doi: 10.1016/0304-3770(95)00456-A

Ranaldi, M. M., and Gagnon, M. M. (2008). Trace metal incorporation in otoliths of black bream (*Acanthopagrus butcheri* Munro), an indicator of exposure to metal contamination. *Water Air Soil Pollut.* 194, 31–43. doi: 10.1007/s11270-008-9696-x

Rate, A. W., Robertson, A. E., and Borg, A. T. (2000). Distribution of heavy metals in near-shore sediments of the Swan River estuary, Western Australia. *Water Air Soil Pollut.* 124, 155–168. doi: 10.1023/A:1005289203825

Robson, B. J., and Hamilton, D. P. (2003). Summer flow event induces a cyanobacterial bloom in a seasonal Western Australian estuary. *Mar. Freshw. Res.* 54, 139–151. doi: 10.1071/MF02090

Scholz, V. V., Martin, B. C., Meyer, R., Schramm, A., Fraser, M. W., Nielsen, L. P., et al. (2021). Cable bacteria at oxygen-releasing roots of aquatic plants: a widespread and diverse plant-microbe association. *New Phytol.* 232, 2138–2151. doi: 10.1111/nph.17415

Scholz, V. V., Müller, H., Koren, K., Nielsen, L. P., and Meckenstock, R. U. (2019). The rhizosphere of aquatic plants is a habitat for cable bacteria. *FEMS Microbiol. Ecol.* 95:fiz062. doi: 10.1093/femsec/fiz062

Short, F., Carruthers, T., Dennison, W., and Waycott, M. (2007). Global seagrass distribution and diversity: a bioregional model. *J. Exp. Mar. Biol. Ecol.* 350, 3–20. doi: 10.1016/j.jembe.2007.06.012

Shute, S. (2007). *Tributyltin and Heavy Metal Survey in the Swan River*. Prepared for the Swan River Trust. Report No. 581/1. Wembley, WA: Oceanica Consulting Pty Ltd.

Sigman, D. M., Casciotti, K. L., Andreani, M., Barford, C., Galanter, M., and Böhlke, J. K. (2001). A bacterial method for the nitrogen isotopic analysis of nitrate in seawater and freshwater. *Anal. Chem.* 73, 4145–4153. doi: 10.1021/ac010088e

Simmons, W. J. (1975). Determination of low concentrations of cobalt in small samples of plant material by flameless atomic absorption spectrophotometry. *Anal. Chem.* 47, 2015–2018. doi: 10.1021/ac60362a013

Skrzypek, G. (2013). Normalization procedures and reference material selection in stable HCNOS isotope analyses: an overview. *Anal. Bioanal. Chem.* 405, 2815–2823. doi: 10.1007/s00216-012-6517-2

Statham, P. J. (2012). Nutrients in estuaries - an overview and the potential impacts of climate change. *Sci. Total Environ.* 434, 213–227. doi: 10.1016/j.scitotenv.2011.09.088

Steffy, L. Y., and Kilham, S. S. (2004). Elevated δ15N in stream biota in areas with septic tank systems in an urban watershed. *Ecol. Appl.* 14, 637–641. doi: 10.1890/03-5148

Sutherland, M. D., Dafforn, K. A., Scanes, P., Potts, J., Simpson, S. L., Sim, V. X. Y., et al. (2017). Links between contaminant hotspots in low flow estuarine systems and altered sediment biogeochemical processes. *Estuar. Coast. Shelf Sci.* 198, 497–507. doi: 10.1016/j.ecss.2016.08.029

Tarquinio, F., Hyndes, G. A., Laverock, B., Koenders, A., and Säwström, C. (2019). The seagrass holobiont: understanding seagrass-bacteria interactions and their role in seagrass ecosystem functioning. *FEMS Microbiol. Lett.* 366:fnz057. doi: 10.1093/femsle/fnz057

Terrados, J., Borum, J., Duarte, C. M., Fortes, M. D., Kamp-Nielsen, L., Agawin, N. S. R., et al. (1999). Nutrient and mass allocation of South-east Asian seagrasses. *Aquat. Bot.* 63, 203–217. doi: 10.1016/S0304-3770(99)00004-2

Touchette, B. W., and Burkholder, J. M. (2000). Review of nitrogen and phosphorus metabolism in seagrasses. *J. Exp. Bot.* 250, 133–167. doi: 10.1037/h0034880

Vogwill, R., and Oldmeadow, D. (2018). *IF14 Groundwater Sampling and analysis Report*. Harare: Prepared for Department of Parks and Wildlife.

Wagner, S., Hoefer, C., Puschenreiter, M., Wenzel, W. W., Oburger, E., Hann, S., et al. (2020). Arsenic redox transformations and cycling in the rhizosphere of *Pteris vittata* and *Pteris quadriaurita*. *Environ. Exp. Bot.* 177:104122. doi: 10.1016/j.envexpbot.2020.104122

Wang, X., Yao, H., Wong, M. H., and Ye, Z. (2013). Dynamic changes in radial oxygen loss and iron plaque formation and their effects on Cd and As accumulation in rice (*Oryza sativa* L.). *Environ. Geochem. Health* 35, 779–788. doi: 10.1007/s10653-013-9534-y

Wickham, H. (2009). *ggplot2: Elegant Graphics for Data Analysis*, 2nd Edn. New York, NY: Springer.

Yamamuro, M., Kayanne, H., and Yamano, H. (2003). δ15N of seagrass leaves for monitoring anthropogenic nutrient increases in coral reef ecosystems. *Mar. Pollut. Bull.* 46, 452–458. doi: 10.1016/S0025-326X(02)00463-0

Yamamuro, M., Umezawa, Y., and Koike, I. (2001). Seasonality in nutrient concentrations and stable isotope ratios of *Halophila ovalis* growing on the intertidal flat of SW Thailand. *Limnology* 2, 199–205. doi: 10.1007/s10201-001-8036-2

Ye, Y., and Doak, T. G. (2009). A parsimony approach to biological pathway reconstruction/inference for genomes and metagenomes. *PLoS Comput. Biol.* 5:e1000465. doi: 10.1371/journal.pcbi.1000465

Conflict of Interest: The authors declare that the research was conducted in the absence of any commercial or financial relationships that could be construed as a potential conflict of interest.

Publisher's Note: All claims expressed in this article are solely those of the authors and do not necessarily represent those of their affiliated organizations, or those of the publisher, the editors and the reviewers. Any product that may be evaluated in this article, or claim that may be made by its manufacturer, is not guaranteed or endorsed by the publisher.

frontiers in Plant Science

ORIGINAL RESEARCH
published: 10 February 2022
doi: 10.3389/fpls.2022.805065

Photoacclimation and Light Thresholds for Cold Temperate Seagrasses

Romy Léger-Daigle[1], Fanny Noisette[1], Simon Bélanger[2], Mathieu Cusson[3] and Christian Nozais[2]*

[1] Québec-Océan and Institut des Sciences de la Mer de Rimouski, Université du Québec à Rimouski, Rimouski, QC, Canada, [2] Québec-Océan and Département de Biologie, Chimie et Géographie, Université du Québec à Rimouski, Rimouski, QC, Canada, [3] Québec-Océan and Département des Sciences Fondamentales, Université du Québec à Chicoutimi, Chicoutimi, QC, Canada

Water quality deterioration is expected to worsen the light conditions in shallow coastal waters with increasing human activities. Temperate seagrasses are known to tolerate a highly fluctuating light environment. However, depending on their ability to adjust to some decline in light conditions, decreases in daily light quantity and quality could affect seagrass physiology, productivity, and, eventually, survival if the *Minimum Quantum Requirements* (MQR) are not reached. To better understand if, how, and to what extent photosynthetic adjustments contribute to light acclimation, eelgrass (*Zostera marina* L.) shoots from the cold temperate St. Lawrence marine estuary (Rimouski, QC, Canada) were exposed to seven light intensity treatments (6, 36, 74, 133, 355, 503, and 860 μmol photons m^{-2} s^{-1}, 14:10 light:dark photoperiod). Photosynthetic capacity and efficiency were quantified after five and 25 days of light exposure by Pulse Amplitude Modulated (PAM) fluorometry to assess the rapid response of the photosynthetic apparatus and its acclimation potential. Photoacclimation was also studied through physiological responses of leaves and shoots (gross and net primary production, pigment content, and light absorption). Shoots showed proof of photosynthetic adjustments at irradiances below 200 μmol photons m^{-2} s^{-1}, which was identified as the threshold between limiting and saturating irradiances. Rapid Light Curves (RLC) and net primary production (NPP) rates revealed sustained maximal photosynthetic rates from the highest light treatments down to 74 μmol photons m^{-2} s^{-1}, while a compensation point (NPP = 0) of 13.7 μmol photons m^{-2} s^{-1} was identified. In addition, an important package effect was observed, since an almost three-fold increase in chlorophyll content in the lowest compared to the highest light treatment did not change the leaves' light absorption. These results shed new light on photosynthetic and physiological processes, triggering light acclimation in cold temperate eelgrass. Our study documents an MQR value for eelgrass in the St. Lawrence estuary, which is highly pertinent in the context of conservation and restoration of eelgrass meadows.

Keywords: photophysiology, PAM fluorometry, *Zostera marina*, subarctic, light attenuation and limitation, photosynthesis, eelgrass

OPEN ACCESS

Edited by:
Jan de Vries,
University of Göttingen, Germany

Reviewed by:
Jessica Pazzaglia,
University of Naples Federico II, Italy
Zhijian Jiang,
South China Sea Institute of Oceanology, Chinese Academy of Sciences (CAS), China
Yan Xiang Ow,
National University of Singapore, Singapore

****Correspondence:***
Romy Léger-Daigle
romy.leger-daigle@uqar.ca

Specialty section:
This article was submitted to Marine and Freshwater Plants, a section of the journal Frontiers in Plant Science

Received: *29 October 2021*
Accepted: *11 January 2022*
Published: *10 February 2022*

Citation:
Léger-Daigle R, Noisette F, Bélanger S, Cusson M and Nozais C (2022) Photoacclimation and Light Thresholds for Cold Temperate Seagrasses. Front. Plant Sci. 13:805065. doi: 10.3389/fpls.2022.805065

INTRODUCTION

Human-induced environmental stressors contribute to the degradation of light conditions in vegetated coastal ecosystems through changes in water quality. Water quality is especially compromised through increased particle loading in coastal zones from the watershed (Kemp et al., 1983; Hemminga and Duarte, 2000). In addition, excessive anthropogenic nitrogen inputs indirectly limit light penetration in the water column as it stimulates phytoplanktonic and epiphytic algal growth (Kemp et al., 1983; Borum, 1985; Sand-Jensen and Borum, 1991), competing with benthic autotrophs for light (Agusti et al., 1994; Heuvel et al., 2019). The light limitation has been singled out as the primary cause of seagrass loss worldwide (Hauxwell et al., 2001; Short et al., 2011). For example, *Zostera marina* L. (1753; eelgrass), the prevalent seagrass in temperate North Atlantic coastal habitats (Green and Short, 2003), was declining in 2007 at an estimated rate of 1.4% per year (Short et al., 2011). This decline in global spatial cover was attributed to the combined effects of natural environmental pressures (e.g., extreme weather events, ice scouring, and terrestrial runoffs) and anthropogenic disturbances (e.g., land use, sand mining, coastal development, aquatic recreational, and commercial activities) (Green and Short, 2003; Hauxwell et al., 2003; Unsworth et al., 2018) through deterioration of light conditions in coastal waters. Specifically, changes in light intensity, spectral composition, or regime have been shown to strongly impact eelgrass distribution, growth, and survival, and ultimately alter coastal habitats and communities (Dennison, 1987; Zimmerman et al., 1991; Nielsen et al., 2002; Ralph et al., 2007).

Alteration of eelgrass meadow dynamics can profoundly disturb shallow coastal ecosystems because of their critical role in these habitats. Eelgrass meadows provide many ecosystem services and fulfill major ecological roles for coastal communities associated with the complex habitat structure they provide and its associated fauna (Duffy, 2006). Because of its significant ecological role, *Z. marina* was recognized as an Ecologically Significant Species in Canada in 2009 (Cooper et al., 2009). A decline in eelgrass abundance could damper their water purification role through particle depositions and nutrient uptake (Nelson and Waaland, 1997; Hemminga and Duarte, 2000) and contribute even more to the degradation of light conditions in meadows (Maxwell et al., 2017). Eelgrass biological responses to changing light conditions deserve attention, especially in Western North Atlantic coastal waters, where underwater light conditions are altered by sustained human activities (Waycott et al., 2009). This is especially the case in boreal and subarctic environments, where strong seasonality and extreme weather events can cause light attenuation in the water column over periods from a few days to several weeks through, for instance, ice cover, freshet, or terrestrial runoffs, inducing browning of the coastal waters (Murphy et al., 2021).

Changes in light intensity can alter subcellular processes and induce a response to adjust and optimize photosynthesis. As described by Falkowski and Raven (2007), incident light influences the electron transport in the thylakoid membranes (electron transport chain, ETC) downstream of photosystem II (PSII), in which photons are captured by accessory pigments and funneled toward the chl*a* of the reaction center. There, electrons are retrieved from H_2O molecules to feed the ETC. Electron transport supplies the Calvin cycle with NAPDH and ATP. The most common ways to monitor photosynthesis are through the electron transport rate (ETR) in the ETC and CO_2/O_2 fluxes. Manipulation of PSII by Pulse Amplitude Modulated (PAM) fluorometry provides insights into the functioning of the photosynthetic apparatus. This technique reveals the relative importance of the different pathways competing for photon energy: photochemistry, fluorescence, and heat dissipation, complementing the information gathered on primary productivity (Schreiber, 2004).

Following a change in light intensity, biological responses to optimize photosynthesis can occur on different biological and timescales (McMahon et al., 2013; Bertelli and Unsworth, 2018). For example, rapid adjustments to a new constant irradiance take place in a matter of days through subcellular photosynthetic changes (Lambers et al., 2008). On the other hand, photoacclimation, i.e., photosynthetic, physiological, and morphological adjustments to light conditions may take weeks to months, and occur from subcellular to plant scale (McMahon et al., 2013; Schubert et al., 2018). At shoot scale, an increase in leaf surface or photosynthetic biomass, often approximated by an increase of the above or below-ground biomass ratio, helps maintain carbon balance by decreasing the proportion of non-photosynthetic tissues relative to photosynthetic ones (Olesen and Sand-Jensen, 1993). In addition, higher pigment content can counteract low light levels by increasing leaf absorptance (Beer et al., 2014), i.e., the fraction of incident photons harvested by leaf tissues (Kirk, 1994; Zimmerman, 2003). Furthermore, the photosynthetic apparatus responds to low light conditions by optimizing photon use at the subcellular level, thus enhancing photosynthetic efficiency (Bertelli and Unsworth, 2018). However, despite a more efficient photon use, insufficient photon availability leads to a decreased electron transport rate and, consequently, to a lower photosynthetic capacity. Photoacclimation is achieved when the plant has reached a new steady state, reflecting optimization of photosynthesis under its new light environment (Lambers et al., 2008; Bertelli and Unsworth, 2018). At some point, the photophysiological adjustments can no longer compensate for the too few incident photons, and shoot mortality can occur if carbon balance cannot be maintained and metabolic costs exceed carbon fixation by photosynthesis (Longstaff and Dennison, 1999; Ralph et al., 2007; Bertelli and Unsworth, 2018).

There have been attempts to estimate the *Minimum Light Requirements* (MLR) needed for growth and survival for *Z. marina*. This MLR is expressed as a percentage of surface irradiance and traditionally determined by the light intensity measured at the maximum depth limit of a seagrass species or population (Dennison et al., 1993). However, the MLR calculated for seagrasses by Duarte (1991) (i.e., 11% of surface irradiance) is not well suited for cold temperate intertidal ecosystems which experience less daylight than tropical species (Lee et al., 2007; Bulmer et al., 2016; Eriander, 2017). Light requirements can also be regarded as the light intensity under which the shoot

respiratory demands amount photosynthesis (Ralph et al., 2007), referred to as *Minimum Quantum Requirements* for growth (MQR) and expressed as photosynthetically active radiation (PAR) intensity. Although rarely encountered in literature (Ralph et al., 2007), this latter proxy is more appropriate when studying photoacclimation in a context of conservation since it provides an absolute minimum light intensity to which seagrasses can acclimate and survive. Therefore, it becomes relevant to reassess these light requirements when studying specific species or even populations, especially for management and conservation purposes (Collier et al., 2012; Bertelli and Unsworth, 2018).

This study aims to characterize the photoacclimation responses of *Z. marina* in controlled conditions along a natural gradient of PAR intensity experienced by an intertidal eelgrass population from the cold temperate St. Lawrence Estuary (Quebec, Canada, ca. 48.5°N). Rapid adjustments to changes in irradiance after five days were quantified by examining tissue-scale photosynthetic responses (i.e., photosynthetic apparatus efficiency and capacity). Photoacclimation was also assessed by examining the evolution of the photosynthetic and physiological adjustments after 25 days of light exposure *via* measurements of photosynthetic apparatus efficiency and capacity, pigment content, and shoot-scale primary production. Based on the observations of Bertelli and Unsworth (2018), shoots metabolism should have reached a new stable state by that time. Compared to physiological responses, the photosynthetic apparatus should respond first, after only a few days of light exposure (Collier et al., 2012; Bertelli and Unsworth, 2018). These rapid adjustments are expected to occur with light decrease until PAR intensity becomes too low to support photosynthetic activity and maintain carbon balance. We hypothesized that photoacclimation would occur as soon as PAR becomes limiting to optimize photon absorption and electron transport, thus maintaining photosynthetic rates. This should be achieved through increased chlorophyll concentration and absorptance, increased photon use, and lower saturating light intensity.

MATERIALS AND METHODS

Sample Collection

Whole eelgrass shoots were collected on the intertidal eelgrass meadow in East Rimouski, Quebec, Canada (48°27′42.24″N 68°31′25.92″O) on July 8, 2020, and placed in a cooler with seawater for transport to the Pointe-au-Père research station located a few kilometers away. The next day, shoots with their root system and surrounding sediments were transplanted into individual plastic cores (5 cm deep, 2.5 cm diameter). Transplanted shoots were approximately 20 cm in height, had intact roots, and three rhizome internodes. Prior to the experiment, shoots were placed in experimental tanks four days for acclimation, with a 14:10 photoperiod (light:dark, h) and under 860 μmol photon m^{-2} s^{-1}, which corresponds to the mean light intensity measured over a tide cycle during daytime in the same meadow in summer 2020 (Léger-Daigle, unpublished results).

Experimental Design and System

Seven PAR treatments (6, 36, 74, 133, 355, 503, and 860 μmol m^{-2} s^{-1}) were used to test for eelgrass light adjustment and acclimation responses. This range of light intensities was established to achieve a high resolution of the photoacclimation response in the lower irradiances. Most of the light intensities were chosen for their ecological significance. For instance, 36 and 133 μmol photons m^{-2} s^{-1} are close to the light compensation point for growth and the maximum specific growth rate of *Z. marina,* respectively (Olesen and Sand-Jensen, 1993). Furthermore, the 6 and 860 μmol photons m^{-2} s^{-1} treatments correspond to the mean PAR intensity measured, respectively, under the seasonal sea ice cover in winter (Horner and Schrader, 1982) and during daytime in summer in Rimouski. The latter light treatment, therefore, acts as a control treatment. The other three light intensities (i.e., 74, 355, and 503 μmol photons m^{-2} s^{-1}) were selected to achieve exponential increments throughout the studied range.

The experiment was carried out in a flow-through system in two separate tanks, in which the PAR treatments were randomly assigned (**Figure 1**). For each PAR treatment, nine shoots were randomly and evenly distributed in three transparent independent containers (three individual plastic cores per container). The shoots served as units of replication, although shoots from the same containers were considered pseudo-replicates and accounted for in the statistical treatment. The containers were continuously and directly supplied with sand-filtered seawater pumped a few kilometers offshore of the research station. Water temperature remained constant at 11 ± 0.01°C. Lighting was ensured by LED growth lights mimicking the sunlight emission spectrum (model GHBH-640W–120V, RayonLed, Montreal, CA, United States). Light intensity was attenuated with gray filters (LEE Filters, Burbank, CA, United States) to reach the targeted PAR, without changing spectral quality. Filters were suspended above the three containers of each treatment. The natural daylight hours of that time of year, a 14:10 photoperiod (light:dark, h), were recreated by an autonomous timer.

Eelgrass shoots were kept in the containers for 25 days, during which epiphytes were manually cleaned off the leaves twice a week. Rapid photosynthetic adjustments were assessed after five days of exposure for each light treatment. Photosynthetic responses were measured again at the end of the experiment (on day 25) to compare these responses to those of day 5 (rapid adjustments) and assess photoacclimation (**Figure 1**). Physiological responses were also measured on day 25 to appreciate acclimation responses to the different light treatments. Finally, leaf surface (cm^2) was measured with ImageJ software (Rasband, 2019).

Photosynthetic Measurements

The photophysiological responses of eelgrass were determined by non-invasive PAM fluorometry with a Diving PAM-II (Heinz Walz GmbH, Effeltrich, Germany). Rapid Light Curves (RLCs) were used to assess photosynthesis (White and Critchley, 1999; Ralph and Gademann, 2005). Particularly, fluorescence is

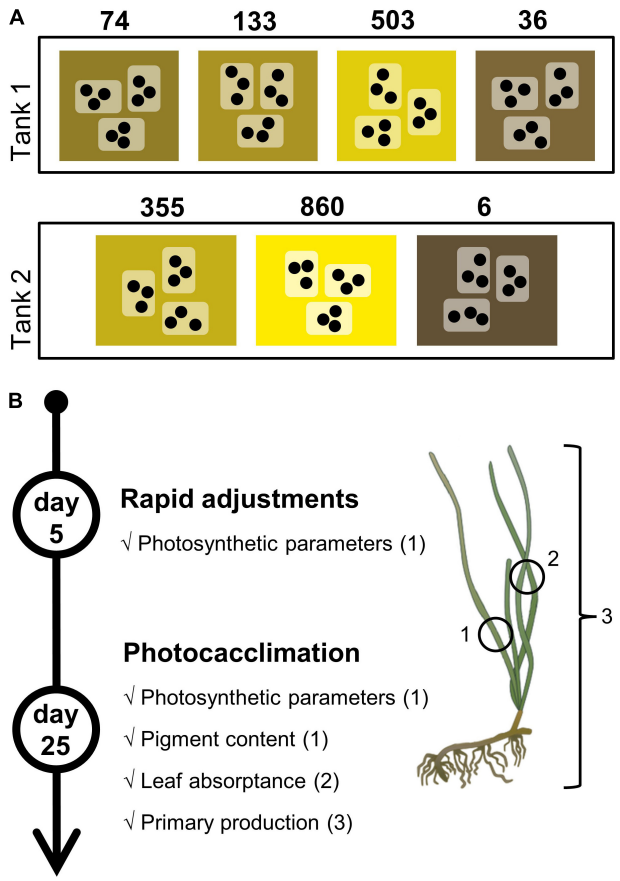

FIGURE 1 | Schematic representation of the experimental system and sampling design. **(A)** Experimental flowthrough system with the two tanks in which were randomly assigned the seven light intensity treatments (numbers in μmol photons m^{-2} s^{-1}), to which nine shoots (●: sediment core with a single shoot) were exposed while distributed in three transparent plastic containers. **(B)** Sampling timeline for rapid adjustments and photoacclimation assessment. Numbers in parenthesis refer to the part of the shoot used for measurements. 1: second leaf, 5 cm above the sheath; 2: green mature leaf fragment; 3: whole shoot. For every variable, n = 9 shoots per treatment, except for primary production where n = 6 shoots per treatment.

measured through a range of PAR intensity and allows calculation of quantum yields (maximum: Fv/Fm; and effective: YII), ETR, and quenching coefficients (photochemical: qP; and non-photochemical: NPQ) for each actinic light step. RLCs usually exhibit three regions from which photosynthetic parameters can be estimated: (i) in the light-limited region of the RLC, the initial slope of the ETR-PAR relationship (alpha, α) is used as a proxy for photosynthetic efficiency (Schreiber, 2004). (ii) As PAR intensity increases, the onset of light saturation (E_k) is reached, the ETC saturates and the ETR reaches a plateau (ETR_{max}) which serves as a proxy for photosynthetic capacity (Schreiber, 2004). Mathematically, E_k corresponds to the intersection of alpha and ETR_{max}. Physiologically, E_k is the light intensity where neither photochemical reactions (qP) nor heat dissipation (NPQ) dominates fluorescence quenching (Henley, 1993). (iii) In the high end of the PAR range of the RLC, a drop of the ETR can occur, indicating photoinhibition (Henley, 1993).

Rapid Light Curves (RLCs) were carried out on each shoot, on the second leaf, approximately 5 cm above the top of the sheath (Beer et al., 2001), after five and 25 days of light exposure, and around midday every time. The RLCs consisted of 10 actinic light steps (38, 68, 98, 137, 190, 288, 432, 637, 954, and 1246 μmol photons m^{-2} s^{-1}) lasting 10 s each. Leaves were shaded with the leaf clip no more than 10 s before the start of the RLC (Ralph and Gademann, 2005). The PAM calculates the ETR using the equation of Beer et al. (2001):

$$ETR = YII \times PAR \times AF \times 0.5 \quad (1)$$

where YII is the effective quantum yield of photosystem II, PAR corresponds to the actinic light intensity generated by the PAM, AF refers to the absorption factor, and 0.5 refers to the even distribution of photons between PSII and PSI (Beer et al., 2001). The YII is automatically calculated based on fluorescence ratios, according to Genty et al. (1989). The AF was set at 0.44, corresponding to the mean fraction of absorbed light for eelgrass (Beer et al., 1998). This AF value of 0.44 was established for populations from higher latitudes (66°N) and is, therefore, not entirely appropriate for our study. It was, however, used in this study to compare results between the beginning and the end of the experiment, and with other studies. This default AF was later replaced by other absorption factors, which were determined spectrophotometrically (see section "Light absorption") for more accurate calculations of ETRs.

The ETR values were then fitted against the PAR steps to the double exponential decay function described in Platt et al. (1980) to extract the photosynthetic parameters alpha, E_k, and ETR_{max}. This was performed with the software R (R Core Team, version 4.1.1) using the *fitPGH* function and a Port regression algorithm (*fitmethod*) in the Phytotools package (Silsbe and Malkin, 2015). RLCs with no saturation of the electron transport, even at the highest actinic light, were omitted from the analysis since they reflected underlying technical problems.

Physiological Measurements

Pigment Composition

At the end of the experiment, the second leaf of every single shoot was collected and stored at −80°C for pigment analysis. Leaves were ground using a mortar and pestle in 100% acetone on ice and under green light. Photosynthetic and accessory pigments were extracted in 10 ml acetone for 20 h. Upon extraction, chl*a*, chl*b*, and total carotenoids were quantified spectrophotometrically by measuring absorbance at 470, 645, and 662 nm using a Genesys 10UV Scanning (Thermo Electro Corporation, Madison, WI, United States). Pigment concentrations were calculated using Lichtenthaler (1987) equations and standardized to leaf fresh weight (FW).

Light Absorption

Since ETR is estimated based on the absorbed PAR, the method for quantifying the fraction of absorbed light can significantly influence the measured photosynthetic rates

(Runcie and Durako, 2004). According to Ralph et al. (2007), leaf absorptance should be corrected for light absorption by non-photosynthetic components of photosynthetic tissues. However, the Absorption Factor (AF) used for ETR calculations (Equation 1) is often estimated in a way that makes it impossible to differentiate non-photosynthetic from photosynthetic light absorption (Durako, 2007). Furthermore, the relationship between pigment content and light absorption makes it inadequate to use a single absorption factor for photoacclimation studies (Manassa et al., 2017).

Light absorption was determined using a Lambda850 spectrophotometer (PerkinElmer, Waltham, MA, United States) equipped with a 150 mm integrating sphere. Absorptance measurements were performed on samples collected at the end of the experiment and on any green and mature leaf remaining after pigment analysis. Leaf fragments were suspended at the center of the integrating sphere with a clip-style sample holder (Labsphere Inc., North Sutton, NH, United States) (Moss and Loomis, 1952; Boss et al., 2018). The reflectance ports of the sphere were closed with a white Spectralon reflectance standard, and the beam was angled by 85°. This configuration represents an optimal geometry of absorbance measurement by ensuring the detection of nearly all photons scattered by the leaf. To our knowledge, this technique has never been used for *Zostera marina* leaf absorptance. The spectral absorbance ($D\lambda$) was converted into leaf spectral absorptance ($A\lambda$) as

$$A\lambda = (1 - 10^{-D\lambda}) \quad (2)$$

Leaf AF was calculated as the spectral average of $A\lambda$ between 400 and 700 nm. We distinguished the total absorption factor from the absorption factor due to the photosynthetic components of the leaf. Therefore, AF_{total} represents the fraction of absorbed light by the leaf's photosynthetic and non-photosynthetic components. The measured absorptance was corrected for non-photosynthetic light absorption by subtracting the absorptance in the near infrared (at 750 nm), assumed to be non-photosynthetic (Rühle and Wild, 1979; Cummings and Zimmerman, 2003; Durako, 2007). Photosynthetic absorptance ($A_P\lambda$) was, thus, obtained with the following correction:

$$A_P\lambda = (A\lambda - A_{750}) \quad (3)$$

where A_{750} is the total leaf absorptance at 750 nm. Leaf photosynthetic absorptance (AF_{photo}) was calculated as the spectral average of $A_P\lambda$ between 400 and 700 nm. The estimated AF_{total} and AF_{photo} were used for the correction of photosynthetic rates (ETR_{max}) *a posteriori*.

Primary Production and Respiration

Net primary production (NPP) and respiration (R) were assessed at the end of the experiment by measuring the variation of O_2 concentration during light and dark incubations, respectively, using a non-invasive oxygen meter Fibox4 (PreSens, Regensburg, Germany) (Noisette et al., 2013). Each shoot was gently cleaned of epiphytes and sediments and individually incubated in 0.2 μm filtered seawater in a 300 ml sealed glass bottle. Each incubation lasted 3 h, during which four measurements were made 20 min apart in the dark and then under the respective light treatment. Bottles were gently shaken every 10 min. Incubations were run in a water bath to keep the temperature close to 11°C. Net and gross primary production (GPP) and respiration rates were calculated using the following equations:

$$NPP = \frac{(\alpha light * vol)}{photosynthetic\ leaf\ surface} \quad (4)$$

$$GPP = \frac{(\alpha light * vol) - (\alpha dark * vol)}{photosynthetic\ leaf\ surface} \quad (5)$$

$$R = \frac{\alpha dark * vol}{total\ leaf\ surface} \quad (6)$$

where $\alpha light$ and $\alpha dark$ are the slopes of the oxygen concentration variation along time (μmol O_2 L^{-1} h^{-1}), respectively for the light and dark incubations, and *vol* is the volume of the glass bottles (L). GPP and NPP were standardized to photosynthetic leaf surface (only the green parts of the leaves in cm^2), whereas respiration was standardized to the total leaf surface. Leaf surfaces represent only one side of the leaves. Rates are expressed as μmol O_2 cm^{-2} h^{-1}.

Statistical Analyses

Relationships between photosynthetic and physiological parameters against light treatment were modeled by fitting hierarchical generalized additive models (HGAM) (Pedersen et al., 2019). The maximum of basis functions was set to $k = 7$, since light intensity, the principal predictor, had seven levels (even though it was treated as a continuous variable). The identity of the containers in which shoots were kept during the experiment was included as a random factor to account for any undesired added variance among containers.

For photosynthetic parameters analysis, HGAMs were structured with date-specific smoothers to account for the additional temporal aspect of the data (day 5 and day 25). This allowed appreciating the evolution of the functional response between the beginning (rapid adjustment responses) and the end (acclimation responses) of the experiment. Shoot id was also included in the model as a random variable. HGAM for analysis of the corrected ETR_{max} was structured in the same way, only with the method for absorptance estimation (default AF of 0.44, spectrophotometrically measured AF_{total} and AF_{Photo}) as a grouping factor.

Gross primary production measured at the shoot scale was fitted to an HGAM model rather than a classic photosynthesis-irradiance (PI) curve. A PI curve usually follows the photosynthetic rate of an individual throughout a range of increasing light intensities (Falkowski and Raven, 2007). Here, the curve is shaped by multiple individuals, all of which are acclimated to their respective light environments (x-axis). Therefore, the physiological mechanisms behind the observed response are not the same as with a classic PI curve.

Graphical analysis of the models sometimes suggested thresholds. In these cases, T-tests were carried out to confirm the presence of such a threshold in the response of a variable among

light treatments. This was done for both alpha and E_k on day 5, between 133 and 355 μmol photons m^{-2} s^{-1}. Data were tested for normality and homoscedasticity with the Shapiro and Fligner tests, respectively, and using light treatment as a factor. Statistical analyses were carried out with R (R Core Team, version 4.1.1).

RESULTS

Rapid Photosynthetic Adjustments

Photosynthetic Efficiency and Capacity

Five days after the beginning of the light exposure, photosynthetic efficiency, estimated with alpha, varied significantly with irradiance exposure ($p < 0.001$, **Table 1**) and followed a non-linear trend. Eelgrass shoots from the 74 μmol photons m^{-2} s^{-1} treatment showed the most efficient electron transport at a low light intensity, as indicated by the peak of alpha at 0.173 (**Figure 2A**). Above and below this irradiance, alpha decreased strongly. The ETR_{max} increased linearly with the increase of irradiance exposure ($p < 0.001$, **Figure 2B**), ranging from 24.6 to 62.7 μmol electrons m^{-2} s^{-1} at 6 and 860 μmol photons m^{-2} s^{-1}, respectively. On day 5, the onset of light saturation (E_k) increased significantly with light treatment ($p < 0.001$; **Figure 2C**).

As shown by the patterns depicted by the models for the three photosynthetic parameters, functional responses reached a threshold of around 200 μmol photons m^{-2} s^{-1} after five days of experimenting. Alpha and E_k were significantly different under 133 μmol photons m^{-2} s^{-1} compared to 355 μmol photons m^{-2} s^{-1} (T-test, $p = 0.005$ and 0.023, respectively). Both parameters did not vary significantly above 355 μmol photons m^{-2} s^{-1}. Furthermore, E_k did not change with light treatment beneath 133 μmol photons m^{-2} s^{-1}, with mean values close to 200 μmol photons m^{-2} s^{-1}.

Photoacclimation

Photosynthetic Apparatus Comparison Between Day 5 and Day 25

The relationship between alpha and light treatment changed significantly between day 5 and day 25 ($p < 0.001$, **Table 1** and **Figure 2A**), leading at the end to a consistent alpha among all the light treatments ($p = 0.187$, HGAM). As of 355 μmol photons m^{-2} s^{-1} and above, alpha significantly increased between day 5 and day 25 based on the non-overlapping confidence intervals (Crawley, 2013). The increase in ETR_{max} with light treatments was similar on day 5 and day 25 ($p = 0.302$), as supported by the overlapping confidence intervals. Conversely, E_k increased differently with light treatment on day 5 and day 25 ($p < 0.001$, **Table 1**), showing a greater slope at day 5 compared to day 25. The CIs for the two dates cease to overlap as of 355 μmol photons m^{-2} s^{-1} and beyond.

Pigments and Light Absorption

After 25 days of light exposure, chlorophyll contents in the eelgrass leaves decreased with increasing irradiance ($p < 0.001$ for both chl*a* and chl*b*, **Table 1**). Chl*a* and chl*b* contents were over two times higher in the four lower light treatments (133 μmol photons m^{-2} s^{-1} and beneath) than at 860 μmol photons m^{-2} s^{-1} (**Figure 3A**). Total carotenoids followed a similar trend, although the relationship was less pronounced ($p = 0.002$, **Table 1**).

The light harvesting efficiency (AF_{total}) of eelgrass leaves was minimal in the mid-range irradiances ($p = 0.032$, **Table 1** and **Figure 3B**). AF_{total} ranged from 0.47 in the 503 μmol photons m^{-2} s^{-1} treatment to 0.59 and 0.58 under 6 and 860 μmol photons m^{-2} s^{-1}, respectively. Photosynthetic absorptance (AF_{photo}, $p = 0.413$, **Table 1**) did not change with light treatment. By the end of the experiment, eelgrass shoots captured on average 55% ($AF_{total} = 0.55 \pm 0.02$ SE) of incident light while only 18% ($AF_{photo} = 0.18 \pm 0.01$ SE) of incident photons were trapped by the photosynthetic apparatus.

Correcting Electron Transport Rates for Photosynthetic Light Absorption

Correction of the electron transport rates, by replacing the default AF value of 0.44 in the ETR equation with the measured AF_{total} (refer to section "Light Absorption"), significantly affected the relationship between ETR_{max} and light treatment by increasing its intercept rather than the overall trend ($p < 0.001$, **Figure 4**). Further correction of the photosynthetic rates with the AF_{photo} led to a stronger change of the relationship ($p < 0.001$), yielding to ETR_{max} values 67% lower than the rates calculated with the default AF (**Figure 4**). ETR_{max} increased significantly with increasing irradiance, regardless of the method for absorptance estimation (HGAM model, **Table 1**, $p < 0.001$ with default AF, AF_{total}, and AF_{photo}).

Shoot-Scale Primary Production

Gross primary production rates increased from 0.56 μmol O_2 cm^{-2} h^{-1} in the lowest light treatment up to a peak of 2.04 μmol O_2 cm^{-2} h^{-1} at 355 μmol photons m^{-2} s^{-1} (**Figure 5**). NPP rates increased from 0.29 to 1.0 μmol O_2 cm^{-2} h^{-1}, from the 6 to the 74 μmol photons m^{-2} s^{-1} treatments. Above that irradiance level, NPP reached a plateau (**Figure 5**). Dark respiration (R) rates in the 355 and 860 μmol photons m^{-2} s^{-1} treatments averaged -0.55 ± 0.08 SE and -0.53 ± 0.03 SE μmol O_2 cm^{-2} h^{-1}, respectively, whereas the other light treatments yielded an overall mean respiration rate of -0.28 ± 0.02 SE μmol O_2 cm^{-2} h^{-1}.

An MQR for our light acclimated eelgrass shoots was estimated from the NPP-irradiance HGAM model considering a mean respiration rate of 0.35 ± 0.02 SE μmol O_2 cm^{-2} h^{-1} for a light intensity of 0 μmol photons m^{-2} s^{-1}. This MQR was estimated to occur at 13.7 μmol photons m^{-2} s^{-1}, the irradiance at which photosynthesis (GPP) would equal respiration (NPP = 0).

DISCUSSION

This experimental study assessed the capacity of *Z. marina* shoots to adjust and acclimate to light through a broad range of irradiances from 6 to 860 μmol photons m^{-2} s^{-1}. Short-term photosynthetic adjustments measured after five days of exposure and photoacclimation processes after 25 days were

TABLE 1 | Output of the hierarchical generalized additive models (HGAM) analyses.

		F	*p*-value	R^2 (adj.)	Dev. expl.	*n*
Alpha	date	3.807	0.000239*	0.433	47.9%	113
	s(PAR) on day5	12.775	< 0.001*			
	s(PAR) on day25	1.381	0.187			
	s(container)	0.212	0.300			
	s(id)	0.000	0.735			
ETR_{max}	date	−1.037	0.302	0.72	78%	113
	s(PAR) on day5	38.725	< 0.001*			
	s(PAR) on day25	72.502	< 0.001*			
	s(container)	0.001	0.4356			
	s(id)	0.494	0.0394*			
E_k	date	−4.135	7.29e−05*	0.62	65.3%	113
	s(PAR) on day5	60.507	< 0.001*			
	s(PAR) on day25	33.609	< 0.001*			
	s(container)	0.001	0.456			
	s(id)	0.112	0.307			
corrected ETR_{max}	0.44-AF	4.094	6.88e−05*	0.781	79%	159
	0.44-AP	−12.987	< 0.001*			
	AF-AP	−17.081	< 0.001*			
	s(PAR) with 0.44	42.732	< 0.001*			
	s(PAR) with AF	116.152	< 0.001*			
	s(PAR) with AP	14.177	0.000237*			
	s(container)	0.058	0.349388			
Chl*a*	s(PAR)	31.53	< 0.001*	0.551	56.5%	58
	s(container)	0.000	0.593			
Chl*b*	s(PAR)	19.73	2.24e−07*	0.45	47%	58
	s(container)	0.000	0.711			
Carotenoids	s(PAR)	8.759	0.00247*	0.153	17%	58
	s(container)	0.000	0.90185			
AF_{total}	s(PAR)	3.535	0.0324*	0.0868	11.2%	83
	s(container)	0.000	0.4054			
AF_{photo}	s(PAR)	1.139	0.413	0.0111	2.97%	83
	s(container)	0.000	0.996			
GPP	s(PAR)	13.189	1.8e−06*	0.568	61.7%	41
	s(container)	1.315	0.112			
NPP	s(PAR)	91.013	< 0.001*	0.863	87.4%	82
	s(container)	3.504	0.0142*			

The table shows the F statistics and p-values for each predictor, and adjusted R-squared (R^2 adj.), deviance explained and sample size (n) for each model. Smoothed variables are identified with s(). Statistical significance is identified with an asterisk (*).

observed in response to light attenuation. Rapid adjustments of the photosynthetic apparatus after five days revealed a light intensity threshold between 133 and 355 μmol photons m^{-2} s^{-1} at which photosynthetic parameters started to change compared to the higher light treatments. Furthermore, photoacclimation revealed a second threshold around 74 μmol photons m^{-2} s^{-1} at which photoacclimation mechanisms were optimal (**Figure 6**) and below which photosynthesis and primary production were impeded.

Rapid Photosynthetic Adjustments

Rapid responses of the photosynthetic apparatus already occurred after five days of exposure to new light conditions, as previously demonstrated by other studies (Collier et al., 2012; Bertelli and Unsworth, 2018). Globally, the photosynthetic capacity (ETR_{max}) increased linearly with increasing light treatment, hence leading to the increase of the saturation irradiance (E_k), as reported in previous studies (Ralph and Gademann, 2005; Ochieng et al., 2010; Bertelli and Unsworth, 2018) and is a direct consequence of the light limitation of the electron transport chain (ETC). The peak of photosynthetic efficiency (alpha) reached under 74 μmol photons m^{-2} s^{-1}, and its plateau above 355 μmol photons m^{-2} s^{-1} suggests that electron transport was most efficient at 74 μmol photons m^{-2} s^{-1}. From 133 μmol photons m^{-2} s^{-1} and below, E_k had stabilized around 200 μmol photons m^{-2} s^{-1}, which is higher than the treatment intensity. These changes illustrate the optimization of electron input into the ETC when incident PAR intensity decreases. Above 355 μmol photons m^{-2} s^{-1}, alpha stabilized, implying that these light intensities did not

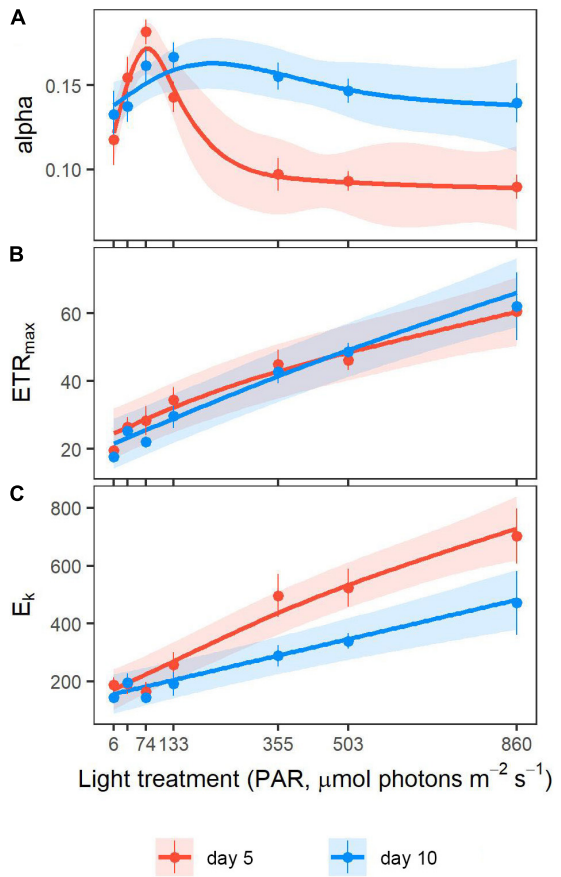

FIGURE 2 | Photosynthetic parameters derived from Rapid Light Curves (RLCs) after 5 (red) and 25 (blue) days of light exposure. Dotted values are mean ± SE (n = 5–9 shoots) for each light treatment. Lines correspond to the values fitted by hierarchical generalized additive models (HGAM) with a 95% CI. **(A)** Alpha (initial slope of the RLC), **(B)** maximum electron transport rate (ETR_{max}, µmol electrons m^{-2} s^{-1}), and **(C)** onset of light saturation (E_k, µmol photons m^{-2} s^{-1}).

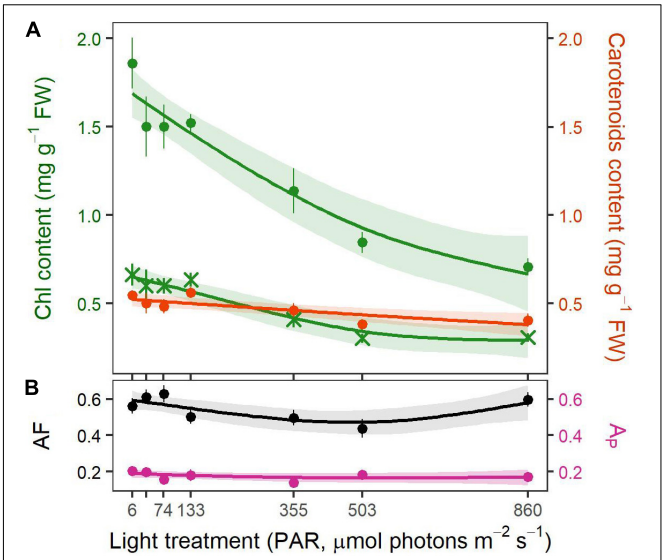

FIGURE 3 | Pigment content and absorptance of eelgrass leaves for each light treatment at the end of the experiment. **(A)** Chl*a* (green circles), chl*b* (green x), and total carotenoids (orange) contents (mg pigment g^{-1} FW). **(B)** Total absorption factor (AF_{total}, black) and photosynthetic absorption factor (AF_{photo}, purple). Dotted values are mean ± SE (n = 8–9 shoots). Lines represent the fitted values from HGAM models with a 95% CI.

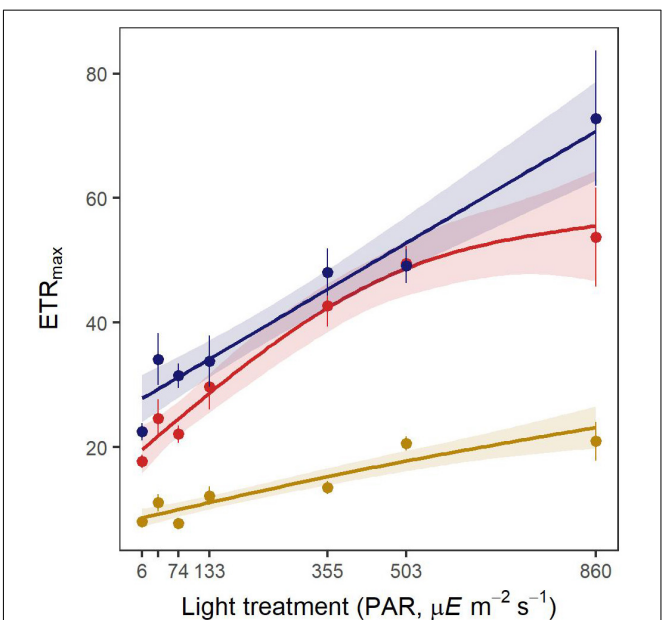

FIGURE 4 | Maximum electron transport rates (ETR_{max}, µmol electrons m^{-2} s^{-1}) for each light treatment at the end of the experiment. Dotted values are mean ± SE (n = 5–9 shoots) uncorrected ETR_{max} (red, with default AF of 0.44) and rates corrected with the measured AF_{total} and AF_{photo} (blue and yellow, respectively). Lines represent the fitted values from HGAM models with a 95% CI.

necessitate any photosynthetic adjustments from the shoots, probably because they were closer to the natural PAR intensities to which the shoots were acclimated *in situ* at the time of collection (mean irradiance of ca. 860 µmol m^{-2} s^{-1} during daylight hours in July). Photosynthetic adjustments occurred below 355 µmol photons m^{-2} s^{-1}, as evidenced by the increased photosynthetic efficiency (alpha). The irradiance of their implementation is, therefore, somewhere between 133 and 355 µmol photons m^{-2} s^{-1}.

Despite adjustments of alpha, processes on the acceptor side of PSII caused a limitation of ETR_{max} in low-light treatments. Indeed, a rate-limiting step in the ETC or a slow Rubisco activity associated with low-light conditions can lower the maximum rate of electron transport by slowing down the turnover rate (or reoxidation) of PSII (Sukenik et al., 1987; Han, 2001; Behrenfeld et al., 2004). Our results suggest photosystem turnover was much slower in shoots from the 133 µmol m^{-2} s^{-1} light treatment and beneath than the higher treatments. This is supported by the sharp increase of the fluorescence signal (F) in these lower irradiances (Ralph and Gademann, 2005), as revealed by the fluorescence kinetics obtained during RLCs

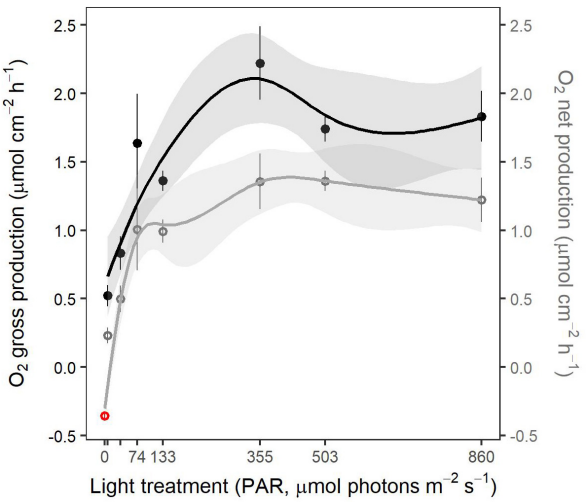

FIGURE 5 | Net primary production (NPP) and gross primary production (GPP) standardized by photosynthetic leaf surface (µmol O_2 h^{-1} cm^{-2}) of whole eelgrass shoots from each light treatment at the end of the experiment. Dotted values are mean ± SE (n = 5–6 shoots). NPP at 0 µmol photons m^{-2} s^{-1} (red circle) is the mean respiration rate measured throughout the range of light treatments (n = 41). Lines represent the fitted values from HGAM models with a 95% CI.

(**Supplementary Figure 1**). This increasingly limited capacity of the ETC, accompanied by an increase of alpha, leads to its quicker saturation (E_k). This dynamic between the three photosynthetic parameters amongst themselves and with light intensity is a characteristic response of the photosynthetic apparatus to highly fluctuating irradiances (Behrenfeld et al., 2004). This potential for such rapid photosynthetic adjustments enables eelgrass to achieve efficient photosynthesis in the highly variable light conditions of the intertidal zone (Anthony et al., 2004; Manassa et al., 2017; Bertelli and Unsworth, 2018).

Photoacclimation

After 25 days of light exposure, the photosynthetic responses differed partly from those observed after five days. In the three highest light treatments (355, 503, and 860 µmol m^{-2} s^{-1}), alpha increased between the beginning and the end of the experiment, leading the shoots to exhibit similar efficiencies regardless of the treatment. However, their ETR_{max} did not change between days 5 and 25. These shoots showed a decrease in their E_k since an increase of alpha unaccompanied by a change of ETR_{max} inevitably leads to a decrease of E_k. In the lower light treatments (133 µmol m^{-2} s^{-1} and beneath), shoots exhibited little to no change of their photosynthetic parameters between the beginning and the end of the experiment. Accordingly, Bertelli and Unsworth (2018) reported a quick (after five days) and then stable photosynthetic response for similar low light intensities (from 3 to 155 µmol m^{-2} s^{-1}).

Photosynthetic responses shifted between 133 and 355 µmol photons m^{-2} s^{-1}, supporting the observations made on day 5. The change of the photosynthetic parameters with time in the three above-mentioned highest light treatments and the E_k plateau around 200 µmol photons m^{-2} s^{-1} suggest that this specific irradiance level draws the line between limiting and non-limiting irradiances. It is indeed the lowest light intensity needed to saturate the ETC, even after acclimation of the shoots. It was used hereafter to distinguish low-light (i.e., limiting or non-saturating) from high-light (i.e., saturating) treatments. Schwarz (2004) reported a similar saturating light intensity for subtropical intertidal and subtidal shoots of *Zostera capricorni*, with E_k ranging from 195 to 242 µmol photons m^{-2} s^{-1}. Furthermore, I_k values (the equivalent of E_k, only obtained from PI curves instead of RLCs) ranging from 198 to 220 µmol photons m^{-2} s^{-1} were reported by Goodman et al. (1995) for subtropical *Z. marina* regardless of their experimental light exposure.

In high-light treatments, as alpha increased between days 5 and 25, plants likely became better acclimated to low PAR intensities. In other words, these shoots developed a more efficient use of photons when light is scarce, but not when it is saturating (i.e., their respective light treatments). Effective quantum yield (YII) at the light treatment intensity did not change either (**Supplementary Figure 2**) while it increased from day 5 to day 25 in the low end of the PAR range of the RLCs. This enhanced efficiency under low PAR for high-light acclimated shoots is likely a secondary effect of a structural change in the ETC such as the size or redox state of the plastoquinone pool, PSII:PSI ratio, or trans-thylakoid pH variations (Wilson and Huner, 2000; Yang et al., 2017). The E_k measured in plants from high-light treatments dropped by more than 100 µmol m^{-2} s^{-1} between day 5 and 25 which resulted in plants being exposed to irradiances higher than their saturating irradiances. In addition, these shoots exhibited important non-photochemical quenching (NPQ, **Supplementary Figure 3**) due to greater heat dissipation when the ETC is saturated (Falkowski and Raven, 2007). This important heat dissipation in shoots with a constantly supersaturated ETC may have prevented cellular damage related to oxygen build-up and reactive oxygen species (ROS) formation (Badger, 1985; Ralph et al., 2002).

As for low-light (6–133 µmol m^{-2} s^{-1}) acclimated shoots, photosynthetic parameters remained the same as on day 5, with high alpha and low ETR_{max} and E_k compared to the high-light treatments. E_k remained similar after 25 days of low-light exposure, implying that the ETC still would not saturate with less than 200 µmol photons m^{-2} s^{-1}, which is well above the irradiances of the low-light treatments. These findings suggest that photoacclimatory mechanisms were already fully set as of day 5, probably underpinned by the rapid regulation of genes involved in photosynthesis a couple of days after exposure to severe light attenuation (Davey et al., 2018). The NPQ kinetics (**Supplementary Figure 3**) suggests the preservation of photoprotection mechanisms throughout the range of light tested. The NPQ of low-light acclimated shoots saturated more quickly than in the high-light acclimated shoots, indicating efficient dissipation of excess energy as soon as ETC saturates. Similar NPQ plateaus regardless of the light treatment suggest that maximal photoprotective ability was comparable among treatments, even though it was reached at lower light intensities for low-light acclimated shoots. This can be attributed to the naturally important xanthophyll pool found in plants

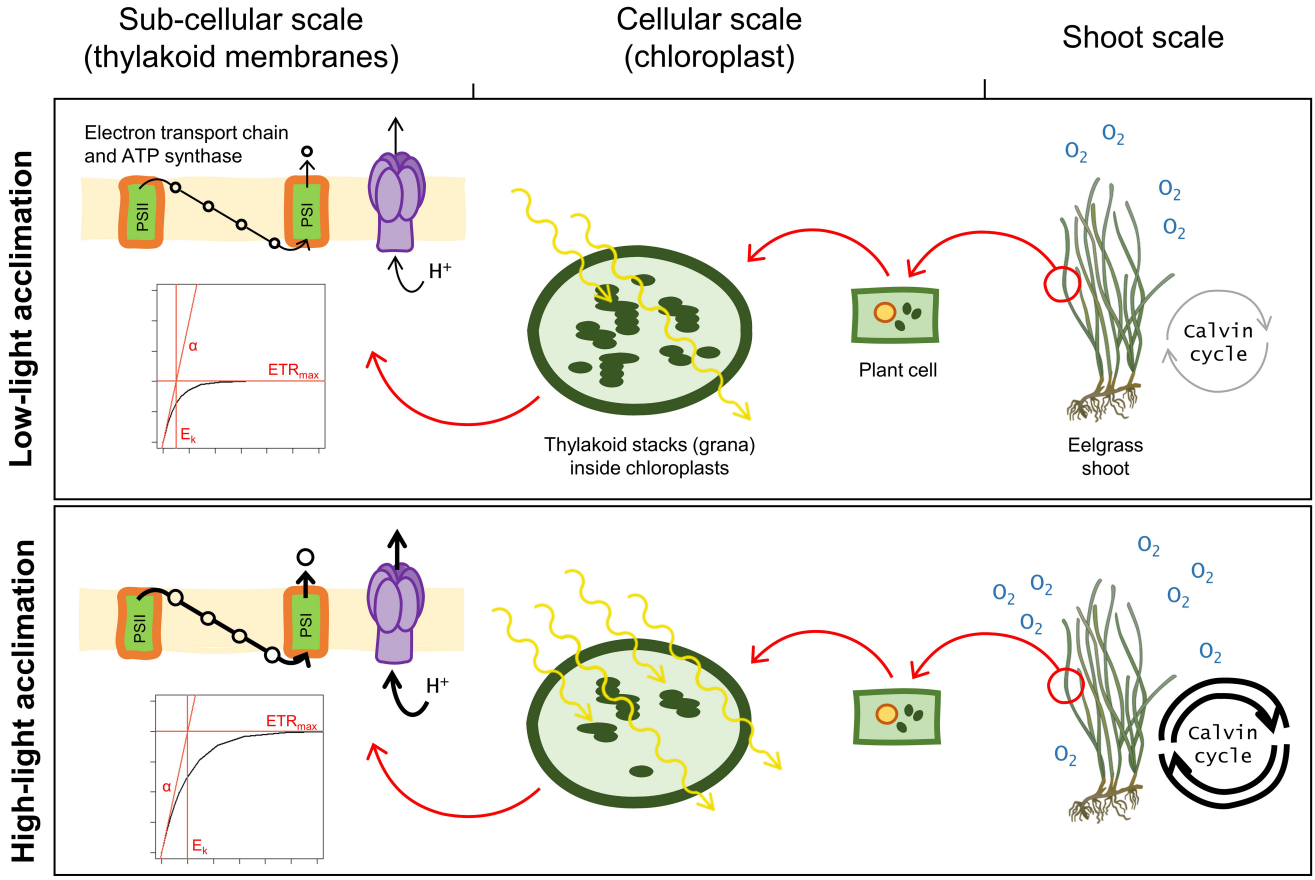

FIGURE 6 | Photoacclimation responses of eelgrass shoots to low and high light, observed after 25 days of light exposure. The limit between low and high light was drawn at 200 μmol photons m^{-2} s^{-1}, based on E_k measurements. The low-light acclimation response illustrated here only sums up the observations made for the 74 and the 133 μmol photons m^{-2} s^{-1} treatments, which are irradiances for which photoacclimation was sufficient to prevent any shoot decay. The figure shows the highest photosynthetic capacity (ETR_{max}) and the onset of light saturation (E_k) of the high-light acclimated shoots compared to the low-light acclimated ones, suggesting a more efficient electron transport chain. Photosynthetic efficiency (alpha) was similar in both light conditions. Higher pigment contents in low-light acclimated shoots are illustrated by an increased number of thylakoids inside the chloroplasts. Light absorption, represented by the wavy yellow arrows, was constant amongst light conditions. Low-light acclimated shoots had lower primary production (GPP), and presumably a lower Calvin cycle activity than high-light acclimated ones.

from highly variable light environments (Demmig-Adams et al., 1999) such as intertidal meadows. These observations differ from those reported by Ralph and Gademann (2005), where low-light (50 μmol m^{-2} s^{-1}) acclimated eelgrass shoots had a reduced ability for excess energy dissipation compared to high-light (300 μmol m^{-2} s^{-1}) acclimated ones for a similar exposure duration.

Overall, pigment content decreased with increasing light intensity, chl*a* and chl*b*, showing greater variations than carotenoids. This relationship between chl*a* and *b* content and light is consistent with previous studies (Cummings and Zimmerman, 2003; Silva et al., 2013; Bertelli and Unsworth, 2018). The subtle change in carotenoid contents with light intensity can be related to the preservation of heat dissipation mechanisms, as mentioned above, and/or to an optimization of light harvesting in low-light environments (Silva et al., 2013; Davey et al., 2018). Changes in pigment contents are often considered as photoacclimatory mechanisms enabling better light absorption (Ralph et al., 2007; Schubert et al., 2018). However, the adaptation of seagrasses to the aquatic life, consisting of concentrating the chloroplasts in the leaf epidermis to optimize inorganic carbon acquisition (Hemminga and Duarte, 2000; Enríquez, 2005), leads to a strong package effect (Cummings and Zimmerman, 2003; Enríquez, 2005; Durako, 2007). This phenomenon is caused by self-shading of overlapping pigments (Cummings and Zimmerman, 2003) and results in a non-linear relationship between pigment content and light absorption (or absorptance), overriding the influence of pigment content on leaf optical properties. The occurrence of a strong package effect was supported in our study by an almost three-fold increase in chl*a* content in low-light treatments without any significant increase in absorptance (**Figure 6**).

Leaf absorptance was influenced by the strong natural variability of its optical properties and therefore not considered as a relevant proxy of eelgrass photoacclimatory response. For instance, leaf absorptance can vary substantially within

and among shoots and with the physiological state of the photosynthetic tissues (Vähätalo et al., 1998; Enríquez, 2005; Durako, 2007). As previously shown, the photosynthetic capacity increased with PAR intensity, regardless of the absorptance coefficient used. Thus, the choice of absorptance coefficient does not affect the observed functional response of photosynthetic tissues to light intensity. However, the use of absorptance coefficients that are not corrected for non-photosynthetic light absorption (default AF and AF_{total}) leads to an important overestimation of photosynthetic rates (Runcie and Durako, 2004). ETRs should always be estimated using photosynthetic absorptance (AF_{photo}), especially if those rates are to be compared or linked to other quantitative photosynthetic or physiological parameters. Furthermore, from the lack of relationship between pigment content and leaf absorptance, we can infer that a change in pigment content with time (as an acclimation mechanism) did not affect absorptance. Thus, leaf absorptance probably remained the same throughout the experiment, which makes the comparison of photosynthetic parameters between days 5 and 25 valid even though absorptance was only measured at the end.

Net primary production and GPP rates measured at the shoot scale increased with an irradiance of up to 74 and 355 μmol photons m^{-2} s^{-1}, respectively. The peak of GPP at 355 μmol photons m^{-2} s^{-1} suggests that this light intensity at which the highest rates of photosynthesis occur is the light optimum for acclimated eelgrass shoots. Beneath this irradiance (or most likely beneath 200 μmol m^{-2} s^{-1}), primary production is limited by light availability. On the other hand, the NPP plateau reached 74 μmol photons m^{-2} s^{-1}, well beneath the light optimum suggested by GPP, which can be attributed to higher dark respiration rates at 355 μmol photons m^{-2} s^{-1}, affecting the overall shape of the HGAM model. Rates of primary production were over two times higher than those reported by Beer et al. (1998) and Dennison and Alberte (1985, 1986) for acclimated shoots and similar light intensities. This discrepancy can be partly explained by the standardization of oxygen fluxes by leaf surface while the whole shoot (below-ground tissues included) was incubated. Standardization by total dry weight would have been more convenient but was precluded by the destructive nature of pigment and absorptance analyses. However, the NPP plateau is close to the light saturation point of 100 μmol photons m^{-2} s^{-1} for *Z. marina,* defined by Dennison and Alberte (1982, 1985), although this value was estimated through PI curves. The plateau of GPP above 355 μmol photons m^{-2} s^{-1} while electron transport keeps increasing may be explained by an increase in photorespiration (Beer et al., 1998) to counteract oxygen build-up and prevent photodamage (Kozaki and Takeba, 1996). The different saturating intensities for NPP and GPP can be explained by the dark respiration rates, which were two times higher in the 355 and 860 μmol photons m^{-2} s^{-1} treatments.

The *Minimum Quantum Requirements* of 13.7 μmol photons m^{-2} s^{-1}, derived from predicted values of the HGAM model, was inside the range of values for compensation points (10–25 μmol photons m^{-2} s^{-1}) found by Dennison and Alberte (1982, 1985), although these values were, again, obtained from classic PI curves. The MQR of 13.7 μmol photons m^{-2} s^{-1} (0.69 mol m^{-2} d^{-1} according to our experimental setup) is much lower than the average light intensity (4.91 mol m^{-2} d^{-1}) at the minimum depth limit of a New Zealand *Z. muelleri* population, as measured by Bulmer et al. (2016) at the minimum depth limit for a New Zealand *Zostera muelleri* population. This difference between the two studies may be related to species-specific responses to light changes (Touchette and Burkholder, 2000). Our lowest light treatment, a light intensity of 6 μmol m^{-2} s^{-1}, would be too low to support primary production. Hence, the impaired photosynthetic efficiency (alpha) and the poor photosynthetic capacity (ETR_{max}) measured at 6 μmol photons m^{-2} s^{-1} support the hypothesis for deterioration of the photosynthetic apparatus. NPP, however, was positive at this irradiance, although close to zero. These shoots might have survived off their carbohydrate reserves (rhizomes) for the experiment duration (Olesen and Sand-Jensen, 1993; Ralph et al., 2007; Silva et al., 2013). A longer experiment would have confirmed if 6 μmol photons m^{-2} s^{-1} were insufficient to support basic metabolism, in which case shoot mortality would have been observed once starch reserves depleted.

The findings brought up by this study could be helpful in the context of conservation and restoration of cold temperate *Z. marina* meadows. We identified multiple light thresholds with different ecological and physiological significance. For instance, the lowest PAR intensity at which eelgrass exhibited a positive NPP, identified as the MQR, was around 13.7 μmol m^{-2} s^{-1}. However, the maximum NPP was reached around 74 μmol m^{-2} s^{-1} through the implementation of photoacclimation mechanisms. *Z. marina* should further thrive under irradiances around 200 μmol m^{-2} s^{-1} since this PAR intensity was considered as saturating and, thus, did not limit photosynthesis and should allow the build-up of carbohydrate reserves. Similar conclusions were drawn by Thom et al. (2008), reporting minimum requirements of 3 mol photons m^{-2} day^{-1} for long-term survival and of 7 mol m^{-2} day^{-1} for light-saturated growth for a northeastern Pacific eelgrass population from similar latitude. These numbers draw near to our light thresholds of 74 μmol m^{-2} s^{-1} (3.7 mol m^{-2} day^{-1}) and 200 μmol m^{-2} s^{-1} (10.1 mol m^{-2} day^{-1}), respectively. The light thresholds identified in our study are, in our opinion, more accurate than the information usually obtained from classic PI curves. Furthermore, using production rates from acclimated shoots provide insights into the photoacclimatory potential of this species or population, whereas PI curves rather reflect acclimation to one specific light intensity. Therefore, the MQR of 13.7 μmol photons m^{-2} s^{-1} and the saturating irradiance of 200 μmol m^{-2} s^{-1} are more useful in a context of conservation than the usual compensation (I_c) and saturation (I_{sat}) points derived from PI curves. However, the light intensities used in our study did not mimic natural light regimes, which are governed by photoperiod, tides, and water column light attenuation variability. Thus, the thresholds identified here must be seen as averages instead of integrated light intensities (mol photons m^{-2} day^{-1}). An experimental setup with light treatments recreating natural photoperiods would have allowed calculating representative daily PAR intensities. Nonetheless, our results give valuable insights into the photoacclimatory ability of *Z. marina*

and highlight key compensatory mechanisms encompassing different biological scales and allowing them to thrive in very fluctuating light environments.

Ecological Implications and Concluding Remarks

Our study demonstrated the ability of the *Zostera marina* to maintain its photosynthetic rates throughout an extensive range of irradiances through a quick response of its photosynthetic apparatus to changing light intensity. Under experimental conditions, these adjustments were only observed beneath 200 μmol photons m^{-2} s^{-1}, which was here identified as the threshold between limiting and saturating irradiances. After five days of light exposure, shoots from light-limited treatments had already implemented photoacclimatory mechanisms through increased photosynthetic efficiency and lower photosynthetic capacity. Shoots exposed to non-limiting irradiances exhibited a slower acclimation. Primary production rates measured after 25 days of light exposure resulted from underlying changes at cellular and subcellular scales. In high-light acclimated shoots, light intensity exceeded what was needed for ETC saturation (E_k), which likely underpinned photoprotective mechanisms (photorespiration and heat dissipation through NPQ). Once light became limiting (as of 200 μmol m^{-2} s^{-1} and beneath), photoacclimation allowed shoots to maintain photosynthetic rates and carbon balance, as illustrated by the NPP plateau from 74 μmol photons m^{-2} s^{-1} and above. Beneath this light intensity, primary production was not maximal, because limited by light availability but still positive. The apparent optimization of photosynthetic efficiency, regardless of the light treatment, as evidenced by alpha on day 25, supports the ability of eelgrass to acclimate to a wide range of light intensities. Severe light limitation, i.e., when irradiance falls beneath the MQR of 13.7 μmol photons m^{-2} s^{-1}, possibly led to a deterioration of the photosynthetic apparatus and consumption of carbohydrate reserves. A reduction of underwater light intensity beneath 13.7 μmol m^{-2} s^{-1} for a prolonged period caused, for instance, by drastic eutrophication, intense sustained human activities (e.g., dredging), or by local sea-level rise could have an impact at meadow-scale through shoot density decline, narrower distribution area, or shoaling of the meadow.

The ability to quickly respond to changing light conditions is critical in cold temperate intertidal ecosystems where underwater light intensity can change considerably and rapidly over a tidal cycle with weather conditions and depending on the seasons (Anthony et al., 2004). Shoots have demonstrated a quick response to sudden light limitation and high tolerance to high intensities. Photoacclimation ability is as important as quick adjustments to changing light in the long-term. Indeed, seagrass habitats are expected to change, especially with regard to underwater light conditions, with climate change and human-induced disturbances (Hauxwell et al., 2003; Short et al., 2011). Seagrasses with a high potential for photoacclimation would cope better with these changes.

DATA AVAILABILITY STATEMENT

The raw data supporting the conclusions of this article will be made available by the authors, without undue reservation.

AUTHOR CONTRIBUTIONS

RL-D, FN, CN, and MC devised the work plan for the experiment. RL-D and FN carried out the experiments. RL-D carried out the sample and statistical analyses, with input from FN, MC, and CN. RL-D wrote the first manuscript, which was then improved with editorial inputs from all authors. All authors have read and agreed to the published version of the manuscript.

FUNDING

This study was supported by a FAST research grant (18FARIMA20) from the Canadian Space Agency awarded to SB, MC, and CN, and by a Natural Sciences and Engineering Research Council of Canada (NSERC) Discovery Program grant (RGPIN-2019-05993) awarded to CN.

ACKNOWLEDGMENTS

We would like to thank the fellow students from Bélanger's, Nozais', and Noisette's teams for their input and support at every stage of the project. We are also grateful to Nathalie Morin for her help and expertise at the research station in Pointe-au-Père. We also thank the editor and reviewers for their insightful comments on our manuscript.

SUPPLEMENTARY MATERIAL

The Supplementary Material for this article can be found online at: https://www.frontiersin.org/articles/10.3389/fpls.2022.805065/full#supplementary-material

Supplementary Figure 1 | Maximum (Fm', dashed lines) and steady-state fluorescence signals (F, solid lines) for each light treatment (μmol photons m^{-2} s^{-1}) during Rapid Light Curves (RLCs) at the beginning and the end of the experiment (day 5 in red and day 25 in blue). Lines are mean values (n = 5–9) with a 95% CI.

Supplementary Figure 2 | Effective quantum yield (YII) of photosystem II (PSII) (dashed lines) and electron transport rate (ETR, solid lines) for each light treatment (μmol photons m^{-2} s^{-1}) during RLCs at the beginning and the end of the experiment (day 5 in red and day 25 in blue). Lines are mean values (n = 5–9) with a 95% CI.

Supplementary Figure 3 | Photochemical coefficients (qP, dashed lines) and non-photochemical quenching coefficients (NPQ, solid lines) for each light treatment (μmol photons m^{-2} s^{-1}) during RLCs at the beginning and the end of the experiment (day 5 in red and day 25 in blue). Lines are mean values (n = 5–9) with a 95% CI.

REFERENCES

Agusti, S., Enriquez, S., Frost-Christensen, H., Sand-Jensen, K., and Duarte, C. M. (1994). Light harvesting among photosynthetic organisms. *Funct. Ecol.* 8:273. doi: 10.2307/2389911

Anthony, K. R. N., Ridd, P. V., Orpin, A. R., Larcombe, P., and Lough, J. (2004). Temporal variation of light availability in coastal benthic habitats: effects of clouds, turbidity, and tides. *Limnol. Oceanogr.* 49, 2201–2211. doi: 10.4319/lo.2004.49.6.2201

Badger, M. R. (1985). Photosynthetic oxygen exchange. *Annu. Rev. Plant Physiol. Plant Mol. Biol.* 36, 27–53. doi: 10.1146/annurev.pp.36.060185.000331

Beer, S., Björk, M., and Beardall, J. (2014). *Photosynthesis in the Marine Environment*. Oxford, UK: John Wiley & Sons.

Beer, S., Björk, M., Gademann, R., and Ralph, P. (2001). "Measurements of photosynthetic rates in seagrasses," in *Global Seagrass Research Methods*, eds F. T. Short and R. Coles (London: Elsevier), 183–198. doi: 10.1016/B978-044450891-1/50010-4

Beer, S., Vilenkin, B., Weil, A., Veste, M., Susel, L., and Eshel, A. (1998). Measuring photosynthetic rates in seagrasses by pulse amplitude modulated (PAM) fluorometry. *Mar. Ecol. Prog. Ser.* 174, 293–300. doi: 10.3354/meps174293

Behrenfeld, M. J., Prasil, O., Babin, M., and Bruyant, F. (2004). In search of a physiological basis for covariations in light-limited and light-saturated photosynthesis: photosynthetic variability in algae. *J. Phycol.* 40, 4–25. doi: 10.1046/j.1529-8817.2004.03083.x

Bertelli, C. M., and Unsworth, R. K. F. (2018). Light stress responses by the eelgrass. *Front. Environ. Sci.* 6:39. doi: 10.3389/fenvs.2018.00039

Borum, J. (1985). Development of epiphytic communities on eelgrass (*Zostera marina*) along a nutrient gradient in a Danish estuary. *Mar. Biol.* 87, 211–218. doi: 10.1007/BF00539431

Boss, E., D'Sa, E. J., Freeman, S., Fry, E., Mueller, J. L., Pegau, S., et al. (2018). "Ocean Optics and Biogeochemistry Protocols for Satellite Ocean Colour Sensor Validation," in *Inherent Optical Property Measurements and Protocols: Absorption Coefficient*, eds A. R. Neeley and A. Mannino ((Dartmouth, NS: IOCCG).

Bulmer, R., Kelly, S., and Jeffs, A. (2016). Light requirements of the seagrass, Zostera muelleri, determined by observations at the maximum depth limit in a temperate estuary, New Zealand. *N. Z. J. Mar. Freshw. Res.* 50, 183–194. doi: 10.1080/00288330.2015.1120759

Collier, C. J., Waycott, M., and Ospina, A. G. (2012). Responses of four Indo-West Pacific seagrass species to shading. *Mar. Pollut. Bull.* 65, 342–354. doi: 10.1016/j.marpolbul.2011.06.017

Cooper, S., Schmidt, A., and Barrell, J. (2009). *Does Eelgrass (Zostera marina) Meet the Critetia as An Ecologically Significant Species?*. Moncton, NB: Fisheries and Oceans Canada.

Crawley, M. J. (2013). *The R Book*, 2nd Edn. Chichester: John Wiley & Sons.

Cummings, M. E., and Zimmerman, R. C. (2003). Light harvesting and the package effect in the seagrasses *Thalassia testudinum* Banks ex König and *Zostera marina* L.: optical constraints on photoacclimation. *Aquat. Bot.* 75, 261–274. doi: 10.1016/S0304-3770(02)00180-8

Davey, P. A., Pernice, M., Ashworth, J., Kuzhiumparambil, U., Szabó, M., Dolferus, R., et al. (2018). A new mechanistic understanding of light-limitation in the seagrass *Zostera muelleri*. *Mar. Environ. Res.* 134, 55–67. doi: 10.1016/j.marenvres.2017.12.012

Demmig-Adams, B., Adams, W. W., Ebbert, V., and Logan, B. A. (1999). "Ecophyciology of the Xanthophyll Cycle," in *The Photochemistry of Carotenoids Advances in Photosynthesis*, eds H. A. Frank, A. Young, G. Britton, and R. J. Cogdell (Dordrecht: Kluwer Academic Publishers).

Dennison, W. C. (1987). Effects of light on seagrass photosynthesis, growth and depth distribution. *Aquat. Bot.* 27, 15–26. doi: 10.1016/0304-3770(87)90083-0

Dennison, W. C., and Alberte, R. S. (1982). Photosynthetic responses of *Zostera marina* L. (Eelgrass) to in situ manipulations of light intensity. *Oecologia* 55, 137–144. doi: 10.1007/BF00384478

Dennison, W. C., and Alberte, R. S. (1985). Role of daily light period in the depth distribution of *Zostera marina* (eelgrass). *Mar. Ecol. Prog. Ser.* 25, 51–61. doi: 10.3354/meps025051

Dennison, W. C., and Alberte, R. S. (1986). Photoadaptation and growth of *Zostera marina* L. (eelgrass) transplants along a depth gradient. *J. Exp. Mar. Biol. Ecol.* 98, 265–282. doi: 10.1016/0022-0981(86)90217-0

Dennison, W. C., Orth, R. J., Moore, K. A., Stevenson, J. C., Carter, V., Kollar, S., et al. (1993). Assessing Water Quality with Submersed Aquatic Vegetation. *BioScience* 43, 86–94. doi: 10.2307/1311969

Duarte, C. M. (1991). Seagrass depth limits. *Aquat. Bot.* 40, 363–377. doi: 10.1016/0304-3770(91)90081-F

Duffy, J. (2006). Biodiversity and the functioning of seagrass ecosystems. *Mar. Ecol. Prog. Ser.* 311, 233–250. doi: 10.3354/meps311233

Durako, M. J. (2007). Leaf optical properties and photosynthetic leaf absorptances in several Australian seagrasses. *Aquat. Bot.* 87, 83–89. doi: 10.1016/j.aquabot.2007.03.005

Enríquez, S. (2005). Light absorption efficiency and the package effect in the leaves of the seagrass *Thalassia testudinum*. *Mar. Ecol. Prog. Ser.* 289, 141–150. doi: 10.3354/meps289141

Eriander, L. (2017). Light requirements for successful restoration of eelgrass (*Zostera marina* L.) in a high latitude environment – Acclimatization, growth and carbohydrate storage. *J. Exp. Mar. Biol. Ecol.* 496, 37–48. doi: 10.1016/j.jembe.2017.07.010

Falkowski, P. G., and Raven, J. A. (2007). *Aquatic Photosynthesis*, 2nd Edn. Princeton: Princeton University Press.

Genty, B., Briantais, J.-M., and Baker, N. R. (1989). The relationship between the quantum yield of photosynthetic electron transport and quenching of chlorophyll fluorescence. *Biochim. Biophys. Acta* 990, 87–92. doi: 10.1016/S0304-4165(89)80016-9

Goodman, J. L., Moore, K. A., and Dennison, W. C. (1995). Photosynthetic responses of eelgrass (*Zostera marina* L.) to light and sediment sulfide in a shallow barrier island lagoon. *Aquat. Bot.* 50, 37–47. doi: 10.1016/0304-3770(94)00444-Q

Green, E. P., and Short, F. T. (2003). *World Atlas of Seagrasses*. Berkeley, USA: UNEP World Conservation Monitoring Centre.

Han, B. (2001). Photosynthesis–irradiance response at physiological level: a mechanistic model. *J. Theor. Biol.* 213, 121–127. doi: 10.1006/jtbi.2001.2413

Hauxwell, J., Cebrián, J., Furlong, C., and Valiela, I. (2001). Macroalgal canopies contribute to eelgrass (*Zostera marina*) decline in temperate estuarine ecosystems. *Ecology* 82, 1007–1022. doi: 10.1890/0012-96582001082[1007:MCCTEZ]2.0.CO;2,

Hauxwell, J., Cebrián, J., and Valiela, I. (2003). Eelgrass *Zostera marina* loss in temperate estuaries: relationship to land-derived nitrogen loads and effect of light limitation imposed by algae. *Mar. Ecol. Prog. Ser.* 247, 59–73. doi: 10.3354/meps247059

Hemminga, M. A., and Duarte, C. M. (2000). *Seagrass Ecology*, 1st Edn. Cambridge, UK: Cambridge University Press, doi: 10.1017/CBO9780511525551

Henley, W. J. (1993). Measurement and interpretation of photosynthetic light-response curves in algae in the context of photoinhibition and diel changes. *J. Phycol.* 29, 729–739. doi: 10.1111/j.1529-8817.1995.tb02565.x

Heuvel, M. R., Hitchcock, J. K., Coffin, M. R. S., Pater, C. C., and Courtenay, S. C. (2019). Inorganic nitrogen has a dominant impact on estuarine eelgrass distribution in the Southern Gulf of St. Lawrence, Canada. *Limnol. Oceanogr.* 64, 2313–2327. doi: 10.1002/lno.11185

Horner, R., and Schrader, G. C. (1982). Relative Contributions of Ice Algae. *Arctic* 35, 485–503. doi: 10.14430/arctic2356

Kemp, W. M., Twilley, R. R., Stevenson, J. C., Boynton, W. R., and Means, J. C. (1983). The decline of submerged vascular plants in upper Chesapeake Bay: summary of results concerning possible causes. *Mar. Technol. Soc. J.* 17, 78–89.

Kirk, J. T. O. (1994). *Light and Photosynthesis in Aquatic Ecosystems*, 2nd Edn. Cambridge, UK: Cambridge University Press, doi: 10.1017/CBO9780511623370

Kozaki, A., and Takeba, G. (1996). Photorespiration protects C3 plants from photooxidation. *Nature* 384, 557–560.

Lambers, H., Chapin, F. S., and Pons, T. L. (2008). *Plant Physiological Ecology*. New York, NY: Springer New York, doi: 10.1007/978-0-387-78341-3

Lee, K.-S., Park, S. R., and Kim, Y. K. (2007). Effects of irradiance, temperature, and nutrients on growth dynamics of seagrasses: a review. *J. Exp. Mar. Biol. Ecol.* 350, 144–175. doi: 10.1016/j.jembe.2007.06.016

Lichtenthaler, H. K. (1987). Chlorophylls and carotenoids: pigments of photosynthetic biomembranes. *Methods Enzymol.* 148, 350–382.

Longstaff, B. J., and Dennison, W. C. (1999). Seagrass survival during pulsed turbidity events: the effects of light deprivation on the seagrasses *Halodule*

pinifolia and *Halophila ovalis*. *Aquat. Bot.* 65, 105–121. doi: 10.1016/S0304-3770(99)00035-2

Manassa, R. P., Smith, T. M., Beardall, J., Keough, M. J., and Cook, P. L. M. (2017). Capacity of a temperate intertidal seagrass species to tolerate changing environmental conditions: significance of light and tidal exposure. *Ecol. Indic.* 81, 578–586. doi: 10.1016/j.ecolind.2017.04.056

Maxwell, P. S., Eklöf, J. S., van Katwijk, M. M., and Boström, C. (2017). The fundamental role of ecological feedback mechanisms for the adaptive management of seagrass ecosystems - a review: review of feedbacks in seagrass. *Biol. Rev.* 92, 1521–1538. doi: 10.1111/brv.12294

McMahon, K., Collier, C., and Lavery, P. S. (2013). Identifying robust bioindicators of light stress in seagrasses: a meta-analysis. *Ecol. Indic.* 30, 7–15. doi: 10.1016/j.ecolind.2013.01.030

Moss, R. A., and Loomis, W. E. (1952). Absorption spectra of leaves. *Plant Physiol.* 27, 370–391.

Murphy, G. E. P., Dunic, J. C., Adamczyk, E. M., Bittick, S. J., Côté, I. M., Cristiani, J., et al. (2021). From coast to coast to coast: ecology and management of seagrass ecosystems across Canada. *Facets* 6, 139–179. doi: 10.1139/facets-2020-0020

Nelson, T. A., and Waaland, J. R. (1997). Seasonality of eelgrass, epiphyte, and grazer biomass and productivity in subtidal eelgrass meadows subjected to moderate tidal amplitude. *Aquat. Bot.* 56, 51–74. doi: 10.1016/S0304-3770(96)01094-7

Nielsen, S. L., Sand-Jensen, K., Borum, J., and Geertz-Hansen, O. (2002). Depth colonization of eelgrass (*Zostera marina*) and macroalgae as determined by water transparency in Danish coastal waters. *Estuaries* 25, 1025–1032. doi: 10.1007/BF02691349

Noisette, F., Egilsdottir, H., Davoult, D., and Martin, S. (2013). Physiological responses of three temperate coralline algae from contrasting habitats to near-future ocean acidification. *J. Exp. Mar. Biol. Ecol.* 448, 179–187. doi: 10.1016/j.jembe.2013.07.006

Ochieng, C., Short, F., and Walker, D. (2010). Photosynthetic and morphological responses of eelgrass (*Zostera marina* L.) to a gradient of light conditions. *J. Exp. Mar. Biol. Ecol.* 382, 117–124. doi: 10.1016/j.jembe.2009.11.007

Olesen, B., and Sand-Jensen, K. (1993). Seasonal acclimatization of eelgrass *Zostera marina* growth to light. *Mar. Ecol. Prog. Ser.* 94, 91–99.

Pedersen, E., Miller, D., Simpson, G., and Ross, N. (2019). Hierarchical generalized additive models in ecology: an introduction with mgcv. *Peerj* 7:e6876. doi: 10.7717/peerj.6876

Platt, T., Gallegos, C., and Harrison, W. G. (1980). Photoinhibition of photosynthesis in natural assemblages of marine phytoplankton. *J. Mar. Res.* 38, 103–111.

Ralph, P. J., Durako, M. J., Enríquez, S., Collier, C. J., and Doblin, M. A. (2007). Impact of light limitation on seagrasses. *J. Exp. Mar. Biol. Ecol.* 350, 176–193. doi: 10.1016/j.jembe.2007.06.017

Ralph, P. J., and Gademann, R. (2005). Rapid light curves: a powerful tool to assess photosynthetic activity. *Aquat. Bot.* 82, 222–237. doi: 10.1016/j.aquabot.2005.02.006

Ralph, P. J., Polk, S. M., Moore, K. A., Orth, R. J., and Smith, W. O. (2002). Operation of the xanthophyll cycle in the seagrass *Zostera marina* in response to variable irradiance. *J. Exp. Mar. Biol. Ecol.* 271, 189–207. doi: 10.1016/S0022-0981(02)00047-3

Rasband, W. (2019). *ImageJ*. Bethesda, MD: National Institutes of Health.

Rühle, W., and Wild, A. (1979). The intensification of absorbance changes in leaves by light-dispersion: differences between high-light and low-light leaves. *Planta* 146, 551–557. doi: 10.1007/BF00388831

Runcie, J. W., and Durako, M. J. (2004). Among-shoot variability and leaf-specific absorptance characteristics affect diel estimates of in situ electron transport of *Posidonia australis*. *Aquat. Bot.* 80, 209–220. doi: 10.1016/j.aquabot.2004.08.001

Sand-Jensen, K., and Borum, J. (1991). Interactions among phytoplankton, periphyton, and macrophytes in temperate freshwaters and estuaries. *Aquat. Bot.* 41, 137–175. doi: 10.1016/0304-3770(91)90042-4

Schreiber, U. (2004). "Pulse-Amplitude-Modulation (PAM) fluorometry and saturation pulse method: an overview," in *Chlorophyll A Fluorescence: A Signature of Photosynthesis. Advances in Photosynthesis and Respiration*, Vol. 19, eds G. C. Papageorgiou and Govindjee (Dordrecht: Springer), 279–319.

Schubert, N., Freitas, C., Silva, A., Costa, M. M., Barrote, I., Horta, P. A., et al. (2018). Photoacclimation strategies in northeastern Atlantic seagrasses: Integrating responses across plant organizational levels. *Sci. Rep.* 8:14825. doi: 10.1038/s41598-018-33259-4

Schwarz, A. (2004). Contribution of photosynthetic gains during tidal emersion to production of *Zostera capricorni in* a North Island. *Mar. Freshw. Res.* 38, 809–818. doi: 10.1080/00288330.2004.9517280

Short, F. T., Polidoro, B., Livingstone, S. R., Carpenter, K. E., Bandeira, S., Bujang, J. S., et al. (2011). Extinction risk assessment of the world's seagrass species. *Biol. Conserv.* 144, 1961–1971. doi: 10.1016/j.biocon.2011.04.010

Silsbe, G. M., and Malkin, S. Y. (2015). *Phytoplankton Production Tools*. Available online at: https://CRAN.R-project.org/package=phytotools [accessed on Feb 14, 2015].

Silva, J., Barrote, I., Costa, M. M., Albano, S., and Santos, R. (2013). Physiological responses of *Zostera marina* and *Cymodocea nodosa* to light-limitation stress. *PLoS One* 8:e81058. doi: 10.1371/journal.pone.0081058

Sukenik, A., Bennett, J., and Falkowski, P. (1987). Light-saturated photosynthesis — Limitation by electron transport or carbon fixation? *Biochim. Biophys. Acta* 891, 205–215. doi: 10.1016/0005-2728(87)90216-7

Thom, R. M., Southard, S. L., Borde, A. B., and Stoltz, P. (2008). Light Requirements for Growth and Survival of Eelgrass (*Zostera marina* L.) in Pacific Northwest (USA) Estuaries. *Estuaries Coasts* 31, 969–980. doi: 10.1007/s12237-008-9082-3

Touchette, B. W., and Burkholder, J. M. (2000). Overview of the physiological ecology of carbon metabolism in seagrasses. *J. Exp. Mar. Biol. Ecol.* 250, 169–205. doi: 10.1016/S0022-0981(00)00196-9

Unsworth, R. K. F., Ambo-Rappe, R., Jones, B. L., La Nafie, Y. A., Irawan, A., Hernawan, U. E., et al. (2018). Indonesia's globally significant seagrass meadows are under widespread threat. *Sci. Total Environ.* 634, 279–286. doi: 10.1016/j.scitotenv.2018.03.315

Vähätalo, A., Søndergaard, M., Schlüter, L., and Markager, S. (1998). Impact of solar radiation on the decomposition of detrital leaves of eelgrass *Zostera marina*. *Mar. Ecol. Prog. Ser.* 170, 107–117. doi: 10.3354/meps170107

Waycott, M., Duarte, C. M., Carruthers, T. J. B., Orth, R. J., Dennison, W. C., Olyarnik, S., et al. (2009). Accelerating loss of seagrasses across the globe threatens coastal ecosystems. *Proc. Natl. Acad. Sci. U.S.A.* 106, 12377–12381. doi: 10.1073/pnas.0905620106

White, A. J., and Critchley, C. (1999). Rapid light curves: a new fluorescence method to assess the state of the photosynthetic apparatus. *Photosynth. Res.* 59, 63–72.

Wilson, K. E., and Huner, N. P. A. (2000). The role of growth rate, redox-state of the plastoquinone pool and the trans-thylakoid DpH in photoacclimation of Chlorella vulgaris to growth irradiance and temperature. *Planta* 212, 93–102.

Yang, X. Q., Zhang, Q. S., Zhang, D., and Sheng, Z. T. (2017). Light intensity dependent photosynthetic electron transport in eelgrass (*Zostera marina* L.). *Plant Physiol. Biochem.* 113, 168–176. doi: 10.1016/j.plaphy.2017.02.011

Zimmerman, R. C. (2003). A biooptical model of irradiance distribution and photosynthesis in seagrass canopies. *Limnol. Oceanogr.* 48, 568–585. doi: 10.4319/lo.2003.48.1_part_2.0568

Zimmerman, R. C., Reguzzoni, J. L., Wyllie-Echeverria, S., Josselyn, M., and Alberte, R. S. (1991). Assessment of environmental suitability for growth of *Zostera marina* L. (eelgrass) in San Francisco Bay. *Aquat. Bot.* 39, 353–366. doi: 10.1016/0304-3770(91)90009-T

Conflict of Interest: The authors declare that the research was conducted in the absence of any commercial or financial relationships that could be construed as a potential conflict of interest.

frontiers in Marine Science

MINI REVIEW
published: 21 February 2022
doi: 10.3389/fmars.2022.821614

Effects of Epiphytes on the Seagrass Phyllosphere

Kasper Elgetti Brodersen and Michael Kühl*

Marine Biological Section, Department of Biology, University of Copenhagen, Helsingør, Denmark

The seagrass phyllosphere consists of a dynamic mosaic of physico-chemical microgradients that modulate light harvesting, gas and nutrient exchange between the photosynthetic leaves and the surrounding water-column. The phyllosphere is thus of vital importance for seagrass growth and fitness. However, unfavorable environmental conditions such as water-column hypoxia, increasing temperature and high nutrient inputs that are predicted to increase in frequency and severity in the Anthropocene, can render the leaf microenvironment into a hostile microhabitat that is challenging or even harmful for the plants—especially if leaves are covered by epiphytic biofilms. Here we summarize effects of epiphytic biofilms on seagrass leaves and discuss how they change and affect the biogeochemical processes and chemical conditions in the seagrass phyllosphere. During night-time, water-column hypoxia can lead to anoxic conditions at the leaf/epiphyte interface, reducing diffusive O_2 supply and thus O_2 availability for plant respiration and transport to below-ground tissues. Furthermore, anoxia in epiphytic biofilms can also enable anaerobic microbial processes that can lead to harmful nitric oxide production *via* denitrification. Such microenvironmental stress conditions at night-time are exacerbated by increasing temperatures. In the light, the leaf epiphytic biofilm community often results in lower leaf photosynthetic activity and efficiency due to epiphyte-induced shading and a combination of O_2 build-up and CO_2 reduction in the phyllosphere owing to thicker total diffusional pathways, phyllosphere basification and epiphytic carbon fixation. Furthermore, absorbed light energy in the epiphytic biofilm can also drive an increase in the leaf surface temperature relative to the surrounding seawater potentially aggravating heating events in the surrounding seawater. In combination, all these above-mentioned diurnal effects of epiphytes result in higher compensation photon irradiance of epiphyte-covered leaves and thus higher light requirements of seagrasses.

Keywords: Anthropocene, light, microenvironment, oxygen, pH, photosynthesis, temperature, toxins

OPEN ACCESS

Edited by:
Alberto Basset,
University of Salento, Italy

Reviewed by:
Dirk de Beer,
Max Planck Society, Germany

****Correspondence:***
Kasper Elgetti Brodersen
kasper.elgetti.brodersen@bio.ku.dk

Specialty section:
This article was submitted to Marine Ecosystem Ecology, a section of the journal Frontiers in Marine Science

Received: *24 November 2021*
Accepted: *31 January 2022*
Published: *21 February 2022*

Citation:
Brodersen KE and Kühl M (2022) Effects of Epiphytes on the Seagrass Phyllosphere. Front. Mar. Sci. 9:821614. doi: 10.3389/fmars.2022.821614

INTRODUCTION

Seagrasses are marine angiosperms that have adapted to a life in an aqueous environment rooted in reduced, anoxic sediments by evolving internal gas channels (aerenchyma) enabling low-resistance, intra-plant gas transport to below-ground tissues (Armstrong, 1979; Colmer, 2003), and leaves with primary photosynthetic tissue in the epidermis that lack stomata and bares a thin cuticle

(Larkum et al., 2006). Seagrasses are highly productive marine plants that form densely populated meadows, which provide important ecosystem services, such as: (i) increasing the pH and O_2 level in the surrounding water-column during daytime with positive effects on calcifying organisms like corals (Greve et al., 2003; Ricart et al., 2021); (ii) providing coastal protection against erosion owing to leaf-induced wave attenuation (Ward et al., 1984; Fonseca and Cahalan, 1992); (iii) offering versatile feeding and nursery grounds especially for juvenile fish (Bertelli and Unsworth, 2014); (iv) absorbing nutrients such as N and P leading to improved water quality (McRoy and Barsdate, 1970; Pernice et al., 2016); (v) efficient sequestration of fixed carbon into the sediment and thus mitigating climate change (Duarte et al., 2005; Fourqurean et al., 2012). Healthy and productive seagrass leaf canopies are thus important for ensuring a good environmental state of marine waters, especially in coastal regions. However, seagrasses are challenged by global climate change and regional anthropogenic stressors encompassing rising seawater temperatures, ocean deoxygenation, and coastal eutrophication that have detrimental effects on plant performance and health (Waycott et al., 2009; Raun and Borum, 2013; Brodersen et al., 2015a,b, 2020a,b; Pedersen et al., 2016; Noisette et al., 2020; Rasmusson et al., 2020; Nguyen et al., 2021).

Increasing temperature can e.g., lead to a negative O_2 balance in the seagrass plant, owing to a decreasing net photosynthesis above the plant's temperature optimum (about 24°C in temperate seagrasses and > 30°C in tropical species). This is due to enzyme capacity limitations and denaturation of proteins involved in photosynthesis, whereas the plant respiration rate continues to increase strongly with increasing temperature (Staehr and Borum, 2011; Pedersen et al., 2016). Ocean deoxygenation can also result in inadequate plant aeration *via* limited O_2 diffusion into the seagrass leaves, which especially affects the below-ground tissue at night-time and can lead to increased mortality owing to sulfide intrusion (Holmer and Bondgaard, 2001; Pedersen et al., 2004; Borum et al., 2005). Coastal eutrophication, leads to algal blooms in the water-column and enhanced epiphyte growth on seagrass leaves (Borum et al., 1984; Borum, 1985; Frankovich and Fourqurean, 1997; Burkholder et al., 2007; Ralph et al., 2007), which shade the leaves during daytime (Brush and Nixon, 2002; Brodersen et al., 2015a). This leads to reduced leaf photosynthesis (Sand-Jensen, 1977; Brodersen et al., 2015a) and increases the water-column and leaf biofilm O_2 demand during night-time (Diaz and Rosenberg, 2008; Brodersen et al., 2015a). All of the above-mentioned environmental challenges often act in synergy and thus deteriorate seagrass health. Leaf epiphytic biofilm communities also challenge their seagrass host by generating an extreme leaf microenvironment, especially in the epiphyte micro-understory, leading to carbon limitation and enhanced photorespiration during daytime, and low O_2 availability and potentially phytotoxic nitric oxide (NO) production in the leaf microenvironment at night-time (Brodersen et al., 2020a,b; Noisette et al., 2020). Furthermore, leaf infection with the pathogenic marine slime mold-like protist *Labyrinthula*, also known as wasting disease, have previously shown to cause large scale die-off events of seagrass meadows (Sullivan et al., 2013; Trevathan-Tackett et al., 2018); a disease that is predicted to worsen with global warming and increased precipitation (Sullivan et al., 2018). Seagrasses can alleviate epiphyte colonization *via* production of zosteric acid (ZA) an effective antifoulant (Newby et al., 2006) that has been shown to reduce bacterial and fungal attachment and formation on surfaces (Villa et al., 2010; Jendresen and Nielsen, 2019). However, although the production of ZA can reduce the initial colonization of leaves with epiphytes, such defense mechanism appears insufficient to avoid overgrowth under coastal eutrophication events. Epifauna can also mitigate the epiphyte pressure on seagrass leaves as they function as grazers in seagrass meadows (Orth and Van Montfrans, 1984; Orth et al., 1984), where this reduction in leaf epiphyte biomass likely positively effects nutrient cycling in the ecosystems *via* epifaunal nutrient excretion. Last not least, leaf epiphytes have also been shown to be beneficial for seagrasses by enhancing the bioavailable amount of inorganic nitrogen *via* mineralization of dissolved organic nitrogen accommodated by microorganisms on the leaf surface; thus, enhancing the productivity and growth rate of the hosting seagrass meadows (Tarquinio et al., 2018).

In this mini-review, we focus on the seagrass leaf phyllosphere and how its microenvironment is affected by environmental change in the Anthropocene, especially eutrophication-induced epiphyte overgrowth of leaves that can have strong detrimental impact on seagrasses in future oceans (e.g., York et al., 2016).

THE PHYSICAL MICROENVIRONMENT OF THE SEAGRASS LEAF PHYLLOSPHERE

Impedance of Mass Transfer in the Phyllosphere

Epiphytic biofilms strongly affect the light microclimate as well as the mass and heat transfer across the leaf tissue surface (**Figure 1**; Brodersen et al., 2015a; Noisette et al., 2020). Seagrass leaves (and most other flow exposed aquatic surfaces) are surrounded by a diffusive boundary layer (DBL) that is generated by impeded water movement toward the leaf surface, leading to unstirred water conditions close to the leaf surface where mass transfer is predominated by diffusion (Jørgensen and Revsbech, 1985; Koch, 1994; Hurd, 2000). The average transport time for a molecule *via* molecular diffusion scales with the square of the distance, and mass transfer impedance imposed by the DBL thus depends strongly on its thickness. The DBL thickness is affected by factors like the flow velocity and the leaf surface topography, where low flow conditions and more rough leaf surfaces increase the DBL thickness (Jørgensen and Des Marais, 1990; Lichtenberg et al., 2017). Epiphytic biofilms can strongly accentuate such mass transfer impedance by increasing the total diffusional distance (TDD, i.e., the combined thickness of the biofilm and the overlying DBL thickness) between the seagrass leaf and the surrounding water, in combination with active removal of e.g., O_2 in the epiphytic biofilm in darkness imposing strong O_2 limitation (Brodersen et al., 2015a, 2020a,b).

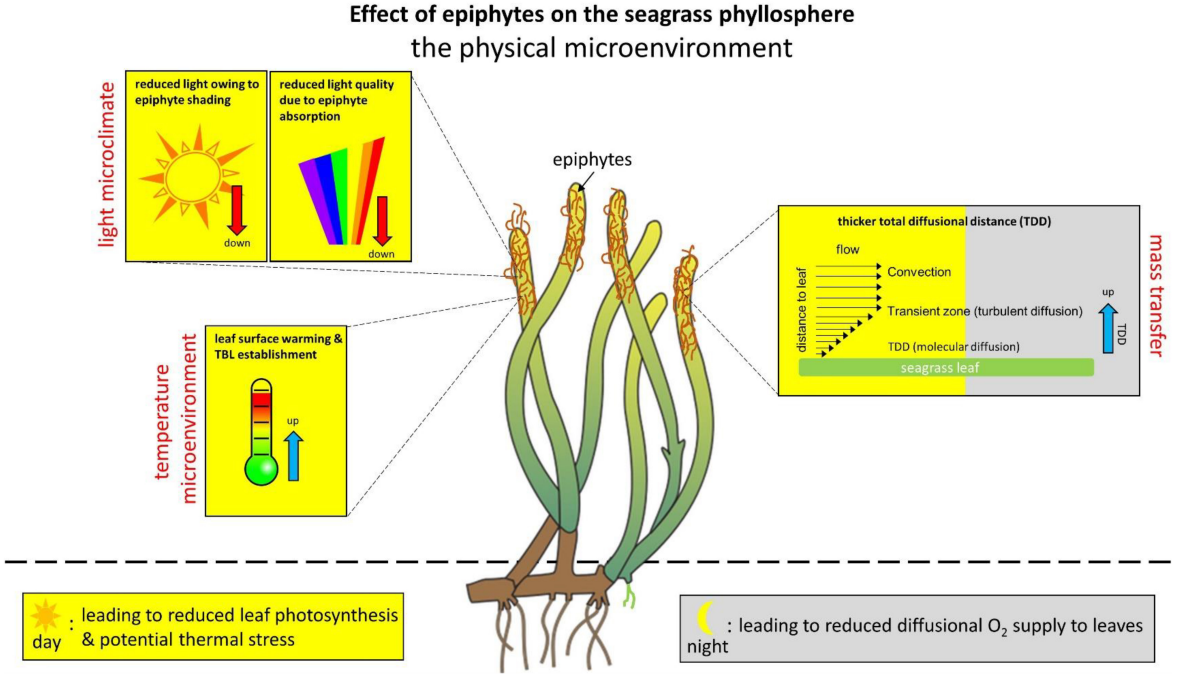

FIGURE 1 | Effect of epiphytes on the physical microenvironment in the seagrass phyllosphere. The changes in the phyllosphere physical microenvironment are shown as an effect on seagrass leaves with epiphytic biofilms as compared with bare leaves and/or bare leaf parts. The seagrass phyllopshere dynamics are shown over diel cycles, where the yellow marked areas represent alterations during daytime and gray marked areas represent changes during night-time. Blue arrows indicate an increase. Red arrows indicate a decrease.

Light-Driven Heating of the Phyllosphere

Absorbed solar radiation in densely pigmented epiphytic biofilms and tissues can lead to local heating, which is dissipated toward the overlying water *via* a leaf thermal boundary layer (TBL; Jimenez et al., 2008; Noisette et al., 2020). The TBL acts as an insulating barrier and therefore impedes heat dissipation (i.e., the rate of convective dissipation of heat) from the tissue surface (Jimenez et al., 2008, 2011; Brodersen et al., 2014). High irradiance can increase the leaf surface temperature up to ∼0.8°C relative to the ambient seawater (Noisette et al., 2020) and such leaf surface warming correlates linearly with the incident irradiance (under similar flow conditions) and is further enhanced by epiphytic overgrowth. The TBL thickness increases with decreasing flow velocity, increasing leaf surface topography and epiphytic overgrowth (Noisette et al., 2020), and is often much thicker than the TDD (∼4 times wider) under slow to moderate flow velocities. Such seagrass leaf surface warming can potentially aggravate negative responses to extreme heat events and ongoing global warming, especially in regions where seagrasses live close to their thermal stress tolerance, but the role of the phyllosphere temperature microenvironment remains largely unexplored.

Changes in the Light Microclimate of the Phyllosphere

The presence of epiphytes reduces both light quality and quantity reaching the seagrass leaf surface (Drake et al., 2003; Brodersen et al., 2015a; Noisette et al., 2020). The presence of epiphytes has been shown to reduce the photon scalar irradiance of photosynthetically active radiation (PAR; 400–700 nm) at the seagrass leaf surface by about 50%, depending on epiphyte thickness, composition and density (Brodersen et al., 2015a; Noisette et al., 2020); however, reductions of >90% as compared to bare leaves have been recorded (Brodersen et al., 2015a). Depending on the structure of the epiphytic biofilms, compaction of the epiphytic biofilm under high flow conditions can further decrease the light intensity reaching the leaf surface (Noisette et al., 2020).

In the upper more loose epiphyte canopy, this decrease in scalar irradiance is mainly uniform across wavelengths within the PAR region, whereas blue and red light are strongly absorbed by algae in the understory of epiphytic biofilms (spanning the innermost < 1 mm above the leaf tissue surface) (Brodersen et al., 2015a). Such dramatic reduction in the blue and red wavelengths reaching the seagrass leaf surface below the epiphyte canopy leads to an unfavorable light microenvironment predominated by green light that is not effectively absorbed by the seagrass leaf chlorophylls (*a* and *b*). Consequently, epiphyte-covered leaves typically have an increased compensation photon irradiance, i.e., the photon irradiance required for producing enough O_2 through photosynthesis to meet the plants own respiratory needs (Brodersen et al., 2015a). Furthermore, sediment resuspension and sedimentation of fine particles on seagrass leaves, which likely is promoted by epiphyte cover due to exopolymer excretion, also negatively affect light transmission through

the water-column and the seagrass leaf microenvironment (Erftemeijer and Lewis, 2006; York et al., 2015; Brodersen et al., 2017a).

On top of declining light availability in turbid waters affected e.g., by eutrophication or dredging, epiphyte-induced reduced light quality at the seagrass leaf surface can thus further deprive the light microclimate to near or below minimal photon requirements for a positive net O_2 balance (Brodersen et al., 2015a). This can lead to high seagrass mortality rates in heavily exposed areas, due to the relatively high light requirements of seagrass (approx. 10–20% of the sea surface irradiance depending on seagrass species); with *Z. marina* placed in the high-end of the light requirement scale at ∼20% of the sea surface irradiance (Duarte, 1991; Dennison et al., 1993; Ballesteros et al., 2007; Larkum et al., 2018).

Microscale light measurements have mainly been performed on temperate *Zostera sp*. with epiphytes largely consisting of bacteria and microalgae dominated by green, brown and red algae; where the dominating algae group determines the color morph of the epiphytic community (i.e., typically green during spring and red in the autumn; Borum et al., 1984). However, calcifying epiphytes often appear white in color (often seen in the Mediterranean and the tropics) and therefore likely rather reflect light than absorb it; as e.g., observed with the skeleton in corals (Enriquez et al., 2005; Wangpraseurt et al., 2012; Brodersen et al., 2014). But such effects of epiphyte community compositions needs to be verified experimentally and thus deserves further attention in future studies.

THE CHEMICAL MICROENVIRONMENT OF THE SEAGRASS LEAF PHYLLOSPHERE

Leaf epiphytes also strongly affect the chemical microenvironment of the seagrass phyllosphere over diel cycles, generating extreme microenvironmental conditions for the seagrass leaf exposed to the epiphyte micro-understory, as compared with bare leaves (**Figure 2**). In the light, photosynthesis (both in the seagrass leaf and epiphytic biofilm) leads to a strong increase in O_2 concentration in the seagrass phyllosphere of epiphyte-covered leaves due to restricted mass transfer over the TDD (Brodersen et al., 2015a, 2020a,b; Noisette et al., 2020). This results in markedly reduced efficiency of seagrass leaf photosynthesis due to enhanced photorespiration, as the high O_2 to CO_2 ratio favors the oxygenase function of RuBisCO, which leads to reduced carbon fixation *via* leaf photosynthesis (Buapet and Björk, 2016; Larkum et al., 2018; Brodersen et al., 2020a; Rasmusson et al., 2020). Actually, in seagrass leaves covered by thick and dense epiphytic biofilms, the vast majority of the O_2 production in the seagrass phyllosphere is produced by the epiphytes (i.e., photosynthesis by the epiphyte community can account for up to ∼70% of the total O_2 production in the seagrass phyllosphere in light [Mazzella and Alberte, 1986; Noisette et al., 2020; Zhang et al., 2022]), and leaf epiphytes have also been shown to cause oxidative stress in seagrass (Costa et al., 2015).

During night-time, seagrasses are completely dependent on passive diffusion of O_2 from the surrounding water-column into the leaves (Greve et al., 2003; Pedersen et al., 2004; Borum et al., 2005, 2006). Epiphytic biofilms intervene with such diffusive O_2 supply *via* epiphyte respiration and an increased TDD leading to reduced plant respiration rates and hypoxic phyllosphere conditions, as well as establishment of anoxic microzones in the epiphyte micro-understory (Brodersen et al., 2020a,b; Noisette et al., 2020). In such epiphyte-driven anoxic microhabitats anaerobic microbial processes can produce phytotoxins such as nitric oxide (NO) *via* denitrification (Noisette et al., 2020), which can potentially be very harmful to the plant (Beligni and Lamattina, 2001; Arasimowicz and Floryszak-Wieczorek, 2007; Kumar et al., 2015). Anoxia in the seagrass phyllosphere can thus lead to multiple detrimental effects on the intra-plant conditions, however, leaf-associated microorganisms may also be beneficial to the seagrass plant. Epiphytic microbiota have thus been shown to increase the nitrogen availability for seagrasses by mineralizing amino acids *via* heterotrophic metabolism (Tarquinio et al., 2018), which may be further supplemented by diazotrophic cyanobacteria (Hamisi et al., 2013). Biogeochemical processes in the epiphytic biofilms may thus increase the nitrogen uptake of seagrass leaves and enable enhanced plant productivity and growth in nitrogen-limited waters. The nitrogen cycle and dynamics in the seagrass phyllosphere is, however, not well described and deserves further attention in future studies.

The leaf photosynthetic activity is likewise negatively affected by epiphytes as compared with bare leaves (Sand-Jensen, 1977; Drake et al., 2003), largely due to epiphyte-induced shading (Brodersen et al., 2015b; Larkum et al., 2018). Reduced photosynthesis leads to decreased carbohydrate synthesis and thus increases the risk of plant starvation (Falkowski and Raven, 2013), as well as less efficient O_2 transport to distal roots and parts of the rhizome *via* the aerenchyma. The latter can lead to anaerobic metabolism in below-ground tissues and intrusion of phytotoxins like hydrogen sulfide into the seagrass plant from the surrounding sediment (Borum et al., 2006; Brodersen, 2016; Brodersen et al., 2018a).

In epiphyte-covered seagrass leaves, especially thick and dense microalgal biofilm communities, leaf photosynthesis drives a pronounced phyllosphere basification up to a pH of about 10. This leads to marked shifts in the phyllosphere carbon speciation from CO_2 toward bicarbonate (HCO_3^-) and even further to carbonate ions (CO_3^{2-}), resulting in a CO_2 and HCO_3^- availability below the plants CO_2 compensation point of about 0.6 μM CO_2 for active leaf photosynthesis (Brodersen et al., 2020a). The phyllosphere basification, and thus strong reduction in CO_2 and HCO_3^- availability, correlates with increasing irradiance and TDD (Brodersen et al., 2020a). In regions where the epiphytic community is dominated by calcifying epiphytes, such epiphyte-induced carbon limitation challenge in the light may be alleviated, as calcification generates CO_2 owing to its effect on the carbonate system equilibria and thereby likely supplies inorganic carbon for RuBisCO (McConnaughey, 1991; Riebesell et al., 2000; Van Dam et al., 2021). Furthermore, aerobic respiration by grazing leaf epifauna (e.g., Orth and Van Montfrans, 1984) may also decrease the O_2/CO_2 ratio in the

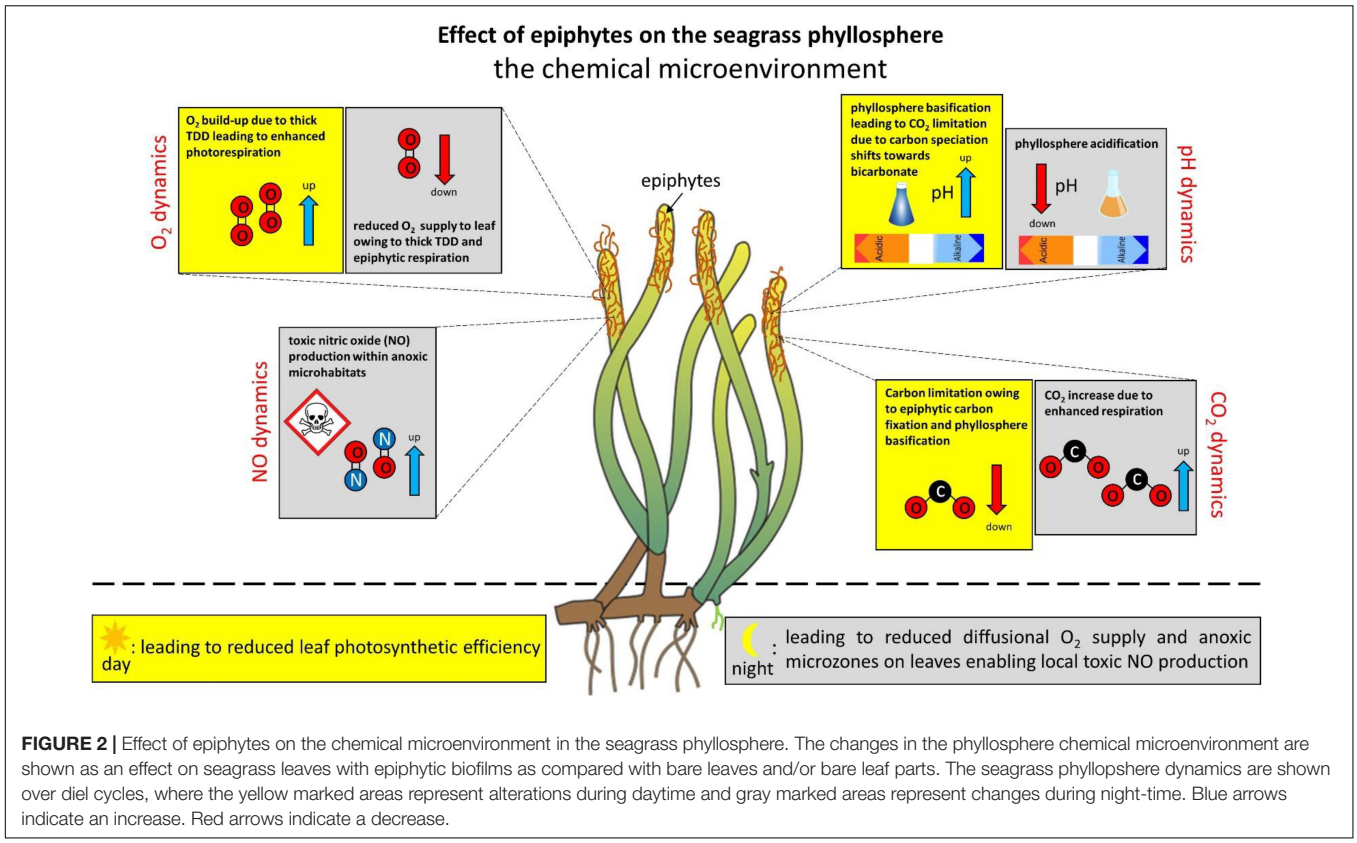

FIGURE 2 | Effect of epiphytes on the chemical microenvironment in the seagrass phyllosphere. The changes in the phyllosphere chemical microenvironment are shown as an effect on seagrass leaves with epiphytic biofilms as compared with bare leaves and/or bare leaf parts. The seagrass phyllopshere dynamics are shown over diel cycles, where the yellow marked areas represent alterations during daytime and gray marked areas represent changes during night-time. Blue arrows indicate an increase. Red arrows indicate a decrease.

seagrass phyllosphere. However, these speculations need to be verified experimentally and therefore deserve further attention in future studies. In darkness, on the other hand, the leaf surface pH of epiphyte-covered leaves reaches pH 7, as compared to a more or less constant value of pH 8 on the leaf surface of bare seagrass leaves, which is similar to the bulk water-column, in both light and darkness (Brodersen et al., 2020a).

Phyllosphere basification in combination with epiphytic carbon fixation can thus induce inorganic carbon limitation in seagrasses, where densely epiphyte-covered seagrass leaves have a strong dependence on HCO_3^- utilization for maintaining efficient photosynthesis-driven carbon fixation (Brodersen et al., 2020a). Seagrasses possess several CO_2 concentration mechanisms (Beer et al., 1980, 2002; Beer and Rehnberg, 1997; Larkum et al., 2017) such as extracellular carbonic anhydrase (CA) that catalyzes the conversion of HCO_3^- to CO_2 through dehydration, as well as active transport of HCO_3^- into epidermal cells and subsequent conversion to CO_2 by intracellular CA (Beer and Rehnberg, 1997; Borum et al., 2016; Larkum et al., 2017). However, such carbon-concentration machinery, which can be up- and downregulated depending on external environmental conditions (Kim et al., 2018), is energetically more expensive for seagrasses as compared with passive uptake of CO_2 *via* diffusion (Raven et al., 2014; Larkum et al., 2018). Extreme conditions in the chemical phyllosphere microenvironment can thus reduce leaf photosynthesis and respiration, as well as enable microbial production of reduced toxic compounds within anoxic microzones. This can lead to seagrass die-off events owing to inadequate internal plant aeration and chemical suffocation, respectively.

EFFECTS OF LEAF PHYLLOSPHERE CONDITIONS ON THE SEAGRASS RHIZOSPHERE

The leaf microenvironment largely controls the internal O_2 balance of the seagrass plant over diurnal cycles and thereby the transport of O_2 down to the below-ground rhizome and roots of seagrasses (reviewed in Brodersen et al., 2018a). Seagrasses release O_2 into the rhizosphere at the base of the leaf (i.e., basal leaf meristem), the root/shoot junctions (i.e., nodes), and at tips (i.e., apical root meristem) of actively growing roots (Pedersen et al., 1998; Jensen et al., 2005; Frederiksen and Glud, 2006; Koren et al., 2015; Brodersen et al., 2016). Such radial O_2 loss (ROL) forms oxic microzones, which: (i) protect the seagrass plant against intrusion of reduced toxic compounds such as H_2S produced in the surrounding anoxic sediment (Brodersen et al., 2015b, 2018a,b; Martin et al., 2019), and (ii) mobilize nutrients by means of stimulating microbial processes (Welsh et al., 1996; Nielsen et al., 2001; Brodersen et al., 2018b) and chemical solubilization (Brodersen et al., 2017b).

The oxidation capacity of the seagrass below-ground tissue is determined by the efficiency of O_2 transport from the leaves and the following O_2 release into the sediment, whereas the sediment oxygenation is a balance between the below-ground

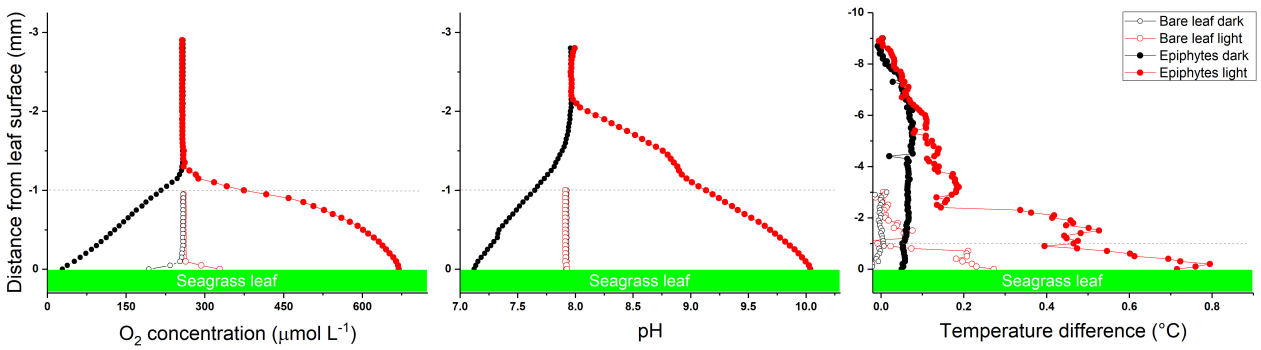

FIGURE 3 | Microsensor profiles of O_2, pH and temperature at the surface of seagrass leaves with (*epiphytes*) and without (*bare leaves*) epiphytes. Data originates from Brodersen et al. (2020a) and Noisette et al. (2020). The dashed line at 1 mm distance from the leaf tissue surface marks the approximate thickness of the epiphytic biofilm layer. Red symbols and lines represent measurements in light. Black symbols and lines measurements in darkness. Microprofiling data of leaves with epiphytes show that in light the phyllosphere becomes hyperoxic, strongly basified and heated (solid red symbols as compared to open red symbols), whereas phyllopshere hyperoxia and acidification occurs in darkness (solid black symbols as compared with open black symbols); strongly affecting seagrass health and performance.

tissue O_2 release and the sediment O_2 demand (Borum et al., 2006; Brodersen, 2016; Brodersen et al., 2018a). Within the seagrass rhizosphere, ROL leads to marked reductions in the sediment sulfide concentrations through spontaneous chemical and biological oxidation of H_2S (Brodersen et al., 2015b, 2018b; Martin et al., 2019) resulting in an acidification of the seagrass rhizosphere through production of sulfuric acid (Brodersen et al., 2015b, 2016, 2018b). Rhizosphere acidification can also lead to phosphate solubilization in carbonate-rich sediments *via* protolytic dissolution of Ca-phosphates, while other important nutrients such as ammonium and Fe(II) can be mobilized *via* stimulation of the microbial community by plant exudates (Brodersen et al., 2017b); sulfate-reducing bacteria can e.g., fix dinitrogen (Welsh et al., 1996; Nielsen et al., 2001) and solubilize Fe(II) and P through reductive dissolution of insoluble Fe(III)oxyhydroxides (Brodersen et al., 2017b). Changes in the seagrass phyllosphere microenvironment can thus have strong effects on the biogeochemical processes and chemical conditions in the seagrass rhizosphere, and thereby the capacity of the below-ground tissue to detoxify reduced compounds and mobilize nutrients in the surrounding sediment. Inadequate internal plant aeration, and subsequent diminished oxic microzones in the rhizosphere, can thus lead to toxic sulfide intrusion and plant starvation, which may kill the plants if persisting over long time periods (Pedersen et al., 2004; Holmer and Hasler-Sheetal, 2014; Brodersen et al., 2015b).

TECHNIQUES FOR MONITORING THE PHYLLOSPHERE MICROENVIRONMENT

The seagrass phyllosphere represents at thin mm-thick zone surrounding the seagrass leaf and in some cases also encompasses epiphytic biofilms colonizing the leaf surface. Traditionally, microenvironmental analyses of the phyllosphere and rhizosphere of plants have involved use of electrochemical and fiber-optic microsensors (Kühl and Revsbech, 2001; Kühl, 2005; Pedersen et al., 2020; Revsbech, 2021) with tip sizes typically ranging from ∼5 to 100 µm. Such microsensors enable minimally invasive profiling of physical (light, temperature, diffusivity) and chemical (gases and ions) analytes at high specificity and spatio-temporal resolution around and within plant tissue at specific locations, and their application has gained many fundamental insights to the seagrass microenvironment (see previous sections; **Figure 3**). While it is possible to use microsensors to map 2D transects and even 3D grids of microprofiles, e.g., over plant tissue topographies (Lichtenberg et al., 2017), it remains a major challenge to align microsensor measurements and account for spatial heterogeneity in samples with pronounced structural complexity. In recent years, microenvironmental studies of seagrasses are increasingly complemented by chemical imaging approaches, especially for 2D mapping with optical sensors embedding or appressed to the below-ground seagrass tissue (reviewed in Scholz et al., 2021). The use of magnetic sensor particles in combination with luminescence lifetime imaging has also enabled 2D mapping of O_2 over natural flow-exposed surfaces and biofilms (Fabricius-Dyg et al., 2012) and recently, a first application studying the heterogeneous O_2 microenvironment of epiphytic biofilms on seagrass leaves was reported (Brodersen et al., 2020b). Suitable sensor particles have been developed for a variety of analytes in the aquatic environment (Moßhammer et al., 2019), and we envision that this approach can relatively easily be extended to imaging other chemical species (e.g., pH) in the seagrass phyllosphere. Furthermore, combining such sensor particle-based imaging with e.g., light sheet or confocal microscopy systems could enable true 3D mapping of the chemical phyllosphere microenvironment.

CONCLUSION AND PERSPECTIVES

Coastal eutrophication is a major environmental stressor stimulating dense epiphytic biofilm growth on seagrass leaves.

Increased epiphyte colonization shades the seagrass leaves, and the increasing diffusion distance between the leaf and surrounding water can result in phyllosphere basification, warming and hyperoxia, leading to carbon limitation and enhanced photorespiration in the light. During darkness, anoxic stress in the seagrass phyllosphere owing to restricted diffusional O_2 supply across the epiphytic biofilm layer from the surrounding water-column and/or heterotrophic activity in the biofilm can induce production of reduced toxic substances that can diffuse into the plant tissue and potentially cause increased mortality. Finally, reduced leaf O_2 evolution or diffusional supply from the adjacent water decreases O_2 transport to the root/rhizome system and subsequent release to the reduced sediment increasing the risk of H_2S intrusion and plant nutrient limitation.

The biomass of the seagrass leaf-associated epiphytic communities is largely driven by progressive enrichment of seawater with minerals and nutrients, wherefore leaf epiphyte blooms mainly follow algal blooms in the water-column that mostly occur during spring (April-May) and autumn (Aug-Sep) time in northern temperate waters (Borum et al., 1984). These time windows thus represent the most critical periods during the annual growth season of the seagrass plant. Furthermore, ocean acidification can lead to a shift in the seagrass epiphyte community structure by increasing the fleshy/calcareous algal taxa ratio (Campbell and Fourqurean, 2014), which may impose further shading and impede mass transfer in seagrasses owing to the increased epiphytic biomass load on the seagrass leaves. This is supported by recent findings near CO_2 seeps, where seagrass leaves often appear free of calcifying epiphytes (e.g., Mishra et al., 2020); however, the underlying mechanisms for epiphyte colonization at CO_2 seeps are not well understood. Future climate conditions with heavier precipitation driving more frequent coastal eutrophication events, in combination with ocean acidification, can thus potentially lead to enhanced and shifting leaf epiphyte communities putting seagrass ecosystems at risk of local-extinction, especially in combination with further environmental stress factors such as ocean deoxygenation and/or extreme heating events.

However, pronounced knowledge gaps about the seagrass leaf microenvironment and the role of leaf epiphytes on seagrass plant fitness prevail and encompass: (i) a detailed determination of the nitrogen cycling in the phyllosphere to better understand the role of epiphytic biofilms for plant nutrition and potential production of phytotoxins, (ii) a better understanding of the optical properties of the seagrass leaf tissue and the leaf microenvironmental landscape, including how it is affected by leaf epiphytes, and (iii) how leaves and epiphytism in seagrass acclimate to future climate conditions, including seagrass expansion to cold and light-limiting Artic regions.

AUTHOR CONTRIBUTIONS

KB and MK developed the concept for this review and wrote the manuscript. Both authors contributed to the article and approved the submitted version.

FUNDING

We would like to acknowledge financial support from the Carlsberg Foundation (KB: project no. CF16-0899), the Villum Foundation (KB: project no. 00028156), and the Independent Research Fund Denmark (MK: project no. DFF-8021-00308B).

REFERENCES

Arasimowicz, M., and Floryszak-Wieczorek, J. (2007). Nitric oxide as a bioactive signalling molecule in plant stress responses. *Plant Sci.* 172, 876–887. doi: 10.1016/j.plantsci.2007.02.005

Armstrong, W. (1979). "Aeration in higher plants," in *Advances in Botanical Research*, Vol. 7, ed. H. W. Woolhouse (London: Academic Press), 225–332. doi: 10.1016/S0065-2296(08)60089-0

Ballesteros, E., Cebrian, E., and Alcoverro, T. (2007). Mortality of shoots of *Posidonia oceanica* following meadow invasion by the red alga *Lophocladia lallemandii*. *Botanica Marina* 50, 8–13. doi: 10.1515/BOT.2007.002

Beer, S., Bjork, M., Hellblom, F., and Axelsson, L. (2002). Inorganic carbon utilization in marine angiosperms (seagrasses). *Funct. Plant Biol.* 29, 349–354. doi: 10.1071/PP01185

Beer, S., and Rehnberg, J. (1997). The acquisition of inorganic carbon by the seagrass *Zostera marina*. *Aquatic Bot.* 56, 277–283. doi: 10.1016/S0304-3770(96)01109-6

Beer, S., Shomer-Ilan, A., and Waisel, Y. (1980). Carbon metabolism in seagrasses: II. Patterns of photosynthetic CO_2 incorporation. *J. Exp. Bot.* 31, 1019–1026. doi: 10.1093/jxb/31.4.1019

Beligni, M., and Lamattina, L. (2001). Nitric oxide in plants: the history is just beginning. *Plant Cell Environ.* 24, 267–278. doi: 10.1046/j.1365-3040.2001.00672.x

Bertelli, C. M., and Unsworth, R. K. (2014). Protecting the hand that feeds us: seagrass (*Zostera marina*) serves as commercial juvenile fish habitat. *Mar. Pollut. Bull.* 83, 425–429. doi: 10.1016/j.marpolbul.2013.08.011

Borum, J. (1985). Development of epiphytic communities on eelgrass (*Zostera marina)* along a nutrient gradient in a Danish estuary. *Mar. Biol.* 87, 211–218. doi: 10.1007/BF00539431

Borum, J., Kaas, H., and Wium-Andersen, S. (1984). Biomass variation and autotrophic production of an epiphyte-macrophyte community in a coastal Danish area: II. Epiphyte species composition, biomass and production. *Ophelia* 23, 165–179. doi: 10.1080/00785326.1984.10426612

Borum, J., Pedersen, O., Greve, T. M., Frankovich, T. A., Zieman, J. C., Fourqurean, J. W., et al. (2005). The potential role of plant oxygen and sulphide dynamics in die-off events of the tropical seagrass, *Thalassia testudinum*. *J. Ecol.* 93, 148–158. doi: 10.1111/j.1365-2745.2004.00943.x

Borum, J., Pedersen, O., Kotula, L., Fraser, M. W., Statton, J., Colmer, T. D., et al. (2016). Photosynthetic response to globally increasing CO_2 of co-occurring temperate seagrass species. *Plant Cell Environ.* 39, 1240–1250. doi: 10.1111/pce.12658

Borum, J., Sand-Jensen, K., Binzer, T., Pedersen, O., and Greve, T. (2006). "Oxygen movement in seagrasses," in *Seagrasses: Biology, Ecology and Conservation*, eds A. W. D. Larkum, J. R. Orth, and C. M. Duarte (Dordrecht: Springer), 255–270. doi: 10.1007/1-4020-2983-7_10

Brodersen, K. E. (2016). *The Seagrass Rhizosphere*. Ph.D. thesis. Sydney: University of Technology Sydney.

Brodersen, K. E., Hammer, K. J., Schrameyer, V., Floytrup, A., Rasheed, M. A., Ralph, P. J., et al. (2017a). Sediment resuspension and deposition on seagrass leaves impedes internal plant aeration and promotes phytotoxic H_2S intrusion. *Front. Plant Sci.* 8:657. doi: 10.3389/fpls.2017.00657

Brodersen, K. E., Koren, K., Moßhammer, M., Ralph, P. J., Kühl, M., and Santner, J. (2017b). Seagrass-mediated phosphorus and iron solubilization in tropical sediments. *Environ. Sci. Technol.* 51, 14155–14163. doi: 10.1021/acs.est.7b03878

Brodersen, K. E., Koren, K., Lichtenberg, M., and Kühl, M. (2016). Nanoparticle-based measurements of pH and O_2 dynamics in the rhizosphere of *Zostera marina* L.: effects of temperature elevation and light/dark transitions. *Plant Cell Environ.* 39, 1619–1630. doi: 10.1111/pce.12740

Brodersen, K. E., Koren, K., Revsbech, N. P., and Kühl, M. (2020a). Strong leaf surface basification and CO_2 limitation of seagrass induced by epiphytic biofilm microenvironments. *Plant Cell Environ.* 43, 174–187. doi: 10.1111/pce.13645

Brodersen, K. E., Kühl, M., Trampe, E., and Koren, K. (2020b). Imaging O_2 dynamics and microenvironments in the seagrass leaf phyllosphere with magnetic optical sensor nanoparticles. *Plant J.* 104, 1504–1519. doi: 10.1111/tpj.15017

Brodersen, K. E., Kühl, M., Nielsen, D. A., Pedersen, O., and Larkum, A. W. (2018a). "Rhizome, root/sediment interactions, aerenchyma and internal pressure changes in seagrasses," in *Seagrasses of Australia*, eds A. Larkum, G. Kendrick, and P. Ralph (Cham: Springer), 393–418. doi: 10.1007/978-3-319-71354-0_13

Brodersen, K. E., Siboni, N., Nielsen, D. A., Pernice, M., Ralph, P. J., Seymour, J., et al. (2018b). Seagrass rhizosphere microenvironment alters plant-associated microbial community composition. *Environ. Microbiol.* 20, 2854–2864. doi: 10.1111/1462-2920.14245

Brodersen, K. E., Lichtenberg, M., Paz, L.-C., and Kühl, M. (2015a). Epiphyte-cover on seagrass (*Zostera marina* L.) leaves impedes plant performance and radial O_2 loss from the below-ground tissue. *Front. Mar. Sci.* 2:58. doi: 10.3389/fmars.2015.00058

Brodersen, K. E., Nielsen, D. A., Ralph, P. J., and Kühl, M. (2015b). Oxic microshield and local pH enhancement protects *Zostera muelleri* from sediment derived hydrogen sulphide. *New Phytol.* 205, 1264–1276. doi: 10.1111/nph.13124

Brodersen, K. E., Lichtenberg, M., Ralph, P. J., Kühl, M., and Wangpraseurt, D. (2014). Radiative energy budget reveals high photosynthetic efficiency in symbiont-bearing corals. *J. R. Soc. Interface* 11:20130997. doi: 10.1098/rsif.2013.0997

Brush, M. J., and Nixon, S. W. (2002). Direct measurements of light attenuation by epiphytes on eelgrass *Zostera marina*. *Mar. Ecol. Progr. Series* 238, 73–79. doi: 10.3354/meps238073

Buapet, P., and Björk, M. (2016). The role of O_2 as an electron acceptor alternative to CO_2 in photosynthesis of the common marine angiosperm *Zostera marina* L. *Photosynthesis Res.* 129, 59–69. doi: 10.1007/s11120-016-0268-4

Burkholder, J. M., Tomasko, D. A., and Touchette, B. W. (2007). Seagrasses and eutrophication. *J. Exp. Mar. Biol. Ecol.* 350, 46–72. doi: 10.1016/j.jembe.2007.06.024

Campbell, J. E., and Fourqurean, J. W. (2014). Ocean acidification outweighs nutrient effects in structuring seagrass epiphyte communities. *J. Ecol.* 102, 730–737. doi: 10.1111/1365-2745.12233

Colmer, T. D. (2003). Long-distance transport of gases in plants: a perspective on internal aeration and radial oxygen loss from roots. *Plant Cell Environ.* 26, 17–36. doi: 10.1046/j.1365-3040.2003.00846.x

Costa, M. M., Barrote, I., Silva, J., Olivé, I., Alexandre, A., Albano, S., et al. (2015). Epiphytes modulate *Posidonia oceanica* photosynthetic production, energetic balance, antioxidant mechanisms, and oxidative damage. *Front. Mar. Sci.* 2:111. doi: 10.3389/fmars.2015.00111

Dennison, W. C., Orth, R. J., Moore, K. A., Stevenson, J. C., Carter, V., Kollar, S., et al. (1993). Assessing water quality with submersed aquatic vegetation. *BioScience* 43, 86–94. doi: 10.2307/1311969

Diaz, R. J., and Rosenberg, R. (2008). Spreading dead zones and consequences for marine ecosystems. *Science* 321, 926–929. doi: 10.1126/science.1156401

Drake, L. A., Dobbs, F. C., and Zimmerman, R. C. (2003). Effects of epiphyte load on optical properties and photosynthetic potential of the seagrasses *Thalassia testudinum* Banks ex König and *Zostera marina* L. *Limnol. Oceanogr.* 48(Part 2), 456–463. doi: 10.4319/lo.2003.48.1_part_2.0456

Duarte, C. M. (1991). Seagrass depth limits. *Aquatic Bot.* 40, 363–377. doi: 10.1016/0304-3770(91)90081-F

Duarte, C. M., Middelburg, J., and Caraco, N. (2005). Major role of marine vegetation on the oceanic carbon cycle. *Biogeosciences* 2, 1–8. doi: 10.5194/bg-2-1-2005

Enriquez, S., Méndez, E. R., and Iglesias-Prieto, R. (2005). Multiple scattering on coral skeletons enhances light absorption by symbiotic algae. *Limnol. Oceanogr.* 50, 1025–1032. doi: 10.4319/lo.2005.50.4.1025

Erftemeijer, P. L. A., and Lewis, R. R. R. (2006). Environmental impacts of dredging on seagrasses: a review. *Mar. Pollut. Bull.* 52, 1553–1572. doi: 10.1016/j.marpolbul.2006.09.006

Fabricius-Dyg, J., Mistlberger, G., Staal, M., Borisov, S. M., Klimant, I., and Kühl, M. (2012). Imaging of surface O_2 dynamics in corals with magnetic micro optode particles. *Mar. Biol.* 159, 1621–1631. doi: 10.1007/s00227-012-1920-y

Falkowski, P. G., and Raven, J. A. (2013). *Aquatic Photosynthesis*. New Jersey, NJ: Princeton University Press.

Fonseca, M. S., and Cahalan, J. A. (1992). A preliminary evaluation of wave attenuation by four species of seagrass. *Estuarine Coastal Shelf Sci.* 35, 565–576. doi: 10.1016/S0272-7714(05)80039-3

Fourqurean, J. W., Duarte, C. M., Kennedy, H., Marba, N., Holmer, M., Mateo, M. A., et al. (2012). Seagrass ecosystems as a globally significant carbon stock. *Nat. Geosci.* 5, 505–509. doi: 10.1038/ngeo1477

Frankovich, T. A., and Fourqurean, J. W. (1997). Seagrass epiphyte loads along a nutrient availability gradient, Florida Bay, USA. *Mar. Ecol. Progr. Series* 159, 37–50. doi: 10.3354/meps159037

Frederiksen, M. S., and Glud, R. N. (2006). Oxygen dynamics in the rhizosphere of *Zostera marina*: a two-dimensional planar optode study. *Limnol. Oceanogr.* 51, 1072–1083. doi: 10.4319/lo.2006.51.2.1072

Greve, T. M., Borum, J., and Pedersen, O. (2003). Meristematic oxygen variability in eelgrass (*Zostera marina*). *Limnol. Oceanogr.* 48, 210–216. doi: 10.4319/lo.2003.48.1.0210

Hamisi, M., Díez, B., Lyimo, T., Ininbergs, K., and Bergman, B. (2013). Epiphytic cyanobacteria of the seagrass *Cymodocea rotundata*: diversity, diel nifH expression and nitrogenase activity. *Environ. Microbiol. Rep.* 5, 367–376. doi: 10.1111/1758-2229.12031

Holmer, M., and Bondgaard, E. J. (2001). Photosynthetic and growth response of eelgrass to low oxygen and high sulfide concentrations during hypoxic events. *Aquatic Bot.* 70, 29–38. doi: 10.1016/S0304-3770(00)00142-X

Holmer, M., and Hasler-Sheetal, H. (2014). Sulfide intrusion in seagrasses assessed by stable sulfur isotopes—a synthesis of current results. *Front. Mar. Sci.* 1:64. doi: 10.3389/fmars.2014.00064

Hurd, C. L. (2000). Water motion, marine macroalgal physiology, and production. *J. Phycol.* 36, 453–472. doi: 10.1046/j.1529-8817.2000.99139.x

Jendresen, C. B., and Nielsen, A. T. (2019). Production of zosteric acid and other sulfated phenolic biochemicals in microbial cell factories. *Nat. Commun.* 10, 1–10. doi: 10.1038/s41467-019-12022-x

Jensen, S. I., Kühl, M., Glud, R. N., Jørgensen, L. B., and Prieme, A. (2005). Oxic microzones and radial oxygen loss from roots of *Zostera marina*. *Mar. Ecol. Progr. Series* 293, 49–58. doi: 10.3354/meps293049

Jimenez, I. M., Kühl, M., Larkum, A., and Ralph, P. J. (2008). Heat budget and thermal microenvironment of shallow-water corals: do massive corals get warmer than branching corals? *Limnol. Oceanogr.* 53, 1548–1561. doi: 10.4319/lo.2008.53.4.1548

Jimenez, I. M., Kühl, M., Larkum, A. W., and Ralph, P. J. (2011). Effects of flow and colony morphology on the thermal boundary layer of corals. *J. R. Soc. Interface* 8, 1785–1795. doi: 10.1098/rsif.2011.0144

Jørgensen, B. B., and Des Marais, D. J. (1990). The diffusive boundary layer of sediments: oxygen microgradients over a microbial mat. *Limnol. Oceanogr.* 35, 1343–1355. doi: 10.4319/lo.1990.35.6.1343

Jørgensen, B. B., and Revsbech, N. P. (1985). Diffusive boundary layers and the oxygen uptake of sediments and detritus. *Limnol. Oceanogr.* 30, 111–122. doi: 10.4319/lo.1985.30.1.0111

Kim, M., Brodersen, K. E., Szabó, M., Larkum, A. W., Raven, J. A., Ralph, P. J., et al. (2018). Low oxygen affects photophysiology and the level of expression of two-carbon metabolism genes in the seagrass *Zostera muelleri*. *Photosynthesis Res.* 136, 147–160. doi: 10.1007/s11120-017-0452-1

Koch, E. (1994). Hydrodynamics, diffusion-boundary layers and photosynthesis of the seagrasses *Thalassia testudinum* and *Cymodocea nodosa*. *Mar. Biol.* 118, 767–776. doi: 10.1007/BF00347527

Koren, K., Brodersen, K. E., Jakobsen, S. L., and Kühl, M. (2015). Optical sensor nanoparticles in artificial sediments – a new tool to visualize O_2 dynamics around the rhizome and roots of seagrasses. *Environ. Sci. Technol.* 49, 2286–2292. doi: 10.1021/es505734b

Kühl, M. (2005). Optical microsensors for analysis of microbial communities. *Methods Enzymol.* 397, 166–199. doi: 10.1016/S0076-6879(05)97010-9

Kühl, M., and Revsbech, N. P. (2001). "Biogeochemical microsensors for boundary layer studies," in *The Benthic Boundary Layer*, eds B. P. Boudreau and B. B. Jørgensen (New York, NY: Oxford University Press), 180–210.

Kumar, A., Castellano, I., Patti, F. P., Palumbo, A., and Buia, M. C. (2015). Nitric oxide in marine photosynthetic organisms. *Nitric Oxide* 47, 34–39. doi: 10.1016/j.niox.2015.03.001

Larkum, A. W., Pernice, M., Schliep, M., Davey, P., Szabo, M., Raven, J. A., et al. (2018). "Photosynthesis and metabolism of seagrasses," in *Seagrasses of Australia*, eds A. Larkum, G. Kendrick, and P. Ralph (Cham: Springer), 315–342. doi: 10.1007/978-3-319-71354-0_11

Larkum, A. W. D., Davey, P. A., Kuo, J., Ralph, P. J., and Raven, J. A. (2017). Carbon-concentrating mechanisms in seagrasses. *J. Exp. Bot.* 68, 3773–3784. doi: 10.1093/jxb/erx206

Larkum, A. W. D., Orth, R. J., and Duarte, C. M. (2006). *Seagrasses: Biology, Ecology and Conservation*. Berlin: Springer.

Lichtenberg, M., Nørregaard, R. D., and Kühl, M. (2017). Diffusion or advection? Mass transfer and complex boundary layer landscapes of the brown alga *Fucus vesiculosus*. *J. R. Soc. Interface* 14:20161015. doi: 10.1098/rsif.2016.1015

Martin, B. C., Bougoure, J., Ryan, M. H., Bennett, W. W., Colmer, T. D., Joyce, N. K., et al. (2019). Oxygen loss from seagrass roots coincides with colonisation of sulphide-oxidising cable bacteria and reduces sulphide stress. *ISME J.* 13, 707–719. doi: 10.1038/s41396-018-0308-5

Mazzella, L., and Alberte, R. S. (1986). Light adaptation and the role of autotrophic epiphytes in primary production of the temperate seagrass, *Zostera marina* L. *J. Exp. Mar. Biol. Ecol.* 100, 165–180. doi: 10.1016/0022-0981(86)90161-9

McConnaughey, T. (1991). Calcification in *Chara corallina*: CO_2 hydroxylation generates protons for bicarbonate assimilation. *Limnol. Oceanogr.* 36, 619–628. doi: 10.4319/lo.1991.36.4.0619

McRoy, C. P., and Barsdate, R. J. (1970). Phosphate absorption in eelgrass. *Limnol. Oceanogr.* 15, 6–13. doi: 10.4319/lo.1970.15.1.0006

Mishra, A. K., Santos, R., and Hall-Spencer, J. (2020). Elevated trace elements in sediments and seagrasses at CO_2 seeps. *Mar. Environ. Res.* 153:104810. doi: 10.1016/j.marenvres.2019.104810

Moßhammer, M., Brodersen, K. E., Kühl, M., and Koren, K. (2019). Nanoparticle- and microparticle-based luminescence imaging of chemical species and temperature in aquatic systems: a review. *Microchim. Acta* 186:126. doi: 10.1007/s00604-018-3202-y

Newby, B. Z., Cutright, T., Barrios, C. A., and Xu, Q. (2006). Zosteric acid—An effective antifoulant for reducing fresh water bacterial attachment on coatings. *JCT Res.* 3, 69–76. doi: 10.1007/s11998-006-0007-4

Nguyen, H. M., Ralph, P. J., Marín-Guirao, L., Pernice, M., and Procaccini, G. (2021). Seagrasses in an era of ocean warming: a review. *Biol. Rev.* 96, 2009–2030. doi: 10.1111/brv.12736

Nielsen, L. B., Finster, K., Welsh, D. T., Donelly, A., Herbert, R. A., De Wit, R., et al. (2001). Sulphate reduction and nitrogen fixation rates associated with roots, rhizomes and sediments from *Zostera noltii* and *Spartina maritima* meadows. *Environ. Microbiol.* 3, 63–71. doi: 10.1046/j.1462-2920.2001.00160.x

Noisette, F., Depetris, A., Kühl, M., and Brodersen, K. E. (2020). Flow and epiphyte growth effects on the thermal, optical and chemical microenvironment in the leaf phyllosphere of seagrass (*Zostera marina*). *J. R. Soc. Interface* 17:20200485. doi: 10.1098/rsif.2020.0485

Orth, R. J., Heck, K. L., and van Montfrans, J. (1984). Faunal communities in seagrass beds: a review of the influence of plant structure and prey characteristics on predator-prey relationships. *Estuaries* 7, 339–350. doi: 10.2307/1351618

Orth, R. J., and Van Montfrans, J. (1984). Epiphyte-seagrass relationships with an emphasis on the role of micrograzing: a review. *Aquatic Bot.* 18, 43–69. doi: 10.1016/0304-3770(84)90080-9

Pedersen, O., Binzer, T., and Borum, J. (2004). Sulphide intrusion in eelgrass (*Zostera marina* L.). *Plant Cell Environ.* 27, 595–602. doi: 10.1111/j.1365-3040.2004.01173.x

Pedersen, O., Borum, J., Duarte, C. M., and Fortes, M. D. (1998). Oxygen dynamics in the rhizosphere of *Cymodocea rotundata*. *Mar. Ecol. Progr. Series* 169, 283–288. doi: 10.3354/meps169283

Pedersen, O., Colmer, T. D., Borum, J., Zavala-Perez, A., and Kendrick, G. A. (2016). Heat stress of two tropical seagrass species during low tides–impact on underwater net photosynthesis, dark respiration and diel *in situ* internal aeration. *New Phytol.* 210, 1207–1218. doi: 10.1111/nph.13900

Pedersen, O., Revsbech, N. P., and Shabala, S. (2020). Microsensors in plant biology: in vivo visualization of inorganic analytes with high spatial and/or temporal resolution. *J. Exp. Bot.* 71, 3941–3954. doi: 10.1093/jxb/eraa175

Pernice, M., Sinutok, S., Sablok, G., Commault, A. S., Schliep, M., Macreadie, P. I., et al. (2016). Molecular physiology reveals ammonium uptake and related gene expression in the seagrass *Zostera muelleri*. *Mar. Environ. Res.* 122, 126–134. doi: 10.1016/j.marenvres.2016.10.003

Ralph, P. J., Tomasko, D., Moore, K., Seddon, S., and Macinnis-Ng, C. M. (2007). "Human impacts on seagrasses: eutrophication, sedimentation, and contamination," in *Seagrasses: Biology, Ecology and Conservation*, eds A. W. D. Larkum, R. J. Orth, and C. M. Duarte (Cham: Springer), 567–593. doi: 10.1007/1-4020-2983-7_24

Rasmusson, L. M., Buapet, P., George, R., Gullström, M., Gunnarsson, P. C., and Björk, M. (2020). Effects of temperature and hypoxia on respiration, photorespiration, and photosynthesis of seagrass leaves from contrasting temperature regimes. *ICES J. Mar. Sci.* 77, 2056–2065. doi: 10.1093/icesjms/fsaa093

Raun, A. L., and Borum, J. (2013). Combined impact of water column oxygen and temperature on internal oxygen status and growth of *Zostera marina* seedlings and adult shoots. *J. Exp. Mar. Biol. Ecol.* 441, 16–22. doi: 10.1016/j.jembe.2013.01.014

Raven, J. A., Beardall, J., and Giordano, M. (2014). Energy costs of carbon dioxide concentrating mechanisms in aquatic organisms. *Photosynthesis Res.* 121, 111–124. doi: 10.1007/s11120-013-9962-7

Revsbech, N. P. (2021). Simple sensors that work in diverse natural environments: the micro-Clark sensor and biosensor family. *Sensors Actuators B: Chem.* 329:129168. doi: 10.1016/j.snb.2020.129168

Ricart, A. M., Ward, M., Hill, T. M., Sanford, E., Kroeker, K. J., Takeshita, Y., et al. (2021). Coast-wide evidence of low pH amelioration by seagrass ecosystems. *Global Change Biol.* 27, 2580–2591. doi: 10.1111/gcb.15594

Riebesell, U., Zondervan, I., Rost, B., Tortell, P. D., Zeebe, R. E., and Morel, F. M. (2000). Reduced calcification of marine plankton in response to increased atmospheric CO_2. *Nature* 407, 364–367. doi: 10.1038/35030078

Sand-Jensen, K. (1977). Effect of epiphytes on eelgrass photosynthesis. *Aquatic Bot.* 3(Suppl. C), 55–63. doi: 10.1016/0304-3770(77)90004-3

Scholz, V. V., Brodersen, K. E., Kühl, M., and Koren, K. (2021). Resolving chemical gradients around seagrass roots–a review of available methods. *Front. Mar. Sci.* 1597. doi: 10.3389/fmars.2021.771382

Staehr, P. A., and Borum, J. (2011). Seasonal acclimation in metabolism reduces light requirements of eelgrass (*Zostera marina*). *J. Exp. Mar. Biol. Ecol.* 407, 139–146. doi: 10.1016/j.jembe.2011.05.031

Sullivan, B. K., Sherman, T. D., Damare, V. S., Lilje, O., and Gleason, F. H. (2013). Potential roles of *Labyrinthula* spp. in global seagrass population declines. *Fungal Ecol.* 6, 328–338. doi: 10.1016/j.funeco.2013.06.004

Sullivan, B. K., Trevathan-Tackett, S. M., Neuhauser, S., and Govers, L. L. (2018). Review: host-pathogen dynamics of seagrass diseases under future global change. *Mar. Pollut. Bull.* 134, 75–88. doi: 10.1016/j.marpolbul.2017.09.030

Tarquinio, F., Bourgoure, J., Koenders, A., Laverock, B., Säwström, C., and Hyndes, G. A. (2018). Microorganisms facilitate uptake of dissolved organic nitrogen by seagrass leaves. *ISME J.* 12, 2796–2800. doi: 10.1038/s41396-018-0218-6

Trevathan-Tackett, S. M., Sullivan, B. K., Robinson, K., Lilje, O., Macreadie, P. I., and Gleason, F. H. (2018). Pathogenic *Labyrinthula* associated with Australian seagrasses: considerations for seagrass wasting disease in the southern hemisphere. *Microbiol. Res.* 206, 74–81. doi: 10.1016/j.micres.2017.10.003

Van Dam, B., Zeller, M., Lopes, C., Smyth, A., Böttcher, M., Osburn, C., et al. (2021). Calcification-driven CO_2 emissions exceed "Blue Carbon" sequestration in a carbonate seagrass meadow. *Sci. Adv.* 7:eabj1372. doi: 10.1126/sciadv.abj1372

Villa, F., Albanese, D., Giussani, B., Stewart, P. S., Daffonchio, D., and Cappitelli, F. (2010). Hindering biofilm formation with zosteric acid. *Biofouling* 26, 739–752. doi: 10.1080/08927014.2010.511197

Wangpraseurt, D., Larkum, A. W., Ralph, P. J., and Kühl, M. (2012). Light gradients and optical microniches in coral tissues. *Front. Microbiol.* 3:316. doi: 10.3389/fmicb.2012.00316

Ward, L. G., Kemp, W. M., and Boynton, W. R. (1984). The influence of waves and seagrass communities on suspended particulates in an estuarine embayment. *Mar. Geol.* 59, 85–103. doi: 10.1016/0025-3227(84)90089-6

Waycott, M., Duarte, C. M., Carruthers, T. J. B., Orth, R. J., Dennison, W. C., Olyarnik, S., et al. (2009). Accelerating loss of seagrasses across the globe threatens coastal ecosystems. *Proc. Natl. Acad. Sci. U.S.A.* 106, 12377–12381. doi: 10.1073/pnas.0905620106

Welsh, D. T., Wellsbury, P., Bourguès, S., de Wit, R., and Herbert, R. A. (1996). Relationship between porewater organic carbon content, sulphate reduction and nitrogen fixation (acetylene reduction) in the rhizosphere of *Zostera noltii*. *Hydrobiologia* 329, 175–183. doi: 10.1007/BF00034556

York, P. H., Carter, A. B., Chartrand, K., Sankey, T., Wells, L., and Rasheed, M. A. (2015). Dynamics of a deep-water seagrass population on the Great Barrier Reef: annual occurrence and response to a major dredging program. *Sci. Rep.* 5:13167. doi: 10.1038/srep13167

York, P. H., Smith, T. M., Coles, R. G., McKenna, S. A., Connolly, R. M., Irving, A. D., et al. (2016). Identifying knowledge gaps in seagrass research and management: an Australian perspective. *Mar. Environ. Res.* 127, 163–172. doi: 10.1016/j.marenvres.2016.06.006

Zhang, Q., Kühl, M., and Brodersen, K. E. (2022). Effects of epiphytic biofilm activity on the photosynthetic activity, pH and inorganic carbon microenvironment of seagrass leaves (Zostera marina L.). *Front. Mar. Sci.* 9:835381.

Conflict of Interest: The authors declare that the research was conducted in the absence of any commercial or financial relationships that could be construed as a potential conflict of interest.

Publisher's Note: All claims expressed in this article are solely those of the authors and do not necessarily represent those of their affiliated organizations, or those of the publisher, the editors and the reviewers. Any product that may be evaluated in this article, or claim that may be made by its manufacturer, is not guaranteed or endorsed by the publisher.

frontiers in Marine Science

ORIGINAL RESEARCH
published: 16 March 2022
doi: 10.3389/fmars.2022.822485

Temperature Effects on Leaf and Epiphyte Photosynthesis, Bicarbonate Use and Diel O_2 Budgets of the Seagrass *Zostera marina* L.

*Aske Bang Hansen†, Anne Sofie Pedersen†, Michael Kühl and Kasper Elgetti Brodersen**

Marine Biological Section, Department of Biology, University of Copenhagen, Helsingør, Denmark

Ocean warming along with nutrient enrichment are major stressors causing global seagrass decline. While the effects of global warming on metabolic parameters in seagrasses are well described, the effect of increasing temperature on the epiphytic overgrowth of seagrass leaves and the consequences for the seagrass plant are poorly understood. Here, we investigated the effects of elevating temperature on the photosynthetic efficiency of the seagrass species *Zostera marina* L. and its associated epiphytes, to explore how ocean warming might affect epiphytism in seagrasses. Gas exchange and final pH measurements on bare seagrass leaves, leaves with epiphytes, and epiphytes separated from seagrass leaves were used to quantify photosynthesis and respiration rates, and the inorganic carbon extraction capacity of leaves and epiphytes as a function of photon scalar irradiance and temperature (12, 17, 22, and 27°C). Seagrass without epiphytic biofilm had a high ability to exploit the incoming irradiance regardless of the light intensity and temperature, shown as continuously high light use efficiency and maximum net photosynthesis rates. The presence of epiphytic biofilm on the seagrass leaves impaired plant photosynthesis by increasing light requirements and reducing the photosynthetic efficiency (especially at 27°C). Epiphytes showed the lowest respiration rates in darkness and had the highest oxygen surplus over diel cycles up to 22°C, whereas bare leaves had the highest diel oxygen surplus at 27°C. Both bare leaves and epiphytes lost the ability to utilize bicarbonate at 27°C, and epiphytes also did not show use of bicarbonate at 12°C. Our results indicate a competitive advantage for epiphytes in cold CO_2-rich environments, whereas seagrass with bare leaves could be less affected under elevated seawater temperatures.

Keywords: biofilm, CO_2, epiphytes, global warming, photosynthesis, respiration, seagrass

OPEN ACCESS

Edited by:
Christian Grenz, UMR 7294 Institut Méditerranéen d'Océanographie (MIO), France

Reviewed by:
Peter Anton Upadhyay Staehr, Aarhus University, Denmark
Nadine Schubert, University of Algarve, Portugal

***Correspondence:**
Kasper Elgetti Brodersen
kasper.elgetti.brodersen@bio.ku.dk

†These authors have contributed equally to this work and share first authorship

Specialty section:
This article was submitted to Marine Ecosystem Ecology, a section of the journal Frontiers in Marine Science

Received: *25 November 2021*
Accepted: *08 February 2022*
Published: *16 March 2022*

Citation:
Hansen AB, Pedersen AS, Kühl M and Brodersen KE (2022) Temperature Effects on Leaf and Epiphyte Photosynthesis, Bicarbonate Use and Diel O_2 Budgets of the Seagrass Zostera marina L. Front. Mar. Sci. 9:822485. doi: 10.3389/fmars.2022.822485

INTRODUCTION

Seagrass meadows are among the most productive and diverse coastal benthic ecosystems (Larkum et al., 2006; Unsworth and Cullen-Unsworth, 2017). Seagrasses colonize organic rich and reduced sediments, where the phytotoxin hydrogen sulfide is produced by anaerobic bacterial sulfate reduction (Blaabjerg et al., 1998; Nielsen et al., 2001). Via their internal gas-filled aerenchymal tissue, seagrasses exhibit efficient gas transport to their belowground tissues (Borum et al., 2006; Brodersen et al., 2014, 2018), where it supplies the belowground biomass with oxygen and can protect the seagrass rhizosphere from hydrogen sulfide intrusion, which otherwise can be fatal to

the plant (Brodersen et al., 2015a,b, 2017; Brodersen, 2016). Many crucial ecosystem services are provided by seagrass meadows such as fisheries production (Bertelli and Unsworth, 2014; Unsworth and Cullen-Unsworth, 2014, 2017; Unsworth et al., 2019), coastal protection from erosion (Fonseca and Cahalan, 1992), efficient carbon sequestration in the oxygen-depleted seagrass sediments (e.g., Fourqurean et al., 2012; Macreadie et al., 2015; Cullen-Unsworth and Unsworth, 2018) and reduction of microbiological contaminants (Lamb et al., 2017). Seagrass meadows are thus of high ecological and economic value (Costanza et al., 1997; Unsworth et al., 2019) and the ongoing decline in seagrass habitats due to anthropogenic stress can therefore lead to decreasing biodiversity, which further contributes to negative effects induced by climate change.

Anthropogenic impacts, such as coastal development and eutrophication, are major drivers behind the global decline in seagrass meadows (Orth et al., 2006; Waycott et al., 2009). Eutrophication is facilitating epiphytic overgrowth of microalgae and bacteria on the surface of seagrass leaves, which is an increasing problem in coastal waters, due to accelerating nutrient runoff from land (Borum, 1985). Furthermore, nutrient-driven enhanced macroalgal growth can potentially outcompete seagrass species (Ballesteros et al., 2007). While the colonization of microalgae and the presence of plant detritus on the seagrass leaf surface can serve as a food source for small herbivores (Cullen-Unsworth and Unsworth, 2018), the presence of epiphytic biofilms can strongly influence plant fitness (Sand-Jensen, 1977). Epiphytic biofilm growth on seagrass leaves leads to dramatic changes in the seagrass phyllosphere (Brodersen and Kühl, 2022), i.e., the dynamic microhabitat forming at the leaf tissue surface of the seagrass plant (Brodersen et al., 2020a,b; Noisette et al., 2020). The presence of epiphytic biofilms impedes O_2 and heat transfer between the leaf area and the ambient water, and both light availability and light quality reaching the seagrass leaves is highly diminished (Brodersen et al., 2015a; Noisette et al., 2020); all negatively affecting seagrass performance and health. However, leaf microorganisms can also be beneficial to seagrasses, as they can facilitate uptake of dissolved organic nitrogen by leaves and thus potentially benefit seagrass growth and productivity (Tarquinio et al., 2018).

The ocean has a high heat capacity and has absorbed > 90% of heat induced by the ongoing increase of greenhouse gases in the atmosphere (Levitus et al., 2000; Resplandy et al., 2019), which drives ongoing ocean warming (Gattuso and Hansson, 2011). Temperature is a primary parameter controlling the distribution of seagrass species from tropical to temperate regions, as evident by the higher temperature optima of photosynthesis in tropical seagrass species (Pedersen et al., 2016), where some species can endure short-term exposure to water temperatures of up to 42°C. Several vital processes within seagrasses are temperature dependent such as the diffusive transport of gases and solutes, rates of photosynthesis and respiration, and the enzymatic capacity of RuBisCO (Staehr and Borum, 2011). The plant's metabolic rates (e.g., photosynthesis and respiration) and thus nutrient demand increases with increasing temperature toward an optimum temperature, above which increasing deactivation of metabolic processes and/or denaturation of vital metabolic macromolecules (e.g., proteins) lead to increasing plant stress (Staehr and Borum, 2011). Seagrass respiration exhibits a stronger response with increasing temperature than photosynthetic processes (Dennison, 1987). Consequently, a disbalance at high temperatures may affect the light requirements and depth distribution of e.g., eelgrass (*Zostera marina* L.), since a higher irradiance is needed to compensate the increasing oxygen demands to maintain a positive carbon-balance (Staehr and Borum, 2011). High temperatures, above the plant's photosynthetic temperature optima, can thus lead to a negative diel O_2 balance in the seagrass plant due to reduced leaf photosynthesis and increased tissue respiration, which strongly reduces the internal plant aeration (Staehr and Borum, 2011; Pedersen et al., 2016). The interactions between plant, sediment, and the water column, also strongly depend on the water temperature. As temperature increases, the oxygen solubility in the water decreases, and the intra-plant oxygen content is lowered e.g., due to increasing respiration, which leads to a reduction in the plant tolerance to anoxia (Raun and Borum, 2013). This becomes apparent during night-time or low light levels, when seagrass' respiration can be limited by the availability of dissolved O_2 in the water column, since the supply is sustained solely by the relatively slow diffusion of O_2 into the leaf through the diffusive boundary layer (DBL) (Brodersen et al., 2015a; Pedersen et al., 2016). This makes the plant highly susceptible to hydrogen sulfide intrusion (Brodersen et al., 2015b), which can lead to chemical asphyxiation. Especially, seagrass communities inhabiting shallow intertidal waters can experience impeded photosynthetic activity due to extreme light levels, temperatures, O_2 fluctuations and pH changes (Pedersen et al., 2016).

The increase in atmospheric CO_2 equilibrates with seawater affecting the speciation of inorganic carbon and leading to ocean acidification (Albert et al., 2020). This can influence some marine phototrophs positively since it is favorable to use CO_2 as an inorganic carbon source (Riebesell et al., 2018), while calcifying organisms are facing increasing difficulties in depositing calcium carbonate. Different bicarbonate utilization strategies have been detected in temperate seagrasses (Borum et al., 2016; Kim et al., 2018; Larkum et al., 2018). External carbonic anhydrase (CA) can catalyze the conversion of bicarbonate to CO_2 at the leaf surface (Borum et al., 2016; Kim et al., 2018; Larkum et al., 2018), while local acidification of the diffusive boundary layer (DBL) via proton pumps on the leaf surface might cause a local decrease in pH and thus enhanced conversion of bicarbonate to CO_2 for photosynthesis (Borum et al., 2016). Such CO_2 concentrating mechanisms are energy consuming for the plant, which only makes them favorable in CO_2 poor environments (Raven et al., 2014). Theoretically, seagrasses are able to use bicarbonate (HCO_3^-) as a carbon source when they are able to rise pH above 9 using the pH drift approach (Sand-Jensen et al., 1992).

Eelgrass (*Z. marina* L.) has been shown to exhibit temperature optima at 20–25°C for growth and photosynthesis under saturating light, while light limiting conditions can reduce the optimum temperature by up to 10°C (Beca-Carretero et al., 2018). The photosynthetic saturation

level and the compensation photon irradiance of *Z. marina* generally increase with increasing temperatures (Marsh et al., 1986). Q10 values for light-saturated photosynthesis and dark respiration of 1.5–1.7 and 2.4, respectively, have been determined over the temperature range of 0–35°C (Marsh et al., 1986). *Z. marina* plants originating from the northern part of their distribution range (i.e., subarctic populations) show higher sensitivity to extreme temperatures with faster declines in photosynthesis and increases in respiration (Beca-Carretero et al., 2018). Compared to other seagrass species such as *Ruppia maritima* L., *Z. marina* appears less tolerant to higher temperatures (e.g., Evans et al., 1986), which also corresponds with their respective seasonal community dynamics. Primary productivity cycles of *Z. marina* and its epiphytes have been suggested to be closely interrelated (Penhale, 1977), where the epiphyte community photosynthesis can double the total primary production of *Z. marina* leaves (Mazzella and Alberte, 1986), while at the same time having detrimental effects on leaf photosynthesis owing to shading (Sand-Jensen, 1977; Brodersen et al., 2015a) and carbon limitation (Brodersen et al., 2020a). Such knowledge is important to determine critical temperature thresholds for productivity and survival of *Z. marina* under future climate change conditions. *Z. marina* thus seems to have relatively high ability to acclimate to environmental change considering its wide latitudinal distribution (Staehr and Borum, 2011; Assis et al., 2020); plants exhibit a higher ability to utilize low irradiance during winter, whereas no difference in optimum temperatures has been found between winter- and summer-acclimated plants (Staehr and Borum, 2011).

Although temperature effects on seagrass leaf photosynthesis are well described, almost nothing is known about how increasing temperature affects leaf/epiphyte interactions and how epiphyte growth on leaves affects the ability of seagrasses to withstand increasing seawater temperatures. In this study, we investigated acute temperature effects on the respiration and photosynthesis of eelgrass (*Z. marina*) leaves and their epiphytic biofilms using a combination of gas exchange and pH measurements on leaf fragments in closed incubation chambers. We analyze and compare how increasing temperature affects (i) the balance between autotrophy and heterotrophy, (ii) the photosynthetic efficiency, and (iii) the potential to use bicarbonate in photosynthesis in bare seagrass leaves, leaves covered by an epiphytic biofilm, as well as in epiphytes separated from the seagrass leaves. The experiments aimed to obtain a better understanding of how increasing seawater temperature may affect the ability of seagrasses to withstand ongoing ocean warming and increased epiphytic overgrowth.

MATERIALS AND METHODS

Seagrass and Sediment Sampling

Whole specimens of the common seagrass species *Zostera marina* L. and marine sediment were collected in early April 2021 at the coast of Julebæk, North Zealand, Denmark (56°03′29.2″N; 12°34′40.7″E). Seagrass plants with and without epiphytic biofilms on their leaves were collected in the shallow (< 2 m) coastal brackish water with a salinity of 18. The average water temperature in April is about 10°C. The specimens were immediately transported to nearby laboratory facilities at the Marine Biology Section (University of Copenhagen) in Elsinore, where the seagrass plants and collected sediment were placed in a large aquarium containing constantly aerated seawater from the sampling site kept at 16–18°C. The seagrass samples were exposed to an incident photon irradiance (400–700 nm) of 100 μmol photons m^{-2} s^{-1} as provided by a metal-halide lamp (14:10 h light/dark cyclus; MEGACHROME, Giesemann Aquaristic Gmbh, Nettetal, Germany). The water temperature in the sampling area rapidly increases from about 10–20°C from April to June, and the holding aquarium temperature was adjusted to reflect the *in-situ* water temperature at the sampling site at the time of the experimental measurements (e.g., Staehr and Borum, 2011). The incubation photon irradiance mimicked the approximate daily average photon irradiance at the sampling site at the depth of the seagrass meadow (e.g., Staehr and Borum, 2011). The plants were acclimated to the aquarium conditions for 1 week prior to the start of the experiments. Leaves with a similar fluffy coating of filamentous epiphytes were selected for the experiments. The epiphytic biofilm community composition was assumed to predominantly consist of green algae, brown algae, diatoms, and bacteria as previously shown by Borum et al. (1984). To minimize dissimilarities between the seagrass leaves selected for the experiment, the youngest and the oldest leaves from each individual plant were excluded (Brodersen et al., 2020a).

Gas Exchange Measurements

We quantified the net O_2 exchange in darkness (respiration) and under defined photon irradiance levels (net photosynthesis) by placing seagrass leaf segments of a known area in small custom-made glass chambers (1.8 mL). The chambers were equipped with small oxygen sensor spots (OXSP5, PyroScience GmbH, Aachen, Germany) fixed on the inside with a transparent silicone glue (SPGLUE ELASTOSIL E43, WACKER Chemical Corporation, Adrian MI, United States). An optical fiber, mounted on a holder enclosing each chamber, was pointing at and sending red excitation light to the oxygen sensor spot and collected the resulting O_2-dependent infrared luminescence. The optical fibers were connected to a 4-channel optical O_2 sensor system (FireSting-O2; FSO2-C4, PyroScience GmbH, Aachen, Germany), which was connected to a PC running Pyroscience Oxygen Logger software (PyroScience GmbH, Germany) that logged and stored the data. A temperature sensor was connected to the system and was used to perform temperature-compensated O_2 measurements over the experimental temperature range of 12–22°C. Prior to the measurements, each of the four applied microrespiration chambers was calibrated at two known O_2 levels using a sodium sulfite (Na_2SO_3) solution for the 0% air saturation calibration and air saturated seawater (prepared by aeration with an air pump) for the 100% air saturation calibration. The calibration was repeated before conducting the experiment under 27°C due to drifting calibrations at high temperature.

To manipulate and control the temperature, the closed gas exchange chambers with seawater and seagrass leave sections were placed in an aquarium with thermostated DI-water. To obtain the desired water temperatures in the aquarium and thereby the measuring chambers, we used a combination of a cooling system (Heto Cooling bath type CBN 8-30, HETO-HOLTEN A/S, Allerød, Denmark) and an aquarium heater (Aquael EasyHeater 25W, Suwałki Poland) submerged into the aquarium. A submersed water pump (Universal mini pump 5W, TUNZE, Austin TX, United States) placed in the aquarium ensured sufficient water circulation and homogeneous temperature distribution in the experimental chambers.

The aquarium was placed above two magnetic stirrers (IKA Magnetic Stirrers RCT basic, IKA®-Werke GmbH & Co. KG, Staufen, Germany) and each measuring chamber was equipped with a small magnet to ensure sufficient mixing in the experimental chambers during incubations. Small plankton nets (0.2 mm mask width) were placed above the magnet to protect the specimens from mechanical impact form the stirring magnet. To ensure that the specimens were exposed to equivalent photon irradiances, the three chambers and a control chamber only containing air saturated, filter-sterilized (0.2 μm) seawater and a magnet, were positioned with the same distance to an adjustable fiber-optic tungsten halogen lamp (KL-2500LCD, Schott GmbH, Germany) equipped with a tri-furcated fiber bundle, each mounted with a collimating lens. Photon scalar irradiance in the experimental chambers for defined lamp settings were determined through measurements with a calibrated photon scalar irradiance sensor (3 mm diameter) connected to a calibrated irradiance meter (ULM-500, Walz GmbH, Effeltrich, Germany).

For each experimental run, three leaf segments from one seagrass specimen were used: One leaf segment without visible epiphyte cover (bare leaf, 35 mm lengths), one segment with epiphyte cover (leaf with epiphytes, 30 mm length), and epiphytes which were gently scraped off a leaf segment with a scalpel (epiphytes, 40 mm). All leaf segments originated from the middle part of the leaves to avoid the youngest and oldest regions and thus to minimize age and genetic differences between investigated leaf segments (Brodersen et al., 2020a); where leaf segments with epiphyte cover refer to leaves with 100% areal epiphytic biofilm cover and bare leaves to leaf segments with 0% areal epiphytic biofilm cover. Different leaf segment lengths were used to aim for a similar total photosynthetic biomass between samples (here, determined as a similar DW), while also ensuring a water volume of 1.8 mL in all measuring chambers. The seagrass leaf segments (bare and with epiphytes) and the epiphytes were placed in three custom-made microrespiration chambers containing air saturated and filter-sterilized (0.2 μm) seawater with a salinity of 18.

Four biological replicates were used in the gas exchange experiment (n = 4), one replicate per experimental run. Each replicate was exposed to water temperatures of 12, 17, 22, and 27°C (for a minimum of 30 min prior to onset of measurements); where the high temperature treatment of 27°C represents possible maximal temperatures during summer-time within the investigated meadow under future global warming. Running each temperature treatment, the specimens were alternately exposed to darkness and increasing light irradiances (100, 300, and 600 μmol photons m^{-2} s^{-1}) for 8 min at each light condition. This time interval resulted in a constant linear change in O_2 concentration during incubations. The experiment started out and ended in darkness.

To obtain photosynthesis and respiration rates per gram dry weight (g DW^{-1}), the seagrass leaf segments were placed in an oven and the specimen dry weight was measured after 48 h exposure to 60°C. Respiration and net photosynthesis rates were calculated by multiplying the slope of the linear O_2 concentration vs. time curve (nmol L^{-1} h^{-1}) with the volume of water in the measuring chamber (L) divided by the sample dry weight. Post-illumination respiration (i.e., respiration rates measured after a light period) was measured as the immediate O_2 depletion rate in darkness after light exposure to a given photon scalar irradiance and was used as a proxy for respiration in the previous light period. Gross photosynthetic rates were calculated by adding the absolute values of the respective respiration rates (i.e., dark respiration or the post-illumination respiration rates measured immediately after the light period at each experimental photon irradiance level) to the respective net photosynthetic rates: GP (E) = NP (E) + |R (E) |. Control measurements in chambers without leaves or epiphytes did not show any O_2 production or consumption under all tested experimental conditions. Such control incubations are performed to allow for potential correction of measurements on samples due to minor microbial contamination in the measuring chambers leading to undesired microbial-mediated O_2 production and/or consumption.

pH Drift Measurements

To estimate the dissolved inorganic carbon (DIC) extraction capacity and maximal pH tolerance of the seagrass leaves and the epiphytes, pH drift measurements were performed according to Brodersen et al. (2020a). A final pH of > 9 in such drift experiments indicates the ability of the specimens to utilize bicarbonate as an additional inorganic carbon source in photosynthesis (Pedersen et al., 2016). For each experimental run, a total of four biological replicates were used (n = 4). We used four seagrass leaf segments without visible epiphyte cover (bare leaf, 35 mm length), four leaf segments with epiphyte cover (leaf with epiphytes, 30 mm length), and 4 samples of epiphytes gently scraped off from 4 seagrass leaves with a scalpel (epiphytes, scraped off a 40 mm long leaf segment). Different segment lengths were used to ensure similar photosynthetic biomass (here, determined as a similar g DW). The leaf segments and the epiphyte samples were placed in separate falcon tubes with 35 mL filter-sterilized (0.2 μm) seawater with a salinity of 18, which allowed for a headspace in each tube to minimize photorespiration during the long-term incubations (cf. Pedersen et al., 2016). To manipulate and control the temperature, all tubes were positioned in a DI water-filled thermostated aquarium similar to the one used for gas exchange measurements. A lamp (MIA worldlight, LP300Q-4K.24_RY; MIA Light GmbH, Gronau, Germany) was placed on top of the aquarium to provide the specimens with a constant saturating photon scalar irradiance of 600 μmol photons m^{-2} s^{-1}. Light levels were quantified with a

photon scalar irradiance sensor (3 mm diameter) connected to a calibrated irradiance meter (ULM-500, Walz GmbH, Effeltrich, Germany). The experiment was conducted four times with the following water temperatures: 12, 17, 22, and 27°C. The experiment proceeded 45 h under each temperature before the final pH levels was measured in each sample; this incubation time was chosen after several repetitive measurements at different timescales, i.e., 24, 36, and 48 h showing how pH approached a stable maximum value. The pH measurements were done with a calibrated pH minisensor (BlueLine pH combination electrode; SI Analytics GmbH, Mainz, Germany) connected to a pH meter (PHM220 Lab pH Meter; Radiometer Analytical SAS, Lyon, France) and calibrated with commercial pH buffers of pH 7 and 10 (VWR Chemicals, Pennsylvania, United States).

Data Calculations and Analysis

The software program OriginPro 2020 (OriginLab Corporation, Northampton MA, United States) was used to create photosynthesis vs. irradiance curves, and for fitting and analyzing the experimental data. Non-linear regression fits of the calculated net photosynthesis (NP) and gross photosynthesis (GP) rates normalized to dry weight as a function of photon scalar irradiance (E), were used to obtain photosynthetic parameters (described below). We fitted an exponential saturation model for gross photosynthesis vs. irradiance curves (Webb et al., 1974):

$$GP\,(E) = GP_{MAX} \cdot (1 - exp\,(-\alpha \cdot E/GP_{MAX})) \quad (1)$$

and used a similar model with an additional respiration term for fitting net photosynthesis vs. irradiance curves (Spilling et al., 2010):

$$NP\,(E) = NP_{MAX} \cdot (1 - exp\,(-\alpha \cdot E/NP_{MAX})) + R(E) \quad (2)$$

Here, P_{MAX} is the calculated photosynthetic rate at saturating photon irradiance, α is the light utilization efficiency related to the photosynthetic activity, i.e., the slope of the P vs. E curve, and R(E) is the respiration rate of the seagrass leaves and/or epiphytes at the respective photon scalar irradiance.

The compensation irradiance, i.e., the photon scalar irradiance above which a sample exhibits net photosynthetic production of O_2, E_C, was determined from the obtained photosynthetic parameters as:

$$E_c = NP_{MAX} \cdot LOG10\,((1 + R/NP_{MAX})/ - \alpha) \quad (3)$$

The photon scalar irradiance at the onset of photosynthesis saturation (E_k) was calculated as:

$$E_k = NP_{MAX}/\alpha \quad (4)$$

To evaluate the sensitivity of the different photosynthesis parameters of leaves and epiphytes to temperature changes, a calculation of Q_{10} was made for NP_{MAX}, α_{np} (from NP), R, GP_{MAX}, and α_{gp} (from GP):

$$Q_{10} = (Parameter_{T2}/Parameter_{T1})^{(10/(T_2 - T_1))} \quad (5)$$

where $Parameter_{T2}$ and $Parameter_{T1}$ are the metabolic parameters of the leaves/epiphytes measured at two given temperatures, i.e., 22 and 12°C, respectively.

The total daily net oxygen production, DP, of the leaves and epiphytes was estimated as a function of increasing temperature assuming 14 h of light exposure at differing light irradiances followed by 10 h of darkness. The 14 h of light exposure were divided into 7 intervals each lasting 2 h (i.e., 5–7, 7–9, 9–11, 11–13, 13–15, 15–17, and 17–19). For each time interval, a photon irradiance average was calculated. The data on diel photon irradiance originated from Staehr et al. (2018).

The net photosynthesis under each averaged photon irradiance interval was calculated with equation 2 using the averaged photon irradiance determined for each of the pre-defined 7 time-intervals (*t1-t7*).

The daily net oxygen production of the leaves and epiphytes was calculated as:

$$DP = (\sum_{t=1}^{t=7} NP(E)) \; - \; (R\,x\,10) \quad (6)$$

where *NP(E)* is the net oxygen production at the given average photon irradiance for a given 2 h time interval, *R* is the dark respiration, and *t* represent the respective pre-defined time intervals.

Student's *t*-tests were used to statistically analyze data and compare treatments. The significance level was set to $p < 0.05$. Statistical tests were performed in Microsoft Excel.

RESULTS AND DISCUSSION

Our study provides evidence that the seagrass *Z. marina* L. performs better under elevated temperatures (27°C) in terms of photosynthetic performance (e.g., light use efficiency and maximum net photosynthesis) and diel O_2 balance, when no epiphytic biofilm is present on the surface of the leaves. Simultaneously, the seagrass bare leaves also performed better than their associated epiphytes originating from the leaves.

Photosynthesis and Respiration

Net photosynthesis increased with increasing photon scalar irradiance until saturation (**Figures 1A–L**), and with increasing temperature except for leaves with epiphytes, and for epiphytes originating from *Z. marina* L. leaves at 27°C. Such response to increasing irradiance and temperature is similar to previous studies on bare seagrass leaves (Ralph et al., 2007; Staehr and Borum, 2011; Pedersen et al., 2016). At 27°C, only bare seagrass leaves showed a positive net photosynthesis at a photon scalar irradiance of 100 μmol photons m^{-2} s^{-1}. Respiration increased with temperature and varied to a lesser degree with photon scalar irradiance, as determined from comparing dark respiration and post-illumination respiration rates (**Figures 1A–L**). This is

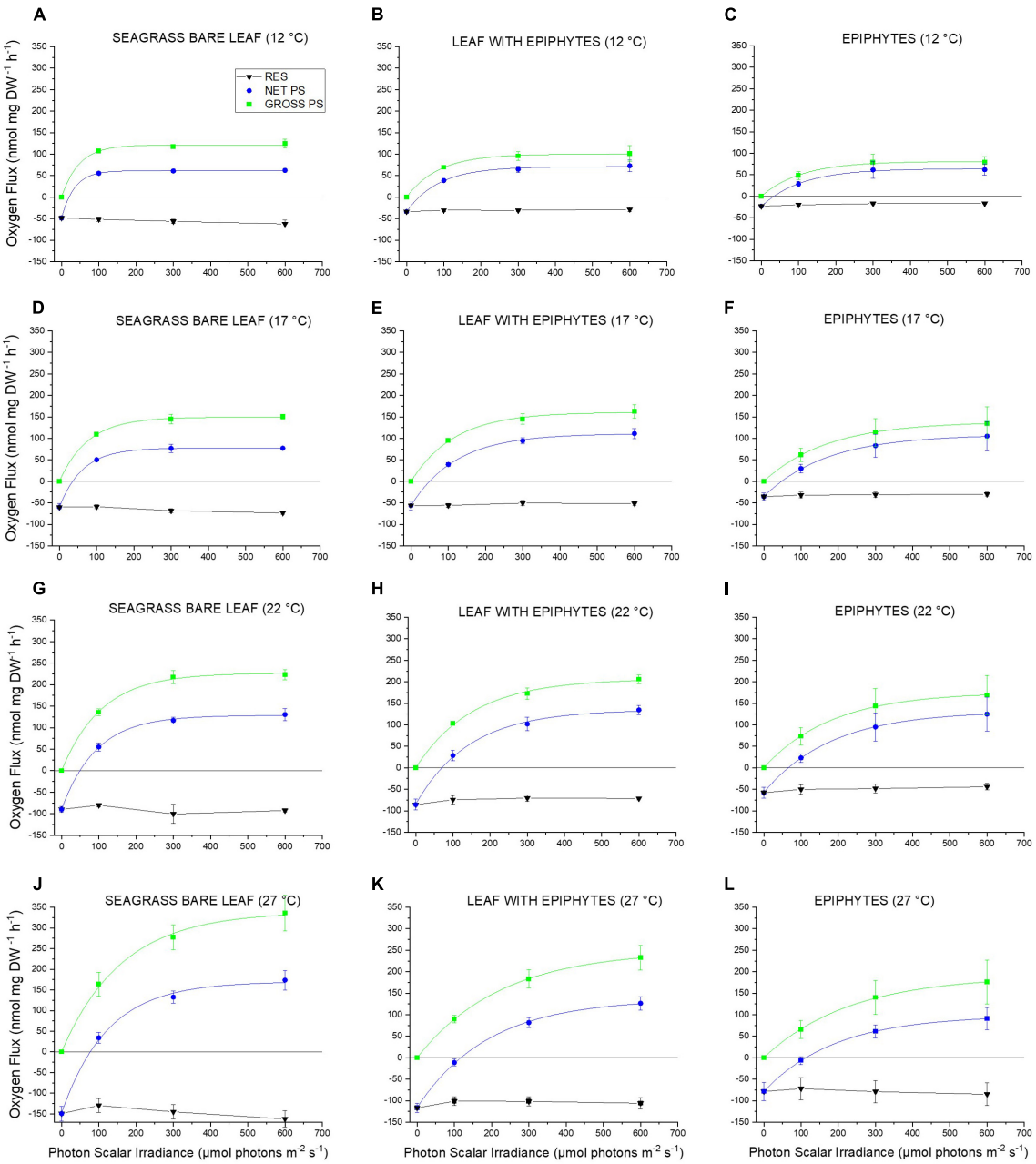

FIGURE 1 | (A–L) Respiration, net and gross O_2 production rates as a function of incident photon scalar irradiance for *Z. marina* L. leaves with and without epiphytes, as well as, for epiphytes originating from *Z. marina* L. leaves. The respiration, net and gross photosynthesis rates were measured for photon scalar irradiances (PAR, 400–700 nm) of 0, 100, 300, and 600 µmol photons m^{-2} s^{-1} and temperatures of 12, 17, 22, and 27°C. Black symbols and lines shows respiration. Blue symbols and lines show net photosynthesis. Zero net O_2 production ($Y = 0$) indicates the compensation photon irradiance of the seagrass leaves and epiphytes. Green symbols and lines show gross photosynthesis. Symbols with error bars represent mean values ± SEM; $n = 4$, biological replicates. All non-linear regression curve fits had an R^2 of ≥ 0.99. Detailed information about our statistical models can be found in **Supplementary Notes 1** and **Supplementary Tables 1–24**.

similar to previous studies that also found a strong temperature dependency of the dark respiration rate for seagrass leaves (Staehr and Borum, 2011; Pedersen et al., 2016). Gross photosynthesis rates increased with increasing photon scalar irradiance until saturation and with elevated temperatures (**Figures 1A–L**). The gross photosynthesis of the bare leaves was highest at all temperatures besides at 17°C, where the gross photosynthesis rate of all samples was very similar and reached a maximum gross photosynthesis rate of ∼150 nmol O_2 mg DW^{-1} h^{-1} (**Figure 1**). Epiphytes exhibited the lowest gross photosynthesis rates at 12, 22, and 27°C as compared to bare leaves and leaves with epiphytes.

Maximum net photosynthesis (NP_{MAX}) increased strongly from 12 to 22°C in all samples (**Figure 2A**). NP_{MAX} for the bare leaves showed a similar increase from 22 to 27°C, while the increase in leaves with epiphytes became less pronounced, and separated epiphytes showed a decrease in NP_{MAX} (**Figure 2A**). Bare seagrass leaves exhibited higher NP_{MAX} at 27°C compared to leaves with epiphytic cover and epiphytes originating from *Z. marina* L. leaves. This impediment by epiphytic biofilm of the seagrass metabolic parameters and thus photosynthetic performance is similar to previous studies (Staehr and Borum, 2011; Brodersen et al., 2015a, 2020a; Noisette et al., 2020). Accumulation of gases within the seagrass phyllosphere in light, due to thicker diffusive boundary layers (DBL) and total diffusive distances (TDD) caused by the epiphyte cover, limits the exchange of gases and nutrients (Brodersen et al., 2015a, 2020a; Noisette et al., 2020), and thus the NP_{MAX}.

The dark respiration rate (R) also increased strongly with increasing temperature (**Figure 2B**). However, while the respiration of leaves with epiphytes and separated epiphytes displayed a quasi-linear increase with temperature (R^2 = 0.99 and R^2 = 0.98), the respiration of bare seagrass leaves respiration rate increased quasi-exponentially (R^2 = 0.99) (**Figure 2B**). The separated epiphytes exhibited the lowest respiration rate under all measured temperatures (**Figure 2B**). The respiration rates of bare seagrass leaves exceeded respiration rates of leaves with epiphytes at 12 and 27°C, whereas the respiration rates were similar at 17 and 22°C (**Figure 2B**). The low dark respiration rate of the epiphytes observed under elevated temperatures (27°C) (**Figure 2B**), could suggest that the epiphytes are better at adapting to the rising seawater temperature. However, the Q_{10} relationship between respiration rate and photosynthesis rate of the epiphytes, revealed a negative correlation (**Table 1**), explaining their low NP_{MAX} values at elevated temperatures (27°C). Such general increase in dark respiration with increasing temperature of seagrass leaves is similar to previous studies (Staehr and Borum, 2011; Pedersen et al., 2016), where Staehr and Borum (2011) found Q_{10} values for dark respiration ranging from 1.4 to 3.9, which is very similar to our results with Q10 ranging from 1.9 to 2.5 (**Table 1**).

The light utilization efficiency (α) of the bare *Z. marina* L. leaves was higher at all experimental temperatures, as compared to leaves with epiphytic cover and separated epiphytes (**Figure 2C**). The light use efficiency was lowest in samples with epiphytes separated from the leaves. Leaves with epiphytes and the separated epiphytes light utilization efficiency increased with temperature reaching a maximum at 22°C, followed by a decrease at higher temperature (**Figure 2C**). Bare leaves exhibited a marked drop in light utilization efficiency from 12°C (maximum) to 17°C (minimum). This decrease of the bare leaves was thus in contrast to leaves with epiphytes and separated epiphytes, and was followed by an increasing efficiency in bare leaves from 22 to 27°C (**Figure 2C**). An earlier investigation of the seagrass phyllosphere (Brodersen et al., 2015a), concluded that the presence of epiphytic biofilm diminishes both the quantity and quality of light available for the seagrass leaf, which might explain the lower light utilization efficiencies in leaves with epiphytes and separated epiphytes. These observations emphasize the ability of the bare leaves to maintain a higher NP_{MAX} under elevated temperatures. This statement was supported by the positive relation between the Q_{10} values of photosynthesis rates compared to respiration rates for bare leaves (**Table 1**). Our estimated light use efficiencies (α) for *Z. marina* and its epiphytes were the same order of magnitude as previous findings in Danish waters (e.g., Staehr and Borum, 2011). However, we note that the relatively high estimated α value for bare seagrass leaves at 12°C may be overestimated owing to limited measurements of O_2 evolution under sub-saturating photon irradiances for bare leaves at this specific temperature treatment (see **Figure 1**), which challenges the used calculation of α.

The photon scalar irradiance at the onset of photosynthesis saturation (E_k) of the leaves and epiphytes increased with increasing temperature, with the bare leaf showing lowest E_K values at all temperatures, as compared to the separated epiphytes and leaves with epiphytes (**Figure 2D**). At 27°C, separated epiphytes and leaves with epiphytes reached the onset of light saturation at higher light levels (i.e., 193μmol photons m^{-2} s^{-1} and 194 μmol photons m^{-2} s^{-1}), as compared to the bare leaves (123 μmol photons m^{-2} s^{-1}) (**Figure 2D**). Similarly, the compensation irradiance (E_c), i.e., the photon scalar irradiance above which leaves/epiphytes exhibited a net O_2 production and thus an autotrophic carbon balance, increased quasi-exponentially (R^2 = 0.99) with temperature for all samples (**Figure 2E**). Epiphytes separated from the leaves and leaves with epiphytes displayed a stronger increase in E_c with increasing temperature, as compared to bare leaves exhibiting the lowest E_c values at all temperatures (**Figure 2E**). Student's *t*-tests confirmed significant differences ($p < 0.05$) between E_c values of the bare leaves, of the epiphytes separated from the leaves, and of the leaves with epiphytes. The temperature dependency of E_c thus increased the light irradiance demand of the specimens to maintain a positive carbon balance. The lower light compensation level (E_c) observed in bare leaves (**Figure 2E**), also demonstrated by Staehr and Borum (2011), was accompanied by a lower onset of photosynthesis saturation point (E_k) (**Figure 2D**) indicating that bare leaves were less temperature dependent/affected (e.g., Wieland and Kühl, 2000). In contrast, leaves with epiphytes exhibited the highest E_c levels over all experimental temperatures (**Figure 2E**). The high irradiance requirement reflects the impediment of the seagrass by the epiphytic cover; that is, the biofilm was shading the incoming irradiance, affecting both the light quality and quantity reaching the leaf surface (Brodersen et al., 2015a), increasing the light requirement of the epiphyte covered leaf. Thus under future warmer ocean conditions, *Z. marina* might become limited to shallow waters with sufficiently high irradiance. The water clarity in coastal waters is challenged by ongoing eutrophication by accelerating land runoff, which is promoting algal blooms and epiphytic growth on the seagrass leaves (Borum, 1985; Brodersen et al., 2020a). Furthermore, shallow coastal habitats often experience fluctuating temperatures, O_2 levels, and pH changes that constitute a threat to seagrass growth and survival both during the day and at nighttime (Greve et al., 2003; Borum et al., 2005; Pulido Pérez and Borum, 2010; Raun and Borum, 2013;

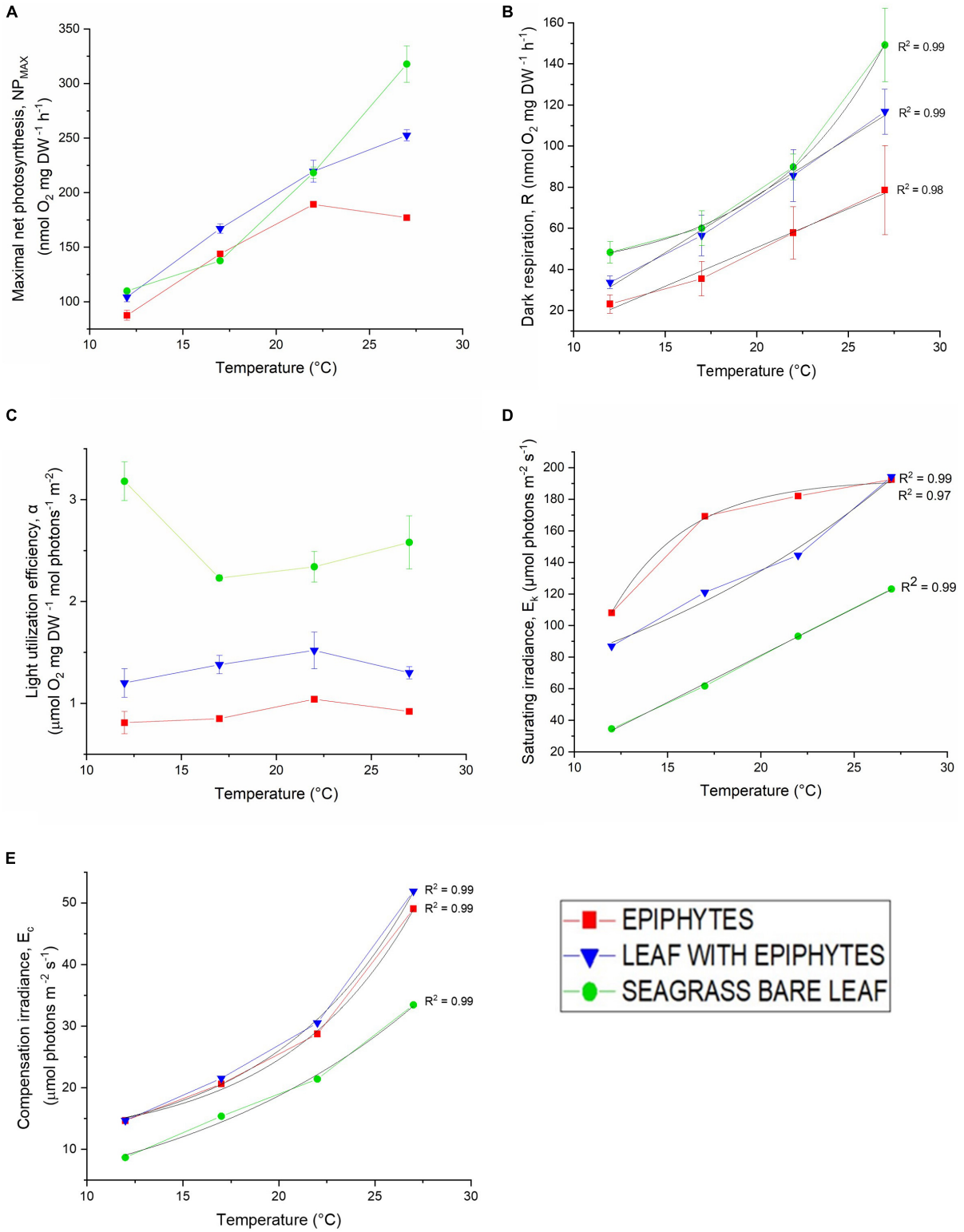

FIGURE 2 | (A) Maximum photosynthesis rate (*Pmax*), **(B)** dark respiration (*R*), **(C)** light use efficiency (α), **(D)** photon scalar irradiance at the onset of photosynthesis saturation (E_k), and **(E)** compensation photon scalar irradiance (E_c) as a function of increasing temperature (12, 17, 22, and 27°C). Red symbols and lines represent epiphytes originating from *Z. marina* L. leaves. Blue symbols and lines represent *Z. marina* L. leaves with epiphytes. Green symbols and lines represent bare *Z. marina* L. leaves. Black lines show fitted exponential or linear function for the photosynthetic parameters: R, E_c and E_k; all with $R^2 \geq 0.97$. Symbols with error bars represent mean values ± SEM; $n = 4$, biological replicates.

TABLE 1 | Q_{10} values for photosynthetic parameters: dark respiration, maximum net and gross photosynthesis, and their respective light use efficiencies (α), of *Z. marina* L. leaves with and without epiphytes, and for epiphytes originating from *Z. marina* leaves.

	Net PS	Alpha (α)	Respiration	Gross PS	Alpha (α)
Epiphytes	2.16	1.28	2.46	2.18	1.26
Leaf with epiphytes	2.10	1.27	2.52	2.07	1.16
Bare seagrass leaf	1.99	0.74	1.85	1.87	0.81

*Temperature range: 12–22°C. Values are calculated from averaged photosynthetic parameters derived from the fitted exponential saturation models at increasing temperature (all with $R^2 \geq 0.99$, see **Figure 1**; thus, representing an original biological replication of 4). A value of 2 in the temperature range of 12–22°C means a doubling of photosynthesis and respiration with a temperature increase of 10°C.*

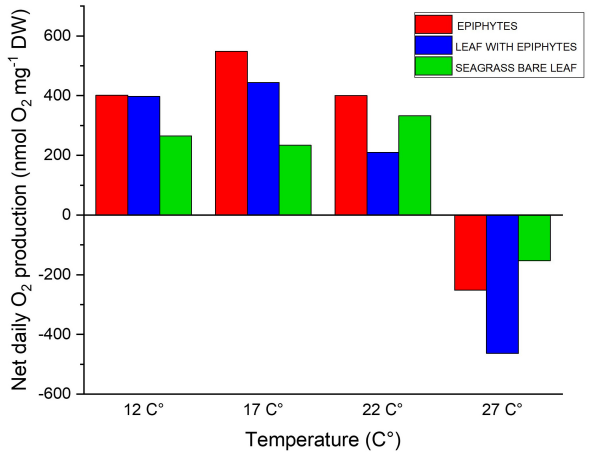

FIGURE 3 | Diel oxygen budget as function of increasing temperatures (12, 17, 22, and 27°C), illustrating the daily net oxygen surplus of the leaf and epiphyte communities. Red bars represent epiphytes originating from *Z. marina* leaves. Blue bars represent *Z. marina* leaves with epiphytes. Green bars represent bare *Z. marina* leaves. The daily net oxygen production was calculated from the fitted exponential saturation models at increasing temperature (see **Figure 1**; all with a $R^2 \geq 0.99$) using an *in situ* measured 14h:10 h light/dark cycle (Staehr et al., 2018). The averaged exponential saturation fits were calculated from a biological replication of 4.

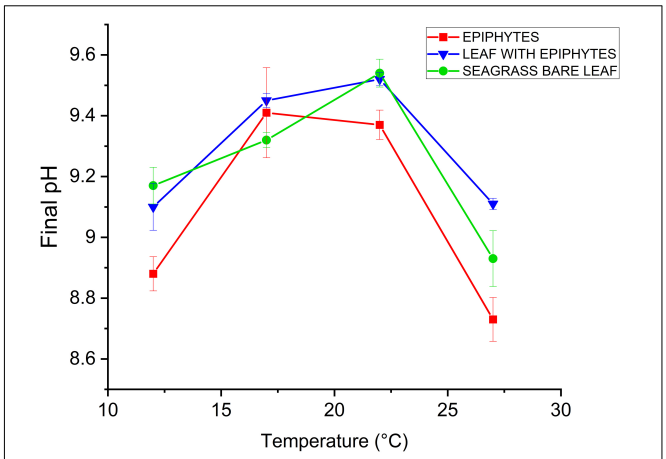

FIGURE 4 | Inorganic carbon extraction capacity as a function of increasing temperature (12, 17, 22, and 27°C). Red symbols and lines represent epiphytes originating from *Z. marina* leaves. Blue symbols and lines represent *Z. marina* leaves with epiphytes. Green symbols and lines represent bare *Z. marina* leaves. Data point with error bars represent means ± SEM ($n = 4$, biological replicates).

Brodersen et al., 2015a,b; Koren et al., 2015; Brodersen et al., 2020a,b; Rasmusson et al., 2020).

Net Daily Oxygen Production

The net daily oxygen production (DP) calculations provided an overview of the net oxygen budget of the bare leaves, leaves with epiphytes and epiphytes separated from the leaves over a diel cycle with 14 h of light exposure followed by 10 h of darkness. The epiphytes had highest oxygen surplus over diel cycles when exposed to 12–22°C, with up to 2.3-fold higher values compared to the seagrass (**Figure 3**). This dominance by the epiphytes, at the lower temperature, suggests a competitive advantage for the epiphytes in cold waters. Thus, the bare leaves displayed an optimum at about 22°C in the diel oxygen budget (**Figure 3**), and exceeded the epiphytes and especially the leaves with epiphytes at 27°C, due the lower temperature impact and higher tolerance (**Table 1**). At 27°C, an oxygen deficit (i.e., negative DP) was observed for all specimens, indicating onset of hypoxic/anoxic stress conditions; with the lowest oxygen deficiency determined for the bare leaves and the highest oxygen deficiency observed on leaves with epiphytes (**Figure 3**). Bare seagrass leaves were apparently less affected by the increasing temperature. This was supported by our calculated Q_{10} values over the temperature range of 12–22°C showing a doubling of respiration, maximum gross, and net photosynthesis rates (**Table 1**). Bare leaves showed a higher Q_{10} value for photosynthesis than respiration, as compared to leaves with epiphytes and separated epiphytes that both displayed higher Q_{10} values for respiration as compared to photosynthesis (**Table 1**). Such negative DP at high seawater temperature can be detrimental to the seagrass plant as H_2S intrusion from the surrounding sediment may occur (Pedersen et al., 2004; Borum et al., 2005; Holmer et al., 2009; Holmer and Hasler-Sheetal, 2014). Considering the ability of *Z. marina* to acclimate to the different seasonal conditions (Staehr and Borum, 2011), seagrass performance is expected to increase, if the experiments described above were conducted with summer acclimated plant tissue. Further investigations of the seasonal epiphytic biofilm composition and performance, especially epiphytes growing on seagrass leaves throughout the summer/autumn season is thus needed (Borum et al., 1984).

Final pH Measurements: Dissolved Inorganic Carbon Extraction Capacity

A maximal final pH of 9.5 was observed for bare *Z. marina* L. leaves under 22°C (**Figure 4**). This result is very similar to recent studies of final pH in other seagrass species, i.e., pH

9.6 in *Thalassia hemprichii* and *Enhalus acoroides* (Pedersen et al., 2016) and pH 9.6 in *Z. marina* L. (Brodersen et al., 2020a). The carbon extraction capacity curves for all specimens (**Figure 4**) indicate that their CO_2 concentration mechanisms (CCMs) are temperature dependent and were mostly affected by the lowest and highest seawater temperatures, corresponding to normal temperature-induced effects on seagrass enzymes like the CO_2-concentrating enzyme carbonic anhydrase (CA) (e.g., Staehr and Borum, 2011). The separated epiphytes exhibited the lowest bicarbonate extraction capacity, both under the lowest temperature (12°C; pH 8.9) and the highest temperatures (22 and 27°C), while they exhibited a maximum final pH of 9.4 at 17°C (**Figure 4**). Leaves with epiphytes and bare leaves reached their maximum final pH of 9.5 at 22°C (**Figure 4**). A steep decline in final pH was found between 22 and 27°C for all samples, where only leaves with epiphytes reached pH > 9 at temperatures of 27°C (**Figure 4**). This indicates that bare *Z. marina* L. leaves and the separated epiphytes apparently lost their ability to utilize bicarbonate in their photosynthesis at 27°C (**Figure 4**; as the specimens exhibited final pH values < 9). This observation emphasizes that the bicarbonate utilization strategies (CCMs, e.g., Larkum et al., 2017) likely are too energy consuming (Borum et al., 2016) when the temperature is markedly exceeding the normal habitual temperature range (here, at 27°C). Other explanations for the apparent lost or reduced (i.e., for leaves with epiphytes) ability to use bicarbonate at 27°C, are that high temperature-induced increased tissue and/or epiphytic biofilm respiration leads to increased CO_2 concentrations in the aerenchyma that can diffuse and thus concentrate CO_2 around RuBisCO. Nevertheless, the inorganic carbon extraction capacity was not only specimen specific (i.e., seagrass vs. associated epiphytes) but also temperature dependent (**Figure 4**). Seagrass and the epiphytes originating from *Z. marina* L. are therefore expected to experience lower photosynthetic efficiency under future elevated seawater temperatures surpassing 27°C.

Furthermore, with the lowest inorganic carbon extraction capacities at all temperatures, except from (17°C), the epiphytes originating from *Z. marina* L. appear to have less efficient CCMs compared to the seagrass leaves. This is inline with previous findings showing that simple filamentous algae often lack effective CCMs (Hepburn et al., 2011). Several members of the epiphytic biofilm community originating from *Z. marina* L. could thus constitute obligate CO_2 users. If this is the case, the epiphytes will be restricted by lack of inorganic carbon sources, as the photosynthetic activity of obligate CO_2 users are limited at low CO_2 concentrations (Albert et al., 2020). Such epiphytes would benefit from ocean acidification. Whether the seagrass did or did not have epiphytic cover, did not show an indicative difference in the inorganic carbon extraction capacity (**Figure 4**). However, one must assume that the presence of epiphytic biofilm and consequently a change in the seagrass phyllosphere will have significance for the seagrass' bicarbonate utilization ability. As demonstrated by Brodersen et al. (2020a), the presence of epiphytic biofilm can lead to a reduced photosynthetic efficiency due to basification of the phyllosphere and increasing DBL thickness; hence, cause inorganic carbon limitation. Furthermore, epiphytes extend the diffusion distance between the leaf and the ambient water, and thus impede gas movement in between, moreover, constitute a competitor for the inorganic carbon sources (Brodersen et al., 2020a). In our study, the observed peak in the final pH at 17°C (**Figure 4**) along with the results from the gas exchange experiments demonstrate that the epiphytes originating from *Z. marina* L. exhibited optimal photosynthetic performance at 17–22°C. Hence, this increased dependency on sufficient CO_2 availability and supply at high seawater temperatures (27°C), may put seagrass leaves and associated epiphytes at enhanced risk of carbon limitation under future climate conditions.

Here, we investigated eelgrass plants and their epiphyte communities sampled at the beginning of the growth season (April) under the spring epiphyte-bloom (Borum et al., 1984). The results are therefore more likely to reflect how plants and epiphytes may be impacted in the early summer months in northern European waters (here Northern Øresund, Denmark), where the maximal water temperature increases about 10°C over a 3-month period (i.e., from ∼10°C in April to ∼23°C in July), and where the plants generally have higher chlorophyll *a* and nitrogen content, as compared to the late summer months and the autumn epiphyte-bloom (Borum et al., 1984; Staehr and Borum, 2011). Our results (e.g., the increase in critical light requirement with increasing temperature) might therefore be slightly overestimated as compared to the situation for summer-acclimated plants and epiphyte communities. Furthermore, rates of respiration are expected to be peaking at slightly lower temperatures in our spring-acclimated seagrass and epiphyte communities (Staehr and Borum, 2011). Temperate seagrass meadows growing in more open waters with frequent circulation/mixing of the water body are also less likely to experience such high temperatures as investigated in this study (i.e., 27°C) and the derived negative daily O_2 production and loss of the ability to utilize bicarbonate as a response to increasing water temperatures. It is also important to note that the potential role of species adaptation and how species originating from latitudinal gradients respond to climate change was not considered in this study (e.g., Short and Neckles, 1999). To further elucidate and predict if one of the specimens (i.e., seagrass leaf or associated epiphytes) will benefit from the changing environmental conditions induced by global climate change, investigations of metabolic responses in different seasonal epiphytic biofilm communities need to be conducted. Furthermore, experimental temperature treatments above 27°C and with longer-term exposure to different temperatures, could provide more detailed information about *Z. marina* L. acclimation/adaptation capabilities. However, water temperatures above 27°C are highly unlikely at the seagrass sampling site (open water in Denmark). Another major challenge as a consequence of global warming are marine heat waves (MHW) (Nguyen et al., 2021). MHWs can exceed the average temperature for more than 5 days in a row and may present a bigger threat to marine organisms than the current progressive temperature increase (Nguyen et al., 2021). Thus, investigations of the resilience of seagrass and associated epiphytes to these frequent extreme thermal events could supply

crucial information about future changes in seagrass-epiphyte interactions and potential effects on plant fitness. Finally, similar measurements should be performed in tropical environments, where seagrasses may be living at water temperatures closer to their thermal stress thresholds, to further elucidate the global impact of ocean warming on the intricate seagrass/epiphyte relationship.

CONCLUSION

Based on our measurements of a low light compensation level (E_c), high light utilization efficiency (α), and high maximum net photosynthesis rates (NP_{MAX} values) at all temperatures for bare leaves we conclude that bare seagrass leaves are less affected by elevated temperatures as compared to seagrass leaves with epiphyte cover and the epiphytes themselves. The high E_k values of leaves with epiphytes and separated epiphytes are likely caused by self-shading. The experiments also confirmed impairment of metabolic rates (i.e., photosynthesis and respiration) when the seagrass leaves had epiphytic cover, revealing that the presence of epiphytic biofilm makes the seagrass more vulnerable to elevated temperatures, e.g., due to thicker DBLs and TDDs, as well as diminished availability of light and inorganic carbon. Epiphytes originating from *Z. marina* L. exhibited the highest temperature dependency, and thus most susceptible to effects of ocean warming. Moreover, epiphytes displayed less efficient CCMs, implying that the epiphytes will benefit from ocean acidification. Seagrass without epiphytes will be less affected by elevated temperatures and marine heat waves. Increasing seawater temperatures in future oceans may thus affect *Z. marina* leaf-epiphytes interactions as the presence of epiphytes can negatively affect *Z. marina* plants responses to temperature increases. Hence, we found a ∼2-fold faster decrease in the net daily O_2 balance over the temperature range of 17–27°C for leaves with epiphytes as compared to bare leaves, increasing the risk of inadequate internal plant aeration. Such shift in seagrass-epiphyte interactions may induce stress responses in the plant triggering, for example, increased production of zosteric acid with antifouling activity that can reduce the initial colonization of leaves with microorganisms (Villa et al., 2010) and thus likely improve the plants O_2 balance.

DATA AVAILABILITY STATEMENT

The original contributions presented in the study are included in the article/**Supplementary Material**, further inquiries can be directed to the corresponding author/s.

AUTHOR CONTRIBUTIONS

KEB designed the research and supervised experimental work. MK provided infrastructure, additional supervision, and input to data analysis. AH and AP conducted the experiments, analyzed the data, and wrote the manuscript with editorial help from MK and KEB. All authors contributed to the article and approved the submitted version.

FUNDING

This study was funded by grants from the Villum Foundation (00028156) to KEB and the Independent Research Fund Denmark (DFF-8021-00308B) to MK.

ACKNOWLEDGMENTS

We thank Mary Gonzalez and Victoria Thuesen for technical assistance. We thank Peter A. Staehr for providing the light data used to calculate the diel O_2 balances.

SUPPLEMENTARY MATERIAL

The Supplementary Material for this article can be found online at: https://www.frontiersin.org/articles/10.3389/fmars.2022.822485/full#supplementary-material

REFERENCES

Albert, G., Hepburn, C. D., Pajusalu, L., Paalme, T., Pritchard, D. W., and Martin, G. (2020). Could ocean acidification influence epiphytism? A comparison of carbon-use strategies between *Fucus vesiculosus* and its epiphytes in the Baltic Sea. *J. Appl. Phycol.* 32, 2479–2487. doi: 10.1007/s10811-019-01953-z

Assis, J., Fragkopoulou, E., Frade, D., Neiva, J., Oliveira, A., Abecasis, D., et al. (2020). A fine-tuned global distribution dataset of marine forests. *Sci. Data* 7:119. doi: 10.1038/s41597-020-0459-x

Ballesteros, E., Cebrian, E., and Alcoverro, T. (2007). Mortality of shoots of *Posidonia oceanica* following meadow invasion by the red alga *Lophocladia lallemandii*. *Bot. Mar.* 50, 8–13. doi: 10.1515/BOT.2007.002

Beca-Carretero, P., Olesen, B., Marbà, N., and Krause-Jensen, D. (2018). Response to experimental warming in northern eelgrass populations: comparison across a range of temperature adaptations. *Mar. Ecol. Prog. Ser.* 589, 59–72. doi: 10.3354/meps12439

Bertelli, C. M., and Unsworth, R. K. (2014). Protecting the hand that feeds us: seagrass (*Zostera marina*) serves as commercial juvenile fish habitat. *Mar. Pollut. Bull.* 83, 425–429. doi: 10.1016/j.marpolbul.2013.08.011

Blaabjerg, V., Mouritsen, K. N., and Finster, K. (1998). Diel cycles of sulphate reduction rates in sediments of a *Zostera marina* bed (Denmark). *Aquat. Microb. Ecol.* 15, 97–102. doi: 10.3354/ame015097

Borum, J. (1985). Development of epiphytic communities on eelgrass (*Zostera marina*) along a nutrient gradient in a Danish estuary. *Mar. Biol.* 87, 211–218. doi: 10.1007/BF00539431

Borum, J., Kaas, H., and Wium-Andersen, S. (1984). Biomass variation and autotrophic production of an epiphyte-macrophyte community in a coastal Danish area: II. Epiphyte species composition, biomass and production. *Ophelia* 23, 165–179. doi: 10.1080/00785326.1984.10426612

Borum, J., Pedersen, O., Greve, T. M., Frankovich, T. A., Zieman, J. C., Fourqurean, J. W., et al. (2005). The potential role of plant oxygen and sulphide dynamics in die-off events of the tropical seagrass, *Thalassia testudinum*. *J. Ecol.* 93, 148–158. doi: 10.1111/j.1365-2745.2004.00943.x

Borum, J., Pedersen, O., Kotula, L., Fraser, M. W., Statton, J., Colmer, T. D., et al. (2016). Photosynthetic response to globally increasing CO2 of co-occurring temperate seagrass species. *Plant Cell Environ.* 39, 1240–1250. doi: 10.1111/pce.12658

Borum, J., Sand-Jensen, K., Binzer, T., Pedersen, O., and Greve, T. (2006). "Oxygen movement in seagrasses," in *Seagrasses: Biology, Ecology and Conservation*, eds A. W. D. Larkum, J. R. Orth, and C. M. Duarte (Dordrecht: Springer), 255–270. doi: 10.1007/1-4020-2983-7_10

Brodersen, K. E. (2016). *The Seagrass Rhizosphere.* Ph.D. thesis. Sydney, NSW: University of Technology Sydney.

Brodersen, K. E., and Kühl, M. (2022). Effects of epiphytes on the seagrass phyllosphere. *Front. Mar. Sci.* 9:821614. doi: 10.3389/fmars.2022.821614

Brodersen, K. E., Hammer, K. J., Schrameyer, V., Floytrup, A., Rasheed, M. A., Ralph, P. J., et al. (2017). Sediment resuspension and deposition on seagrass leaves impedes internal plant aeration and promotes phytotoxic H2S intrusion. *Front. Plant Sci.* 8:657. doi: 10.3389/fpls.2017.00657

Brodersen, K. E., Koren, K., Revsbech, N. P., and Kühl, M. (2020a). Strong leaf surface basification and CO2 limitation of seagrass induced by epiphytic biofilm microenvironments. *Plant Cell Environ.* 43, 174–187. doi: 10.1111/pce.13645

Brodersen, K. E., Kühl, M., Nielsen, D. A., Pedersen, O., and Larkum, A. W. (2018). "Rhizome, root/sediment interactions, aerenchyma and internal pressure changes in seagrasses," in *Seagrasses of Australia*, eds A. Larkum, G. Kendrick, and P. Ralph (Cham: Springer), 393–418. doi: 10.1007/978-3-319-71354-0_13

Brodersen, K. E., Kühl, M., Trampe, E., and Koren, K. (2020b). Imaging O2 dynamics and microenvironments in the seagrass leaf phyllosphere with magnetic optical sensor nanoparticles. *Plant J.* 104, 1504–1519. doi: 10.1111/tpj.15017

Brodersen, K. E., Lichtenberg, M., Paz, L.-C., and Kühl, M. (2015a). Epiphyte-cover on seagrass (*Zostera marina* L.) leaves impedes plant performance and radial O2 loss from the below-ground tissue. *Front. Mar. Sci.* 2:58. doi: 10.3389/fmars.2015.00058

Brodersen, K. E., Nielsen, D. A., Ralph, P. J., and Kühl, M. (2014). A split flow chamber with artificial sediment to examine the below-ground microenvironment of aquatic macrophytes. *Mar. Biol.* 161, 2921–2930. doi: 10.1007/s00227-014-2542-3

Brodersen, K. E., Nielsen, D. A., Ralph, P. J., and Kühl, M. (2015b). Oxic microshield and local pH enhancement protects *Zostera muelleri* from sediment derived hydrogen sulphide. *New Phytol.* 205, 1264–1276. doi: 10.1111/nph.13124

Costanza, R., d'Arge, R., de Groot, R., Farber, S., Grasso, M., Hannon, B., et al. (1997). The value of the world's ecosystem services and natural capital. *Nature* 387, 253–260. doi: 10.1038/387253a0

Cullen-Unsworth, L. C., and Unsworth, R. (2018). A call for seagrass protection. *Science* 361, 446–448. doi: 10.1126/science.aat7318

Dennison, W. C. (1987). Effects of light on seagrass photosynthesis, growth and depth distribution. *Aquat. Bot.* 27, 15–26. doi: 10.1016/0304-3770(87)90083-0

Evans, A. S., Webb, K. L., and Penhale, P. A. (1986). Photosynthetic temperature acclimation in two coexisting seagrasses, *Zostera marina* L. and *Ruppia maritima* L. *Aquat. Bot.* 24, 185–197. doi: 10.1016/0304-3770(86)90095-1

Fonseca, M. S., and Cahalan, J. A. (1992). A preliminary evaluation of wave attenuation by four species of seagrass. *Estuar. Coast. Shelf Sci.* 35, 565–576. doi: 10.1016/S0272-7714(05)80039-3

Fourqurean, J. W., Duarte, C. M., Kennedy, H., Marba, N., Holmer, M., Mateo, M. A., et al. (2012). Seagrass ecosystems as a globally significant carbon stock. *Nat. Geosci.* 5, 505–509. doi: 10.1038/ngeo1477

Gattuso, J.-P., and Hansson, L. (2011). *Ocean Acidification*. Oxford: Oxford University press. doi: 10.1093/oso/9780199591091.001.0001

Greve, T. M., Borum, J., and Pedersen, O. (2003). Meristematic oxygen variability in eelgrass (*Zostera marina*). *Limnol. Oceanogr.* 48, 210–216. doi: 10.4319/lo.2003.48.1.0210

Hepburn, C., Pritchard, D., Cornwall, C., McLeod, R., Beardall, J., Raven, J., et al. (2011). Diversity of carbon use strategies in a kelp forest community: implications for a high CO2 Ocean. *Glob. Chang. Biol.* 17, 2488–2497. doi: 10.1111/j.1365-2486.2011.02411.x

Holmer, M., and Hasler-Sheetal, H. (2014). Sulfide intrusion in seagrasses assessed by stable sulfur isotopes—a synthesis of current results. *Front. Mar. Sci.* 1:64. doi: 10.3389/fmars.2014.00064

Holmer, M., Pedersen, O., Krause-Jensen, D., Olesen, B., Hedegård Petersen, M., Schopmeyer, S., et al. (2009). Sulfide intrusion in the tropical seagrasses *Thalassia testudinum* and *Syringodium filiforme*. *Estuar. Coast. Shelf Sci.* 85, 319–326. doi: 10.1016/j.ecss.2009.08.015

Kim, M., Brodersen, K. E., Szabó, M., Larkum, A. W., Raven, J. A., Ralph, P. J., et al. (2018). Low oxygen affects photophysiology and the level of expression of two-carbon metabolism genes in the seagrass *Zostera muelleri*. *Photosynth. Res.* 136, 147–160. doi: 10.1007/s11120-017-0452-1

Koren, K., Brodersen, K. E., Jakobsen, S. L., and Kühl, M. (2015). Optical sensor nanoparticles in artificial sediments – a new tool to visualize O2 dynamics around the rhizome and roots of seagrasses. *Environ. Sci. Technol.* 49, 2286–2292. doi: 10.1021/es505734b

Lamb, J. B., van de Water, J. A. J. M., Bourne, D. G., Altier, C., Hein, M. Y., Fiorenza, E. A., et al. (2017). Seagrass ecosystems reduce exposure to bacterial pathogens of humans, fishes, and invertebrates. *Science* 355, 731–733. doi: 10.1126/science.aal1956

Larkum, A. W. D., Davey, P. A., Kuo, J., Ralph, P. J., and Raven, J. A. (2017). Carbon-concentrating mechanisms in seagrasses. *J. Exp. Bot.* 68, 3773–3784. doi: 10.1093/jxb/erx206

Larkum, A. W. D., Orth, R. J., and Duarte, C. M. (2006). *Seagrasses: Biology, ecology and conservation*. Dordrecht: Springer. doi: 10.1007/978-1-4020-2983-7

Larkum, A. W., Pernice, M., Schliep, M., Davey, P., Szabo, M., Raven, J. A., et al. (2018). "Photosynthesis and metabolism of seagrasses," in *Seagrasses of Australia*, eds A. W. D. Larkum, G. A. Kendrick, and P. J. Ralph (Cham: Springer), 315–342. doi: 10.1007/978-3-319-71354-0_11

Levitus, S., Antonov, J. I., Boyer, T. P., and Stephens, C. (2000). Warming of the world ocean. *Science* 287, 2225–2229. doi: 10.1126/science.287.5461.2225

Macreadie, P. I., Trevathan-Tackett, S. M., Skilbeck, C. G., Sanderman, J., Curlevski, N., Jacobsen, G., et al. (2015). Losses and recovery of organic carbon from a seagrass ecosystem following disturbance. *Proc. R. Soc. B Biol. Sci.* 282:20151537. doi: 10.1098/rspb.2015.1537

Marsh, J. A. Jr., Dennison, W. C., and Alberte, R. S. (1986). Effects of temperature on photosynthesis and respiration in eelgrass (*Zostera marina* L.). *J. Exp. Mar. Biol. Ecol.* 101, 257–267. doi: 10.1016/0022-0981(86)90267-4

Mazzella, L., and Alberte, R. S. (1986). Light adaptation and the role of autotrophic epiphytes in primary production of the temperate seagrass, *Zostera marina* L. *J. Exp. Mar. Biol. Ecol.* 100, 165–180. doi: 10.1016/0022-0981(86)90161-9

Nguyen, H. M., Ralph, P. J., Marín-Guirao, L., Pernice, M., and Procaccini, G. (2021). Seagrasses in an era of ocean warming: a review – under review in biological reviews. *Biol. Rev.* 96, 2009–2030. doi: 10.1111/brv.12736

Nielsen, L. B., Finster, K., Welsh, D. T., Donelly, A., Herbert, R. A., De Wit, R., et al. (2001). Sulphate reduction and nitrogen fixation rates associated with roots, rhizomes and sediments from *Zostera noltii* and *Spartina maritima* meadows. *Environ. Microbiol.* 3, 63–71. doi: 10.1046/j.1462-2920.2001.00160.x

Noisette, F., Depetris, A., Kühl, M., and Brodersen, K. E. (2020). Flow and epiphyte growth effects on the thermal, optical and chemical microenvironment in the leaf phyllosphere of seagrass (*Zostera marina*). *J. R. Soc. Interface* 17:20200485. doi: 10.1098/rsif.2020.0485

Orth, R. J., Carruthers, T. J. B., Dennison, W. C., Duarte, C. M., Fourqurean, J. W., Heck, K. L. Jr., et al. (2006). A global crisis for seagrass ecosystems. *BioScience* 56, 987–999. doi: 10.1641/0006-3568(2006)56[987:AGCFSE]2.0.CO;2

Pedersen, O., Binzer, T., and Borum, J. (2004). Sulphide intrusion in eelgrass (*Zostera marina* L.). *Plant Cell Environ.* 27, 595–602. doi: 10.1111/j.1365-3040.2004.01173.x

Pedersen, O., Colmer, T. D., Borum, J., Zavala-Perez, A., and Kendrick, G. A. (2016). Heat stress of two tropical seagrass species during low tides–impact on underwater net photosynthesis, dark respiration and diel in situ internal aeration. *New Phytol.* 210, 1207–1218. doi: 10.1111/nph.13900

Penhale, P. A. (1977). Macrophyte-epiphyte biomass and productivity in an eelgrass (*Zostera marina* L.) community. *J. Exp. Mar. Biol. Ecol.* 26, 211–224. doi: 10.1016/0022-0981(77)90109-5

Pulido Pérez, C., and Borum, J. (2010). Eelgrass (*Zostera marina*) tolerance to anoxia. *J. Exp. Mar. Biol. Ecol.* 385, 8–13. doi: 10.1016/j.jembe.2010.01.014

Ralph, P. J., Durako, M. J., Enríquez, S., Collier, C. J., and Doblin, M. A. (2007). Impact of light limitation on seagrasses. *J. Exp. Mar. Biol. Ecol.* 350, 176–193. doi: 10.1016/j.jembe.2007.06.017

Rasmusson, L. M., Buapet, P., George, R., Gullström, M., Gunnarsson, P. C., and Björk, M. (2020). Effects of temperature and hypoxia on respiration,

photorespiration, and photosynthesis of seagrass leaves from contrasting temperature regimes. *ICES J. Mar. Sci.* 77, 2056–2065. doi: 10.1093/icesjms/fsaa093

Raun, A. L., and Borum, J. (2013). Combined impact of water column oxygen and temperature on internal oxygen status and growth of *Zostera marina* seedlings and adult shoots. *J. Exp. Mar. Biol. Ecol.* 441, 16–22. doi: 10.1016/j.jembe.2013.01.014

Raven, J. A., Beardall, J., and Giordano, M. (2014). Energy costs of carbon dioxide concentrating mechanisms in aquatic organisms. *Photosynth. Res.* 121, 111–124. doi: 10.1007/s11120-013-9962-7

Resplandy, L., Keeling, R. F., Eddebbar, Y., Brooks, M., Wang, R., Bopp, L., et al. (2019). Quantification of ocean heat uptake from changes in atmospheric O2 and CO2 composition. *Sci. Rep.* 9:20244. doi: 10.1038/s41598-019-56490-z

Riebesell, U., Aberle-Malzahn, N., Achterberg, E. P., Algueró-Muñiz, M., Alvarez-Fernandez, S., Arístegui, J., et al. (2018). Toxic algal bloom induced by ocean acidification disrupts the pelagic food web. *Nat. Clim. Change* 8, 1082–1086. doi: 10.1038/s41558-018-0344-1

Sand-Jensen, K. (1977). Effect of epiphytes on eelgrass photosynthesis. *Aquat. Bot.* 3(Suppl. C), 55–63. doi: 10.1016/0304-3770(77)90004-3

Sand-Jensen, K., Pedersen, M. F., and Nielsen, S. L. (1992). Photosynthetic use of inorganic carbon among primary and secondary water plants in streams. *Freshw. Biol.* 27, 283–293. doi: 10.1111/j.1365-2427.1992.tb00540.x

Short, F. T., and Neckles, H. A. (1999). The effects of global climate change on seagrasses. *Aquat. Bot.* 63, 169–196. doi: 10.1016/S0304-3770(98)00117-X

Spilling, K., Titelman, J., Greve, T. M., and Kühl, M. (2010). Microsensor measurements of the external and internal microenvironment of *Fucus vesiculosus* (phaeophyceae). *J. Phycol.* 46, 1350–1355. doi: 10.1111/j.1529-8817.2010.00894.x

Staehr, P. A., and Borum, J. (2011). Seasonal acclimation in metabolism reduces light requirements of eelgrass (*Zostera marina*). *J. Exp. Mar. Biol. Ecol.* 407, 139–146. doi: 10.1016/j.jembe.2011.05.031

Staehr, P. A., Asmala, E., Carstensen, J., Krause-Jensen, D., and Reader, H. (2018). Ecosystem metabolism of benthic and pelagic zones of a shallow productive estuary: spatio-temporal variability. *Mar. Ecol. Prog. Ser.* 601, 15–32. doi: 10.3354/meps12697

Tarquinio, F., Bourgoure, J., Koenders, A., Laverock, B., Säwström, C., and Hyndes, G. A. (2018). Microorganisms facilitate uptake of dissolved organic nitrogen by seagrass leaves. *ISME J.* 12, 2796–2800. doi: 10.1038/s41396-018-0218-6

Unsworth, R. K. F., and Cullen-Unsworth, L. C. (2014). "Biodiversity, ecosystem services, and the conservation of seagrass meadows," in *Coastal Conservation*, eds B. Maslo and J. Lockwood (Cambridge: Cambridge University Press), 95–130. doi: 10.1017/CBO9781139137089.005

Unsworth, R. K. F., and Cullen-Unsworth, L. C. (2017). Seagrass meadows. *Curr. Biol.* 27, R443–R445. doi: 10.1016/j.cub.2017.01.021

Unsworth, R. K. F., Nordlund, L. M., and Cullen-Unsworth, L. C. (2019). Seagrass meadows support global fisheries production. *Conserv. Lett.* 12, 1–8. doi: 10.1111/conl.12566

Villa, F., Albanese, D., Giussani, B., Stewart, P. S., Daffonchio, D., and Cappitelli, F. (2010). Hindering biofilm formation with zosteric acid. *Biofouling* 26, 739–752. doi: 10.1080/08927014.2010.511197

Waycott, M., Duarte, C. M., Carruthers, T. J. B., Orth, R. J., Dennison, W. C., Olyarnik, S., et al. (2009). Accelerating loss of seagrasses across the globe threatens coastal ecosystems. *Proc. Natl. Acad. Sci. U.S.A.* 106, 12377–12381. doi: 10.1073/pnas.0905620106

Webb, W. L., Newton, M., and Starr, D. (1974). Carbon dioxide exchange of *Alnus rubra*. *Oecologia* 17, 281–291. doi: 10.1007/BF00345747

Wieland, A., and Kühl, M. (2000). Irradiance and temperature regulation of oxygenic photosynthesis and O2 consumption in a hypersaline cyanobacterial mat (Solar Lake, Egypt). *Mar. Biol.* 137, 71–85. doi: 10.1007/s002270000331

Conflict of Interest: The authors declare that the research was conducted in the absence of any commercial or financial relationships that could be construed as a potential conflict of interest.

Publisher's Note: All claims expressed in this article are solely those of the authors and do not necessarily represent those of their affiliated organizations, or those of the publisher, the editors and the reviewers. Any product that may be evaluated in this article, or claim that may be made by its manufacturer, is not guaranteed or endorsed by the publisher.

frontiers in Marine Science

ORIGINAL RESEARCH
published: 28 March 2022
doi: 10.3389/fmars.2022.861998

The Importance of Dead Seagrass (*Posidonia oceanica*) Matte as a Biogeochemical Sink

Eugenia T. Apostolaki[1], Laura Caviglia[2], Veronica Santinelli[2], Andrew B. Cundy[3], Cecilia D. Tramati[2,4], Antonio Mazzola[2,4] and Salvatrice Vizzini[2,4]*

[1] Institute of Oceanography, Hellenic Centre for Marine Research, Heraklion, Greece, [2] Department of Earth and Marine Sciences, University of Palermo, Palermo, Italy, [3] School of Ocean and Earth Science, National Oceanography Centre (Southampton), University of Southampton, Southampton, United Kingdom, [4] Consorzio Nazionale Interuniversitario per le Scienze del Mare, Rome, Italy

OPEN ACCESS

Edited by:
Stacey Marie Trevathan-Tackett, Deakin University, Australia

Reviewed by:
Mohammad Rozaimi, Universiti Kebangsaan Malaysia, Malaysia
Nerea Piñeiro Juncal, University of Santiago de Compostela, Spain
Anna Lafratta, Edith Cowan University, Australia

***Correspondence:**
Eugenia T. Apostolaki
eapost@hcmr.gr

Specialty section:
This article was submitted to Marine Biogeochemistry, a section of the journal Frontiers in Marine Science

Received: *25 January 2022*
Accepted: *07 March 2022*
Published: *28 March 2022*

Citation:
Apostolaki ET, Caviglia L, Santinelli V, Cundy AB, Tramati CD, Mazzola A and Vizzini S (2022) The Importance of Dead Seagrass (Posidonia oceanica) Matte as a Biogeochemical Sink. Front. Mar. Sci. 9:861998. doi: 10.3389/fmars.2022.861998

We assessed the potential of dead seagrass *Posidonia oceanica* matte to act as a biogeochemical sink and provide a coherent archive of environmental change in a degraded area of the Mediterranean Sea (Augusta Bay, Italy). Change in sediment properties (dry bulk density, grain size), concentration of elements (C_{org}, C_{inorg}, N, Hg) and stable isotope ratios ($\delta^{13}C$, $\delta\ ^{15}N$) with sediment depth were measured in dead *P. oceanica* matte and unvegetated (bare) sediments in the polluted area, and an adjacent *P. oceanica* meadow. Principal Component Analysis (PCA) revealed a clear clustering by habitat, which explained 72% of variability in our samples and was driven mainly by the accumulation of N and Hg in finer sediments of the dead matte. Assessment of the temporal trends of C_{org}, N and Hg concentrations in the dead matte revealed changes in the accumulation of these elements over the last 120 years, with an increase following the onset of industrial activities 65 y BP (i.e., yr. 1950) that was sustained even after seagrass loss around 35 y BP. Despite a decrease in Hg concentrations in the early 1980s following the onset of pollution abatement, overall Hg levels were 2-fold higher in the local post-industrial period, with a Hg enrichment factor of 3.5 in the dead matte. Mean stocks of C_{org}, N and Hg in 25 cm thick sediment deposits (4.08 ± 2.10 kg C_{org} m^{-2}, 0.14 ± 0.04 kg N m^{-2}, 0.19 ± 0.04 g Hg m^{-2}) and accumulation in the last 120 yr (35.3 ± 19.6 g C_{org} m^{-2} y^{-1}, 1.2 ± 0.4 g N m^{-2} y^{-1}, 0.0017 ± 0.0004 g Hg m^{-2} y^{-1}) were higher in the dead matte than bare sediment or adjacent *P. oceanica* meadow. Our results indicate that dead *P. oceanica* matte maintained its potential as a biogeochemical sink and, like its living counterpart, dead matte can serve as an effective archive to allow for reconstructing environmental change in coastal areas of the Mediterranean where severe perturbations have led to *P. oceanica* loss. Appropriate management for contaminated areas should be prioritized to prevent release of pollutants and carbon from dead mattes.

Keywords: blue carbon, nutrient filters, contamination, seagrass degradation, anthropogenic impact, seagrass archives

INTRODUCTION

There is an increasing appreciation of the role of seagrass ecosystems as nature-based climate solutions due to their effective carbon sequestration (Macreadie et al., 2021). As blue carbon (BC) sinks, seagrass meadows sequester organic carbon through metabolism (Duarte et al., 2010) and trapping of allochthonous particles (Gacia and Duarte, 2001), which results in the formation of biogenic reefs comprised of senescent plant tissue and sediment. These reefs show increased carbon preservation as their sub-surface anoxic conditions favor slow decomposition and effectively retain buried carbon (Duarte et al., 2013). This is particularly impressive in the case of the Mediterranean endemic seagrass species, *Posidonia oceanica* (L.) Delile, which can form extensive deposits called 'matte' (Boudouresque et al., 2015) that can be up to 6.5 m thick (Lo Iacono et al., 2008) and 9,000 yr. old (Monnier et al., 2021). *P. oceanica* is a slow-growing, perennial, long-lived seagrass that owes the capacity to form these mattes to the vertical growth of its rhizomes that raise the matte over time, while the highly recalcitrance nature of its modules (Kaal et al., 2018) favors slow decay rates (Mateo et al., 1997). It has been well documented that these mattes act as significant sinks for carbon, storing up to 88 kg C_{org} m^{-2} in their top meter of sediment (Serrano et al., 2016b; Mazarrasa et al., 2017b; Apostolaki et al., 2019; Monnier et al., 2021), which places *P. oceanica* meadows among the top blue carbon sinks compared to other seagrass species around the world (Lavery et al., 2013; Thorhaug et al., 2017; Röhr et al., 2018; Serrano et al., 2018; Sousa et al., 2019).

Less studied, yet seemingly equally important, is the capacity of *P. oceanica* mattes to sequester and retain nutrients and contaminants, and the consequent role of seagrass meadows in the mitigation of coastal eutrophication and contamination in the Mediterranean Sea. Anthropogenic activities around Mediterranean coasts and industrialization have increased the levels of nutrients, such as nitrogen (N), in the water column and studies, albeit very limited so far, have documented that part of the N incorporated in *P. oceanica* tissues is stored in their underlying sediments (Mateo et al., 1997; Apostolaki et al., 2019), supplemented also by the high capacity of these meadows to trap suspended N-bearing particles from the bottom water above the canopy (Gacia et al., 2002). Similarly, *P. oceanica* shoots tend to accumulate trace elements in their tissues (Bonanno and Orlando-Bonaca, 2017), while the meadows enhance the deposition of fine organic-rich particles that have strong binding affinity with trace elements and, thereby, immobilizing a large quantity of pollutants in their substrates (Serrano et al., 2011). As such, the *P. oceanica* matte represents an important archive of anthropogenic disturbances that has helped to reconstruct environmental change and identify thresholds of ecosystem processes following perturbations (Serrano et al., 2011; Serrano et al., 2013; Leiva-Dueñas et al., 2021).

Intensification of anthropogenic activities around the coasts of the Mediterranean has resulted in an accelerating degradation of *P. oceanica* ecosystems (de los Santos et al., 2019), with important implications for the role of this species in the biogeochemical cycles of the Mediterranean Sea. The loss of *P. oceanica* foliar canopy results in the exposure of matte, which is then comprised only of the underlying rhizomes and roots, and sediment particles and is often called 'dead matte'. Being indicative of seagrass degradation, dead *P. oceanica* mattes have been traditionally considered a habitat of poor ecological quality, failing to attract considerable research attention or management. However, there has been early evidence of the importance of these ecosystems (Borg et al., 2006) and their very recent use as a substrate for successful transplantation and regeneration of *P. oceanica* meadows (Calvo et al., 2021) could revalorize dead mattes in the current consensus for ocean restoration. In fact, dead mattes may persist for several years or even decades (Boudouresque et al., 2015). This feature could allow the assessment of historical fluctuations in areas with unknown local history, where severe pressure has resulted in complete disappearance of the meadows. This would advocate an implementation of relative conservation actions, but at present we lack a generalized understanding of the fate of stocks in dead mattes that is necessary to build a comprehensive framework to support environmental management of these degraded matte areas.

Currently it is unclear whether dead mattes maintain their chrono-stratigraphy coherently and their biogeochemical sinks intact, and there is still a significant knowledge deficit in the fate of carbon and nutrient following cover loss. Apparently, in the absence of leaves there would be no seagrass metabolic capture, as seagrass productivity is a key factor regulating the magnitude of carbon storage (Mazarrasa et al., 2018), while a potential decrease in trapping of allochthonous matter is also expected to occur. Seagrass loss may pose a risk of erosion and subsequent remineralisation of historic stores of organic matter which have been built-up in seagrass sediments over centuries, or even millennia in the case of *P. oceanica*, as the upper, previously anoxic layers of sediment can become exposed to oxic conditions (Pendleton et al., 2015; Lovelock et al., 2017). However, the vulnerability to decomposition depends on the microbial activity and recalcitrance of the residual organic matter (Spivak et al., 2019), which in turn varies among seagrass species. *P. oceanica* cover loss does not necessarily lead to erosion, but it can result in increase in mineralization of organic matter at least in the rhizosphere (Piñeiro-Juncal et al., 2021) and it is the balance between the decomposition and preservation and the environmental conditions that would ultimately determine the magnitude of elemental loss.

Here, we study the potential of dead seagrass *P. oceanica* matte to act as a biogeochemical sink. We do so by reconstructing the historical trends in concentration and accumulation of carbon, nitrogen and mercury in sediments beneath dead *P. oceanica* matte and unvegetated (bare) sediments in a highly contaminated coastal marine area in the Mediterranean Sea (Augusta Bay, Italy), and in sediments beneath an adjacent *P. oceanica* meadow. More widely, we address the capacity of dead mattes to provide a coherent archive of environmental change in degraded areas along the Mediterranean coastlines.

MATERIALS AND METHODS

Study Site

The study was performed in Augusta Bay, a semi-enclosed basin located in eastern Sicily (Italy), delimited to the north by Santa Croce Cape and to the south by Santa Panagia Cape (**Figure 1**). The north-eastern side of the bay is occupied by Augusta Harbour, where major commercial and industrial activities commenced after World War II. The area hosts the largest European petrochemical complex and the most important chloro-alkali plant in Italy, which was active from 1954 to 2005, and until the early 1980s had been discharging waste waters into the sea across the *Vallone della Neve River* without treatment. Consequently, high accumulations of mercury (Hg) have been reported in the marine environment of Augusta Bay (Bellucci et al., 2012), with major Hg discharges continuing until the construction of a demercurization and waste treatment plant in 1983, in accordance with the national law (G.U.R.I, L.319/1976). Two breakwaters built in the 1960s have delimited Augusta Harbour from the open sea, and the presence of two narrow inlets (Levante, which is 400 m wide and 40 m deep, and Scirocco, which is 300 m wide and 13 m deep) together with a general cyclonic water circulation (ICRAM, 2008) (**Figure 1**) prevented higher water exchange and facilitated further accumulation of contaminants (Sprovieri et al., 2011).

Through the Scirocco Inlet, Augusta Harbour connects with the coastal area of Priolo Bay, defined by the European Commission Habitat Service (94/43/EEC) as a Site of Community Importance (SCI). The outflows of bottom water export contaminants from the Harbour to Priolo Bay through this inlet (Di Leonardo et al., 2014; Signa et al., 2017). Consequently, high contents of Hg (1.3 ± 0.2 mg kg^{-1}), Cd (0.2 ± 0.0 mg kg^{-1}), Ni (46.2 ± 7.2 mg kg^{-1}) and PAHs ($\Sigma PAHs_{18}$ 164.4 ng g^{-1}), exceeding sediment quality guidelines, have been detected in the surface sediments of Priolo Bay (Di Leonardo et al., 2014). Priolo Bay shows complex current dynamics with a general water flow moving from NE to SW and a local current parallel to the coast (Di Leonardo et al., 2014). The large input of contaminants during the last century caused gradual regression of the *Posidonia oceanica* seagrass meadow extending in the area until its complete loss in the late 1970s (Costantini, 2015; Di Leonardo et al., 2017). Currently, the seabed is characterized by sand and dead seagrass matte (Di Leonardo et al., 2014).

The north-western sector of Augusta Bay is covered by extensive and abundant *P. oceanica* meadows in Xifonio Gulf, around 3 - 7 km away from August Harbour and the

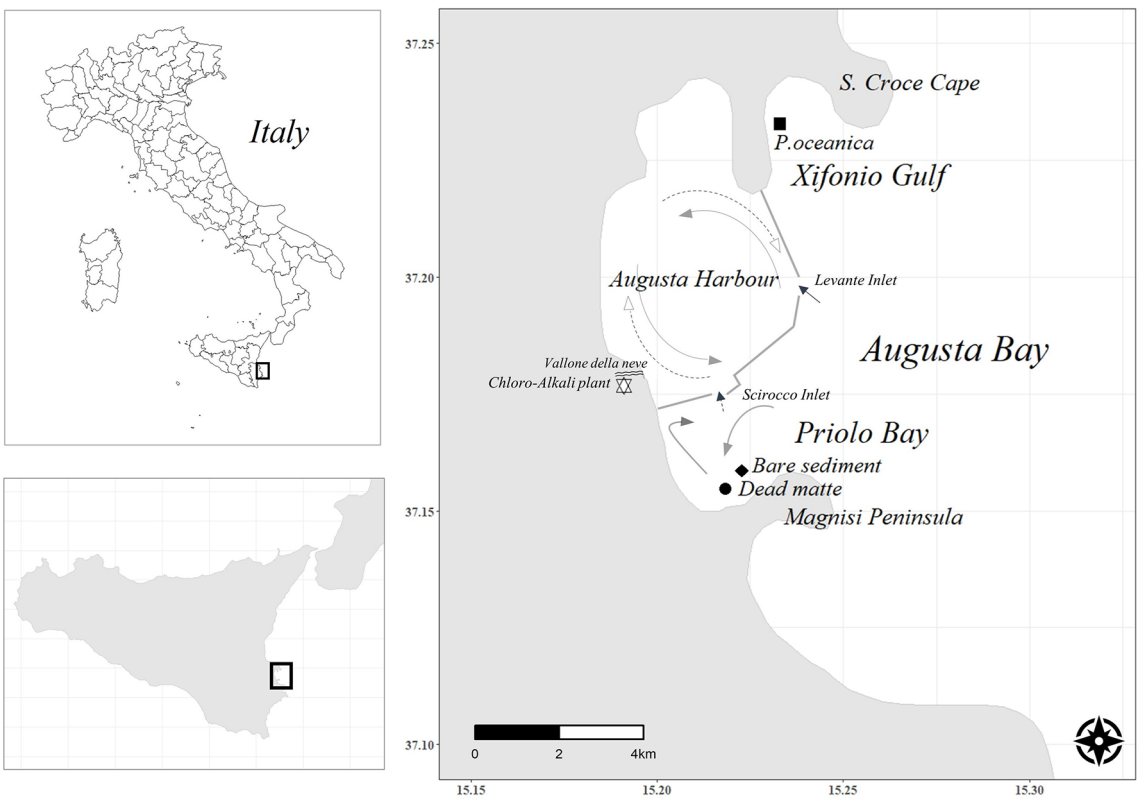

FIGURE 1 | Map of Augusta Bay (Ionian Sea, southern Italy, eastern Sicily). Arrows indicate the main currents (modified from ICRAM, 2008 and Di Leonardo et al., 2014). The grey segments indicate the breakwaters built in the 1960s that delimit connection of Augusta Harbour from the open sea through the Scirocco and Levante inlets. The chloro-alkali plant (indicated with a star) and the mouth of the river Vallone della Neve are also shown. The sampling stations (dead matte and bare sediment at Priolo Bay, and Posidonia oceanica at Xifonio Gulf) are reported.

petrochemical industries. The meadow expands at 13 m depth, with shoot density of 363 ± 20 shoots m^{-2} and leaf area index of 6.6 m^2 leaves m^{-2} (Costantini, 2015). Hg concentration in *P. oceanica* leaves is 0.09 ± 0.02 mg kg^{-1} (S. Vizzini, unpubl. data), close to the Hg mean reported from areas with minimal contamination (0.04 ± 0.00 mg kg^{-1}, (Lafabrie et al., 2008).

Sampling and Analytical Methods

Three stations were selected, each one characterised by a different habitat but at similar water depth (*ca.* 12 m). Two stations were located at Priolo Bay: one characterized by the presence of dead *P. oceanica* matte, hereafter called 'dead matte', and the other characterized by unvegetated sediments, hereafter called 'bare sediment' (**Figure 1**). Another station was sampled at Xifonio Gulf, within the *P. oceanica* meadow, hereafter called '*P. oceanica* meadow'. Sediment cores were collected at each station in July 2015 by scuba-divers in duplicate (around 10 m apart from each other) to allow the assessment of spatial and temporal variability, using a hand-corer consisted of a 60 cm long and 7.4 cm wide PVC pipe. Compression was estimated by measuring the outer, inner, and total length of the core. Prior to any calculation, the thickness of each sediment slice was corrected by applying a compression correction factor. The compression factor was on average 0.76 for dead matte cores, 0.86 for bare sediment cores and 0.65 for *P. oceanica* cores. Sediment samples were immediately frozen at -20°C.

The cores were sliced into 1 cm sections for the first 10 cm and every 2 cm for the remaining sediment. Subsamples of each slice from the first ten cm of sediment were homogenized to correspond to a slice thickness of 0 – 10 cm of sediment, which was used for granulometry analysis. Wet samples were previously left in a H_2O_2 solution (3 - 10%) to eliminate organic matter. Subsequently, sediment fractions (gravel > 2 mm, sand 2 mm - 63 μm, silt/clay < 63 μm) were oven-dried at 60°C, separated by dry sieving using a set of sieves up to 63 μm, and weighed.

The remaining sediment of each slice was freeze-dried for 48 hours and powdered for the determination of dry bulk density, elemental concentration and isotopic composition of carbon and nitrogen and mercury concentration per slice. For the determination of concentration of total carbon and nitrogen (C_{tot}, N) and nitrogen isotopic composition ($\delta^{15}N$), sediment aliquots were weighed in tin capsules and analysed using an isotope ratio mass spectrometer (Thermo IRMS Delta Plus XP) coupled with an elemental analyser (Thermo EA-1112). For the determination of organic carbon (C_{org}) a fraction of each sediment sample was acidified in silver capsules prior to the analysis in the EA-IRMS system according to Nieuwenhuize et al. (1994) to eliminate carbonates. For carbon stable isotope ($\delta^{13}C$) determination, each sample was acidified with HCl 2N until bubbling stopped to remove carbonates, centrifuged and the supernatant removed by pipette; sample was then washed with Milli-Q water, centrifuged, oven dried after supernatant removal and weighed in tin capsules. Analytical uncertainty based on replicate measurements of internal standards (Acetanilide for C and N, International Atomic Energy Agency IAEA- CH-6 for $\delta^{13}C$ and IAEA-NO-3 for $\delta^{15}N$) was 0.02%, 0.05%, 0.1‰ and 0.2‰ for C, N, $\delta^{13}C$ and $\delta^{15}N$, respectively. The concentration of inorganic carbon (C_{inorg}) was calculated as the difference between the concentration of C_{tot} and C_{org}.

To quantify aluminium (Al) and mercury (Hg) concentration, dry sediment sub-samples (0.2 g each) were mineralised using an automatic microwave digestion system (MARS 5, CEM) with a solution of 67–70% HNO_3, 30% HF, 30% H_2O_2 and Milli-Q water at a ratio of 6:2:0.4:1.6 according to the USEPA (1996) method. Hg concentration was determined using a hydride generation system linked to ICP-OES with a reductant solution, consisting of 0.2% sodium (Na) borohydride and 0.05% Na hydroxide. Samples were analysed by inductively coupled plasma optical emission spectrometry (ICP-OES, Optima 8000, PerkinElmer). Analytical quality control was performed using Marine sediment NIST 2702 (National Institute of Standards and Technology) as the Certified Reference Material (CRM) (recovery percentage was between 88% and 101%). RSD was lower than 10%; LOQ was 0.003 mg kg^{-1}. Hg data were normalised to Al measured at the corresponding slices to account for the difference in grain size and minerology (e.g., Ackermann, 1980; Di Leonardo et al., 2007).

The activity of ^{210}Pb was determined in selected sub-samples at dead matte core 1 and 2 and *P. oceanica* core 1. P. *oceanica* core 2 and both bare sediment cores thought to be unsuitable for dating due to their sandy nature and high bioturbation and the potential to be highly mixed. The activity was determined through the measurement of its granddaughter ^{210}Po, using alpha spectrometry. This method is based on that outlined in (Flynn, 1968) and used double acid leaching (with freshly prepared *aqua regia*, 3:1 conc. HCl: conc. HNO_3) of the dried sediment sample followed by auto-deposition of the Po in the leachate onto silver polished discs. ^{209}Po was added as an isotopic yield tracer. Samples were counted over three days on a Canberra Alpha spectrometry Quad system. The limit of detection was 0.1 Bq kg^{1}.

Calculations and Data Analysis

Mass and sediment accumulation rates (MAR, g cm^{-2} y^{-1} and SAR, cm y^{-1}) were calculated from ^{210}Pb data using the Constant Flux: Constant Sedimentation CF: CS model (Robbins, 1978) of ^{210}Pb dating, which gives an average sediment accumulation rate over the datable cumulative mass or core depth, respectively, and *via* the Constant Rate of Supply (CRS) model (Appleby and Oldfield, 1978). While the CF:CS model has been shown to be robust in many marine settings, the CRS model allows for the assessment of variations in sediment accumulation rate over time, although it makes the fundamental assumption that ^{210}Pb supply is dominantly atmospheric (rather than supplied on sediment particles), which may not apply in dynamic sedimentary environments such as Augusta Bay where significant sediment in-wash or remobilization occurs. Application of the CRS model here indicated no large-scale inflections or variations in sediment accumulation rate in the cores dated, in line with the assumptions used in the CF:CS model. So, while we used both methods here to evaluate sediment accumulation rates, we used the CF:CS model as the primary

model for age control. Supported ^{210}Pb activities (*ca.* 12 Bq kg^{-1}) were estimated using average activities in older, deeper sediments, effectively the activity at which ^{210}Pb declines to near-constant values at depth in older core material (Cundy and Croudace, 1996). For the simple or CF: CS model, the sedimentation rate was calculated by plotting the natural logarithm of the unsupported ^{210}Pb activity ($^{210}Pb_{excess}$) against depth and determining the least-squares fit. Inventories of excess ^{210}Pb (in Bq m^{-2}) per core were calculated as the sum of excess ^{210}Pb activity multiplied by the DBD and slice thickness of each core slice.

Analysis of Covariance (ANCOVA) was used to examine whether there were significant differences in the temporal profiles of geochemical variables among dead matte and *P. oceanica* habitat. Given the low number of cores per habitat, we used 'core' as the categorical variable instead of 'habitat', while 'age' was the continuous explanatory variable. The residuals were checked for normality using the Shapiro-Wilk test and for homogeneity of variance using the Levene' s test. When necessary, data were $\log_{10}$ transformed. When a significant interaction occurred among the explanatory variables, a linear regression was used to assess the change in geochemical variables along the years for each core separately. A linear regression was also used to estimate possible variation in the distribution of elements downcore in the case of bare sediment cores, as we were not able to ascribe dates to those cores (see below).

A paired t-test was used to identify the impact of contamination in Priolo Bay, by comparing the mean concentrations of elements before and after the onset of industrial activities in dead matte cores, based on the ^{210}Pb geochronology. Prior to the analysis, the data were checked for normality using the Shapiro-Wilk test.

Principal component analysis (PCA) was performed to identify patterns of variance between habitats. The PCA was performed using an Euclidean distance matrix considering the vertical profile of DBD, C_{org}, C_{inorg}, N, Hg:Al, δ^{13}C and δ^{15}N per core, while the granulometric data of the 0 – 10 cm sediment slice were extened to the whole core. Compositional data (grain size fractions and elemental concentrations) were transformed using the log center ratio (Aitchison, 1986) and all data were standardized using z-scores. Permutational multivariate analysis of variance was used (PERMANOVA, n perm. = 999) (Anderson, 2001) to detect potential significant differences in the ordination of habitats based on their vertical profiles.

Elemental stocks were estimated as the cumulative product of element concentration, DBD and decompressed sediment slice thickness and were standardized to 25 cm of sediment thickness. We also standardized the estimates of stocks to sediment thickness of one meter to allow comparisons, by fitting a linear regression of cumulative stock per slice against sediment depth. Accumulation rate of elements were standardized to the last 120 years (the effective age limit of ^{210}Pb dating) by multiplying the corresponding stock with SAR.

Mixing models using δ^{13}C were applied [R package simmr: Stable Isotope Mixing Models in R (Parnell et al., 2013)] to estimate the contribution of potential sources of organic matter to the sediment C_{org} in the three different habitats. As the deeper layers may have undergone post-depositional diagenesis processes, mixing models were applied just for the first 5 cm of sediment depth. The end-members included in the model were: particulate organic matter (POM; δ^{13}C = -22.9 ± 0.3‰), seagrass leaves (*P. oceanica*; δ^{13}C = -12.0 ± 1.0‰) and the macroalgae (*Caulerpa prolifera* and *Dictyopteris polypodioides*; averaged δ^{13}C = -16.5 ± 5.6‰). δ^{13}C data for POM and macroalgae were retrieved from Signa et al. (2017), while those of *P. oceanica* leaves are unpublished (S. Vizzini data).

All the analyses were performed using R version 3.6.1 (R Core Team, 2021).

RESULTS

The total activity of ^{210}Pb showed a quasi-exponential decline with sediment depth in dead matte core 1, reaching supported activities (*ca.* 12 *Bq* kg^{-1}) at 19 - 20 cm of sediment depth (**Figure 2**). The application of the CF:CS rate model yielded a SAR of 0.19 ± 0.03 cm y^{-1} (MAR = 0.14 g cm^{-2} y^{-1}). We did not reach these background activities at the base of the core material available for dating (11 - 12 cm) in dead matte 2, as activities were still higher than supported activities in this shorter core, and SAR was estimated at 0.19 ± 0.21 cm y^{-1} (MAR = 0.11 g cm^{-2} y^{-1}). SAR of the *P. oceanica* core 1 was 0.21 ± 0.77 cm y^{-1} (MAR = 0.12 g cm^{-2} y^{-1}). Mixing of sediment profiles (and the very sandy composition of the sediment, see below) precluded the estimation of SAR by ^{210}Pb in bare sediment cores and *P. oceanica* core 2. For the latter, we used the SAR of *P. oceanica* core 1 to calculate the corresponding accumulation rates. The $^{210}Pb_{excess}$ inventories of dead matte 1 (3,605 ± 469 Bq m^{-2}) and dead matte 2 (2,884 ± 490 Bq m^{-2}) were higher than that of *P. oceanica* 1 (2,711 ± 461 Bq m^{-2}) (**Figure 3**).

The sediments beneath each habitat were mainly sandy, but those of dead matte had two to three-fold higher silt/clay content (**Table 1**). The vertical distribution of elemental concentrations and isotopic composition differed between habitats, with dead matte cores showing a higher range and larger variability within the sediment profile. The temporal distribution of geochemical variables studied over the last 120 years differed between dead matte and *P. oceanica* cores, although the way age affected the variation depended on the core studied and not all cores showed a significant variation with time (**Figures 4A, B** and **Table S1**). The range of DBD in dead matte cores (0. 29 - 0.78 g cm^{-3} with mean 0.52 ± 0.16 g cm^{-3}) was similar to that in *P. oceanica* cores (0.15 - 0.91 g cm^{-3} and mean 0.49 ± 0.16 g cm^{-3}), but *P. oceanica* cores showed a decrease in DBD towards the present day (**Figure 4A**). Overall, high variation in the investigated variables was evident for dead matte cores from 12 cm sediment depth up to the sediment surface, which, based on the chrono-stratigraphy of the cores, corresponds to the period of 1950 (i.e., the onset of industrial activity) to present (i.e., 2015, when cores were collected). A significant increase towards present was measured for C_{org} and N in dead matte 1, while

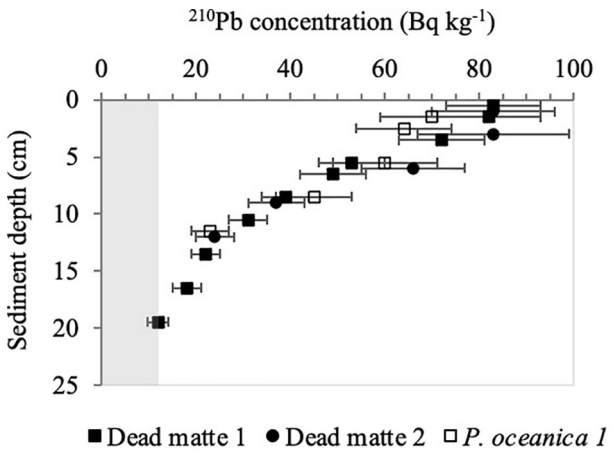

FIGURE 2 | Total ^{210}Pb activity (Bq kg^{-1} ± SE) with sediment depth. Shaded area represents the supported activity (12 Bq kg^{-1}).

both dead matte cores showed significantly more ^{15}N-enriched and ^{13}C-depleted values. Overall, the range and mean (± STDEV) of C_{org} (1.65 – 3.50 and 2.28 ± 0.44% DW) and N (0.02 - 0.2 and 0.08 ± 0.05% DW) in *P. oceanica* cores showed generally lower values than in the dead matte ones, with only the N concentration of *P. oceanica* core 1 showing a significant increase towards the present (**Figures 4A, B**). The δ^{13}C and δ^{15}N ranges were similar between habitats, with *P. oceanica* core 1 showing higher δ^{13}C and δ^{15}N values and core 2 lower δ^{15}N values towards the present. The range of Hg concentration (0.28 – 3.18 mg kg^{-1}) was above the local background value (BGV 0.28 mg kg^{-1}; Romano et al. (2021)) almost along the whole sediment profile of the dead matte cores. Hg was marginally at the BGV only at the base of the cores. Hg and Hg:Al showed a major increase starting at around 65 y BP (after yr. 1950) and high accumulation during the 1960s and 1970s. On the contrary, Hg concentration was constantly below the BGV in the *P. oceanica* cores, with 0.02 – 0.20 mg kg^{-1} range and a 24-fold lower mean (0.08 ± 0.05 mg kg^{-1}) than in the dead matte cores (1.84 ± 0.92 mg kg^{-1}). Paired t-tests between pre- and post-industrial mean values for dead matte revealed a significant increase in Hg ($t = 6.5$, $P < 0.05$) and Hg:Al ($t = -488$, $P < 0.001$) and a significant depletion in the δ^{13}C signal ($t = -10.6$, $P < 0.05$) after 1950 (post-industrial period). By dividing the maximum Hg concentration in the post-industrial period with the median one during the pre-industrial period, we calculated an enrichment factor for Hg of 3.5 at the dead matte habitat.

The range of DBD in bare sediment cores (0.40 – 1.18 g cm^{-3} and mean 0.83 ± 0.23 g cm^{-3}) was higher than that in dead matte cores (**Table 1**). Both C_{org} and N concentrations showed an increase towards the surface of the bare sediment cores, but this increase was not as pronounced as in the case of the dead matte cores (**Figure 4A**). Hg concentration showed a different pattern from that found in the dead matte cores, with decreasing values

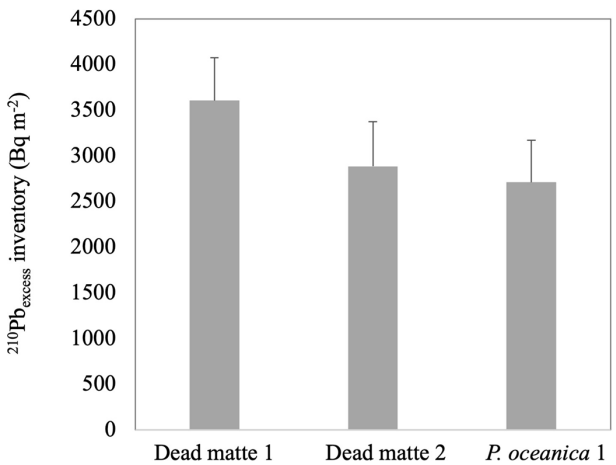

FIGURE 3 | Inventories of ^{210}Pb$_{excess}$ (Bq m^{-2}) at each core and habitat. Errors are based on uncertainties on the ^{210}Pb measurements used in the inventory calculations.

TABLE 1 | Range (min – max) and mean (± STDEV) values of sediment properties over the top 25 cm of substrate per habitat.

Habitat		Gravel > 2 mm (%)	Sand 63 μm - 2 mm (%)	Silt/Clay < 63 μm (%)	DBD (g cm^{-3})	C_{org} (% DW)	C_{inorg} (% DW)	$\delta^{13}C$ (‰)	N (% DW)	$\delta^{15}N$ (‰)	Hg (mg kg^{-1})
Dead matte	Min	–	–	–	0.29	1.24	6.23	-17.1	0.09	0.6	0.28
	Max	–	–	–	0.78	6.56	13.46	-14.1	0.17	3.3	3.18
	Mean	5.62	63.68	30.72	0.52	3.48	8.25	-15.1	0.13	2.2	1.84
	STDEV	0.06	6.67	6.74	0.16	1.15	1.51	0.6	0.02	0.6	0.92
Bare sediment	Min	–	–	–	0.40	0.18	8.25	-19.1	0.02	0.2	0.21
	Max	–	–	–	1.18	0.54	13.37	-18.0	0.04	2.4	0.92
	Mean	4.95	80.59	14.46	0.83	0.30	11.03	-18.6	0.03	1.0	0.36
	STDEV	2.81	1.71	4.51	0.23	0.09	1.28	0.3	0.01	0.6	0.19
P. oceanica meadow	Min	–	–	–	0.15	1.65	6.94	-16.0	0.03	0.4	0.02
	Max	–	–	–	0.91	3.50	11.08	-13.3	0.10	4.8	0.20
	Mean	2.69	89.17	8.15	0.49	2.28	8.19	-15.0	0.06	2.5	0.08
	STDEV	2.13	3.71	1.58	0.16	0.44	1.10	0.6	0.02	1.3	0.05

towards the surface. Dead matte cores contained, on average, 12 times higher C_{org} (3.48 ± 1.15% DW), 5 times higher N (0.13 ± 0.02% DW), 5 times higher Hg (1.84 ± 0.92 mg kg^{-1}), and 2 times higher $\delta^{15}N$ values (2.25 ± 0.6 ‰) than bare sediments (C_{org} 0.30 ± 0.09% DW, N 0.03 ± 0.01% DW, Hg 0.36 ± 0.19 mg kg^{-1}, $\delta^{15}N$ 1.00 ± 0.6 ‰) (**Figures 4A, B**). Only C_{inorg} was higher in bare sediments (8.25 – 13. 37% DW, 11.03 ± 1.28% DW) than in dead matte (6.23 – 13.46% DW, 8.25 ± 1.51% DW).

Two principal components explained 72% of the total variability in the vertical profiles among the habitats (**Figure 5**). The three habitats are well separated along the PC1 axis, which accounted for 48% of total variability, while PC2, explaining 24% of total variability, separated *P. oceanica* meadow from the other two habitats. Dead matte was characterised by a higher silt/clay, Hg:Al and N content, while bare sediment had higher DBD and C_{inorg} content. PERMANOVA showed a strong clustering of habitats based on their corresponding profiles (**Table S2**, $P < 0.001$).

Dead matte supported on average 7 times higher C_{org} stock (4.08 ± 2.10 kg C_{org} m^{-2}) and 3 times higher N stock (0.14 ± 0.04 kg N m^{-2}) than bare sediment (0.55 ± 22.13 kg C_{org} m^{-2}, 0.05 ± 0.01 kg N m^{-2}) in the top 25 cm of sediment (**Table 2**). Dead matte also supported higher C_{org} and N stocks than *P. oceanica* (2.88 ± 0.53 kg C_{org} m^{-2}, 0.07 ± 0.01 kg N m^{-2}), but the difference was not that pronounced. Bare sediments supported the highest C_{inorg} stocks (22.13 ± 3.04 kg C_{inorg} m^{-2}), with 3-fold higher values than in both dead matte (8.85 ± 1.97 kg C_{inorg} m^{-2}) and *P. oceanica* (10.89 ± 4.7 kg C_{inorg} m^{-2}). Mean stocks extrapolated in the top meter in dead matte were 179 ± 118 Mg C_{org} ha^{-1}, 399 ± 113 Mg C_{inorg} ha^{-1} and 6.1 ± 2.3 Mg N ha^{-1}, in *P. oceanica* were 124 ± 20 Mg C_{org} ha^{-1}, 457 ± 178 Mg C_{inorg} ha^{-1} and 3.1 ± 0.7 Mg N ha^{-1} and in bare sediments were 24 ± 6 Mg C_{org} ha^{-1}, 977 ± 164 Mg C_{inorg} ha^{-1} and 2.1 ± 0.2 Mg N ha^{-1}. The difference in Hg stock between habitats was very high, with dead matte (0.19 ± 0.04 g Hg m^{-2}) having 2-fold higher mean than that in bare sediment (0.09 ± 0.01 g Hg m^{-2}) and 26-fold higher than that in *P. oceanica* (0.007 ± 0.004 g Hg m^{-2}).

The mixing model outcome indicated that the contribution of different sources to the organic carbon was similar between the dead matte and *P. oceanica* meadow, while it differed at the bare sediment (**Figure S1**). Seagrass detritus contributed on average 32% and 36% in dead matte and *P. oceanica* meadow, respectively. The overall contribution of other sources (i.e., macroalgae *D. polyploides* and *C. prolifera*, and POM) to the organic carbon pool was higher than that of seagrass; macroalgae contributed in total 52% and 51% in dead matte and *P. oceanica* meadow, respectively, while POM contributed the remaining 16% and 12%, respectively. Macroalgae (*D. polyploides* and *C. prolifera*) and POM were the main contributors to the bare sediment (44% and 38%, respectively).

Over the last 120 years, the rate of accumulation of C_{org} and N was higher in dead matte (35.3 ± 19.6 g C_{org} m^{-2} y^{-1}, 1.2 ± 0.4 g N m^{-2} y^{-1}) than in *P. oceanica* (24.3 ± 3.7 g C_{org} m^{-2} y^{-1}, 0.6 ± 0.1 g N m^{-2} y^{-1}). The accumulation rate of Hg was especially higher in dead matte than that in *P. oceanica* (i.e., by 27-fold; 0.0017 ± 0.0004 g Hg m^{-2} y^{-1} and 0.00006 ± 0.00003 g Hg m^{-2} y^{-1} in dead matte and *P. oceanica*, respectively). The C_{inorg} accumulation rate was lower in the dead matte than in *P. oceanica* (74.4 ± 22.8 g C_{inorg} m^{-2} y^{-1} and 91.6 ± 33.9 g C_{inorg} m^{-2} y^{-1} in dead matte and *P. oceanica*, respectively). More than half of the stocks in the dead matte were accumulated after the onset of industrial activities, with a large part even after seagrass loss (**Figure 6**).

DISCUSSION

Our data analysis revealed that dead *P. oceanica* matte is an important biogeochemical sink and a valid archive for reconstructing Hg contamination in Augusta Bay. The vertical and temporal trends in geochemical variables studied here reflect the change in environmental conditions following the onset of industrial development in Augusta Harbour after World War II. The release of contaminants from 1950 (Bellucci et al., 2012) and the concurrent human intervention in water circulation with the

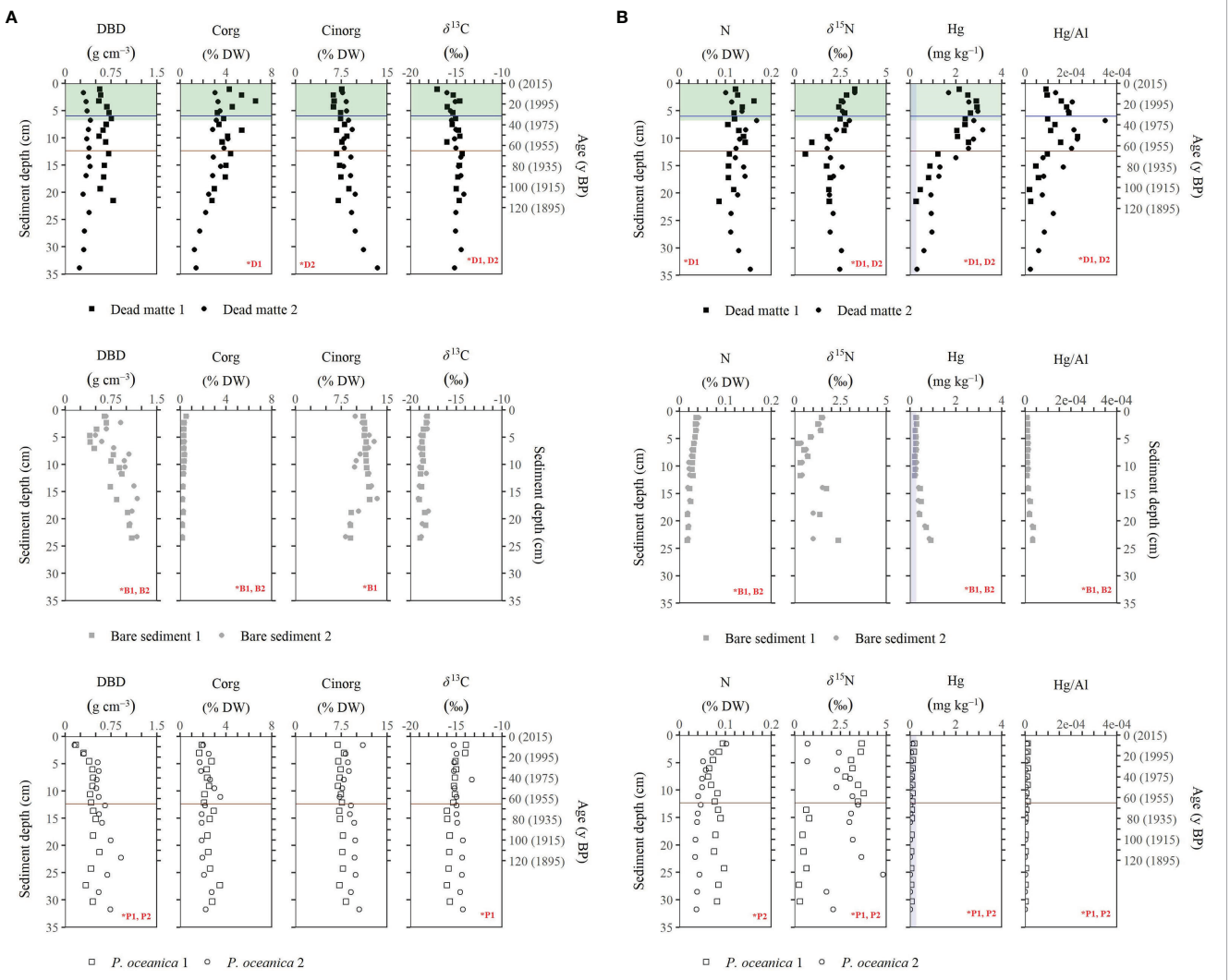

FIGURE 4 | Vertical profiles of **(A)** dry bulk density, C_{org}, C_{inorg} and $\delta^{13}C$ and **(B)** N, $\delta^{15}N$, Hg, Hg:Al with sediment depth for each core collected per habitat. Temporal trend for the last 120 years is also provided for dead matte and *P. oceanica* cores (only distribution with sediment depth is given after 120 yr. BP). The grey shaded area in the Hg profile indicates the local background value (BGV) of 0.28 mg kg^{-1} (Romano et al., 2021). The brown line indicates the onset of industrial activities in Augusta Bay, while the blue one indicates the commissioning of the demercurization plant and waste treatment. The green shaded area indicates the period of seagrass loss. Red asterisks indicate significant linear relationship with age for dead matte and *P. oceanica* cores and with depth for bare sediment cores (D, dead matte; B, bare sediment, *P. oceanica* meadow).

building of breakwaters in the early 1960s resulted in the accumulation of elements in the southern part of the bay (Sprovieri et al., 2011) and the subsequent higher post-industrial contamination levels in Priolo Bay through export of contaminants from Augusta Harbour (Di Leonardo et al., 2014).

Dead matte had high capacity to accumulate elements, as seen by the increase of C_{org}, N and $\delta^{15}N$ values over the past 120 years and the higher N and Hg association with fine sediments shown by the PCA. Post-industrial concentrations in *P. oceanica* cores remained at pre-industrial levels, despite slight and occasional (i.e., not consistent among cores) increases in N, $\delta^{15}N$ and Hg, which fall inside the natural temporal and spatial variability within seagrass meadows (Kennedy et al., 2010; Bonanno and Orlando-Bonaca, 2017). The strong separation of habitats shown in statistical analyses reflected their corresponding geochemical profiles, with organic-rich sediments of both *Posidonia* mattes supporting higher organic stocks, as opposed to the coarse, high density and inorganic-rich bare sediment. The concentration of C_{inorg} does not necessarily differ among seagrass and adjacent bare sediments (Mazarrasa et al., 2015) and the magnitude of C_{inorg} accumulation varies considerably among habitats and seagrass species, depending on the balance between carbonates precipitation, dissolution and sedimentation and the environmental conditions, implying that in the given study the lower C_{inorg} stocks in *Posidonia* mattes should reflect enhanced dissolution of carbonates in seagrass sediments

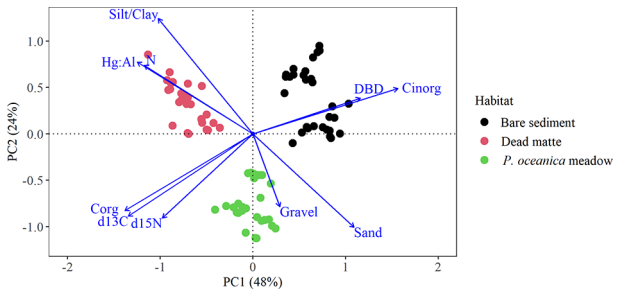

FIGURE 5 | PCA biplot of the vertical profiles (standardized to the top 25 cm) of dry bulk density, grain size fractions (gravel, sand, silt/clay), and elements (C_{org}, C_{inorg}, N, $\delta^{13}C$, $\delta^{15}N$, Hg:Al) for all habitats.

(Saderne et al., 2019). The capacity of seagrass sediments to support larger organic stocks than bare sediments has been shown previously (e.g., (Serrano et al., 2016c; Thorhaug et al., 2017; Gullström et al., 2018), including *P. oceanica* meadows (Apostolaki et al., 2019). That capacity has been related to the intense metabolism (Duarte et al., 2010) and high trapping capacity of seagrass shoots (Gacia and Duarte, 2001) and the slow decay of seagrass sediments due to the recalcitrant nature of *P. oceanica* detritus (Mateo et al., 1997; Kaal et al., 2018). This is the first study though to show that, even when dead, the *P. oceanica* matte maintained high C_{org} and N stocks. The dead matte accumulated sediments at a rate (1.9 ± 0.9 mm y^{-1}, on average) close to the mean reported for the species (2.1 ± 0.4 mm y^{-1}; Serrano et al. (2016b)) and supported stocks in the top meter that were inside the range reported for other *P. oceanica* meadows in the western and eastern parts of the Mediterranean basin (Mazarrasa et al., 2017b; Apostolaki et al., 2019). The stocks were standardized to 1 m sediment thickness for the sake of comparison between habitats studied here and elsewhere, but normalization by a period of accumulation rather than depth should be more effective in providing robust comparisons. Unfortunately, the absence of a valid chronological record from bare sediment cores precluded unvegetated sediments from this comparison. The upper ~10 cm of sediment in bare sediment cores seemed to be eroded or mixed rapidly, indicative of low retention capacity of superficial sandy unvegetated sediments (Thorhaug et al., 2017). However, the comparison of *Posidonia* mattes for the past 120 years revealed that dead matte retained its sink capacity even 30 years after the death of the shoots.

Other studies that examined the effect of decline or complete loss of other seagrass species on BC storage have reported extensive decreases in stocks (Marbà et al., 2015; Dahl et al., 2016; Thorhaug et al., 2017; Arias-Ortiz et al., 2018; Trevathan-Tackett et al., 2017; Githaiga et al., 2019; Salinas et al., 2020; Moksnes et al., 2021). These decreases are usually attributed to erosion following canopy loss and the subsequent enhancement in mineralization of previously buried C_{org} under newly oxic conditions. In our case, however, erosion of dead matte had been minimal, as seen by the comparison of $^{210}Pb_{excess}$ inventories across *Posidonia* matte cores. It should be noted here that differences in sedimentary setting and sediment composition, and possibly in ^{210}Pb supply dynamics between Priolo Bay and Xifonio Gulf presumably yielded different $^{210}Pb_{excess}$ inventories and therefore the use of the $^{210}Pb_{excess}$ inventory of Xifonio Gulf as a reference for assessing possible erosion should be considered with caution. Nevertheless, the sedimentary record stretches to the present day, and, based on elemental and isotopic compositions and profiles, it seems that there has been continuous sediment accumulation in dead matte. In fact, there have been other occasions where no erosion was detected following cover loss of several seagrass species, including *P. oceanica* (Macreadie et al., 2014; Salinas et al., 2020; Piñeiro-Juncal et al., 2021). The fate of stocks following disturbance in BC ecosystems is not thoroughly understood (Spivak et al., 2019) and the magnitude of elemental loss will ultimately depend on the interplay between local environmental settings and biogeochemical conditions that drive the balance between decomposition and preservation of organic matter. Here, it appears that the chronic loading of effluents from intensive industrial activities increased the sediment pools and gradually resulted in loss of foliar canopy but did not disrupt the matte in the given short time period. The specific geomorphology of the dead matte area with mild hydrodynamics (ICRAM, 2008) and moderate depth, where the wave-orbital motions potentially causing sediment resuspension and erosion are expected to be

TABLE 2 | Mean ± STDEV of C_{org}, C_{inorg} and N stocks in the top 25 cm of sediment at each habitat.

Habitat	C_{org} stock (kg m^{-2})	C_{inorg} stock (kg m^{-2})	N stock (kg m^{-2})	Hg stock (g m^{-2})
Dead matte	4.08 ± 2.10	8.85 ± 1.97	0.14 ± 0.04	0.19 ± 0.04
Bare sediment	0.55 ± 0.11	22.13 ± 3.04	0.05 ± 0.01	0.09 ± 0.01
P. oceanica meadow	2.88 ± 0.53	10.89 ± 4.37	0.07 ± 0.01	0.007 ± 0.004

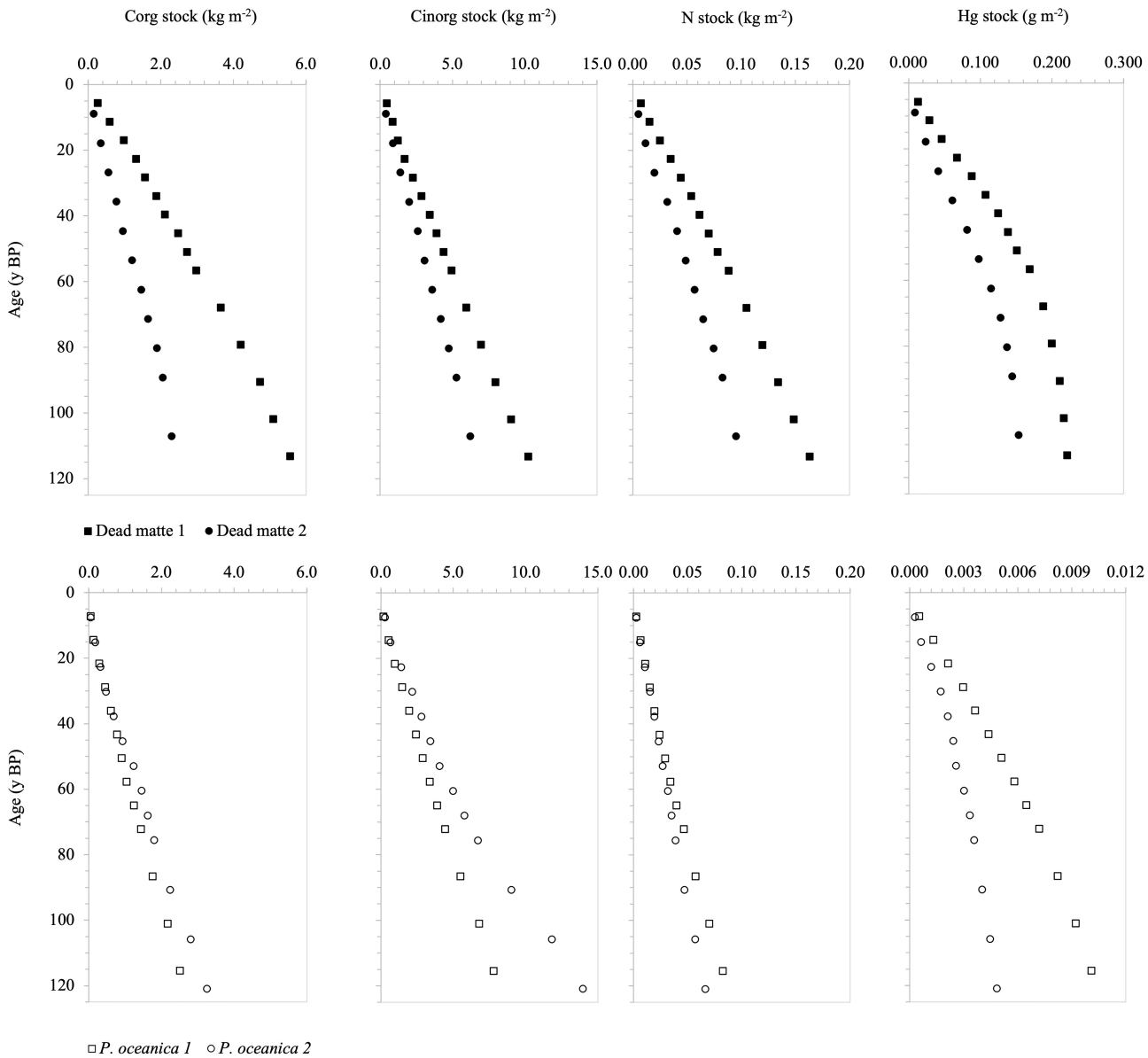

FIGURE 6 | Temporal trend of C_{org}, C_{inorg}, N and Hg stocks in dead matte and *P. oceanica* cores over approx. the last 120 yr. Note the different scale in Hg stock.

limited (Fonseca and Bell, 1998; Samper-Villarreal et al., 2016), and the establishment of the breakwaters, which further attenuated water movement (Sprovieri et al., 2011), provided protection from physical disturbance and significant erosion. The absence of mechanical damage such as anchoring, that can lead to extensive erosion of dead matte patches (Abadie et al., 2016), also provided a degree of physical protection. Although we have not measured the mineralization rate of sedimentary organic pools, available data from the area show microbial degradation of organic matter (Oliveri et al., 2016). It appears that any microbial priming and increase in efflux of CO_2 (Trevathan-Tackett et al., 2018) must have been counterbalanced by the continuous deposition of organic matter and the recalcitrant nature of seagrass detritus, limiting the long-term loss of sediment C_{org}. A similar situation has been described in fish-farm impacted seagrass sediments, where continuous deposition of fish farm effluents had led to enhancement of mineralization and efflux of CO_2 and dissolved nitrogen (Apostolaki et al., 2010) and at the same time to increase in the sedimentary organic matter pools (Apostolaki et al., 2011), suggesting that continuous deposition may outpace the deriving effluxes or that there may be a time lag between efflux and considerable decrease in organic matter pools. Perhaps this could be a unique characteristic of

P. oceanica dead matte, owing to its intrinsic properties where rhizomes and roots promote stability (Dahl et al., 2021; Piñeiro-Juncal et al., 2021) while slow decay rates (Mateo et al., 1997) and refractory sediment organic matter (Kaal et al., 2018) limit the loss of stored elements even for several decades after seagrass loss, at least where the interaction between the environmental conditions and the physical setting does not induce the erosional process.

The colonization of the dead matte by macroalgae may have partly contributed to carbon preservation and further sequestration in dead matte cores. Dead *P. oceanica* mattes are often colonized by other seagrass (*Cymodocea nodosa* and *Halophila stipulacea*) and/or macroalgae with root-like rhizoids (e.g., *Caulerpa* spp.) (Boudouresque et al., 2015), that may contribute both to metabolic production and trapping of elements through their leaves, and to the stabilization of the upper layers of the matte through their roots and rhizoids. Indeed, macroalgae contributed around 50% to the organic matter pool in dead matte, and macroalgae like *C. prolifera* found here possess a high capacity to trap allochthonous particles (Hendriks et al., 2009). The depletion of $\delta^{13}C$ signal found in post-industrial period also suggests enhancement in trapping of allochthonous material towards the present, which typically has more ^{13}C-depleted values than seagrasses, and reflects nutrient enrichment in the area, as also seen in other meadows under human pressure (Mazarrasa et al., 2017a). Additional studies are necessary to assess the contribution of other macrophytes to the storage capacity and fate of carbon following colonization of dead matte by different macrophytes, especially in the context of changing seagrass biogeography of the Mediterranean where *C. nodosa* and *H. stipulacea* are expected to expand (Chefaoui et al., 2016; Wesselmann et al., 2021a) contributing to the BC storage in the region (Apostolaki et al., 2019; Wesselmann et al., 2021b).

The 2.5-fold increase in Hg levels of the dead matte and the enrichment factor of 3.5 in the post-industrial period indicates the severe contamination by Hg in Priolo Bay and reflects the capacity of dead matte to serve as an environmental archive, similar to the case of living *Posidonia* mattes (Serrano et al., 2011; Serrano et al., 2016a; Lafratta et al., 2019). The vertical resolution of the dead matte cores was 6 – 9 years which provided a sufficient record to reconstruct the history of contamination. The temporal variation of Hg aligns well with the described pattern of Hg in the area from unvegetated sediments (Sprovieri et al., 2011; Bellucci et al., 2012; Di Leonardo et al., 2014; Romano et al., 2021), showing an initial increase after the 1950s, and a further increment between the 1960s and 1980s with a peak around 1970 – 1975. A declining concentration trend was seen after the 1980s which followed the establishment of demercurization and waste treatment plants in 1983 (Bellucci et al., 2012). Hg and C_{org} concentrations were positively interrelated ($P < 0.01$) in dead matte, showing the strong binding of Hg in organic-rich superficial seagrass sediments (Serrano et al., 2013). The capacity of bioaccumulation by seagrasses has been well documented (Sanz-Lazaro et al., 2012; Malea et al., 2019) and it is believed to be the result of active uptake from leaves and roots and absorption in seagrass detritus after burial, as well as trapping of metal-bearing particles from the water column. However, despite the correlation between the two elements, normalization of Hg to C_{org} clearly indicates the high accumulation of Hg during the 1960 – 1980 period, suggesting that the increase in Hg is not merely controlled by the availability of organic matter. In fact, Hg in the area is mainly immobilized and is available predominantly as Hg^0 and secondarily as HgS, while only a minor part (< 2%) accounts for the labile fraction (Oliveri et al., 2016). The disproportion of Hg with organic matter is indicative of highly contaminated areas with large quantities of anthropogenically derived Hg, such as Augusta Bay (Di Leonardo et al., 2007; Oliveri et al., 2016). High values of Hg have been reported from other industrial-impacted *P. oceanica* meadows [0.56 ± 0.14 mg kg^{-1}, Lafabrie et al. (2007); 1.79 ± 0.01 mg kg^{-1}, Di Leo et al. (2013)]. However, in our case even after remedial measures the Hg levels remained high and certainly higher than the BGV of 0.28 mg kg^{-1} (Romano et al., 2021), with a mean value of 2.55 ± 0.44 mg kg^{-1}. Recent increases or still high Hg concentrations locally in Augusta Harbour have been measured before, mainly in unvegetated sediments (Bellucci et al., 2012; Romano et al., 2021) but also in a dead matte core once (Di Leonardo et al., 2017) and have been attributed to the mobilization of polluted sediment caused by dredging and ship traffic (Bellucci et al., 2012). It is important to note here that pre-industrial Hg levels in Priolo Bay (dead matte area) were already higher than BGV (1.02 ± 0.51 mg kg^{-1}), which is in accordance with previous measurements in unvegetated sediments (Sprovieri et al., 2011; Bellucci et al., 2012; Di Leonardo et al., 2014; Romano et al., 2021) and dead matte (Di Leonardo et al., 2017) from the area. This suggests that there had already been human development in the area and that the pre-industrial period considered here is relatively short (~ 55 years) and certainly not representative of baseline conditions, as shown in samples older than 2800 ^{14}C yr BP in *P. oceanica* matte from the northwest Mediterranean, where Hg concentration was as low as 0.007 ± 0.001 mg kg^{-1} (Serrano et al., 2013).

The coarse, high density and organic-poor unvegetated sediments showed limited capacity to retain Hg, as seen by the Hg profile and the 5-fold lower mean value in bare sediments compared to that in dead matte. Hg was at the BVG throughout the top 10 cm while it increased above BGV at the 10 – 20 cm sediment thickness (mean 0.57 ± 0.2 mg kg^{-1}, median 0.47 mg kg^{-1}), indicating the resuspension of surface sediments and the subsequent accumulation of Hg in deeper sediments. Nevertheless, the 5-fold higher Hg concentration of bare sediment compared to *P. oceanica* meadow in Xifonio Gulf showed the severe contamination of Priolo Bay and the lack of correlation between C_{org} and Hg in bare sediments points to the industrially derived loading of Hg. The analysis of Hg content in *P. oceanica* leaves from Xifonio Gulf clearly shows that the meadow is not subjected to contamination by Hg, with a mean content of 0.09 ± 0.016 mg kg^{-1} (S. Vizzini, unpubl. data) close to the mean reported for leaves from areas with minimal contamination (0.04 ± 0.00 mg kg^{-1}, Lafabrie et al. (2008)) and generally close to the low end of the range reported for *P.*

oceanica leaves in the Mediterranean Sea (0.01 – 0.27 mg kg^{-1}, Bonanno and Orlando-Bonaca (2017)). Similarly, the mean Hg concentration in the *P. oceanica* sediments (0.08 ± 0.05 mg kg^{-1}) fell closer to the lower values reported from *P. oceanica* rhizosphere (0.02 – 1.79 mg kg^{-1}, Bonanno and Orlando-Bonaca (2017)), albeit, as also seen in the case of dead matte, this is higher than what are considered pre-anthropogenic levels (Serrano et al., 2013).

The two dead matte cores showed small differences in concentrations, stocks, and accumulation rates of elements, possibly reflecting the spatial variation in deposition within the dead matte. Nevertheless, the variables that are indicative of nutrient enrichment (i.e., C_{org}, N, $\delta^{15}N$) had similar temporal trends between the replicate cores, with increasing values towards the present, while the temporal trends in Hg followed the well described pattern of Hg accumulation in the Bay. Furthermore, their mean values were higher than the corresponding means in *P. oceanica* and bare sediment cores, indicating that the changes observed in the dead matte over the last 65 years were related mainly to the increase in nutrient and Hg deposition from human activities in Augusta Harbour and less to changes in the composition of sediment.

The interpretation of our data suggests that dead *P. oceanica* mattes act as biogeochemical sinks and may be used as archives to identify environmental and ecosystem shifts in areas with unknown environmental history, reinforcing the paramount importance of seagrasses, and *P. oceanica* in particular, also after their death. Potential losses of C_{org} and N due to an increase in mineralization following seagrass loss must have been decelerated by the physical setting and/or counterbalanced by chronic loading from industrial activities and allochthonous sequestration. However, detailed studies are needed to elucidate the fate of carbon following natural recolonization of the matte by different macrophytes and, therefore, to evaluate the opportunity for active recolonization actions (i.e., plant transplantation) aimed at the stabilisation of sediment and associated nutrients and contaminants. Further studies are also necessary to determine the decomposition rate, and CO_2 and nutrient fluxes of dead matte and consequent risk of release of stored C_{org} and pollutants following possible element mobilization. In this framework, new management schemes for highly contaminated areas should be elaborated and prioritized to prevent pollutant and carbon release, including the protection and conservation of dead mattes, and the development of adequate remediation actions (*e.g.*, seagrass restoration) avoiding sediment dredging and mobilization, practices widely advocated and adopted so far.

DATA AVAILABILITY STATEMENT

The raw data supporting the conclusions of this article will be made available by the authors, without undue reservation.

AUTHOR CONTRIBUTIONS

SV and AM conceived the research idea and designed the sampling. SV and CT conducted field work. AC and CT performed the laboratory analyses. EA and LC analyzed the data. EA wrote the first draft of the manuscript. All authors contributed to the article and approved the submitted version.

FUNDING

The study was funded by the project TETIDE, PON01_03112, Italian Ministry of University and Research (MIUR) and by the project Marine Hazard, PON03PE_00203_1, Italian Ministry of Education, University and Research (MIUR).

ACKNOWLEDGMENTS

We thank Andrea Savona, Antonino M. Vaccaro and Rossella Di Leonardo for sampling, Adele E. Aleo for helping with laboratory analyses, and Victoria Litsi Mizan for helping with the graphical representation of the results. AC is grateful to colleagues in GAU-Radioanalytical, University of Southampton, for radiochemical analysis. We highly acknowledge constructive criticism by the three reviewers.

SUPPLEMENTARY MATERIAL

The Supplementary Material for this article can be found online at: https://www.frontiersin.org/articles/10.3389/fmars.2022.861998/full#supplementary-material

REFERENCES

Abadie, A., Lejeune, P., Pergent, G., and Gobert, S. (2016). From Mechanical to Chemical Impact of Anchoring in Seagrasses: The Premises of Anthropogenic Patch Generation in *Posidonia Oceanica* Meadows. *Mar. Pollut. Bull.* 109, 61–71. doi: 10.1016/j.marpolbul.2016.06.022

Ackermann, F. (1980). A Procedure for Correcting Grain Size Effect in Heavy Metal Analysis of Estuarine and Coastal Sediments. *Env. Tech. Lett.* 1, 518–527. doi: 10.1080/09593338009384008

Aitchison, J. (1986). *The Statistical Analysis of Compositional Data* (London: Chapman and Hall Ltd.), 416.

Anderson, M. J. (2001). A New Method for Nonparametric Multivariate Analysis of Variance. *Austral Ecol.* 2632, 46. doi: 10.1111/j.1442-9993.2001.01070.pp.x

Apostolaki, E. T., Holmer, M., Marba, N., and Karakassis, I. (2010). Degrading Seagrass (*Posidonia Oceanica*) Ecosystems: A Source of Dissolved Matter to the Mediterranean. *Hydrobiologia* 649, 13–23. doi: 10.1007/s10750-010-0255-2

Apostolaki, E. T., Holmer, M., Marba, N., and Karakassis, I. (2011). Reduced Carbon Sequestration in a Mediterranean Seagrass (*Posidonia Oceanica*) Ecosystem Impacted by Fish Farming. *Aquac. Environ. Interact.* 2, 49–59. doi: 10.3354/aei00031

Apostolaki, E. T., Vizzini, S., Santinelli, V., Kaberi, H., Andolina, C., and Papathanassiou, E. (2019). Exotic *Halophila Stipulacea* is an Introduced

Carbon Sink for the Eastern Mediterranean Sea. *Sci. Rep-uk.* 9, 9643. doi: 10.1038/s41598-019-45046-w

Appleby, P. G., and Oldfield, F. (1978). The Calculation of Lead-210 Dates Assuming a Constant Rate of Supply of Unsupported ^{210}Pb to the Sediment. *Catena* 5, 1–8. doi: 10.1016/S0341-8162(78)80002-2

Arias-Ortiz, A., Serrano, O., Masque, P., Lavery, P. S., Mueller, U., Kendrick, G. A., et al. (2018). A Marine Heatwave Drives Massive Losses From the World's Largest Seagrass Carbon Stocks. *Nat. Clim. Change* 81, 9. doi: 10.1038/s41558-018-0096-y

Bellucci, L. G., Giuliani, S., Romano, S., Albertazzi, S., Mugnai, C., and Frignani, M. (2012). An Integrated Approach to the Assessment of Pollutant Delivery Chronologies to Impacted Areas: Hg in the Augusta Bay (Italy). *Environ. Sci. Technol.* 46, 2040–2046. doi: 10.1021/es203054c

Bonanno, G., and Orlando-Bonaca, M. (2017). Trace Elements in Mediterranean Seagrasses: Accumulation, Tolerance and Biomonitoring. A Review. *Mar. Pollut. Bull.* 125, 8–18. doi: 10.1016/j.marpolbul.2017.10.078

Borg, J. A., Rowden, A. A., Attrill, M. J., Schembri, P. J., and Jones, M. B. (2006). Wanted Dead or Alive: High Diversity of Macroinvertebrates Associated With Living and "Dead" *Posidonia Oceanica* Matte. *Mar. Biol.* 149, 667–677. doi: 10.1007/S00227-006-0250-3

Boudouresque, C. F., Pergent, G., Pergent-Martini, C., Ruitton, S., Thibaut, T., and Verlaque, M. (2015). The Necromass of the *Posidonia Oceanica* Seagrass Meadow: Fate, Role, Ecosystem Services and Vulnerability. *Hydrobiologia* 781, 1–18. doi: 10.1007/s10750-015-2333-y

Calvo, S., Calvo, R., Luzzu, F., Raimondi, V., Assenzo, M., Cassetti, F. P., et al. (2021). Performance Assessment of *Posidonia Oceanica* (L.) Delile Restoration Experiment on Dead Matte Twelve Years After Planting—Structural and Functional Meadow Features. *Water-sui* 13, 724. doi: 10.3390/w13050724

Chefaoui, R. M., Assis, J., and Duarte, C. M. (2016). And Serrão, ELarge-Scale Prediction of Seagrass Distribution Integrating Landscape Metrics and Environmental Factors: The Case of *Cymodocea Nodosa* (Mediterranean–Atlantic). *A.Ecol. Model* 39, 123–137. doi: 10.1016/s0304-3800(02)00199-0

Costantini, C. (2015). Ripristino Dei Fondali Degradati E Recupero Del Paesaggio Sommerso Nell' Area Mediterranea. PhD Thesis (Italy: Univerisita di Palermo).

Cundy, A. B., and Croudace, I. W. (1996). Sediment Accretion and Recent Sea-Level Rise in the Solent, Southern England: Inferences From Radiometric and Geochemical Studies. *Estuar. Coast. Shelf. Sci.* 43, 449–467. doi: 10.1006/ecss.1996.0081

Dahl, M., Björk, M., and Gullström, M. (2021). Effects of Seagrass Overgrazing on Sediment Erosion and Carbon Sink Capacity: Current Understanding and Future Priorities. *Limnol. Oceanogr. Lett.* 6, 309–319. doi: 10.1002/lol2.10211

Dahl, M., Deyanova, D., Lyimo, L. D., Näslund, J., Samuelsson, G. S., Mtolera, M. S. P., et al. (2016). Effects of Shading and Simulated Grazing on Carbon Sequestration in a Tropical Seagrass Meadow. *J. Ecol.* 104, 654–664. doi: 10.1111/1365-2745.12564

de los Santos, C. B., Krause-Jensen, D., Alcoverro, T., Marbà, N., Duarte, C. M., Katwijk, M. M., et al. (20193356). Recent Trend Reversal for Declining European Seagrass Meadows. *Nat. Commun.* 10, 3356. doi: 10.1038/s41467-019-11340-4

Di Leo, A., Annicchiarico, C., and Cardellichio, N. (2013). Trace Metal Distributions in Posidonia Oceanica and Sediments From Taranto Gulf (Ionian Sea, Southern Italy). *Mediterr. Mar. Sci.* 14, 204–213. doi: 10.12681/mms.316

Di Leonardo, R., Bellanca, A., Capotondi, L., Cundy, A., and Neri, R. (2007). Possible Impacts of Hg and PAH Contamination on Benthic Foraminiferal Assemblages: An Example From the Sicilian Coast, Central Mediterranean. *Sci. Total Environ.* 388, 168–183. doi: 10.1016/j.scitotenv.2007.08.009

Di Leonardo, R., Mazzola, A., Cundy, A. B., Tramati, C. D., and Vizzini, S. (2017). Trace Element Storage Capacity of Sediments in Dead Posidonia Oceanica Mat From a Chronically Contaminated Marine Ecosystem. *Environ. Toxicol. Chem.* 36, 49–58. doi: 10.1002/etc.3539

Di Leonardo, R., Mazzola, A., Tramati, C. D., Vaccaro, A., and Vizzini, S. (2014). Highly Contaminated Areas as Sources of Pollution for Adjoining Ecosystems: The Case of Augusta Bay (Central Mediterranean). *Mar. Pollut. Bull.* 89, 417–426. doi: 10.1016/j.marpolbul.2014.10.023

Duarte, C. M., Kennedy, H., Marbà, N., and Hendriks, I. (2013). Assessing the Capacity of Seagrass Meadows for Carbon Burial: Current Limitations and Future Strategies. *Ocean Coast. Manage* 83, 32–38. doi: 10.1016/j.ocecoaman.2011.09.001

Duarte, C. M., Marba, N., Gacia, E., Fourqurean, J. W., Beggins, J., Barrón, C., et al. (2010). Seagrass Community Metabolism: Assessing the Carbon Sink Capacity of Seagrass Meadows. *Global Biogeochem. Cy* 24, GB4032. doi: 10.1029-2010GB003793

Flynn, W. W. (1968). The Determination of Low Levels of Polonium-210 in Environmental Materials. *Anal. Chim. Acta* 43, 221–227. doi: 10.1016/s0003-2670(00)89210-7

Fonseca, M., and Bell, S. (1998). Influence of Physical Setting on Seagrass Landscapes Near Beaufort, North Carolina, USA. *Mar. Ecol. Prog. Ser.* 171, 109–121. doi: 10.3354/meps171109

Gacia, E., and Duarte, C. M. (2001). Sediment Retention by a Mediterranean *Posidonia Oceanica* Meadow: The Balance Between Deposition and Resuspension. *Estuar. Coastal Shelf. Sci.* 52, 505–514. doi: 10.1006/ecss.2000.0753

Gacia, E., Duarte, C. M., and Middelburg, J. J. (2002). Carbon and Nutrient Deposition in a Mediterranean Seagrass (*Posidonia Oceanica*) Meadow. *Limnol. Oceanogr.* 47, 23–32. doi: 10.4319/lo.2002.47.1.0023

Githaiga, M. N., Frouws, A. M., Kairo, J. G., and Huxham, M. (2019). Seagrass Removal Leads to Rapid Changes in Fauna and Loss of Carbon. *Front. Ecol. Evol.* 7. doi: 10.3389/fevo.2019.00062

Gullström, M., Lyimo, L. D., Dahl, M., Samuelsson, G. S., Eggertsen, M., Anderberg, E., et al. (2018). Blue Carbon Storage in Tropical Seagrass Meadows Relates to Carbonate Stock Dynamics, Plant–Sediment Processes, and Landscape Context: Insights From the Western Indian Ocean. *Ecosystems* 21551, 566. doi: 10.1007/s10021-017-0170-8

Hendriks, I. E., Bouma, T. J., and Morris, E. P. (2009). Effects of Seagrasses and Algae of the *Caulerpa* Family on Hydrodynamics and Particle-Trapping Rates. *Mar. Biol.* 157, 473–481. doi: 10.1007/S00227-009-1333-8

Lo Iacono, C., Mateo, M. A., Gràcia, E., Guasch, L., Carbonell, R., Serrano, L., et al. (2008). Very High-Resolution Seismo-Acoustic Imaging of Seagrass Meadows (Mediterranean Sea): Implications for Carbon Sink Estimates. *Geophys. Res. Lett.* 35, L18601. doi: 10.1029/2008gl034773

ICRAM-Istituto Centrale per la Ricerca scientifica e tecnologica Applicata al Mare (2008). *Progetto Preliminare Di Bonifica Dei Fondali Della Rada Di Augusta Nel Sito Di Interesse Nazionale Di Priolo—Elaborazione Definitiva*. (Rome: ICRAM) 182, BoI-Pr-SI-PR-Rada di Augusta-03.22.

Kaal, J., Serrano, O., del Río, J. C., and Rencoret, J. (2018). Radically Different Lignin Composition in Posidonia Species may Link to Differences in Organic Carbon Sequestration Capacity. *Org. Geochem.* 124, 247–256. doi: 10.1016/j.orggeochem.2018.07.017

Kennedy, H., Beggins, J., Duarte, C. M., Fourqurean, J. W., Holmer, M., Marba, N., et al. (20104026). Seagrass Sediments as a Global Carbon Sink: Isotopic Constraints. *Global Biogeochem. Cy* 24, GB4026. doi: 10.1029/2010GB003848

Lafabrie, C., Pergent, G., Kantin, R., Pergent-Martini, C., and Gonzalez, J. L. (2007). Trace Metals Assessment in Water, Sediment, Mussel and Seagrass Species - Validation of the Use of *Posidonia Oceanica* as a Metal Biomonitor. *Chemosphere* 68, 2033–2039. doi: 10.1016/j.chemosphere.2007.02.039

Lafabrie, C., Pergent-Martini, C., and Pergent, G. (2008). Metal Contamination of *Posidonia Oceanica* Meadows Along the Corsican Coastline (Mediterranean). *Environ. Pollut.* 151, 262–268. doi: 10.1016/j.envpol.2007.01.047

Lafratta, A., Serrano, O., Masqué, P., Mateo, M. A., Fernandes, M., Gaylard, S., et al. (2019). Seagrass Soil Archives Reveal Centennial-Scale Metal Smelter Contamination While Acting as Natural Filters. *Sci. Total Environ.* 649, 1381–1392. doi: 10.1016/j.scitotenv.2018.08.400

Lavery, P. S., Mateo, M.-Á., Serrano, O., and Rozaimi, M. (2013). Variability in the Carbon Storage of Seagrass Habitats and Its Implications for Global Estimates of Blue Carbon Ecosystem Service. *PloS One* 8, e73748. doi: 10.1371/journal.pone.0073748.t008

Leiva-Dueñas, C., Cortizas, A. M., Piñeiro-Juncal, N., Díaz-Almela, E., Garcia-Orellana, J., and Mateo, M. A. (2021). Long-Term Dynamics of Production in Western Mediterranean Seagrass Meadows: Trade-Offs and Legacies of Past Disturbances. *Sci. Total Environ.* 754, 142117. doi: 10.1016/j.scitotenv.2020.142117

Lovelock, C. E., Atwood, T., Baldock, J., Duarte, C. M., Hickey, S., Lavery, P. S., et al. (2017). Assessing the Risk of Carbon Dioxide Emissions From Blue Carbon Ecosystems. *Mar. Policy* 15257, 265. doi: 10.1016/j.marpol.2015.12.020

Macreadie, P. I., Anton, A., Raven, J. A., Beaumont, N., Connolly, R. M., Friess, D. A., et al. (2019). The Future of Blue Carbon Science. *Nat. Commun.* 10, 3998. doi: 10.1038/s41467-019-11693-w

Macreadie, P. I., Costa, M. D. P., Atwood, T. B., Friess, D. A., Kelleway, J. J., Kennedy, H., et al. (2021). Blue Carbon as a Natural Climate Solution. *Nat. Rev. Earth Environ.* 2, 826–839. doi: 10.1038/s43017-021-00224-1

Macreadie, P. I., York, P. H., Sherman, C. D. H., Keough, M. J., Ross, D. J., Ricart, A. M., et al. (2014). No Detectable Impact of Small-Scale Disturbances on 'Blue Carbon' Within Seagrass Beds. *Mar. Biol.* 161, 2939–2944. doi: 10.1007/s00227-014-2558-8

Malea, P., Mylona, Z., and Kevrekidis, T. (2019). Improving the Utility of the Seagrass *Posidonia Oceanica* as a Biological Indicator of Past Trace Element Contamination. *Ecol. Indic.* 107, 105596. doi: 10.1016/j.ecolind.2019.105596

Marbà, N., Arias-Ortiz, A., Masqué, P., Kendrick, G. A., Mazarrasa, I., Bastyan, G. R., et al. (2015). Impact of Seagrass Loss and Subsequent Revegetation on Carbon Sequestration and Stocks. *J. Ecol.* 103, 296–302. doi: 10.1111/1365-2745.12370

Mateo, M. A., Romero, J., Perez, M., Littler, M. M., and Littler, D. S. (1997). Dynamics of Millenary Organic Deposits Resulting From the Growth of the Mediterranean Seagrass *Posidonia Oceanica*. *Estuar. Coastal Shelf. Sci.* 44, 103 110. doi: 10.1006/ecss.1996.0116

Mazarrasa, I., Marbà, N., Garcia-Orellana, J., Masqué, P., Arias-Ortiz, A., and Duarte, C. M. (2017a). Dynamics of Carbon Sources Supporting Burial in Seagrass Sediments Under Increasing Anthropogenic Pressure. *Plant Physiol.* 62, 1451–1465. doi: 10.1104/pp.115.2.599

Mazarrasa, I., Marbà, N., Garcia-Orellana, J., Masqué, P., Arias-Ortiz, A., and Duarte, C. M. (2017b). Effect of Environmental Factors (Wave Exposure and Depth) and Anthropogenic Pressure in the C Sink Capacity of *Posidonia Oceanica* Meadows. *Proc. Natl. Acad. Sci.* 62, 1436–1450. doi: 10.1073/pnas.0905620106

Mazarrasa, I., Marba, N., Lovelock, C. E., Serrano, O., Lavery, P. S., Fourqurean, J. W., et al. (2015). Seagrass Meadows as a Globally Significant Carbonate Reservoir. *Biogeosci. Discussions* 124107, 4138. doi: 10.5194/bgd-12-4993-2015

Mazarrasa, I., Samper-Villarreal, J., Serrano, O., Lavery, P. S., Lovelock, C. E., Marbà, N., et al. (2018). Habitat Characteristics Provide Insights of Carbon Storage in Seagrass Meadows. *Mar. Pollut. Bull.* 134106, 117. doi: 10.1016/j.marpolbul.2018.01.059

Moksnes, P., Röhr, M. E., Holmer, M., Eklöf, J. S., Eriander, L., Infantes, E., et al. (2021). Major Impacts and Societal Costs of Seagrass Loss on Sediment Carbon and Nitrogen Stocks. *Ecosphere* 12, e03658. doi: 10.1002/ecs2.3658

Monnier, B., Pergent, G., Mateo, M.Á., Carbonell, R., Clabaut, P., and Pergent-Martini, C. (2021). Sizing the Carbon Sink Associated With *Posidonia Oceanica* Seagrass Meadows Using Very High-Resolution Seismic Reflection Imaging. *Mar. Environ. Res.* 170, 105415. doi: 10.1016/j.marenvres.2021.105415

Nieuwenhuize, J., Maas, Y. E. M., and Middelburg, J. J. (1994). Rapid Analysis of Organic Carbon and Nitrogen in Particulate Materials. *Mar. Chem.* 45, 217–224. doi: 10.1016/0304-4203(94)90005-1

Oliveri, E., Manta, D. S., Bonsignore, M., Cappello, S., Tranchida, G., Bagnato, E., et al. (2016). Mobility of Mercury in Contaminated Marine Sediments: Biogeochemical Pathways. *Mar. Chem.* 186, 1–10. doi: 10.1016/j.marchem.2016.07.002

Parnell, A. C., Phillips, D. L., Bearhop, S., Semmens, B. X., Ward, E. J., Moore, J. W., et al. (2013). Bayesian Stable Isotope Mixing Models. *Environmetrics* 24, 387–399. doi: 10.1002/env.2221

Pendleton, L., Donato, D. C., Murray, B. C., Crooks, S., Jenkins, W. A., Sifleet, S., et al. (2015). Estimating Global "Blue Carbon" Emissions From Conversion and Degradation of Vegetated Coastal Ecosystems. *PloS One* 7, e43542. doi: 10.1371/journal.pone.0043542

Piñeiro-Juncal, N., Kaal, J., Moreira, J. C. F., Cortizas, A. M., Lambais, M. R., Otero, X. L., et al. (2021). Cover Loss in a Seagrass *Posidonia Oceanica* Meadow Accelerates Soil Organic Matter Turnover and Alters Soil Prokaryotic Communities. *Org. Geochem.* 151, 104140. doi: 10.1016/j.orggeochem.2020.104140

R Core Team (2021) *R: A Language and Environment for Statistical Computing*. Available at: https://www.R-project.org/.

Robbins, J. A. (1978). "Geochemical and Geophysical Applications of Radioactive Lead," in *The Biogeochemistry of Lead in the Environment Part a*. Ed. J. O. Nriagu (Amsterdam: Elsevier Scientific), 285–293.

Röhr, M. E., Holmer, M., Baum, J. K., Björk, M., Boyer, K., Chin, D., et al. (2018). Blue Carbon Storage Capacity of Temperate Eelgrass (*Zostera Marina*) Meadows. *Global Biogeochem. Cy* 32, 1457–1475. doi: 10.1029/2018gb005941

Romano, E., Bergamin, L., Croudace, I. W., Pierfranceschi, G., Sesta, G., and Ausili, A. (2021). Measuring Anthropogenic Impacts on an Industrialised Coastal Marine Area Using Chemical and Textural Signatures in Sediments: A Case Study of Augusta Harbour (Sicily, Italy). *Sci. Total Environ.* 755, 142683. doi: 10.1016/j.scitotenv.2020.142683

Saderne, V., Geraldi, N. R., Macreadie, P. I., Maher, D. T., Middelburg, J. J., Serrano, O., et al. (20191106). Role of Carbonate Burial in Blue Carbon Budgets. *Nat. Commun.* 10, 1106. doi: 10.1038/s41467-019-08842-6

Salinas, C., Duarte, C. M., Lavery, P. S., Masque, P., Arias-Ortiz, A., Leon, J. X., et al. (2020). Seagrass Losses Since Mid-20th Century Fuelled CO_2 Emissions From Soil Carbon Stocks. *Global Change Biol.* 26, 4772–4784. doi: 10.1111/gcb.15204

Samper-Villarreal, J., Lovelock, C. E., Saunders, M. I., Roelfsema, C., and Mumby, P. J. (2016). Organic Carbon in Seagrass Sediments is Influenced by Seagrass Canopy Complexity, Turbidity, Wave Height, and Water Depth. *Limnol. Oceanogr.* 61, 938–952. doi: 10.1002/lno.10262

Sanz-Lazaro, C., Malea, P., Apostolaki, E. T., Kalantzi, I., Marin, A., and Karakassis, I. (2012). The Role of the Seagrass *Posidonia Oceanica* in the Cycling of Trace Elements. *Biogeosciences* 9, 2497–2507. doi: 10.5194/bg-9-2497-2012

Serrano, O., Almahasheer, H., Duarte, C. M., and Irigoien, X. (2018). Carbon Stocks and Accumulation Rates in Red Sea Seagrass Meadows. *Sci. Rep-uk.* 8, 1 13. doi: 10.1038/s41598-018-33182-8

Serrano, O., Davis, G., Lavery, P. S., Duarte, C. M., Martinez-Cortizas, A., Mateo, M.-Á., et al. (2016a). Reconstruction of Centennial-Scale Fluxes of Chemical Elements in the Australian Coastal Environment Using Seagrass Archives. *Sci. Total Environ.* 541, 883–894. doi: 10.1016/j.scitotenv.2015.09.017

Serrano, O., Lavery, P. S., López-Merino, L., Ballesteros, E., and Mateo, M. A. (2016b). Location and Associated Carbon Storage of Erosional Escarpments of Seagrass Posidonia Mats. *Front. Mar. Sci.* 3. doi: 10.3389/fmars.2016.00042

Serrano, O., Martínez-Cortizas, A., Mateo, M. A., Biester, H., and Bindler, R. (2013). Millennial Scale Impact on the Marine Biogeochemical Cycle of Mercury From Early Mining on the Iberian Peninsula. *Global Biogeochem. Cy* 27, 21–30. doi: 10.1029/2012gb004296

Serrano, O., Mateo, M. A., Dueñas-Bohórquez, A., Renom, P., López-Sáez, J. A., and Cortizas, A. M. (2011). The *Posidonia Oceanica* Marine Sedimentary Record: A Holocene Archive of Heavy Metal Pollution. *Sci. Total Environ.* 409, 4831 4840. doi: 10.1016/j.scitotenv.2011.08.001

Serrano, O., Ricart, A. M., Lavery, P. S., Mateo, M.-Á., Arias-Ortiz, A., Masqué, P., et al. (2016c). Key Biogeochemical Factors Affecting Soil Carbon Storage In Posidonia Meadows. *Biogeosciences* 134581, 4594. doi: 10.4225/75/56b2fd48b92d5

Signa, G., Mazzola, A., Tramati, C. D., and Vizzini, S. (2017). Diet and Habitat Use Influence Hg and Cd Transfer to Fish and Consequent Biomagnification in a Highly Contaminated Area: Augusta Bay (Mediterranean Sea). *Environ. Pollut.* 230, 394–404. doi: 10.1016/j.envpol.2017.06.027

Sousa, A. I., da Silva, J. F., Azevedo, A., and Lillebø, A. I. (2019). Blue Carbon Stock in *Zostera Noltei* Meadows at Ria De Aveiro Coastal Lagoon (Portugal) Over a Decade. *Sci. Rep-uk.* 9, 14387. doi: 10.1038/s41598-019-50425-4

Spivak, A. C., Sanderman, J., Bowen, J. L., Canuel, E. A., and Hopkinson, C. S. (2019). Global-Change Controls on Soil-Carbon Accumulation and Loss in Coastal Vegetated Ecosystems. *Nat. Geosci.* 12, 685–692. doi: 10.1038/s41561-019-0435-2

Sprovieri, M., Oliveri, E., Leonardo, R. D., Romano, E., Ausili, A., Gabellini, M., et al. (2011). The Key Role Played by the Augusta Basin (Southern Italy) in the Mercury Contamination of the Mediterranean Sea. *J. Environ. Monitor* 13, 1753–1760. doi: 10.1039/c0em00793e

Thorhaug, A., Poulos, H. M., López-Portillo, J., Ku, T. C. W., and Berlyn, G. P. (2017). Seagrass Blue Carbon Dynamics in the Gulf of Mexico: Stocks, Losses From Anthropogenic Disturbance, and Gains Through Seagrass Restoration. *Sci. Total Environ.*, 605–606, 626–636. doi: 10.1016/j.scitotenv.2017.06.189

Trevathan-Tackett, S. M., Thomson, A. C. G., Ralph, P. J., and Macreadie, P. I. (2018). Fresh Carbon Inputs to Seagrass Sediments Induce Variable Microbial Priming Responses. *Sci. Total Environ.* 621, 1–7. doi: 10.1016/j.scitotenv.2017.11.193

Trevathan-Tackett, S. M., Wessel, C., Cebrián, J., Ralph, P. J., Masqué, P., and Macreadie, P. I. (2017). Effects of Small-Scale, Shading-Induced Seagrass Loss on Blue Carbon Storage: Implications for Management of Degraded Seagrass Ecosystems. *I. J. Appl. Ecol.* 55, 1351–1359. doi: 10.1111/1365-2664.13081

USEPA - United States Environmental Protection Agency (1996). *Method 3052. Microwave Assisted Acid Digestion of Siliceous and Organically Based Matrices* (Washington, DC: USEPA).

Wesselmann, M., Chefaoui, R. M., Marbà, N., Serrao, E. A., and Duarte, C. M. (2021a). Warming Threatens to Propel the Expansion of the Exotic Seagrass *Halophila Stipulacea*. *Front. Mar. Sci.* 8. doi: 10.3389/fmars.2021.759676

Wesselmann, M., Geraldi, N. R., Duarte, C. M., Garcia-Orellana, J., Díaz-Rúa, R., Arias-Ortiz, A., et al. (2021b). Seagrass (*Halophila Stipulacea*) Invasion Enhances Carbon Sequestration in the Mediterranean Sea. *Global Change Biol.* 27, 2592–2607. doi: 10.1111/gcb.15589

Conflict of Interest: The authors declare that the research was conducted in the absence of any commercial or financial relationships that could be construed as a potential conflict of interest.

frontiers | Frontiers in Marine Science

ORIGINAL RESEARCH
published: 10 May 2022
doi: 10.3389/fmars.2022.835381

Effects of Epiphytic Biofilm Activity on the Photosynthetic Activity, pH and Inorganic Carbon Microenvironment of Seagrass Leaves (*Zostera marina* L.)

Qingfeng Zhang, Michael Kühl and Kasper Elgetti Brodersen *

Marine Biological Section, Department of Biology, University of Copenhagen, Helsingør, Denmark

Epiphytic biofilms on seagrass leaves can lead to extreme microenvironmental conditions for the encapsulated leaf limiting both its photosynthesis and respiration. Yet, little is known about how the biological activity of the biofilm itself changes the seagrass phyllosphere microenvironment and dynamics. We used microsensors to measure O_2 concentrations and pH gradients and calculate fluxes of O_2, CO_2 and bicarbonate (HCO_3^-) around seagrass leaves (*Z. marina* L.) covered with artificial, inactive biofilms and natural epiphytic biofilms. A sterilized seawater-agar matrix was used to make an artificial "inactive" biofilm on seagrass leaves with the same thickness as the natural leaf epiphytic biofilm, which impeded turbulent exchange of gases but did not have microbial activity. We compared the concentration profiles and fluxes of O_2 and inorganic carbon of the "active" and "inactive" biofilm to investigate the effect of microbial activity and molecular diffusion in seagrass leaf biofilms. In light, the O_2 flux of leaves with inactive biofilm was only 31% of the leaves with active biofilm, indicating that the photosynthesis of the microbial community in the biofilm makes up the majority of O_2 production in the leaf microenvironment. During darkness, the O_2 concentration profiles and O_2 fluxes were almost identical in the "active" and "inactive" biofilms. The pH profiles showed the same trend with an increase in pH of ~1.0 in the "active" biofilms and ~0.3 pH units in the "inactive" biofilms in the light, and both showing a decrease of ~0.3 pH units in darkness compared to the bulk seawater. Our measurements thus demonstrate strong photosynthesis in the epiphyte layer driving phyllosphere basification and inorganic carbon limitation. The calculated CO_2 concentration on the leaf surface decreased to 0.09 μmol L^{-1} in the epiphytic biofilm in the light compared to leaf surface CO_2 concentrations of 13.8 μmol L^{-1} on bare seagrass leaves, and the CO_2 influxes were only 3.0% and 5.4% of O_2 effluxes for leaves with "active" and "inactive" biofilm, respectively. Calculations also showed that HCO_3^- influxes in light accounted for 91-97% of the total inorganic carbon influx to the seagrass leaf, although the HCO_3^- utilization *via* CO_2 concentration mechanisms is energy-consuming. Besides increasing mass

OPEN ACCESS

Edited by:
Tilmann Harder, University of Bremen, Germany

Reviewed by:
Christina C. Roggatz, University of Hull, United Kingdom
Pimchanok Buapet, Prince of Songkla University, Thailand

***Correspondence:**
Kasper Elgetti Brodersen
kasper.elgetti.brodersen@bio.ku.dk

Specialty section:
This article was submitted to Marine Ecosystem Ecology, a section of the journal Frontiers in Marine Science

Received: *14 December 2021*
Accepted: *14 March 2022*
Published: *10 May 2022*

Citation:
Zhang Q, Kühl M and Brodersen KE (2022) Effects of Epiphytic Biofilm Activity on the Photosynthetic Activity, pH and Inorganic Carbon Microenvironment of Seagrass Leaves (Zostera marina L.). Front. Mar. Sci. 9:835381. doi: 10.3389/fmars.2022.835381

transfer impedance, leaf epiphytic biofilm activity thus strongly affects the seagrass leaf microenvironment in the light by inducing higher O_2 concentration and pH, increasing CO_2 limitation and reducing the leaf photosynthetic efficiency.

Keywords: biofilm, carbon, pH, photosynthesis, seagrass

INTRODUCTION

Seagrass meadows are important ecosystems in aquatic environments (Terrados and Borum, 2004). They are found along temperate and tropical coastlines on all continents besides Antarctica, with a documented areal cover of ~125.000 km^2 globally and an estimated cover of >160.000 km^2 with moderate or high confidence (Unsworth and Cullen-Unsworth, 2017; McKenzie et al., 2020). Seagrass meadows are highly productive habitats that maintain high biological diversity of invertebrates, fish and marine mammals, and represent important nursery grounds for juvenile fish (Terrados and Borum, 2004). Seagrass meadows filter terrestrial runoff, reducing pollution and exceeding nutrients (Short and Short, 1984; Lemmens et al., 1996). As a rooted plant, seagrass decreases turbidity and hinders sediment erosion or suspension (Short and Short, 1984) and store substantial amounts of carbon into the sediment (Duarte et al., 2005; Fourqurean et al., 2012). Therefore, seagrass meadows are a considerable carbon sink and play an important role in mitigating climate change (Cullen-Unsworth and Unsworth, 2018). Since 1980, seagrass meadows have been disappearing worldwide at a rate of ~110 km^2 yr^{-1} mainly due to coastal development, poor water quality and climate change as the main threats (Waycott et al., 2009). Protection of seagrass meadows and better understanding of seagrass ecology are key to reversing this decreasing trend.

Coastal eutrophication is a major threat to seagrass ecosystems (Sand-Jensen, 1977; Borum, 1985; Drake et al., 2003). It stimulates epiphyte overgrowth on seagrass leaves affecting the leaf microenvironment, leading to extreme leaf physicochemical conditions for the plant (Ruesink, 2016; Brodersen et al., 2020a; Brodersen et al., 2020b). The epiphytic biofilm microenvironment can e.g., become hyperoxic and basified in the light and turn hypoxic or even anoxic in the dark (Noisette et al., 2020; Brodersen et al., 2020a; Brodersen et al., 2020b). Thick epiphytic biofilms can attenuate more than 50% of the incident photon irradiance of photosynthetically active radiation (PAR; 400–700 nm) and induce leaf surface warming of about 0.6°C, i.e., three times higher than bare leaves without epiphytes in the light (Noisette et al., 2020). Such dramatic microenvironmental changes in the leaf phyllosphere impact the seagrass function and fitness, as well as, the microbial metabolism of the biofilm (Sand-Jensen, 1977; Brodersen et al., 2015a). In Danish waters, bacteria, diatoms and brown algae are commonly present in the epiphytic community with green algae mostly found in spring, and cyanobacteria and red algae mostly present in autumn (Wium-Andersen and Borum, 1984).

The activity of the microbial community in the epiphytic biofilm is an important factor for driving the dynamic nature of the seagrass phyllosphere, where epiphyte respiration and photosynthesis strongly affect the concentrations of essential solutes and gases within the seagrass leaf microenvironment, and microbes compete for dissolved inorganic carbon during the daytime and intensely consume oxygen at night, leading to an often negative relationship between the epiphyte biomass and seagrass photosynthesis (Drake et al., 2003; Brodersen et al., 2015a; Brodersen et al., 2020a; Brodersen et al., 2020b; Noisette et al., 2020). Furthermore, phytotoxic compounds such as nitric oxide (NO) can be produced in the epiphytic biofilm during phyllosphere anoxia *via* anaerobic biochemical processes that can be detrimental to the seagrass leaf and plant (Noisette et al., 2020).

Epiphytes can also obstruct the flow over the leaf surface, impede turbulent transport and slow down solute exchange between the seagrass leaf and the surrounding water *via* molecular diffusion (Koch, 1994). The epiphyte layer thickness together with the diffusive boundary layer (DBL) thickness above the epiphyte/seawater interface constitutes the total diffusion distance (TDD) (Jørgensen and Revsbech, 1985; Jørgensen and Des Marais, 1990). The TDD on leaves with epiphytes is much larger (often up to 10 times thicker) than on bare leaves, and therefore extends the molecular diffusion time and restricts nutrients and gas exchange between seagrass leaves and the surrounding water (Koch, 1994; Noisette et al., 2020). The limited molecular transport impedes the supplement of substrates and metabolic products accumulate within the biofilm, which exacerbate the negative impact of the epiphytic microbiota. In the light, high pH and O_2 levels in the leaf microenvironment reduce the leaf photosynthetic efficiency due to carbon limitation and enhanced photorespiration, which negatively affects the fitness of the seagrass plant (Brodersen et al., 2020a; Brodersen et al., 2020b). Within the basified epiphytic biofilm, CO_2 is rapidly consumed due to abiotic (e.g., high-pH induced change in the carbon speciation towards HCO_3^- and CO_3^{2-}) and biotic (e.g., photosynthetic DIC assimilation) factors, and the carbonate species mostly exist in the form of HCO_3^- (Brodersen et al., 2020a). Most seagrass are able to utilize HCO_3^- as an inorganic carbon source for leaf photosynthesis by using CO_2 concentration mechanisms (CCM), such as facilitated by carbonic anhydrase (CA). However, CCMs are energy-consuming processes that reduce the leaf photosynthetic efficiency (Koch et al., 2013). Furthermore, high O_2 and low CO_2 levels enhance RuBisCO oxygenase activity promoting photorespiration, which further reduces the photosynthetic efficiency of seagrass leaves (Brodersen et al., 2020a). However, to which extent the biological activity of the epiphytic biofilm contributes to the phyllosphere dynamics and affects photosynthesis and inorganic carbon availability for the seagrass leaf remains largely unknown.

In this study, we used a pre-sterilized agar matrix to simulate an "inactive" epiphytic biofilm on seagrass leaves, which impeded mass transfer but did not have microbial activity. We compared the natural "active" and artificial "inactive" biofilm of similar thickness to distinguish between effects of epiphytic microbial activity and mass transfer impedance on seagrass leaf photosynthesis and respiration, as well as the inorganic carbon availability. We also performed comparative measurements on bare seagrass leaves and leaves with the epiphytic biofilm removed.

MATERIALS AND METHODS

Seagrass Sampling

Specimens of *Zostera marina* L. with and without epiphytic biofilms on leaves were collected from shallow coastal waters (<2m depth) at Julebæk, North Zealand, Denmark (56°03'29.2"N; 12°34'40.7"E) during spring (March – May, 2021). The seagrass and the sediment around the roots were transported to the laboratory at the nearby Marine Biological Section (Helsingør, University of Copenhagen, Denmark) and were kept in reservoirs with constantly aerated water (20°C; salinity = 18) under a 12h:12h light/dark cycle (at a photon irradiance of ~200 μmol photons m^{-2} s^{-1} provided by metal-halide lamps, PAR=400-700 nm).

Experimental Procedures and Leaf Encapsulation in Agar Matrix

Seagrass leaf fragments (~8 cm long, cut near the tip from healthy seagrass leaves of similar age with no signs of deterioration) were bend into a slight U-shape, where the ends were mounted on black glass slides with black electrical tape. Microsensor measurements were conducted on the upper side of the leaf fragments (**Figures 1A, B**). Microprofiles of O_2 concentration and pH were first measured (see below) on leaves with epiphytes. Then the epiphytic community was carefully removed with a surgical razorblade, and gradients were measured on the epiphyte-removed (epi-removed) leaves. After these initial measurements, the leaves were briefly placed into a melting agar solution (1.5% w/w, 40°) using filter-sterilized seawater (0.2 μm, with a salinity of 18) to have the agar matrix covering the leaf surface. Briefly, this was done in a custom-made mold with removable glass slides as side walls, which controlled the volume of agar solution to precisely adjust the thickness of the agar matrix (**Figure 1C**). Small screws were positioned beneath both ends of the bare seagrass leaf fragments to bend the leaf slightly (**Figure 1C**), which create a small range of distance from the surface of the agar to the leaf surface, allowing us to perform measurements precisely where the agar encapsulation and thereby the TDD was as thick as the former epiphytic community. The outer limit of the DBL was determined as where the linear O_2 concentration gradient intercepts with the extrapolated bulk water O_2 concentration, and the TDD as the distance between the outer limit of the DBL and the seagrass leaf tissue surface. The depth profiles of O_2 concentration and pH were also measured on bare leaves without visible biofilm growing on the surface. The O_2 concentration and pH gradients were measured on each sample in darkness (i.e., 0 μmol photons m^{-2} s^{-1}) and in light (230 μmol photons m^{-2} s^{-1}). Before measuring each profile, leaf samples were exposed to dark/light conditions for more than 30 minutes until the pH or O_2 concentration at the leaf surface kept constant for minimum 5 minutes; to ensure steady state conditions while microprofiling. The natural epiphytic biofilm was defined as "active" and the artificial biofilm as "inactive" due to the sterilization processes (i.e., using filter-sterilized seawater and boiling the agarose solution) during the casting procedure.

Microsensor Calibration and Measurements

We used O_2 and pH microsensors to measure concentration gradients and calculate chemical fluxes around the seagrass leaves. A Clark-type O_2 microsensor with a tip size of ~25 μm (OX-25, Unisense A/S, Denmark) was linearly calibrated from signal readings in 100% air saturated seawater and anoxic water (using an alkaline ascorbate solution) at experimental temperature and salinity. A pH microelectrode with a tip size of ~100 μm (pH-100, Unisense A/S, Denmark) was calibrated using sensor potential readings against a reference electrode (REF-RM; Unisense A/S, Denmark) in commercial pH buffer solutions (pH 4, pH 7 and pH 10; Hach.com), at experimental salinity and temperature. The length of the sensitive pH glass in pH-100 is 150-250 μm, which limits the spatial resolution in the vertical direction to about 150-250 μm.

The microsensors and the reference electrode were connected to a multichannel microsensor meter (Unisense A/S, Denmark),

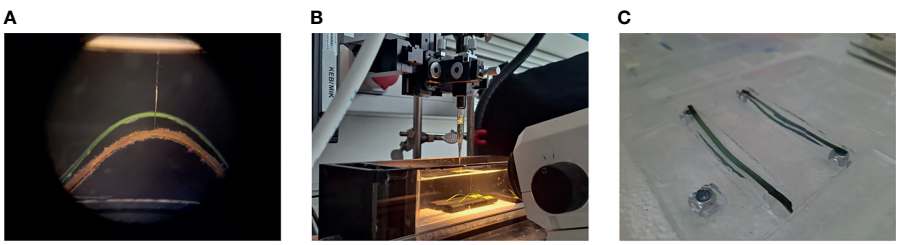

FIGURE 1 | Experimental setup. Example of the bare seagrass leaf (green) and leaf with epiphytes (brown) fixed on the microscope glass slides **(A)**. Leaf fragments in the flow chamber in front of the stereo microscope, and with a microsensor mounted on the motorized micromanipulator above the seagrass leaf samples **(B)**. Bare seagrass leaves and epiphyte-removed leaves in the custom-made mold made by glass slides to shape and determine the volume/height of the agar encapsulation **(C)**.

and the microsensors were mounted on a motorized micromanipulator system (Unisense A/S, Denmark). Both the multichannel microsensor system and the micromanipulator were connected to a PC, where data acquisition and sensor positioning was controlled *via* software (SensorSuite Profiler v3.2, Unisense A/S, Denmark). Microsensor positioning was relative to the seagrass leaf surface, as determined by manually handling the micromanipulator while observing the leaf surface and microsensor tip *via* a stereo microscope.

All microsensor measurement were performed on seagrass leaf fragments fixed onto black glass slides in a flow-chamber supplied with a constant flow (~1 cm s^{-1}) of aerated seawater (at 18° and a salinity of 18) pumped from a supporting aquarium tank beneath the flow chamber (**Figure 1B**). Further information on the experimental setup and procedure can be found in Brodersen et al. (2014) and Noisette et al. (2020). Three or more technical replicates were measured at nearby position on each leaf fragment originating from 5 seagrass plants with natural epiphytic biofilm on the leaves and 4 seagrass plants without epiphytic biofilm; i.e., bare leaves (n = 12-15).

Total Inorganic Carbon Measurements

We used a calibrated total organic carbon analyzer (TOC-L; Shimadzu, Japan) to measure the total dissolved inorganic carbon concentration (DIC) in the bulk seawater around the seagrass leaves during the experiment (n=3). Samples were acidified and sparged to convert DIC into gaseous CO_2 that was quantified with a non-dispersive infrared detector (NDIR).

Microsensor Data Calculations

Assuming that the carbonate system was in equilibrium and thus that pH and the calculated CO_2 and HCO_3^- profiles represent steady-state concentrations (De Beer et al., 1997; De Beer et al., 2000; Brodersen et al., 2020a), concentration profiles of CO_2 and HCO_3^- were calculated from the measured pH microprofiles and the measured DIC in the seawater (Dickson and Millero, 1987; Millero, 2010):

$$DIC = [CO_2] + [HCO_3^-] + [CO_3^{2-}],$$

$$[HCO_3^-] = \frac{DIC \cdot k_1 \cdot [H^+]}{[H^+]^2 + k_1 \cdot [H^+] + k_1 \cdot k_2},$$

$$[CO_2] = \frac{DIC \cdot [H^+]^2}{[H^+]^2 + k_1 \cdot [H^+] + k_1 \cdot k_2},$$

where k_1 is the equilibrium constant of CO_2 hydrolysis to bicarbonate and k_2 is the equilibrium constant of bicarbonate to carbonate conversion at experimental temperature and salinity taken from Mehrbach et al. (1973), Dickson and Millero (1987), and Dickson (2010) ($k_1 = 9.952 \cdot 10^{-7}$, $k_2 = 5.482 \cdot 10^{-10}$, temperature of 18°, salinity=18).

Fluxes of chemical species were calculated according to Fick's first law of diffusion:

$$J = -D \cdot \frac{dC}{dz},$$

where D is the diffusion coefficient of either O_2, CO_2 and HCO_3^- in seawater at experimental temperature and salinity (tabulated values available at www.unisense.com), and $\frac{dC}{dz}$ is the slope of the linear concentration gradient in the DBL.

Data Analysis

We conducted statistical analyses in SPSS (IBM SPSS Statistics 28.0.0). We used independent sample t-tests to assess (1) the differences of O_2 fluxes among the four treatments (i.e., leaf with epiphytes, epiphytes removed, leaf with agar encapsulation and bare leaf) and (2) the difference of carbon fluxes (i.e., CO_2 fluxes and HCO_3^- fluxes) of seagrass leaves with natural epiphytic biofilms and agar coatings (n=15). Furthermore, the confidence interval of the 95% confidence level was calculated using Student's t-distribution to describe the range of our results.

RESULT AND DISCUSSION

Our experiments demonstrated that the presence and activity of epiphytic biofilms on seagrass leaves can induce major changes in the leaf phyllosphere microenvironment during daytime, inducing hyperoxia and increased pH that limited CO_2 availability and reduced the photosynthetic activity and efficiency of the seagrass leaf.

Phyllosphere Diffusion Distance, O_2 and pH Dynamics

The total diffusion distance (TDD = DBL + biofilm thickness) on leaves with epiphytes was 710 ± 91 μm, as compared to 105 ± 9 μm after removing the natural "active" epiphytic biofilm. The thickness of the agar matrix encapsulation and thus the TDD was the same as the thickness of the former epiphytic biofilm covered seagrass leaf. The DBL of bare leaves was 90 ± 6 μm thick. The biological variation in the TDDs and DBLs between the same type of leaf samples were mainly due to the respective thickness of the natural epiphytic biofilm and the surface roughness, respectively (Hurd, 2000; Brodersen et al., 2015a).

Oxygen Dynamics

Oxygen concentration profiles measurements on leaves with epiphytes showed that the oxygen concentration increased from 265 μmol L^{-1} in the bulk 100% air saturated water to 552 μmol L^{-1} at the leaf surface in the light, and decreased to 110 μmol L^{-1} in the dark (**Figure 2A** and **Table 1**; n=5 biological replicates). Similar measurements on seagrass leaves covered with agar (i.e., "inactive" biofilm) showed a similar decrease in darkness, while the increase in oxygen concentration was much less in the light reaching 363 μmol L^{-1} (**Figure 2A** and **Table 1**). A much smaller shift in oxygen concentration between dark and light conditions was measured on the surface of bare leaves and leaves with removed epiphytes surface (**Figure 2B**). The oxygen fluxes from the leaf surface into the active biofilm and from bare leaves to bulk water (i.e., 260 and 233 nmol cm^{-2} h^{-1}, respectively) was 1.7 to 3.2-fold higher than fluxes from leaves after removal of epiphytes and bare seagrass leaves with agar in the light (**Figure 6A**; **Tables 1** and **2**). The oxygen uptake in the dark of bare leaves and leaves after removal of epiphytes was 1.3

to 1.6-fold higher in the dark (231 and 218 nmol cm^{-2} h^{-1}, respectively), as compared to leaves with active or inactive epiphytic biofilms (**Figure 6A**; **Tables 1** and **2**). Such extreme diel changes in the leaf O_2 microenvironment induced by epiphytic biofilm are similar to findings in recent studies (Brodersen et al., 2020a; Noisette et al., 2020).

pH Dynamics

The pH gradients in the active and inactive epiphytic biofilms on seagrass leaves were caused by the balance between photosynthetic CO_2 uptake and respiratory CO_2 production, as well as the proton transport. The pH of the bulk seawater was 7.9, and increased towards the leaf surface in light reaching a pH maximum of pH 8.9 and 8.2 at the surface of seagrass leaves with an active and inactive biofilm, respectively, while pH decreased to a pH 7.6 in the dark (**Figure 3A** and **Table 1**). Such marked phyllosphere basification in the epiphytic biofilm micro-understory is similar to previous studies (Brodersen et al., 2020a). We found no significant changes in pH on bare seagrass leaves and leaves after removal of their epiphytes (**Figure 3B**). This can to some extent be explained by the spatial resolution of the pH microsensor, which is about 150-250 µm and thus larger than the thickness of the DBL on bare leaves. This also strongly limited our CO_2 and HCO_3^- calculations for these leaf types (see below).

Effect of Epiphytes on Dissolved Inorganic Carbon Availability

We calculated CO_2 and HCO_3^- concentrations from measured pH microprofiles and the total concentration of dissolved inorganic carbon (DIC) in the seawater (**Figures 4A** and **5A**). The total DIC in the seawater was 15.1 ± 0.4 mg L^{-1} (or 1257.2 ± 35 µmol L^{-1}). The CO_2 concentration decreased from 14.8 to 0.1 µmol L^{-1} at the leaf surface under the natural epiphytic biofilm in the light (**Figure 4A**), as compared to leaf surface CO_2 concentrations of 9.7 µmol L^{-1} and 13.8 µmol L^{-1} on leaves with inactive biofilm and on epiphyte-removed leaves, respectively (**Figure 4** and **Table 1**). Compared to the leaves without biofilms, the relatively low CO_2 concentration at the leaf surface under inactive and active biofilms (i.e., 9.7 and 0.1 µmol L^{-1}, respectively) indicate a limited CO_2

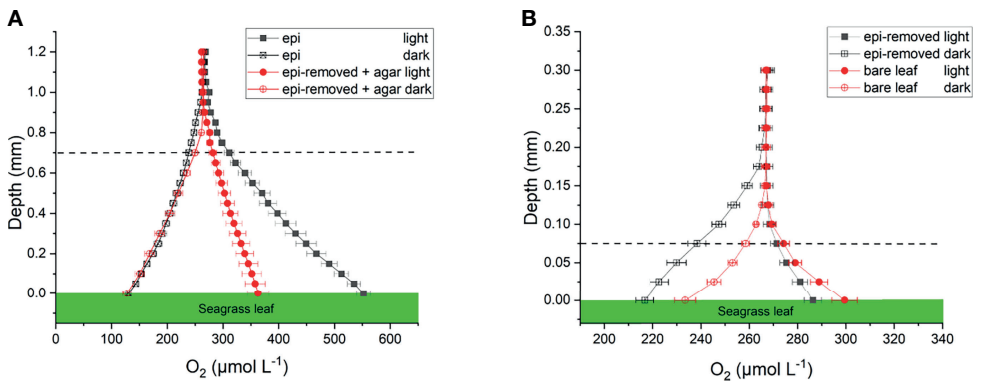

FIGURE 2 | Oxygen concentration profiles measured on seagrass leaves with epiphytes (epi) and leaves where epiphytes were removed (epi-removed) and covered with agar **(A)**, as well as on bare leaves and leaves where epiphytes were removed **(B)** in darkness (0 µmol photons m^{-2} s^{-1}) and light (230 µmol photons m^{-2} s^{-1}). The error bars indicate standard error of mean (SEM); n =15 (replicates with epi, epi-removed and epi-removed + agar), n =12 (bare leaves). Note the different scale on the x- and y-axis between the panels. Dashed line indicates the total diffusion distance (i.e., the surface of the leaf, biofilm or ager + the diffusive boundary layer).

TABLE 1 | O_2, CO_2, HCO_3^- concentrations and pH on the seagrass leaf surface, and O_2, CO_2, HCO_3^- and total carbon flux (mean ± SEM) from leaf surfaces into active (i.e., epi) or inactive biofilm (i.e., epi-removed + agar).

	epi		epi-removed + agar		epi-removed		bare leaf	
	Light	**Dark**	**Light**	**Dark**	**Light**	**Dark**	**Light**	**Dark**
Concentration								
O_2 (µmol L^{-1})	552 ± 12	131 ± 3	363 ± 19	128 ± 8	286 ± 4	217 ± 4	299 ± 5	233 ± 4
pH	8.9 ± 0.1	7.6 ± 0.0	8.2 ± 0.1	7.6 ± 0.0	7.9 ± 0.0	7.9 ± 0.0	7.9 ± 0.0	7.9 ± 0.0
CO_2 (µmol L^{-1})	0.1 ± 0.2	29.7 ± 2.5	9.7 ± 1.3	33.5 ± 24.7	13.8 ± 0.5	13.7 ± 0.5	13.7 ± 0.2	13.5 ± 0.5
HCO_3^- (µmol L^{-1})	920.3 ± 36.9	1236.9 ± 0.8	1169.8 ± 19.2	1250.1 ± 0.6	1264.4 ± 1.5	1264.2 ± 1.1	1264.1 ± 0.7	1264.6 ± 2.0
Flux (nmol cm^{-2} h^{-1})								
O_2	300 ± 58	-162 ± 23	81 ± 11	-164 ± 8	137 ± 22	-218 ± 25	234 ± 25	-231 ± 26
CO_2	-8.1 ± 1.4	14.6 ± 1.8	-4.4 ± 0.5	19.6 ± 1.8				
HCO_3^-	-226.3 ± 15.6	1.1 ± 1.3	-46.4 ± 12.2	2.9 ± 1.8				
Total Carbon	-234.4 ± 17.0	15.7 ± 3.1	-50.7 ± 12.7	22.6 ± 3.5	-0.5 ± 0.4	0.4 ± 0.4	-1.7 ± 0.6	-0.8 ± 0.3

Positive value indicates efflux, negative value indicates influx; n =15 (replicates with epi, epi-removed and epi-removed + agar), n =12 (bare leaves). Note that the CO_2 and HCO_3^- concentrations and fluxes are based on calculated estimates (see the Materials and Methods *section for further information).*

TABLE 2 | Results of the independent sample t-tests (p-value) on O_2 fluxes among our four treatments (i.e., leaves with epiphytes, epiphytes removed, leaves with agar encapsulation and bare leaves) and carbon fluxes (i.e., CO_2 fluxes and HCO_3^- fluxes) on leaves with epiphytes and leaves with agar encapsulation.

		O_2 flux	
		Light	**Dark**
epi	epi-removed +agar	0.008	0.287
	epi-removed	0.045	0.031
	bare leaf	0.357	0.02
epi-removed +agar	epi-removed	0.016	0.027
	bare leaf	<0.001	0.022
bare leaf	epi-removed	0.005	0.364
		C flux	
		light	**dark**
epi	epi-removed +agar	<0.001	<0.001
		CO_2 flux	
		light	**dark**
epi	epi-removed +agar	0.012	0.028
		HCO_3^- flux	
		light	**dark**
epi	epi-removed +agar	<0.001	0.202

availability and supply for the seagrass leaves (**Figure 4A** and **Table 1**). In the inactive biofilm, the thicker TDD reduced the CO_2 availability by 29.9%, whereas in the active biofilm the CO_2 availability was reduced by 99.3% in the light (**Figure 4A**). Moreover, the contribution of CO_2 to the total inorganic carbon influx to the seagrass/epiphyte community also decreased from 12.6% at the epiphyte/water interface (i.e., active biofilm surface), to 8.6% at the leaf/agar interface (i.e., the leaf surface under inactive biofilm), to only 3.3% at the leaf/epiphyte interface (i.e., the leaf surface under the active biofilm). Thus, indicating strong CO_2 consumption by the epiphytic biofilm community markedly reducing the CO_2 availability for the underlying seagrass leaf. The low CO_2 availability at the seagrass leaf surface is thus likely a combined effect of (1) a high-pH induced change in the phyllosphere carbonate system speciation towards bicarbonate, (2) diffusion-limited CO_2 supply to the leaf surface due to thick total diffusion pathways induced by the epiphytic layer, and (3) CO_2 fixation by the photosynthetic organisms within the leaf epiphytic biofilm itself.

The HCO_3^- concentration decreased from 1235 ± 35 to 920 ± 37 μmol L^{-1} through the active epiphytic biofilm in the light, as compared to a leaf surface HCO_3^- concentration of 1170 ± 19 μmol L^{-1} under the inactive biofilm and 1264 ± 2 umol L-1 on the bare leaf surface (**Figure 5** and **Table 1**). The HCO_3^- accounted for 91.4 and 96.7% of the total inorganic carbon flux into the seagrass leaf under the artificial inactive biofilm and active epiphytic biofilm, respectively (**Figures 6B, D** and **Table 1**). Furthermore, the total inorganic carbon flux (i.e., the sum of CO_2 and HCO_3^- fluxes) was 234 ± 8 nmol cm^{-2} h^{-1} on leaves with epiphytes, which was 4.6-fold higher compared to the flux on leaves with artificial inactive biofilm ($p<0.001$), and was consistent with the HCO_3^- influx was 4.9-fold higher than in leaves with inactive biofilm ($p<0.001$, **Figures 6C, D** and **Tables 1**, **2**).

For the CO_2 and HCO_3^- calculation, we assumed a constant DIC concentration and that the carbonate system was in equilibrium within the biofilm/ager. However, as the CO_2 was rapidly produced or consumed and the equilibrium between CO_2 and HCO_3^- is slow, the carbonate system may be out of equilibrium in the steep gradient along the biofilm (because of different diffusivities of CO_2 and HCO_3^-; i.e., diffusion coefficient of $1.5274 \cdot 10^{-5}$ cm^2 s^{-1} for CO_2 and $0.9689 \cdot 10^{-5}$ cm^2 s^{-1} for HCO_3^- at experimental temperature and salinity), which could induce an error to the calculations (De Beer et al., 1997). Therefore, the pH measurements were first conducted when the pH signal was stable to minimize this uncertainty (e.g., De Beer et al., 2000; Brodersen et al., 2020a).

Epiphytic Microenvironment and Leaf Photosynthesis

The leaf epiphyte community showed higher net photosynthetic rates as compared to leaves with inactive biofilm, where the

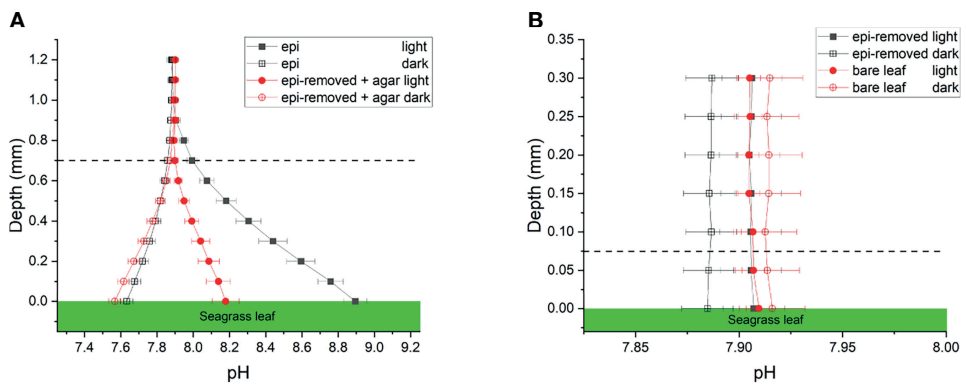

FIGURE 3 | pH profiles measured on seagrass leaves with epiphytes (epi) and leaves where epiphytes were removed (epi-removed) and covered with agar **(A)**, as well as on bare leaves and leaves where epiphytes were removed **(B)** in darkness (0 μmol photons m^{-2} s^{-1}) and light (230 μmol photons m^{-2} s^{-1}). The error bars indicate SEM; n =15 (replicates with epi, epi-removed and epi-removed + agar), n =12 (bare leaves). Note the different scale of the x- and y-axis between panels. Dashed line indicates the total diffusion distance (i.e., the surface of the leaf, biofilm or ager + the diffusive boundary layer).

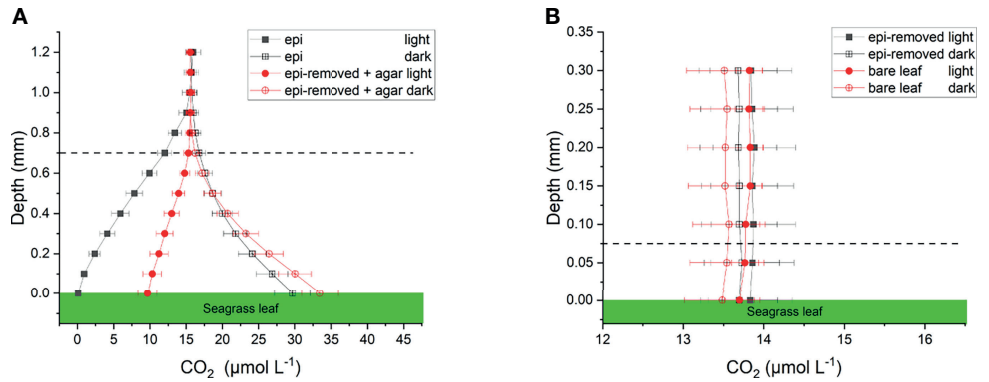

FIGURE 4 | Calculated CO_2 profiles over seagrass leaves with epiphytes (epi) and leaves where epiphytes were removed (epi-removed) and covered with agar **(A)**, as well as on bare leaves and leaves where epiphytes were removed **(B)** in darkness (0 µmol photons m^{-2} s^{-1}) and light (230 µmol photons m^{-2} s^{-1}). The error bars indicate SEM; n =15 (replicates with epi, epi-removed and epi-removed + agar), n =12 (bare leaves). Calculated based on measured pH microprofiles and total DIC measurements in seawater. Note the different scale on the x- and y-axis between panels. Dashed line indicates the total diffusion distance (i.e., the surface of the leaf, biofilm or ager + the diffusive boundary layer).

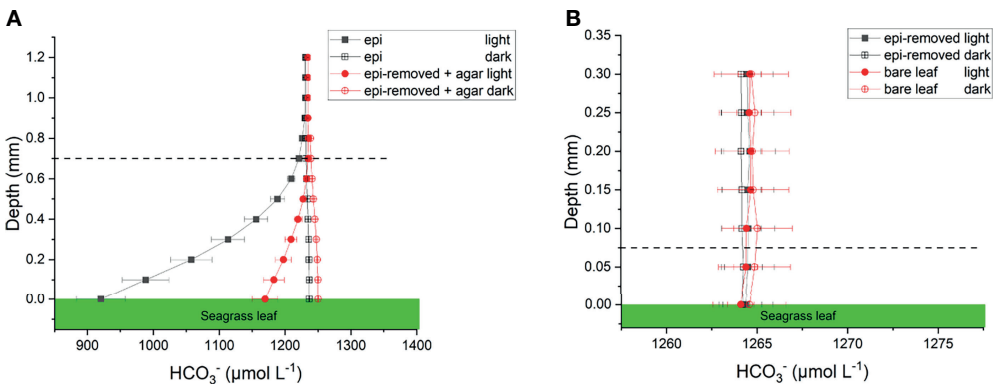

FIGURE 5 | Calculated HCO_3^- profiles on seagrass leaves with epiphytes (epi) and leaves where epiphytes were removed (epi-removed) and covered with agar **(A)**, as well as on bare leaves and leaves where epiphytes were, removed **(B)** in darkness (0 µmol photons m^{-2} s^{-1}) and light (230 µmol photons m^{-2} s^{-1}). The error bars indicate SEM; n =15 (replicates with epi, epi-removed and epi-removed + agar), n =12 (bare leaves). Calculated based on measured pH microprofiles and total DIC measurements in seawater. Note the different scale on the x- and y-axis between panels. Dashed line indicates the total diffusion distance (i.e., the surface of the leaf, biofilm or ager + the diffusive boundary layer).

oxygen flux of leaves with inactive biofilm was 31% of the leaf with active biofilm (p=0.008; **Figure 6A** and **Tables 1**, **2**). The photosynthesis of the microbial community thus composed most of the oxygen production in the seagrass leaf microenvironment (about 69%); which might actually be underestimated as the epiphyte micro-understory is receiving less light of lower quality owing to shading effects and predominantly blue and red light absorption in the uppermost part of the natural epiphytic biofilm (Brodersen et al., 2015a; Brodersen and Kühl, 2022). The oxygen concentration profiles and oxygen flux were almost the same in active and inactive biofilm during darkness (p=0.287; **Figures 2A**, **6A** and **Tables 1**, **2**), indicating that the activity of the microbial community in the epiphytic biofilm contributed little to the respiration of the combined leaf/epiphyte community. The oxygen concentration gradient was thus mainly formed because of the effect of the TDD on molecular diffusion in our experiments. The apparent low dark respiration in the natural biofilm could be due to low bacterial biomass and/or that dark respiration often only accounts for ~10% of photosynthesis rates at light-saturation in microalgae (Geider & Osborne, 1989), and we note that other epiphytic biofilms might show a stronger effect on O_2 availability for the seagrass leaf in darkness due to higher respiration rates.

The total inorganic carbon influxes across the seagrass leaves were of similar magnitude as the corresponding oxygen effluxes for leaves with epiphytes and leaves with inactive biofilm in the light (i.e., CO_2/O_2 flux ratios of about 0.90 and 0.63, respectively) (**Figures 6A, B** and **Table 1**). However, the CO_2 influxes were

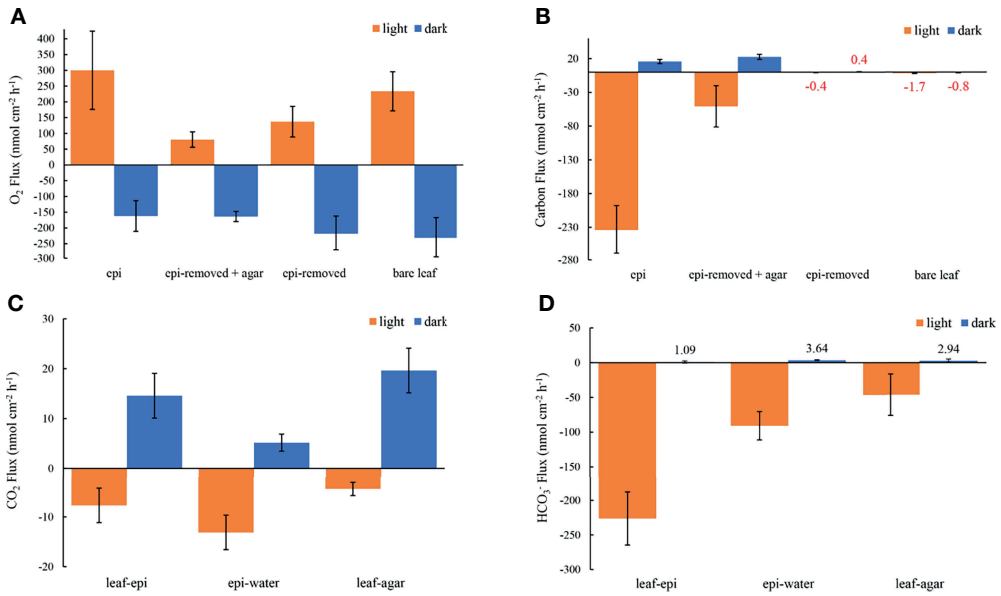

FIGURE 6 | Measured O_2 fluxes at seagrass leaf surfaces **(A)**, the estimated carbon fluxes as the sum of CO_2 and HCO_3^- fluxes at leaf surfaces **(B)**, the estimated CO_2 fluxes and HCO_3^- fluxes from leaf to epiphyte, from epiphyte to water and from leaf to agar (**C**, **D**, respectively) in darkness (0 µmol photons m^{-2} s^{-1}, blue) and light (230 µmol photons m^{-2} s^{-1}, orange). The error bars indicate the confidence interval of 95% confidence level according to the Student's t distribution; n =15 (replicates with epi, epi-removed and epi-removed + agar), n =12 (bare leaves). Positive values denote efflux and negative values denote influx across the respective interface. Note in panel b, that it was not really possible to calculate the total carbon flux for leaves with the epiphytes removed and for the bare leaves, both with very thin DBLs, due to the limited spatial resolution of the pH microsensor (mean values are marked with red color code).

only 3.0% and 5.4% of oxygen effluxes for leaves with active epiphytic biofilm and leaves with inactive biofilm, respectively (**Figures 6A, C** and **Table 1**); i.e., similar to findings in a previous study on *Z. marina* leaves with epiphytic biofilms (Brodersen et al., 2020a) and other marine organisms like symbiont-bearing foraminifera (Köhler-Rink and Kühl, 2005) and corals (De Beer et al., 2000). Some of this discrepancy can be explained by (1) that O_2 acts as an alternative electron acceptor to CO_2 in photosynthesis *via* photorespiration in *Z. marina* plants (Buapet and Björk, 2016), and/or (2) that the O_2/CO_2 ratio at the site of RuBisCo differs from the leaf surface concentrations and fluxes due to internal carbon concentration mechanisms involving enhanced local enzymatic dehydration of HCO_3^- to CO_2 facilitated by CA, (Köhler-Rink and Kühl, 2005; De Beer et al., 2000), as well as CO_2 supply mechanism likely involving the aerenchyma. The leaf or leaf/epiphytes community thus consumed CO_2 rapidly in light, and especially the natural active biofilm strongly impeded CO_2 supply from the bulk seawater to the underlying leaf, causing low CO_2 concentration and low CO_2 influxes into seagrass leaves with epiphytes. Such DIC competition between plants and epiphytic biofilms is similar to other aquatic plants (e.g., Jones et al., 2002; Wijewardene et al., 2022) and makes seagrass highly dependent on HCO_3^- utilization. The low CO_2 availability limits seagrass leaf photosynthesis (**Figure 6A**) when comparing the O_2 production of epiphyte-removed leaves and the epiphyte-removed and agar encapsulated (i.e., inactive biofilm) leaves, which both excluded microbial activity. Here, the O_2 efflux on epiphyte-removed leaves was 1.7-fold higher than from the leaves with inactive biofilms (p=0.016; **Figure 6A** and **Tables 1**, **2**), which can be attributed to the reduced-CO_2 leaf microenvironment. Furthermore, the O_2 efflux of epiphyte-removed leaves was only 58% compared to natural bare leaves (p=0.005; **Figure 6A** and **Tables 1**, **2**) indicating that leaves under epiphytic biofilms were of lower fitness and health; although the respiration was of similar order of magnitude (p=0.364; **Figure 6A** and **Tables 1**, **2**).

The activity of epiphytic biofilm thus results in dramatic changes in the seagrass leaf microenvironment, as O_2 concentration and pH increased in light, and most DIC (73.2-98.2%) facilitated by CA existed in the form of HCO_3^- within the basified phyllosphere. Most seagrasses including *Zostera marina* L. are able to utilize HCO_3^- as source of inorganic carbon in photosynthesis (Koch et al., 2013), and our results showed that the HCO_3^- influx was 29.5-fold higher than the CO_2 influx in light, accounting for 96.7% of the total inorganic carbon influx to the leaf surface under the active biofilm (**Figures 6B, C** and **Table 1**). However, the direct uptake of HCO_3^- and intracellular conversion of HCO_3^- to CO_2 or extracellular conversion by extracellular carbonic anhydrase are all energy-consuming CO_2 concentration mechanisms (CCM), reducing the efficiency of carbon assimilation and energy storage (Lucas, 1985; Larkum et al., 1989; Larsson and Axelsson, 1999; Hellblom et al., 2001; Beer et al., 2002; Hellblom and Axelsson, 2003). Another energy-expensive potential CCM is using proton pumps to locally acidify the leaf surface, which for seagrasses have been suggested several times in previous studies (e.g., Beer et al., 2002; Borum et al.,

2016). Here, the hypothesis is that acid zones on the leaf surface of marine plants increase the CO_2 availability for photosynthesis-driven carbon fixation through local stimulation of CO_2 formation, *via* low-pH driven conversion of HCO_3^- to CO_2, within the leaf diffusive boundary layers by proton (H^+) extrusion (Beer et al., 2002). However, our detailed pH measurements in high spatiotemporal resolution (~0.1 mm) within the leaf DBL did not show any indications of a general acidification of the seagrass leaf DBL as a possible CO_2 concentration mechanism (**Figure 3**); even not in the pH measurements on leaves with agar that artificially increased the TDD and thereby allowed for several point measurements with the pH microsensor within the artificially increased proton diffusion pathway. However, if such leaf surface acidification mechanism, exists, as indicated by utilizing pH buffers in previous studies (Larkum et al., 2017), it must be very localized within separated leaf micro-acid zones. In darkness, the respiration of seagrass leaves and epiphytic biofilm lead to hypoxic conditions on the leaf surface driven by the DBL and TDD decreasing the diffusive O_2 supply from the surrounding water to the plant. Such decreased availability of oxygen makes seagrass more susceptible to suffocation and H_2S intrusion from the surrounding sediment due to restricted intra-diffusional O_2 transport to below-ground tissues *via* the aerenchyma (Brodersen et al., 2015b). Under global warming, such inadequate internal tissue and rhizosphere aeration may be further aggravated owing to temperature-induced enhanced epiphyte and leaf respiration.

In a previous study of epiphytic biofilms on *Z. marina* L., the pH reached 9.6 in a very dense and thick epiphytic biofilm (1.2 mm) in the light (300 μmol photons m^{-2} s^{-1}), and CO_2 microsensor measurements showed that the CO_2 concentration decreased to 0 μmol L^{-1} ~0.2 mm above the leaf surface, which is consistent with our measurements and calculations (Brodersen et al., 2020a). High O_2 and low CO_2 concentrations on the leaf surface reduce the O_2 efflux and CO_2 influx, causing O_2 accumulation intracellularly and low intracellular CO_2 concentrations, which impede leaf photosynthesis and enhance photorespiration (Mass et al., 2010), thus representing a threat to seagrass photosynthetic performance and overall health (Sand-Jensen et al., 1992; Raven et al., 2014; Buapet and Björk, 2016). Furthermore, a previous study demonstrated reduced seagrass gross photosynthetic rates at high pH, high O_2 and low DIC seawater, with a maximum decrease in gross photosynthetic rate of 75% detected in *Zostera marina*; thus, further supporting our finding that the basified leaf microenvironment induced by epiphytic biofilms in the light has strong negative impacts on seagrass leaf photosynthesis (Buapet et al., 2013). Combined with increased respiration under global warming, such epiphyte-induced reduced leaf photosynthesis may lead to a negative oxygen and carbon balance in exposed seagrass plants; putting key ecosystem services at risk of ceasing. Eutrophication stimulates epiphytic biofilm overgrowth of seagrass leaves (Borum, 1985), where a previous study has shown 3 to 5-fold higher epiphyte biomass in nitrogen and phosphorus-enriched seawater compared to ambient seawater (Jaschinski and Sommer, 2008). Coastal eutrophication is therefore likely to put more stress on exposed seagrass meadows. However, it is important to mention that epiphytes can also be beneficial to the plant hosts. Microorganisms, can e.g., facilitate uptake of dissolved organic nitrogen by seagrass leaves (Tarquinio et al., 2018).

In conclusion, we found that microbial activity in epiphytic biofilms mostly affected the seagrass leaf chemical microenvironment in the light: causing (1) high O_2 and pH conditions and (2) strong consumption of inorganic carbon, which leads to low carbon availability for the seagrass plant. Furthermore, leaves with the epiphytes removed produced less oxygen than the bare leaf and thus exhibited lower photosynthetic capacity. In the basified phyllosphere, the relatively low CO_2 concentration and thus intensified demand for energy-requiring HCO_3^- utilization limited leaf photosynthesis, and the high O_2 and low CO_2 concentration in the cell will increase photorespiration and further reduce the photosynthetic efficiency. In eutrophic coastal waters, the overgrowth of seagrass leaves with epiphytic biofilm resulting in thicker TDD and strong microbial activity can thus lead to intense diurnal changes in the seagrass leaf chemical microenvironment that can have negative impacts on seagrass performance and therefore is a potential hazard for seagrass fitness and vital ecosystem function.

DATA AVAILABILITY STATEMENT

The original contributions presented in the study are included in the article/supplementary material. Further inquiries can be directed to the corresponding author.

AUTHOR CONTRIBUTIONS

KB and MK designed experiments and provided essential infrastructure. QZ performed the experiments and analyzed the data (supervised by KB). QZ wrote the manuscript with editorial help from all co-authors. All authors have given approval to the final version of the manuscript.

FUNDING

This research project was funded by grants from the Villum Foundation (KB; 00028156) and the Independent Research Fund Denmark (MK; DFF-8021-00308B).

ACKNOWLEDGMENTS

We thank Nikola Medic, Victoria Thuesen, Mary Gonzales and Cecilie Appeldorff (UCPH) for technical assistance.

REFERENCES

Beer, S., Bjork, M., Hellblom, F., and Axelsson, L. (2002). Inorganic Carbon Utilization in Marine Angiosperms (Seagrasses). *Funct. Plant Biol.* 29, 349–354. doi: 10.1071/PP01185

Borum, J. (1985). Development of Epiphytic Communities on Eelgrass (*Zostera Marina*) Along a Nutrient Gradient in a Danish Estuary. *Mar. Biol.* 87 (2), 211–218. doi: 10.1007/BF00539431

Borum, J., Pedersen, O., Kotula, L., Fraser, M. W., Statton, J., Colmer, T. D., et al. (2016). Photosynthetic Response to Globally Increasing CO_2 of Co-Occurring Temperate Seagrass Species. *Plant Cell Environ.* 39 (6), 1240–1250. doi: 10.1111/pce.12658

Brodersen, K. E., Koren, K., Revsbech, N. P., and Kühl, M. (2020a). Strong Leaf Surface Basification and CO_2 Limitation of Seagrass Induced by Epiphytic Biofilm Microenvironments. *Plant Cell Environ.* 43 (1), 174–187. doi: 10.1111/pce.13645

Brodersen, K. E., and Kühl, M. (2022). Effects of Epiphytes on the Seagrass Phyllosphere. *Front. Mar. Sci.* 9, 821614. doi: 10.3389/fmars.2022.821614

Brodersen, K. E., Kühl, M., Trampe, E., and Koren, K. (2020b). Imaging O_2 Dynamics and Microenvironments in the Seagrass Leaf Phyllosphere With Magnetic Optical Sensor Nanoparticles. *Plant J.* 104 (6), 1504–1519. doi: 10.1111/tpj.15017

Brodersen, K. E., Lichtenberg, M., Paz, L. C., and Kühl, M. (2015a). Epiphyte-Cover on Seagrass (*Zostera Marina L.*) Leaves Impedes Plant Performance and Radial O_2 Loss From the Below-Ground Tissue. *Front. Mar. Sci.* 2, 58. doi: 10.3389/fmars.2015.00058

Brodersen, K. E., Nielsen, D. A., Ralph, P. J., and Kühl, M. (2014). A Split Flow Chamber With Artificial Sediment to Examine the Below-Ground Microenvironment of Aquatic Macrophytes. *Mar. Biol.* 161 (12), 2921–2930. doi: 10.1007/s00227-014-2542-3

Brodersen, K. E., Nielsen, D. A., Ralph, P. J., and Kühl, M. (2015b). Oxic Microshield and Local P H Enhancement Protects *Zostera Muelleri* From Sediment Derived Hydrogen Sulphide. *N. Phytol.* 205 (3), 1264–1276. doi: 10.1111/nph.13124

Buapet, P., and Björk, M. (2016). The Role of O2 as an Electron Acceptor Alternative to CO2 in Photosynthesis of the Common Marine Angiosperm *Zostera Marina* L. *Photosynth. Res.* 129 (1), 59–69. doi: 10.1007/s11120-016-0268-4

Buapet, P., Rasmusson, L. M., Gullström, M., and Björk, M. (2013). Photorespiration and Carbon Limitation Determine Productivity in Temperate Seagrasses. *PloS. One.* 8 (12), e83804. doi: 10.1371/journal.pone.0083804

Cullen-Unsworth, L. C., and Unsworth, R. (2018). A Call for Seagrass Protection. *Science* 361 (6401), 446–448. doi: 10.1126/science.aat7318

De Beer, D., Glud, A., Epping, E., and Kûhl, M. (1997). A Fast-Responding CO_2 Microelectrode for Profiling Sediments, Microbial Mats, and Biofilms. *Limnol. Oceanogr.* 42 (7), 1590–1600. doi: 10.4319/lo.1997.42.7.1590

De Beer, D., Kühl, M., Stambler, N., and Vaki, L. (2000). A Microsensor Study of Light Enhanced CA_2^+ Uptake and Photosynthesis in the Reef-Building Hermatypic Coral Favia sp. *Mar. Ecol. Prog. Ser.* 194, 75–85. doi: 10.3354/meps194075

Dickson, A. G. (2010). The Carbon Dioxide System in Seawater: Equilibrium Chemistry and Measurements. *Guide to Best Practices for Ocean Acidification Research and Data Reporting.* (Luxembourg: Publications Office of the European Union). 1, 17–40. doi: 10.1016/0198-0149(87)90021-5

Dickson, A. G., and Millero, F. J. (1987). A Comparison of the Equilibrium Constants for the Dissociation of Carbonic Acid in Seawater Media. *Deep Sea Res. Part A Oceanogr. Res. Pap.* 34 (10), 1733–1743. doi: 10.1016/0198-0149(87)90021-5

Drake, L. A., Dobbs, F. C., and Zimmerman, R. C. (2003). Effects of Epiphyte Load on Optical Properties and Photosynthetic Potential of the Seagrasses *Thalassia testudinum* Banks Ex König and *Zostera marina* L. *Limnol. Oceanogr.* 48 (1part2), 456–463. doi: 10.4319/lo.2003.48.1_part_2.0456

Duarte, C. M., Middelburg, J., and Caraco, N. (2005). Major Role of Marine Vegetation on the Oceanic Carbon Cycle. *Biogeosciences* 2, 1–8. doi: 10.5194/bg-2-1-2005

Fourqurean, J. W., Duarte, C. M., Kennedy, H., Marba, N., Holmer, M., Mateo, M. A., et al. (2012). Seagrass Ecosystems as a Globally Significant Carbon Stock. *Nat. Geosci.* 5 (7), 505–509. doi: 10.1038/ngeo1477

Geider, R. J., and Osborne, B. A. (1989). Respiration and Microalgal Growth: A Review of the Quantitative Relationship Between Dark Respiration and Growth. *N. Phytol.* 112 (3), 327–341. doi: 10.1111/j.1469-8137.1989.tb00321.x

Hellblom, F., and Axelsson, L. (2003). External HCO_3^- Dehydration Maintained by Acid Zones in the Plasma Membrane Is An Important Component of the Photosynthetic Carbon Uptake in *Ruppia cirrhosa*. *Photosynth. Res.* 77, 173–181. doi: 10.1023/A:1025809415048

Hellblom, F., Beer, S., Björk, M., and Axelsson, L. (2001). A Buffer Sensitive Inorganic Carbon Utilization System in *Zostera marina*. *Aquat. Bot.* 69, 55–62. doi: 10.1016/S0304-3770(00)00132-7

Hurd, C. L. (2000). Water Motion, Marine Macroalgal Physiology, and Production. *J. Phycol.* 36 (3), 453–472. doi: 10.1046/j.1529-8817.2000.99139.x

Jørgensen, B. B., and Des Marais, D. J. (1990). The Diffusive Boundary Layer of Sediments: Oxygen Microgradients Over a Microbial Mat. *Limnol. Oceanogr.* 35 (6), 1343–1355. doi: 10.4319/lo.1990.35.6.1343

Jørgensen, B. B., and Revsbech, N. P. (1985). Diffusive Boundary Layers and the Oxygen Uptake of Sediments and Detritus 1. *Limnol. Oceanogr.* 30 (1), 111–122. doi: 10.4319/lo.1985.30.1.0111

Jaschinski, S., and Sommer, U. (2008). Top-Down and Bottom-Up Control in an Eelgrass–Epiphyte System. *Oikos* 117 (5), 754–762. doi: 10.1111/j.0030-1299.2008.16455.x

Jones, J. I., Young, J. O., Eaton, J. W., and Moss, B. (2002). The Influence of Nutrient Loading, Dissolved Inorganic Carbon and Higher Trophic Levels on the Interaction Between Submerged Plants and Periphyton. *J. Ecol.* 90 (1), 12–24. doi: 10.1046/j.0022-0477.2001.00620.x

Koch, E. (1994). Hydrodynamics, Diffusion-Boundary Layers and Photosynthesis of the Seagrasses *Thalassia Testudinum* and *Cymodocea Nodosa*. *Mar. Biol.* 118 (4), 767–776. doi: 10.1007/BF00347527

Koch, M., Bowes, G., Ross, C., and Zhang, X. H. (2013). Climate Change and Ocean Acidification Effects on Seagrasses and Marine Macroalgae. *Global Change Biol.* 19, 103–132. doi: 10.1111/j.1365-2486.2012.02791.x

Köhler-Rink, S., and Kühl, M. (2005). The Chemical Microenvironment of the Symbiotic Planktonic Foraminifer *Orbulina Universa*. *Mar. Biol. Res.* 1 (1), 68–78. doi: 10.1080/17451000510019015

Larkum, A. W. D., Davey, P. A., Kuo, J., Ralph, P. J., and Raven, J. A. (2017). Carbon-Concentrating Mechanisms in Seagrasses. *J. Exp. Bot.* 68 (14), 3773–3784. doi: 10.1093/jxb/erx206

Larkum, A. W. D., Roberts, G., Kuo, J., and Strother, S. (1989). "Gaseous Movement in Seagrasses," in *Biology of Seagrasses. A Treatise on the Biology of Seagrasses with Special Reference to the Australian Region* (Amsterdam: Elsevier Science Publishers BV), 686–722.

Larsson, C., and Axelsson, L. (1999). Bicarbonate Uptake and Utilization in Marine Macroalgae. *Eur. J. Phycol.* 34, 79–86. doi: 10.1080/09670269910001736112

Lemmens, J. W. T. J., Clapin, G., Lavery, P., and Cary, J. (1996). Filtering Capacity of Seagrass Meadows and Other Habitats of Cockburn Sound, Western Australia. *Mar. Ecol. Prog. Ser.* 143, 187–200. doi: 10.3354/meps143187

Lucas, W. J., and Berry, J. A. (1985). Inorganic Carbon Uptake by Aquatic Photosynthetic Organisms *Physiol. Plant.* 65 (1985), 539–543. doi: 10.1111/j.1399-3054.1985.tb08687.x

Mass, T., Genin, A., Shavit, U., Grinstein, M., and Tchernov, D. (2010). Flow Enhances Photosynthesis in Marine Benthic Autotrophs by Increasing the Efflux of Oxygen From the Organism to the Water. *Proc. Natl. Acad. Sci.* 107 (6), 2527–2531. doi: 10.1073/pnas.0912348107

McKenzie, L. J., Nordlund, L. M., Jones, B. L., Cullen-Unsworth, L. C., Roelfsema, C., and Unsworth, R. K. (2020). The Global Distribution of Seagrass Meadows. *Environ. Res. Lett.* 15 (7), 074041. doi: 10.1088/1748-9326/ab7d06

Mehrbach, C., Culberson, C. H., Hawley, J. E., and Pytkowicx, R. M. (1973). Measurement of the Apparent Dissociation Constants of Carbonic Acid In Seawater at Atmospheric Pressure. *Limno.Oceanogr* 18 (6), 897–907. doi: 10.4319/lo.1973.18.6.0897

Millero, F. J. (2010). Carbonate Constants for Estuarine Waters. *Mar. Freshw. Res.* 61 (2), 139–142. doi: 10.1071/MF09254

Noisette, F., Depetris, A., Kühl, M., and Brodersen, K. E. (2020). Flow and Epiphyte Growth Effects on the Thermal, Optical and Chemical Microenvironment in the Leaf Phyllosphere of Seagrass (*Zostera Marina*). *J. R. Soc. Inter.* 17 (171), 20200485. doi: 10.1098/rsif.2020.0485

Raven, J. A., Beardall, J., and Giordano, M. (2014). Energy Costs of Carbon Dioxide Concentrating Mechanisms in Aquatic Organisms. *Photosynth. Res.* 121, 111–124. doi: 10.1007/s11120-013-9962-7

Ruesink, J. L. (2016). Epiphyte Load and Seagrass Performance are Decoupled in an Estuary With Low Eutrophication Risk. *J. Exp. Mar. Biol. Ecol.* 481, 1–8. doi: 10.1016/j.jembe.2016.03.022

Sand-Jensen, K. A. J. (1977). Effect of Epiphytes on Eelgrass Photosynthesis. *Aquat. Bot.* 3, 55–63. doi: 10.1016/0304-3770(77)90004-3

Sand-Jensen, K. A. J., Pedersen, M. F., and Nielsen, S. L. (1992). Photosynthetic Use of Inorganic Carbon Among Primary and Secondary Water Plants in Streams. *Freshw. Biol.* 27 (2), 283–293. doi: 10.1111/j.1365-2427.1992.tb00540.x

Short, F. T., and Short, C. A. (1984). "The Seagrass Filter: Purification of Estuarine and Coastal Waters," in *The Estuary as a Filter* (Cambridge, Massachusetts: Academic Press), p. 395–413.

Tarquinio, F., Bourgoure, J., Koenders, A., Laverock, B., Säwström, C., and Hyndes, G. A. (2018). Microorganisms Facilitate Uptake of Dissolved Organic Nitrogen by Seagrass Leaves. *ISME J.* 12 (11), 2796–2800. doi: 10.1038/s41396-018-0218-6

Terrados, J., and Borum, J. (2004). "Why are Seagrasses Important? Goods and Services Provided by Seagrass Meadows," in *European Seagrasses* (The M&MS Project), p. 8–10.

Unsworth, R. K., and Cullen-Unsworth, L. C. (2017). Seagrass Meadows. *Curr. Biol.* 27 (11), R443–R445. doi: 10.1016/j.cub.2017.01.021

Waycott, M., Duarte, C. M., Carruthers, T. J., Orth, R. J., Dennison, W. C., Olyarnik, S., et al. (2009). Accelerating Loss of Seagrasses Across the Globe Threatens Coastal Ecosystems. *Proc. Natl. Acad. Sci.* 106 (30), 12377–12381. doi: 10.1073/pnas.0905620106

Wijewardene, L., Wu, N., Fohrer, N., and Riis, T. (2022). Epiphytic Biofilms in Freshwater and Interactions With Macrophytes: Current Understanding and Future Directions. *Aquat. Bot.* 176, 103467. doi: 10.1016/j.aquabot.2021.103467

Wium-Andersen, S., and Borum, J. (1984). Biomass Variation and Autotrophic Production of an Epiphyte-Macrophyte Community in a Coastal Danish Area: I. Eelgrass (*Zostera Marina* L.) Biomass and Net Production. *Ophelia* 23 (1), 33–46. doi: 10.1080/00785236.1984.10426603

Conflict of Interest: The authors declare that the research was conducted in the absence of any commercial or financial relationships that could be construed as a potential conflict of interest.

Publisher's Note: All claims expressed in this article are solely those of the authors and do not necessarily represent those of their affiliated organizations, or those of the publisher, the editors and the reviewers. Any product that may be evaluated in this article, or claim that may be made by its manufacturer, is not guaranteed or endorsed by the publisher.

frontiers | Frontiers in Marine Science

ORIGINAL RESEARCH
published: 22 July 2022
doi: 10.3389/fmars.2022.920699

Influence of Rising Water Temperature on the Temperate Seagrass Species Eelgrass (*Zostera marina* L.) in the Northeast USA

Holly K. Plaisted[1], Erin C. Shields[2,3], Alyssa B. Novak[4], Christopher P. Peck[5], Forest Schenck[6], Jillian Carr[7], Paul A. Duffy[5], N. Tay Evans[6], Sophia E. Fox[8], Stephen M. Heck[9], Robbie Hudson[10], Trevor Mattera[11], Kenneth A. Moore[3], Betty Neikirk[2,3], David B. Parrish[2,3], Bradley J. Peterson[9], Frederick T. Short[12] and Amanda I. Tinoco[9]*

[1]Northeast Coastal and Barrier Network, United States National Park Service, Kingston, RI, United States, [2]Chesapeake Bay National Estuarine Research Reserve in Virginia, Gloucester Point, VA, United States, [3]Virginia Institute of Marine Science, William & Mary, Gloucester Point, VA, United States, [4]Department of Earth and Environment, Boston University, Boston, MA, United States, [5]Neptune and Company, Inc., Denver, CO, United States, [6]Habitat Program, Massachusetts Division of Marine Fisheries, Boston, MA, United States, [7]Massachusetts Bays National Estuary Partnership, Boston, MA, United States, [8]Cape Cod National Seashore, United States National Park Service, Wellfleet, MA, United States, [9]School of Marine and Atmospheric Science, Stony Brook University, Stony Brook, NY, United States, [10]College of the Environment and Life Sciences, University of Rhode Island, Kingston, RI, United States, [11]Piscataqua Region Estuaries Partnership, Habitat Program, Durham, NH, United States, [12]Jackson Estuarine Laboratory, Department of Natural Resources and the Environment, University of New Hampshire, Durham, NH, United States

OPEN ACCESS

Edited by:
Kasper Elgetti Brodersen, University of Copenhagen, Denmark

Reviewed by:
Michael Alan Rasheed, James Cook University, Australia
Martin Dahl, Södertörn University, Sweden

***Correspondence:**
Holly K. Plaisted
holly_plaisted@nps.gov

Specialty section:
This article was submitted to Marine Ecosystem Ecology, a section of the journal Frontiers in Marine Science

Received: *14 April 2022*
Accepted: *10 June 2022*
Published: *22 July 2022*

Citation:
Plaisted HK, Shields EC, Novak AB, Peck CP, Schenck F, Carr J, Duffy PA, Evans NT, Fox SE, Heck SM, Hudson R, Mattera T, Moore KA, Neikirk B, Parrish DB, Peterson BJ, Short FT and Tinoco AI (2022) Influence of Rising Water Temperature on the Temperate Seagrass Species Eelgrass (Zostera marina L.) in the Northeast USA. Front. Mar. Sci. 9:920699. doi: 10.3389/fmars.2022.920699

Sea surface temperature (SST) has increased worldwide since the beginning of the 20th century, a trend which is expected to continue. Changes in SST can have significant impacts on marine biota, including population-level shifts and alterations in community structure and diversity, and changes in the timing of ecosystem events. Seagrasses are a group of foundation species that grow in shallow coastal and estuarine systems, where they provide many ecosystem services. Eelgrass, *Zostera marina* L., is the dominant seagrass species in the Northeast United States of America (USA). Multiple factors have been cited for losses in this region, including light reduction, eutrophication, and physical disturbance. Warming has the potential to exacerbate seagrass loss. Here, we investigate regional changes in eelgrass presence and abundance in relation to local water temperature using monitoring data from eight sites in the Northeastern USA (New Hampshire to Maryland) where a consistent monitoring protocol, SeagrassNet, has been applied. We use a hurdle model consisting of a generalized additive mixed model (GAMM) with binomial and beta response distributions for modeling eelgrass presence and abundance, respectively, in relation to the local summer average water temperature. We show that summer water temperature one year prior to monitoring is a significant predictor of eelgrass presence, but not abundance, on a regional scale. Above average summer temperatures correspond to a decrease in probability of eelgrass presence (and increased probability of eelgrass absence) the following year. Cooler than average temperatures in the preceding year, down to approximately 0.5°C below the site average, are associated with the highest predicted probability of eelgrass presence. Our findings

suggest vulnerability in eelgrass meadows of the Northeast USA and emphasize the value of unified approaches to seagrass monitoring, conservation and management at the seascape scale.

Keywords: seagrass (Zostera), climate change, monitoring, sea surface temperature, *Zostera marina*

INTRODUCTION

Sea surface temperature (SST) has increased worldwide since the beginning of the 20th century (Hartmann et al., 2013; NOAA, 2016a; NOAA, 2016b). In the Northern Hemisphere, SST is projected to rise by approximately 0.05 to 0.5°C per decade to the end of the 21st century (Alexander et al., 2018), with warming expected to be amplified in shallow coastal waters (Oczkowski et al., 2015). The primary cause of increasing SST is climate warming due to increasing amounts of greenhouse gases being released into the atmosphere by anthropogenic activities, such as the burning of fossil fuels (IPCC, 2018). These gases reduce the amount of heat that is radiated from the Earth's surface back into space and the upper ocean is absorbing over ninety percent of the excess heat retained by the Earth (Bindoff et al., 2007). Changes in SST have been shown to vary with season, year, and region (Hartmann et al., 2013) and can have significant impacts on marine biota, including population shifts, alterations in community structure and diversity, and changes in plant phenology and the timing of other ecosystem-level events and processes (Parmesan and Yohe, 2003; Doney et al., 2012).

Seagrasses are a group of foundation species that grow in shallow coastal and estuarine waters. They form extensive meadows ranging from a few square meters to hundreds of square kilometers and can be found along every continent except Antarctica (Green and Short, 2003). Seagrass meadows provide many ecosystem services such as improved water quality and clarity, increased biodiversity and habitat, sediment stabilization, and nutrient accumulation (Orth et al., 2006). Seagrass meadows also store significant quantities of carbon in biomass and sediments (Fourqurean et al., 2012), minimize exposure of bacterial pathogens to humans, fish, and invertebrates (Lamb et al., 2017; Reusch et al., 2021) and support global fisheries (Unsworth et al., 2018). Despite their importance, seagrasses are among the most threatened ecosystems on earth, with global trends of loss occurring since 1880 (Waycott et al., 2009; UNEP, 2020; Dunic et al., 2021). The primary causes of loss are sustained pressure from coastal development, declines in water quality, and climate change, including thermal stress due to rising SST (Short and Wyllie-Echeverria, 1996; Waycott et al., 2009; Wilson and Lotze, 2019).

The response of seagrass species to increased water temperature depends on their relative thermal tolerances and their optimum temperatures for photosynthesis, respiration, and growth (Short and Neckles, 1999; Björk et al., 2008). Temperature stress on seagrasses can result in altered growth rates, distribution shifts, changes in patterns of sexual reproduction, and mortality. Temperature stress has been linked to seagrass mortality in the Mediterranean Sea (Díaz-Almela et al., 2009; Jordà et al., 2012), Australia (Seddon et al., 2000; Nowicki et al., 2017; Strydom et al., 2020), southeast Asia, and the Caribbean (Hall et al., 2016; Zieman et al., 1999), and shifts in the species composition of communities dominated by *Zostera marina* L. (eelgrass; Shields et al., 2019). Likewise, increased SST has been linked to the northward expansion of *Halophila decipiens* into the Mediterranean Sea (Gerakaris et al., 2020) and an increase in flowering intensity and frequency in *Posidonia oceanica* and *Zostera japonica* (Ruiz et al., 2017; Qin et al., 2019). Environmental factors, such as hypersalinity (Durako and Howarth, 2017; Wilson and Dunton, 2018), shallow water depths (Collier and Waycott, 2014), limited circulation (Koch and Erskine, 2001; Binzer et al., 2005), and reduced oxygen and light (Moore and Jarvis, 2008) can amplify the impacts of temperature stress on seagrass meadows (Lefcheck et al., 2017).

The ability of seagrasses to resist the effects of stressors and recover from disturbance depends on multiple biotic and abiotic factors (O'Brien et al., 2018). Recovery of seagrass meadows following heat-induced disturbance and mortality has been attributed to increased genetic diversity (Reusch et al., 2005) and the presence of viable seed banks (Moore and Jarvis, 2008; Strydom et al., 2020). The self-reinforcing feedback mechanisms present in continuous seagrass meadows create conditions that promote further seagrass growth and may buffer against disturbance (Maxwell et al., 2017). Fragmented and sparse meadows of slow-growth species may have reduced capacity to buffer stresses due to minimal ability to modify their habitat, therefore, prospects for recovery will rely on long-distance dispersal of seeds and vegetative expansion (Nowicki et al., 2017). Prolonged periods without recovery can lead to regime shifts in which conditions are no longer habitable for seagrass. For example, Moksnes et al. (2018) document a local regime shift following the loss of eelgrass along the Swedish West Coast.

Eelgrass is the most widely distributed seagrass species in temperate marine environments of the Northern Hemisphere. The species has a wide temperature tolerance with an optimal range between 10 and 25°C (Moore et al., 2006; Lee et al., 2007). Exposure to temperatures above 25°C have been shown to cause plant mortality (Greve et al., 2003; Reusch et al., 2005; Moore and Jarvis, 2008; Moore et al., 2014). For example, in Northern Europe the performance and survival of eelgrass was severely impacted when plants were exposed to water temperatures ≥25°C during a series of heat waves (Reusch et al., 2005; Nejrup and Pedersen, 2008; Ehlers et al., 2008). Likewise, complete vegetative dieback was observed in Chesapeake Bay, VA following a heat wave where waters exceeded 30°C (Moore and Jarvis, 2008). Moore et al. (2014) also suggested that short-term exposure to rapidly increasing temperature by 4-5°C above the average of normal summer months can result in widespread diebacks.

Here, we use data from eight SeagrassNet monitoring sites located along the northeastern coast of the United States of

America (USA) (New Hampshire to Maryland) to investigate changes in eelgrass presence and abundance in relation to summer water temperature. SeagrassNet is a global seagrass monitoring network that uses a standardized monitoring protocol to detect and document seagrass habitat changes and relate them to environmental trends. The SeagrassNet program began in 2001 in the Western Pacific and now includes 126 sites in 33 countries (Short et al., 2006; Short et al., 2014). Along the east coast of the USA, it is estimated that up to 50% of all eelgrass habitat has been lost in the past century, and the prospects for recovery in most of this area are low (Green and Short, 2003). More recently, a global assessment of seagrass trajectories found eelgrass extent to be in rapid decline in the region (Turschwell et al., 2021) where mean SST is warming at a rate of 0.4°C per decade (Alexander et al., 2018), and summer SST has increased more than 2°C since 1902 (Karmalkar and Horton, 2021). The large geographic coverage of our dataset and time-period in which it spans provide an opportunity to investigate the influence of changing temperature regimes on eelgrass in the Northeast USA.

METHODS

Eelgrass Monitoring

Eelgrass was monitored annually at eight SeagrassNet monitoring sites located along a latitudinal gradient on the northeastern Atlantic coastline of the USA (**Figure 1**). The sites vary in their geomorphic setting, surrounding land use, tide range, bed size, and sources of disturbance (**Supplemental Material**). Summer (June-August) temperatures at each site reflect primarily site latitude (**Table 1**), geomorphic setting, residence time, and proximity to oceanic flushing. A SeagrassNet site includes three 50-m transects that parallel the shoreline along an increasing depth gradient. SeagrassNet monitoring sites are chosen to be representative of seagrass in the area of interest (Short et al., 2005). Seagrass abundance is measured within twelve permanent 0.25 m^2 quadrats positioned at random locations along the transects.

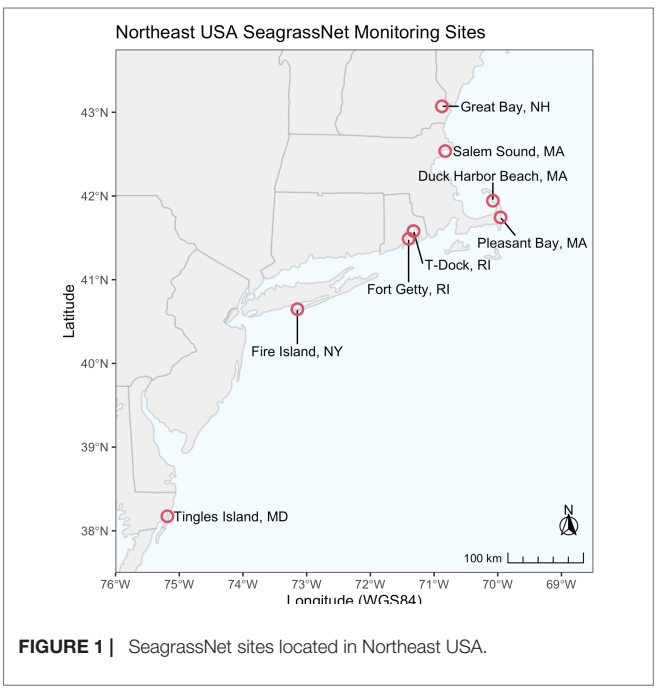

FIGURE 1 | SeagrassNet sites located in Northeast USA.

Eelgrass was monitored annually at most sites over nine- to 17-year periods between 2003 and 2021. The years in which monitoring occurred varied among sites (**Figure 2**). We examined eelgrass percent cover as an abundance metric that integrates shoot density and canopy height, measured during the season of peak biomass. Although widgeongrass (*Ruppia maritima*) grows throughout the region, it was present in only three sites and was therefore excluded from quantitative analyses. To standardize depth among sites and control for the effect of light availability, we restricted our analyses to the shallowest transect at which eelgrass occurred at each site.

Water Temperature

Continuous temperature records were obtained from various sources either within or near the eight SeagrassNet sites. Temperature was measured directly within four of the sites using temperature loggers (Onset Computer Co. Onset, MA) deployed near the substrate surface at one end of the shallow transect. At the other four sites, water temperature records from nearby locations representative of the monitoring stations were acquired through publicly available internet sources (**Table 1**). We investigate the effect of the previous year's mean summer (June 1 – August 31) water temperature on eelgrass percent cover. Evidence suggests that the negative effects of high thermal stress on eelgrass persists into the following growing season (Lefcheck et al., 2017). Daily mean summer temperatures were derived from the continuous temperature records. This level of aggregation was necessary to account for different temperature sampling intervals among sites. Annual summer mean water temperatures were then calculated for each site using the daily mean records. Additionally, to control for the confounding effect of latitude on water temperature, and the likely adaptation of eelgrass to local temperature (DuBois et al., 2022), summer water temperatures within each site were centered prior to modeling (**Table 1**).

Statistical Analysis

Eelgrass percent cover varied on a near-continuous interval from 0 to 100% (i.e., [0,1]) across all quadrats and sites during the period of interest. All instances of percent cover measurements equal to 1 were converted to 0.99 for model parsimony because there is not a meaningful ecological difference between the two values. However, since there is an ecologically important distinction between absence (percent cover = 0) and presence (percent cover > 0) of eelgrass, we used a hurdle model to accommodate the presence of zeros in the data (Cragg, 1971; Potts and Elith, 2006). This modeling framework has the added benefit of allowing for inference on two separate ecologically meaningful processes related to eelgrass: presence and abundance.

The hurdle model presence and abundance component consisted of a generalized additive mixed model (GAMM) with

TABLE 1 | SeagrassNet site locations and time period average of the daily average summertime water temperatures (used for centering) within each site.

SeagrassNet Site	Coordinates	Average Daily Mean Temperature (June-Aug.)	Temperature Record Time Periods	n Years	Water temperature data source
Great Bay, New Hampshire	N 43° 2.5632' W 70° 31.8294'	20.9°C	2006-2012, 2014-2020	14	Great Bay National Estuarine Research Reserve (NOAA National Estuarine Research Reserve System (NERRS) 2021); distance from monitoring transect 2.5 km
Salem Sound, Massachusetts	N 42° 19.9080' W 70° 29.4000'	15.7°C	2011, 2013-2019	8	Within monitoring transect
Duck Harbor Beach, Massachusetts	N 41° 34.0560' W 69° 34.3980'	20.7°C	2003-2018, 2020	17	Within monitoring transect
Pleasant Bay, Massachusetts	N 41° 27.0600' W 69° 34.3980'	22.3°C	2004-2018, 2020	16	Within monitoring transect
T-Dock, Rhode Island	N 41° 34.8402' W 71° 19.2798'	20.8°C	2005-2012, 2016	9	Narragansett Bay National Estuarine Research Reserve (NOAA National Estuarine Research Reserve System (NERRS) 2021); T-Wharf Surface, distance from monitoring transect 0.25 km
Fort Getty, Rhode Island	N 41° 29.6400' W 71° 23.8602'	21.2°C	2005-2007, 2010-2011	5	University of Rhode Island URI 169 Quonset Point, Surface Sonde (NERACOOS, 2021); distance from monitoring transect 10 km
Fire Island, New York	N 41° 6.0000' W 70° 31.8240'	24.3°C	2006, 2008, 2010-2016, 2019-2020	11	Long Island Shore, Smith Point Bridge (LIShore 2021); distance from monitoring transect 6 km; and within monitoring transect (2019-2020)
Tingles Island, Maryland	N 38° 6.7440' W 75° 6.5640'	27.0°C	2009-2018, 2020	11	Within monitoring transect

binomial and beta response distributions, respectively. Each mean response was modeled as a smooth function [denoted $s(\cdot)$] of both year and the centered average water temperature in the preceding year using thin-plate regression splines (Wood, 2003). Site and quadrat were included as nested random effects to account for unmeasured differences (heterogeneity) among SeagrassNet sites. The full model specification and model diagnostics are included in **Supplemental Material**.

All analyses were carried out using the R Statistical Computing Environment (R Core Team, 2021). Each hurdle model component GAMM was fit using the mgcv package (Wood, 2011; Wood et al., 2016) and visualized using the gratia package (Simpson, 2021).

RESULTS

Summary of Eelgrass Cover and Site Temperature

The time-periods in which eelgrass cover was surveyed varied across the region. All sites but one had at least 10 years of eelgrass data. Average eelgrass percent cover over all years of monitoring across the region ranged from 0 to 100 percent and averaged 34.5 percent. The frequency of eelgrass presence/absence along a transect fluctuated over the sample years within sites, with some sites having relatively infrequent observations of eelgrass presence and chronically low to no cover (**Figure 2**).

Site mean summer temperature across the region ranged from 15.7°C (Salem Sound) to 27.0°C (Tingles Island) (**Table 1**). **Figure 3** illustrates the variability in summer temperature across the region and shows that the range of summer temperature is narrower in some sites than others.

GAMM

Centered average water temperature in the preceding year was found to be a statistically significant nonlinear predictor of eelgrass presence in the following year (approximate p-value < 0.0001, **Table 2**). For preceding years that are hotter

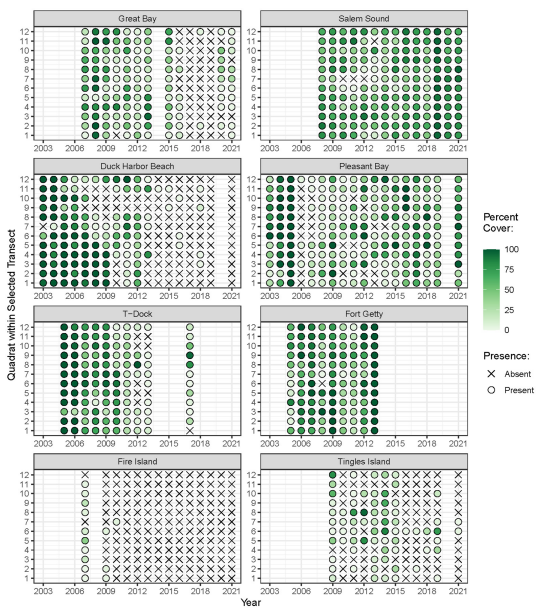

FIGURE 2 | Monitoring years and percent cover of eelgrass (*Zostera marina* L.) within each quadrat over time. Absence of plant cover is depicted with an × symbol.

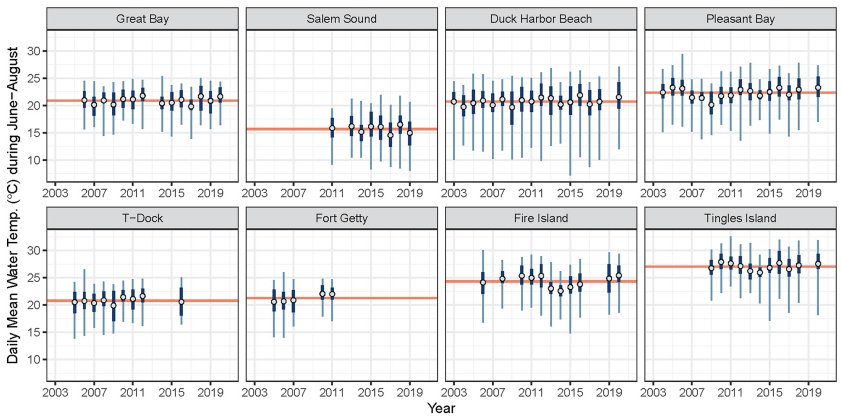

FIGURE 3 | Average daily mean water temperature during June-August each year (blue open circle) for associated years in which eelgrass cover was surveyed. Interquartile range and range of observed daily mean water temperatures are plotted in dark and light blue, respectively. The time period average (mean of all daily means) is plotted as horizontal red line. Water temperature data were not available for all years at all sites. Displayed here are only the temperature records used in the analysis.

than average (i.e., greater than the time-period average), an increase in average summer water temperature by 0.5°C or more for that year is associated with a linear decrease in the predicted probability of eelgrass presence the subsequent year (**Figure 4**). Cooler than average temperatures in the preceding year, down to approximately 0.5°C below the time-period average, are associated with the highest predicted probability of eelgrass presence. For eelgrass abundance, however, centered average water temperature in the preceding year was not found to be a statistically significant predictor (approximate *p*-value = 0.7820, **Table 3**).

DISCUSSION

We analyzed eight monitoring data sets from locations along a latitudinal gradient in the Northeastern USA to investigate associations between summer water temperature and eelgrass presence and abundance on a regional scale. We found that above average summer temperatures corresponded to a decreased probability of eelgrass presence (and increased probability of eelgrass absence) the following year. Our results showed that temperatures down to 0.5°C below the site average, corresponded to the highest probability of eelgrass presence. In contrast, we detected no association between eelgrass abundance (when present) and prior summer average temperature. However, eelgrass must survive to grow, so the lack of a statistically significant association between eelgrass abundance and prior year summer temperature cannot be taken outside of the context of the negative association between eelgrass presence and average summer temperature and highlights the importance of considering multiple fitness metrics when assessing species' response to temperature (Hughes et al., 2019). Overall, these

TABLE 2 | Eelgrass presence/absence component GAMM (binomial response distribution with logit link function) summary.

Parametric coefficients:				
	Estimate	**Std. Error**	***z* value**	**Pr(>|z|)**
Intercept	1.54	0.89	1.73	0.0842
Approximate significance of smooth terms:				
	edf	**Reference *df***	**χ^2Statistic**	***p-value***
s(Site)	6.74	7	252.87	< 0.0001
s(Quadrat within Site)	13.64	95	17.66	0.0653
s(Centered Avg. Temperature)	2.89	9	377.17	< 0.0001
s(Year)	4.50	9	1292.77	< 0.0001
Standard deviations of random effects:				
	Std. Deviation			
s(Site)	2.47			
s(Quadrat within Site)	0.39			
Deviance explained = 45.5%				
n = 1092				

[edf, effective degrees of freedom].

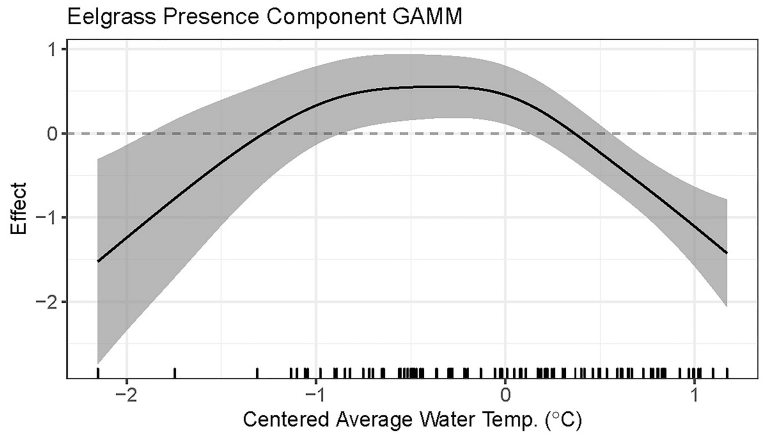

FIGURE 4 | Plot of the presence component GAMM fitted smooth with 95% confidence interval for the effect of centered average water temperature in the preceding year on eelgrass presence.

findings suggest eelgrass meadows in the Northeast USA are vulnerable to warming and, further, this vulnerability increases as water temperatures rise above the summer mean.

The recovery of seagrass meadows following disturbances can vary greatly, depending on the resilience of the meadow, (i.e., its ability to absorb changes and continue to persist; Holling, 1973). Even when water temperatures are below thermal thresholds, high temperature can interact with other stressors to exacerbate declines and prevent recovery. Because more light is required at higher temperatures for eelgrass to maintain a positive carbon balance (Marsh et al., 1986; Moore et al., 1997; Staehr and Borum, 2011; Beca-Carretero et al., 2018), light limitation and temperature increases can combine to cause eelgrass declines (Moore et al., 2014). Salo and Pedersen (2014) found that synergistic effects of high temperature and low salinity resulted in higher eelgrass mortality rates and lower leaf production. Additionally, Neckles et al. (1993) showed that high summer temperatures exacerbated the negative effects of epiphytes on eelgrass growth. As water temperatures continue to increase, these types of negative interactions are likely to worsen. The light experienced by eelgrass at the different SeagrassNet sites is influenced by water depth, tidal range, and water quality. Management actions that aim to improve water quality and clarity may also increase eelgrass resilience to higher temperatures.

In addition, ecological feedback mechanisms play a major role in the resilience of seagrass ecosystems (Maxwell et al., 2017). The degradation of seagrass meadows, and subsequent loss of self-reinforcing feedbacks (wherein seagrasses create conditions promoting further seagrass growth), can lead to a positive feedback loop in which recovery capacity is reduced, which can lead to conditions that are unsuitable for seagrass (Duarte et al., 2009). Thus, the ecological consequences of reduced eelgrass

TABLE 3 | Eelgrass abundance, given presence, component GAMM (beta response distribution with logit link function) summary.

Parametric coefficients:				
	Estimate	**Std. Error**	***z* value**	**Pr(>|*z*|)**
Intercept	-0.27	0.26	-1.06	0.2880
Approximate significance of smooth terms:				
	edf	**Reference *df***	**χ^2 Statistic**	***p-value***
s(Site)	6.66	7	98.61	< 0.0001
s(Quadrat within Site)	0.00	93	0.00	0.8490
s(Centered Avg. Temperature)	0.00	9	0.00	0.7820
s(Year)	3.79	9	1464.38	< 0.0001
Standard deviations of random effects:				
	Std. Deviation			
s(Site)	0.71			
s(Quadrat within Site)	0.00			
Deviance explained = 33.9%				
n = 713				

[edf, effective degrees of freedom].

presence with higher-than-average summer temperature may differ considerably among meadows with chronically high versus low eelgrass presence. Moreover, eelgrass meadows of the Northeast USA are part of seascapes and exist as metapopulations (Olsen et al., 2004). Connectivity among populations is critical for sustaining the eelgrass resources and the ecological services they provide at the local and regional scale (Kendrick et al., 2012). To prevent irreversible eelgrass losses as waters warm, proactive management actions are needed such as transplanting or seeding declining meadows with heat-tolerant genotypes and reducing synergistic stressors such as reduced light due to nutrient loading or turbidity from coastal construction, as well as mechanical disturbance to the bottom (such as dock construction over eelgrass or fishing practices that involve dredging or dragging gear along the seafloor; Neckles et al., 2005).

An important component of future targeted management actions to enhance eelgrass resilience to warming may include transplanting and seeding of genotypes that are more tolerant to warm waters into areas experiencing declines (Björk et al., 2008; Unsworth et al., 2015). For instance, Plaisted et al. (2020) planted eelgrass shoots collected from multiple populations into mesocosms and found resilience to reduced light and increased sediment organic matter to be positively associated with source population genetic diversity. Transplant and seeding of heat tolerant genotypes should occur at the seascape scale (de la Torre-Castro et al., 2014; Unsworth et al., 2015). For example, the distribution of eelgrass over a large latitudinal temperature gradient within the northeast region suggests southerly populations, adapted to warmer conditions, could boost resiliency at northern sites. However, a study of the seagrass species *Posidonia oceanica* found that transplants originating from the cool-edge of the thermal range performed equally well to warm-edge transplants when transplanted into the warm-edge of the thermo-geographical range, suggesting cool-edge seagrass populations may be more resilient to warming than expected (Bennett et al., 2022). Transplanting of eelgrass to areas that natural dispersal is rare or nonexistent raises other concerns which include spreading non-native epibiont species (Carman and Grunden, 2010) and disease (Groner et al., 2016). Also, eelgrass from southerly locations is potentially adapted to latitudinal gradients other than temperature, such as day length or seasonality (Clausen and Clausen, 2013; Clausen et al., 2014; Jueterbock et al., 2021).Finally, eelgrass restoration has experienced low success rates due to a variety of factors, including high seed loss due to seed predation and bioturbation, and high seedling mortality due to light availability and physical disturbances, as examples (Infantes et al., 2016).

Local-scale mosaics in environmental stress can also lead to gradients in heat-tolerance among eelgrass meadows (DuBois et al., 2022). Importantly, these local temperature mosaics are disassociated from latitudinal gradients (Helmuth et al., 2006) and can occur over spatial scales within the natural dispersal range of eelgrass and eelgrass associated species. For example, in our study, eelgrass in Great Bay, NH experiences average mean summertime temperatures 5°C warmer than Salem Sound, MA despite its more northerly locale and thus could be a possible source of heat-tolerant eelgrass. The potential for local-scale population differentiation to buffer the effects of warming without the same potential pitfalls of transplanting eelgrass across larger geographic distances highlights the importance of identifying local phenotypic variation among meadows and protecting eelgrass populations that span a variety of environmental conditions within regions. To identifyi gradients of heat-tolerance, monitoring of seagrass presence, abundance and distribution, as well as water temperature must occur at wider spatial scales than that which we present here.

Temperature stress may also result in distribution shifts of seagrass species. For example, Shields et al. (2019) documented a shift in species composition from eelgrass to a more transient sub-dominant species, *Ruppia maritima* (widgeongrass) in response to increasing summer temperature regimes. Although not included in the present study, increases in widgeongrass following eelgrass declines at both Tingles Island, MD and Fire Island, NY have been observed (Peck and Plaisted, in prep.). These two species co-occur in many areas, and widgeongrass has a higher optimum growth temperature (Evans et al., 1986); therefore, it has the potential to expand into areas where eelgrass recovery is limited by stressful water temperatures. Widgeongrass expansion has been documented in a variety of systems where it co-occurs with eelgrass, including San Diego, CA (Johnson et al., 2003), northwest Mexico (Lopez-Calderon et al., 2010), and the Chesapeake Bay (Shields et al., 2018; Richardson et al., 2018). The ability of widgeongrass to at least temporarily replace eelgrass after its decline may be a crucial mechanism of resiliency for these seagrass meadows. Widgeongrass ecosystem functions, including trapping sediment and improving water clarity, may create a positive feedback loop for the recolonization of eelgrass, though the extent to which this occurs remains an important area of research.

Although our study was limited by the data that were available, our results indicate that eelgrass presence on a regional scale is threatened by warming waters. Furthermore, differences in mean eelgrass presence and abundance among sites coupled with the known importance of self-reinforcing feedbacks in seagrass ecosystems (Duarte et al., 2009; Maxwell et al., 2017) suggests that sites with greater eelgrass presence and abundance may be more resilient to temperature stress than sites with chronically low eelgrass metrics. Proactive seeding of vulnerable sites with heat-tolerant eelgrass may be an important tool to combat eelgrass losses associated with rising temperatures in the Northeast USA. These topics warrant future research including continued regional monitoring of seagrass and water temperature at temporal and spatial scales necessary to answer both local and seascape level questions (Unsworth et al., 2019; Neckles et al., 2012). In summary, by using yearly percent cover data paired with high frequency temperature data, we were able to assess the impacts of warming on this important foundation species at a regional scale. Predictions of future response to dominant driving variables under warming conditions and factors limiting recovery are needed for managers to identify and minimize vulnerability to loss or degradation and reverse declining trajectories of seagrass ecosystems.

CONCLUSION

Our study exemplifies the value of long-term monitoring in tracking change in seagrass meadows and relating patterns to key drivers. The factors leading to eelgrass presence and abundance are complex, though our finding of reduced eelgrass presence with increased summer temperature supports other work linking eelgrass loss to additive effects of high thermal stress (Lefcheck et al., 2017). Discussion of the management action needed to improve the success of eelgrass must include an awareness of the role of temperature in exacerbating other stressors.

DATA AVAILABILITY STATEMENT

Publicly available datasets were analyzed in this study. This data can be found here: https://datadryad.org/stash/share/sRVnIbj397_nghEFD9DdVGSbqjHwVVM85bmBZyZl9DM.

AUTHOR CONTRIBUTIONS

HP, ES, AN, CP, and FS contributed to study conception, data compilation and analysis, conception of tables and figures, results interpretation and manuscript writing. PD contributed to statistical analyses, results interpretation and writing. JC, NE, SF, SH, RH, KM, BN, BP, FTS, and AT contributed to study conception, results interpretation, and writing. TM and DP contributed results interpretation and writing. All authors contributed to the article and approved the submitted version.

FUNDING

Funding for various aspects of SeagrassNet were provided by The David and Lucile Packard Foundation, the Oak Foundation, the New Hampshire Charitable Foundation and Tom Haas, and the University of New Hampshire. Funding for the herein analysis and manuscript was provided by the Northeast Coastal and Barrier Inventory and Monitoring Network of the US National Park Service.

ACKNOWLEDGMENTS

We thank the many staff, interns, researchers, and students who contributed to the collection of the data used in this collaborative project. Thanks also to the organizations for their support in implementing and maintaining SeagrassNet monitoring sites in the Northeast USA: University of New Hampshire; Piscataqua Region Estuaries Partnership; Massachusetts Division of Marine Fisheries; Save The Bay, Rhode Island; Narragansett Bay National Estuarine Research Reserve; US National Park Service: Northeast Coastal and Barrier Network, Cape Cod National Seashore, Fire Island National Seashore, and Assateague Island National Seashore. Thank you to Sara Stevens for initial review and editing. We especially thank Drs Hilary Neckles and Blaine Kopp formerly of the US Geological Survey for establishing four SeagrassNet sites, and Dr. Neckles specifically for her leadership in the initial conception of this paper, as well as her dedication to maintaining the seagrass monitoring program at Cape Cod National Seashore and advancing seagrass monitoring, research and management throughout the Northeast USA.

SUPPLEMENTARY MATERIAL

The Supplementary Material for this article can be found online at: https://www.frontiersin.org/articles/10.3389/fmars.2022.920699/full#supplementary-material

REFERENCES

Alexander, M. A., Scott, J. D., Friedland, K. D., Mills, K. E., Nye, J. A., Pershing, A. J., et al. (2018). Projected Sea Surface Temperatures Over the 21st Century: Changes in the Mean, Variability and Extremes for Large Marine Ecosystem Regions of Northern Oceans. *Elem Sci. Anth* 6, 9. doi: 10.1525/elementa.191

Beca-Carretero, P., Olesen, B., Marbà, N. and Krause-Jensen, D. (2018). Response to Experimental Warming in Northern Eelgrass Populations: Comparison Across a Range of Temperature Adaptations. *Mar. Ecol. Prog. Ser.* 589, 59–72. doi: 10.3354/meps12439

Bennett, S., Alcoverro, T., Kletou, D., Antoniou, C., Boada, J., Buñuel, X., et al. (2022). Resilience of Seagrass Populations to Thermal Stress Does Not Reflect Regional Differences in Ocean Climate. *New Phytol.* 233, 1657–1666. doi: 10.1111/nph.17885

Bindoff, N. L., IPCC, Willebrand, J., Artale, V., Cazenave, A., Gregory, J. M., Gulev, S., et al. (2007). "Climate Change," in *The Physical Science Basis*. Ed. Solomon, S., et al (Cambridge: Cambridge Univ. Press), 385–428.

Binzer, T., Borum, J. and Pedersen, O. (2005). Flow Velocity Affects Internal Oxygen Conditions in the Seagrass *Cymodocea nodosa*. *Aquat. Botany.* 83, 239–247. doi: 10.1016/j.aquabot.2005.07.001

Björk, M., Short, F. T., Mcleod, E. and Beer, S. (2008). *Managing Seagrasses for Resilience to Climate Change* (Gland, Switzerland: IUCN), 56pp.

Carman, M. R. and Grunden, D. W. (2010). First Occurrence of the Invasive Tunicate *Didemnum Vexillum* in Eelgrass Habitat. *Aquat. Invasions* 5, 23–29. doi: 10.3391/ai.2010.5.1.4

Clausen, K. K. and Clausen, P. (2013). Earlier Arctic Springs Cause Phenological Mismatch in Long-Distance Migrants. *Oecologia* 173, 1101–1112. doi: 10.1007/s00442-013-2681-0

Clausen, K. K., Krause-Jensen, D., Olesen, B. and Marbà, N. (2014). Seasonality of Eelgrass Biomass Across Gradients in Temperature and Latitude. *Mar. Ecol. Prog. Ser.* 506, 71–85. doi: 10.3354/meps10800

Collier, C. and Waycott, M. (2014). Temperature Extremes Reduce Seagrass Growth and Induce Mortality. *Mar. pollut. Bull.* 83 (2), 483–490. doi: 10.1016/j.marpolbul.2014.03.050

Cragg, J. G. (1971). Some Statistical Models for Limited Dependent Variables With Application to the Demand for Durable Goods. *Econometrica J. Econometric Soc.*, 39, 829–844. doi: 10.2307/1909582

de la Torre-Castro, M., Di Carlo, G. and Jiddawi, N. S. (2014). Seagrass Importance for a Small-Scale Fishery in the Tropics: The Need for Seascape Management. *Mar. pollut. Bull.* 83, 398–407. doi: 10.1016/j.marpolbul.2014.03.034

Díaz-Almela, E., Marbà, N., Martínez, R., Santiago, R. and Duarte, C. (2009). Seasonal Dynamics of *Posidonia oceanica* in Magalluf Bay (Mallorca, Spain): Temperature Effects on Seagrass Mortality. *Limnol. Oceanogr.* 54, 2170–2182. doi: 10.4319/lo.2009.54.6.2170

Doney, S. C., Mary Ruckelshaus, M., Duffy, J. E., Barry, J. P., Chan, F., English, C. A., et al. (2012). Climate Change Impacts on Marine Ecosystems. *Annu. Rev. Mar. Sci.* 4, 11–37. :1. doi: 10.1146/annurev-marine-041911-111611

Duarte, C. M., Conley, D. J., Carstensen, J. and S´anchez-Camacho, M. (2009). Return to Neverland: Shifting Baselines Affect Eutrophication Restoration Targets. *Estuaries Coasts* 32 (5), 29–36. doi: 10.1007/s12237-008-9111-2

DuBois, K., Pollard, K. N., Kauffman, B. J., Williams, S. L. and Stachowicz, J. J. (2022). Local Adaptation in a Marine Foundation Species: Implications for Resilience to Future Global Change. *Global Change Biol.* 00, 1–15. doi: 10.1111/gcb.16080

Dunic, J. C., Brown, C. J., Connolly, R. M., Turschwell, M. P. and Côté, I. M. (2021). Long-Term Declines and Recovery of Meadow Area Across the World's Seagrass Bioregions. *Glob. Change Biol.* 27, 4096–4109. doi: 10.1111/gcb.15684

Durako, M. J. and Howarth, J. F. (2017). Leaf Spectral Reflectance Shows *Thalassia testudinum* Seedlings More Sensitive to Hypersalinity Than Hyposalinity. *Front. Plant Sci.* 8. doi: 10.3389/fpls.2017.01127

Ehlers, A., Worm, B. and Reusch, B. H. (2008). Importance of Genetic Diversity in Eelgrass (*Zostera marina*) for its Resilience to Global Warming. *Mar. Ecol. Prog. Ser.* 355, 1–7. doi: 10.3354/meps07369

Evans, A. S., Webb, K. L. and Penhale, P. A. (1986). Photosynthetic Temperature Acclimation in Two Coexisting Seagrasses, *Zostera marina* L. And *Ruppia maritima* L. *Aquat. Bot.* 24, 185–197. doi: 10.1016/0304-3770(86)90095-1

Fourqurean, J. W., Duarte, C. M., Kennedy, H., Marbà, N., Holmer, M., Mateo, M. A., et al. (2012). Seagrass Ecosystems as a Globally Significant Carbon Stock. *Nat. Geosci.* 5, 505–509. doi: 10.1038/ngeo1477

Gerakaris, V., Lardi, P. and Issaris, Y. (2020). First Record of the Tropical Seagrass Species *Halophila decipiens* Ostenfeld in the Mediterranean Sea. *Aquat. Bot.* Volume 160. doi: 10.1016/j.aquabot.2019.103151

Green, E. P. and Short, F. T. (Eds.) (2003). *World Atlas of Seagrasses* (Berkeley: University of California Press).

Greve, T. M., Borum, J. and Pedersen, O. (2003). Meristematic Oxygen Variability in Eelgrass (*Zostera marina*). *Limnology Oceanography* 48, 210–216. doi: 10.4319/lo.2003.48.1.0210

Groner, M. L., Maynard, J., Breyta, R., Carnegie, R. B., Dobson, A., Friedman, C. S., et al. (2016). Managing Marine Disease Emergencies in an Era of Rapid Change. *Philos. Trans. R. Soc. London. Ser. B Biol. Sci.* 371 (1689), 20150364. doi: 10.1098/rstb.2015.0364

Hall, M., Furman, B., Merello, M. and Durako, M. (2016). Recurrence of *Thalassia testudinum* Seagrass Die-Off in Florida Bay, USA: Initial Observations. *Mar. Ecol. Prog. Ser.* 560, 243–249. doi: 10.3354/meps11923

Hartmann, D. L., Klein Tank, A. M. G., Rusticucci, M., Alexander, L. V., Brönnimann, S., Charabi, Y., et al. (2013). "Chapter 2: Observations: Atmosphere and Surface", in IPCC AR5 WG1 2013, 159–254.

Helmuth, B., Broitman, B. R., Blanchette, C. A., Gilman, S., Halpin, P., Harley, C. D. G., et al. (2006). Mosaic Patterns of Thermal Stress in the Rocky Intertidal Zone: Implications for Climate Change. *Ecol. Monogr.* 76, 461–479. doi: 10.1890/0012-9615(2006)076[0461:MPOTSI]2.0.CO;2

Holling, C. S. (1973). Resilience and Stability of Ecological Systems. *Annu. Rev. Ecol. Syst.* 4, 1–23. doi: 10.1146/annurev.es.04.110173.000245

Hughes, A. R., Hanley, T. C., Moore, A. F. P., Ramsay-Newton, C., Zerebecki, R. A. and Sotka, E. E. (2019). Predicting the Sensitivity of Marine Populations to Rising Temperatures. *Front. Ecol. Environ.* 17 (1), 17–24. doi: 10.1002/fee.1986

Infantes, E., Eriander, L. and Moksnes, P. O. (2016). Eelgrass (*Zostera marina*) Restoration on the West Coast of Sweden Using Seeds. *Mar. Ecol. Prog. Ser.* 546, 31–45. doi: 10.3354/meps11615

IPCC (2018). *Global Warming of 1.5°C. An IPCC Special Report on the Impacts of Global Warming of 1.5°C Above Pre-Industrial Levels and Related Global Greenhouse Gas Emission Pathways, in the Context of Strengthening the Global Response to the Threat of Climate Change, Sustainable Development, and Efforts to Eradicate Poverty*. Eds. Masson-Delmotte, V., Zhai, P., Pörtner, H. O., Roberts, D., Skea, J., Shukla, P. R., Pirani, A., Moufouma-Okia, W., Péan, C., Pidcock, R., Connors, S., Matthews, J. B. R., Chen, Y., Zhou, X., Gomis, M. I., Lonnoy, E., Maycock, T., Tignor, M. and Waterfield, T.

Johnson, M. R., Williams, S. L., Lieberman, C. H. and Solbak, A. (2003). Changes in the Abundance of the Seagrasses *Zostera marina* L. (Eelgrass) and *Ruppia maritima* L. (Widgeongrass) in San Diego, California, Following an El Niño Event. *Estuaries* 26 (1), 106–115.

Jordà, G., Marbà, N. and Duarte, C. (2012). Mediterranean Seagrass Vulnerable to Regional Climate Warming. *Nat. Clim. Change* 2, 821–824. doi: 10.1038/NCLIMATE1533

Jueterbock, A., Duarte, B., Coyer, J., Olsen, J. L., Kopp, M. E. L., Smolina, I., et al. (2021). Adaptation of Temperate Seagrass to Arctic Light Relies on Seasonal Acclimatization of Carbon Capture and Metabolism. *Front. Plant Sci.* Vol. 12. doi: 10.3389/fpls.2021.745855

Karmalkar, A. V. and Horton, R. M. (2021). Drivers of Exceptional Coastal Warming in the Northeastern United States. *Nat. Clim. Change* 11, 854–860. doi: 10.1038/s41558-021-01159-7

Kendrick, G. A., Waycott, M., Carruthers, T. J. B., Cambridge, M. L., Hovey, R., Krauss, S. L. et al. (2012). The Central Role of Dispersal in the Maintenance and Persistence of Seagrass Populations. *Bioscience* 62, 56–65. doi: 10.1525/bio.2012.62.1.10

Koch, M. S. and Erskine, J. M. (2001). Sulfide as a Phytotoxin to the Tropical Seagrass *Thalassia testudinum*: Interactions With Light, Salinity and Temperature. *J. Exp. Mar. Biol. Ecol.* 266, 81–95. doi: 10.1016/S0022-0981(01)00339-2

Lamb, J., Van de Water, J., Bourne, D., Altier, C., Hein, M., Fiorenza, E., et al. (2017). Seagrass Ecosystems Reduce Exposure to Bacterial Pathogens of Humans, Fishes, and Invertebrates. *Science* 355, 731. doi: 10.1126/science.aal1956

Lee, K. S., Park, S. and Kim, Y. (2007). Effects of Irradiance, Temperature, and Nutrients on Growth Dynamics of Seagrasses: A Review. *J. Exp. Mar. Biol. Ecology.* 350, 144–175. doi: 10.1016/j.jembe.2007.06.016

Lefcheck, J. S., Wilcox, D. J., Murphy, R. R., Marion, S. R. and Orth, R. J. (2017). Multiple Stressors Threaten the Imperiled Coastal Foundation Species Eelgrass (*Zostera marina*) in Chesapeake Bay, USA. *Global Change Biol.* 23 (9), 3474–3483. doi: 10.1111/gcb.13623

LIShore (Accessed 12 February 2021). (2021). a project of the School of Marine and Atmospheric Sciences at Stony Brook University in collaboration with the LIShore partners.

Lopez-Calderon, J., Riosmena-Rodríguez, R., Rodríguez-Baron, J. M., Carrión-Cortez, J., Torre, J., Meling-López, A., et al. (2010). Outstanding Appearance of *Ruppia maritima* Along Baja California Sur, México and Its Influence in Trophic Networks. *Mar. Biodiversity* 40 (4), 293–300. doi: 10.1007/s12526-010-0050-3

Marsh, J. A., Dennison, W. C. and Alberte, R. S. (1986). Effects of Temperature on Photosynthesis and Respiration in Eelgrass (*Zostera marina* L.). *J. Exp. Mar. Biol. Ecol.* 101, 257–267. doi: 10.1016/0022-0981(86)90267-4

Maxwell, P. S., Eklöf, J. S., van Katwijk, M. M., O'Brien, K. R., de la Torre-Castro, M., Boström, C., et al. (2017). The Fundamental Role of Ecological Feedback Mechanisms for the Adaptive Management of Seagrass Ecosystems—a Review. *Biol. Rev.* 92, 1521–1538. doi: 10.1111/brv.12294

Moksnes, P. O., Eriander, L., Infantes, E., Holmer, M., et al. (2018). Local Regime Shifts Prevent Natural Recovery and Restoration of Lost Eelgrass Beds Along the Swedish West Coast. *Estuaries Coasts* 41, 1712–1731. doi: 10.1007/s12237-018-0382-y

Moore, K. A. and Jarvis, J. C. (2008). Environmental Factors Affecting Recent Summertime Eelgrass Diebacks in the Lower Chesapeake Bay: Implications for Long-Term Persistence. *J. Coast. Res.* 55, 135–147. doi: 10.2112/SI55-014

Moore, K. A., Shields, E. C. and Parrish, D. B. (2014). Impacts of Varying Estuarine Temperature and Light Conditions on *Zostera marina* (Eelgrass) and Its Interactions With *Ruppia maritima* (Widgeongrass). *Estuaries Coasts* 37, 20–30. doi: 10.1007/s12237-013-9667-3

Moore, K. A., Short, F. T., Orth, R. J., and Duarte, C. M., (2006). "Zostera: Biology, Ecology, and Management," in *Seagrasses: Biology, Ecology and Conservation*. Ed. Larkum, A. W. D., et al (Dordrecht: Springer), 323–345.

Moore, K. A., Wetzel, R. L. and Orth, R. J. (1997). Seasonal Pulses of Turbidity and Their Relations to Eelgrass (*Zostera marina* L.) Survival in an Estuary. *J. Exp. Mar. Biol. Ecol.* 215, 115–134. doi: 10.1016/S0022-0981(96)02774-8

Neckles, H. A., Kopp, B. S. and Peterson, B. J (2012). Integrating Scales of Seagrass Monitoring to Meet Conservation Needs. *Estuaries Coasts* 35, 23–46. doi: 10.1007/s12237-011-9410-x

Neckles, H. A., Short, F. T., Barker, S. and Kopp, B. S. (2005). Disturbance of Eelgrass (*Zostera marina* L.) by Commercial Mussel (*Mytilus Edulis*) Harvesting Inmaine: Dragging Impacts and Habitat Recovery. *Mar. Ecol. Prog. Ser.* 285, 57–73. doi: 10.3354/meps285057

Neckles, H. A., Wetzel, R. L. and Orth, R. J. Pooler, P. (1993). Relative Effects of Nutrient Enrichment and Grazing on Epiphyte-Macrophyte (*Zostera marina* L.) Dynamics. *Oecologia* 93 (2), 285–295. doi: 10.1007/BF00317683

Nejrup, L. and Pedersen, M. (2008). Effects of Salinity and Water Temperature on the Ecological Performance of *Zostera marina*. *Aquat. Botany.* 88, 239–246. doi: 10.1016/j.aquabot.2007.10.006

NOAA (National Oceanic and Atmospheric Administration) (2016a) *Extended Reconstructed Sea Surface Temperature (ERSST.V4)* (National Centers for Environmental Information). Available at: www.ncdc.noaa.gov/data-access/

marineocean-data/extended-reconstructed-sea-surface-temperature-ersst (Accessed March 2016).

NOAA (National Oceanic and Atmospheric Administration) (2016b) *NOAA Merged Land Ocean Global Surface Temperature Analysis (NOAAGlobalTemp): Global Gridded 5° X 5° Data* (National Centers for Environmental Information). Available at: www.ncdc.noaa.gov/data-access/marineocean-data/noaa-global-surface-temperature-noaaglobaltemp (Accessed June 2016).

NOAA National Estuarine Research Reserve System (NERRS) (2021). *System-Wide Monitoring Program. Data Accessed From the NOAA NERRS Centralized Data Management Office Website*. Available at: http://www.nerrsdata.org (Accessed 12 February 2021).

Northeastern Regional Association of Coastal Ocean Observing Systems (NERACOOS) *Graduate School of Oceanography, Marine Ecosystems Research Laboratory* (University of Rhode Island). Available at: http://www.neracoos.org/erddap/tabledap/URI_169-QP_SurfaceSonde.graph (Accessed February 2021).

Nowicki, R., Thomson, J., Burkholder, D., Fourqurean, J. and Heithaus, M. (2017). Predicting Seagrass Recovery Times and Their Implications Following an Extreme Climate Event. *Mar. Ecol. Prog. Ser.* 567, 79–93. doi: 10.3354/meps12029

O'Brien, K. R., Waycott, M., Maxwell, P., Kendrick, G. A., Udy, J. W., Ferguson, A. J. P., et al. (2018). Seagrass Ecosystem Trajectory Depends on the Relative Timescales of Resistance, Recovery and Disturbance. *Mar. pollut. Bull.* Volume 134, 166–176. doi: 10.1016/j.marpolbul.2017.09.006

Oczkowski, A., McKinney, R., Ayvazian, S., Hanson, A., Wigand, C. and Markham, E. (2015). Preliminary Evidence for the Amplification of Global Warming in Shallow, Intertidal Estuarine Waters. *PloS One* 10 (10), e0141529. doi: 10.1371/journal.pone.0141529

Olsen, J. L., Stam, W. T., Coyer, J. A., Reusch, T. B. H., Billingham, M., Boström, C., et al. (2004). North Atlantic Phylogeography and Large-Scale Population Differentiation of the Seagrass *Zostera marina* L. *Mol. Ecol.* 13, 1923–1941. doi: 10.1111/j.1365-294X.2004.02205.x

Orth, R. J., Carruthers, T. J. B., Dennison, W. C., Duarte, C. M., Fourqurean, J. W., Heck, K. L. J., et al. (2006). A Global Crisis for Seagrass Ecosystems. *Bioscience* 56 (12), 987–996. doi: 10.1641/0006-3568(2006)56[987:AGCFSE]2.0.CO;2

Parmesan, C. and Yohe, G. (2003). A Globally Coherent Fingerprint of Climate Change Impacts Across Natural Systems. *Nature* 421, 37–42. doi: 10.1038/nature01286

Peck, C. P. and Plaisted, H. K. "Northeast Coastal and Barrier I&M Network Parks: Estuarine Nutrient Enrichment Monitoring Data Summary and Trend Analysis," in *Natural Resource Data Series NPS/NCBN/NRDS—TBD* (Fort Collins, Colorado: National Park Service).

Plaisted, H. K., Novak, A. B., Weigel, S. and Short, F. T. (2020). Correction to: Eelgrass Genetic Diversity Influences Resilience to Stresses Associated With Eutrophication. *Estuaries Coasts* 43, 1584. doi: 10.1007/s12237-020-00696-2

Potts, J. M. and Elith, J. (2006). Comparing Species Abundance Models. *Ecol. Model.* 199 (2), 153–163. doi: 10.1016/j.ecolmodel.2006.05.025

Qin, L., Kim, S. H., Song, H., Suonan, Z., Kim, H., Kwon, O., et al. (2019). Influence of Regional Water Temperature Variability on the Flowering Phenology and Sexual Reproduction of the Seagrass *Zostera marina* in Korean Coastal Waters. *Estuaries Coasts*. 43, 449–462. doi: 10.1007/s12237-019-00569-3

R Core Team (2021). *R: A Language and Environment for Statistical Computing* (Vienna, Austria: R Foundation for Statistical Computing). Available at: https://www.R-project.org/.

Reusch, T. B. H., Ehlers, A. H., Hammerli, A. and Worm, B. (2005). Ecosystem Recovery After Climatic Extremes Enhanced by Genotypic Diversity. *Proc. Natl. Acad. America* 102, 2826–2831. doi: 10.1073/pnas.0500008102

Reusch, T. B. H., Schubert, P. R., Marten, S. M., Gill, D., Karez, R., Busch, K., et al. (2021). Lower Vibrio Spp. Abundances in *Zostera marina* Leaf Canopies Suggest a Novel Ecosystem Function for Temperate Seagrass Beds. *Mar. Biol.* 168, 149. doi: 10.1007/s00227-021-03963-3

Richardson, J. P., Lefcheck, J. S. and Orth, R. J. (2018). Warming Temperatures Alter the Relative Abundance and Distribution of Two Cooccurring Foundational Seagrasses in Chesapeake Bay, USA. *Mar. Ecol. Prog. Ser.* 599, 65–74. doi: 10.3354/meps12620

Ruiz, H., Ballantine, D. L. and Sabater, H. (2017). Continued Spread of the Seagrass *Halophila stipulacea* in the Caribbean: Documentation in Puerto Rico and the British Virgin Islands. *Gulf Caribb. Res.* 28, SC5–SC7. doi: 10.18785/gcr.2801.05

Salo, T. and Pedersen, M. F. (2014). Synergistic Effects of Altered Salinity and Temperature on Estuarine Eelgrass (*Zostera marina*) Seedlings and Clonal Shoots. *J. Exp. Mar. Biol. Ecol.* 457, 143–150. doi: 10.1016/j.jembe.2014.04.008

Seddon, S., Connolly, R. M. and Edyvane, K. S. (2000). Large-Scale Seagrass Dieback in Northern Spencer Gulf, South Australia. *Aquat. Bot.* 66, 297–310. doi: 10.1016/S0304-3770(99)00080-7

Shields, E. C., Moore, K. A. and Parrish, D. B. (2018). Adaptations by *Zostera marina* Dominated Seagrass Meadows in Response to Water Quality and Climate Forcing. *Diversity* 10 (4), 125. doi: 10.3390/d10040125

Shields, E. C., Parrish, D. and Moore, K. (2019). Short-Term Temperature Stress Results in Seagrass Community Shift in a Temperate Estuary. *Estuaries Coasts* 42, 755–764. doi: 10.1007/s12237-019-00517-1

Short, F., Coles, R., Fortes, M., Victor, S., Salik, M., Isnain, I., et al. (2014). Monitoring in the Western Pacific Region Shows Evidence of Seagrass Decline in Line With Global Trends. *Mar. pollut. Bull.* 83, 408–416. doi: 10.1016/j.marpolbul.2014.03.036

Short, F. T., Koch, E. W., Creed, J. C., Magalhães, K. M., Fernandez, E. and Gaeckle, J. L. (2006). SeagrassNet Monitoring Across the Americas: Case Studies of Seagrass Decline. *Mar. Ecol.* 27, 277–289. doi: 10.1111/j.1439-0485.2006.00095.x

Short, F. T., McKenzie, L. J., Coles, R. G. and Gaeckle, J. L. (2005). *SeagrassNet Manual for Scientific Monitoring of Seagrass Habitat – Caribbean Edition* (Durham, NH, USA: University of New Hampshire), 74 pp. Available at: http://www.SeagrassNet.org.

Short, F. T. and Neckles, H. A. (1999). The Effects of Global Climate Change on Seagrasses. *Aquat. Bot.* 63, 169–196. doi: 10.1016/S0304-3770(98)00117-X

Short, F. T. and Wyllie-Echeverria, S. (1996). Natural and Human-Induced Disturbance of Seagrasses. *Environ. Conserv.* 23 (1), 17–27. doi: 10.1017/S0376892900038212

Simpson, G. L. (2021) *Gratia: Graceful 'ggplot'-Based Graphics and Other Functions for Gams Fitted Using 'Mgcv'*. Available at: https://CRAN.R-project.org/package=gratia.

Staehr, P. A. and Borum, J. (2011). Seasonal Acclimation in Metabolism Reduces Light Requirements of Eelgrass (*Zostera marina*). *J. Exp. Mar. Biol. Ecol.* 407, 139–146. doi: 10.1016/j.jembe.2011.05.031

Strydom, S., Murray, K., Wilson, S., Huntley, B., Rule, M., Heithaus, M., et al. (2020). Too Hot to Handle: Unprecedented Seagrass Death Driven by Marine Heatwave in a World Heritage Area. *Glob. Change Biol.* 26, 3525–3538. doi: 10.1111/gcb.15065

Turschwell, M. P., Connolly, R. M., Dunic, J. C., Sievers, M., Buelow, C. A., Pearson, R. M., et al. (2021). Anthropogenic Pressures and Life History Predict Trajectories of Seagrass Meadow Extent at a Global Scale. *Proc. Natl. Acad. Sci. Nov* 118 (45), e2110802118. doi: 10.1073/pnas.2110802118

United Nations Environment Programme (UNEP) (2020). *Out of the Blue: The Value of Seagrasses to the Environment and to People* (Nairobi: UNEP).

Unsworth, R. K., Collier, C. J., Waycott, M., Mckenzie, L. J. and Cullen-Unsworth, L. C. (2015). A Framework for the Resilience of Seagrass Ecosystems. *Mar. pollut. Bull.* 100 (1), 34–46. doi: 10.1016/j.marpolbul.2015.08.016

Unsworth, R. K. F., McKenzie, L. J., Collier, C. J., Cullen-Unsworth, L. C., Duarte, C. M., et al. (2019). Global Challenges for Seagrass Conservation. *Ambio* 48, 801–815. doi: 10.1007/s13280-018-1115-y

Unsworth, R. K. F., Nordlund, L. M. and Cullen-Unsworth, L. C. (2018). Seagrass Meadows Support Global Fisheries Production. *Conserv. Lett.* 12, e12566 doi: 10.1111/conl.12566

Waycott, M., Duarte, C. M., Carruthers, T. J. B., Orth, R., Dennison, W. C., Olyarnike, S., et al. (2009). Accelerating Loss of Seagrasses Across the Globe Threatens Coastal Ecosystems. *PNAS* 106 (30), 12377–12381. doi: 10.1073/pnas.0905620106

Wilson, S. S. and Dunton, K. H. (2018). Hypersalinity During Regional Drought Drives Mass Mortality of the Seagrass *Syringodium filiforme* in a Subtropical Lagoon. *Estuaries Coasts* 41 (3), 855–865. doi: 10.1007/s12237-017-0319-x

Wilson, K. L. and Lotze, H. K. (2019). Climate Change Projections Reveal Range Shifts of Eelgrass *Zostera marina* in the Northwest Atlantic. *Mar. Ecol. Prog. Ser.* 620, 47–62. doi: 10.3354/meps12973

Wood, S. N. (2011). Fast Stable Restricted Maximum Likelihood and Marginal Likelihood Estimation of Semiparametric Generalized Linear Models. *J. R. Stat. Society: Ser. B (Statistical Methodology)* 73 (1), 3–36. doi: 10.1111/j.1467-9868.2010.00749.x

Wood, S. N., Pya, N. and Säfken, B. (2016). Smoothing Parameter and Model Selection for General Smooth Models. *J. Am. Stat. Assoc.* 111 (516), 1548–1563. doi: 10.1080/01621459.2016.1180986

Wood S. N. (2003). Thin Plate Regression Splines. *J. R. Stat. Society: Ser. B (Statistical Methodology)* 65 (1), 95–114. doi: 10.1111/1467-9868.00374

Zieman, J., Fourqurean, J. and Frankovich, T. (1999). Seagrass Die-Off in Florida Bay: Long-Term Trends in Abundance and Growth of Turtle Grass, *Thalassia testudinum*. *Estuaries* 22, 460–470. doi: 10.2307/1353211

Conflict of Interest: Authors CP and PD are employed by Neptune and Company, Inc. The remaining authors declare that the research was conducted in the absence of any commercial or financial relationships that could be construed as a potential conflict of interest.

Publisher's Note: All claims expressed in this article are solely those of the authors and do not necessarily represent those of their affiliated organizations, or those of the publisher, the editors and the reviewers. Any product that may be evaluated in this article, or claim that may be made by its manufacturer, is not guaranteed or endorsed by the publisher.

frontiers | Frontiers in Marine Science

TYPE Original Research
PUBLISHED 28 July 2022
DOI 10.3389/fmars.2022.867986

OPEN ACCESS

EDITED BY
Fanny Noisette,
Université du Québec à Rimouski,
Canada

REVIEWED BY
Ludovic Pascal,
Université du Québec à Rimouskii,
Canada
Dominique Davoult,
Sorbonne Universités, France

*CORRESPONDENCE
Irene Olivé
irene.olive@szn.it

SPECIALTY SECTION
This article was submitted to Marine Biogeochemistry, a section of the journal Frontiers in Marine Science

RECEIVED 01 February 2022
ACCEPTED 01 July 2022
PUBLISHED 28 July 2022

CITATION
Olivé I, García-Robledo E, Silva J, Pintado-Herrera MG, Santos R, Kamenos NA, Cuet P and Frouin P (2022) Contribution of the seagrass *Syringodium isoetifolium* to the metabolic functioning of a tropical reef lagoon.
Front. Mar. Sci. 9:867986.
doi: 10.3389/fmars.2022.867986

Contribution of the seagrass *Syringodium isoetifolium* to the metabolic functioning of a tropical reef lagoon

Irene Olivé[1,2]*, Emilio García-Robledo[3], João Silva[4], Marina G. Pintado-Herrera[5], Rui Santos[4], Nicholas A. Kamenos[2,6], Pascale Cuet[7] and Patrick Frouin[7]

[1]Integrated Molecular Ecology Department, Stazione Zoologica Anton Dohrn, Naples, Italy, [2]School of Geographical & Earth Sciences, University of Glasgow, Glasgow, United Kingdom, [3]Biology Department, University of Cadiz, Cadiz, Spain, [4]Marine Plant Ecology Research Group, Centre for Marine Sciences, University of Algarve, Faro, Portugal, [5]Physics and Chemistry Department, University of Cadiz, Cadiz, Spain, [6]Department of Ecology and Environmental Sciences, Umeå Marine Sciences Centre, Umeå University, Umeå, Sweden, [7]UMR ENTROPIE, LabEx CORAIL, University of Reunion, Reunion, France

Seagrasses are gaining attention thanks to their metabolism and potential major role as carbon sinks, with further implications as nature-based solutions against climate change. Despite their recognized importance and the growing number of studies published, there is still a striking paucity of information on seagrass metabolism and contribution to biogeochemical cycles for some seagrass species and ocean areas. In this study we assessed the metabolic balance and nutrient cycling contribution of seagrasses to the benthic compartment of a tropical reef lagoon in Reunion Island, providing original information on a barely studied seagrass species (*Syringodium isoetifolium*) and a poorly studied ocean region (West Indian Ocean). We measured the net productivity, respiration and the metabolic balance in different components of the lagoon benthic compartment (i.e. seagrass, sediment, and benthic community) and the water-sediment nutrient benthic fluxes at differently impacted sites within the lagoon. The biogeochemical environmental variability, including inorganic and organic indicators of anthropogenic contamination, was also assessed at each site.

Large spatial variability was detected in the metabolic balance of each benthic component assessed, also associated with the natural and/or anthropic-driven environmental variability found in the lagoon. The seagrass *S. isoetifolium* was net autotrophic across the lagoon and contributed to the lagoon benthic metabolism with net plant productivity exceeding by one order of magnitude the plant respiration. The lowest seagrass metabolism was detected at the impacted site. The metabolic balance of the sediment was heterotrophic but the high productivity of *S. isoetifolium* contributed to reducing the heterotrophy of the whole benthic community. The lagoon-wide benthic metabolic balance was slightly heterotrophic, but the associated uncertainty

ranged from autotrophy to heterotrophy. Nutrient concentrations in the lagoon were low and the benthic community capacity for nutrient retention (uptake) and removal (denitrification and anammox) indicated potential for buffering moderate nutrient inputs into the lagoon. Organic contaminants of emerging concern (CECs) were low but detectable in the lagoon, especially in highly frequented beach areas, arising as an environmental quality indicator of interest.

KEYWORDS

benthic community, metabolic balance, nutrient fluxes, productivity, reef lagoon, respiration, seagrass

1 Introduction

Within the coral reef systems, the reef lagoonal benthic communities (*sensu lato*) play a key role in the overall reef primary production (Gattuso et al., 1998; Heil et al., 2004), significantly contributing to inorganic carbon (CO_2) fluxes and organic matter remineralization (Gattuso et al., 1998; Borges et al., 2006). The impacts of local anthropogenic pressures, such as eutrophication (Bell, 1992) or the increase of contaminants of emerging concern (CECs) (Reid et al., 2019), and climate change (Hughes et al., 2003) pose a serious threat to the biodiversity, resilience and functioning of these valuable ecosystems. As a consequence of natural or human-driven pressures, shifts in the composition of benthic primary producer and productivity are expected, implying changes in the benthic metabolism, the sediment biogeochemical composition, and the nutrient water-sediment fluxes (Eyre and Ferguson, 2002; Smetacek and Zingone, 2013). Nutrient fluxes in the benthic compartment are controlled by biogeochemical processes closely tied to the metabolic activity of the benthic community (Risgaard-Petersen and Ottosen, 2000; Barrón et al., 2006). Changes in the physico-chemical environmental conditions may impact the biological community (composition, functional role and productivity), which in turn may also modify the chemical and physical conditions and processes taking place in the sediments, ultimately affecting nutrient fluxes, cycling and storage capacity of the benthic compartment (Eyre and Ferguson, 2002). The study of the metabolic status of the benthic reef compartment, in terms of production and respiration and nutrient fluxes, is thus essential for the determination of the metabolic status (i.e. auto- or heterotrophic) of coral reef systems and for forecasting their potential to cope and respond to events of natural or anthropogenic-induced environmental forcing (Eyre and Ferguson, 2002; Taddei et al., 2007).

While microphytobentos represents the main primary producer in unvegetated soft-bottom lagoons (Taddei et al., 2007; Hochard et al., 2012), the presence of marine macrophytes, macroalgae and seagrasses, is also frequent in the reef lagoons and may constitute important contributors to primary production and the overall metabolic balance of reef system (Gattuso et al., 1998; Heil et al., 2004). Seagrasses are considered "foundation" species with the capacity to modify the physico-chemical environment around them creating suitable conditions for themselves and for the associated community (Dayton, 1972; Ricart et al., 2021). Moreover, seagrass meadows are gaining further momentum among the scientific and stake-holder communities because of the ecosystem services attributed to them and their potential as nature-based solutions for climate change mitigation (Seddon et al., 2020; Macreadie et al., 2021). The characteristic below-ground rhizomatic-root system of seagrasses physically connects the water mass and the sediment altering the diffusive water-sediment nutrient fluxes and further modifying the magnitude and velocity of the biogeochemical processes that occur both in the water and the sediment (Bouma et al., 2009). Among the valuable essential services attributed to seagrasses (Orth et al., 2006), those related to water oxygenation (Duarte et al., 2010), nutrient cycling (Eyre and Ferguson, 2002) and carbon sequestration (Fourqurean et al., 2012) are closely linked to seagrass productivity and metabolic balance. Indeed, seagrass meadows are considered among the most productive coastal systems on Earth (Duarte and Chiscano, 1999). However, despite the studies published, information on seagrass metabolism is yet inconclusive and large uncertainties remain on the quantification of seagrass net metabolic contribution to the system productivity and nutrient fluxes (Duarte et al., 2010; Van Dam Bryce et al., 2021; Ward et al., 2022). Large inter- and intraspecific variability has been described in seagrass productivity (Duarte et al., 2010). This plasticity has been associated to spatio-temporal variability (Enríquez et al., 2004; Olivé et al., 2013), environmental forcing derived from natural- or anthropogenic-driven perturbations, such as diseases, nutrient-derived eutrophication, or warming (Olivé et al., 2009; Graham et al., 2021), and "top-down" control of the associated community (Martínez-Crego et al., 2014).

Despite their recognized importance and the growing number of studies published in the last decades, seagrasses have been traditionally overlooked in coral reef systems (Duarte et al., 2008). At present, there is a particular striking paucity of information on seagrass metabolism and contribution to biogeochemical cycles in some tropical areas, such as the West Indian Ocean (Duarte et al., 2010; Ward et al., 2022). Moreover, information available on tropical seagrasses is biased and very limited information is available for some species, such is the case of *Syringodium isoetifolium* (Duarte et al., 2010; Ward et al., 2022). To help fulfilling this gap, this work provides novel and original information on the metabolism of a poorly studied seagrass species (i.e. *S. isoetifolium*) and a poorly studied ocean region (i.e. West Indian Ocean).

This work aims at evaluating the productivity and metabolic contribution of a tropical seagrass to the metabolism and nutrient cycling of the benthic compartment in a reef lagoon system, considering the environmental biogeochemical variability associated to the lagoon. This was addressed by evaluating the metabolic balance of different benthic components (i.e. seagrass, sediment, and whole benthic community) and the nutrient fluxes of the benthic community across a tropical reef lagoon. We used the reef lagoon in Reunion Island (West Indian Ocean) as a model system and the seagrass *S. isoetifolium* as a model species. The fast-growing species *S. isoetifolium* is the only seagrass present in Reunion (Cuvillier et al., 2017). It thrives in sandy bottoms along the inner reef lagoon and its coverture can reach up to 30% of the lagoon (Cuvillier et al., 2017). Despite its limited extension, the reef lagoon is exposed to different levels of natural and anthropogenic environmental pressure (Chazottes et al., 2008; Clavier et al., 2008). Indeed, time-series analysis have revealed large seascape variability of *S. isoetifolium* communities across the lagoon associated with natural (e.g. storms, grazing) and anthropogenic (e.g. warming, nutrient inputs) environmental forcing (Cuvillier et al., 2017). However, the productivity and metabolic assessment of the seagrass *S. isoetifolium* in the lagoon remains unexplored. Oxygen was chosen as the main descriptor to assess productivity and explore the metabolic balance in the different components of the benthic compartment of the lagoon together with its spatial variability. The oxygen metabolic balance has been commonly used as a physiological indicator of the metabolic status across organismal scales (Gillooly et al., 2001), benthic communities (Roth et al., 2019), and the benthic compartment (Revsbech et al., 1981; Glud, 2008). Oxygen fluxes are also closely associated with other nutrient fluxes (e.g. carbon (Duarte et al., 2010) and nitrogen (Risgaard-Petersen, 2003). Nitrogen fluxes in the benthic compartment were also assessed to evaluate the potential role of the benthic community as sink or source of nutrients in the lagoon as well as testing the potential of the benthic lagoon community to face increases in the nutrient load.

2 Material and methods

2.1 Study site

Reunion Island (Mascarene Archipelago, Western Indian Ocean) has been identified as a marine hotspot of biodiversity for coral reefs with highest ecological value (Roberts et al., 2002). The coral reef systems of Reunion Island (S 21°, E 55°) are restricted to the western and southern coasts of the island. This study was conducted in La Saline fringing reef (9 km long, up to 500 m wide, 1 to 1.5 m deep), which is the most extensive reef of Reunion Island (Tedetti et al., 2020). The lagoon is exposed to semidiurnal tides ranging from 0.1 m (neap) to 0.9 m (spring). The sediment in the reef lagoon is mainly composed of coarse sand, scattered with coral fragments, over a limestone substrate (Clavier et al., 2008). The lagoon is considered an oligotrophic system with low nutrient levels, though local areas potentially exposed to nutrient inputs, mainly through groundwater discharges and runoff from land, have been reported along the lagoon (Clavier et al., 2008; Tedetti et al., 2020).

Monospecific beds of the seagrass *Syringodium isoetifolium* were selected according to previous works and three different stations were set along the reef lagoon as a representative of different environmental pressures (i.e. nutrient enrichment associated to submarine groundwater discharge and human pressure) (Chazottes et al., 2008; Cuvillier et al., 2017). "Saint-Gilles" (Site A, STG, S 21.07020°; E 055.22031°) was selected as pristine meadow with low anthropogenic pressure and little or no nutrient enrichment; "Passe Ermitage" (Site B, PAS, S 21.08629°; E 055.22705°), located close to an intermittent stream receiving the effluent of a sewage plant, was selected as impacted site exposed to high submarine groundwater discharge, nutrient inputs, and hydrodynamics; and "Saline" (Site C, SAL, S 21.09597°; E 055.23338°), a frequented beach area, was selected as representative of intermediate impact with moderate human pressure and average nutrient availability (**Figure 1**).

At each station, we measured the main environmental biogeochemical descriptors (including physico-chemical parameters, inorganic nutrients, and organic contaminants of emerging concern, CECs) and studied three different components of benthic compartment: i) seagrasses (plant and meadow level), ii) sediment, and iii) the whole benthic community (which includes the sediment, seagrasses, and its associated benthic community, such as benthic infauna, epiphytes, etc.). Field work was conducted in June 2018.

2.2 Environmental biogeochemical descriptors

Descriptors of the water mass in the lagoon around the seagrass meadows were monitored using a combination of

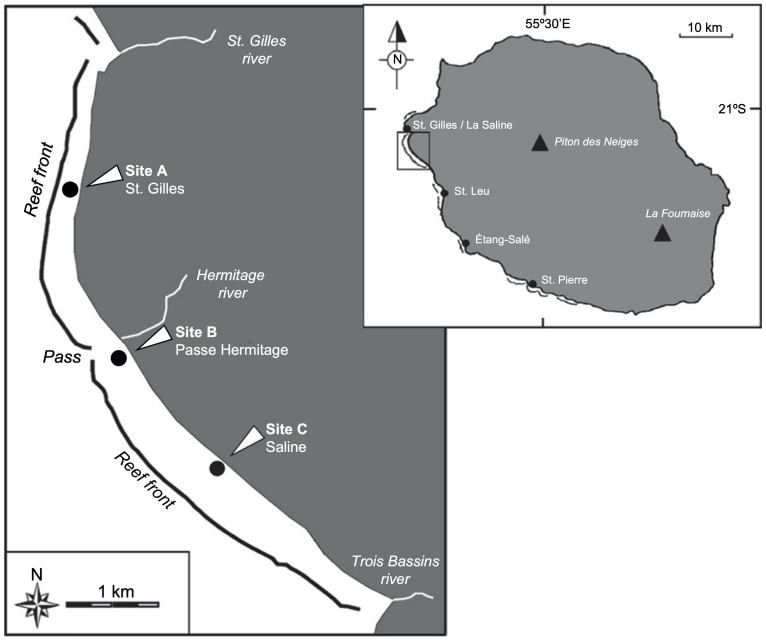

FIGURE 1
Sampling locations at Reunion Island. "Saint-Gilles" (STG, site A), "Passe Ermitage" (PAS, site B) and "Saline" (SAL, site C). Modified from Clavier et al. (2008).

autonomous sensors and analytical techniques. Temperature, dissolved oxygen (PreSens®), and irradiance (Odyssey Integrating PAR sensor, Dataflow Systems) were measured *in situ* at each sampling location. Water samples for salinity, nutrients, pH and alkalinity analysis were also taken at the sampling locations for later analysis at University of La Reunion. Salinity was measured using a multiparameter probe (YSI 6920). Ammonium analyses were performed spectrophotometrically (Kontron Uvikon 922) according to the indo-phenol blue method following Aminot and Kerouel (2004). Nitrate, nitrite, and phosphate were measured using a Seal Autoanalyzer III and standard analysis methods. Potentiometric determination of pH (Radiometer TIM865 titrator with combined pH electrode pHC2401-8) was performed at 25°C using Tris/HCl and 2-aminopyridine/HCl buffers in synthetic seawater to calibrate the electrode (Dickson et al., 2007). Alkalinity was determined by potentiometric titration using 0.01 M HCl in NaCl to approximate the ionic strength of seawater using Certified Reference Material from A. Dickson laboratory (Scripps Institution of Oceanography) as standard.

Sediment samples around the seagrass meadows were collected using Plexiglas tubes (i.d. 5 cm, length 30 cm, n = 3). Organic matter content of the first centimetre was measured as loss on ignition (burned at 550 °C for 4 hours). Chlorophyll content was measured in the top one cm, extracting the photosynthetic pigments with 100% methanol for 24 hours at 4 °C (Thompson et al., 1999) and determining the pigment content spectrophotometrically as previously described (Ritchie, 2008). Selected emerging organic contaminants (CECs), among the most widely detected in the sediment, such as polycyclic fragrances, nitro musks, triclosan (antibacterial) and methyl triclosan (its metabolite), nonylphenol isomers (surfactant), DEET (insect repellent), UV filters and organophosphorus flame retardants (OPFRs) were analysed by in-cell clean-up pressurised liquid extraction (PLE) followed by gas chromatography-triple quadrupole mass spectrometry (GC-MS/MS; SCION 456-GC and SCION TQ, Bruker). Limits of detection (lod) of the method, calculated using a signal to noise ratio of 3:1, ranged between 0.003 and 2.4 ng g^{-1}. Further details on the extraction and detection methodology can be found in Pintado-Herrera et al. (2016).

2.3 Seagrass metabolism

The net productivity and respiration of *S. isoetifolium* individuals were evaluated measuring oxygen evolution during *in situ* incubations (Olivé et al., 2017) with PreSens® optodes. At each location (site A, B and C), plants (circa 10-15 cm rhizome bearing 5-7 shoots) were randomly collected, gently cleaned, and incubated in gas-tight zip-bags (PPC+PET) with its own surrounding water. At each site, two rounds of incubations were performed around solar noon (noon ± 3 hour). On each round, incubations for net plant productivity (NPP)

(transparent chambers, n = 5) and respiration (R) (darkened chambers, n = 5) were performed. Seagrass structural descriptors (biomass and morphometry) were also recorded after the incubations for rates normalisation. Productivity and respiration of seagrass meadow at each site was calculated considering the biomass of seagrass per area at each of the studied sites. Daily productivity, respiration, and metabolic balance budgets of *S. isoetifolium* plant and meadow were calculated assuming a 12 h daylight photoperiod as it was in Reunion Island during the sampling period. The metabolic balance was calculated as the output between daily productivity and respiration. Since incubations ran at noon (i.e. maximum irradiance), seagrass productivity measurements were most likely maximised (Olivé et al., 2016), so the daily budgets calculated, for both plant and meadow, can be considered a proxy of maximum productivity and metabolic balance.

2.4 Sediment metabolism

2.4.1 Sampling procedure

Three small cores (10 cm length, 4 cm i.d., n = 3 per site) enclosing sediment were randomly collected within the seagrass meadows at each sampling site (A, B and C) for microsensor measurements. Cores and *in situ* water (≈ 20 L) were transported immediately to the laboratory (within 30 minutes after collection) and maintained at 26 °C, similar to *in situ* water temperature.

2.4.2 Sediment microprofiles

Diffusive fluxes (O_2) of the water-sediment were evaluated using oxygen microelectrodes in the laboratory on collected cores. Cores were maintained in a temperature-controlled aquarium at 26 °C with bubbling to ensure adequate oxygen saturation and water turbulence. Cores were exposed to light conditions (white LED, ≈ 50 µmol quanta m^{-2} s^{-1}) for one hour before starting the measurements and, subsequently, to dark conditions for another hour. A minimum of 3 microprofiles were measured in each core in both light and dark conditions using Clark type oxygen microelectrodes (Unisense, Denmark). The microsensor tip was 50 µm in diameter and profiles were calibrated using O_2 concentrations in the vigorously bubbled overlying water as 100% O_2 saturation and the signal at anoxic depths as zero. Microsensors were connected to a picoammeter (Multimeter, Unisense, Denmark) and driven into the sediment using a motorised micromanipulator (MM33, Unisense, Denmark) in vertical steps of 100 µm. O_2 fluxes across the sediment-water interface were calculated by Fick's first law of diffusion, using the vertical gradient in the diffusive boundary layer following the equation:

$$J\left(mmolO_2m^{-2}h^{-1}\right) = D_0\frac{\partial[O_2]}{\partial z}$$

Where, D_0 is the diffusion coefficient of oxygen in water at the temperature and salinities of the sample and $\partial[O_2]/\partial z$ is the oxygen concentration gradient measured in the diffusive boundary layer. Daily metabolic fluxes and budgets were calculated assuming a 12 h daylight photoperiod.

2.5 Benthic community metabolism and water-sediment fluxes

2.5.1 Sampling procedure

Six sediment cores (30 cm length, 5.6 cm i.d., n = 6 per site) enclosing the whole community, i.e. sediment + seagrass + the associated benthic community (e.g. benthic infauna, epiphytes, etc), were randomly collected within the seagrass meadows at each sampling site (A, B, C) for community incubations. Transportation and laboratory setting up was conducted as for sediment cores (section 2.4.1).

2.5.2 Community incubations

Total oxygen and nutrient fluxes between the benthic community and the overlying water were measured by sediment core incubations. Three cores were maintained at dark conditions, whereas the other three were maintained illuminated (white LED, ≈50 µmol quanta m^{-2} s^{-1}). To ensure turbulence in the water column during the incubation, magnetic stirrers were mounted inside each core and driven by an external rotating magnet. Thirty minutes before the start of the incubations, $15N-NO_3^-$, was added to each one of the cores to reach a final concentration of 5 µM (initial $14-NO_3^-$, concentration in the cores ranged 0.4-0.8 µM) to trace processes of the N cycle (i.e. denitrification and anammox). Stirring was kept on and cores left without the stopper to avoid changes in the oxygen concentration of the water. Initial water samples for nutrients (i.e. nitrate, nitrite and ammonium) were collected and initial oxygen concentration was measured using one oxygen microsensor (Unisense, Denmark). The sediment cores were then sealed by closing the tubes with rubber stoppers and kept closed for 3-3.8 hours of incubation. Water samples were withdrawn from the cores using a syringe before closing the cores with the stoppers and at the end of the incubation.

The change in concentration of gases and nutrients in the water column were used to calculate the benthic community-water fluxes as a mass balance following the equation:

$$J = \frac{C_{final} - C_{initial}}{t} \times \frac{V}{A}$$

Where: $C_{initial}$ and C_{final} were the concentrations measured before closing with the stopper and immediately after the

incubation, respectively; t was the incubation time; V was the water volume and A was the area of the sediment. Samples for nutrients were filtered through a 0.2 µm nylon filter into a polyethylene vial and stored at -18 °C until later analysis. Nutrients concentration was analysed at Cadiz University as described in García-Robledo et al. (2014). Samples for the determination of 15N-N_2 were collected and preserved with $ZnCl_2$ for later analysis. The excess concentration of $^{29}N_2$ and $^{30}N_2$ was measured in a CF-IRMS at the Centre for Geomicrobiology, Aarhus University (Denmark). Rate calculations were done according to Thamdrup and Dalsgaard (2002). Daily fluxes and budgets were calculated assuming a 12 h daylight photoperiod.

2.6 Statistical Analysis

One-way ANOVAs were performed to determine differences among the three sites studied in the environmental parameters as well as in oxygen and nutrient fluxes measured on each component (i.e. seagrasses, sediment, benthic community) in both light and darkness. The significance level was set at α = 0.05. Data were transformed (square-root) when necessary to meet parametric conditions. If -parametric conditions were not meet after transformation, a non-parametric Kruskal-Wallis test was applied. To link the biogeochemical descriptors and the oxygen fluxes measured on each component of the lagoon, a Spearman's Rank correlation analysis was conducted considering the normalized mean values at each station (i.e. n=3 ranks, station A, B and C) using the IBM SPSS software. Lineal regression model was run between nutrient fluxes and initial nutrients concentration. Unless otherwise indicated, statistical analysis was performed in R (version 4.1.1, R Core Team 2021) using RStudio (version 2021.09.0). Values along the text are mean ± standard deviation (SD) to give indication about the variability of the data. Bars in figures represent mean ± standard error of the mean (SEM) to give indication of the uncertainty in the estimate of the mean (Cumming et al., 2007). Standard deviation of daily budgets was calculated considering error propagation of the mean (Laffers, 2010).

3 Results

3.1 General biogeochemical description

Biogeochemical descriptors of both water and sediment measured at each site are shown in **Table 1**. Nutrient concentrations (NH_4^+, NO_2^-, NO_3^-, PO_4^{3-},) were low (< 0.5 µM), with the pristine location (St A) showing the lowest N concentrations (**Table 1**, $p < 0.001$). The organic matter content in the sediment was less than 5% and chlorophyll concentration remained lower than 10 µg g^{-1}, with the highest values measured at site C (**Table 1**).

The presence of organic contaminants of emerging concern (CECs) in the sediment was generally low across the lagoon (lower than 3.72 ng g^{-1} DW). The main organic contaminants found in the sediment were sunscreen UV filters, organophosphate flame retardants (OPFRs) and nonylphenols (NPs), which were detected at all three sites studied (**Table 1**). The higher concentrations of CECs were detected at site C (i.e. 3.7 ng g^{-1} DW of UV filter octocrylene, OC, and 0.9 ng g^{-1} DW of OPFR tri-n-butyl phosphate, TnBP, **Table 1**). (See **Table S1** in **Supplemental Material** for a complete list of CECs analysed but not detected).

3.2 Seagrass metabolism

The plant metabolic balance, understood as the balance between productivity and respiration, was autotrophic in all sites studied and averaged plant net productivity of *S. isoetifolium* significantly exceeded respiration by more than 6-fold (85 ± 9 and 14 ± 3 µmol O_2 g DW^{-1} h^{-1}, respectively, **Figure 2**; **Table S2**). However, net productivity and respiration trends differed among locations (**Figure 2**, $p < 0.001$ and $p < 0.01$, respectively, **Table S2**). Plants growing in the pristine location of St. Gilles (STG, Site A) showed the highest productivity, while those growing at the impacted site Passe Hermitage (PAS, Site B) showed the highest respiration (106 ± 14 and 19 ± 7 µmol O_2 g DW^{-1} h^{-1}, respectively). The daily plant metabolic balance (PMB) was autotrophic in all sites studied but the PMB in the pristine location (Site A) was double of the impacted site (Site B) (**Figure 2**).

The plant and meadow structure also differed among the 3 locations sampled. Plant morphotype (leaf length and above/below biomass ratio) and shoot density were lower at Passe Hermitage (site B) (*authors' personal observation*). Accordingly, seagrass biomass per area was significantly lower at Site B while similar biomass was recorded at sites A and C (276 ± 122; 53 ± 14; 320 ± 133 g DW m^{-2}, for St A, B and C, respectively, $p < 0.001$). These differences resulted in significantly lower meadow net productivity and respiration at site B under light and dark conditions, respectively (**Figure 3**, $p < 0.001$, **Table S2**). Overall, the daily meadow metabolic balance (MMB) in all sites was autotrophic. However, the daily metabolic balance inferred for the meadow at Site B was around the 10% of that estimated at sites A and C (**Figure 3**). The mean daily metabolic balance estimated for *S. isoetifolium* meadows in the Reunion lagoon was 204.14 ± 21.97 mmol O_2 m^{-2} d^{-1}.

3.3 Sediment metabolism

Oxygen microprofiles showed that oxygen was quickly consumed in the first 2-3 mm of the sediment at the three

TABLE 1 Lagoon biogeochemical descriptors.

Compartment	Parameter (units)	Site A (STG) Mean ± SD (n)	Site B (PAS) Mean ± SD (n)	Site C (SAL) Mean ± SD (n)	ANOVA
Water	Irradiance (µmol quanta m^{-2} s^{-1})	702 ± 203 (51)	998 ± 210 (29)	665 ± 199 (40)	p < 0.001; A, C < B
Water	Salinity	34.52	34.61	34.76	
Water	Temperature (°C)	26.9 ± 0.5 (20)	25.9 ± 0.4 (19)	27.2 ± 0.2 (19)	p < 0.001; A, C > B (*)
Water	O_2 (uM)	222 ± 21 (20)	176 ± 16 (19)	224 ± 29 (19)	p < 0.001; A, C > B
Water	pH_{TOT}	8.04 ± 0.01 (3)	7.97 ± 0.01 (3)	8.09 ± 0.01 (3)	p < 0.001; C > A > B
Water	TA (µmol/kg)	2287 ± 3 (3)	2261 ± 1 (3)	2187 ± 2 (3)	p < 0.001; A > B > C
Water	NH_4^+ (µM)	0.29 ± 0.01 (3)	0.37 ± 0.01 (3)	0.48 ± 0.02 (3)	p < 0.001; A < B < C
Water	NO_3^- (µM)	0.13 ± 0.01 (3)	0.20 ± 0.01 (3)	0.24 ± 0.01 (3)	p < 0.001; A < B < C
Water	NO_2^- (µM)	0.06 ± 0.00 (3)	0.10 ± 0.01 (3)	0.10 ± 0.00 (3)	p < 0.001; A < B, C
Water	PO_4^{3-} (µM)	0.16 ± 0.01 (3)	0.12 ± 0.00 (3)	0.09 ± 0.01 (3)	p < 0.001; A > B > C
Sediment	OM (%)	3.4 ± 0.05 (5)	3.7 ± 0.44 (4)	5.04 ± 0.28 (5)	p < 0.001; A, B < C
Sediment	Chl a (µg g^{-1})	7.87	6.63	9.06	
Sediment			CECs (ng g^{-1} DW)		
	Fragrances				
	Galaxolide	lod	lod	0.075	
	Tonalide	0.108	lod	0.137	
	UV Filters				
	OC	2.644	1.153	3.709	
	4-MBC	0.180	0.262	0.562	
	EHMC	0.123	0.082	0.217	
	BP-3	0.092	lod	0.252	
	OPFRs				
	TnBP	0.484	0.204	0.911	
	TiBP	0.027	lod	0.03	
	TEHP	0.008	lod	0.009	
	Other CECs				
	NPs	2.463	1.870	1.767	

Data are mean values ± standard deviation (sample size). Irradiance, salinity, temperature, oxygen (O2), pHTOT (25°C, total scale), total alkalinity (TA), ammonium (NH4+), nitrate (NO3-), nitrite (NO2-), and phosphate (PO43-) were measured in water. Organic matter (OM), chlorophyll a (Chl a), and contaminants of emerging concern (CECs) were measured in the first 3 centimetres of the sediment. CECs are UV filters (Octocrylene (OC), 4-methylbenzylidene camphor (4-MBC), Ethylhexyl methoxycinnamate (EHMC), and Benzophenone 3 (BP3)); organophosphate flame retardants (OPFRs) (tri-n-butyl phosphate (TnBP), tri-iso-butyl phosphate (TiBP), and tris-2-ethylhexyl phosphate (TEHP)); and nonylphenol isomers (NPs). (DW) indicates dry weight and (lod) indicates levels below the detection limit. In case no SD value is indicated, mean values refer to a pooled sample. ANOVA results are indicated as statistical significance (p-value) and Tukey HSD pos-hoc analysis for sites. (*) indicates non-parametric data.

sampling sites. In the site A (STG), net production profiles showed a clear production peak below the sediment-water interface, extending the oxygen penetration depth to 3-4 mm. Site B (PAS) showed the lowest oxygen penetration depth, being as low as 1 mm in some dark profiles (Figure S1).

Despite occasional profiles showing net production under light conditions, sediment oxygen fluxes were negative (i.e. oxygen consumption) (Figure 4). Among locations studied, the pristine site (St A) showed the lowest oxygen consumption in the sediment in both light and dark conditions (Figure 4, significant in darkness $p < 0.05$, Table S2). The daily metabolic oxygen balance in the sediment component (SMB, only sediment) was net heterotrophic in all sites (Figure 4). The average daily metabolic balance in the lagoon for the sediment component was -16.31 ± 4.20 mmol O_2 m^{-2} d^{-1}.

3.4 Benthic community metabolism and nutrient fluxes

The benthic community metabolism (i.e. sediment, seagrasses, and the associated benthic community) was net autotrophic in light conditions, releasing oxygen at a rate of 1.4 to 1.9 mmol m^{-2} h^{-1}, being similar in the three sites studied (Figure 5; Table S2). In darkness, oxygen was consumed at rates of 1.2 to 4 mmol m^{-2} h^{-1}, with the highest consumption rates measured at site C. The averaged daily metabolic balance in the lagoon for the benthic community (CMB) was -8.63 ± 24.86 mmol O_2 m^{-2} d^{-1}, that is, a net consumption of O_2 although the high variability associated to this value covers the range from autotrophic to heterotopic net balance.

In general, the benthic community consumed both ammonium and nitrate under light and dark conditions,

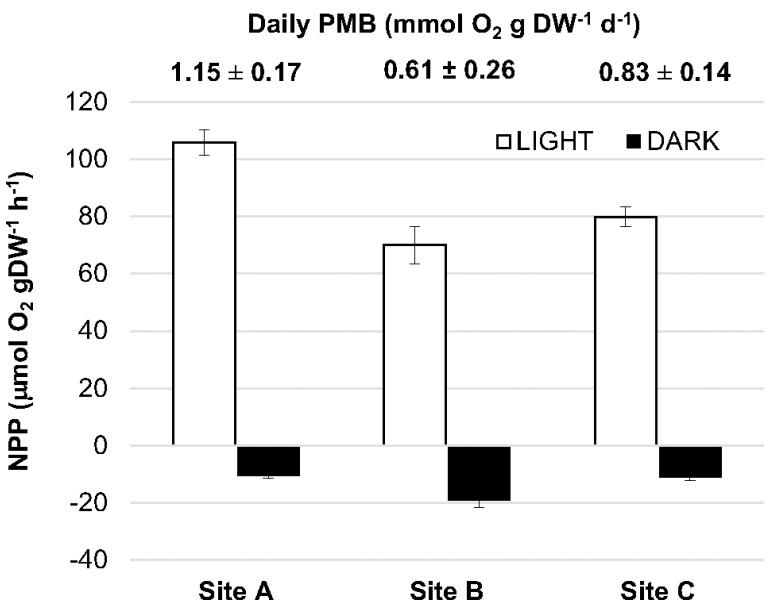

FIGURE 2
Net plant oxygen production of *S. isoetifolium* measured in light (net plant productivity, NPP, white columns) and in darkness (respiration, R, black columns) at "Saint-Gilles" (STG, site A), "Passe Ermitage" (PAS, site B) and "Saline" (SAL, site C). Bars are mean ± SEM. Numbers above indicate the daily plant metabolic balance (PMB) for each site (mean ± SD).

although the large heterogeneity in the rates measured resulted in large deviations from the mean value and therefore no significant differences were found between sites (Figures 6A, B Table S2). Nitrate consumption by denitrification and anammox was low (< 0.1 µmol m^{-2} h^{-1}) and a minor fraction of the total nitrate consumption (0.1-1.1%) but it was measured at significant rates in the three sites ($p < 0.05$, t-test). No differences were detected among stations in nitrate

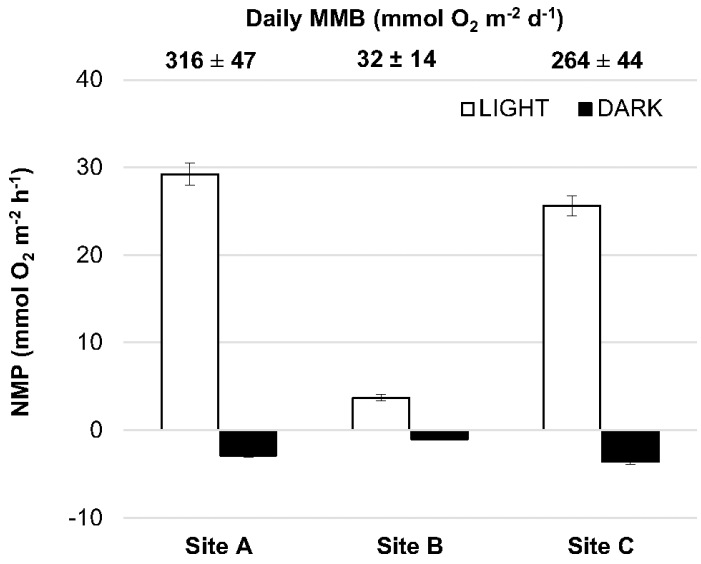

FIGURE 3
Seagrass net meadow productivity measured in light (white columns) and dark (black columns) conditions. Bars are mean ± SEM. Numbers above indicate the daily seagrass meadow metabolic balance (MMB) (mean ± SD) for each site.

consumption but for denitrification in darkness (Table S2). Daily denitrification rates ranged from 0.02 to 1.4 μmol m^{-2} d^{-1}, with higher rates measured at station A while anammox rates varied between 0.5 and 2.2 μmol m^{-2} d^{-1} with no clear trend found among sites (Figure 6C).

Initial nutrient concentrations measured in the core incubations were higher than those measured in samples collected *in situ*, especially for ammonium (Figure 6D, Table 1, respectively). This likely resulted in net consumption fluxes higher than those expected at *in situ* concentrations. Similarly, the measured ammonium fluxes are much higher than nitrate fluxes despite the similar trace levels found *in situ* for both nutrients.

4 Discussion

This study provides the first metabolic dataset for the seagrass *Syringodium isoetifolium* in the West Indian Ocean. The seagrass community in the Reunion lagoon was net autotrophic and contributed to the lagoon benthic metabolism. Large variability among sites was detected in the metabolic balance of each one of the benthic components assessed (i.e. seagrass, sediment, community) also associated with the natural and/or anthropic-driven environmental variability found in the lagoon. The metabolic balance of the benthic compartment in Reunion was slightly heterotrophic but highly variable. The high productivity and autotrophic metabolic balance of *S. isoetifolium* helped decreasing the sediment net heterotrophy. No significant nutrient inputs were detected in this study and the benthic community showed potential capacity for maintaining the lagoon oligotrophic condition *via* nitrogen retention (uptake by microphytobenthos and seagrasses) and removal (denitrification and anammox) but other sources of contamination, such as organic CECs, may potentially affect the benthic community and metabolism in the lagoon and should be considered in the future studies.

4.1 Biogeochemistry of Reunion lagoon

Biogeochemical descriptors measured in the water column were in the range of those previously reported in the Reunion lagoon (Tedetti et al., 2020). Nutrients measured in the water mass, as well as organic matter and chlorophyll in the sediment, were low and within the range expected for a tropical oligotrophic sandy lagoon (van Tussenbroek, 2011; Bayraktarov and Wild, 2014). Environmental pressures in the lagoon have been historically attributed to nutrients loads from watershed associated to increasing urbanization and agriculture (Cuet, 1989). However, the low nutrient concentration measured in this study does not support the hypothesis that Reunion lagoon is experiencing significant nutrients load or facing eutrophication risk, even at the "impacted" site of Passe Hermitage.

Together with inorganic nutrients, submarine groundwater discharges and rivers may also carry organic matter and

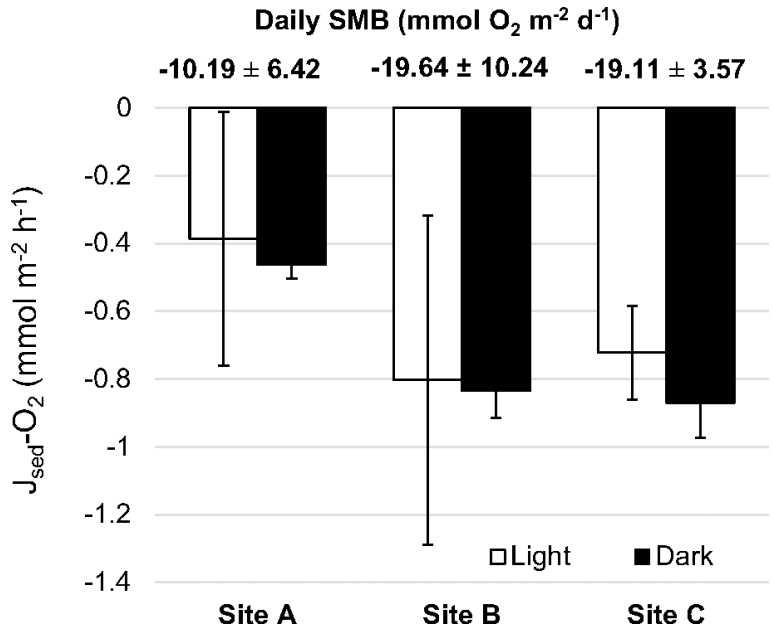

FIGURE 4
Sediment metabolic fluxes of oxygen measured in light (white columns) and dark (black columns) conditions. Bars are mean ± SEM. Numbers above indicate the daily sediment metabolic balance (SMB) (mean ± SD) for each site.

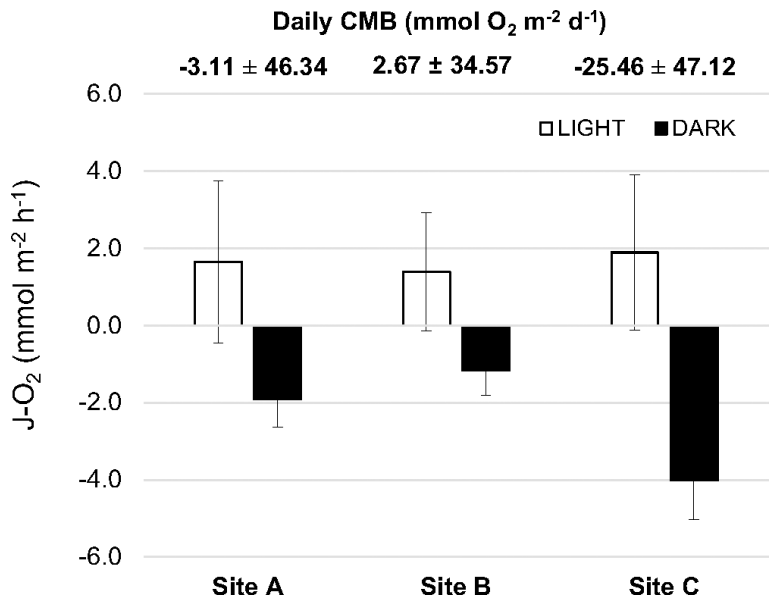

FIGURE 5
Community metabolic fluxes of oxygen measured in light (white columns) and dark (black columns) conditions. Positive rates mean net release from the community to the water column whereas negative values represent net consumption rates from the benthic community. Bars are mean ± SEM. Numbers above indicate the daily benthic community metabolic balance (CMB) (mean ± SD) for each site.

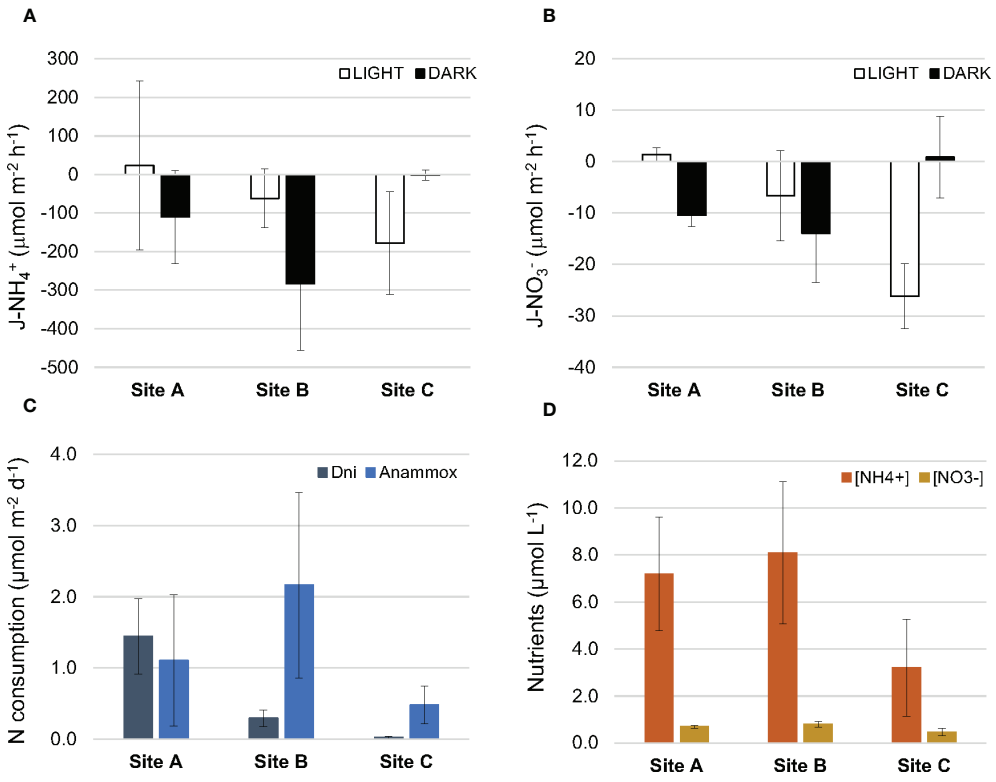

FIGURE 6
Net community fluxes of ammonium **(A)**, and nitrate **(B)**. Daily community nitrogen consumption rates (denitrification (Dni) and anammox) **(C)**. Nutrient concentrations (ammonium and nitrate) recorded in the water at the beginning of the incubation **(D)**. Bars are mean ± SEM.

contaminants to the lagoon (Tedetti et al., 2020). Organic contaminants are a growing threat in marine systems and their toxicity has been largely demonstrated (Soares et al., 2008; Miller et al., 2021). In this study, we analysed the presence of organic contaminants of emerging concern (CECS) as potential sources of anthropogenic pressure, providing the first report on CECs in the sediment of Reunion lagoon. In general, the number and concentration of organic contaminants detected in the lagoon were low in comparison with other coral reef ecosystems and tropical areas (Kawahata et al., 2004; Mitchelmore et al., 2019). Even though, CECs were still detectable in the sediment, which is particularly relevant considering the sandy matrix of Reunion lagoon and the low affinity of organic contaminants for sandy substrates (Pignatello, 2012). The main groups of CECs found in the sediment were the UV filters, widely used as sunscreen, organophosphorus flame retardants (OPFRs), widely used as plasticizers, and detergent-like nonionic surfactant nonylphenols (NPs). UV filters (sunscreen) were the most detected CECs in the lagoon at concentrations similar than those reported in several coastal areas (Tsui et al., 2015; Apel et al., 2018) while NPs and OPFRs concentrations were lower compared to other coral reef and coastal areas (Kawahata et al., 2004; Chen et al., 2019). River flow, runoff, and groundwater discharges carrying industrial and urban wastewater are considered main entries of CECs into coral reef systems (Kroon et al., 2020). However, the higher concentrations of UV filters detected at Saline (Site C), a popular frequented beach area, are likely due to sunscreen being directly released into the environment during recreational activities. This site also showed the higher percentage of organic matter, which may further favours CECs accumulation in the sediment due to the known interaction and affinity of organic pollutants with sediment organic matter (Pignatello, 2012). Benthic organisms may further accumulate CECs, as it has been recently reported for UV filters in belowground tissues of seagrasses (Agawin et al., 2022). Once incorporated, CECs may disrupt metabolic pathways in benthic organisms altering the metabolic balances at different trophic levels, with possible wider consequences in the marine food web and biogeochemical fluxes (Kawahata et al., 2004; Tsui et al., 2015; Miller et al., 2021). A significant negative correlation (Spearman's rank correlation, **Table S3**) was found between CECs (e.g. UV filters OC, 4-MBC, EHMC and BP-3, and OPFRs TnBP, TiBP, and TEHP) and the respiration rates in the 3 compartments studied (i.e. seagrass meadow, community and, to a less extend, sediment) as well as with the community metabolic balance (CMB). Although not conclusive, the reported negative correlations may indicate a potential negative effect of CECs on the mitochondrial functioning and metabolic routes as a result of oxidative damage, as it has been described in other species (Yeh et al., 2017; Leitão et al., 2021), which may impact in the respiration rates of seagrasses and the lagoon system. Although further work is needed, the presence of CECs in Reunion lagoon may constitute an environmental driver of pressure also contributing to the high metabolic variability detected in the benthic compartment (see discussion below). Our results highlight the need of considering new emerging contaminants together with classical biogeochemical descriptors to properly describe the environmental context and detect potential drivers of pressure for the benthic community in areas of high ecological value, such as tropical coral reefs.

4.2 Metabolic balance in the lagoon compartments

4.2.1 Seagrass metabolism

Plants of *S. isoetifolium* in Reunion showed a positive metabolic balance, understood as the balance between photosynthesis and respiration, confirming the autotrophic contribution of seagrasses to coral reef systems. The positive metabolic output resulted from plant photosynthesis largely exceeding respiration in all the sites assessed. The average daily metabolic balance calculated for seagrass meadows in Reunion (204.14 ± 21.97 mmol O_2 m^{-2} d^{-1}) falls within the range attributed to seagrass communities (Duarte et al., 2010) and within other tropical small-species (Anton et al., 2020). We also note our estimate should be considered as optimized since seagrass metabolism was assessed at noon when seagrass productivity is likely to be maximised (Olivé et al., 2016).

The net productivity, respiration, and metabolic balance of *S. isoetifolium* plants displayed large variability (up to two-fold) among the sites studied. Large intraspecific plasticity has been attributed to the metabolism of seagrasses, as well as other physiological and morphological traits, associated with environmental drivers (Olivé et al., 2013; Enríquez et al., 2019; Peralta et al., 2021). Differences in the metabolic balance of plants found at the different sites likely reflected the exposure to different environmental conditions. We hypothesised that plants in site B were potentially exposed to higher environmental pressure, such as nutrients or contamination from sewage loads. The lower metabolic balance of plants was recorded at the impacted site B (PASS) and was mainly due to a higher oxygen consumption (i.e. respiration) in darkness, though the net productivity recorded at this site was also the lowest. Increased respiration associated with nutrient enrichment has been already documented as a metabolic response of seagrasses (Burkholder et al., 2007). However, nutrients, organic matter, and organic contaminants levels remained low at the three sites studied. Hydrodynamics may also affect morphological and physiological traits in seagrasses, for instance favouring the development of the anchoring system, decreasing the above/belowground biomass ratio, and the proportion of autotrophic tissues (Peralta et al., 2006). Plants at site B (PAS) were indeed exposed to a higher hydrodynamic regime, due to the proximity to the reef pass (Tedetti et al., 2020), likely contributing to the lower metabolism recorded at this site.

After integrating *S. isoetifolium* metabolism per area projected, seagrass meadows at Reunion also resulted in net autotrophic systems but the daily productivity greatly varied, up to 10-fold, among locations. Together with metabolic traits, morphological descriptors of *S. isoetifolium* also differed among locations. Previous monitoring of seagrass meadows conducted in Reunion revealed large variations in seagrass seascape coverage along the recent decades in the reef lagoon (Cuvillier et al., 2017). In agreement with seascape monitoring, we detected more than 5-fold variation in the seagrass biomass per area among the sites studied with significant lower biomass at site B (PAS). Both natural, physical (e.g. hydrodynamics) and biotic disturbances (e.g. grazing), as well as anthropogenic pressures (e.g. grubbing, nutrient inputs) have been pointed as main drivers conditioning seagrass meadows stability in Reunion (Cuvillier et al., 2017). Reduced growth rates and shoot density has been further described as a response of seagrass to environmental forcing, such as eutrophication (Olivé et al., 2009) and hydrodynamic perturbation events (Peralta et al., 2006). Higher energetic demands at plant level together with environmental forcing likely affected growth rates and biomass partitioning of *S. isoetifolium* resulting in significantly lower biomass cover at impacted location (PAS). This, in turn, scaled-up into significantly lower net metabolism and lower autotrophic contribution of seagrass meadows in the impacted site.

4.2.2 Sediment metabolism

The average daily metabolic balance calculated for the sediment component (-16.31 ± 4.20 mmol O_2 m^{-2} d^{-1}) was in the range reported in *in situ* sediment incubations conducted in the same locations (Taddei et al., 2007), reflecting a net oxygen consumption by the sediment likely being a carbon dioxide source.

The sediment oxygen fluxes measured in the sediment-water interface with microsensors were negative, i.e. net heterotrophic, even under light conditions at the irradiance levels set in the laboratory. The presence of benthic microalgae, microphytobenthos, was confirmed by the detection of chlorophyll a and c in the sediments of the three locations. Chlorophyll a concentration in the first centimetre of the sediment ranged from 6 to 9 μg g^{-1}, equivalent to 43 to 59 mg m^{-2}. These values were in the range of concentrations measured in other coral reef sediments where sediments are net autotrophic and microphytobenthos has been shown to be a relevant primary producer in the benthic compartment (Heil et al., 2004; Hochard et al., 2012; Cox et al., 2020). Despite the similar biomass of microphytobenthos (based on the chlorophyll concentrations) suggesting certain relevance of the microphytobenthos biomass in the benthic compartment, our measurements showed that the sediment was net heterotrophic. The relatively low light intensity reached in the laboratory, compared to the *in situ* light levels recorded in the field in this study and reported in other studies (Taddei et al., 2007), may have limited photosynthesis of microphytobenthos during the microsensor measurements. Some oxygen microprofiles showed net oxygen production, reflecting the potential for microphytobenthonic productivity. The larger variability in the sediment fluxes reported under light conditions was caused by the occasional presence of net productive spots with high gross productivity, even at the low light intensity set in the lab conditions. *In situ* oxygen microprofiles could provide further relevant information about the contribution of benthic microalgae to the metabolism of the coral reef sediment (Glud et al., 2000). However, such measurements are technically complex and were not carried out during the present study. Future studies should therefore consider the *in situ* use of microsensors, to fully characterise the metabolic role of microphytobenthos in the coral reef system of Reunion island.

4.2.3 Community metabolism

Oxygen fluxes between the benthic community and the water column measured with core incubations integrated the metabolism of the whole benthic community, including the sediment, seagrasses, and the associated benthic community.

The large variability of the values measured in diffusive (sediment) and community fluxes at each site did not allow the detection of significant changes in the metabolic balance among the three sites studied, however noticeable differences could be observed between the contribution of the sediment alone and the whole community to the net oxygen consumption. As it could be expected, oxygen fluxes measured in dark conditions were 2-4 times higher than the values obtained for the sediment with microsensors, reflecting the increase in oxygen consumption by the other community components (seagrasses and associated benthic community). Despite including the seagrasses, the respiration rates of the community were in the same range of those reported for bare sediment measured using *in situ* benthic incubation chambers close to our study sites (Taddei et al., 2007; Taddei et al., 2008). The respiration of the sediment was about 21-25% of the community respiration in sites A and C, increasing up to 70% in site B. The high contribution of the community in the respiratory rates measured in sites A and C revealed that the benthic community has a relevant role in the net oxygen consumption in the sandy areas of the reef lagoon. Previous studies in the lagoon had however considered only the bare sediment (Taddei et al., 2007; Taddei et al., 2008), excluding the contribution of the community associated with the seagrass meadows. On the other hand, the lowest contribution of the benthic community to the oxygen consumption rates in darkness was detected in Passe Hermitage (St B), which also held the lowest seagrass coverage and biomass.

The major contribution of the seagrasses to the benthic community metabolism was detected during light conditions. Unlike the sediment component, the benthic community was

net autotrophic at the three stations, shifting the role of the lagoon to a net oxygen producer. Similarly to the microphytobenthonic productivity measured in the sediment, the irradiance during the laboratory incubations was low compared to *in situ* values, likely limiting the net oxygen production by the seagrass community. *In situ* community incubations similar to those performed in the bare sediments by Taddei et al. (2007) could provide useful information about the metabolic activity of the seagrass meadows, further supporting the relevance of the benthic compartment in the net production of the reef lagoon as our results suggest.

4.2.4 Lagoon-wide metabolic balances

Lagoon-wide, the mean daily benthic community metabolic balance estimated for the lagoon was slightly heterotrophic (-8.63 ± 24.86 mmol O_2 m^{-2} d^{-1}). However, the high uncertainty associated to this value does not allow to assertively characterize the system as net heterotrophic but close to zero oscillating between autotrophy and heterotrophy. Mean O_2 fluxes varied *circa* 10-fold among sites studied with large variability also associated within each site. The large metabolic variability found on the species *S. isoetifolium* across reduced spatial scales (hundreds of metres) has been also described in other seagrass species (Olivé et al., 2013). Moreover, the sediment and the community metabolism also varied significantly across the lagoon highlighting the need of considering spatial variability when calculating global metabolic budgets. As Clavier et al. (2008) noted for temporal scales, metabolic budgets measured in limited areas and then extrapolated to larger areas without considering the associated variability may entail large inaccuracies when used in ecosystem models.

Despite this variability, the global metabolic balance of the benthic community was less heterotrophic than the sediment compartment (-8.63 ± 24.86 and -16.31 ± 4.20 mmol O_2 m^{-2} d^{-1}, respectively). Although seagrass beds coverage in Reunion Island is relatively low and limited to one single species, this study reveals the major role that seagrasses may hold in contributing to the autotrophic metabolic balance of reef lagoon. In order to get a closer estimate of the contribution of seagrass meadows to the community metabolism, we performed a scaling-up exercise. The productivity of seagrass meadow (NMP), measured under natural light conditions, was recalculated for the irradiance used in the laboratory for the sediment and community incubations (i.e. laboratory LED lights) using the PI curves parameters for *S. filiforme* provided by Major and Dunton (2000). At the laboratory irradiance, the NMP of seagrass meadows was reduced by circa 85% (i.e. 4.38 ± 0.59, 0.56 ± 0.16, 3.84 ± 0.52 mmol O_2 m^{-2} h^{-1}, for St. A, B and C, respectively) falling within the same order of magnitude of metabolic rates measured in the sediment and the benthic community (**Figures 4** and **5**). When adding the seagrass contribution to the oxygen fluxes measured in the sediment (i.e. sediment + seagrass), the NPP values obtained (3.99, -0.25, 3.11 mmol O_2 m^{-2} h^{-1}, for St A, B, C, respectively) fit closer to the community fluxes measured in the laboratory (1.65, 1.39, 1.89 mmol O_2 m^{-2} h^{-1}, for St A, B and C, respectively, **Figure 5**). Indeed, estimated mean daylight fluxes for the lagoon calculated from sediment + seagrass data closely matched those obtained for the benthic community (2.29 and 1.65 mmol O_2 m^{-2} h^{-1}, respectively). These results highlight the major role that seagrass *S. isoetifolium* plays in turning the benthic metabolism of the Reunion lagoon from net heterotrophy into net autotrophy and further confirm seagrasses as a key component to consider when calculating benthic fluxes and global metabolism in the benthic compartment.

4.2.5 Nutrient fluxes

Nitrogen fluxes in the community incubations were also assessed to evaluate the potential role of the benthic community as sink or source of nutrients in the lagoon. *In situ* nitrogen and phosphorus nutrient concentrations were below 0.5 µM at the three stations, confirming the low nutrient availability in the water column and the oligotrophic conditions of the lagoon. However, the sampling of the cores for community incubations likely induced a perturbation in the low nutrient conditions of the water column. Ammonium concentrations measured in the water column inside the cores ranged from 1 to 5 µM, being 2-10 times higher than the concentrations measured *in situ* (about 0.5 µM). Ammonium accumulates in the porewater (Capone et al., 1992) and the increased concentrations measured in the cores suggest that sediment resuspension during the collection or later manipulation of the sediment cores and the release of porewater ammonium may have taken place. Nitrate concentrations in the water column during the incubations were similar to those measured *in situ*, suggesting that nitrate did not accumulate in the porewater as has also been measured in other coral reef sediments (Capone et al., 1992) and the sediment manipulation did not cause a relevant increase in the nitrate concentration inside the cores.

Ammonium and nitrate fluxes were significantly and negatively correlated with the concentration of each nutrient at the beginning of the incubation (linear regression, $p < 0.01$, **Table S4**), likely reflecting the nutrient limitation status of the community. At low nutrient concentrations, fluxes were close to zero or even positive whereas negative values (i.e. net consumption) were detected in samples with higher initial nitrogen concentrations. The increase in ammonium concentration caused by the slight sediment disturbance resulted in increased ammonium consumption. Similarly, the increase in nitrate concentrations caused by isotope addition proportionally increased nitrate consumption rates. In both cases, the increase in nutrient concentration resulted in a proportional increase in nutrient flux to the benthic compartment. These results indicate the capacity of the benthic ecosystem for nutrient uptake when nutrient concentrations increase in the water column. Nutrient fluxes in seagrass communities has been shown to be proportional to the nutrient concentrations in the water column at low concentrations, being consequence of nutrient uptake by the

different components of the community (seagrasses and microphytobenthos) (Cornelisen and Thomas, 2006). Therefore, slight and sporadic increases in nutrient loading to the reef could be buffered by the nutrient retention capacity of the seagrass benthic community, which absorbs nutrients from the water column at a rate proportional to the concentration of nutrients in the water column. Nutrient discharges from groundwater systems have been described in the area (Tedetti et al., 2020) and the potential nutrient uptake from the seagrass community (Alexandre et al., 2011) might dampen the negative impacts of nutrient enrichment in oligotrophic ecosystem such as the Reunion Island lagoon.

The nitrate flux towards the benthic community also included denitrification and anammox processes. Nitrate transformations to nitrogen gas were detected in the community incubations at the three sites confirming the presence of this process in the sediments of the reef lagoon. Rates measured were low as could be expected by the low nitrate levels found in the lagoon, resulting in rates similar to those found in subtropical seagrass sediments (Salk et al., 2017). Dissimilatory reduction of nitrate to ammonium (DNRA) was not measured in this study and it might induce the underestimation of denitrification and anammox rates (Song et al., 2013; Salk et al., 2017). However, DNRA rates in intact sediment cores are commonly low and the impact on denitrification and anammox rates are negligible (Song et al., 2016). On average, only 0.4-1.2% of the nitrate flux to the sediment was converted to dinitrogen (N_2) and removed from the system. While the nutrients incorporated by the photosynthetic community can return to the system through the degradation of their biomass, denitrification and anammox processes imply a loss of nitrogen from the system. These nitrogen consumption processes of the benthic compartment, although slow, remove a fraction of the nutrient load of the ecosystem, likely contributing to the maintenance of the oligotrophic conditions of the lagoon.

Data availability statement

The datasets presented in this study can be found in online repositories. The names of the repository/repositories and accession number(s) can be found below: ZENODO repository (https://doi.org/10.5281/zenodo.6822296).

Author contributions

IO, EG-R, JS, RS, NK, PC, and PF contributed to conception and design of the study; IO, EG-R, JS, PC, and PF conducted field work; IO, EG-R, MP-H, and PC conducted laboratory analysis; IO and EG-R organized and analysed the database; IO wrote the first draft of the manuscript; EG-R and MP-H wrote sections of the manuscript. All authors contributed to manuscript revision, read, and approved the submitted version.

Funding

This research was supported by funding from the European Union's Horizon 2020 research and innovation programme under grant agreements No 654182 (ENVRIplus project, TNA-MACRORE) and No 752250 (Marie Skłodowska-Curie grant scheme MSCA-IF-EF-ST, SEAMET). This study received funding from the Integrative Marine Ecology Department from Stazione Zoologica Anton Dohrn; from the 2014-2020 European Regional Development Fund (ERDF) Operational Programme; the Department of Economy, Knowledge, Business and University of the Regional Government of Andalusia (Spain) (FEDER-UCA18-107225); from the Portuguese national funds from FCT - Foundation for Science and Technology through projects UIDB/04326/2020, UIDP/04326/2020 and LA/P/0101/2020.

Acknowledgments

Authors thank the ENVRIplus project for providing TransNational Access (TNA) to OSU-Réunion stations - MACRORE project. IO was supported by a postdoctoral grant (H2020-MSCA-IF-2016-752250). EG-R is supported by the Spanish Ramon y Cajal Program (RYC2019-027675-I). The authors thank Sophie Bureau, for her valuable help and her technical support in the field.

Conflict of interest

The authors declare that the research was conducted in the absence of any commercial or financial relationships that could be construed as a potential conflict of interest.

Publisher's note

Supplementary material

The Supplementary Material for this article can be found online at: https://www.frontiersin.org/articles/10.3389/fmars.2022.867986/full#supplementary-material

References

Agawin, N. S. R., Sunyer-Caldú, A., Díaz-Cruz, M. S., Frank-Comas, A., García-Márquez, M. G., and Tovar-Sánchez, A. (2022). Mediterranean Seagrass posidonia oceanica accumulates sunscreen UV filters. *Mar. Pollut. Bull.* 176, 113417. doi: 10.1016/j.marpolbul.2022.113417

Alexandre, A., Silva, J., Bouma, T. J., and Santos, R. (2011). Inorganic nitrogen uptake kinetics and whole-plant nitrogen budget in the seagrass zostera noltii. *J. Exp. Mar. Biol. Ecol.* 401, 7–12. doi: 10.1016/j.jembe.2011.03.008

Aminot, A., and Kerouel, R. (2004). *Hydrologie des écosystèmes marins: Paramètres et analyses* (Paris: IFREMER).

Anton, A., Baldry, K., Coker, D. J., and Duarte, C. M. (2020). Drivers of the low metabolic rates of seagrass meadows in the red Sea. *Front. Mar. Sci.* 7. doi: 10.3389/fmars.2020.00069

Apel, C., Tang, J., and Ebinghaus, R. (2018). Environmental occurrence and distribution of organic UV stabilizers and UV filters in the sediment of Chinese bohai and yellow seas. *Environ. Pollut.* 235, 85–94. doi: 10.1016/j.envpol.2017.12.051

Barrón, C., Duarte, C. M., Frankignoulle, M., and Borges, A. V. (2006). Organic carbon metabolism and carbonate dynamics in a Mediterranean seagrass (Posidonia oceanica), meadow. *Estuar. Coast.* 29 (3), 417–426. doi: 10.1007/BF02784990

Bayraktarov, E., and Wild, C. (2014). Spatiotemporal variability of sedimentary organic matter supply and recycling processes in coral reefs of tayrona national natural park, Colombian Caribbean. *Biogeosciences* 11 (11), 2977–2990. doi: 10.5194/bg-11-2977-2014

Bell, P. R. F. (1992). Eutrophication and coral reefs–some examples in the great barrier reef lagoon. *Water Res.* 26 (5), 553–568. doi: 10.1016/0043-1354(92)90228-V

Borges, A. V., Schiettecatte, L. S., Abril, G., Delille, B., and Gazeau, F. (2006). Carbon dioxide in European coastal waters. *Estuar. Coast. Shelf. Sci.* 70, 375–387. doi: 10.1016/j.ecss.2006.05.046

Bouma, T. J., Olenin, S., Reise, K., and Ysebaert, T. (2009). Ecosystem engineering and biodiversity in coastal sediments: posing hypotheses. *Helgoland. Mar. Res.* 63 (1), 95–106. doi: 10.1007/s10152-009-0146-y

Burkholder, J. M., Tomasko, D. A., and Touchette, B. W. (2007). Seagrasses and eutrophication. *J. Exp. Mar. Biol. Ecol.* 350 (1–2), 46–72. doi: doi: 10.1016/j.jembe.2007.06.024

Capone, D. G., Dunham, S. E., Horrigan, S. G., and Duguay, L. (1992). Microbial nitrogen transformations in unconsolidated coral reef sediments. *Mar. Ecol. Prog. Ser.* 80, 75–88. doi: 10.1016/j.jembre.2007.06

Chazottes, V., Reijmer, J. J. G., and Cordier, E. (2008). Sediment characteristics in reef areas influenced by eutrophication-related alterations of benthic communities and bioerosion processes. *Mar. Geol.* 250 (1), 114–127. doi: 10.1016/j.margeo.2008.01.002

Chen, M., Gan, Z., Qu, B., Chen, S., Dai, Y., and Bao, X. (2019). Temporal and seasonal variation and ecological risk evaluation of flame retardants in seawater and sediments from bohai bay near tianjin, China during 2014 to 2017. *Mar. pollut. Bull.* 146, 874–883. doi: 10.1016/j.marpolbul.2019.07.049

Clavier, J., Chauvaud, L., Cuet, P., Esbelin, C., Frouin, P., Taddei, D., et al. (2008). Diel variation of benthic respiration in a coral reef sediment (Reunion island, Indian ocean). *Estuar. Coast. Shelf. Sci.* 76 (2), 369–377. doi: 10.1016/j.ecss.2007.07.028

Cornelisen, C. D., and Thomas, F. I. M. (2006). Water flow enhances ammonium and nitrate uptake in a seagrass community. *Mar. Ecol. Prog. Ser.* 312, 1–13. doi: 10.3354/MEPS312001

Cox, T. E., Cebrian, J., Tabor, M., West, L., and Krause, J. W. (2020). Do diatoms dominate benthic production in shallow systems? a case study from a mixed seagrass bed. *Limnol. Oceanog. Lett.* 5 (6), 425–434. doi: 10.1002/lol2.10167

Cuet, P. (1989). *Influence des résurgences d'eaux douces sur les caractéristiques physico-chimiques et métaboliques de l'écosystème récifal à la réunion (Océan indien)*. Thèse de doctorat Chimie de l'environnement. http://www.theses.fr/1989AIX30044, Université d,Aix-Marseille III

Cumming, G., Fidler, F., and Vaux, D. L. (2007). Error bars in experimental biology. *J. Cell Biol.* 177 (1), 7–11. doi: 10.1083/jcb.200611141

Cuvillier, A., Villeneuve, N., Cordier, E., Kolasinski, J., Maurel, L., Farnier, N., et al. (2017). Causes of seasonal and decadal variability in a tropical seagrass seascape (Reunion island, south western Indian ocean). *Estuar. Coast. Shelf. Sci.* 184, 90–101. doi: 10.1016/j.ecss.2016.10.046

Dayton, P. (1972). Toward an understanding of community resilience and the potential effects of enrichment to the benthos at McMurdo sound, Antarctica. *Proc. Colloquium. Conserv. Prob. Antarctica.* 81–96.

Dickson, A. G., Sabine, C. L., and Christian, J. R. (2007). *Guide to best practices for ocean CO2 measurements*. Canada: PICES special publication 3, 191 pp.

Duarte, C. M., and Chiscano, C. L. (1999). Seagrass biomass and production: a reassessment. *Aquat. Bot.* 65 (1), 159–174. doi: 10.1016/S0304-3770(99)00038-8

Duarte, C., Dennison, W., Orth, R., and Carruthers, T. (2008). The charisma of coastal ecosystems: addressing the imbalance. *Estuar. Coast.* 31 (2), 233–238. doi: 10.1007/s12237-008-9038-7

Duarte, C. M., Marbà, N., Gacia, E., Fourqurean, J. W., Beggins, J., Barrón, C., et al. (2010). Seagrass community metabolism: Assessing the carbon sink capacity of seagrass meadows. *Global Biogeochem. Cyc.* 24 (4), GB4032. doi: 10.1029/2010gb003793

Enríquez, S., Marbà, N., Cebrián, J., and Duarte, C. M. (2004). Annual variation in leaf photosynthesis and leaf nutrient content of four Mediterranean seagrasses. *Botanica Mar.* 47, 295–306. doi: 10.1515/BOT.2004.035

Enríquez, S., Olivé, I., Cayabyab, N., and Hedley, J. D. (2019). Structural complexity governs seagrass acclimatization to depth with relevant consequences for meadow production, macrophyte diversity and habitat carbon storage capacity. *Sci. Rep.* 9 (1), 14657. doi: 10.1038/s41598-019-51248-z

Eyre, B. D., and Ferguson, A. J. P. (2002). Comparison of carbon production and decomposition, benthic nutrient fluxes and denitrification in seagrass, phytoplankton, benthic microalgae- and macroalgae-dominated warm-temperate Australian lagoons. *Mar. Ecol. Prog. Ser.* 229, 43–59. doi: 10.3354/meps229043

Fourqurean, J. W., Duarte, C. M., Kennedy, H., Marba, N., Holmer, M., Mateo, M. A., et al. (2012). Seagrass ecosystems as a globally significant carbon stock. *Nat. Geosci.* 5 (7), 505–509. doi: 10.1038/ngeo1477

García-Robledo, E., Corzo, A., and Papaspyrou, S. (2014). A fast and direct spectrophotometric method for the sequential determination of nitrate and nitrite at low concentrations in small volumes. *Mar. Chem.* 162, 30–36. doi: 10.1016/j.marchem.2014.03.002

Gattuso, J. P., Frankignoulle, M., and Wollast, R. (1998). Carbon and carbonate metabolism in coastal aquatic ecosystems. *Annu. Rev. Ecol. Systemat.* 29 (1), 405–434. doi: 10.1146/annurev.ecolsys.29.1.405

Gillooly, J. F., Brown, J. H., West, G. B., Savage, V. M., and Charnov, E. L. (2001). Effects of size and temperature on metabolic rate. *Science* 293 (5538), 2248–2251. doi: 10.1126/science.1061967

Glud, R. N. (2008). Oxygen dynamics of marine sediments. *Mar. Biol. Res.* 4 (4), 243–289. doi: 10.1080/17451000801888726

Glud, R. N., Gundersen, J. K., and Ramsing, N. B. (2000). ""Electrochemical and optical oxygen microsensors for in situ measurements. in in situ monitoring of aquatic systems: Chemical analysis and speciation,"," in *In situ monitoring of aquatic systems*. Ed. G. Horvai (Chichester, New York: Wiley), 20–73.

Graham, O. J., Aoki, L. R., Stephens, T., Stokes, J., Dayal, S., Rappazzo, B., et al. (2021). Effects of seagrass wasting disease on eelgrass growth and belowground sugar in natural meadows. *Front. Mar. Sci.* 8. doi: 10.3389/fmars.2021.768668

Heil, C. A., Chaston, K., Jones, A., Bird, P., Longstaff, B., Costanzo, S., et al. (2004). Benthic microalgae in coral reef sediments of the southern great barrier reef, Australia. *Coral. Reefs.* 23 (3), 336–343. doi: 10.1007/s00338-004-0390-1

Hochard, S., Pinazo, C., Rochelle-Newall, E., and Pringault, O. (2012). Benthic pelagic coupling in a shallow oligotrophic ecosystem: Importance of microphytobenthos and physical forcing. *Ecol. Model.* 247, 307–318. doi: 10.1016/j.ecolmodel.2012.07.038

Hughes, T. P., Baird, A. H., Bellwood, D. R., Card, M., Connolly, S. R., Folke, C., et al. (2003). Climate change, human impacts, and the resilience of coral reefs. *Science* 301 (5635), 929–933. doi: 10.1126/science.1085046

Kawahata, H., Ohta, H., Inoue, M., and Suzuki, A. (2004). Endocrine disrupter nonylphenol and bisphenol a contamination in Okinawa and ishigaki islands, Japan--within coral reefs and adjacent river mouths. *Chemosphere* 55 (11), 1519–1527. doi: 10.1016/j.chemosphere.2004.01.032

Kroon, F. J., Berry, K. L. E., Brinkman, D. L., Kookana, R., Leusch, F. D. L., Melvin, S. D., et al. (2020). Sources, presence and potential effects of contaminants of emerging concern in the marine environments of the great barrier reef and Torres strait, Australia. *Sci. Tot. Environ.* 719, 135140. doi: 10.1016/j.scitotenv.2019.135140

Laffers, R. (2010). *Error propagation calculator*. Available at: https://www.eoas.ubc.ca/ciurses/eosc252/ error-propagation-calculator-fj.htm.

Leitão, I., Leclercq, C. C., Ribeiro, D. M., Renaut, J., Almeida, A. M., Martins, L. L., et al. (2021). Stress response of lettuce (Lactuca sativa) to environmental contamination with selected pharmaceuticals: A proteomic study. *J. Proteomics* 245, 104291. doi: 10.1016/j.jprot.2021.104291

Macreadie, P. I., Costa, M. D. P., Atwood, T. B., Friess, D. A., Kelleway, J. J., Kennedy, H., et al. (2021). Blue carbon as a natural climate solution. *Nat. Rev. Earth Environ.* 2 (12), 826–839. doi: 10.1038/s43017-021-00224-1

Major, K. M., and Dunton, K. H. (2000). Photosynthetic performance in syringodium filiforme: seasonal variation in light-harvesting characteristics. *Aquat. Bot.* 68 (3), 249–264. doi: 10.1016/S0304-3770(00)00115-7

Martínez-Crego, B., Olivé, I., and Santos, R. (2014). CO2 and nutrient-driven changes across multiple levels of organization in *Zostera noltii* ecosystems. *Biogeosciences* 11 (24), 7237–7249. doi: 10.5194/bg-11-7237-2014

Miller, I. B., Pawlowski, S., Kellermann, M. Y., Petersen-Thiery, M., Moeller, M., Nietzer, S., et al. (2021). Toxic effects of UV filters from sunscreens on coral reefs revisited: regulatory aspects for "reef safe" products. *Environ. Sci. Europe.* 33 (1), 74. doi: 10.1186/s12302-021-00515-w

Mitchelmore, C. L., He, K., Gonsior, M., Hain, E., Heyes, A., Clark, C., et al. (2019). Occurrence and distribution of UV-filters and other anthropogenic contaminants in coastal surface water, sediment, and coral tissue from Hawaii. *Sci. Tot. Environ.* 670, 398–410. doi: 10.1016/j.scitotenv.2019.03.034

Olivé, I., García-Sánchez, M. P., Brun, F. G., Vergara, J. J., and Pérez-Lloréns, J. L. (2009). Interactions of light and organic matter under contrasting resource simulated environments: the importance of clonal traits in the seagrass *Zostera noltii*. *Hydrobiologia* 629, 199–208. doi: 10.1007/s10750-009-9773-1

Olivé, I., Silva, J., Costa, M. M., and Santos, R. (2016). Estimating seagrass community metabolism using benthic chambers: The effect of incubation time. *Estuar. Coast.* 39 (1), 138–144. doi: 10.1007/s12237-015-9973-z

Olivé, I., Silva, J., Lauritano, C., Costa, M. M., Ruocco, M., Procaccini, G., et al. (2017). Linking gene expression to productivity to unravel long- and short-term responses of seagrasses exposed to CO2 in volcanic vents. *Sci. Rep.* 7, 42278. doi: 10.1038/srep42278

Olivé, I., Vergara, J. J., and Pérez-Lloréns, J. L. (2013). Photosynthetic and morphological photoacclimation of the seagrass *Cymodocea nodosa* to season, depth and leaf position. *Mar. Biol.* 160, 285–297. doi: 10.1007/s00227-012-2087-2

Orth, R. J., Carruthers, T. J. B., Dennison, W. C., Duarte, C. M., Fourqurean, J. W., Heck, K. L., et al. (2006). A global crisis for seagrass ecosystems. *Bioscience* 56, 987–996. doi: 10.1641/0006-3568(2006)56[987:AGCFSE]2.0.CO;2

Peralta, G., Brun, F. G., Pérez-Lloréns, J. L., and Bouma, T. J. (2006). Direct effects of current velocity on the growth, morphometry and architecture of seagrasses: a case study on *Zostera noltii*. *Mar. Ecol. Prog. Ser.* 327, 135–142. doi: 10.3354/meps327135

Peralta, G., Godoy, O., Egea, L. G., de los Santos, C. B., Jiménez-Ramos, R., Lara, M., et al. (2021). The morphometric acclimation to depth explains the long-term resilience of the seagrass *Cymodocea nodosa* in a shallow tidal lagoon. *J. Environ. Manage.* 299, 113452. doi: 10.1016/j.jenvman.2021.113452

Pignatello, J. J. (2012). Dynamic interactions of natural organic matter and organic compounds. *J. Soils. Sed.* 12 (8), 1241–1256. doi: 10.1007/s11368-012-0490-4

Pintado-Herrera, M. G., González-Mazo, E., and Lara-Martín, P. A. (2016). In-cell clean-up pressurized liquid extraction and gas chromatography–tandem mass spectrometry determination of hydrophobic persistent and emerging organic pollutants in coastal sediments. *J. Chromatogr. A.* 1429, 107–118. doi: 10.1016/j.chroma.2015.12.040

Reid, A. J., Carlson, A. K., Creed, I. F., Eliason, E. J., Gell, P. A., Johnson, P. T. J., et al. (2019). Emerging threats and persistent conservation challenges for freshwater biodiversity. *Biol. Rev.* 94 (3), 849–873. doi: 10.1111/brv.12480

Revsbech, N. P., JØrgensen, B. B., and Brix, O. (1981). Primary production of microalgae in sediments measured by oxygen microprofile, H14CO3 - fixation, and oxygen exchange methods1. *Limnol. Oceanog.* 26 (4), 717–730. doi: 10.4319/lo.1981.26.4.0717

Ricart, A. M., Ward, M., Hill, T. M., Sanford, E., Kroeker, K. J., Takeshita, Y., et al. (2021). Coast-wide evidence of low pH amelioration by seagrass ecosystems. *Global Change Biol.* 27, 2580–2591. doi: 10.1111/gcb.15594

Risgaard-Petersen, N. (2003). Coupled nitrification-denitrification in autotrophic and heterotrophic estuarine sediments: On the influence of benthic microalgae. *Limnol. Oceanog.* 48 (1), 93–105. doi: 10.4319/lo.2003.48.1.0093

Risgaard-Petersen, N., and Ottosen, L. D. M. (2000). Nitrogen cycling in two temperate zostera marina beds: seasonal variation. *Mar. Ecol. Prog. Ser.* 198, 93–107. doi: 10.3354/meps198093

Ritchie, R. J. (2008). Universal chlorophyll equations for estimating chlorophylls a, b, c, and d and total chlorophylls in natural assemblages of photosynthetic organisms using acetone, methanol, or ethanol solvents. *Photosynthetica* 46 (1), 115–126. doi: 10.1007/s11099-008-0019-7

Roberts, C. M., McClean, C. J., Veron, J. E. N., Hawkins, J. P., Allen, G. R., McAllister, D. E., et al. (2002). Marine biodiversity hotspots and conservation priorities for tropical reefs. *Science* 295 (5558), 1280–1284. doi: 10.1126/science.1067728

Roth, F., Wild, C., Carvalho, S., Rädecker, N., Voolstra, C. R., Kürten, B., et al. (2019). An *in situ* approach for measuring biogeochemical fluxes in structurally complex benthic communities. *Methods Ecol. Evol.* 10 (5), 712–725. doi: 10.1111/2041-210X.13151

Salk, K. R., Erler, D. V., Eyre, B. D., Carlson-Perret, N., and Ostrom, N. E. (2017). Unexpectedly high degree of anammox and DNRA in seagrass sediments: Description and application of a revised isotope pairing technique. *Geochim. Cosmochim. Acta* 211, 64–78. doi: 10.1016/j.gca.2017.05.012

Seddon, N., Chausson, A., Berry, P., Girardin, C. A. J., Smith, A., and Turner, B. (2020). Understanding the value and limits of nature-based solutions to climate change and other global challenges. *Philos. Trans. R. Soc. B.: Biol. Sci.* 375 (1794), 20190120. doi: 10.1098/rstb.2019.0120

Smetacek, V., and Zingone, A. (2013). Green and golden seaweed tides on the rise. *Nature* 504 (7478), 84–88. doi: 10.1038/nature12860

Soares, A., Guieysse, B., Jefferson, B., Cartmell, E., and Lester, J. N. (2008). Nonylphenol in the environment: A critical review on occurrence, fate, toxicity and treatment in wastewaters. *Environ. Int.* 34 (7), 1033–1049. doi: 10.1016/j.envint.2008.01.004

Song, G. D., Liu, S. M., Kuypers, M. M. M., and Lavik, G. (2016). Application of the isotope pairing technique in sediments where anammox, denitrification, and dissimilatory nitrate reduction to ammonium coexist. *Limnol. Oceanog.: Methods* 14 (12), 801–815. doi: 10.1002/lom3.10127

Song, G. D., Liu, S. M., Marchant, H., Kuypers, M. M. M., and Lavik, G. (2013). Anammox, denitrification and dissimilatory nitrate reduction to ammonium in the East China Sea sediment. *Biogeosciences* 10 (11), 6851–6864. doi: 10.5194/bg-10-6851-2013

Taddei, D., Bucas, G., Clavier, J., Cuet, P., and Frouin, P. (2007). Carbon fluxes at the water sediment interface in reunion island fringing reef. *West. Indian Ocean. J. Mar. Sci.* 6 (2), 137–146.

Taddei, D., Cuet, P., Frouin, P., Esbelin, C., and Clavier, J. (2008). Low community photosynthetic quotient in coral reef sediments. *Comptes. Rendus. Biol.* 331 (9), 668–677. doi: 10.1016/j.crvi.2008.06.006

Tedetti, M., Bigot, L., Turquet, J., Guigue, C., Ferretto, N., Goutx, M., et al. (2020). Influence of freshwater discharges on biogeochemistry and benthic communities of a coral reef ecosystem (La réunion island, Indian ocean). *Front. Mar. Sci.* 7. doi: 10.3389/fmars.2020.596165

Thamdrup, B., and Dalsgaard, T. (2002). Production of N2 through anaerobic ammonium oxidation coupled to nitrate reduction in marine sediments. *Appl. Environ. Microbiol.* 68 (3), 1312–1318. doi: 10.1128/AEM.68.3.1312-1318.2002

Thompson, R. C., Tobin, M. L., Hawkins, S. J., and Norton, T. A. (1999). Problems in extraction and spectrophotometric determination of chlorophyll from epilithic microbial biofilms: towards a standard method. *J. Mar. Biol. Assoc. Unite. Kingdom.* 79 (3), 551–558. doi: 10.1017/S0025315498000678

Tsui, M. M. P., Leung, H. W., Kwan, B. K. Y., Ng, K.-Y., Yamashita, N., Taniyasu, S., et al. (2015). Occurrence, distribution and ecological risk assessment of multiple classes of UV filters in marine sediments in Hong Kong and Japan. *J. Haz. Mat.* 292, 180–187. doi: 10.1016/j.jhazmat.2015.03.025

Van Dam Bryce, R., Zeller Mary, A., Lopes, C., Smyth Ashley, R., Böttcher Michael, E., Osburn Christopher, L., et al. (2021). Calcification-driven CO2 emissions exceed "Blue carbon" sequestration in a carbonate seagrass meadow. *Sci. Adv.* 7 (51), eabj1372. doi: 10.1126/sciadv.abj1372

van Tussenbroek, B. I. (2011). Dynamics of seagrasses and associated algae in coral reef lagoons. *Hidrobiológica* 21 (3), 293–310.

Ward, M., Kindinger, T. L., Hirsh, H. K., Hill, T. M., Jellison, B. M., Lummis, S., et al. (2022). Reviews and syntheses: Spatial and temporal patterns in seagrass metabolic fluxes. *Biogeosciences* 19 (3), 689–699. doi: 10.5194/bg-19-689-2022

Yeh, A., Marcinek, D. J., Meador, J. P., and Gallagher, E. P. (2017). Effect of contaminants of emerging concern on liver mitochondrial function in Chinook salmon. *Aquat. Toxicol.* 190, 21–31. doi: 10.1016/j.aquatox.2017.06.011

Advantages of publishing in Frontiers

OPEN ACCESS
Articles are free to read for greatest visibility and readership

FAST PUBLICATION
Around 90 days from submission to decision

HIGH QUALITY PEER-REVIEW
Rigorous, collaborative, and constructive peer-review

TRANSPARENT PEER-REVIEW
Editors and reviewers acknowledged by name on published articles

Frontiers
Avenue du Tribunal-Fédéral 34
1005 Lausanne | Switzerland

Visit us: www.frontiersin.org
Contact us: frontiersin.org/about/contact

REPRODUCIBILITY OF RESEARCH
Support open data and methods to enhance research reproducibility

DIGITAL PUBLISHING
Articles designed for optimal readership across devices

FOLLOW US
@frontiersin

IMPACT METRICS
Advanced article metrics track visibility across digital media

EXTENSIVE PROMOTION
Marketing and promotion of impactful research

LOOP RESEARCH NETWORK
Our network increases your article's readership